PRECISION ORBIT DETERMINATION FROM GPS RECEIVER NAVIGATION SOLUTIONS

by

Scott Shannon Carter

B.S. Astronautical Engineering
United States Air Force Academy
(1994)

SUBMITTED TO THE DEPARTMENT OF AERONAUTICS AND ASTRONAUTICS IN PARTIAL FULFILLMENT OF THE REQUIREMENTS FOR THE DEGREE OF

MASTER OF SCIENCE

at the

MASSACHUSETTS INSTITUTE OF TECHNOLOGY

June 1996

Signature of Author_____
Department of Aeronautics and Astronautics
June 1996

Certified by_____
Dr. Ronald J. Proulx
Thesis Supervisor, CSDL

Certified by_____
Dr. Paul J. Cefola
Thesis Supervisor, CSDL
Lecturer, Department of Aeronautics and Astronautics

Accepted by_____
Professor Harold Y. Wachman
Chairman, Departmental Graduate Committee

[This page intentionally left blank.]

PRECISION ORBIT DETERMINATION FROM GPS RECEIVER NAVIGATION SOLUTIONS

by

Scott S. Carter

Submitted to the Department of Aeronautics and Astronautics
on May 10, 1996 in partial fulfillment of the requirements
for the Degree of Master of Science

ABSTRACT

Satellite tracking techniques have traditionally been limited to ground-based stations that measure a satellite's range, azimuth, elevation and range rate. The advent of high accuracy Global Positioning System (GPS) navigation techniques, however, offers alternative methods. This thesis investigates the use of GPS navigation solutions (earth-centered, earth-fixed position and velocity information) as an observation source in a weighted least-squares orbit determination process. Such an orbit determination scheme could limit dependence upon the costly and complex ground-based tracking facilities for low and medium earth orbit satellites, while providing real-time information for on-board instrumentation and mission management. This investigation included modification of the Draper Laboratory version of the Goddard Trajectory Determination System (Draper R&D GTDS) to include coordinate systems compatible with the Fifth Fundamental Catalogue (FK5) and an inertial true equator and equinox of date frame. Solid earth tide modeling was introduced for numerical integration techniques and refined for semianalytic methods. The accuracy of the navigation solution-derived orbits (and the ability of Draper R&D GTDS to model spacecraft motion) is determined for the Ocean Topography Experiment (TOPEX), Technology for Autonomous Operational Survivability (TAOS), and Extreme Ultraviolet Explorer (EUVE) through comparison to high quality, independently generated "truth" solutions (Precise Orbit Ephemerides, or POEs).

Thesis Supervisor: Dr. Ronald J. Proulx
Title: Technical Staff Engineer, The Charles Stark Draper Laboratory, Inc.

Thesis Supervisor: Dr. Paul J. Cefola
Title: Lecturer, Department of Aeronautics and Astronautics
Program Manager, The Charles Stark Draper Laboratory, Inc.

[This page intentionally left blank.]

Acknowledgments

Many individuals deserve recognition for the completion of this work, and I can only hope to minimize incidental omission. Paul Cefola and Ron Proulx provided not only the technical expertise and guidance for this project, but also tremendous opportunities for personal and professional development. Ms. Fern Kinion (previously of the United States Air Force Academy), Mr. John Sweeney and Ms. Joan Chiffer (Draper Education Office) warrant special recognition for offering the opportunity to participate in the Draper Fellowship program. Wayne McClain, John Loud, Rick Metzinger, Jasjit Heckathorn, and Linda Alger (all Draper personnel) have supported this work in various manners. Kenn Gold (UC-Boulder), Joseph Guinn (JPL) and Stephanie Lowery (Johnson Space Center) were extremely helpful in obtaining appropriate data for analysis purposes. Richard Hujsak (Logicon) supplied software associated with the solid earth tide modeling, and Don Danielson (Naval Postgraduate School) provided insight for the averaged tidal representation. Pat Johnson (GSFC) was tremendously helpful in the transfer of SLP data bases, and Nikita Zelensky (GSFC) provided an interpolation scheme for the POE solutions. Chris Sabol (USAF Phillips Laboratory), Viola Hill-Raben (NOAA) and Lt. Scott Wallace (USAF Phillips Laboratory) were helpful in obtaining geomagnetic activity information. Larry Young and Steven Lichten (JPL) provided technical insight on various types of space-based GPS receivers. Ed Doll (GSFC) assisted in understanding the internal operation of GTDS. Prof. Robert Culp and Prof. George Born (UC-Boulder) were helpful in providing a point of contact for the EUVE information.

As any author knows, support external to the work environment is often as important as technical advice. I am grateful to my mom, dad, and sister for the unselfish encouragement provided in my career development. Maryann Mossa and Brian Tidwell have enriched my life to a degree far beyond what is expected of any individual. Lisa Michael and Katy Trainor were tremendously helpful during times of frustration. Thanks goes out to Scott Wallace, Kent Engebretson, and Naresh Shah who provided insight in the academic, military and social environments. Finally, to the Good Lord whose grace has offered hope for the whole world.

This thesis was prepared at The Charles Stark Draper Laboratory, Inc., with support from Draper Laboratory's DFY96 IR&D Task 636.

[This page intentionally left blank.]

Contents

[This page intentionally left blank.]

List of Figures

[This page intentionally left blank.]

List of Tables

Chapter 1

Introduction

1.1 Statement of Objectives

The ability to determine the past, present, and often future location of a spacecraft is an essential component to any space mission. Without such knowledge, personnel could miss their communications relay, infer incorrect scientific measurements, or misinterpret visual images. The goal of orbit determination is to provide such a description of a satellite's location based upon a series of measurements.

Orbit determination is a statistical process that estimates a satellite's location at a given epoch using a prescribed set of initial conditions and information from various observation sources. Should the equations of motion and a priori initial conditions perfectly describe the satellite's path, the process would become completely deterministic, and no measurements would be required. Unfortunately, both the models and the available initial conditions are corrupted by noise (called process noise), making it is necessary to introduce additional information in the form of measurements, which have their own uncertainties (referred to as measurement noise).

Information from the models and measurements are combined to develop a "best estimate" of the satellite's trajectory. This estimated orbit is defined as

the state that corresponds closest to that of the true orbit, minimizing the weighted sum of the squares of the differences between the observations and the true orbit [18]. Assuming future conditions will be representative of those experienced during the fit (weight least-squares) process, this estimate of the satellite's orbit can then be used to predict future motion.

Traditionally, ground-based tracking stations provided measurements in the form of a satellite's range, azimuth, elevation and range rate to support this weighted least-squares differential correction process. However, these measurements contain station-dependent biases and are inherently limited to the time periods that the station is able to acquire a signal from the satellite, which can sometimes be very short in duration. Although the amount of available information can be increased through a network of these tracking stations, the cost associated with maintaining such a network prohibits continuous coverage of the satellite.

The advent of high accuracy Global Positioning System (GPS) navigation techniques introduces alternatives for measurement sources to support the orbit determination process. A GPS receiver (GPSR) placed on-board a satellite provides continuous tracking in the form of navigation solutions; that is, the position and velocity of the spacecraft. Use of this information in place of the traditional measurements could limit dependence upon the costly and complex ground-based tracking facilities for low and medium earth orbit satellites, while providing real-time information for on-board instrumentation [26]. The only limitation arises from the fact that the satellite must be able to properly acquire signals from the GPS constellation, a

problem for high eccentricity and geosynchronous orbits, or interplanetary missions.

The objective of this thesis is to investigate the use of commercial (C/A) navigation solutions from a low-cost, single frequency GPSR as an observation data type in the orbit determination process. Mean and osculating element sets are produced for three satellites carrying GPSRs, and comparison to high quality, independently generated truth ephemerides indicates the feasibility of using the navigation solutions in moderate accuracy applications. A secondary objective is to utilize these high accuracy truth orbits to evaluate the modeling process of the orbit determination software.

1.2 The Global Positioning System (GPS)

The Global Positioning System (GPS) is a constellation of twenty-four satellites whose fundamental objective is to provide navigation and timing support to military personnel. The constellation operates at an altitude of approximately 20200 km in four nearly circular orbit planes inclined 55 degrees with respect to the earth's equator. Given this geometry, if twenty-one of the twenty-four satellites are operational and the planes are evenly spaced in right ascension, reception from four satellites at any ground-based location is assured [40]. To optimize global visibility, the phasing within each plane is not constant [41]. The suitability of such a system to a variety of fields has expanded the role of GPS into the civilian sector to help satisfy needs in areas such as surveying and navigation.

A low earth orbit satellite equipped with a GPS receiver (GPSR) can be continuously tracked due to the GPS constellation geometry, a feature not available to ground-based tracking stations. These receivers develop solutions for the user location based upon time differences between GPS satellite transmission and reception by the user satellite.

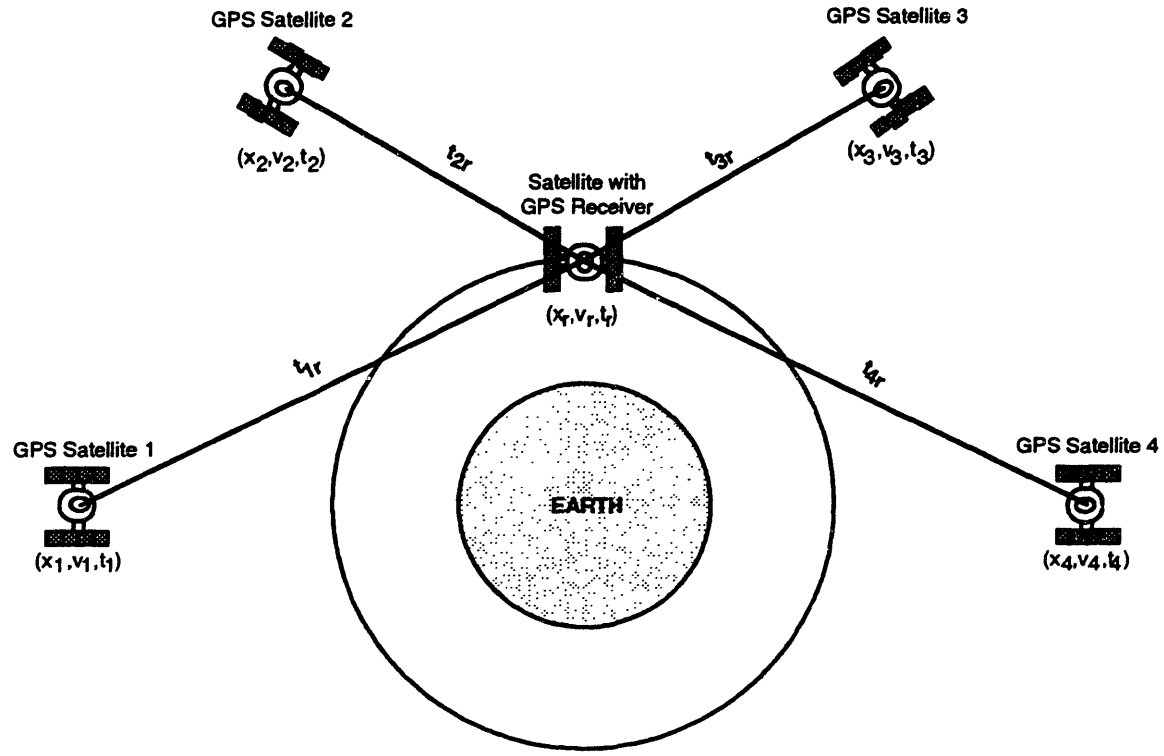

Figure 1.1 GPS Signal Acquisition

Each GPS satellite is equipped with a set of highly stable atomic clocks operating at a fundamental frequency of 10.23 MHz. The two L-band carrier frequencies used in GPS transmissions, 1575.42 (L1) and 1227.6 MHz (L2), are derivatives of this fundamental frequency. Two primary codes, each unique to an individual GPS satellite, are superimposed upon these carrier frequencies and allow the receivers to differentiate signals between satellites. The coarse acquisition (C/A) code is chipped at a rate of 1.023 MHz with a

repeat cycle of 1 μsec, and is used in standard positioning techniques. The precise (P) code is the principal code used in military applications, and has a chipping rate of 10.23 MHz, but consists of a string of 37 week-long segments, each of which can be designated for one GPS satellite. While both codes are written on the L1 frequency, only the P code is encoded on the L2 carrier. In addition to the C/A and P codes, a navigation message is included in each GPS signal. Chipped at 50 Hz, this message includes the ephemeris of the transmitting satellite, various timing information, and an overall status of both the message and the satellite [40].

All of this information is combined into one transmitted GPS signal. The modulation of the code and navigation message onto the carrier is based upon the fundamental concepts of binary phase shift keying (BPSK). BPSK methods utilize 180° phase shifts to convert an analog waveform into a digital modulation form [40].

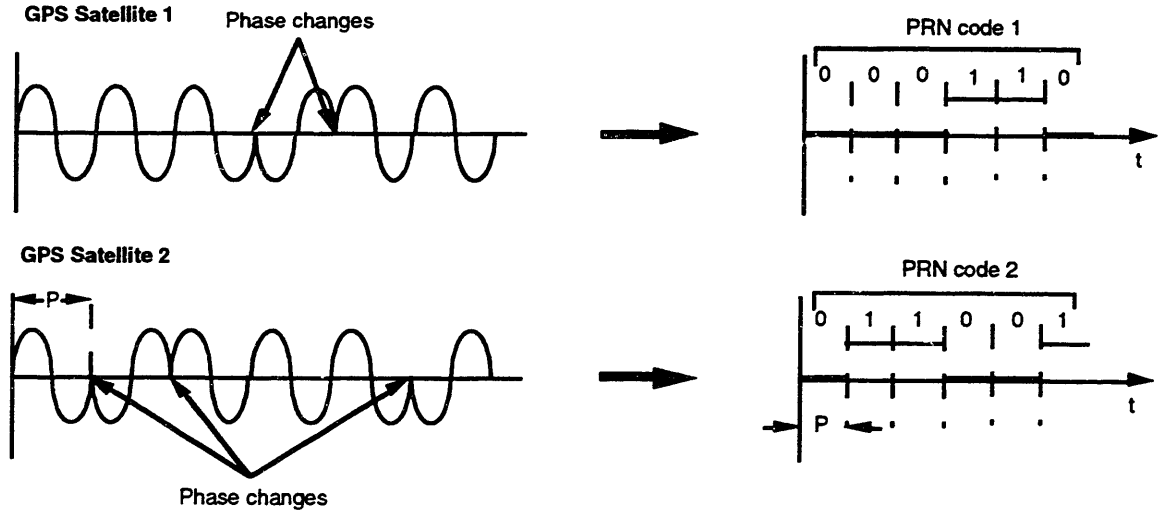

Figure 1.2 PRN Code Generation

Two binary data streams (for instance, the C/A code and navigation message) are combined into one by means of modulo-2 addition. In modulo-2 addition, the following relationships apply:

- $0 + 0 = 0$
- $1 + 0 = 1$
- $0 + 1 = 1$
- $1 + 1 = 0$

The full information content of the incoming GPS signal can be recovered by modulo-2 addition of the proper code and the received signal.

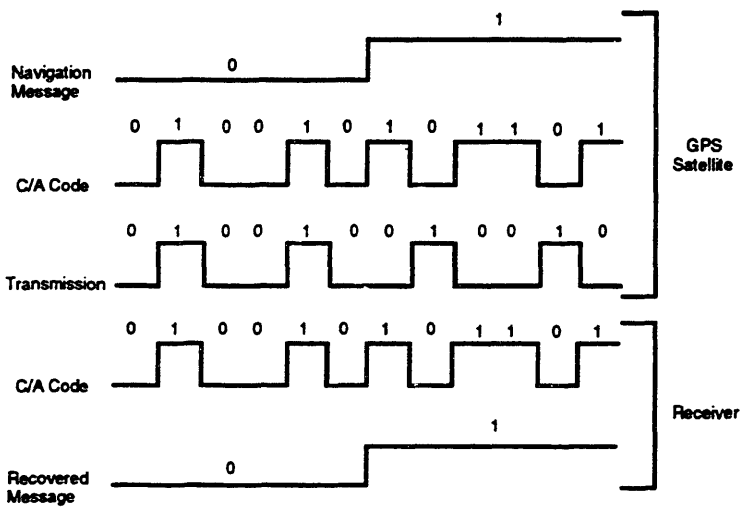

Figure 1.3 Recovery of the Navigation Message for C/A (L1 only) Receiver

The receiver searches for the proper code embedded within the signal by mimicking the procedures that take place in the creation of the codes by the GPS satellites. Therefore, the time that it takes the receiver to search for and acquire the proper code for the incoming signal is proportional to the distance traveled by the signal (plus clock errors and other delay effects).

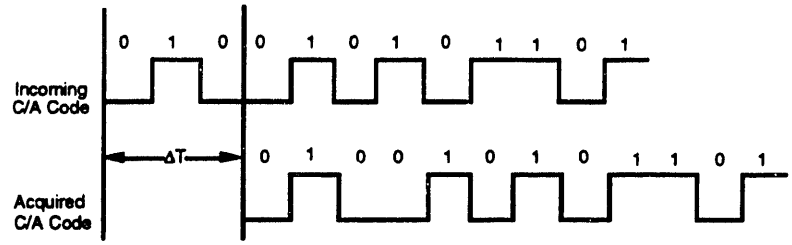

Figure 1.4 Pseudorange Measurement

This time difference is referred to as the *pseudorange*, and is one of two fundamental observables of the GPS system.

$$\rho = c(t_t - t_r + \Delta t_r) + \Delta\rho_e \tag{1.1}$$

where ρ is the pseudorange, t_t is the time of transmission (by the GPS satellite), t_r is the reception time, c is the speed of light, Δt_r is the receiver clock bias, and $\Delta\rho_e$ contains effects of additional error sources (such as ionospheric delay, multipath, etc.). The second observable is known as the *carrier phase*, and represents a difference in phase between the receiver's internal clock and the incoming carrier signal.

Using either the pseudorange or the carrier phase from four satellites, the receiver can determine its earth-centered, earth-fixed (ECEF) coordinates, and the receiver clock bias. This is illustrated by the following set of psuedorange equations.

$$\begin{aligned}
\rho_1 &= \sqrt{(x_1 - x_r)^2 + (y_1 - y_r)^2 + (z_1 - z_r)^2} + c\Delta t_r \\
\rho_2 &= \sqrt{(x_2 - x_r)^2 + (y_2 - y_r)^2 + (z_2 - z_r)^2} + c\Delta t_r \\
\rho_3 &= \sqrt{(x_3 - x_r)^2 + (y_3 - y_r)^2 + (z_3 - z_r)^2} + c\Delta t_r \\
\rho_4 &= \sqrt{(x_4 - x_r)^2 + (y_4 - y_r)^2 + (z_4 - z_r)^2} + c\Delta t_r
\end{aligned} \tag{1.2}$$

where ρ_n is the pseudorange to GPS satellite n, $(x,y,z)_n$ are the ECEF coordinates of GPS satellite n, $(x,y,z)_r$ are the ECEF coordinates of the receiver, c is the speed of light, and Δt_r is the receiver clock bias.

The solution to this set of equations is dependent upon the location of four (or more) GPS satellites and the observed pseudorange (the time difference illustrated in Figure 1.4). A basic assumption in the derivation of this solution is that the GPS and receiver clocks are synchronized such that the pseudorange and carrier phases can be properly measured in the fashion presented above. Also, the navigation message transmitted by each GPS satellite is assumed to be correct for the time of interest. However, the current operation of the GPS system makes both of these assumptions invalid. Intentional degradation of both the ephemeris information contained in the navigation message (known as SA-epsilon) and the GPS on-board clocks (referred to as clock dithering) result in errors in the observable measurements for C/A code users. This feature, known as *selective availability (SA)*, was implemented by the U.S. Air Force to ensure that only authorized users have the opportunity to achieve the highest accuracy results with this system. A separate feature, known as *anti-spoofing (AS)*, limits P-code acquisition to authorized users. Individual navigation solution accuracy under SA and AS is limited to approximately 100 meters for C/A users, while

without SA/AS, the solutions are generally good to between 5 and 20 meters [40].

1.3 Evolution of Spaceborne GPSRs

Although the idea of using GPS for spacecraft navigation has existed since 1976, the first satellite to actually carry a GPSR was Landsat-4 in August 1982. The primary function of the GPSPAC model placed on-board was to provide alternative uses of the GPS system in both real-time and post-flight modes. Unfortunately, the mission was cut short by a memory checksum error after a mere four days [49]. Despite the brevity of the Landsat-4 experiment, several groups have recognized the potential for development in this area and have constructed space-qualified receivers. The current list of manufacturers includes Rockwell International, Motorola, Trimble, Loral, Texas Instruments, Alcatel-Sel, Hitachi, Ashtech, and Alan Osborne and Associates. Appendix A provides a look at some of the available receivers and their characteristics.

The space environment dictates that spaceborne GPSRs differ from the more traditional ground-based receivers. Radiation hardening and more stringent reliability requirements increase the cost and complexity associated with the receivers. Power, size and weight constraints also play a major factor in the integration of a GPSR into a space mission. Because of these limitations and interface requirements, most spaceborne receivers are not off-the-shelf products, but rather ground-based receivers modified to accommodate the needs of the specific mission.

Although these spaceborne receivers can possess multiple functionalities, including time synchronization and attitude determination, this work will focus on the most common use of these GPSRs - navigation. Several spacecraft have augmented their tracking strategies to provide supplemental orbit information by placing a GPSR on-board. Both military and civilian sectors are hoping to utilize GPS as a primary tracking technique in the near future. Table 1.1 summarizes some of the spacecraft that have carried GPSRs.

Table 1.1 Spacecraft Equipped With GPSRs [17,38,49,65,37,55,33]

Spacecraft	Launch Date	Orbit Parameters	Receiver Type
LANDSAT 4	16 July 1982	705 km / 98°	Magnavox GPSPAC
LANDSAT 5	1 March 1984	705 km / 98°	Magnavox GPSPAC
EUVE	7 June 1992	500 km / 28.5°	Motorola GPS/DR
TOPEX	10 April 1992	1336 km / 60°	Motorola GPS/DR
RADCAL	25 June 1993	815 km / 89.5°	Trimble TANS Quadrex (2)
OREX	4 February 1994	450 km / 35°	Toshiba
TAOS	13 March 1994	555 km / 105°	Rockwell AST V
APEX	August 1994	380x2500 km / 70°	Trimble TANS II
STS-69 (Endeavor)	7 September 1995	400 km / 28.5°	Collins
WSF-02	11 September 1995	400 km / 28.5°	Osborne Turbostar
HOPE	late 1990's	380 km / 35°*	undecided
EOS ALT/GLAS	2002	700 km / 94°	undecided

* These numbers are expected to be typical of the HOPE missions.

1.4 Previous Precision Orbit Work Using GPSR Measurements

Most of the precision GPSR studies thus far have focused on use of the raw observables in a differential GPS (DGPS) manner. Information from a network of ground-based receivers is included to eliminate various errors associated with GPS and/or receiver clocks. Single differencing the observables from the same GPS satellite for two receivers (one on the spacecraft, and one on the ground) eliminates most of the errors associated with the common satellite. Double differencing measurements from two receivers for two GPS satellites at common epochs provides the advantage of canceling out the receiver clock errors. Because the largest error sources (SA and clock errors) are eliminated in DGPS, the accuracy of the solution improves.

The most extensively studied mission involving GPS measurements has been TOPEX/POSEIDON. The stringent orbit determination limitations (13 cm radial error) have provided a classic opportunity for development of DGPS techniques for spacecraft applications. The major thrust of the work has come from the Jet Propulsion Laboratory (JPL), the University of Colorado at Boulder, and the University of Texas Center for Space Research (UT/CSR). Using a 20 satellite GPS constellation, and carrier phase information from the TOPEX GPSR and a network of six ground-based GPSRs, Guinn has shown that single difference DGPS techniques can be used to provide an orbit that is, in three-dimensional terms, within 18 cm (4.5 cm in the radial direction) of a high quality "truth" orbit accurate to about 15 cm (3-4 cm radially) [27,61,5,67].

Swift investigated several derivatives of the JPL work by employing both differential and standard (non-differential) techniques. He initially created a reference trajectory with the OMNIS orbit computation system using the JPL fitted DGPS solutions. Double differencing of the carrier phase observables from the TOPEX receiver with information from a network of 15 International GPS Service for Geodynamics (IGS) Rogue receivers resulted in RMS orbit accuracies of 5, 14, and 14 cm in the radial, cross-track and along-track directions, respectively, when compared to his reference trajectory. In a separate experiment, he used the ground-based network of 15 GPSRs to remove SA effects for the GPS satellite orbits. The GPS orbits were then used by the TOPEX GPSR in a non-differential mode. This method produced errors of 5, 18, and 13 cm (radial, cross-track, and along-track) [60].

GPS measurements from other satellites have been utilized in a similar DGPS fashion. Gold [26] and Guinn [28] produced DGPS orbits for the Extreme Ultraviolet Explorer (EUVE) and Technology for Autonomous Operational Survivability (TAOS), respectively, and assessed the quality of these orbits by comparing solutions during overlapping orbit determination (fit) spans. Using a ground-based network of 13 Rogue GPSRs, the EUVE solutions were shown to be accurate to about one meter [26]. The TAOS system utilized 12 ground-based receivers, and the residuals had a 1σ of about three meters [28].

In a somewhat modified form of DGPS, GPSRs were placed on board STS-6 and its payload, the Wake Shield Facility (WSF-02). Double differencing DGPS was performed using the Collins GPSR on *Endeavor* and the TurboStar on-board WSF-02. The relative position between the two receivers was determined within 10 meters. In addition, the observables were double

differenced between each of the on-board receivers and a network of 13 ground-based TurboRogue GPSRs. The converged solutions had a residual RMS of about 3 meters using the psuedorange observable, and 34 cm using carrier phase (TurboStar only) [57].

The Japanese hope to utilize DGPS concepts in their version of a reusable orbiting vehicle (HOPE). In an effort to simulate the environment anticipated for HOPE, a GPSR was placed on-board the Orbital Re-entry Experiment (OREX) spacecraft to evaluate methods of standard point positioning (SPP) and DGPS [37]. Precise GPS clock and orbit information accounting for SA effects was provided by the International GPS Service for Geodynamics (IGS) to produce a truth orbit (although this orbit did not account for ionospheric effects) accurate to about 35 meters. The maximum errors of the least-squares fit process using the broadcast clock information when compared to the truth orbit were on the order of about 225 meters. Comparison of the truth and DGPS orbits (between the OREX receiver and a single ground receiver) showed relative agreement to about 11 meters [50].

Other future missions, like HOPE, envision utilizing similar DGPS techniques as well. Both the EOS ALT/GLAS (GLAS) and GEOSAT Follow-On (GFO/GFO-2) missions require radial orbit accuracies on the order of TOPEX specifications (at much lower altitudes relative to TOPEX) for environmental studies. Drawing on information gleaned from the TOPEX GPS studies, these spacecraft plan on employing high accuracy DGPS concepts to achieve their objectives. Experimental simulations indicate that DGPS will provide sufficient accuracy for both missions (3.0 cm radially for GFO-2; 2.0 cm radially, 7 cm horizontally for GLAS) [55,33].

Other studies, although not as prolific as the DGPS work, have focused on non-differential techniques using GPS measurements. Guinn used GPS navigation solutions (position and clock error of the receiver) from TOPEX to illustrate the concept of autonomously computing maneuver parameters for repeat ground track missions [30]. Langer investigated the feasibility of using navigation solutions with SA effects removed (through a special algorithm provided by the GPS program office) for orbit determination of the RADCAL spacecraft, which required 5 meter post-flight accuracy. Comparison to a DGPS orbit accurate to one meter revealed about a four meter variation, indicating that some missions requiring moderate fit accuracies could take advantage of this special algorithm and use navigation solutions in their orbit determination schemes [38]. Fennessey used navigation solutions covering one day periods from the TAOS spacecraft as observations for a differential correction process as an alternative to the more traditional Space Ground Link System (SGLS) range, elevation, azimuth and range rate (RAER) data. The navigation solution-derived orbits, when compared to Guinn's DGPS orbit, exhibited errors on the order of about 16 meters during the fit interval [17].

1.5 Focus of Current Work

The current generation of GPS satellite receivers primarily focuses on determining a current time position and velocity vector in earth-centered, earth-fixed (ECEF) coordinates and receiver clock parameters [59,16]. By comparing the navigation solutions to the high precision orbits for EUVE and TAOS, Gold and Guinn showed that the errors inherent to the individual

solutions due to SA/AS is on the order of 50 meters, limiting their utility for orbit prediction into the future [26, 28].

Previous work has demonstrated the effectiveness of using pseudorange and carrier phase measurements in a differential mode to obtain a high accuracy assessment of the location of a satellite. However, Fennessey indicates that the bandwidth requirements for using observables can approach 25 megabytes/day per receiver, while the navigation solutions may only require 100 kilobytes/day for an individual receiver - 250 times less [17]. This is a particularly significant difference when considering satellite constellations. The increased data flow and extra ground sites associated with the DGPS techniques could prove expensive when other alternatives exist.

1.6 Use of Navigation Solutions as Observation Data

The current work investigates the direct construction of precision mean (and osculating) element sets using the GPSR on-board navigation solutions as a "replacement" for ground-based tracking data. The ECEF position and velocity data can be preprocessed for entry into a conventional ground-based orbit determination program such as the workstation version of the Goddard Trajectory Determination System (GTDS) used at the Charles Stark Draper Laboratory in Cambridge, MA. Both osculating and mean element sets can then be derived from the differential correction process, and used for ephemeris generation.

Utilization of the GPSR navigation solutions as observation data provides the user with a simple, reliable method of orbit determination, eliminating the

cost and complexity associated with differential techniques or enhancement of on-board receiver software and storage requirements. In addition, the geometry of the GPS constellation ensures continuous tracking of the satellite that ground-based networks cannot provide.

1.7 Navigation Solution Sources for This Work

Navigation solutions and associated "truth" orbits were obtained for three spacecraft over various time periods. These three spacecraft - EUVE, TOPEX, and TAOS - are described below.

1.7.1 The EUVE Mission

The Extreme Ultraviolet Explorer (EUVE) spacecraft was launched in June 1992 into a 500 km, 28° inclination, nearly circular orbit. The NASA spacecraft is dedicated to astronomical observations in the extreme ultraviolet region of the electromagnetic spectrum [26]. As part of its payload, it carries four ultraviolet telescopes to provide the first detailed all-sky survey at these wavelengths. The most likely targets of these telescopes are mature stars, including white dwarfs [65].

An experimental single-frequency GPS receiver was placed on-board the Explorer platform at the manufacturer's (Motorola) expense. The receiver, referred to as a GPS Demonstration Receiver (GPS/DR), is a secondary payload, and hence, does not contribute to the actual mission. Two GPS reception antennae have been included, with a capability of tracking up to twelve GPS satellites (six on each of the antennae) at once. The receiver

provides carrier phase observations every second, and pseudorange and navigation solutions every ten seconds. Characteristics of this receiver are found in Appendix A.

1.7.2 The TOPEX Mission

The TOPEX/POSEIDON spacecraft was launched as a joint NASA/CNES effort on 10 August 1992 into a 1334 km, 66°, nearly circular orbit to provide long-term observation of the global ocean circulation and surface topography [65]. Over its anticipated five year lifetime, the satellite was expected to use two microwave altimeters to observe surface signatures. Earlier missions (GEOSAT and SEASAT) indicated that radial orbit errors are a significant contributor to the uncertainties associated with global circulation models [46]. Therefore, efforts were made to improve orbit determination methods by introducing satellite laser ranging (SLR) and Doppler orbitography and radio positioning integrated by satellite (DORIS).

An experimental GPS/DR built by Motorola (similar to the EUVE version) was included as part of the payload to provide an alternative orbit determination method. The TOPEX GPSR tracks up to six GPS satellites simultaneously and provides carrier phase measurements every second, and pseudorange and navigation solutions every ten seconds [46].

1.7.3 The TAOS Mission

The TAOS spacecraft is a product of the U.S. Air Force Phillips Laboratory launched on 13 March 1994 into a 560 km, 105° inclination, circular orbit. Its purpose is to investigate autonomous navigation options, as well as calibrate other Air Force laser and radio measurements [17].

The Rockwell Advanced Satellite Technology (AST) V six channel, single-frequency GPSR is a significant part of its payload. The receiver provides raw GPS observables on a once per second grid, while navigation solutions are computed once every minute. The TAOS GPSR has not provided tracking data since August 1994 [17].

1.8 Thesis Overview

The remainder of this thesis discusses the details of using GPSR navigation solutions as an observation source, sources of improvement in the orbit determination process, and experimental results from processing actual GPSR navigation solutions for three satellites.

Chapter 2 introduces the reader to fundamentals of the orbit determination software, navigation solutions, the "truth" orbits serving as a reference, and integration of each of these components into a method of analysis. The existing capabilities and fundamental operation of the orbit determination software (Draper R&D GTDS) are presented. This description includes discussions of the pertinent coordinate systems and orbit generator options available in GTDS. The content and format of the navigation solutions and

"truth" orbits are introduced. Finally, a description of the integration of the navigation solutions and orbit determination software is provided.

Chapter 3 describes the various software modifications required to support the study of using navigation solutions as an observation source. A discussion of the J2000 (FK5) coordinate system and its relation to the previous B1950 (FK4) frame is presented. A mathematical derivation of the perturbative effects of solid earth tides is given, followed by a discussion of the differences between instantaneous true of date and true of reference coordinate systems. The software modifications required to support each of these new capabilities are summarized.

Chapter 4 discusses the testing performed to ensure proper implementation of each of these new capabilities. A description of the logic and scope of the testing is followed by various indicators that suggest proper incorporation of these capabilities.

Chapter 5 summarizes the results of using GPSR navigation solutions as a tracking source in orbit determination/prediction for three satellites. The accuracy of the perturbation models within Draper R&D GTDS is indicated through proper application of the "truth" solutions.

Chapter 6 summarizes the findings of this work and offers suggestions for future work in this area.

Appendix A provides a list of the available space-qualified GPSRs and associated characteristics currently on the market.

Appendix B summarizes the code modifications required to support an ECEF input option.

Appendix C lists the software tools developed to support this thesis.

Appendix D is a listing of the new input data cards available that include J2000, solid earth tides, and instantaneous true of date options.

Appendix E describes the manner in which the VAX is configured to properly execute Draper R&D GTDS.

Appendix F discusses the information contained within the newly-developed fundamental constants file that distinguishes execution in the FK4 system from execution in the FK5 system.

Appendix G summarizes the test cases performed in the validation of the incorporation of the new software capabilities added to Draper R&D GTDS. It provides a more detailed form of the items discussed in Chapter 4.

Appendix H summarizes the results of using GPSR navigation solutions in an orbit determination process. It offers a more detailed description of the results presented in Chapter 5.

Chapter 2

GPSR Navigation Solutions in R&D GTDS

2.1 Chapter Introduction

It is imperative for the reader to understand both the data source and orbit generation process in order to fully appreciate the meaning of orbits generated from GPS receiver navigation solutions. This chapter provides background information in both of these areas. The first half of the chapter introduces the orbit determination software (Draper R&D GTDS) and its important features. Following a brief description of software capabilities to acquaint the reader with GTDS terminology, the orbit generators and perturbation techniques relevant to this project are discussed in detail. A fundamental understanding in these areas is vital for the reader to fully appreciate the methods used in developing precision orbits. The second half of the chapter is devoted to describing two data sources pertinent to this work. The content of the GPSR navigation solutions and preprocessing required for their entry into Draper R&D GTDS are described to develop an appreciation of the characteristics associated with this observation source. The Precise Orbit Ephemerides (POEs), high accuracy orbits considered to be the best representation of a satellite's motion available (often referred to as "truth" solutions), are

introduced at the conclusion of the chapter as a reference to compare GPSR-based orbits against.

2.2 Overview of the Goddard Trajectory Determination System

The orbit determination software used to evaluate the underlying concepts of this work is the Draper Research and Development version of the Goddard Trajectory Determination System (hereafter referred to as Draper R&D GTDS), a descendant of the original GTDS developed at NASA/Goddard Space Flight center in the early 1970s. The operational GTDS Math Specification describes the product as "a collection of related computer programs that provide operational support for Earth, lunar, and interplanetary missions and serves as a research and development tool" [25]. The system can be divided into nine major capabilities:

- Ephemeris Generation
- Differential Correction
- Filtering
- Ephemeris Comparison
- Data Management
- Data Simulation
- Permanent File Report Generation
- Error Analysis
- Early Orbit Determination

Each of these capabilities is described in detail in the Goddard Trajectory Determination System (GTDS) User's Guide [25]* . A summary of these descriptions is provided below.

The **EPHEMERIS GENERATION** program develops a state (and, optionally, state partial derivative) history over a specified time span based upon prescribed initial conditions. Orbit generator options include analytic, numerically averaged, and high precision numerical theories for varying accuracy and efficiency requirements. Various perturbation options are available for user specification. Products of this program include an ephemeris output report (which can be sent to an on-line printer) and files that can be subsequently utilized with GTDS and/or other systems (ORB1, ORBIT, and EPHEM).

The **DIFFERENTIAL CORRECTION (DC)** program utilizes estimation theory to evaluate a satellite's orbit and certain associated parameters. An estimate of the initial conditions and a set of observations are used to compute an orbit that minimizes (in a Bayesian weighted least squares sense) the sum of the squares of the residuals between the observed and computed trajectories. Additionally, solve-for parameters such as the drag coefficient or station location can be estimated based upon the observation data. Observation biases are indicated in the tabulated output report, and can be included as solve-for parameters. First and second order statistics (i.e., mean and covariance matrix) are determined for the estimated parameters.

---

* It should be noted that the Operational version of R&D GTDS at Goddard Space Flight Center no longer supports the FILTER program.

The **FILTER** program, like the DC program, utilizes estimation techniques to provide a best estimate of a satellite's orbit. Whereas the DC program is based upon a batch process, however, the FILTER program incorporates two sequential estimate algorithms that account for highly dynamic situations and allow for an estimate that is not necessarily based at a particular epoch. The linear Kalman filter (LKF) and extended Kalman filter (EKF) continuously update the state estimate at each observation time, carrying all the information concerning past measurements in its covariance matrix. This program is currently not operational in GTDS maintained at GSFC, but offers both Cowell and semianaiytic LKF/EKF options at Draper.

The ephemeris **COMPARE** program differences ephemeris information from two GTDS products (ORB1, ORBIT, or EPHEM files). The comparison may be specified for arcs common to both products or any portion of that time period. The differences may be expressed in radial, cross-track, and along-track components or latitude, longitude, and spheroid heights in tabular output. Keplerian and equinoctial element histories and differences for the two ephemerides are produced as well.

The **DATA MANAGEMENT** program creates temporary working files containing information from a GTDS data base for use by other GTDS programs. These working files can either be created as part of the program that will use the files or in a "stand-alone" sense where they will be saved for future executions.

The **DATA SIMULATION** program creates a simulated tracking observations file for a specified location and observation frequency. These files may be

used as inputs to support operations and may include random and bias errors, and the effects of atmospheric refraction, antenna mount errors, and transponder and light time delays.

The permanent **FILE REPORT** program provides a summary report of information contained within various GTDS permanent data bases. This functionality is typically used to determine which data base is appropriate for use in a separate execution.

The **ERROR ANALYSIS** program highlights the effects of uncertainties associated with epoch state, observation quality, and other parameters for a prescribed station-dependent tracking schedule on a specified orbit. It is compatible with observation types modeled within the DC program.

The **EARLY ORBIT** determination program is designed to provide an initial estimate of a satellite orbit when no a priori vector is available to initiate a DC process. GTDS performs this functionality in one of three methods: (1) the Gauss method, (2) the Double R-Iteration Method, and (3) the Range and Angles Method. As few as six tracking observations are required to obtain an initial estimate with the early orbit program.

Although Draper R&D GTDS provides the same major capabilities (plus the FILTER program) as the operational Goddard version, development since it was spun off from the Goddard R&D GTDS has resulted in functional differences within each program. Areas of software development at Draper have included:

- Introduction of the Draper Semianalytic Satellite Theory (DSST) to include enhanced short periodic models and various issues associated with the mean element equations of motion

- Incorporation of the DSST into filtering strategies

- Expansion of the sources and coordinate systems of observation data

- Incorporation of the NORAD General Perturbation (GP) Theories to include SGP, GP4, DP4, HANDE, and SALT

- Incorporation of the NAVSPASUR PPT2 Theory

- Introduction of higher order (50x50) gravity field modeling

Fonte [20] presents an excellent discussion of the historical development of Draper R&D GTDS and modifications made since its inception in 1979.

2.2.1 Operation of Draper R&D GTDS

It is desirable for the reader to have the ability to interpret not only the results of this work, but also the setup used to generate these results. Because the remainder of this thesis will reference various components of the setup, it is logical to introduce the operational concepts of Draper R&D GTDS.

Execution of the desired functionalities within Draper R&D GTDS is controlled by several files. The input card data file identifies the program to

be executed and various options associated with that execution. A separate command file is used to specify relevant data bases and invoke execution of the desired version of Draper R&D GTDS. Because the short periodics input processor is not present in the VAX VMS version, a third file is necessary to override predefined values associated with the short periodics generator (hence, called an overrides file). A typical setup for a VAX VMS Draper R&D GTDS execution is provided in Appendix E.

The input card data files consist of a series of keywords and three associated integer and real field options. Each keyword is a alphanumeric representation of some program option or data quantity. The keywords, in turn, contain options that are specified in the three integer and real fields. The combination of a keyword and its integer and real fields is referred to as a *card*. Figure 2.1 highlights these features with an example of the ELEMENT1 card, used to describe the initial state and associated parameters.

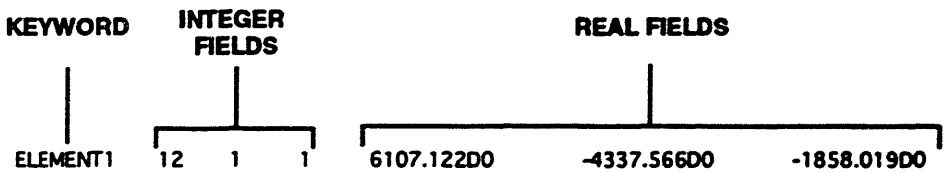

Figure 2.1 Structure of GTDS Card

In this example, the keyword is the ELEMENT1 card; the three integer fields define the coordinate system orientation, coordinate system type, and central body indicator; and the three real fields provide the first three components of the state (in this case, the position vector in kilometers).

To execute a particular GTDS program, a series of these cards is embedded between a CONTROL and FIN card. The CONTROL card specifies which

program is to be exercised, while the FIN card signals the end of the card data file. The structure of the CONTROL card is an exception to the format depicted in Figure 2.1, and is specified in [25].

Various mandatory cards follow the CONTROL card in the data file. These cards are required for execution of a specific program, with the number (from zero to five) being dependent upon the program being executed. An example is the ELEMENT1 card in an ephemeris generation - an initial state is necessary for propagation.

The remainder of the cards are considered optional, and are functionally divided into subdecks that may or may not be particular to one program. For instance, the PFROPT subdeck may only be used within a permanent file report execution, but an OGOPT subdeck may be used in an ephemeris generation, differential correction, filtering process, early orbit determination, and data simulation. These subdecks are offset from the remainder of the card data file by a subdeck identifier (OGOPT, for instance) and an END card.

The relationship between these various components is shown in Figure 2.2, which depicts a typical setup for an ephemeris generation. The mandatory cards for this run specify the initial conditions (EPOCH, ELEMENT1, ELEMENT2), orbit generator options (ORBTYPE), and output options (OUTPUT). The optional cards involve perturbation modeling of drag (DRAG, ATMOSDEN), gravitational potential (MAXDEGEQ, MAXORDEQ, MAXDEGVE, MAXORDVE, POTFIELD), solid earth tides (SETIDE), and solar radiation pressure (SOLRAD). Also, the drag and solar radiation parameters

(DRAGPAR and SOLRDPAR, respectively) are specified as non-solve-for variables, and an ORB1 file is requested (OUTOPT).

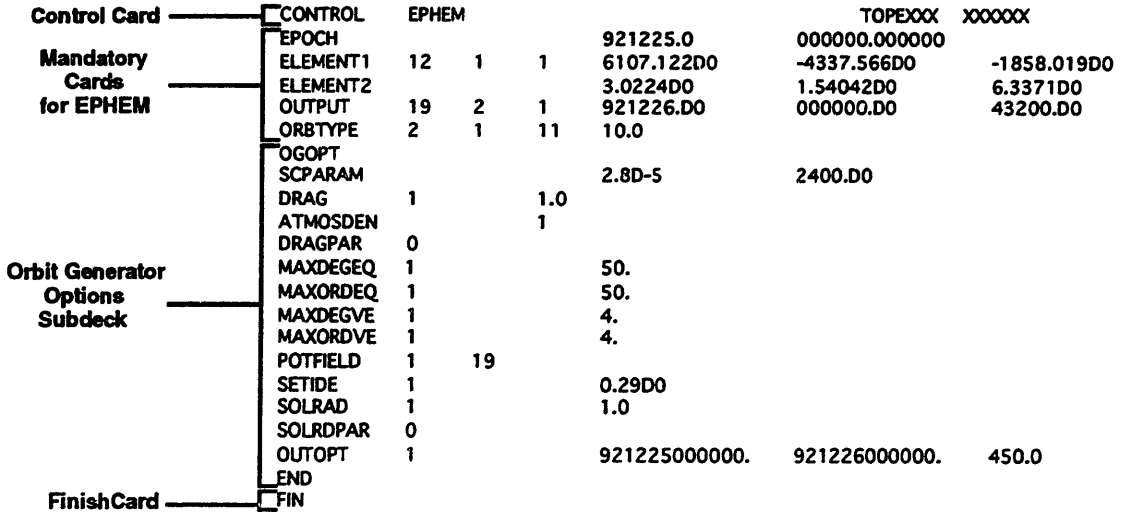

Figure 2.2 Ephemeris Generation Card Data File

GTDS also has the capability to interpret multiple card data files within a single execution, providing a tremendous amount of flexibility to the software package. Concatenated data files are often used to create working files with the data management program for use in a separate program (for instance, a differential correction). They can also be used when the final results of one program are passed to the next through a COMMON block (e.g., from a differential correction to an ephemeris generation).

A more in-depth discussion of the operation of GTDS can be found in [25] and [54].

2.2.2 Draper R&D GTDS Products

Draper R&D GTDS has the capability of producing three types of satellite ephemeris files: the ORBIT file, the EPHEM file, and the ORB1 file. While these files maintain similar content, functional differences dictate distinction in the structure of the files.

ORBIT files serve two functionalities in Draper R&D GTDS. For ephemeris generation purposes, the use of ORBIT files is limited to either Cowell or time-regularized Cowell methods. By selecting option six on the ORBTYPE card (see Appendix D), the user retrieves a set of interpolator coefficients representing the satellite's ephemeris and, optionally, its partial derivatives. These coefficients are used in developing grid points for interpolation schemes in the integration process. The data simulation program also utilizes information from ORBIT files. In order to simulate tracking observations, the program requires position and velocity information over a time period as an input. This position and velocity file is a previously generated ORBIT file from the GTDS ephemeris generation program.

According to [25], EPHEM files are best suited for purposes other than orbit determination, such as tracking data acquisition or maneuver planning. These files could also be used for ephemeris comparison in the Draper R&D GTDS COMPARE program; however, they are seldom used at Draper.

The most extensively used products at Draper are ORB1 files. These files are commonly used in ephemeris comparisons, inputs to future differential corrections (as a Precise Conversion of Elements data type), and inputs to

other non-GTDS post-processing schemes. The user requests an ephemeris for a certain time period at specific intervals on the OUTOPT card to produce the binary ORB1 file. The central body and coordinate system to which the ORB1 file is referenced is by default the same as what is reflected on the OUTPUT card. This project exercises each of the utilities associated with ORB1 files.

2.3 Orbit Generators in Draper R&D GTDS

A direct analytical solution to the perturbed equations of motion is not possible. Instead, perturbation techniques compensate for deviations from classical two-body motion caused by the effects of atmospheric drag, central body gravitational forces, third-body gravitational forces, solar radiation pressure, spacecraft thrusting and other disturbances. The current VAX workstation version of Draper R&D GTDS employs a variety of perturbation techniques to perform its orbit generation function. These techniques have classically been divided into *special* and *general* perturbation methods.

Special perturbation methods deal with the direct numerical integration of the equations of motion, accounting for accelerations due to these perturbations. When small step sizes are used in the integration process, these techniques offer the advantage of high accuracy, but at the expense of longer computational times. Modern computing speeds, however, are diminishing the time involved in this process and driving some individuals toward reliance solely upon these numerical techniques. Draper R&D GTDS offers the following high precision orbit generators:

- Cowell
- Time-regularized Cowell
- Variation of Parameters

The Cowell and Variation of Parameters methods are discussed in detail in sections 2.3.1 and 2.3.2.

General perturbation techniques utilize analytical formulae in conjunction with series approximations to model the effects of perturbations affecting a spacecraft. The disturbance models are limited to develop analytical formulae, reducing the accuracy associated with these techniques. General perturbation methods do not require the multiple time steps used in numerical techniques, and hence are not tied to a specified set of initial conditions [19]. Variation in the initial conditions for special perturbation methods requires reevaluation at each of the integration steps to obtain the desired conditions. The VAX workstation version of Draper R&D GTDS currently offers the following analytical orbit generators:

- Brouwer
- Brouwer-Lyddane
- Brouwer-Lyddane-Gordon
- Vinti
- NORAD Simplified General Perturbation (SGP)
- NORAD GP4
- NORAD DP4
- NORAD HANDE
- NAVSPASUR PPT2 (in progress)

These general perturbation techniques were not utilized for this work, and hence will not be discussed in further detail. However, it should be noted that a fit of the Precise Orbital Ephemerides (POEs, discussed in section 2.7) using these general perturbation theories could provide interesting insight into the actual theories.

A third category that in some respects is a combination of the special and general perturbation techniques has recently gained popularity. The semianalytic method combines the benefits of high accuracy and computational efficiency by separating long period and secular components of the perturbations from the short periodic effects. Osculating equations of motion are converted into a mean representation by stripping the short periodic effects, which are responsible for the short time steps taken in the numerical techniques. The removal of the high frequency terms due to dependence upon the fast variable is accomplished through application of the Generalized Method of Averaging. The perturbations are separated into conservative forces, which are analytically averaged, and non-conservative forces, which are numerically averaged. Conservative perturbations are expressed in Lagrange's VOP equations, and non-conservative forces are represented in Gauss's VOP equations. The mean equations of motion are then propagated to the output request time, when the short periodic effects are included to maintain accuracy. The averaging process allows for much larger step sizes (on the order of days, rather than seconds), bounded by the magnitude of the next higher frequency oscillation [34]. The current version of Draper R&D GTDS contains two semianalytic orbit propagators:

- Draper Semianalytic Satellite Theory
- NORAD Semianalytic Theory (SALT)

A more detailed discussion of Draper Semianalytic Satellite Theory is provided in section 2.3.3.

2.3.1 Cowell Techniques

P.H. Cowell introduced the concept of formulating the equations of motion in terms of rectangular (Cartesian) coordinates and numerically integrating these equations by means of a multistep algorithm in 1908 [56]. The two-body equations of motion are derived through application of Newton's Universal Law of Gravitation and Second Law of Motion to provide:

$$\ddot{\mathbf{r}} + \frac{\mu}{r^3}\mathbf{r} = \mathbf{0} \tag{2.1}$$

where r is the position vector separating the two bodies, and μ is the gravitational parameter. Introduction of perturbative accelerations (a_p) transforms (2.1) into:

$$\ddot{\mathbf{r}} = \mathbf{a}_p - \frac{\mu}{r^3}\mathbf{r} \tag{2.2}$$

This equation can be further broken down into Cartesian coordinates and represented as:

$$\ddot{r}_x = a_x - \frac{\mu}{r^3}x$$
$$\ddot{r}_y = a_y - \frac{\mu}{r^3}y \qquad (2.3)$$
$$\ddot{r}_z = a_z - \frac{\mu}{r^3}z$$

recognizing that

$$r = \sqrt{x^2 + y^2 + z^2} \qquad (2.4)$$

The equations in (2.3) represent a second order differential equation. This could be reduced to a first order differential equation by introducing the velocity vector ($\mathbf{v} = \dot{\mathbf{r}}$) to the left side of the equations. This alternative representation is referred to as a set of Class I differential equations (while 2.3 is a set of Class II differential equations) [24]. By expressing perturbative accelerations in each direction, these equations are integrated over time to provide the position and velocity of the satellite.

As an example, an approximate representation of the perturbative accelerations due to solid earth tides (lunar effects only) is:

$$\mathbf{a}_{tm} = \frac{K_l \mu_m a_e^5 \{[(15/2)(\hat{\mathbf{r}} \cdot \hat{\mathbf{r}}_m)^2 - (3/2)]\mathbf{r} - 3(\hat{\mathbf{r}} \cdot \hat{\mathbf{r}}_m)\hat{\mathbf{r}}_m\}}{|\mathbf{r}_m|^3 |\mathbf{r}|^5} \qquad (2.5)$$

where the subscript m refers to the moon, Kl is Love's constant, μ_m is the universal gravitational constant (G) times the mass of the moon, a_e is the radius of the earth, r_m is the earth centered inertial (ECI) position vector of the moon, and r is the ECI position vector of the satellite [52].

The Class II set of differential equations, with only lunar tidal effects modeled as perturbations, would be:

$$\ddot{r}_x = \left[\left(\frac{K_l a_e^5 \mu_m}{r^5 r_m^3}\right)\left(\frac{15}{2}(\hat{\mathbf{r}}\cdot\hat{\mathbf{r}}_m)^2 - \frac{3}{2}\right) - \frac{\mu_e}{r^3}\right] r_x - \left(\frac{3K_l a_e^5 \mu_m}{r^5 r_m^3}\right)(\hat{\mathbf{r}}\cdot\hat{\mathbf{r}}_m)\hat{r}_{mx}$$

$$\ddot{r}_y = \left[\left(\frac{K_l a_e^5 \mu_m}{r^5 r_m^3}\right)\left(\frac{15}{2}(\hat{\mathbf{r}}\cdot\hat{\mathbf{r}}_m)^2 - \frac{3}{2}\right) - \frac{\mu_e}{r^3}\right] r_y - \left(\frac{3K_l a_e^5 \mu_m}{r^5 r_m^3}\right)(\hat{\mathbf{r}}\cdot\hat{\mathbf{r}}_m)\hat{r}_{my} \qquad (2.6)$$

$$\ddot{r}_z = \left[\left(\frac{K_l a_e^5 \mu_m}{r^5 r_m^3}\right)\left(\frac{15}{2}(\hat{\mathbf{r}}\cdot\hat{\mathbf{r}}_m)^2 - \frac{3}{2}\right) - \frac{\mu_e}{r^3}\right] r_z - \left(\frac{3K_l a_e^5 \mu_m}{r^5 r_m^3}\right)(\hat{\mathbf{r}}\cdot\hat{\mathbf{r}}_m)\hat{r}_{mz}$$

These equations can now be numerically integrated using one of a variety of techniques.

2.3.2 Variation of Parameters

While Cowell methods deal with direct numerical integration of equation (2.2), the variation of parameters (VOP) approach describes satellite motion in terms of element sets, thus providing more insight into the physical effects of the perturbations. This approach is very useful when disturbances are small relative to the unperturbed motion [3], and provides an efficient manner for evaluating perturbing accelerations when the numerical integration process must be restarted frequently (such as with an Extended Kalman Filter), since there is no need to rebuild evaluations at each step [66].

The goal of VOP is to express a set of orbit parameter rates of change in the form:

$$\frac{d\mathbf{c}}{dt} = f(\mathbf{c},t) \qquad (2.7)$$

where c is a vector containing some set of orbital elements. It should be noted that the elements themselves are not constant as in the two-body formulation, but rather time-dependent. These perturbed elements can always be considered as having a corresponding unperturbed two-body representation at any time *t*, although that two-body orbit will vary along with the perturbed elements [44].

Battin's presentation of the VOP equations separates the perturbations into conservative and non-conservative forces [4]. The accelerations due to conservative forces are represented by the gradient of the disturbing potential, while the non-conservative accelerations are in generic vector form. The perturbed equations of motion are given by:

$$\ddot{\mathbf{r}} + \frac{\mu}{r^3}\mathbf{r} = \mathbf{a}_d + \left(\frac{\partial R}{\partial \mathbf{r}}\right)^T \tag{2.8}$$

where:

$\mathbf{a}_d$	is the acceleration due to non-conservative forces
$\left(\frac{\partial R}{\partial \mathbf{r}}\right)^T$	is the acceleration due to conservative forces.

Two vector differential equations can then be expressed from equation (2.8) as:

$$\frac{d\mathbf{r}(\mathbf{c},t)}{dt} = \mathbf{v}(\mathbf{c},t)$$
$$\frac{d\mathbf{v}(\mathbf{c},t)}{dt} + \frac{\mu}{r^3}\mathbf{r}(\mathbf{c},t) = \mathbf{a}_d(\mathbf{c},t) + \left(\frac{\partial R}{\partial \mathbf{r}(\mathbf{c},t)}\right)^T \tag{2.9}$$

Because the elements are no longer constant (as was the case for the two-body problem), the ordinary derivatives should be expressed in terms of partial derivatives through application of the chain rule of differentiation:

$$\frac{d\mathbf{r}}{dt} = \frac{\partial \mathbf{r}}{\partial t} + \frac{\partial \mathbf{r}}{\partial \mathbf{c}}\frac{d\mathbf{c}}{dt}$$
$$\frac{d\mathbf{v}}{dt} = \frac{\partial \mathbf{v}}{\partial t} + \frac{\partial \mathbf{v}}{\partial \mathbf{c}}\frac{d\mathbf{c}}{dt} \tag{2.10}$$

The element rate terms are the only difference between perturbative and two-body motion. Comparison of equations (2.9) and (2.10) reveals the following expressions:

$$\frac{\partial \mathbf{r}}{\partial \mathbf{c}}\frac{d\mathbf{c}}{dt} = 0$$
$$\frac{\partial \mathbf{v}}{\partial \mathbf{c}}\frac{d\mathbf{c}}{dt} = \mathbf{a}_d(\mathbf{c},t) + \left(\frac{\partial R}{\partial \mathbf{r}(\mathbf{c},t)}\right)^T \tag{2.11}$$

Of physical significance is the fact that perturbative and two-body velocities are the same.

The relations in equation (2.11) will now be transformed to a form that will facilitate the derivation process. By premultiplying the first relationship in (2.11) by $(\partial \mathbf{v}/\partial \mathbf{c})^T$ and the second by $(\partial \mathbf{r}/\partial \mathbf{c})^T$, and subtracting the first from the second, a more convenient form is established.

$$\mathbf{L}\frac{d\mathbf{c}}{dt}=\left(\frac{\partial \mathbf{r}}{\partial \mathbf{c}}\right)^{T}\left[\mathbf{a}_{d}+\left(\frac{\partial R}{\partial \mathbf{r}}\right)^{T}\right] \tag{2.12}$$

where

$$\mathbf{L}=\left(\frac{\partial \mathbf{r}}{\partial \mathbf{c}}\right)^{T}\left(\frac{\partial \mathbf{v}}{\partial \mathbf{c}}\right)-\left(\frac{\partial \mathbf{v}}{\partial \mathbf{c}}\right)^{T}\left(\frac{\partial \mathbf{r}}{\partial \mathbf{c}}\right) \tag{2.13}$$

The derivation of the element rates now must be split into two paths dependent upon the source of perturbations. The acceleration due to conservative forces is represented by Lagrange's planetary equations, while non-conservative disturbances are expressed by Gauss's form of the planetary equations.

2.3.2.1 Lagrange's VOP Equations

Lagrange's formulation of the VOP equations deals only with those forces that are conservative, meaning they produce no net work upon an object throughout one circuit. Mathematically, this is represented by setting the non-conservative accelerations ($\mathbf{a}_d$) to zero. Thus, equation (2.12) becomes:

$$\mathbf{L}\frac{d\mathbf{c}}{dt}=\left(\frac{\partial \mathbf{r}}{\partial \mathbf{c}}\right)^{T}\left(\frac{\partial R}{\partial \mathbf{r}}\right)^{T}$$

or

$$\mathbf{L}\frac{d\mathbf{c}}{dt}=\left(\frac{\partial R}{\partial \mathbf{c}}\right)^{T} \tag{2.14}$$

The element rates are then obtained by taking the inverse of the six-dimensional, skew-symmetric Lagrange matrix (**L**).

$$\frac{d\mathbf{c}}{dt} = \mathbf{L}^{-1}\left(\frac{\partial R}{\partial \mathbf{c}}\right)^T \tag{2.15}$$

The elements of the Lagrange matrix are referred to as Lagrangian brackets and are denoted by $[c_i, c_j]$, possessing the following properties:

$$\begin{aligned} [c_i, c_i] &= 0 \\ [c_i, c_j] &= -[c_j, c_i] \\ \frac{\partial}{\partial t}[c_i, c_j] &= 0 \end{aligned} \tag{2.16}$$

The Poisson matrix is an alternative representation and can be shown to be the negative inverse of the Lagrange matrix [7]. Thus,

$$\frac{d\mathbf{c}}{dt} = -\mathbf{P}\left(\frac{\partial R}{\partial \mathbf{c}}\right)^T = \mathbf{P}^T\left(\frac{\partial R}{\partial \mathbf{c}}\right)^T \tag{2.17}$$

The components of the Poisson matrix, referred to as *Poisson brackets,* are referenced in a similar manner as the elements of the Lagrange matrix. Developed from the Keplerian-based Lagrangian brackets according to Battin [4], one representation of the non-zero Poisson brackets is given by:

$$\begin{aligned} (a,\lambda) &= -\frac{2}{na} \quad (e,\omega) = \frac{b}{na^3 e} \quad (e,\lambda) = -\frac{b^2}{na^4 e} \\ (i,\Omega) &= \frac{1}{nab\sin i} \quad (i,\omega) = -\frac{\cot i}{nab} \end{aligned} \tag{2.18}$$

Cefola provides the equinoctial representation of these Poisson brackets [10].

$$(a,\lambda) = -2as_1 \quad (h,k) = -s_1 s_3 \quad (h,p) = -kps_5 \quad (h,q) = -kqs_5$$
$$(h,\lambda) = hs_4 \quad (k,p) = hps_5 \quad (k,q) = hqs_5 \quad (k,\lambda) = ks_4$$
$$(p,q) = -\frac{1}{2}s_3 s_5 I \quad (p,\lambda) = ps_5 \quad (q,\lambda) = qs_5 \tag{2.19}$$

where

$$s_1 = \frac{1}{na^2} \quad s_2 = 1 + p^2 + q^2 \quad s_3 = \sqrt{1 - h^2 - k^2}$$
$$s_4 = \frac{s_1 s_3}{1 + s_3} \quad s_5 = \frac{s_1 s_2}{2s_3} \tag{2.20}$$

with I being the retrograde factor. The appropriate set of brackets is then used in equation (2.17) to determine the element rates, which can be integrated either numerically or analytically to provide a time-varying value of the elements.

2.3.2.2 Gauss' VOP Equations

Unlike Lagrange's VOP equations, Gauss' form is not limited to disturbing functions, but rather works equally well for both conservative and non-conservative forces. Considering only what was defined as non-conservative forces (although the conservative forces could be embedded within this term), equation (2.12) can be rewritten as:

$$\frac{d\mathbf{c}}{dt} = \mathbf{P}^T \left(\frac{\partial \mathbf{r}}{\partial \mathbf{c}} \right)^T \mathbf{a}_d \tag{2.21}$$

Noting that the Poisson matrix is defined as [4]:

$$\mathbf{P} = \frac{\partial \mathbf{c}}{\partial \mathbf{r}}\left[\frac{\partial \mathbf{c}}{\partial \mathbf{v}}\right]^T - \frac{\partial \mathbf{c}}{\partial \mathbf{v}}\left[\frac{\partial \mathbf{c}}{\partial \mathbf{r}}\right]^T \tag{2.22}$$

equation (2.21) can be transformed to:

$$\frac{d\mathbf{c}}{dt} = \frac{\partial \mathbf{c}}{\partial \mathbf{v}}\left(\frac{\partial \mathbf{r}}{\partial \mathbf{r}}\right)^T \mathbf{a}_d - \frac{\partial \mathbf{c}}{\partial \mathbf{r}}\left(\frac{\partial \mathbf{r}}{\partial \mathbf{v}}\right)^T \mathbf{a}_d \tag{2.23}$$

Since the position and velocity components are considered independent:

$$\frac{\partial \mathbf{r}}{\partial \mathbf{r}} = \mathbf{I} \qquad \frac{\partial \mathbf{r}}{\partial \mathbf{v}} = \mathbf{0} \tag{2.24}$$

resulting in

$$\frac{d\mathbf{c}}{dt} = \frac{\partial \mathbf{c}}{\partial \mathbf{v}}\mathbf{a}_d \tag{2.25}$$

Battin presents a convenient form of these Keplerian variational equations in the radial-normal-tangential frame [4], which can be shown as:

$$\begin{aligned}
\frac{da}{dt} &= \frac{2a^2 v}{\mu} a_{dt} \\
\frac{de}{dt} &= \frac{1}{v}\left[2(e+\cos f)a_{dt} - \frac{r\sin f}{a} a_{dn}\right] \\
\frac{di}{dt} &= \frac{r\cos\theta}{h} a_{dh} \\
\frac{d\Omega}{dt} &= \frac{r\sin\theta}{h\sin i} a_{dh} \\
\frac{d\omega}{dt} &= \frac{1}{ev}\left[2\sin f a_{dt} + \left(2e + \frac{r}{a}\cos f\right)a_{dn}\right] - \frac{r\sin\theta\cos i}{h\sin i} a_{dh} \\
\frac{dM}{dt} &= n - \frac{b}{eav}\left[2\left(1+\frac{e^2 r}{p}\right)\sin f a_{dt} + \frac{r}{a}\cos f a_{dn}\right]
\end{aligned} \tag{2.26}$$

The *GTDS Mathematical Specification* provides these equations in an equally valid equinoctial form [24]:

$$
\begin{aligned}
\frac{da}{dt} &= \frac{2\mathbf{v}}{n^2 a}\mathbf{a}_d \\
\frac{dh}{dt} &= \left[\frac{1}{\mu}\left[\left(2\dot{X}_1 Y_1 - X_1\dot{Y}_1\right)\hat{f} - X_1\dot{X}_1\hat{g}\right] + \frac{k}{G}\left(qIY_1 - pX_1\right)\hat{w}\right]\mathbf{a}_d \\
\frac{dk}{dt} &= \left[-\frac{1}{\mu}\left[Y_1\dot{Y}_1\hat{f} - \left(2X_1\dot{Y}_1 - \dot{X}_1 Y_1\right)\hat{g}\right] - \frac{h}{G}\left(qIY_1 - pX_1\right)\hat{w}\right]\mathbf{a}_d \\
\frac{dp}{dt} &= \left[\frac{1+p^2+q^2}{2G}Y_1\hat{w}\right]\mathbf{a}_d \\
\frac{dq}{dt} &= \left[\frac{I\left(1+p^2+q^2\right)}{2G}X_1\hat{w}\right]\mathbf{a}_d \\
\frac{d\lambda}{dt} &= \left[n - \frac{2}{na^3}\mathbf{r} + \beta\left(k\frac{\partial h}{\partial \mathbf{v}} - h\frac{\partial k}{\partial \mathbf{v}}\right) + \frac{1}{na^2}\left(qIY_1 - pX_1\right)\hat{w}\right]\mathbf{a}_d
\end{aligned}
\tag{2.27}
$$

where I is the retrograde factor, n is the mean motion, $\boldsymbol{r}$ and $\boldsymbol{v}$ are Cartesian coordinates in the inertial reference frame, and $\hat{f},\hat{g},\hat{w}$ are unit vectors in the equinoctial reference frame. The position and velocity in the equinoctial orbital frame are represented by:

$$
\begin{aligned}
X_1 &= a\left[\left(1-h^2\beta\right)\cos F + hk\beta\sin F - k\right] \\
Y_1 &= a\left[\left(1-k^2\beta\right)\sin F + hk\beta\cos F - h\right] \\
\dot{X}_1 &= \frac{na^2}{r}\left[hk\beta\cos F - \left(1-h^2\beta\right)\sin F\right] \\
\dot{Y}_1 &= \frac{na^2}{r}\left[\left(1-k^2\beta\right)\cos F - hk\beta\sin F\right]
\end{aligned}
\tag{2.28}
$$

and G and β are defined in the following manner:

$$G = na^2\sqrt{1-h^2-k^2}$$
$$\beta = \frac{1}{1+\sqrt{1-h^2-k^2}} \tag{2.29}$$

2.3.3 Semianalytic Satellite Theory

Semianalytic theories, as stated previously, account for the inherent problems associated with both numerical and analytical techniques to provide high accuracy results in an efficient manner. Numerical integration of the equations of motion requires small integration step sizes to account for high frequency effects, resulting in longer computational times. Analytical theories have limited perturbation modeling capabilities because of the tremendous complexity involved in arriving at a closed form solution to the equations of motion. Semianalytic techniques improve upon numerical schemes by employing larger step sizes to reduce computational times, and are open to non-serial computer architectures. The lack of accuracy associated with pure analytical theories is removed by improved semianalytic perturbation models, which are considered to be the most accurate available at the current time [12]. The result is an orbit propagation scheme that retains accuracy in an efficient manner.

The semianalytic satellite theory is based upon a fundamental set of mean equations of motion analogous to the VOP formulation presented in the previous section. However, where the Lagrangian and Gaussian representation of the equations are functions of the osculating element sets, semianalytic theory utilizes equations expressed in terms of a set of mean elements. These elements are isolated from the high frequency effects

through application of the Generalized Method of Averaging, allowing use of a much larger integration step size to provide an efficient propagation process. The short periodic terms, developed through either analytical or numerical techniques, are then added in at the request time to retain accuracy.

The mean equations of motion are developed from a modified representation of the VOP formulations presented by Lagrange and Gauss. As was previously the case, the magnitude of the perturbations is assumed to be significantly smaller than that of the two-body acceleration. Therefore, the osculating equations of motion can be presented in the form:

$$\begin{aligned} \frac{d\mathbf{c}}{dt} &= \varepsilon F_i(\mathbf{c}, l) \\ \frac{dl}{dt} &= n(\mathbf{c}_1) + \varepsilon F_6(\mathbf{c}, l) \end{aligned} \qquad \text{i=1,2...5} \qquad (2.30)$$

where c is a vector of five slowly-varying elements, l represents the fast variable, n is the mean motion of the spacecraft, and ε is some small parameter associated with the perturbation F. Fonte indicates that in the case of the geopotential, ε takes on the form of the harmonic coefficients (J_2, J_3, ...) [20].

The description that follows is similar to ones provided by McClain [44] and Fonte [20]. The events involved in this process include:

- Describing the osculating equations of motion in (2.30) in terms of mean elements.

- Expanding the perturbing functions in (2.30) in a power series in ε.

- Equating like powers of ε to relate the mean perturbing functions to the osculating perturbing functions.

- Averaging out short periodic effects to provide expressions for short periodic functions and mean equations of motion.

2.3.3.1 *Osculating Element Rates in Terms of Mean Elements*

Because it is desirable to represent these equations in terms of mean elements, it is necessary describe the relationship between the mean and osculating elements. The near identity transformation provides:

$$\begin{aligned} \mathbf{c} &= \bar{\mathbf{c}} + \varepsilon\eta_{i,1}(\bar{\mathbf{c}},\bar{l}) + \varepsilon^2\eta_{i,2}(\bar{\mathbf{c}},\bar{l}) + \ldots \\ l &= \bar{l} + \varepsilon\eta_{6,1}(\bar{\mathbf{c}},\bar{l}) + \varepsilon^2\eta_{6,2}(\bar{\mathbf{c}},\bar{l}) + \ldots \end{aligned} \qquad \text{i=1,2...5} \qquad (2.31)$$

The overbar signifies the mean representation of a value, and the terms εη are defined as short periodic functions. Subscripts on the short periodic functions describe the element (i) and order (j) considered. These short periodic functions are assumed to be 2π periodic in the fast variable; thus,

$$\varepsilon\eta_{i,j}(\bar{\mathbf{c}},\bar{l}) = \varepsilon\eta_{i,j}(\bar{\mathbf{c}},\bar{l}+2\pi) \qquad (2.32)$$

For purposes of this discussion, "short" is defined as being anything with a period shorter than the satellite's orbital period.

Differentiating (2.31) provides a relationship between the mean and osculating element rates.

$$\begin{aligned}\frac{d\mathbf{c}}{dt} &= \frac{d\bar{\mathbf{c}}}{dt} + \varepsilon\frac{\partial\eta_{i,1}}{\partial\bar{\mathbf{X}}}\frac{d\bar{\mathbf{X}}}{dt} + \varepsilon^2\frac{\partial\eta_{i,2}}{\partial\bar{\mathbf{X}}}\frac{d\bar{\mathbf{X}}}{dt} + \ldots \\ \frac{dl}{dt} &= \frac{d\bar{l}}{dt} + \varepsilon\frac{\partial\eta_{6,1}}{\partial\bar{\mathbf{X}}}\frac{d\bar{\mathbf{X}}}{dt} + \varepsilon^2\frac{\partial\eta_{6,2}}{\partial\bar{\mathbf{X}}}\frac{d\bar{\mathbf{X}}}{dt} + \ldots\end{aligned} \qquad \text{i=1,2...5} \qquad (2.33)$$

where $\bar{\mathbf{X}}$ is a vector combining the slowly-varying and fast mean elements.

$$\bar{\mathbf{X}} = \begin{bmatrix}\bar{\mathbf{c}} \\ \bar{l}\end{bmatrix} \qquad (2.34)$$

The mean element rates are assumed to be expressed as functions of only the slowly-varying mean elements and the same small parameter, ε.

$$\begin{aligned}\frac{d\bar{\mathbf{c}}}{dt} &= \varepsilon A_{i,1}(\bar{\mathbf{c}}) + \varepsilon^2 A_{i,2}(\bar{\mathbf{c}}) + \ldots \\ \frac{d\bar{l}}{dt} &= n(\bar{\mathbf{c}}_1) + \varepsilon A_{6,1}(\bar{\mathbf{c}}) + \varepsilon^2 A_{6,2}(\bar{\mathbf{c}}) + \ldots\end{aligned} \qquad \text{i=1,2...5} \qquad (2.35)$$

where $A_{p,q}$ represents the q^{th} order contribution for the p^{th} element to the mean element rates. Note that (2.35) highlights that these functions are dependent only upon the slowly-varying mean elements and not the short periodic functions.

An expression for the osculating element rates in terms of mean elements can be provided by substitution of (2.35) into (2.33).

$$\begin{aligned}\frac{d\mathbf{c}}{dt} &= \left(\varepsilon A_{i,1}(\bar{\mathbf{c}}) + \varepsilon^2 A_{i,2}(\bar{\mathbf{c}}) + \ldots\right) + \left(\varepsilon \frac{\partial \eta_{i,1}}{\partial \bar{\mathbf{X}}} \frac{d\bar{\mathbf{X}}}{dt} + \varepsilon^2 \frac{\partial \eta_{i,2}}{\partial \bar{\mathbf{X}}} \frac{d\bar{\mathbf{X}}}{dt} + \ldots\right) \\ \frac{dl}{dt} &= \left(n(\bar{\mathbf{c}}_1) + \varepsilon A_{6,1}(\bar{\mathbf{c}}) + \varepsilon^2 A_{6,2}(\bar{\mathbf{c}}) + \ldots\right) + \left(\varepsilon \frac{\partial \eta_{6,1}}{\partial \bar{\mathbf{X}}} \frac{d\bar{\mathbf{X}}}{dt} + \varepsilon^2 \frac{\partial \eta_{6,2}}{\partial \bar{\mathbf{X}}} \frac{d\bar{\mathbf{X}}}{dt} + \ldots\right)\end{aligned} \quad \text{i=1,2...5} \quad (2.36)$$

or, grouping like orders of ε,

$$\begin{aligned}\frac{d\mathbf{c}}{dt} &= \varepsilon\left(A_{i,1}(\bar{\mathbf{c}}) + \frac{\partial \eta_{i,1}}{\partial \bar{\mathbf{X}}} \frac{d\bar{\mathbf{X}}}{dt}\right) + \varepsilon^2\left(A_{i,2}(\bar{\mathbf{c}}) + \frac{\partial \eta_{i,2}}{\partial \bar{\mathbf{X}}} \frac{d\bar{\mathbf{X}}}{dt}\right) + \ldots \\ \frac{dl}{dt} &= n(\bar{\mathbf{c}}_1) + \varepsilon\left(A_{6,1}(\bar{\mathbf{c}}) + \frac{\partial \eta_{6,1}}{\partial \bar{\mathbf{X}}} \frac{d\bar{\mathbf{X}}}{dt}\right) + \varepsilon^2\left(A_{6,2}(\bar{\mathbf{c}}) + \frac{\partial \eta_{6,2}}{\partial \bar{\mathbf{X}}} \frac{d\bar{\mathbf{X}}}{dt}\right) + \ldots\end{aligned} \quad \text{i=1,2...5} \quad (2.37)$$

2.3.3.2 Expansion of the Perturbing Functions in ε

The equations found in (2.37) represent the left hand side of (2.30). It is now necessary to express the right hand side of (2.30) in terms of a power series in ε, as seen in (2.37).

The osculating perturbing functions can be expressed in a Taylor series about the mean elements as:

$$F_i(\mathbf{c}, l) = F_i(\bar{\mathbf{c}}, \bar{l}) + \frac{\partial F_i}{\partial \bar{\mathbf{X}}}\left(\mathbf{X} - \bar{\mathbf{X}}\right) + \ldots \qquad \text{i=1,2...5} \qquad (2.38)$$

The set of coefficients for the partial derivatives are the differences between the mean and osculating elements. The near identity transform (2.31) can be rearranged to provide these differences, the short periodic functions.

$$\mathbf{X}-\overline{\mathbf{X}}=\varepsilon\eta_{i,1}+\varepsilon^2\eta_{i,2}+\ldots \qquad \text{i=1,2...6} \qquad (2.39)$$

Thus, (2.38) can be transformed into

$$F_i(\mathbf{c},l)=F_i(\overline{\mathbf{c}},\bar{l})+\frac{\partial F_i}{\partial\overline{\mathbf{X}}}\left(\varepsilon\eta_{i,1}+\varepsilon^2\eta_{i,2}\right)+\ldots \qquad \text{i=1,2...6} \qquad (2.40)$$

Considering the fast variable rate of change expressed in (2.30), it is apparent that the mean motion must be expanded in a Taylor series about the "mean" mean motion as well.

$$n(\mathbf{c}_1)=n(\overline{\mathbf{c}}_1)+\frac{\partial n(\overline{\mathbf{c}}_1)}{\partial\overline{\mathbf{c}}_1}\left(\mathbf{c}_1-\overline{\mathbf{c}}_1\right)+\ldots \qquad (2.41)$$

Using the relationship between the mean motion and semi-major axis, and the near identity transformation, McClain presents an expression for the expansion of the osculating mean motion in powers of ε as [44]:

$$n(\mathbf{c}_1)=n(\overline{\mathbf{c}}_1)+\varepsilon\left(-\frac{3n(\overline{\mathbf{c}}_1)}{2\overline{\mathbf{c}}_1}\eta_{1,1}\right)+\varepsilon^2\left(\frac{15n(\overline{\mathbf{c}}_1)}{8\overline{\mathbf{c}}_1^{\,2}}\eta_{1,1}^2-\frac{3n(\overline{\mathbf{c}}_1)}{2\overline{\mathbf{c}}_1}\eta_{1,2}\right)+\ldots \qquad (2.42)$$

Equations (2.40) and (2.42) reveal that:

$$\varepsilon F_i(\mathbf{c},l) = \varepsilon F_i(\bar{\mathbf{c}},\bar{l}) + \frac{\partial F_i}{\partial \bar{\mathbf{X}}}\left(\varepsilon^2\eta_{i,1} + \varepsilon^3\eta_{i,2}\right)+\ldots$$

$$n(\mathbf{c}_1) + \varepsilon F_6(\mathbf{c},l) = n(\bar{\mathbf{c}}_1) + \varepsilon\left(F_6(\bar{\mathbf{c}},\bar{l}) - \frac{3n(\bar{\mathbf{c}}_1)}{2\bar{\mathbf{c}}_1}\eta_{1,1}\right) \qquad \text{i=1,2...5} \qquad (2.43)$$

$$+\varepsilon^2\left(\frac{\partial F_6}{\partial \bar{\mathbf{X}}}\eta_{6,1} + \frac{15n(\bar{\mathbf{c}}_1)}{8\bar{\mathbf{c}}_1^{\,2}}\eta_{1,1}^2 - \frac{3n(\bar{\mathbf{c}}_1)}{2\bar{\mathbf{c}}_1}\eta_{1,2}\right)+\ldots$$

thus, providing an expression of the right hand side of (2.30).

2.3.3.3 *Equating Like Powers of ε*

Equations (2.37) and (2.43) can be used to replace the left and right hand expressions, respectively, in equation (2.30). Comparison of the terms of like order in ε shows that:

$$F_i(\bar{\mathbf{c}},\bar{l}) = A_{i,1}(\bar{\mathbf{c}}) + \frac{\partial \eta_{i,1}}{\partial \bar{\mathbf{X}}}\frac{d\bar{\mathbf{X}}}{dt}$$

$$F_6(\bar{\mathbf{c}},\bar{l}) - \frac{3n(\bar{\mathbf{c}}_1)}{2\bar{\mathbf{c}}_1}\eta_{1,1} = A_{6,1}(\bar{\mathbf{c}}) + \frac{\partial \eta_{6,1}}{\partial \bar{\mathbf{X}}}\frac{d\bar{\mathbf{X}}}{dt} \qquad \text{i=1,2...5} \qquad (2.44)$$

for first order terms and,

$$\frac{\partial F_i}{\partial \bar{\mathbf{X}}}\eta_{i,1} = A_{i,2}(\bar{\mathbf{c}}) + \frac{\partial \eta_{i,2}}{\partial \bar{\mathbf{X}}}\frac{d\bar{\mathbf{X}}}{dt}$$

$$\frac{\partial F_6}{\partial \bar{\mathbf{X}}}\eta_{6,1} + \frac{15n(\bar{\mathbf{c}}_1)}{8\bar{\mathbf{c}}_1^{\,2}}\eta_{1,1}^2 - \frac{3n(\bar{\mathbf{c}}_1)}{2\bar{\mathbf{c}}_1}\eta_{1,2} = A_{6,2}(\bar{\mathbf{c}}) + \frac{\partial \eta_{6,2}}{\partial \bar{\mathbf{X}}}\frac{d\bar{\mathbf{X}}}{dt} \qquad \text{i=1,2...5} \qquad (2.45)$$

for second order terms. However, further analysis reveals that the rate of change of the elements ($\frac{d\bar{\mathbf{X}}}{dt}$) implicitly contains powers of ε for the first five components ($\bar{\mathbf{c}}$). Thus, to first order:

$$F_i(\bar{\mathbf{c}},\bar{l}) = A_{i,1}(\bar{\mathbf{c}}) + \frac{\partial \eta_{i,1}}{\partial \bar{l}} n(\bar{\mathbf{c}})$$
$$F_6(\bar{\mathbf{c}},\bar{l}) - \frac{3n(\bar{\mathbf{c}}_1)}{2\bar{\mathbf{c}}_1}\eta_{1,1} = A_{6,1}(\bar{\mathbf{c}}) + \frac{\partial \eta_{6,1}}{\partial \bar{l}} n(\bar{\mathbf{c}}) \qquad \text{i=1,2...5} \qquad (2.46)$$

2.3.3.4 *Removal of Short Periodic Functions*

Presence of the short periodic functions, $\eta_{i,j}$, and dependence of the osculating disturbing function, F, on the fast variable in (2.46) prevent expression of the mean equations of motion at this point. It is necessary to remove these high frequency variations for a clear expression of the mean element rates. This stripping of the short periodics is performed by the averaging operation, defined by:

$$\left\langle f(\bar{\mathbf{c}},\bar{l})\right\rangle_{\bar{l}} = \frac{1}{2\pi}\int_0^{2\pi} f(\bar{\mathbf{c}},\bar{l})d\bar{l} \qquad (2.47)$$

Three properties of this operator are significant in the process of removing the short periodic variations. They are:

$$\left\langle g\cdot f(\bar{\mathbf{c}},\bar{l})\right\rangle_{\bar{l}} = g\cdot\left\langle f(\bar{\mathbf{c}},\bar{l})\right\rangle_{\bar{l}}$$
$$\left\langle \frac{\partial f(\bar{\mathbf{c}},\bar{l})}{\partial \bar{\mathbf{X}}}\right\rangle_{\bar{l}} = \frac{\partial}{\partial \bar{\mathbf{X}}}\left\langle f(\bar{\mathbf{c}},\bar{l})\right\rangle_{\bar{l}} \qquad (2.48)$$
$$\left\langle g + f(\bar{\mathbf{c}},\bar{l})\right\rangle_{\bar{l}} = \langle g\rangle_{\bar{l}} + \left\langle f(\bar{\mathbf{c}},\bar{l})\right\rangle_{\bar{l}}$$

where g is any function independent of f.

Utilizing the averaging operator on (2.46) and the properties described above,

$$\left\langle F_i(\bar{\mathbf{c}},\bar{l})\right\rangle_{\bar{l}} = \left\langle A_{i,1}(\bar{\mathbf{c}})\right\rangle_{\bar{l}} + \left\langle \frac{\partial \eta_{i,1}}{\partial \bar{l}} n(\bar{\mathbf{c}}_1)\right\rangle_{\bar{l}}$$
$$\left\langle F_6(\bar{\mathbf{c}},\bar{l})\right\rangle_{\bar{l}} - \left\langle \frac{3n(\bar{\mathbf{c}}_1)}{2\bar{\mathbf{c}}_1}\eta_{1,1}\right\rangle_{\bar{l}} = \left\langle A_{6,1}(\bar{\mathbf{c}})\right\rangle_{\bar{l}} + \left\langle \frac{\partial \eta_{6,1}}{\partial \bar{l}} n(\bar{\mathbf{c}}_1)\right\rangle_{\bar{l}} \qquad \text{i=1,2...6} \qquad (2.49)$$

Because the short periodic functions, $\eta_{i,j}$, are 2π periodic in the mean fast variable,

$$\left\langle \frac{\partial \eta_{i,1}}{\partial \bar{l}} n(\bar{\mathbf{c}}_1)\right\rangle_{\bar{l}} = 0$$
$$\left\langle \frac{3n(\bar{\mathbf{c}}_1)}{2\bar{\mathbf{c}}_1}\eta_{1,1}\right\rangle_{\bar{l}} = 0 \qquad \text{i=1,2...6} \qquad (2.50)$$

resulting in (2.49) being recast as:

$$\left\langle F_i(\bar{\mathbf{c}},\bar{l})\right\rangle_{\bar{l}} = \left\langle A_{i,1}(\bar{\mathbf{c}})\right\rangle_{\bar{l}} \qquad \text{i=1,2...6} \qquad (2.51)$$

Since these disturbing functions are averaged over the mean fast variable the disturbance functions are only dependent upon the slowly-varying mean elements.

$$\overline{F}_i(\bar{\mathbf{c}}) = A_{i,1}(\bar{\mathbf{c}}) \qquad \text{i=1,2...6} \qquad (2.52)$$

The mean equations of motion are then expressed in terms of the slowly-varying mean elements as:

$$\frac{d\bar{\mathbf{c}}}{dt} = \varepsilon \bar{F}_i(\bar{\mathbf{c}})$$
$$\frac{d\bar{l}}{dt} = n(\bar{\mathbf{c}}_1) + \varepsilon \bar{F}_6(\bar{\mathbf{c}}) \qquad \text{i=1,2...5} \qquad (2.53)$$

These equations can now be integrated with a much longer time step because of the lack of a fast variable.

2.3.3.5 Recovery of the Short Periodics

Once the mean equations have been propagated to the proper request time, the short periodics are added in to retain a high level of accuracy. The short periodic functions (which are actually the difference between the osculating and mean disturbing functions) are shown in (2.46) to be:

$$F_i^{sp}(\bar{\mathbf{c}}, \bar{l}) = \frac{\partial \eta_{i,1}}{\partial \bar{l}} n(\bar{\mathbf{c}}_1)$$
$$F_6^{sp}(\bar{\mathbf{c}}, \bar{l}) = \frac{\partial \eta_{6,1}}{\partial \bar{l}} n(\bar{\mathbf{c}}_1) + \frac{3n(\bar{\mathbf{c}}_1)}{2\bar{\mathbf{c}}_1} \eta_{1,1} \qquad \text{i=1,2...5} \qquad (2.54)$$

Rearranging, the short periodic functions are given as:

$$\eta_{i,1} = \frac{1}{n(\bar{\mathbf{c}}_1)} \int_0^{\bar{l}} F_i^{sp}(\bar{\mathbf{c}}, \bar{l}) \partial \bar{l}$$
$$\eta_{6,1} = \frac{1}{n(\bar{\mathbf{c}}_1)} \int_0^{\bar{l}} \left(F_6^{sp}(\bar{\mathbf{c}}, \bar{l}) - \frac{3\eta_{1,1}}{2\bar{\mathbf{c}}_1} \right) \partial \bar{l} \qquad \text{i=1,2...5} \qquad (2.55)$$

2.3.3.6 *Interpolation*

Although the averaged equations of motion allow for larger integration steps, there must exist some manner to evaluate mean element and short periodic coefficients at any request time. Because they are slowly varying, the coefficients are evaluated by interpolation schemes at times not commensurate with the integration grid. The Draper semianalytic theory first evaluates the mean elements at the request time. If the short periodic interpolators are not valid for that request time, an interval is generated that contains time of interest. The short periodic functions are then evaluated from the Fourier series expansions and added to the mean elements to generate an osculating representation.

2.4 Pertinent Coordinate Systems

While Draper R&D GTDS supports a variety of coordinate systems, this discussion focuses only on three types: the mean equator and equinox of fundamental epoch, true equator and equinox of reference time/date, and body-fixed. It should be stressed that other coordinate system options are available within Draper R&D GTDS, and a summary can be found in Figure 3.5 and Appendix D.

2.4.1 Mean Equator and Equinox of Fundamental Epoch

The mean equator and equinox of fundamental epoch reference frames are inertial coordinate systems referenced to a particular fundamental time. The

two epochs most commonly used at present are B1950.0 (Julian date 2433282.423) and J2000.0 (JD 2451545.0).

To define these reference frames, it is necessary to describe a fundamental reference plane and a principal direction along that plane. The principal direction serves as one axis of the coordinate system; a direction perpendicular to that plane acts as a second axis; and the cross-product of the two unit vectors of these two axes (in a right-handed sense) provides the third axis.

Options for the reference plane include the earth's equatorial plane, the ecliptic plane, or some intermediate invariable plane. While the invariable plane is certainly desirable, it is not well determined and, thus, impractical. For some applications, such as interplanetary missions, it is logical to use the ecliptic plane as the fundamental reference plane. However, because most Draper applications involve near-earth missions, the fundamental reference frame is assumed to be the earth's equatorial plane, defined as being perpendicular to the earth's polar axis.

The principal direction of the coordinate system is developed through the introduction of a second, separate plane that intersects the earth's equatorial plane. The earth's orbit about the sun (or, conversely from a geocentric viewpoint, the sun's "orbit" about the earth) defines a plane, referred to as the ecliptic, that intersects the equatorial planes at two points, the *equinoxes*. The vernal equinox (often referred to as the First Point of Aries) is located where the sun's apparent motion causes it to cross the equator from south to north and is considered the principal direction [3].

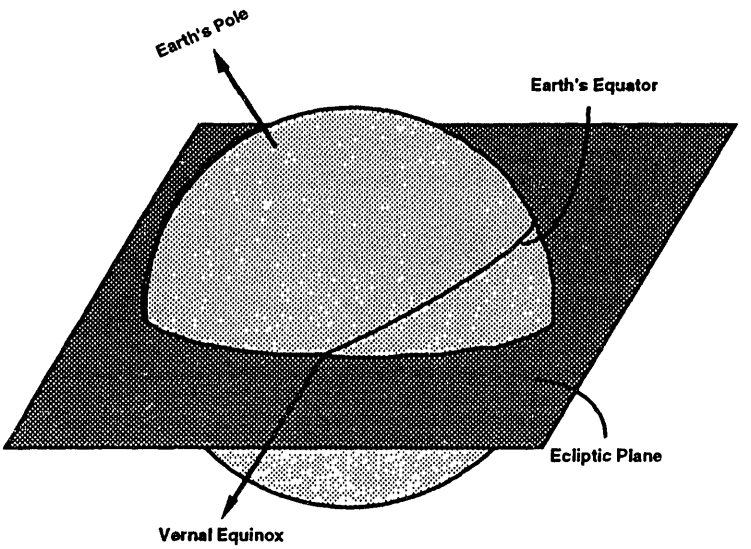

Figure 2.3 Principal Direction of Reference Systems

For the mean equator and equinox of fundamental epoch coordinate systems, the equinox and polar axis (i.e., equatorial plane) are "frozen" at some instant in time (B1950.0 for mean equator and equinox of 1950; J2000.0 for mean equator and equinox of J2000), thus providing a valid inertial coordinate system. A discussion of the difference between the two fundamental reference frames is provided in section 3.2.1.6.

2.4.2 True Equator and Equinox of Reference/Date

There would be no need to define other inertial coordinate systems if the equator and equinox remained fixed with respect to one another. Unfortunately, effects of the sun, moon, and planets on the equatorial and ecliptic planes preclude this situation.

In fact, both the ecliptic and equatorial planes experience motion over time.

The motion of the ecliptic is due to gravitational attraction of the planets on the earth's orbit about the sun, and is referred to as *planetary precession.* The impact of planetary precession includes an eastward drift of the equinox (approximately twelve arc seconds per century) and reduction in the obliquity, the angle between the equatorial and ecliptic planes (approximately forty-seven arc seconds per century) [58].

Motion of the earth's equator contains both long and short periodic components that are a result of the gravitational attractions of the sun, moon and planets on the aspherical earth [56]. The long period motion, called *luni-solar precession,* has an amplitude of approximately 23.5 degrees and a period of about 26,000 years [58]. The combination of planetary and luni-solar precession is defined as *general precession.* Short period motion, referred to as *nutation,* has an amplitude of about nine arc seconds and a period that varies, but can last up to 18.6 years [58].

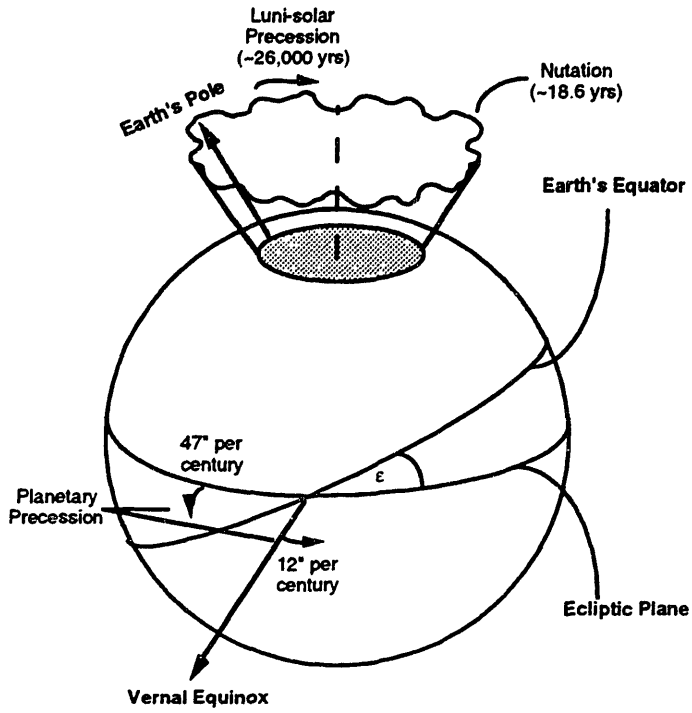

Figure 2.4 Precession and Nutation Effects

General precession and nutation are usually dealt with as separate quantities in astronomy and astrodynamics. By considering precessional effects only, one can describe a coordinate frame corresponding to the mean equator and equinox of date. Then, by accounting for nutational effects, this mean of date frame is transformed into the true equator and equinox of date.

$$\mathbf{X}_{True\ of\ Date} = \underbrace{\mathbf{N}\,\mathbf{P}\,\mathbf{X}_{Mean\ of\ 1950/2000}}_{Mean\ of\ Date} \tag{2.56}$$

Each of these effects is expressed as a 3x3 transformation matrix and dependent upon the geometrical relationship between the equatorial and ecliptic planes. The precession matrix relating the mean equator and equinox of fundamental epoch to the mean equator and equinox of date is determined from the three angles (z_a, θ_a, ζ_a) displayed in Figure 2.5.

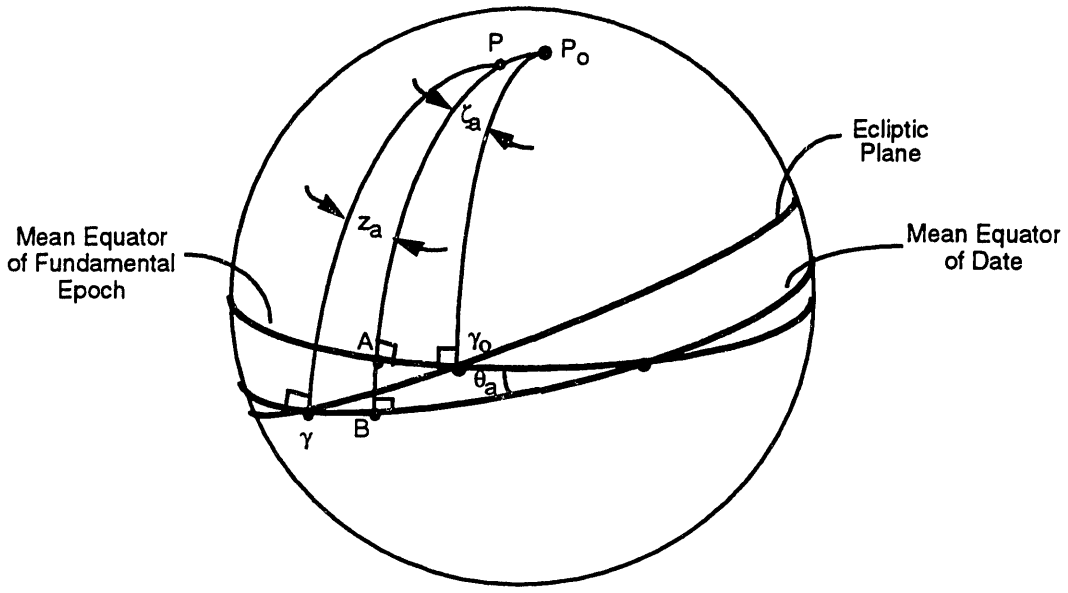

Figure 2.5 Precession Angles (adapted from [41])

The precession matrix (**P**) is then defined by:

$$\mathbf{P} = R_3(-z_a)R_2(\theta_a)R_3(-\zeta_a) \tag{2.57}$$

where the three rotational matrices are defined as:

$$\begin{aligned} R_1(\alpha) &= \begin{bmatrix} 1 & 0 & 0 \\ 0 & \cos\alpha & \sin\alpha \\ 0 & -\sin\alpha & \cos\alpha \end{bmatrix} \\ R_2(\alpha) &= \begin{bmatrix} \cos\alpha & 0 & -\sin\alpha \\ 0 & 1 & 0 \\ \sin\alpha & 0 & \cos\alpha \end{bmatrix} \\ R_3(\alpha) &= \begin{bmatrix} \cos\alpha & \sin\alpha & 0 \\ -\sin\alpha & \cos\alpha & 0 \\ 0 & 0 & 1 \end{bmatrix} \end{aligned} \tag{2.58}$$

Nutation superimposes the short periodic effects of the sun, moon and planets on the mean equator and equinox of date to produce an equator and

equinox true of date. The matrix associated with these short periodic effects is dependent upon deviations in longitude ($\Delta\psi$) and nutation in obliquity ($\Delta\varepsilon$). The relevant relationships are shown in Figure 2.6.

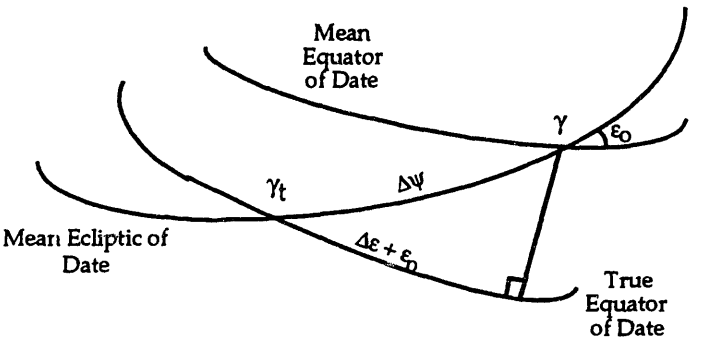

Figure 2.6 Nutation Angles (adapted from [58])

The transformation matrix from mean equator and equinox of date to true equinox and equator of date is given by:

$$\mathbf{N} = R_1(-\varepsilon)R_3(-\Delta\psi)R_1(\varepsilon_0) \tag{2.59}$$

Draper R&D GTDS obtains its precession and nutation information from an external Solar/Lunar/Planetary (SLP) file, which combines precession and nutation information into one matrix without distinguishing between the two.

$$\mathbf{C} = \mathbf{N}(\Delta\varphi, \Delta\varepsilon)\mathbf{P}(z_a, \theta_a, \zeta_a) \tag{2.60}$$

While Draper R&D GTDS cannot currently support a mean equator and equinox of date coordinate system capability, it does possess the option to solve the equations of motion in a true of "reference date" coordinate system. This coordinate system is defined from an equator and equinox that are true

of a particular time, usually midnight of the current day, rather than the request time. The source of the difference, then, between the true of reference and true of date coordinate systems is the evaluation of the precession and nutation matrices. Prior to this work, the instantaneous true equator and equinox of date was not a coordinate system input/output option in Draper R&D GTDS.

2.4.3 Earth-Centered, Earth-Fixed

The earth-centered, earth-fixed (ECEF) coordinate system is a rotating frame referenced to the Greenwich meridian and is based upon the true equator and equinox of date. Draper R&D GTDS uses the ECEF coordinate system in various force model evaluations. The user also has the option of requesting output in this frame, providing a measure of the relative motion of a spacecraft with respect to the earth. Because GPSR navigation solutions are referenced to this frame, an ECEF input capability was added to Draper R&D GTDS. The modifications required for this capability are summarized in Appendix C. Observation modeling in the ECEF frame has existed as an option in Draper R&D GTDS since 1983 [14].

The ECEF coordinate system is related to the true equator and equinox of date frame by a single rotation. The principal direction of the rotating frame is offset from the inertial system due to the earth's rotation. The angular quantity relating the two frames is the Greenwich hour angle, a measure of the difference between the Greenwich meridian and the true vernal equinox in a westerly direction in the plane of the equator [24].

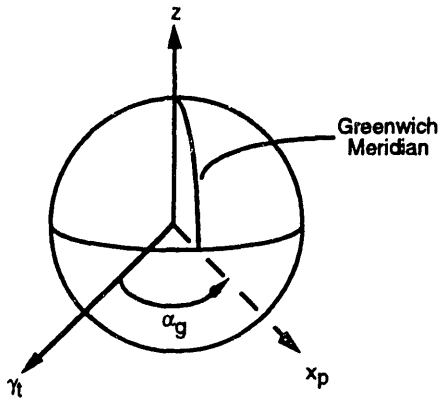

Figure 2.7 Right Ascension of Greenwich

The angle in Figure 2.7 actually represents the right ascension of Greenwich, which is the angular measurement in the eastward direction from the true vernal equinox (γ_t) to the Greenwich meridian (x_p). The Greenwich hour angle, is thus the negative of the right ascension of Greenwich.

Transformation from the true equator and equinox of date to ECEF coordinates is given by:

$$\mathbf{B} = R_3(\alpha_g) = \begin{bmatrix} \cos\alpha_g & \sin\alpha_g & 0 \\ -\sin\alpha_g & \cos\alpha_g & 0 \\ 0 & 0 & 1 \end{bmatrix} \tag{2.61}$$

Therefore, body-fixed coordinates are related to mean equator and equinox of fundamental epoch coordinates by:

$$\mathbf{r}_{ecef} = \mathbf{BCr}_{1950/2000} \tag{2.62}$$

2.5 GPSR Navigation Solutions

GPSR navigation solutions are ECEF position and velocity vectors constructed internally (to the GPSR) from raw pseudorange and carrier phase information. The content of the GPSR navigation solutions is dependent upon the satellite-based receiver and software that translates the telemetry into usable format during ground-based processing. The navigation solutions used for analysis in this work were provided in three different formats: modified RINEX, SP1, and SP3. EUVE navigation solutions were obtained from Johnson Space Center in a modified RINEX format, while TOPEX and TAOS solutions were placed on an anonymous FTP site (address is *bodhi.jpl.nasa.gov, or 128.149.70.66*) by Dr. Joseph Guinn of JPL in SP3 and SP1 formats, respectively.

GPS receiver information is currently stored on the ground in two manners. Data archiving seeks to preserve the information content of the original receiver message through a virtual "one to one transformation" from the binary message to an ASCII format. Common Exchange Formats circumvent the massive storage requirements of Data Archiving by compressing only the pertinent information into a commonly accepted format [31]. Modified RINEX, SP3, and SP1 provide a convenient method of data transfer at the processing level and are thus considered Common Exchange Formats.

The Receiver Independent Exchange (RINEX) format is a standard method of housing the raw observables from a GPSR [31]. Intended to simplify the processing schemes associated with GPSR information, this format consists of a header and the pertinent data. The header contains basic information

including the source, epoch, and interval associated with the observations. The pseudorange and carrier phase measurements are found in the body of the file, organized by time of observation and GPS satellite number. The more precise carrier phase information is generally found on 1 second grids, while pseudorange measurements are provided once every ten seconds. These grid sizes are receiver dependent.

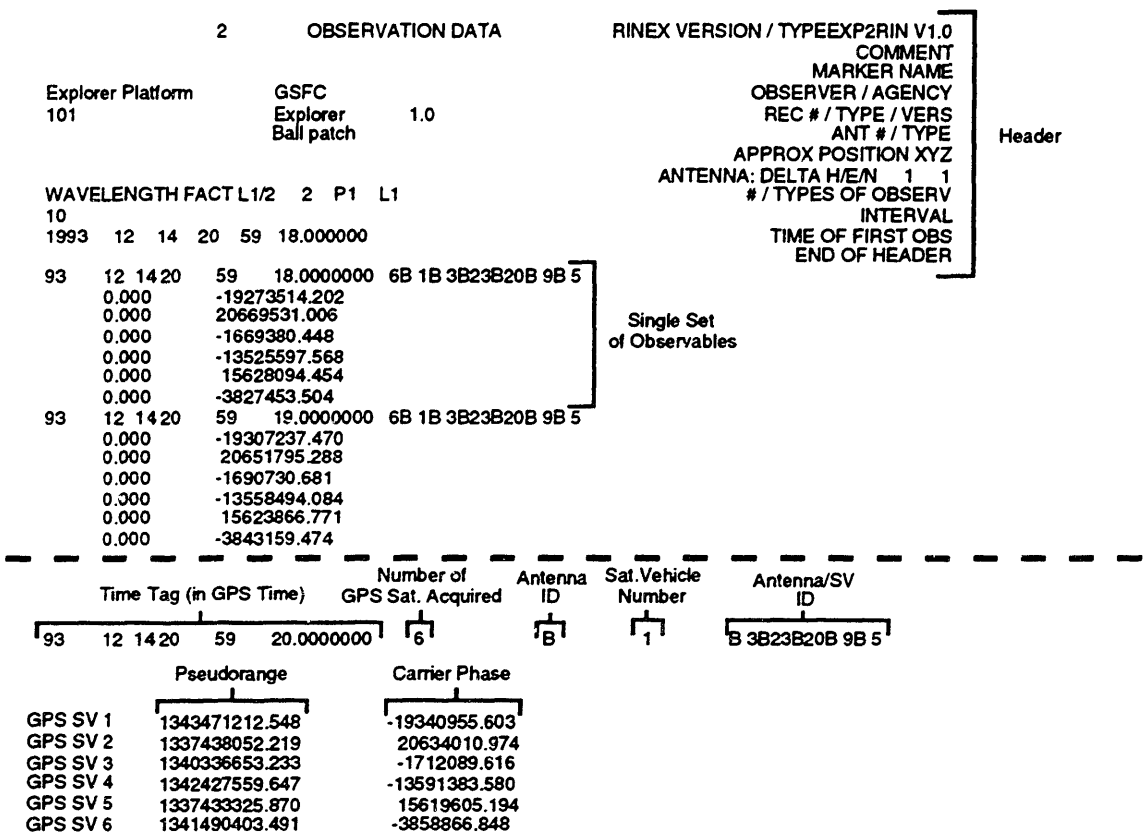

Figure 2.8 RINEX Format for Observables

Technical staff at Johnson Space Center have expanded the GPSR products for EUVE to include a position and velocity file similar to the RINEX format by modifying the software performing the raw binary-ASCII conversion [43]. This file contains four observables of interest: an earth-centered, earth-fixed position and velocity vector, receiver clock error, and time tag. Other

information, such as the number of satellites acquired, their Pseudorandom Number (PRN), and a flag reflecting the quality of the solution (successful or unsuccessful), also exists [16]. The format depicted below is characterized as a modified RINEX format.

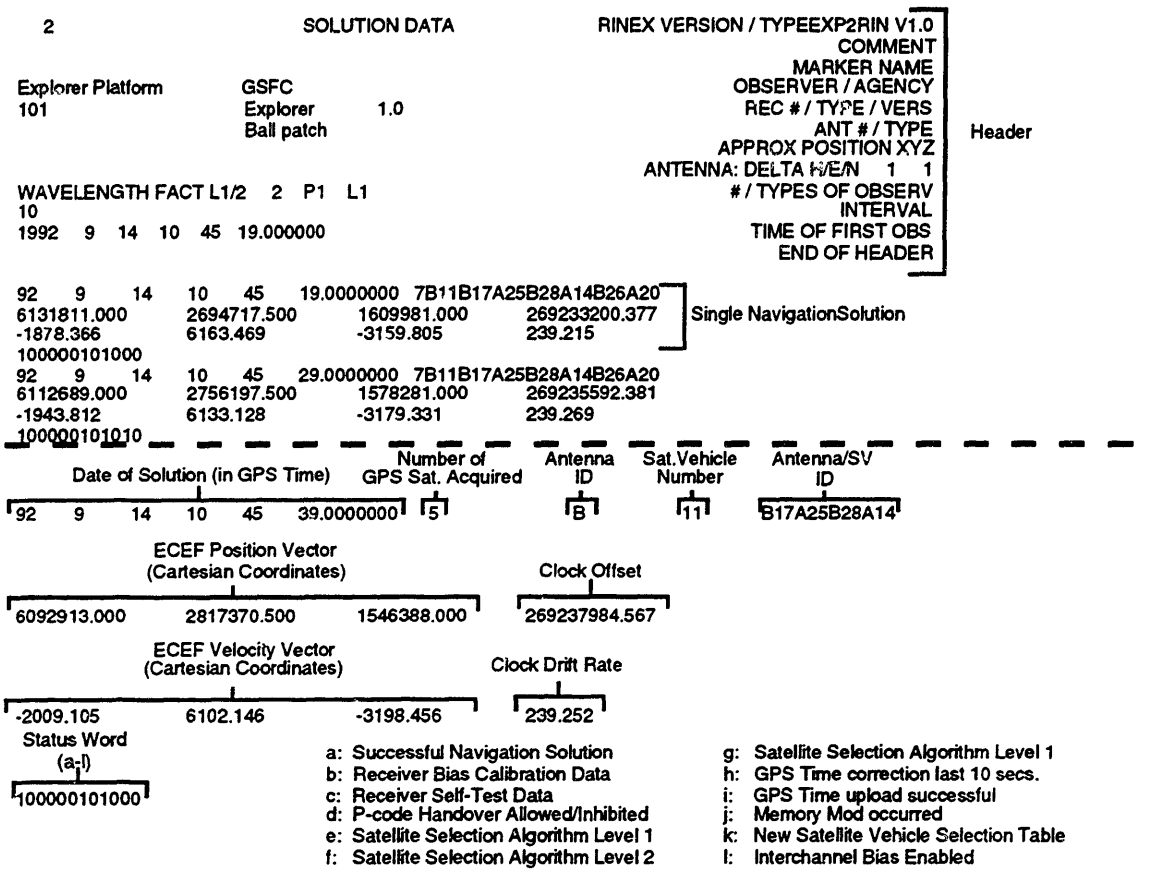

Figure 2.9 Modified RINEX Format for GPSR Navigation Solutions

SP3 format, like RINEX, contains position, velocity, receiver clock error and time information. However, it does not contain the additional information on the process used to derive the solution or its quality. TOPEX GPSR navigation solutions are in SP3 format.

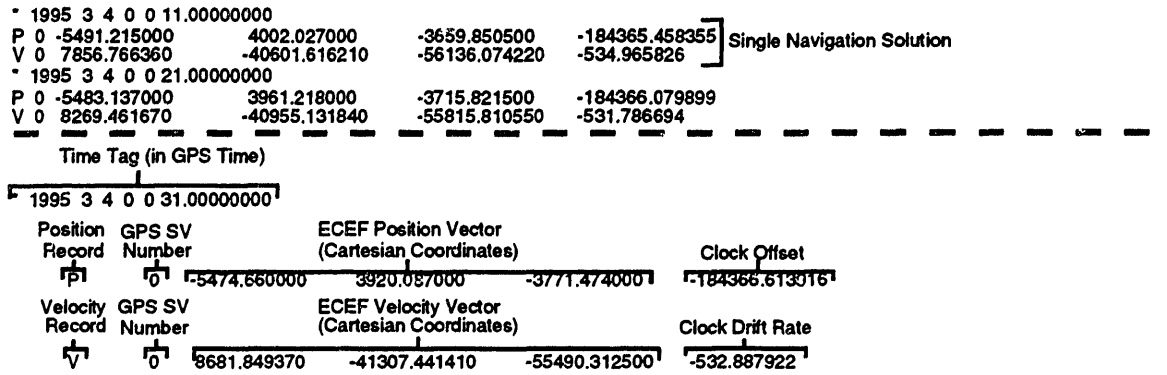

Figure 2.10 SP3 Format for GPSR Navigation Solutions

SP1 format is similar in structure to SP3 format, but does not contain receiver clock error information, as it is incorporated prior to navigation solution generation. Figure 2.11 shows that the time tags are not the usual integer values. TAOS GPSR navigation solutions are in SP1 format. Both SP3 and SP1 formats are products of JPL software.

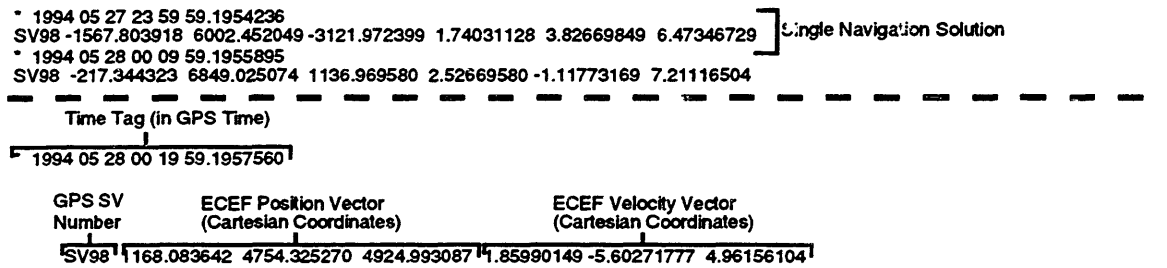

Figure 2.11 SP1 Format for GPSR Navigation Solutions

2.6 GPSR Navigation Solution Preparations

To ensure compatibility with Draper R&D GTDS, the navigation solutions used in this work required several satellite-dependent adjustments. Alterations included binary-ASCII conversion, time rectification, and bias compensation.

The EUVE navigation solutions were contained within a binary file that was a virtual replica of the telemetry flow directly from the satellite. A binary-ASCII conversion routine was provided by Ms. Stephanie Lowery of Johnson Space Center to allow personnel to view the solutions [43]. The TOPEX and TAOS navigation solutions were already in ASCII format when obtained from the JPL FTP site.

The time alterations can be grouped into two categories. The first type of adjustment is a result of timing errors internal to the GPSR. Because of the great significance placed upon time in the GPS system, the receiver's internal clock error is a solve-for variable in the least-squares process along with the coordinates of the receiver (when the receiver has locked onto four GPS satellite signals). This clock error is passed along as part of the navigation solution message (see Figures 2.8-2.10). Since the time tag associated with the estimates is the time that the receiver thinks that it has derived a solution and *not* the actual time, the clock error must be incorporated. In the case of SP1 format navigation solutions (TAOS), this correction has already been applied (see Figure 2.11).

$$t_{correct} = t_{obs} - \delta t_{receiver} \tag{2.63}$$

The second timing adjustment is a result of the difference in time systems between the GPSRs and Draper R&D GTDS. Observation times must be entered into Draper R&D GTDS in Universal Coordinated Time (UTC), while the receivers provide solutions based upon GPS time. GPS time is kept within 1 microsecond of UTC time on a relative scale, but is continuous and not adjusted for leap seconds, resulting in an integer number of seconds

difference between the two time systems. The last common epoch between GPS time and UTC was midnight 5/6 January 1980 [40]. Leap second information can be obtained from the U.S. Naval Observatory [63] or on the internet at *http://tycho.usno.navy.mil.*

Table 2.1 GPS/UTC Time Differences

Beginning of Period (hour 0)	End of Period (hour 24)	GPS Time - UTC (sec)
Janurary 1, 1980	June 30, 1981	0
July 1, 1981	June 30, 1982	1
July 1, 1982	June 30, 1983	2
July 1, 1983	June 30, 1985	3
July 1, 1985	December 31, 1987	4
January 1, 1988	December 31, 1989	5
January 1, 1990	December 31, 1990	6
January 1, 1991	June 30, 1992	7
July 1, 1992	June 30, 1993	8
July 1, 1993	June 30, 1994	9
July 1, 1994	December 31, 1995	10

In addition to these two timing considerations, one modification to the actual TOPEX and EUVE position and velocity navigation solutions is required. A 35 meter cross-track bias was uncovered when performing TOPEX experiments. This error is time dependent and consistent with an offset in the location of the vernal equinox at B1950.0 that ensures compatibility with the FK5 celestial reference system.

The longitudinal offset can be given as [58]:

$$E(T) = 0^{s}.035 + 0^{s}.085(T - T_0)/36524.2198782 \qquad (2.64)$$

where T-$T0$ is the Julian time difference between the current time and B1950.0 (JD 2433282.423). A more detailed discussion of the vernal equinoctial offset at B1950.0 is found in section 3.2.1.6.

To account for this error, the navigation solutions were rotated about the polar axis through the angle, $E(T)$:

$$\mathbf{x}_{\text{modified}} = R_3(E)\mathbf{x}_{\text{original}} \qquad (2.65)$$

where x is either a position or velocity vector.

The 35 meter cross-track error was also observed by Dr. Joseph Guinn at JPL [30]. Application of this rotation bias to the navigation solutions prior to entry into GTDS results in a reduction of the cross-track errors by 30-35 meters for TOPEX. Figure 2.12 highlights the effects of this rotation bias by comparing a navigation solution fit process with a truth solution (the Precise Orbit Ephemerides, POEs, which are discussed in the subsequent section).

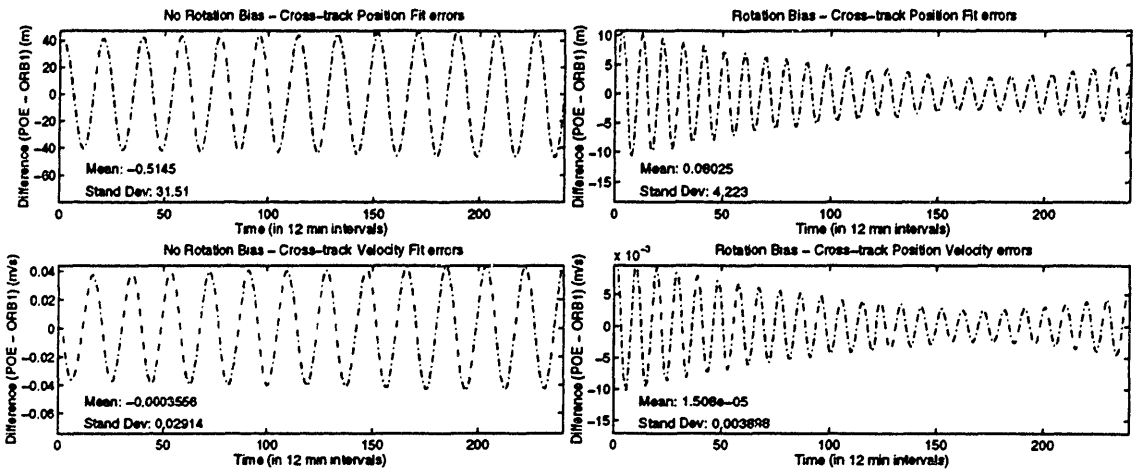

Figure 2.12 Effect of Including Rotation Bias in TOPEX 1992 Navigation Solutions

This rotation bias was tested for both the 1992 and 1995 time frames. The effect was the same for both time periods, indicating that the time-dependent rotation bias modification has the potential to effectively remove the cross-track errors for TOPEX at any time.

EUVE experiments show a similar need to account for the rotation bias. The effect upon cross-track is somewhat less dramatic (on the order of 10 meters), but is compensated for by a 30 meter improvement in the along-track component. Because EUVE is at a lower altitude, the overall effect of this bias is expected to be less. The distribution of the bias is also expected to be more in the along-track component than TOPEX because of a smaller inclination. It should be noted that the TOPEX and EUVE use the same type of receivers, a Motorola GPS Demonstration Receiver (GPSDR). The TAOS navigation solutions do not require compensation for a rotational bias.

After modifications are made, the data sets are thinned such that they meet size limitations (about 48000 observations, maximum) for entry into Draper

R&D GTDS. The large number of observations resulted in TOPEX data sets being thinned to one observation every four minutes, and EUVE data sets including observations every 30 seconds. TAOS navigation solutions were available every 10 minutes and did not require thinning.

Once these alterations were made, the data was converted from its prior format (modified RINEX, SP3 or SP1) to an observation file that can be interpreted by Draper R&D GTDS. Figure 2.13 summarizes the preprocessing steps taken to ensure compatibility between the navigation solutions and Draper R&D GTDS.

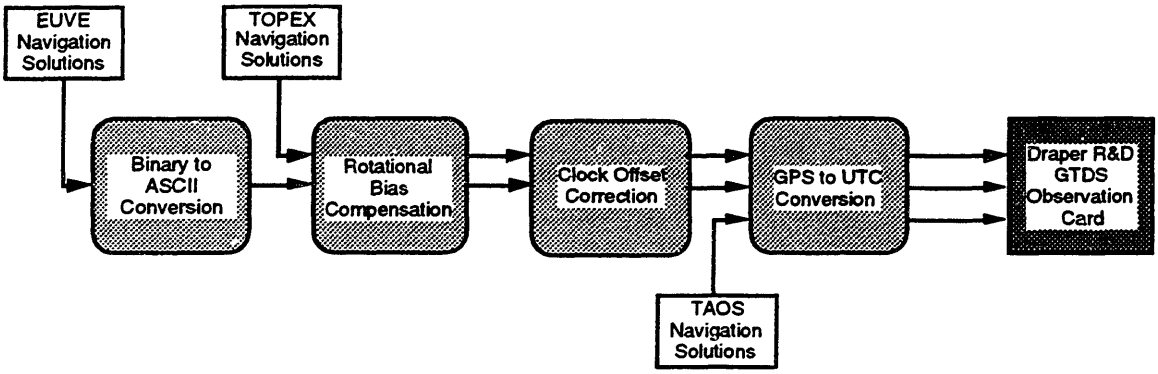

Figure 2.13 Summary of GPSR Navigation Solution Preprocessing

2.7 Precise Orbit Ephemerides (POEs)

The Precise Orbit Ephemerides (POEs) are high quality trajectories used as a truth orbit for referencing other determined orbits (e.g., fitting navigation solutions). These orbits utilize high accuracy observations, such as satellite laser ranging (SLR) or differential GPS tracking information, in the orbit determination process. Each of the satellites used for this work had an associated POE for evaluation purposes.

The TOPEX POEs are by far the most precise and documented reference trajectories. With a 3-D position RMS on the order of about 15 cm, these solutions can certainly be considered absolute truth [67]. The TOPEX POEs were developed at NASA/GSFC through a batch least squares adjustment program (GEODYN) using SLR data [68]. The atmospheric drag and solar radiation pressure models allowed for a variable mean area (VMA) spacecraft cross-sectional area.

A separate version of the TOPEX POEs developed by JPL using differential GPS techniques exists as well. These POEs are accessible at the same internet site as the GSFC POEs, and agree to an accuracy of about 13 cm [29].

The EUVE and TAOS POEs were developed using a differential GPS technique similar to that used for the JPL TOPEX POEs. The EUVE POEs were developed as part of Gold's doctoral thesis at the University of Colorado - Boulder, and have a reported accuracy of about 1 m [26]. The TAOS POEs have a 1σ 3-D position error of about 3 m [28].

The force modeling used in the orbit determination processes for reference orbits were similar for all three spacecraft and included [61]:

- JGM-2 70x70 Gravity Field
- Lunar-Solar Point Mass Gravitational Attraction
- Solid Earth Tides
- Atmospheric Drag (Jacchia-Roberts Density Model)
- Solar Radiation Pressure (Conical Model)

- Earth Radiation Pressure
- Ocean Tides
- Rotational Deformation

In addition to these models, Gold introduced empirical once, twice, and half-per revolution accelerations for the EUVE POEs.

Although the format of the POE file is consistent for the three spacecraft, the information content varies. The most significant difference stems from the lack of an instantaneous inertial true of date representation for the TAOS and EUVE POEs. While the EUVE POEs contain only ECEF vectors, ITOD POEs for TAOS can be generated because of the presence of both ECEF vectors and a Greenwich hour angle at that measurement time. The TOPEX POEs contain the ITOD and ECEF vectors, as well as the Greenwich hour angle. In addition to this ITOD deficiency, the TAOS and EUVE POEs also lack various other less significant header information (e.g., cycle number, start/end times) contained on the TOPEX POEs. The standard POE format is described below in Figure 2.14.

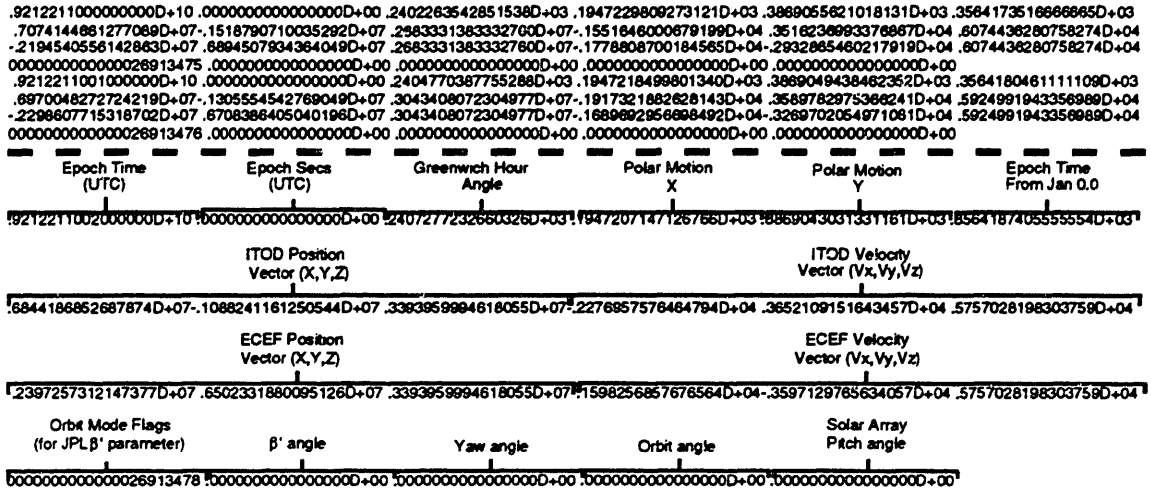

Figure 2.14 Format of POE File

Chapter 3

Incorporation of the J2000 and Instantaneous True of Date Coordinate Systems, and Solid Earth Tides into Draper R&D GTDS

3.1 Chapter Introduction

The orbit determination methods used with a high accuracy data source (such as the POE vectors or GPSR navigation solutions) are critical if the benefits offered by the source are not to be lost in the process noise. Improvements in the Draper R&D GTDS orbit determination process that preclude this from happening are presented in this chapter. The identified software modifications can be grouped into three categories involving the following capabilities: coordinate systems inherently linked to the FK5 fundamental reference frame (often referred to as J2000-based coordinate systems), modeling of lunar and solar solid earth tides, and referencing observations and output to an instantaneous true of date coordinate system.

A discussion of the need for each capability links the software development process and use of GPSR navigation solutions in an orbit determination scheme. The mathematical theory behind the J2000-based coordinate systems, instantaneous true of date coordinate system, and solid earth tides is

presented to demonstrate an understanding of the capabilities being added to Draper R&D GTDS. Various software design considerations are highlighted to rationalize the code development process. Finally, a summary of the code-related changes is given to assist other Draper R&D GTDS users in future developmental projects.

3.1.1 Rationale Behind Software Modifications

With a software package the magnitude of Draper R&D GTDS (as of this writing, the VAX station 4000/90 version contains over 1300 routines), it is imperative for the software developer to understand the reasons for modifications. This section will discuss the motivation for incorporating the J2000 theory, solid earth tides and instantaneous true of date options into Draper R&D GTDS.

3.1.1.1 J2000 Theory

The General Assembly of the International Astronomical Union (IAU) for the 1976 proceedings at Grenoble recommended that a new system of Astronomical Constants be introduced and defined for a new fundamental reference frame [36]. The basis for this new frame, the Fifth Fundamental Catalog (FK5), is derived from observations of the Sun, planets, stars, and lunar occultations from 1900-1977 [22]. The most difficult portion of defining the fundamental frame is determining the location of the equinox. The process involves measuring the sun's declination over a period of time. The information is interpolated to the point in time where the declination

vanishes (i.e., the sun crosses equator). Information from stellar observations is also combined to provide the most accurate assessment of the equinox [39].

Prior to introduction of the FK5 system on January 1, 1984, most of the astrodynamics community operated with the FK4 system. The FK4 frame is based upon the mean equator and equinox at B1950.0 (Julian date, 2433282.423), while the FK5 defines the mean equator and equinox at J2000.0 (Julian date 2451545.0).

The FK5 equinox is offset from the FK4 equinox by an amount that varies slowly over time. Fricke claims this offset, discussed in greater detail in the subsequent section, dates back to Newcomb's Fundamental Catalogue (1899) and is a result of imprecise techniques for measuring the right ascensions of stars of magnitude 4.0-6.0 (the greater the magnitude, the dimmer the star) [22]. As a result, the location of an object described in the FK4 system is different from the FK5 representation.

The astrodynamics community began its transition from FK4-based reference frames to the FK5-based reference frames when the new definitions of the FK5 system took effect on January 1, 1984 [51]. Currently, most of the astrodynamics community uses the FK5 system as its fundamental reference frame. However, when Draper R&D GTDS was spun off from the Goddard R&D GTDS in 1979 [20], the fundamental reference frame in use was the FK4 system. The use of the B1950.0 reference frame limits the compatibility of Draper R&D GTDS software products and information provided by the external community. Introduction of J2000 theory into Draper R&D GTDS

ensures that the software evolves and is consistent with the rest of the astrodynamics community.

3.1.1.2 Solid Earth Tides

In addition to the third-body point-mass effects that the sun and moon can have on a satellite's orbit, these bodies also create perturbations due to solid earth tides. The sun and moon redistribute the mass of the earth through their gravitational attractions, and in turn affect the gravitational field of the earth [52]. Lunar tides are so-called intermediate period effects that have a cycle time of about 14 days and magnitudes of up to 15 meters for a typical satellite orbit. Solar tides result in much longer periodic effects (six months), with magnitudes significantly smaller than lunar tides [23].

To understand the significance of modeling tidal effects within Draper R&D GTDS, one must recall the precision of the data involved. The relatively high-quality data source (GPSR navigation solutions) provides an opportunity to perform orbit determination and prediction with reasonable accuracy. As the data source becomes more accurate, the effect that unmodeled tidal distortion has on modeling the observations becomes a larger percentage of the total error and the need for modeling these effects increases. With other less accurate data sources, this tidal error becomes lost in the process noise.

3.1.1.3 *Instantaneous True Equator and Equinox of Date*

As indicated by the OBSINPUT and OUTPUT cards in Appendix D, Draper R&D GTDS supports a variety of coordinate systems for observation modeling and output. One coordinate system that it did not support prior to this work, however, was one in which the results were referenced to a frame that is true of the time of each data point. Instead, observations and output were based upon a coordinate system true of some reference time (generally the epoch time). Thus, slight variations over time in the equatorial orientation due to nutation (and to a lesser degree, luni-solar precession) were neglected. This is a relatively accurate approximation over small time intervals (the TOPEX orbit, for example, experiences errors on the order of magnitude of 10 meters/day); however, for cases where longer time spans or high precision is required, this approximation is a significant source of error.

The need to support a Draper R&D GTDS instantaneous true of date output capability stemmed from the coordinate systems of the external orbit reference source (the POEs). The POEs provide Cartesian solutions in both inertial true of date (not true of reference) and earth-centered, earth-fixed (ECEF) frames. Comparison of GTDS orbits and POE vectors in ECEF coordinates was straightforward, since Draper R&D GTDS supported the capability to output in ECEF coordinates prior to this work. However, direct comparisons could not be made in the inertial frame of the POE solutions with the existing capabilities. The inertial solutions allow for conversion of the Cartesian differences to orbital element and/or radial/cross-track/along-track differences, which provide unique physical insight into the sources of the errors.

In addition, one of the objectives of this work was to determine the accuracy of the perturbation modeling within Draper R&D GTDS by using the high-quality POE solutions. As will be discussed in the subsequent chapter, it was necessary to perform differential corrections using both the instantaneous true of date (ITOD) and ECEF versions of the POEs. Because the ITOD POEs were referenced to a coordinate system that is true of date and *not* true of reference (TOR), it was necessary to model the observations as instantaneous true of date.

3.2 Mathematical Theory Behind the J2000-Based and Instantaneous True of Date Coordinate Systems and Solid Earth Tides

It is appropriate to discuss the mathematical theories behind the J2000 and ITOD coordinate systems and solid earth tides prior to discussion of the software implementation of these additions. This section first discusses the J2000 theory and, where applicable, provide a comparison to the B1950 theory present in the existing version of Draper R&D GTDS. A brief development of perturbations due to solid earth tides follows. Finally, a mathematical representation for the ITOD coordinate frame is compared to the existing TOR frame.

3.2.1 J2000 Theory

In many respects, the FK5 system is simply an "upgrade" to the previous FK4 system. Theoretical differences can be isolated to astrodynamic constants and

methods of development for parameters measured with respect to the fundamental epoch -- B1950.0 in the case of FK4, and J2000.0 for the FK5.

The differences between FK4 and FK5 are highlighted below and include:

- FK4 vs. FK5 Astrodynamic Constants
- Determination of the mean obliquity and mean Greenwich hour angle
- Precession and nutation formulae
- Determination of the difference between geodetic and geocentric latitude

3.2.1.1 Astrodynamic Constants

When comparing astrodynamic constants associated with the FK4 and FK5 systems, several quantities are notably different. While some parameters, such as the inclination between the lunar equator and the ecliptic, should be expected to vary between fundamental reference frames, most differences are a result of either natural phenomena (i.e., the earth's rotation rate) or improvements in measurement techniques. The values should not necessarily be associated with a fundamental reference frame, but rather the times at which the reference frames are being used.

The various constants that have different values at the time FK5 is being implemented into Draper R&D GTDS are highlighted in Table 3.1. The FK4

values are based upon the preexisting (prior to any modifications due to J2000, solid earth tides or instantaneous true of date) version of R&D GTDS, while FK5 constants are associated with the International Earth Rotation Service (IERS) 1995 definitions.

Table 3.1 Astrodynamic Constants for FK4 and FK5 Systems

Constant	Existing GTDS Value	IERS 1995 Value [53]
Geocentric Gravitational Constant (GM_e)	$3.986008 * 10^{14}$ m^3s^{-2}	$3.986004418 * 10^{14}$ m^3s^{-2}
Universal Gravitational Constant (G)	$6.673*10^{-11}$ $m^3kg^{-1}s^{-2}$	$6.67259*10^{-11}$ $m^3kg^{-1}s^{-2}$
Earth-Moon Mass Ratio (μ)	0.012299970	0.012300034
Sun-Earth Mass Ratio (M_S/M_e)	332953.283	332946.045
Equatorial Radius of the Earth (a_e)	6378140.0 m	6378136.55 m
Earth Flattening (f)	1/298.25	1/298.256421867
Mean Angular Velocity of the Earth (ω)	$7.2921158549*10^{-5}$ rad s^{-1}	$7.2921151467*10^{-5}$ rad s^{-1}
Astronomical Unit (AU)	$1.495979*10^{11}$ m	$1.49597871475*10^{11}$ m
Inclination Between Lunar Equator and Ecliptic	1°32'6"	1°32'33".5

It should be noted that the values of the geocentric gravitational constant (and, hence, the earth-moon and earth-sun ratios) and the earth's equatorial radius are gravity field dependent. This fact is significant for cases where the

gravity field is specified by the user (which is true most of the time for use of Draper R&D GTDS). The subsequent section describes how multiple values of the earth's gravitational constant and equatorial radius are handled.

3.2.1.2 Mean Obliquity

The GTDS Mathematical Specification describes the mean obliquity as the angular difference between the plane of the mean equator of date and the plane of the ecliptic of date [24]. The preexisting version of Draper R&D GTDS contains the following expression for the mean obliquity of date:

$$\varepsilon_m = 23^{\circ}.4457587 - 0^{\circ}.01309404T - 0^{\circ}.88(10^{-6})T^2 + 0^{\circ}.5(10^{-6})T^3 \qquad (3.1)$$

where T is the time in Julian centuries of 36525 days elapsed from B1950.0 (JD2433282.423) [24].

When operating with the FK5 system, the time argument is measured from its reference epoch, J2000.0. The mean obliquity in the FK5 system is given by:

$$\varepsilon_m = 23^{\circ}.43929111 - 0^{\circ}.013004166T - 0^{\circ}.163889(10^{-6})T^2 + 0^{\circ}.503611(10^{-6})T^3 \quad (3.2)$$

where T is the time in Julian centuries of 36525 days elapsed from J2000.0 (JD2451545.0) [58].

3.2.1.3 *Mean Greenwich Hour Angle*

Similarly, the fundamental reference epoch is the distinguishing feature in determination of the mean Greenwich hour angle using FK4 and FK5 theory. The mean Greenwich hour angle is defined as the angle between the hour circle passing through Greenwich, England, and the true vernal equinox, measured westerly in the plane of the equator [24]. Using B1950.0 as the reference epoch, the mean Greenwich hour angle (often referred to as Greenwich mean sidereal time) is defined by:

$$\alpha_{gm} = UT1 + 6^h 38^m 45.^s 836 + 8640184.^s 542T + 0.^s 0929T^2 \qquad (3.3)$$

where T is measured in Julian centuries of 36525 days elapsed from 12 hours UT1 January 0, 1900 (JD2415020.0) to the UT1 time of epoch. Note that the time is measured from 1900 and *not* 1950 [24].

In the FK5 reference frame, the mean Greenwich hour angle is the same angular difference measured at J2000.0, and given by:

$$\alpha_{gm} = UT1 + 6^h 41^m 50.^s 54841 + 8640184.^s 812866T + 0.^s 093104T^2 - 6.^s 2(10^{-6})T^3 \quad (3.4)$$

where T is measured in Julian centuries of 36525 days elapsed from J2000.0 (JD2451545.0) [2].

3.2.1.4 *Precession and Nutation Formulae*

As was stated in section 2.4, precession and nutation are applied to the mean equator and equinox of the fundamental reference frame to produce a true equator and equinox of date. The introduction of the FK5 system in January 1984 altered the expressions governing these effects to reflect evaluation from the new reference epoch (J2000.0).

Section 2.4 indicates the precession matrix is dependent upon three angles defined as ζ_a, z_a, and θ_a. These angles are depicted in Figure 2.5, and can be expressed in the FK4 system (often referred to as Newcomb precession) as:

$$\zeta_a = 2304.^{\circ}9969t + 0.^{\circ}302000t^2 + 0.^{\circ}01808t^3 \tag{3.5}$$

$$z_a = 2304.^{\circ}9969t + 1.^{\circ}092999t^2 + 0.^{\circ}019200t^3 \tag{3.6}$$

$$\theta_a = 2004.^{\circ}2980t - 0.^{\circ}425936t^2 - 0.^{\circ}04160t^3 \tag{3.7}$$

where t is the time in Julian centuries of 36525 days from the desired date to B1950.0 (JD2433282.423) [24].

The corresponding equations in FK5 theory are:

$$\zeta_a = (2306.^{\circ}2181 + 1.^{\circ}39656T - 0.^{\circ}000139T^2)t + (0.^{\circ}30188 - 0.^{\circ}000344T)t^2 + 0.^{\circ}017998t^3 \tag{3.8}$$

$$z_a = (2306.^{\circ}2181 + 1.^{\circ}39656T - 0.^{\circ}000139T^2)t + (1.^{\circ}09468 + 0.^{\circ}000066T)t^2 + 0.^{\circ}018203t^3 \tag{3.9}$$

$$\theta_a = (2004.^{\circ}3109 - 0.^{\circ}85330T - 0.^{\circ}000217T^2)t + (-0.^{\circ}42665 - 0.^{\circ}000217T)t^2 - 0.^{\circ}041833t^3 \tag{3.10}$$

where T is the time in Julian centuries of 36525 days from J2000.0 (JD2451545.0) (ε_0) to some fixed epoch (ε_f), and t is the time in Julian centuries of 36525 days from the fixed epoch (ε_f) to the desired date (ε_d) [35]. These times are depicted in Figure 3.1.

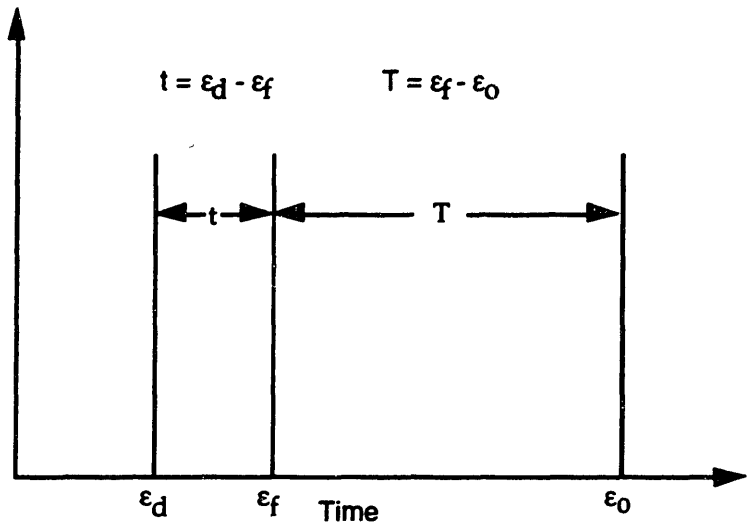

Figure 3.1 Time Arguments in Precession Calculations

These expressions in (3.8-3.10) represent the precession accumulated from a fixed epoch (ε_f) to the time of interest (ε_d). For evaluating precession with respect to the FK5 reference frame in GTDS, the fixed epoch is considered to be J2000.0; thus, the parameter T is set to zero and the angles are representative of the time period between the time of interest and the fundamental epoch. However, there is no requirement that the fixed epoch be equivalent to the fundamental epoch. Instead, precession could be measured between the time of interest and some arbitrary fixed epoch, allowing for representation of a vector in a fundamental frame referenced to that fixed epoch.

These three precession angles can then be used to generate the precession matrix that transforms Cartesian coordinates from the mean equator and equinox of a fundamental epoch (B1950.0 or J2000.0) to the mean equator and equinox of date. The precession matrix is given by:

$$\mathbf{P} = \mathbf{R}_3(-z_a)\mathbf{R}_2(\theta_a)\mathbf{R}_3(-\zeta_a) \tag{3.11}$$

or, in expanded form [42],

$$\mathbf{P} = \begin{bmatrix} \cos z_a \cos\theta_a \cos\zeta_a - \sin z_a \sin\zeta_a & -\cos z_a \cos\theta_a \sin\zeta_a - \sin z_a \cos\zeta_a & -\cos z_a \sin\theta_a \\ \sin z_a \cos\theta_a \cos\zeta_a + \cos z_a \sin\zeta_a & -\sin z_a \cos\theta_a \sin\zeta_a + \cos z_a \cos\zeta_a & -\sin z_a \sin\theta_a \\ \sin\theta_a \cos\zeta_a & -\sin\theta_a \sin\zeta_a & \cos\theta_a \end{bmatrix} \tag{3.12}$$

Section 2.3 points out that transformation from the mean equator and equinox of date to true equator and equinox of date involves applying nutation. The principle term of nutation is dependent upon the longitude of the ascending node of the moon's orbit and has a period of about 18.6 years [15]. The amplitude of the motion (referred to as the *constant of nutation*) is dependent upon the fundamental reference frame being used; for FK4 it is measured at 9."210 [15], while the FK5 value is defined as 9."2025 [58]. In addition, the motion of the true pole is to a much lesser degree dependent upon the mean anomalies and longitudes of the sun and moon [15].

Physical effects due to nutation are accounted for through corrections to the longitude ($\Delta\psi$) and the mean obliquity ($\Delta\varepsilon$), as depicted in Figure 3.2.

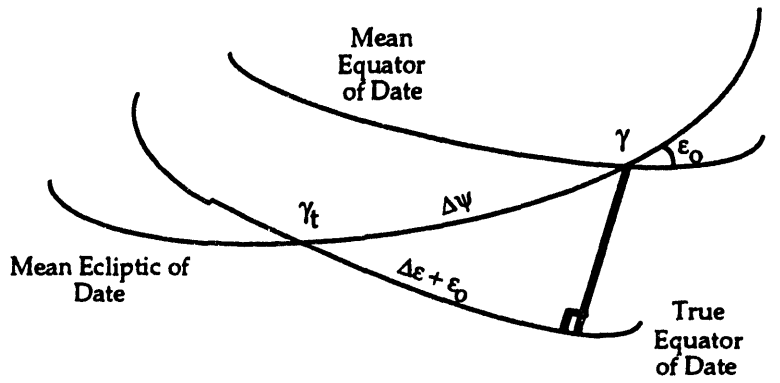

Figure 3.2 The Mean and True Equators of Date (adapted from [58])

A series of three rotations using these terms are performed to transform from the mean equator and equinox of date to the true equator and equinox of date. The transformation is characterized as:

$$\mathbf{N} = \mathbf{R}_1(-\varepsilon)\mathbf{R}_3(-\Delta\psi)\mathbf{R}_1(\varepsilon_o) \tag{3.13}$$

or, in expanded form,

$$\mathbf{N} = \begin{bmatrix} \cos\Delta\psi & -\sin\Delta\psi\cos\varepsilon_o & -\sin\Delta\psi\sin\varepsilon_o \\ \sin\Delta\psi\cos\varepsilon & \cos\Delta\psi\cos\varepsilon\cos\varepsilon_o + \sin\varepsilon\sin\varepsilon_o & \cos\Delta\psi\cos\varepsilon\sin\varepsilon_o - \sin\varepsilon\cos\varepsilon_o \\ \sin\Delta\psi\sin\varepsilon & \cos\Delta\psi\sin\varepsilon\cos\varepsilon_o - \cos\varepsilon\sin\varepsilon_o & \cos\Delta\psi\sin\varepsilon\sin\varepsilon_o + \cos\varepsilon\cos\varepsilon_o \end{bmatrix} \tag{3.14}$$

Development of these correction terms ($\Delta\psi$,$\Delta\varepsilon$) is dependent upon five fundamental arguments (l,l',F,D, and Ω) related to the mean longitudes of the sun and moon, the mean longitudes of the solar and lunar nodes, and the mean ascending node of the moon [58]. The correction terms may be evaluated from:

$$\Delta\psi = \sum_{i=1}^{n} S_i \sin A_i \tag{3.15}$$

and

$$\Delta\varepsilon = \sum_{i=1}^{n} C_i \cos A_i \tag{3.16}$$

where

$$A_i = a_i l + b_i l' + c_i F + d_i D + e_i \Omega \tag{3.17}$$

The coefficients for (3.15), (3.16) and the fundamental arguments are tabulated for 106 terms in [58].

The five fundamental arguments are defined below in Table 3.2.

Table 3.2 Five Fundamental Arguments for Nutation Theory

Symbol	Meaning
l	Mean longitude of the moon - mean longitude of moon's perigee
l′	Mean longitude of the sun - mean longitude of sun's perigee
F	Mean longitude of the moon - mean longitude of moon's node
D	Mean longitude of the moon - mean longitude of the sun
Ω	Longitude of mean ascending node of lunar orbit on ecliptic measured from mean equinox of date

Evaluation of these fundamental arguments is dependent upon the fundamental epoch being used. For FK4 theory, the fundamental epoch is set at 1900 January $0.^{d}5$ (JD2415020.0), and the argument expressions are:

$$
\begin{aligned}
l &= 296°06'16".59 + 1325'198°50'56".79T + 33".09T^2 + 0".0518T^3 \\
l' &= 358°28'33".00 + 99'359°02'59".10T - 0".54T^2 - 0".0120T^3 \\
F &= 11°15'03".20 + 1342'82°01'30".54T - 11".56T^2 - 0".0012T^3 \\
D &= 350°44'14".95 + 1236'307°06'51".18T - 5".17T^2 + 0".0068T^3 \\
\Omega &= 259°10'59".79 - 5'134°08'31".23T + 7".48T^2 + 0".0080T^3
\end{aligned}
\tag{3.18}
$$

where T is measured in Julian centuries of 36525 days elapsed from 1900 January $0.^d5$ (JD2415020.0) [15], and 1^r is equivalent to 360^o.

The FK5 theory uses J2000.0 (JD2451545.0) as its fundamental epoch. The nutation expressions for this frame are based upon the 1980 IAU Theory of Nutation [58] and are described below:

$$
\begin{aligned}
l &= 134°57'46".733 + 1325'198°52'02".633T + 31".310T^2 + 0".064T^3 \\
l' &= 357°31'39".804 + 99'359°03'01".224T - 0".577T^2 - 0".0120T^3 \\
F &= 93°16'18".877 + 1342'82°01'03".137T - 13".257T^2 + 0".011T^3 \\
D &= 297°51'01".307 + 1236'307°06'41".328T - 6".891T^2 + 0".019T^3 \\
\Omega &= 135°02'40".280 - 5'134°08'10".539T + 7".455T^2 + 0".0080T^3
\end{aligned}
\tag{3.19}
$$

where T is measured in Julian centuries of 36525 days elapsed from 2000 January $1.^d5$ (JD2451545.0) [58], and 1^r is equivalent to 360^o.

It is appropriate to point out that Draper R&D GTDS does not currently use the precession angles or fundamental arguments to express mean equator and equinox of the fundamental epoch (B1950.0 or J2000) in mean/true equator and equinox of date. Instead, precession and nutation information is computed by evaluating multiple-day-arc Chebyshev polynomials from a Solar/Lunar/Planetary (SLP) ephemeris file, which also contains precession

and nutation information [24]. SLP ephemeris files are currently maintained by the Testing, Reporting and Maintenance Program (TRAMP) at Draper [62].

Draper R&D GTDS, however, does use combinations of the fundamental nutation arguments to evaluate a transformation matrix from the mean equator and equinox of date to the mean ecliptic and equinox of date reference system. This logic is embedded within subroutine OBLTY. The derivative forms of the fundamental arguments that Draper R&D GTDS recognizes are simply linear combinations of the standard fundamental arguments and are summarized in Table 3.3.

Table 3.3 Relationship Between Standard Nutation Fundamental Arguments and Those Used by R&D GTDS

R&D GTDS Argument	Defined in Terms of Fundamental Arguments	Meaning
CR	$F+\Omega$	Longitude of the Moon
GP	$F+\Omega-l$	Longitude of Perigee of the Moon
G	$F+\Omega-D-l'$	Longitude of Perigee of the Sun
VL	$F+\Omega-D$	Longitude of the Sun
OM	Ω	Longitude of mean ascending node of lunar orbit on ecliptic measured from mean equinox of date

For transformation from mean equator and equinox of date to mean ecliptic and equinox of date, only knowledge of the nutation in obliquity is required (not the nutation in longitude). Therefore, only the values of C_i (the cosine terms) in (3.16) are of interest. R&D GTDS has made the assumption that any values of C_i less than 0."0020 are insignificant and have not been included.

This translates into a maximum of 6 cm error at the surface of the earth per term excluded. To maintain the existing structure of the code, the addition of the FK5 theory makes the same basic assumption.

Although the FK4 nutation series contains 69 coefficient terms, only 15 were identified to be significant according to R&D GTDS criteria. The 1980 IAU Theory of Nutation provides nutation tables that contain 106 coefficient terms, with 16 meeting R&D GTDS limits. By comparing the tables from [58] and [15], one can see that the additional term in the FK5 system has multipliers (a_i, b_i, c_i, d_i, e_i) of (0 1 0 0 0).

3.2.1.5 Geodetic vs. Geocentric Latitude

The relationship between geodetic latitude and geocentric latitude is also dependent upon the fundamental reference frame. This relationship is used within Draper R&D GTDS to determine station coordinates. The expressions for the latitude difference for B1950.0 and J2000.0 fundamental epochs are shown below:

$$\begin{aligned}(\varphi-\varphi')_{FK4} &= 695.''6635\sin(2\varphi)+1.''1731\sin(4\varphi)-0.''0026\sin(6\varphi)\\ (\varphi-\varphi')_{FK5} &= 692.''74\sin(2\varphi)-1.''16\sin(4\varphi)\end{aligned} \tag{3.20}$$

where φ is the geodetic latitude, and φ' is the geocentric latitude.

3.2.1.6 Relating FK4 to FK5

The transition from using the FK4 fundamental reference frame to FK5 as the fundamental frame has resulted in inconsistencies in the representation of

results. Some information is expressed in one system, while the balance is referred to the other. The existence of results in both frames reveals a need to relate the classical (FK4) and more modern (FK5) fundamental coordinate systems. The basic difference between the two frames is an equinox offset that varies slowly over time. This offset is depicted in Figure 3.3 and mathematically represented below.

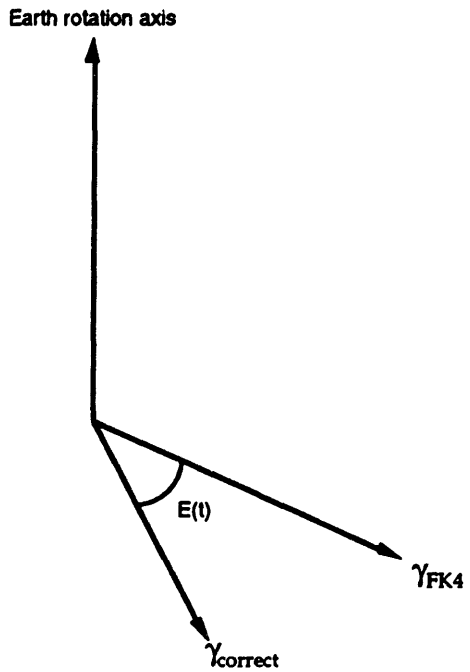

Figure 3.3 FK4 Equinox Offset

$$E(t)_{1950} = 0.^s 035 + 0.^s 085(t - t_{1950})/36524.2198782$$
$$or \qquad (3.21)$$
$$E(t)_{2000} = 0.^s 0775 + 0.^s 085(t - t_{2000})/36525.0$$

where t is the Julian date of the request time, $t1950$ is the Julian date corresponding to B1950.0 (JD2433282.423), $t2000$ is the Julian date corresponding to J2000.0 (JD2451545.0) [36]. Equation (3.21) implies that at B1950.0, the right ascension of every star in the FK4 catalog must be increased

by $0.^{s}035$, while at J2000.0 it must be altered by $0.^{s}0775$ to obtain the equivalent FK5 representation. The motion of the equinox is described by the first-order term, which indicates a $0.^{s}085$ increase every century.

It is important to realize that rotation through this angular offset does not transform satellite coordinates from the FK4 to the FK5 fundamental reference frames. In fact, the FK5 reference frame has experienced precession over the time period separating the two fundamental epochs (around 50 years). Aoki *et al.* present a method for transforming between the FK4 and FK5 systems consistent with the IAU resolutions [1]. A summary of the process includes:

(1) Apply Newcomb precession (based upon FK4 theory) to the FK4 Cartesian coordinates to 1984 January 1, 0^{h}. The precession matrix is constant and given by [58]:

$$\mathbf{P}_1 = \begin{bmatrix} .999965667560 & -.007599409538 & -.003303433841 \\ .007599409535 & .999971123992 & -.000012553023 \\ .003303433846 & -.000012551554 & .999994543569 \end{bmatrix} \qquad (3.22)$$

(2) Apply the right-ascension correction using equation (3.21) at 1984 January 1, 0^{h}. The value for $E(t)$ at this time is $\boldsymbol{0^{s}.0639}$.

(3) Apply precession (based upon FK5 theory) to the Cartesian coordinates from 1984 January 1, 0^{h}, to the fundamental FK5 reference frame. The precession matrix is constant and given by [58]:

$$\mathbf{P}_2 = \begin{bmatrix} .999992390029 & -.003577999042 & -.001554929623 \\ .003577999042 & .999993598937 & -.000002781855 \\ .001554929624 & -.000002781702 & .999998791092 \end{bmatrix} \tag{3.23}$$

This method accounts for the fact that the IAU definitions did not take effect until 1984 January 1, 0^h.

Because this issue deals with two inertial frames at two fundamental epochs, it is possible to represent the transformation from FK4 to FK5 as one constant matrix. The matrix embodies the process described above and is given by [51]:

$$\mathbf{R} = \begin{bmatrix} .9999256794956877 & -.0111814832204662 & -.0048590038153592 \\ .0111814832391717 & .9999374848933135 & -.0000271625947142 \\ .0048590037723143 & -.0000271702937440 & .9999881946023742 \end{bmatrix} \tag{3.24}$$

3.2.2 Solid Earth Tide Theory

As described in section 3.1.1.2, tidal distortion is a perturbation to the earth's geopotential due to gravitational attraction of the sun and moon. Distortion is measured by comparing the expected perturbations due to third body effects with perturbations actually experienced. An approximation of the potential function for tidal distortion is given by:

$$U_3 = -K_l \frac{\mu_3 a_e^5}{|\mathbf{r}_3|^3 |\mathbf{r}|^3} P_2(\hat{\mathbf{r}} \cdot \hat{\mathbf{r}}_3) \tag{3.25}$$

where the subscript 3 refers to the third body (sun or moon), K_l is Love's constant, μ_3 is the universal gravitational constant (G) times the mass of the third body, a_e is the radius of the earth, r_3 is the earth centered inertial

position vector of the third body, r is the ECI position vector of the satellite, and P_2 is the Legendre polynomial [52]. The Love number is determined in a fairly accurate fashion from information provided by geodetic satellite orbits [48].

The acceleration due to these perturbations can be determined by applying the gradient function to these potentials.

$$\mathbf{a}_{t3} = \nabla U_3 = \frac{\partial U_3}{\partial r_x}\hat{x} + \frac{\partial U_3}{\partial r_y}\hat{y} + \frac{\partial U_3}{\partial r_z}\hat{z} \tag{3.26}$$

It should be noted that the argument of the Legendre polynomial P_2 involves the position *unit* vectors, and care must be taken when taking the partial derivatives of the potential functions with respect to the position of the spacecraft (r). The resulting accelerations are given by:

$$\mathbf{a}_{t3} = \frac{K_1 \mu_3 a_e^5 \{[(-15/2)(\hat{\mathbf{r}}\cdot\hat{\mathbf{r}}_3)^2 + (3/2)]\mathbf{r} - 3(\hat{\mathbf{r}}\cdot\hat{\mathbf{r}}_3)\hat{\mathbf{r}}_3\}}{|\mathbf{r}_3|^3 |\mathbf{r}|^5} \tag{3.27}$$

An averaged form of (3.25) is necessary for modeling tidal effects in the semianalytic propagator. It is most convenient to express the orbital parameters in equinoctial form, and reference vectors to the orbital plane. This transforms (3.25) into:

$$U_3 = -\frac{1}{2} K_1 \left(\frac{a_e}{r_3}\right)^3 \left(\frac{a_e}{a}\right)^2 \left(\frac{\mu_3}{a}\right)\left(\frac{a}{r}\right)^3 P_2(\alpha \cos L + \beta \sin L) \tag{3.28}$$

where α and β are the first two components of the third body position with respect to the orbital plane (i.e. $r3 = [\alpha\ \beta\ \gamma]$), and L is the true longitude of the satellite.

Expansion of the Legendre polynomial results in:

$$U_3 = -\frac{1}{2}K_l\left(\frac{a_e}{r_3}\right)^3\left(\frac{a_e}{a}\right)^2\left(\frac{\mu_3}{a}\right)\left(\frac{a}{r}\right)^3\left[\frac{3}{2}(\alpha^2+\beta^2)+\frac{3}{2}(\alpha^2-\beta^2)\cos 2L+3\alpha\beta\sin 2L-1\right] \tag{3.29}$$

Using the averaging techniques presented in 2.3.3.4 and results in [11], the averaged potential function is represented by:

$$\overline{U}_3 = -\frac{1}{2}K_l\left(\frac{a_e}{r_3}\right)^3\left(\frac{a_e}{a}\right)^2\left(\frac{\mu_3}{a}\right)\left(\frac{a}{r}\right)^3 x^3\left[\frac{3}{2}(\alpha^2+\beta^2)-1\right] \tag{3.30}$$

where

$$x = \left(1-h^2-k^2\right)^{-\frac{1}{2}} \tag{3.31}$$

The partial derivatives are then given by:

$$\begin{aligned}
\frac{\partial\overline{U}_3}{\partial\lambda} &= 0 \\
\frac{\partial\overline{U}_3}{\partial a} &= -\frac{3}{a}\overline{U}_3 \\
\frac{\partial\overline{U}_3}{\partial h} &= 3hx^2\overline{U}_3 \\
\frac{\partial\overline{U}_3}{\partial k} &= 3kx^2\overline{U}_3 \\
\frac{\partial\overline{U}_3}{\partial\alpha} &= \frac{1}{2}K_l\left(\frac{a_e}{r_3}\right)^3\left(\frac{a_e}{a}\right)^2\left(\frac{\mu_3}{a}\right)(3\alpha)x^3 \\
\frac{\partial\overline{U}_3}{\partial\beta} &= \frac{1}{2}K_l\left(\frac{a_e}{r_3}\right)^3\left(\frac{a_e}{a}\right)^2\left(\frac{\mu_3}{a}\right)(3\beta)x^3
\end{aligned} \tag{3.32}$$

3.2.3 Instantaneous True of Date

The instantaneous true of date coordinate system is derived from the fundamental reference frame in the manner presented in section 2.4.2. It differs from the inertial true of reference coordinate system in the evaluation of the precession and nutation effects. Using the same notation as in 2.4.2, the relationship between the ITOD and fundamental coordinate systems is given by:

$$\mathbf{x}_{itod} = \left[\mathbf{N}(\Delta\varphi, \Delta\varepsilon)\mathbf{P}(z_a, \theta_a, \zeta_a)\right]_{t=current} \mathbf{x}_{1950/2000} \tag{3.33}$$

This relationship is based upon precession and nutation quantities that are representative of the current time. The inertial true of reference coordinate system, on the other hand, is dependent upon evaluation at some arbitrary reference time (usually midnight of the current day).

$$\mathbf{x}_{tor} = \left[\mathbf{N}(\Delta\varphi, \Delta\varepsilon)\mathbf{P}(z_a, \theta_a, \zeta_a)\right]_{t=t_{ref}} \mathbf{x}_{1950/2000} \tag{3.34}$$

3.3 Design Considerations

The software modifications made for this work were designed to accommodate the three capabilities discussed in sections 3.1 and 3.2. Development of a design that would meet identified functional requirements in an efficient and flexible manner was the primary objective. The functional requirements and key software considerations are addressed below.

3.3.1 Functional Requirements

It is important to clearly identify the objectives prior to inception of any effort, particularly a complicated project. Software development for this project was no exception. The requirements can naturally be categorized into the three capabilities identified in section 3.1. However, before looking at each of these capabilities individually, it is necessary to understand the existing baseline used for development.

3.3.1.1 Existing Software

3.3.1.1.1 Recent R&D GTDS Developments

The baseline version of Draper R&D GTDS that this effort stems from is a combination of several libraries of code. Draper R&D GTDS was introduced to the VAX VMS operating system in 1991 to support the LANDSAT 6 mission [20]. A virtual replica of the 1989 version existing on Draper's IBM MVS mainframe system, this VAX VMS LANDSAT 6 version of Draper R&D GTDS is the ultimate source for all code used in this project [12].

The LANDSAT 6 code was used as a baseline for two major software development projects applicable to this work. Fonte developed a library of modules that supports a 50x50 gravity field modeling capability in 1992-3 [20]. In 1993-4, the LANDSAT 6 version was upgraded for support of the RADARSAT mission launched in November 1995. Fonte's 50x50 modules, however, were not included in the RADARSAT version of the code.

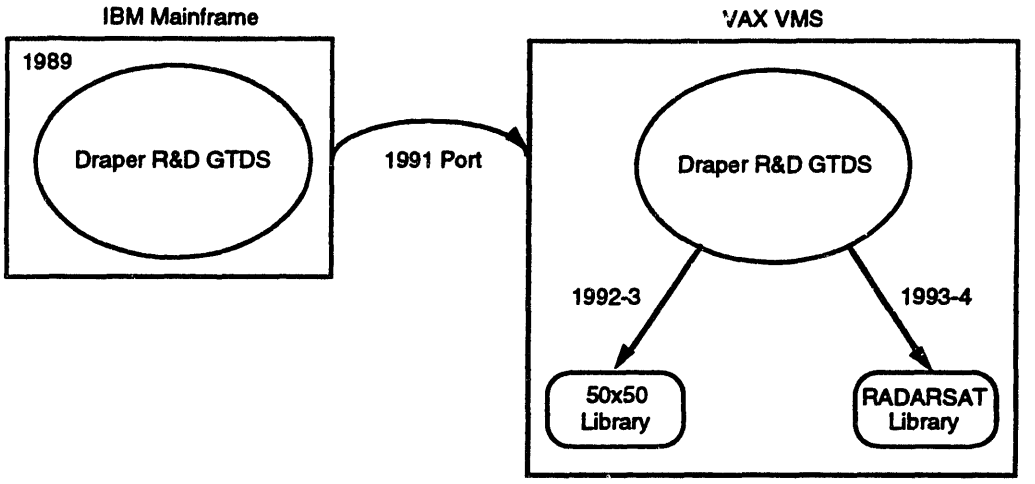

Figure 3.4 Evolution of Draper R&D GTDS Code

One other library of modules was significant for this work. The capability to accept an ECEF representation of the initial state was developed in the PC/DOS version and transported to the VAX VMS environment in 1994. A summary of the changes made to support an ECEF input capability is found in Appendix B.

3.3.1.1.2 Development of Fundamental Source Code for This Work

The most fundamental decision made for this project was determination of the source code for development of the new capabilities. In addition to the VAX VMS version previously discussed, there were also competing versions of Draper R&D GTDS on UNIX workstations (SUN and SGI) and an IBM PC* [21]. The SUN and PC versions each offered a semianalytic short-periodic generator input processor that would facilitate the user in defining options

---

* Draper R&D GTDS was ported to the IBM PC at the U.S. Air Force's Phillips Laboratory with support from Draper Laboratory.

associated with construction of the short periodics. Accurate representation of the short periodics is essential for the development of precision mean elements, and the input processor simplifies the user interface with the software. However, the VAX was the only platform that contained a library of fully tested modules that support 50x50 gravity field modeling.

Ultimately, the VAX was chosen as the platform for software development for a couple of reasons. The 50x50 gravity field modeling was thought to be required in order to show any value associated to incorporating the J2000-based coordinate systems. The improvements expected from inclusion of FK5 would be masked by accuracy degradation caused by lack of 50x50 modeling if the other platforms were chosen. Also, the VAX offered a simple, reliable environment in which to develop software associated with the new capabilities. The link maps, in particular, facilitate the process of identifying modules that were prime for modification due to these new capabilities. However, this would mean that the short periodic input processor would not be available. A separate method for identifying options associated with the short periodics generation process is summarized in Appendix E.

The RADARSAT version of the code was targeted as the baseline source for software development because of its upgrades from the LANDSAT 6 version. However, this necessitated incorporation of the 50x50 modules to ensure sufficient accuracy in the gravity field modeling. Three routines (highlighted in Table 3.4) were identified as having been altered in both the 50x50 and RADARSAT tracks. Changes in each path were identified by differencing the 50x50 and RADARSAT code from the LANDSAT 6 code. A new generation of each of these three routines was created to encompass all changes that had

occurred from the original LANDSAT 6 code. In doing this, both the 50x50 and RADARSAT functionalities were preserved. Finally, the routines required to support the ECEF input coordinate system capability were included.

Table 3.4 Routines Modified in RADARSAT and 50x50 Upgrades

Routine Name	RADARSAT Modification	50x50 Modification
SETOG1	Included ACP Density Model	Included HRMCF, CSBLNK, LUMPCS common blocks; removed STAGE0 common block; included NEWPOT file pointer in FILES; generalized geopotential variables
ELEMGN	Included S-Band Triplet Types	Included HRMCF common block
NUKESBD	Increased number of Newcomb operators to 66538	Increased number of Newcomb operators to 52962

3.3.1.1.3 Coordinate System Functionality in Existing Draper R&D GTDS

It is important to understand the baseline status of the issues being discussed in this section. Since a working version of solid earth tides was not present in any of these versions, this involves only the various coordinate systems present at the onset of the development process. A summary of coordinate system options for various purposes is contained in Table 3.5. A more complete description is found in the card descriptions in Appendix D.

One particular item of note involves the OBSINPUT card, which describes the observations being used in a DC or Filter execution of Draper R&D GTDS.

Table 3.5 Coordinate System Options Prior to Software Development

Option	Input (ELEMENT1)	Integration (ORBTYPE)	Output (OUTPUT)	Observations (OBSINPUT)
1	Mean Equator and Equinox of 1950.0	Mean Equator and Equinox of 1950.0	Mean Equator and Equinox of 1950.0	Mean Equator and Equinox of 1950.0
2	True Equator and Equinox of Reference	True Equator and Equinox of Reference	True Equator and Equinox of Reference	True Equator and Equinox of Reference
3	True Equator and Equinox of Reference		Body-Fixed	Body-Fixed
4	Mean Ecliptic and Equinox of 1950.0		Mean Ecliptic and Equinox of 1950.0	
5	True Ecliptic and Equinox of Reference		True Ecliptic and Equinox of Reference	
6				NORAD True of Date
8	NORAD True of Reference	NORAD True of Reference	NORAD True of Reference	NORAD True of Reference

The information within the integer and real fields does not explicitly include the coordinate system of the observations. Instead, the coordinate system is implicit to the specific observation type number specified in the first integer field. Most types have an associated coordinate system that is implied. However, for the Precise Conversion of Elements (PCE) observation type (which Draper R&D GTDS includes as Cartesian positions and velocities), the

coordinate system is a distinguishing feature of the observation type number. For instance, with PCE card input, there are currently eight individual options differentiated only by the coordinate system of the information. The observation type is read from the OBSPCE card, and a parameter internal to Draper R&D GTDS is set that reflects the implied coordinate system associated with that observation type number.

For the VAX VMS baseline version, the user was required to input the PCE observation coordinate system by an external command file used in conjunction with the debugger rather than the more conventional card inputs.

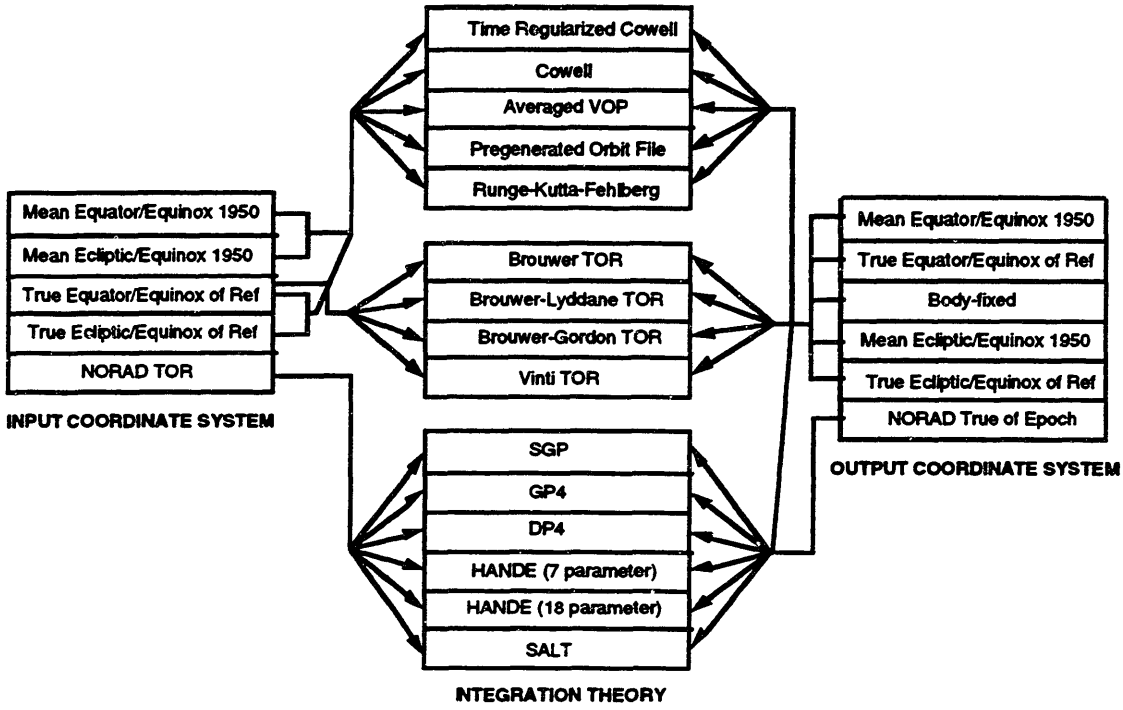

Figure 3.5 Baseline Coordinate System Options

While Table 3.5 identifies the various options available to the user in the baseline version, certain limitations existed on the compatibility of coordinate

systems and orbit generation theories. For example, the analytic theories are inherently designed to use true equator and equinox of reference coordinate system information. Figure 3.5 reflects the actual coordinate system options available to the user in the baseline version.

It should be noted that the integration coordinate systems associated with the numerical integration theories (time regularized Cowell, Cowell, averaged Variation of Parameters, pregenerated ORBIT file, and Runge-Kutta-Fehlberg) can be either mean equator and equinox of 1950.0 or true equator and equinox of a reference date, while the NORAD theories use only the NORAD reference frame as the integration coordinate system.

3.3.1.2 Coordinate System Considerations

The main thrust of the software development process involved incorporation of new coordinate system functionalities, to include the J2000-based and instantaneous true of date capabilities. While it was clear that their development was desirable, there was much discussion over what requirements would be associated with the capabilities.

The most fundamental question addressed involved the final status of the existing FK4-based coordinate systems within Draper R&D GTDS. The options considered were:

(1) Supplementing the existing FK4-based coordinate systems with the more modern FK5-based coordinate systems by adding new functional paths within Draper R&D GTDS.

(2) Supplementing the existing FK4-based coordinate systems with the more modern FK5-based coordinate systems *without* altering the internal operation of a large portion of Draper R&D GTDS.

(3) Replacing the FK4 structure within Draper R&D GTDS with an analogous FK5 system.

Option (1) would achieve the goal of providing the J2000-based coordinate systems without disrupting an existing and proven software package. However, it would also involve creating a new, separate path for the new coordinate system functionalities.

Option (3) offers the advantage of having a structure already in place. Incorporation would simply involve finding references to the FK4 based systems and replacing them with references to the new FK5 system. This option, however, would eliminate the opportunity to test benchmark cases developed for the RADARSAT and LANDSAT versions, based upon FK4 theory.

Option (2) is quite a bit more abstract than the other two alternatives and calls for a more detailed discussion. As section 2.4 indicates, Draper R&D GTDS typically uses coordinate system information in several manners. These include: input processing, parameter initialization, program execution, and post-processing/output. Of these, the input processing and post-processing/output steps require absolute knowledge of coordinate systems. Because each of the new FK5-based coordinate systems has an analog in the

FK4 system (e.g., mean equator and equinox of 1950.0, mean equator and equinox of 2000.0), it is conceivable to limit execution to either the FK4 or FK5 system within the parameter initialization and program execution phases. These steps require information only concerning the relative orientation (whether it is mean of date or instantaneous true of date, referenced to the equator or ecliptic, inertial or body-fixed) and *not* the fundamental epoch of the system being used. By generalizing the meaning of coordinate system variables within the parameter initialization and program execution (which are computationally and time intensive), it would be possible to limit the overall number of software modifications required.

The input processing phase would initially provide absolute knowledge of the coordinate systems to be used throughout execution. This information would be stored in a location not visible to routines during the parameter initialization and program execution phases. It would also be stored in the normal coordinate system locations that the initialization and execution code accesses - common blocks SATPOS (input coordinate system), FRC (integration coordinate system), SECTN (output coordinate system), ESTFLG (observations coordinate system), and SATMAN (maneuver coordinate system). However, before being stored in these normal locations, the information would be generalized in a manner shown in Table 3.6.

Thus, if the user-defined coordinate system options were,

input -- mean equator and equinox of 1950.0
integration -- mean equator and equinox of J2000.0
output -- true equator and equinox of reference (FK5-based)

Table 3.6 Generalized Coordinate System Descriptions

Absolute Coordinate System	Generalized Coordinate System
1 - Mean equator/equinox of 1950.0 11 - Mean equator/equinox of 2000.0	1 - Mean equator/equinox
2 - True equator/equinox of Reference (based on FK4 theory) 12 - True equator/equinox of Reference (based on FK5 theory)	2 - True equator/equinox of Reference
4 - Mean ecliptic/equinox of 1950.0 14 - Mean ecliptic/equinox of 2000.0	4 - Mean ecliptic/equinox
5 - True ecliptic/equinox of Reference (based on FK4 theory) 15 - True ecliptic/equinox of Reference (based on FK5 theory)	5 - True ecliptic/equinox of Reference

the options would be stored in the new common block with values of [1,11,12], while the normal locations would contain [1,1,2]. When absolute knowledge of the coordinate systems is required (i.e. the output phase for labeling, etc.), the code would reference the new common block; otherwise, it would reference the normal locations.

Because it was deemed desirable to maintain the capability of reproducing benchmark cases, option (3) was discarded. Options (1) and (2) were studied in depth to identify specific code-related advantages and disadvantages of each. Using option (1), 101 total routines were identified for modification; for option (2), this total dropped to 82 routines. Of the 101 routines identified in option (1), 31 were routines that would not have to be altered if the second

approach were taken. Conversely, of the 82 routines identified in option (2), 12 were unique.

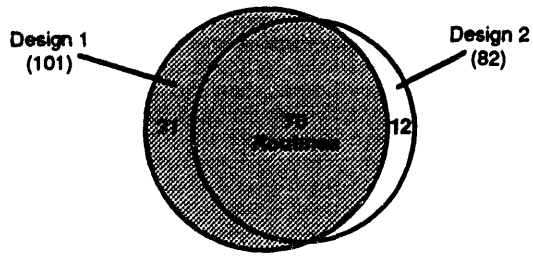

Figure 3.6 Modifications for Options (1) and (2)

It should be noted that these modifications are comprehensive - that is, they include not only the coordinate system issues, but solid earth tides as well.

The driving factor in design choice was the ease with which Draper R&D GTDS users other than the author could understand the modifications made to support this project. Had the number of routines been the only factor considered, clearly the second design would have been more appealing. However, the complexity associated with this design far exceeded that of the first option. In particular, multiple definitions of various coordinate systems would be a tremendous source of confusion for individuals unfamiliar with the design procedures. Therefore, the first design was deemed appropriate for implementing the J2000-based coordinate systems, solid earth tides, and instantaneous true of date output capabilities.

The next major decision involved which programs to include the new coordinate system options for. The factors driving these modifications (i.e., the issues associated with GPSR navigation solutions and POEs) are all related to the orbit generators, differential correction, ephemeris comparison and

possibly the filtering processes within Draper R&D GTDS. While testing of these modifications focuses on these applications, an effort was made to implement the FK5 coordinate system functionality for all programs. Likewise, the instantaneous true of date output capability was included in all applicable programs.

Another important fundamental issue that arose involved the interaction between the FK4 and FK5 coordinate systems. Although it is desirable to have the option of transforming from any one coordinate system to another, it is not realistic because of the current structure of Draper R&D GTDS. The limiting factor involves the manner in which the SLP files are accessed and utilized. Currently, it is possible to access only one set (which consists of one mean equator and equinox of fundamental epoch and one true of date representation of the polynomials) of SLP files at a time. This means that the coordinate system transformations can only be described in one fundamental reference frame at a time, that of the integration reference frame. This limitation prohibits those cases where:

1) the input, output, maneuvers, or observations reference frame is a true of reference or ecliptic coordinate system based upon the FK4 system and the integration coordinate system is FK5 based

or

2) the input, output, maneuvers, or observations reference frame is a true of reference or ecliptic coordinate system based upon the FK5 system and the integration coordinate system is FK4 based.

The cases involving input, output, maneuvers or observations in a mean equator and equinox of fundamental epoch frame remain possible because of the constant transformation matrix between the fundamental FK4 and FK5 systems (see equation 3.24).

It should be noted that the analytic formulae presented in section 3.2.1.4 could be used to circumvent these limitations. Likewise, analytic formulae exist for the equator/ecliptic transformations and could be used. While these methods do not currently reside within Draper R&D GTDS, it very well could be worth the effort to include them in the future to allow for arbitrary input/output options.

An issue related to FK4-FK5 compatibility involves the NORAD coordinate frames. The NORAD frames within Draper R&D GTDS are mean equinox and true equator of date. The mean of date coordinate system is derived by applying precession to the fundamental reference frame as discussed in section 3.2.1.4. However, NORAD nutation transforms from *mean* equator and equinox of date to *mean* equinox and *true* equator of date, as opposed to the *true* equator and equinox of date presented in section 3.2.1.4 [45]. Because the NORAD nutation matrix is developed within Draper R&D GTDS via analytic expressions inherently based upon FK4 theory, it was deemed appropriate to treat the NORAD cases in a manner similar to the FK4 instantaneous true of date systems. Currently, only transformation to and from the NORAD and mean equator and equinox of J2000 coordinate systems is allowed.

As indicated in section 3.1.1.3, the need for a instantaneous true of date capability stems from comparing results to and fitting the POEs. These requirements impact the observation modeling and output functionalities within Draper R&D GTDS. Because the input and integration options did not require instantaneous true of date compatibility, these areas were not addressed.

3.3.1.3 Software Design Considerations

In addition to the questions addressed in the previous section, there were several considerations evaluated from a software standpoint. These included input processing options, coordinate system transformation procedures, solid earth tide modeling structure, and definition of fundamental reference frame-dependent quantities.

Draper R&D GTDS interprets the desires of its users through an input card data file that describes the intended setup of the program. Within this card deck, the user defines the type of program to be run, the necessary information associated with that type of run, and various files and reports containing the desired information that can be generated from the run. Each card contains a keyword, three columns reserved for integer fields, and three columns reserved for real fields. The integer and real fields are numerical values or switches associated with various options as described by the keywords.

Coordinate system options are found in eight different operational cards: ELEMENT1, IMPULSE, OBSINPUT, ORBTYPE, OUTCOORD, OUTOPT,

OUTPUT, and SLPCOORD*. A full description of these cards and the modifications made to support these new coordinate systems is found in Appendix D.

(1) The ELEMENT1 card describes the first three components of the initial state vector at an epoch time. It is a mandatory card used in the ephemeris generation, differential correction, and filter programs in Draper R&D GTDS. The integer fields of the ELEMENT1 card describe the coordinate system orientation, coordinate system type and reference central body associated with this state vector [54].

(2) The IMPULSE card sets impulsive maneuver velocity increments. It is an optional card found in the ephemeris generation, differential correction, and filter programs in Draper R&D GTDS. The integer fields of the IMPULSE card describe the maneuver number, coordinate system reference for that maneuver number, and type of maneuver to be performed [54].

(3) The OBSINPUT card is a mandatory card that specifies the input source of the observations being used in the differential correction, filter or early orbit programs. The integer fields of the OBSINPUT card are defined from the options available for observation sources. Options have been included that

---

* OUTCOORD and SLPCOORD are not used extensively at Draper Laboratories.

differentiate the Precise Conversion of Elements (PCE) observation type by coordinate system, as well as source [54].

(4) The ORBTYPE card is a mandatory card that defines the orbit generator type and its associated parameters for the ephemeris generation, differential correction, and filter programs. For numerical and NORAD theories, the third integer field specifies the coordinate system to be used in the integration process [54]. The analytic theories assume an integration coordinate system of true equator and equinox of a reference time.

(5) The OUTCOORD card is an optional card that defines the output coordinate system orientation by section number. The integer fields describe the flight section number, with the corresponding real fields reflecting the coordinate system orientation [54].

(6) The OUTOPT card is an optional card that describes the selection of the ephemeris output to a file. Information from an ephemeris generation, differential correction or filter run can be directed to an ORBIT, ORB1, or EPHEM file. Generation of EPHEM files requires the coordinate frame indicator as part of the input [54].

(7) The OUTPUT card is a mandatory card that specifies the orbit generator output reports for the ephemeris generation program. The first integer field defines the coordinate system option for

the output reports [54].

(8) The SLPCOORD card is an optional card that describes the coordinate system associated with the SLP files in the ephemeris generation, differential correction, filter, data management, error analysis, and data simulation programs. These files are used to describe planetary locations and coordinate system transformations [54].

The coordinate system options associated with each of these cards (with the exception of the OBSINPUT card, which is discussed later) were augmented with J2000 and instantaneous true of date options. Many integer options were available for describing these new capabilities. The prime motivation in the choice of integers was to make it easy for the user to understand and remember these options when perusing software. The design was based upon a certain symmetry between the FK4 and FK5 systems, and is summarized in Table 3.7. The boldfaced items are products of this project.

Table 3.7 Coordinate System Options for J2000 and True of Date Capabilities

FK4 Option	FK5 Option	Meaning
1	**11**	Mean Equator and Equinox of 1950/2000
2	**12**	True Equator and Equinox of Reference
3	3	Body-Fixed (Output only)
4	**14**	Mean Ecliptic and Equinox of 1950/2000
5	**15**	True Ecliptic and Equinox of Reference
6	--	NORAD True of Date
8	--	NORAD True of Epoch
9	**19**	True Equator and Equinox of Date
10	10	Body-fixed (Input only)

Comparing FK5 options with their FK4 analog, it is clear that the difference between the two integers is ten (e.g. mean equator and equinox of 2000.0 - mean equator and equinox of 1950.0 = 11-1 = 10). The remaining coordinate system options are not specific to a fundamental reference system.

These options are not applicable to every card. SLPCOORD and ORBTYPE possess only mean equator and equinox of fundamental epoch and true equator and equinox of reference options. Setting the SLP coordinate system orientation requires the use of a 3 (for mean equator and equinox of J2000.0) or 4 (for true equator and equinox of reference) for FK5 systems. FK4 options remain unchanged. Deviation from the standard numbering convention is a result of the existing FK5-based SLP files. The Testing, Reporting, and Maintenance Program (TRAMP), which creates the SLP files from a JPL tape, defines the FK5 coordinate system options as 3 and 4. To maintain the existing coordinate system structure for the SLP files as defined by TRAMP, the FK5 SLP coordinate system options were defined as 3 and 4. Because Draper R&D GTDS internally checks the integration coordinate system against this SLP coordinate system, it seemed logical to define the options on the ORBTYPE card in a similar fashion. The alternative was to define these options according to the standard approach given in Table 3.7 (only for mean equator/equinox of 2000.0 and true equator/equinox of reference). Comparison of the number of routines requiring modification in each approach identified the standard numbering procedure as the most appropriate choice (11 routines needed modification using the 3/4 convention, while only 3 were identified for the 11/12 approach).

The OBSINPUT card options differ dramatically from the standard system highlighted in Table 3.7. For non-PCE observation types, the coordinate system is assumed and not part of the OBSINPUT structure. Prior to this work, the PCE coordinate system and source (either GTDS ORB1 file or observation card) had to be deposited in subroutine ESTSET via an external command procedure, a less than desirable method. Cefola introduced a method of differentiating the coordinate systems and sources in the UNIX version of Draper R&D GTDS by coupling them with the PCE observation type [13]. The OBSINPUT card description in Appendix D reveals the choices developed for the VAX version. The choices parallel those made by Cefola in the UNIX version and will facilitate future porting efforts.

While the coordinate system input processing procedures required augmentation of the FK5 options, no input processing methods existed for solid earth tide modeling prior to this work. Therefore, it was necessary to introduce a new card, SETIDE, to relate user-defined parameters related to solid earth tide modeling. The structure of this card was modeled after that of other perturbation cards, such as DRAG. One distinguishing feature, however, is that SETIDE does not support a sectioning functionality (that is, it will either be on or off for the entire program execution). This decision was based upon the lack of a clear understanding of the sectioning capabilities within the current version of Draper R&D GTDS.

The procedures used in Draper R&D GTDS to transform from one coordinate system to another can be categorized into two groups. One method utilizes a combination of two routines, ROTKEY and ROTRAN, specifically designed to perform this function. ROTKEY takes coordinate system and central body

information for the input and output vectors and converts it into a set of "keys" that ROTRAN recognizes. ROTRAN then decodes these keys and performs the translations and transformations at the requested time using information acquired from the SLP files. The second method performs the same functionality as does the ROTKEY/ROTRAN combination, but bypasses these routines and uses the information from the SLP files directly. A call to subroutine EVAL usually accompanies this method in order to evaluate the SLP information at the desired time. Examples of each of these methods are given in Figure 3.7.

```
      SUBROUTINE  OBSPCE  (MSGERR,*)
...
...
      CALL  ROTKEY  (KEYS,  ICENT,I1950,  ICENT,IPCECS)
      CALL  ROTRAN  (XVIN,KEYS,  XVOUT,  TTO)


**************************************************************
**************************************************************
      SUBROUTINE ACCEL(Y,YD,TE)
...
...
      T=TE
...
...
      CALL EVAL(T, IND(14), IND(15), IND(16), IND(17), IND(18),
                NBOPT, XB)
...
...
      IF ((I50 .NE. 1) .AND. (I50 .NE. 11))  GO TO 60
      CALL MA3331(C,X,POS)
      GO TO 70
```

Figure 3.7 Coordinate System Transformation Methods

The first method is highlighted in subroutine OBSPCE, which computes PCE observables. In this example, a call to ROTKEY is made in order to encode the coordinate system (I1950, IPCECS) and central body (ICENT) information into KEYS. ROTRAN then rotates the input Cartesian position and velocity vector (XVIN) from the integration coordinate system (I1950) to the

observation coordinate system (IPCECS) to produce the output vector (XVOUT) at time TTO. A total of 14 routines employ this method.

The second method is shown in a segment extracted from subroutine ACCEL. This routine evaluates the two-body and perturbative accelerations at a given time (TE) based upon the position (Y) and velocity (YD) of the spacecraft. Initially, a call to EVAL is made to evaluate the coordinate system transformation information at time TE. Then, if the initial coordinate system (the integration coordinate system, I50) is mean equator and equinox of a fundamental epoch, the position vector (X) is rotated to the true equator and equinox reference frame by multiplying by the transformation matrix (C) to produce the instantaneous true of date vector (POS) for force evaluation. A total of 20 routines employ this method.

Two design options were available that would include the FK5 based coordinate systems in the transformation process for the ROTKEY/ROTRAN method. The most basic approach would be to expand the range of the "keys" in ROTKEY to include the FK5 based options, ensuring that the representations for the FK4 and FK5 systems were different. The functionalities for the FK5 system within ROTRAN would then be a mirror image for those transformations that have analogs in the FK4 system. Additional options for rotating between the FK4 and FK5 systems would then be added to ROTRAN.

A second, more practical method takes advantage of the symmetry between the FK4 and FK5 options defined in the functional requirements. With this method, the "keys" set in ROTKEY are given the same values for the FK5

system as they were for their analogs in the FK4 system. Thus, an input coordinate system of a mean equator and equinox of 1950.0 retains the same key value as that of a mean equator and equinox of 2000.0 option (1). This approach, in effect, masks the true identity of the transformation from ROTRAN; hence, there is no need to alter ROTRAN for these purposes.

This alternate ROTKEY/ROTRAN method is based upon the premise that the transformation process does not involve FK4-FK5 interaction. To account for these cases, a wrapper routine (CSTRANS) transforms a vector from the input fundamental reference frame to the output fundamental reference frame prior to the ROTKEY/ROTRAN calls. To account for those transformations that currently are not allowed (e.g., FK4-based true equator and equinox of reference input with FK5-based integration), a separate routine (CSERROR) was developed to relay error messages. A driver routine (CSMIX) guides this logic for applicable circumstances.

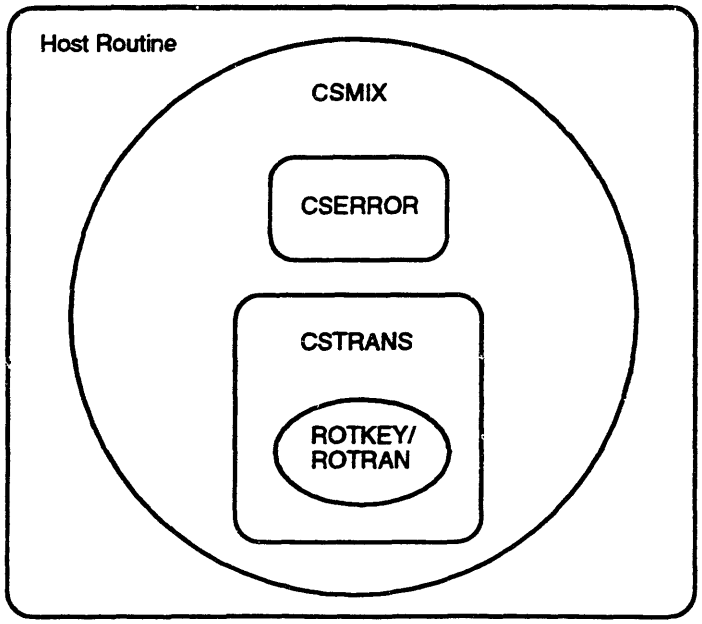

Figure 3.8 New ROTRAN/ROTKEY Logic

While ROTRAN was not modified to support FK5 coordinate system options, it did require changes to support implementation of the instantaneous true of date capabilities. True of date options mirrored true of reference cases where applicable by replacing the transformation matrix from mean of fundamental epoch to true of reference (CREF) with the transformation matrix from mean of fundamental epoch to instantaneous true of date (C). The information describing the fundamental reference frame (FK4-FK5), however, was still masked from ROTRAN in a manner consistent with that illustrated in Figure 3.8.

The solid earth tide modeling structure was implemented in a fashion not unlike that of other perturbative forces (drag, solar radiation pressure, third-body, etc.). Figure 3.9 shows the functionality associated with numerical perturbative force modeling and where solid earth tides were employed.

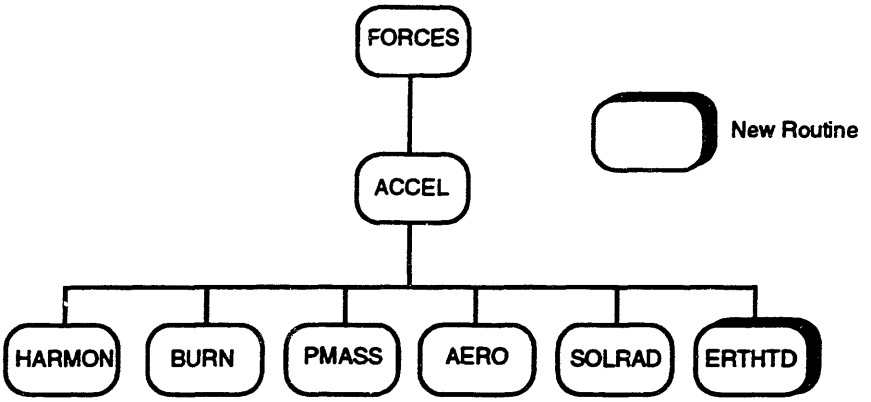

Figure 3.9 Perturbative Force Evaluation Structure

The solid earth tide software was based upon *CELEST* mathematical models and adapted from a routine provided by Hujsak [52]. As previously indicated, solid earth tide modeling is either on or off for the entire run (as opposed to

supporting a modeling by section capability). For numerical integration schemes, solid earth tides are decoupled from third-body lunar/solar perturbations, enabling the user to model with either a combination of third body and tides, one or the other, or neither. For semianalytic theory, solid earth tides can only be included if third-body perturbations are included. Routines PTIDE and TSUM, modeling the averaged tidal effects for the semianalytic propagator, previously existed, but required correction of a sign error for proper implementation. The user has four tidal modeling options that are summarized in Table 3.8 and Appendix D.

Table 3.8 Available Solid Earth Tide Modeling Options

Option	Meaning
1	Consider both lunar and solar tidal effects
2	Consider only solar tidal effects
3	Consider only lunar tidal effects
4	Consider neither lunar or solar tidal effects

The final design consideration involved the various parameters listed in section 3.2.1 that are dependent upon the fundamental reference frame being used. Three approaches that would provide this information were considered:

(1) Place the information in common blocks for either the FK4 or FK5 system, as it currently exists.

(2) Place the information for both the FK4 and FK5 systems in one

external file that will be accessed at a high level during program execution.

(3) Place the information in two separate files (one each for FK4 and FK5 values) and access the appropriate file during program execution.

Option (1) was immediately discarded because of the tedious process involved in switching between FK4 and FK5 systems. Changing systems would require (1) editing the appropriate block data, (2) compiling the modified software, (3) relinking the remaining code with the new objects, and (4) program execution.

Option (2) seemed the most desirable because it provides information for both the FK4 and FK5 system from one file, regardless of which system was being used for program execution. Limiting execution to one set of SLP files, however, resulted in half of this information became extraneous.

Therefore, the decision was made to access the fundamental constants from one external file representative of the fundamental frame being used in program execution. This places the burden of responsibility upon the user to ensure that the astrodynamic constants file and SLP files are compatible.

A couple of options were considered for the location at which this external constants file is read. Because it was necessary information for all programs, it could be read in at the highest level (within ODSEXEC) before any other

tasks were performed. However, it might be desirable to have Draper R&D GTDS perform an internal consistency check on the constants/SLP files.

In this case, it is most convenient to wait until the SLP file information is obtained to avoid having to pass information accessed in ODSEXEC to wherever the SLP file information is retrieved. For most applications, the SLP coordinate system is first revealed within routine SETRUN when the ORBTYPE card is read (by default, the integration coordinate system must be compatible with the SLP coordinate system).

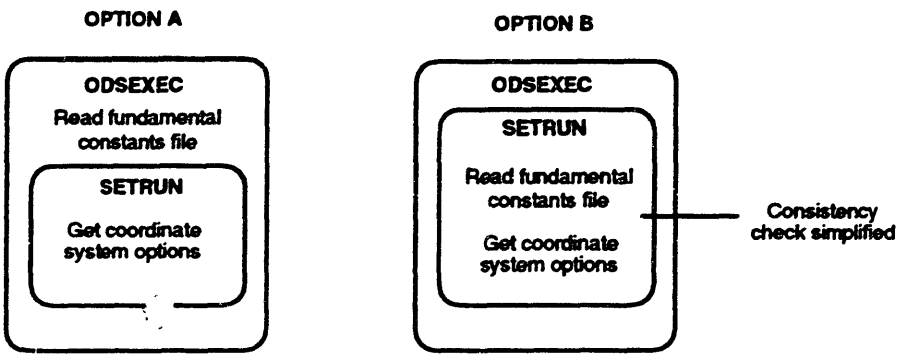

Figure 3.10 Fundamental Constants File Retrieval Options

It should also be noted that the constant values *must* be accessed prior to the processing of optional subdecks because of the need to evaluate certain parameters in some applications. Therefore, it is logical to retrieve information from the constants file after the mandatory card processing, but before the optional card processing.

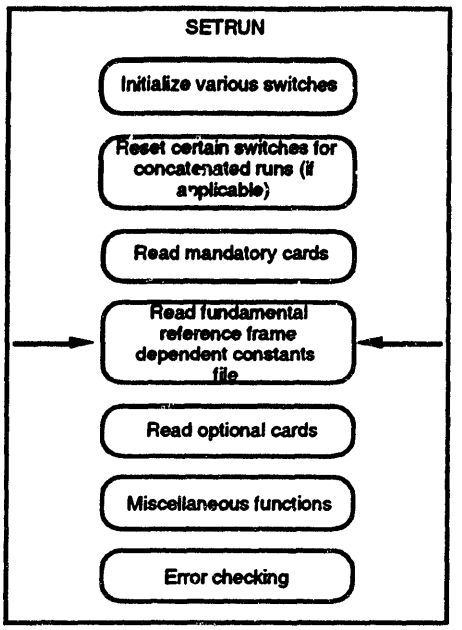

Figure 3.11 Fundamental Constants File Retrieval

Based upon this location for fundamental constants retrieval, the various values within the file are default values. However, because they are read prior to any optional card processing, it is still possible to override their values with the appropriate cards.

New software developed for this functionality includes GET_CSCONS, which retrieves the information from the constants file, and CSCONST, a block data that stores various coefficients from this file. The FK4 and FK5 constant files are called B1950_CSCONST.DAT and J2000_CSCONST.DAT, respectively. Appendix F contains a description of the information contained on these files.

3.4 Summary of Software Modifications

The software modifications required to support the new capabilities involved modifying 90 existing routines and creating 11 new modules. A total of 5527 lines of code were required to make these modifications (3887 lines modified or added to the existing software, and 1640 lines for creation of the 11 new routines). These modifications can be broken into several functional categories, including: input processing, parameter initialization, program execution, and post-processing/output. This section provides examples of the more common forms of modification and an overall summary of the actual modifications made to support the coordinate system and solid earth tide functionalities.

3.4.1 Input Processing Modifications

Thirteen routines were identified for modification at the input processing level, and can be divided into four categories. The routines contain modifications that:

(1) Set a default value for either the input or SLP file coordinate system.

(2) Include logic for the new FK5 coordinate systems mirroring that of the FK4 analogs.

(3) Provide support for the new capabilities through addition of new software.

(4) Alter the ranges of valid values to reflect compatibility with the new coordinate system options.

3.4.1.1 Setting a Default Value

Draper R&D GTDS uses default values either to reflect limitations on a particular functionality, to initialize a parameter with the option of changing that parameter, or to ensure compatibility between the SLP and integration coordinate systems.

Default values reflecting an inherent limitation take the form of a simple assignment statement. The coordinate system is assigned a fixed value based upon the particular application of Draper R&D GTDS being used. An example is found in routine DODSEL, where DODS elements are read from a DODS element data base. These elements are restricted to a true equator and equinox of reference coordinate system and cannot be changed elsewhere (via card, etc.). In order to distinguish between the FK4 and FK5 systems for these instances, logic was implemented that defines the input coordinate system (ICORD) to be compatible with the fundamental frame associated with the integration coordinate system (I50). This assumption limits the user to operating within one system (either FK4 or FK5) for these applications. Because it is desirable to maintain a certain amount of flexibility, the frequency of these occurrences is quite small.

```
      SUBROUTINE  DODSEL  (MSGERR,*,* )
...
...
      IF ((I50 .GT. 10) THEN
         ICORD = 12
      ELSE
         ICORD = 2
      ENDIF
```

Figure 3.12 Default Value Defining Inherent Limitation

Certain applications provide a default value for a coordinate system option, but provide the user with the opportunity to change that value. An example is found in SETOG1 where the coordinate system associated with a generated EPHEM file is defined. Draper R&D GTDS initially assumes a coordinate system of true equator and equinox of reference. However, the user has the option of defining the coordinate system of this file by indicating so on the OUTOPT card (see Appendix D for available options). Should the user either choose not to or fail to indicate the appropriate coordinate system information, the default value is used. Because the default value is a coordinate system based upon an equator and equinox that is true of reference, a method of distinguishing between FK4 and FK5 systems is necessary. As was the case for the invariable default values, the criteria for setting the default value was the integration coordinate system.

```
      SUBROUTINE  SETOG1  (IJK,IIII,*,* )
...
...
      IF ((I50 .EQ. 11) .OR. (I50 .EQ. 12)) THEN
         NREF = 12
      ELSE
         NREF = 2
      ENDIF
...
...
      IF (I1.EQ.3 .AND. I3.GT.0) NREF=I3
```

Figure 3.13 Default Value Overridden By User

The above figure is an excerpt from SETOG1 describing the processing of the OUTOPT card. The integration coordinate system (I50) is used to initially set the default value of the EPHEM file coordinate system (NREF) to either FK4-based (NREF=2) or FK5-based (NREF=12) true equator and equinox of reference. Should the user's desires dictate another coordinate system for the EPHEM file (I1.EQ.3 .AND. I3.GT.0), the value is then modified accordingly (NREF=I3).

The final manner in which Draper R&D GTDS sets default values based upon input information involves the SLP files. Two sets of SLP files exist for each fundamental reference frame - a mean equator and equinox representation, and a true equator and equinox version. The working SLP file (the file actually used in evaluation of the solar, lunar, and planetary information) is defined to reflect the integration reference frame being used. After determining the integration reference frame (I50), Draper R&D GTDS "points" the working SLP file locator (NWSLP) to the appropriate version*.

```
      SUBROUTINE  SETDM  (MSGERR,*,*)
...
...
      IF(I1.EQ.1 .AND. ((I50.EQ.2) .OR. (I50.EQ.12))) NWSLP=NTOD
```

Figure 3.14 Setting Default SLP File Location

In the above example, the SLPFILE card is processed within routine SETDM. The SLPFILE card is not used extensively at Draper, but is responsible for

---

* The working SLP file is nominally set to be the "mean of 1950/2000" file locator. If the integration coordinate system is based upon an equator and equinox that is true of some reference time, the pointer is switched to NTOD.

indicating the source of SLP data in the creation of the SLP working file. After information concerning the source is determined, the proper version of this source must be identified. The solution is to set the working SLP file (NWSLP) pointer to the true of date representation (NTOD) location if the integration coordinate system (I50) is either an FK4- or FK5-based true equator and equinox of reference option.

3.4.1.2 FK5 Logic That Mirrors FK4 Logic

Some routines simply required that FK5 options be included along with FK4 options. In general, these modifications involved conditional statements whose execution was dependent upon coordinate system orientation. Introducing the FK5 analogs along with the appropriate FK4 options was the easy fix. An example of this type of modification is given in OPNORB.

```
      SUBROUTINE  OPNORB  (DAYBEG,SECBEG,  DAYEND,SECEND,
                          TIMDIF,  ICENT,ICOORD,  DAYREF,SECREF,
                          ENDFIL,  IFRN,IFILE)
C
C
      IF  ((ICOORD .EQ. 2  .OR.  ICOORD .EQ. 5) .OR. (ICOORD .EQ. 12
          .OR. ICOORD .EQ. 15))  THEN

          CALL  JULPAK  (DAYREF,SECREF,  ORBREC(27,IFILE),0.D0)
          SECREF  =  SECREF  +  ORBREC (29,IFILE)

      ELSE

          DAYREF  =  DBLNUL
          SECREF  =  DBLNUL

      END IF
```

Figure 3.15 Including FK5 Options in Conditional Statements

OPNORB is responsible for reading the header associated with a GTDS ORB1 position and velocity file. Part of that header information is the coordinate system associated with the ORB1 file. If the ORB1 is based upon a true of reference system (either FK4 or FK5, equator or ecliptic), the reference time

must be read from the header and defined for the rest of the modules. The FK4 logic that performed this function previously existed as

(IF ICOORD.EQ.2 .OR. ICOORD .EQ.5 THEN ...)

However, the same functionality must be preserved for the FK5 systems as well. Therefore, the conditions under which the reference time (DAYREF, SECREF) must be calculated were expanded to include ORB1 coordinate system options (ICOORD) of 12 (FK5-based true equator and equinox of reference) and 15 (FK5-based true ecliptic and equinox of reference).

3.4.1.3 Support of New Capabilities

Input processing modifications required to support new software centered around the fundamental constants file and solid earth tide options. Because these modifications are specific to their particular function, none are illustrated here; rather, they are simply summarized. Routines SETDAF and FILESBD were altered to support file allocation for the fundamental constants file. GET_CSCONS was developed to retrieve information from this external file source within SETRUN. The optional SETIDE card mandated changes to routines SETORB and SETOG1 to support processing for the new card.

3.4.1.4 Range checking

The final category of input processing modifications involves range checking performed by Draper R&D GTDS on card inputs. Should the user indicate an option outside certain boundaries, a message is returned and program

execution is terminated. SETRUN provides an example of this range checking function when the ELEMENT1 card is processed.

```
      SUBROUTINE  SETRUN  (*,*,*)
...
...
      IF  (I1 .LT. 1  .OR.  I1 .GT. 15)  GO TO 170
...
...
C           ********** ERROR! **********
C
C           Illegal data.
C
C
C
      170 ASSIGN 100 TO M
      IERR = 401
      GO TO 840
```

Figure 3.16 Expanding Range Checking for FK5 Options

The first integer field (I1) of the ELEMENT1 card contains the coordinate system orientation option associated with the input state components. When only FK4 systems were considered, the options were limited to 1-8. However, with the introduction of the FK5 systems, this range had to be expanded to 1-15. See Appendix D for the various input coordinate system options.

3.4.1.5 Summary of Input Processing Modifications

A summary of the input processing modifications is provided in Table 3.9.

Table 3.9 Modifications Associated with Input Processing

Routine	Modification
DODSEL	Distinguish default of input coordinate system for FK4 and FK5 true of reference systems
ELERD	Replace character representation of ephemeris comparison files' coordinate systems with integer representation; include FK5 options
ESTFLG	Include observation source number read from OBSINPUT card
FILES	Add fundamental constants file
FRC	Include earth-moon, sun-earth mass ratios to support solid earth tide modeling
OPNORB	Include FK5 true of reference systems in reference date evaluations
SETDAF	Add fundamental constants file
SETDC	Expand range checking of TDRELEM1 card to include FK5 options
SETDM	Expand range checking of SLPCOORD card to include FK5 options; include FK5 true of reference cases for setting working SLP file for SLPFILE processing
SETOG1	Distinguish initial default value for EPHEM file coordinate system for FK4 and FK5 true of reference systems; include SETIDE processing
SETORB	Expand range checking for IMPULSE and OUTCOORD cards to include FK5 options; increase number of card options (NKEY) to 93 in order to support SETIDE card
SETRUN	Introduce call to GET_CSCONS for fundamental constant information; expand range checking for ELEMENT1, OUTPUT, and ORBTYPE cards to include FK5 options; include new options for OBSINPUT card
SWITCH	Include switch for solid earth tide options

3.4.2 Parameter Initialization Modifications

After Draper R&D GTDS has interpreted its users intent from the input card data file, it uses the information to set up the program for execution. Conditional statements determine how various switches are set and parameters are evaluated during this task preparation phase. These initializations can take place either on a one-time basis, or, where applicable, before every iteration of an application (differential correction and filter).

The conditional statements requiring modification can be broken into three categories: those that set switches, those that evaluate necessary parameters, and those that perform a consistency check between the SLP and integration coordinate systems. The modifications are summarized in Table 3.10.

Table 3.10 Modifications Associated with Initialization

Routine	Modification
AVRINT	Include FK5 options for setting C matrix evaluation switches in call to EVAL
CENANG	Include FK5 options for evaluation of direction cosines of central body axis in selenographic cases
CENORI	Include FK5 options for evaluation of the orientation matrix
INEFC	Include FK5 options for setting C matrix evaluation switch in call to EVAL
INTIND	Include FK5 options for evaluation of earth's angular velocity in the true of date reference system
INTOGA	Include FK5 true of reference cases for setting working SLP file
INTOGF	Include FK5 true of reference cases for setting working SLP file

INTOGN	Distinguish default of input coordinate system for FK4 and FK5 true of reference systems in Brouwer mean element cases; include FK5 options for rotation of input vector to integration coordinate system
INTOGV	Include FK5 options for rotation of input vector to integration coordinate system and evaluation of reference time
SECUPD	Include FK5 options in setting integration mode switch
SLPWF	Include FK5 true of reference cases for setting working SLP file
SPINIT	Include FK5 options for setting C matrix evaluation switch in call to EVAL

3.4.3 Program Execution

After all parameters have been initialized or reset, Draper R&D GTDS is prepared to perform the desired task. For the ephemeris generation program, this involves propagating the state through numerical integration or analytic formulae. The filter and differential correction programs add the dimensions of residual determination and state correction. For the file report, this step simply involves retrieving the requested information and preparing it for printing. The remainder of the programs within Draper R&D GTDS have their own definitions of "program execution."

Because the scope of this level is so broad, coordinate system information is used in a wide variety of manners. Therefore, it is inappropriate to attempt to categorize the modifications made at this level without making them program specific. Such a categorization is not presented here; instead, a generic summary of the modifications is provided in Table 3.11.

Table 3.11 Modifications Associated with Program Execution

Routine	Modification
ACCEL	Include FK5 cases for coordinate system transformations
AERO	Include FK5 cases for coordinate system transformations
AMATRX	Replace FK4-based expressions with a generalized expression with information provided by fundamental constants file
ATTPRT	Include FK5 cases for coordinate system transformations
ATTSO	Include FK5 cases for coordinate system transformations; generalize arguments of EVAL call to include FK5 cases
CMATRX	Replace FK4-based expressions with a generalized expression with information provided by the fundamental constants file
CPHALO	Distinguish default of input coordinate system for FK4 and FK5 true of reference systems
ELEMGN	Distinguish default of input coordinate system for FK4 and FK5 true of reference systems; replace FK4-based expressions with a generalized expression with information provided by the fundamental constants file
EPHCMP	Replace 'key' assignments with call to ROTKEY
EPHQLT	Include FK5 options in reading of EPHEM/ORB1 header coordinate system information
GQFUN	Include FK5 cases for coordinate system transformations
HEIGHT	Include FK5 options in parameter evaluation
INPUT1	Replace FK4-based expressions with a generalized expression with information provided by the fundamental constants file
J2SQR	Include FK5 options in parameter evaluation
LMKPRT	Include FK5 cases for coordinate system transformations
LNDMRK	Include FK5 cases for coordinate system transformations; generalize arguments of EVAL call to include FK5 cases
LNDPRT	Include FK5 cases for coordinate system transformations
MANEUV	Include FK5 cases for coordinate system transformations

OBLTY	Replace FK4-based expressions with a generalized expression with information provided by the fundamental constants file
OBSLMK	Include FK5 cases for coordinate system transformations; generalize arguments of EVAL call to include FK5 cases
OBSPCE	Include FK5 cases for coordinate system transformations; include FK5 options in parameter evaluation
OBSTRK	Include FK5 cases for coordinate system transformations
OBSUS1	Include FK5 options in parameter evaluation; generalize arguments of EVAL call to include FK5 cases
SLPEPH	Include FK5 cases for coordinate system transformations
SSTSTN	Include FK5 options in parameter evaluation; generalize arguments of EVAL call to include FK5 cases
THETAG	Replace FK4-based expressions with a generalized expression with information provided by the fundamental constants file
TRANF	Include FK5 cases for coordinate system transformations
TRKPRT	Include FK5 cases for coordinate system transformations
VARFRC	Include FK5 cases for coordinate system transformations

3.4.4 Post-processing/Output Modifications

After Draper R&D GTDS has performed the requested task, it presents results in an understandable manner in the form of output reports and files. A report describing the run, from its inception to its completion, is generated as a text file. In addition, certain products containing information from the run can be created.

The modifications involved in the post-execution phase are a combination of those discussed in the previous sections. Coordinate system information is used in conditional statements that control certain parameter evaluations

and transformation processes. Several switches for EVAL calls are set using coordinate system options. In addition to these functions, coordinate system dependent conditional statements are used for labeling purposes. An example from OUTOUT is shown here.

```
      SUBROUTINE  OUTOUT
...
...
      DATA REFCOR    /' 1950.0 ','INERTIAL',
                      'TOR-1950','INERTIAL',
                      'BODY-FIX','      ',
                      ' 1950.0 ','ECLIPTIC',
                      'TOR-1950','ECLIPTIC',
                      'NORAD   ','INERTIAL',
                      'PSEUDO  ','BODY-FIX',
                      'NOR-REFR','INERTIAL',
                      'TOD-1950','INERTIAL',
                      '12345678','90    ',
                      ' 2000.0 ','INERTIAL',
                      'TOR-2000','INERTIAL',
                      '12345678','90    ',
                      ' 2000.0 ','ECLIPTIC',
                      'TOR-2000','ECLIPTIC',
                      '12345678','90    ',
                      '12345678','90    ',
                      '12345678','90    ',
                      'TOD-2000','INERTIAL'/
...
...
      WRITE(NOUT,2017) OUTOPT(7),OUTOPT(8),(REFCOR(1,INDSEC(26,J)))
```

Figure 3.17 Including FK5 Options in Output Labeling

A summary of the output modifications made to support the new capabilities is found below in Table 3.12.

Table 3.12 Modifications Associated with Post-Program Processing

Routine	Modification
COMPER	Replace 'key' assignments with call to ROTKEY; include FK5 cases for coordinate system transformations
CRDLBL	Expand number of coordinate labels to 19 to include FK5 and instantaneous true of date cases
ELTRAN	Include FK5 cases for coordinate system transformations

EPHEM	Replace 'key' assignments with call to ROTKEY; include FK5 options for OUTOPT card; include FK5 cases for labeling purposes
LCLONE	Include FK5 options for setting C matrix evaluation switch in call to EVAL; include FK5 cases for coordinate system transformations; replace FK4-based expressions with a generalized expression with information provided by the fundamental constants file
LIBR	Include FK5 options for setting C matrix evaluation switch in call to EVAL; include FK5 cases for coordinate system transformations; replace FK4-based expressions with a generalized expression with information provided by the fundamental constants file
MEANOSC	Include FK5 options for setting C matrix evaluation switch in call to EVAL
ORB1	Include FK5 cases for coordinate system transformations
OSCMEAN	Include FK5 options for setting C matrix evaluation switch in call to EVAL
OUT24H	Include FK5 cases for labeling purposes
OUTDC2	Include FK5 cases for labeling purposes; include FK5 options for setting evaluation switch in call to OSCMEAN, MEANOSC, and VECSET; include FK5 options in parameter evaluation
OUTDC6	Include FK5 cases for coordinate system transformations
OUTDC7	Include FK5 cases for labeling purposes
OUTDC8	Include FK5 cases for coordinate system transformations; replace 'key' assignments with call to ROTKEY; distinguish default of output coordinate system for FK4 and FK5 true of reference systems
OUTDC9	Distinguish default of output coordinate system for FK4 and FK5 true of reference systems; include FK5 options for setting evaluation switch in call to OSCMEAN, MEANOSC, and VECSET
OUTEA4	Include FK5 cases for labeling purposes
OUTGPS	Include FK5 cases for labeling purposes

OUTOG2	Include FK5 cases for coordinate system transformations
OUTOG4	Include FK5 cases for coordinate system transformations; replace 'key' assignments with call to ROTKEY
OUTOUT	Include FK5 cases for labeling purposes
OUTPEL	Include FK5 cases for labeling purposes
OUTPMN	Include FK5 cases for labeling purposes
OUTPSC	Include FK5 cases for labeling purposes
OUTSEC	Include FK5 cases for labeling purposes
OUTTEA	Include FK5 cases for labeling purposes; include FK5 options in parameter evaluation
OUTTIC	Include FK5 cases for labeling purposes; include FK5 options in parameter evaluation
OUTWPC	Include FK5 cases for labeling purposes
OUTWSC	Include FK5 cases for labeling purposes
OUTWSD	Include FK5 cases for labeling purposes
OUTWSL	Include FK5 cases for labeling purposes
PRINT	Include FK5 cases for labeling purposes; include FK5 options in parameter evaluation; include FK5 cases for coordinate system transformations
RPTOBS	Include FK5 cases for labeling purposes
SELENO	Include FK5 options for setting C matrix evaluation switch in call to EVAL

3.4.5 Modifications to Routines With Multiple Functionalities

There are several routines that can fall into any of the above categories. These routines are used extensively throughout Draper R&D GTDS and do not limit themselves to one functionality. EVAL is used to determine solar, lunar, and planetary positions and to evaluate transformation matrices from one coordinate system to another. ROTKEY is a routine who's function is to set certain switches used in the transformation from one coordinate system to another. ROTRAN uses the keys set within ROTKEY to perform the

coordinate system transformations. The modifications required for incorporation of the new capabilities for these routines are summarized below.

Table 3.13 Modifications Associated with Routines of Multiple Functionality

Routine	Modification
EVAL	Account for FK5 coordinate systems in consistency check between integration and SLP files; replace FK4-based expressions with a generalized expression with information provided by the fundamental constants file
ROTKEY	Expand number of key options (NCOORD) to 19 to include FK5 systems; FK5 keys are mirror images of FK4 analogs
ROTRAN	Include FK4 and FK5 instantaneous true of date systems for coordinate system transformations; include FK5 true of reference option for coordinate translations

3.4.6 New Draper R&D GTDS Software

Eleven (11) new routines were developed to support the new coordinate system and solid earth tide capabilities. The need for these routines is derived from labeling, transformation, solid earth tide modeling and FK4-FK5 distinction purposes. The new routines are listed below along with a description of their functions.

Table 3.14 Summary of New Routines Added to Draper R&D GTDS

Routine	Purpose
CSCONST	Block Data to house fundamental coordinate system dependent values
CSERROR	Checks for compatibility between coordinate systems in transformation procedures
CSHDC2	Return a coordinate system label to OUTDC2
CSHDC7	Return a coordinate system label to OUTDC7
CSHGPS	Return a coordinate system label to OUTGPS
CSHRPT	Return a coordinate system label to RPTOBS
CSMIX	Driver routine for coordinate system transformations
CSTRANS	Performs coordinate system transformations by calling ROTKEY/ROTRAN; accounts for FK4-FK5 interaction where applicable
ERTHTD	Evaluate accelerations due to solid earth tides
GET_CSCONS	Retrieve fundamental coordinate system dependent values
J2000	Block data that stores transformation matrix between fundamental FK4 and FK5 reference frames

Chapter 4

Testing of the Implementation of the J2000 and Instantaneous True of Date Coordinate Systems and Solid Earth Tides in Draper R&D GTDS

4.1 Chapter Introduction

Chapter 3 summarizes the software development required to support the introduction of the J2000 and ITOD coordinate systems, along with solid earth tides into Draper R&D GTDS. The testing of the changes and additions made to the 101 identified routines is a natural consequence of the development process. This not only validates that the new capabilities were implemented properly, but also ensures that none of the existing functionalities were disturbed.

This chapter describes testing of the final product. Evaluation of the merger between RADARSAT GTDS and Fonte's 50x50 gravity field modeling modifications was necessary to provide a fundamental baseline for software development. A series of standard test cases involving most of the common operations found in Draper R&D GTDS was performed with the final executable to demonstrate that existing functionalities were not altered. Validation of the changes made to support the new capabilities was shown

through progressive testing of the permanent file report, ephemeris generation, differential correction, and ephemeris comparison functions. Finally, the high quality POE information (which provides an independent orbit assessment) was used to highlight the contributions of each of the new capabilities.

4.2 Testing of the RADARSAT/50x50 Merger

As discussed in section 3.3.1.1.2, both the RADARSAT and 50x50 libraries were targeted for inclusion in this work because of upgrades from the LANDSAT 6 version. The merger of the functionalities in the source codes required modification to three routines to encompass all changes made in each path. The alterations are summarized in Table 3.4.

Because the 50x50 gravity field modeling is key to achieving desired accuracy levels, testing of the merged code centered around results presented by Fonte [20]. A combination of three test cases (summarized in Table 4.1) is used to validate the compatibility of the 50x50 class models with the Cowell and DSST orbit propagators, and the differential correction, data management and ephemeris comparison programs.

Table 4.1 Summary of RADARSAT/50x50 Merger Testing

Test Case	Description	References in Appendix G
1	Cowell orbit generator	Figures: G.1-G.2 Table: G.2
2	Cowell differential correction with perturbed initial conditions	Figures: G.3-G.4 Table: G.3
3	21x21 SST fit of orbit created with 50x50 modeling using SST	Figures: G.5-G.8

The first test case was a simple Cowell ephemeris generation using only 50x50 gravity field modeling and third body effects to model spacecraft motion. A LANDSAT 4 Keplerian element set was integrated in the mean equator and equinox of 1950 coordinate system to predict an orbit over a three day time span. The end conditions resulting from the execution using the final software product for this project are compared in Table 4.2 to those seen by Fonte.

Table 4.2 Validation of the Cowell 50x50 Orbit Generator

End conditions	Fonte's Results	New GTDS Results	Δ
X Position (km)	3873.119562949189	3873.119562*82987*	3.3798e-8
Y Position (km)	-430.5243130203381	-430.5243130*354492*	1.5111e-8
Z Position (km)	5925.145802534543	5925.145802*511251*	2.3292e-8
X Velocity (km/s)	5.793182527061727	5.79318252703*6600*	2.5127e-11
Y Velocity (km/s)	-2.597763108551348	-2.59776310854*8536*	2.8120e-12
Z Velocity (km/s)	-3.978183663971041	-3.97818366*4009602*	3.8561e-11

Although the differences are on the sub-millimeter level, their existence is somewhat troubling. It is highly desirable to possess the ability to *exactly* replicate results after significant software modifications are made. However, circumstances do not always allow for that luxury. In this particular instance, the hardware used in the two executions was different. Fonte operated on the VAX 8820 (code-named BIGSIM) under VMS 5 when accomplishing his work in 1992-1993, while this project was carried out on the VAX 4000/90 (ELROND) under the VMS 6 operating system.

The slight difference in results is likely a product of the introduction of a new operating environment. The math libraries associated with the two FORTRAN compilers could be referencing values slightly differently to cause these variations. This hypothesis was tested by introducing the results from a series of test cases discussed in the next section of this chapter.

Four of the test cases have been performed in four different environments. The cases were initially executed on the DECKER VAX 8530 (then located at Princeton, New Jersey) by Dr. David Carter. They were reproduced on BIGSIM by Richard Metzinger in February 1993 when R&D GTDS was being ported to the SUN and SGI platforms. These four cases were then included as part of the software test plan for the RADARSAT project in 1994 on a VAX 4000/90 (BIANCA). The current VAX 4000/90 (ELROND), a slight upgrade from BIANCA, is the final VAX environment that these cases have been tested in.

Table 4.3 VAX Environments for Standard Test Cases

GTDS version	VAX 8530 (DECKER)	VAX 8820 (BIGSIM)	VAX 4000/90 (BIANCA)	VAX 4000/90 (ELROND)
LANDSAT 6	October 1991			
LANDSAT 6		February 1993		
RADARSAT			June 1994	
CURRENT				April 1996

Results from the four test cases were available for the last three environments listed in Table 4.3. Comparison of the results from each of these three environments revealed that the two VAX 4000/90 executions showed the highest level of relative agreement (although in one instance, the differences between BIGSIM and BIANCA were less than the differences between BIANCA and ELROND). ELROND results always agreed better with BIANCA than with BIGSIM. In addition, the magnitudes of these differences were similar to those experienced in Table 4.2, indicating that they are a result of operating in a different environment, and *not* from software modifications.

Satisfied that the 50x50 class models and the Cowell orbit generator worked properly, the next test case was intended to validate the differential correction process using Cowell techniques. Because no Cowell differential correction results were available from Fonte's directories on the VAX, a separate test (highlighted in Figure 4.1) was used for differential correction testing. First, a truth ORB1 file was created by generating a mean equator and equinox of 1950 ephemeris using Cowell techniques. Force modeling included 50x50

geopotential, drag, third body, and solar radiation effects. This ephemeris was then used as an observation source for a separate differential correction/ephemeris generation process using the same Cowell propagator. Although the force models are consistent between the truth execution and the DC/EPHEM process, the initial conditions are perturbed for the DC. By altering the initial conditions, the variational equations are tested in the differential correction process. If working properly, the DC converges back to the initial condition of the truth execution. Comparison of the initial truth ORB1 file and an ORB1 file created from an ephemeris generated using the converged solution will reveal negligible differences.

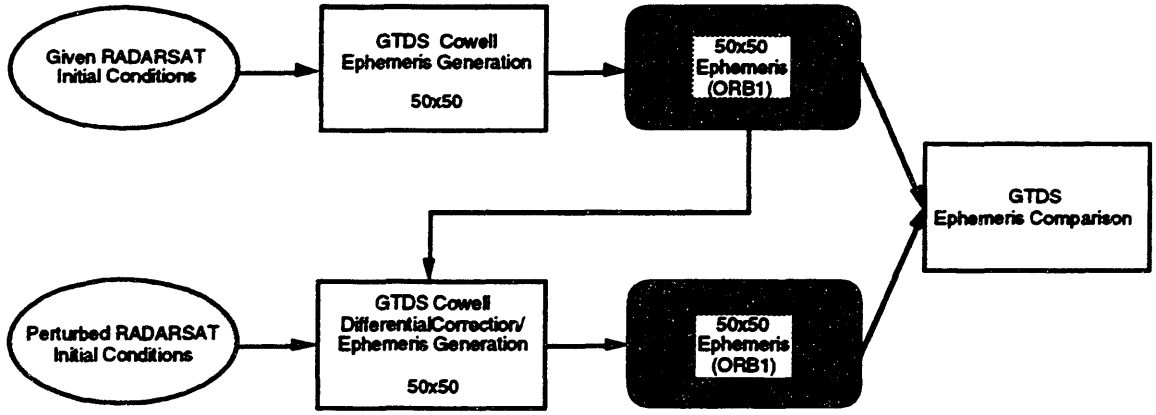

Figure 4.1 Testing of the Cowell Differential Correction

Analysis of the results for this test case is performed by comparing the actual initial conditions for the truth ORB1 with the converged solution in the mean equator and equinox of 1950 reference frame. The differences and standard deviation (from the fit) for each component are shown in Table 4.4 below.

Table 4.4 Comparison of Truth Initial Conditions and Converged Solutions

	Actual Initial Condition (km and km/s)	Converged Solution (km and km/s)	Δ (km and km/s)	1 σ (km and km/s)
X	-3736.803593965437	-3736.803593***80256***	1.4819e-8	1.8207e-5
Y	5523.017887591180	5523.017887***676010***	8.4829e-8	2.7646e-5
Z	-2649.590848037073	-2649.590847***838223***	1.9885e-7	3.1081e-5
VX	-.5134002749726257	-.513400274***8553410***	1.1728e-10	1.8916e-6
VY	2.924254086071665	2.92425408***5898364***	1.7330e-10	2.8533e-6
VZ	6.835193797081531	6.83519379***7165048***	8.3517e-11	3.0873e-6

In addition, the truth ORB1 file and the ORB1 file generated from the last iteration of the differential correction were compared with the GTDS COMPARE program. The maximum position and velocity differences and their associated RMS values are summarized in Table 4.5.

Table 4.5 Comparison of Truth and Converged Orbits for Cowell DC

	Maximum position (km)	Maximum Velocity (km/s)	Position RMS (km)	Velocity RMS (km/s)
Radial	7.0763e-10	3.2279e-10	3.2719e-10	2.7678e-10
Cross-track	5.9873e-11	1.6904e-13	2.9664e-11	1.0239e-13
Along-track	3.1027e-7	5.2725e-13	2.6631e-7	2.7677e-13
Total	3.1027e-7	3.2279e-10	2.6631e-7	2.7678e-10

The final test case performed to validate the merger of the RADARSAT and 50x50 libraries involved a two hundred day fit of the 21x21 GEMT3 Averaged Orbit Generator to the 50x50 GEMT3 Averaged Orbit Generator. This test case is a reproduction of one presented by Fonte in [20]. As shown by Figure 4.2, a

mean equator and equinox of 1950 ORB1 file was created for a DMSP orbit by the SST propagator (using the latest version of GTDS), considering only 50x50 geopotential effects. This ORB1 file was then used as an observation source for a differential correction that considers only the 21x21 portion of the gravitational potential. The ORB1 file generated from the 21x21 fit was then compared to the original 50x50 ORB1 file. In effect, this test case highlighted the impact that an higher order gravity model has on orbit determination.

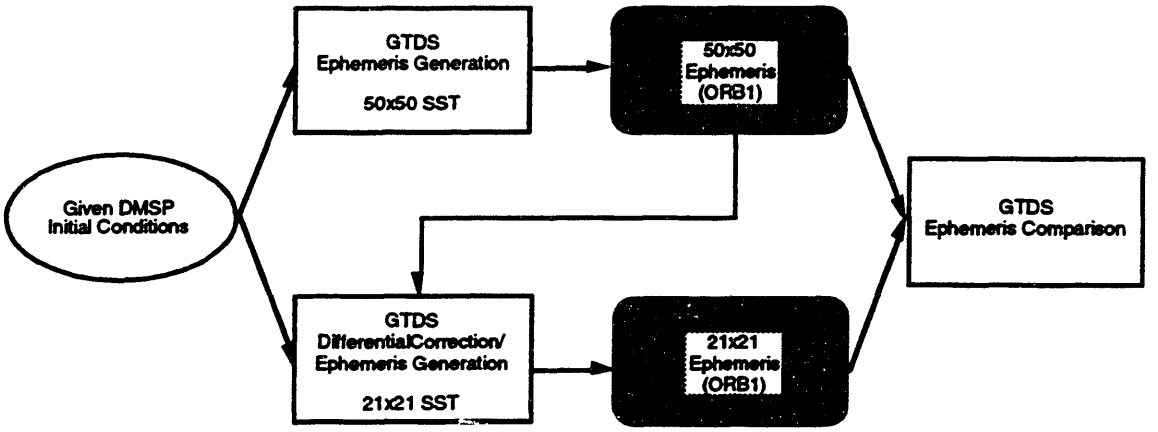

Figure 4.2 Fit of 21x21 GEMT3 Orbit to 50x50 GEMT3 Orbit

The maximum position and velocity differences between the two ORB1 files, as well as the RMS values were compared to those seen by Fonte. The results, summarized in Table 4.6, were identical to the precision provided by the COMPARE program.

Table 4.6 Comparison of 21x21 and 50x50 GEMT3 Orbits

	Maximum position (km)	Maximum Velocity (km/s)	Position RMS (km)	Velocity RMS (km/s)
Radial	5.7267e-2	3.1990e-3	3.3576e-2	1.6680e-3
Cross-track	4.7738e-2	4.1738e-5	1.7800e-2	1.6002e-5
Along-track	3.1515e0	5.9170e-5	1.6392e0	3.4504e-5
Total	3.1519e0	3.1995e-3	1.6396e0	1.6684e-3

4.3 Standard Test Cases

As indicated in the previous section, a series of test cases was developed when Draper R&D GTDS was ported to the SGI UNIX Workstation environment in 1992-93 to confirm that the major functionalities were preserved. The twenty-one tests were targeted toward a subset of the overall Draper R&D GTDS functions, including the ephemeris generation, differential correction, early orbit, permanent file report, ephemeris comparison and data simulation programs. Millimeter and centimeter level agreement was shown across several platforms, including VAX, SUN ...d SGI UNIX workstations, and an IBM mainframe [47]. Similar agreement has been demonstrated for a 486 PC version of Draper R&D GTDS [21]. A list of the twenty-one cases and the functionalities demonstrated by each is shown in Table 4.7.

Table 4.7 Summary of Standard Test Cases

Test Case	Designation	Description
1	L6_PCE_SETUP	SST and Cowell orbit generations
2	L6_PCE_SST	SST DC from ORB1; ephemeris comparison
3	DC_M50_COWELL	Cowell DC from NORAD RAER data
4	EARLY_ORB	Orbit estimate from five sets of observations
5	FILERPT_ATM	File report of Harris-Priester atmospheric density file
6	FILERPT_EPOT	File report of Earth potential file
7	FILERPT_JACC	File report of Jacchia-Roberts atmospheric density file

8	L6_PCE_BL	Brouwer-Lyddane DC from ORB1; ephemeris comparison
9	L6_PCE_BL_DRAG	Brouwer-Lyddane DC from ORB1 considering drag as solve-for; ephemeris comparison
10	EPHEM_BROUWER	Three day ephemeris generation using Brouwer-Lyddane
11	EPHEM_M50_COWELL	Three day ephemeris generation using Cowell
12	EPHEM_M50_COWELL _JACCHIA	Three day ephemeris generation using Cowell with Jacchia-Roberts file
13	EPHEM_TWOBODY	Two day ephemeris generation using Cowell with no perturbations
14	COMPARE	Ephemeris comparison of cases 11 and 12
15	DATASIM	Generates simulated set of observations from given ephemeris
16	DC_SALT	NORAD SALT DC from NORAD RAER data
17	DC_HANDE	HANDE DC from NORAD RAER data
18	DC_GP4	GP4 DC from NORAD RAER data
19	EPHEM_NORAD	One day ephemeris generation using SGP, GP4/DP4, and DP4
20	EPHEM_NORAD_GP4	One day ephemeris generation using GP4
21	L6_PCE_GP4	GP4 DC from ORB1 file

Although these cases did not include 50x50 gravity field modeling, they can be used to verify that existing functionalities were not affected by the introduction of the new capabilities (J2000, ITOD, and solid earth tides). They test the overall operation of Draper R&D GTDS on a much broader scale than the two procedures outlined in the previous section.

Fourteen of the cases were executed using the final version of the software and compared to the results listed in [47]. Unfortunately, cases 15, 16, 17, 18, and 21 in Table 4.7 could not be performed with the new executable because of ambiguity in the setup of the application (i.e., command procedures and overrides files were not available, resulting in uncertainty in the appropriate data files). Test cases 19 and 20 did not have existing VAX values, and thus were not considered. Sub-millimeter agreement was achieved between the two VAX versions for the remaining cases, indicating that these functionalities were preserved during the incorporation of the new capabilities. The results of these test cases using the new executable are summarized in Figures G.9-G.11 and Tables G.5-G.15.

4.4 Testing of the Permanent File Report Program

The permanent file report function was tested primarily to ensure that the FK5-based SLP files provided information in an analogous manner to the FK4-based files. The report contains a header describing the times, fitting procedures, and coordinate system associated with the file. The positions of the sun, moon, and planets, transformation matrices (from mean equator and equinox to selenographic and true of date frames), and coefficients used in the computation of the Greenwich hour angle are provided in ten day intervals. The output of this report is not provided here because of its length; however, it does indicate that the FK5 files are being accessed in a manner consistent with the FK4-based files and are labeled appropriately. The input card data file and command procedure used in this test are shown in section G.3.

4.5 Testing of the Orbit Generators

The primary testing of the new capabilities began with evaluation of the Cowell and SST orbit generators. The Cowell propagator was chosen because of its wide acceptance as a high quality technique, while the SST offers the unique opportunity to produce precision mean elements. Validation of these propagators was imperative for use in orbit determination analyses.

This testing involved two cases designed to demonstrate that the FK5 theory had been properly implemented into Draper R&D GTDS. The first used only two-body mechanics, while the second considered J_2 effects (as seen in Table 4.8).

Table 4.8 FK5 Orbit Generator Test Cases

Test Case	Description	References in Appendix G
1	Two orbits (one based on FK4 theory; the other on FK5) generated using two body mechanics only; ephemerides compared	Figures: G.14-G.30
2	Two orbits (one based on FK4 theory; the other on FK5) generated considering J_2 effects; ephemerides compared	Figures: G.31-G.47

Each case generated two orbits, one based upon FK4 theory, and the other from FK5 theory. Mean equator and equinox of 1950 initial conditions were provided for the ephemeris generations. The state was then propagated using both Cowell and SST techniques in the appropriate reference frame. Output was generated in a mean equator and equinox of J2000 frame and compared

using an external plotting package (see Appendix C for details). This process is summarized in Figure 4.3.

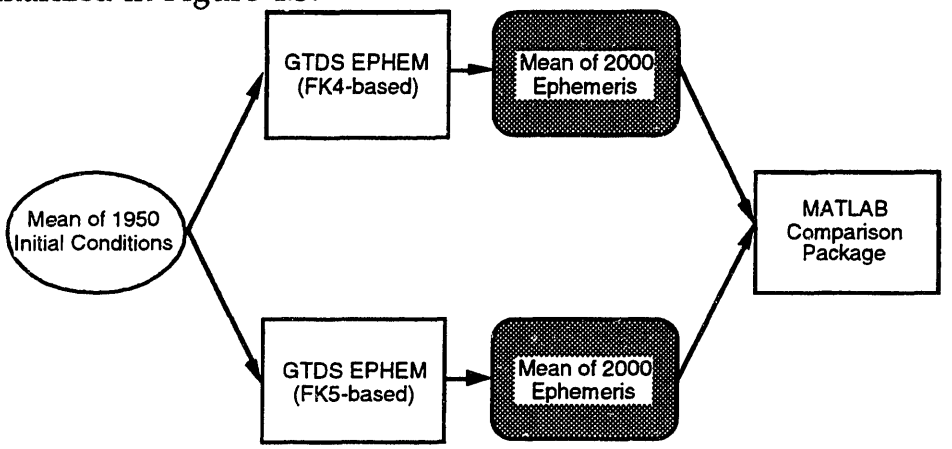

Figure 4.3 Testing of the Implementation of the FK5 Theory

Figure 4.4 is an example of a product of the post-processing package, and represents differences between the ephemerides produced using FK4 and FK5 theories for Cowell and SST propagators.

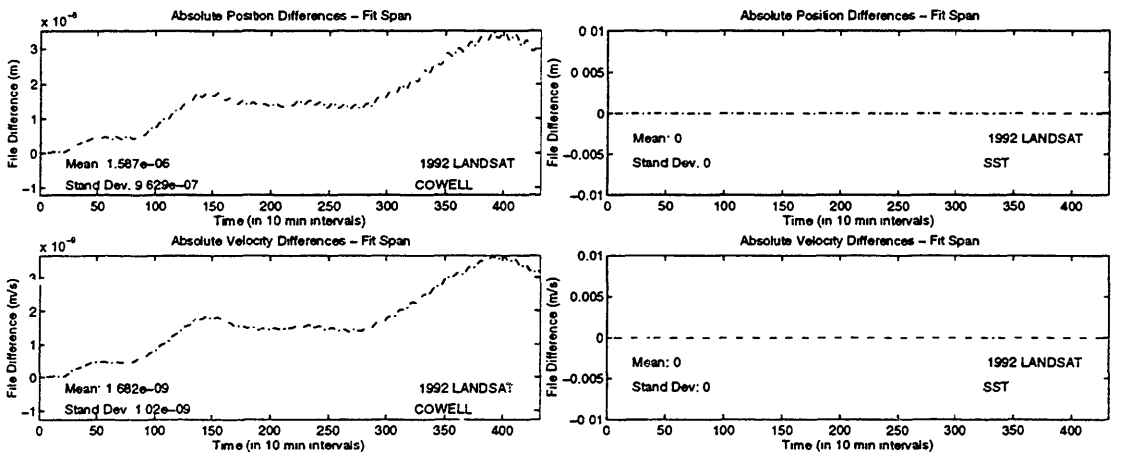

Figure 4.4 Absolute Differences Between FK4/FK5 Two-body Orbits

It suggests that the FK5 theory was implemented in a manner consistent with the way the existing FK4 theory was operating. While the Cowell plot indicates a slight drift in the differences between FK4- and FK5-derived orbits

(a growth that amounts to one meter difference over 2700 years for the LANDSAT 6 orbit), the SST comparison reveals complete agreement for the two-body case.

Because this test case was limited to two-body mechanics, other cases were developed to determine the significance of differences in the force modeling between the two fundamental systems. The most notable case involved adding the second order zonal harmonic (J_2) effects to the two-body orbit. Again, orbits were generated using both FK4 and FK5 theory. A mean equator and equinox of 1950 vector was propagated with both Cowell and SST techniques in the appropriate frames to produce an orbit referenced to the mean equator and equinox of J2000 (see Figure 4.3). Zonal short periodics were activated for the SST execution. The absolute position and velocity differences for the Cowell and SST techniques are shown below in Figure 4.5.

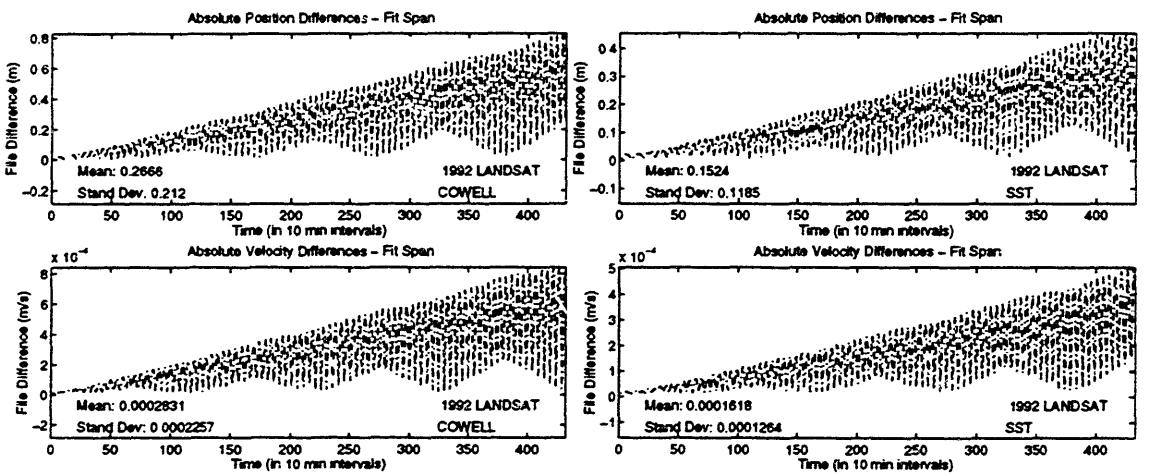

Figure 4.5 Absolute Differences Between FK4/FK5 Orbits with J_2 Considered

Figure 4.5 demonstrates the inherent differences between the FK4 and FK5 theories. Because J_2 effects are the only additional perturbation considered here, the secular growth suggests that the nodal drift rate is key to

understanding these differences. Blitzer indicates that the nodal drift rate is dependent upon the inclination of the satellite [6].

$$\dot{\Omega} = -\frac{3J_2}{2p^2} n \cos i \tag{4.1}$$

where n is the satellite's mean motion, i is the inclination, $J2$ is the second order zonal harmonic coefficient, and

$$p = \frac{a(1-e^2)}{R_e} \tag{4.2}$$

for a given semi-major axis (a), eccentricity (e), and radius of the earth (R_e).

If the representation of the inclination of the satellite when considering second order zonal harmonic effects was fundamentally different for the FK4 and FK5 systems, the nodal drift rates would vary accordingly. Since LANDSAT 6 is inclined at 98° with respect to the earth's equator, the variations are manifest in the cross-track component. Figure 4.6 suggests that this is the case.

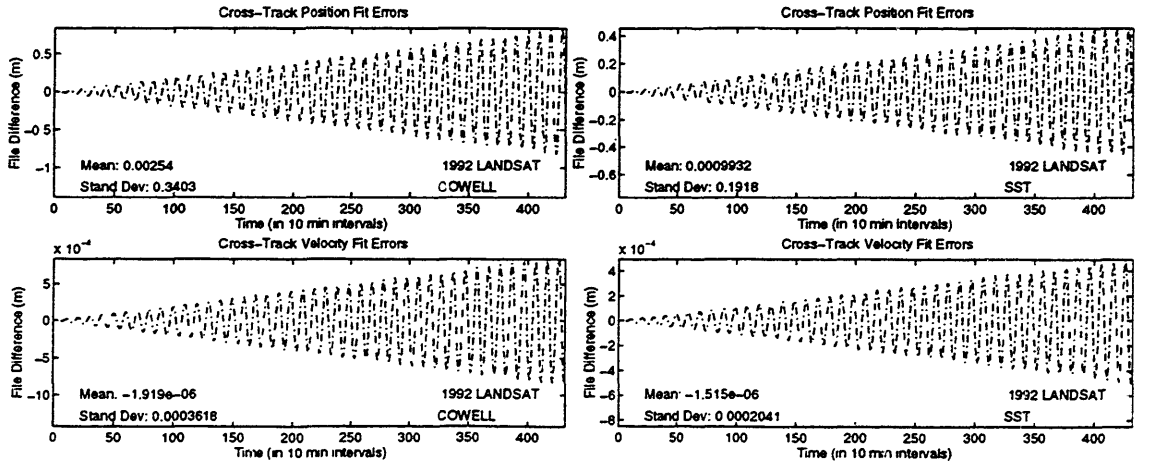

Figure 4.6 LANDSAT 6 Cross-Track Differences for FK4/FK5

To quantify the expected variations, the existing initial conditions for this case were analyzed. Since the J_2 perturbing accelerations are evaluated in the ECEF coordinate system, the representation is the same for the FK4 and FK5 cases at the evaluation level. However, when the perturbing acceleration is transformed to the integration coordinate system, differences are observed. Although the integration coordinate system for these cases were mean equator and equinox of fundamental epoch, the ITOD frames provide more insight for this problem. Conceptually, the FK4 and FK5 ITOD coordinate systems are identical. However, because of the equinox offset and drift rate of the FK4 system (reference section 3.2.1.6), vectors are actually represented differently in the two ITOD systems. Thus, the ITOD frames provide tremendous insight into the fundamental differences between the two systems.

The initial ITOD conditions were calculated using the appropriate SLP files, and the inclination values were determined. The FK4-based ITOD inclination was *98.11233185*, while the FK5-based value was *98.11231366*. These two values were then used to evaluate the anticipated nodal drift rates from equation (4.1). The difference in nodal drift rates suggests that the cross-track error was expected to be approximately 0.8 meters after three days for LANDSAT 6 altitude and eccentricity.

Although the expected cross-track growth is actually slightly larger than the experienced growth, the FK5 theory is likely implemented properly. Differences in the expected and actual values can be attributed to a combination of several factors. First, the 0.8 value assumes that the nodal

errors completely map into the cross-track component (which isn't the case for a 98° inclined orbit). Also, the expected results were derived from first-order J_2 effects (see equation 4.1). Finally, the nodal drift rate is actually changing over the three-day period, but was only evaluated at epoch for this analysis.

One final item of note for this case concerns the differences observed between the Cowell and SST techniques (see Figures 4.5 and 4.6). The slower growth rate seen for the SST is likely the product of an ill-advised input card data file setup. Because osculating Keplerian elements are used as initial conditions, Draper R&D GTDS performs an osculating-to-mean conversion prior to propagation of the mean elements. The iterative procedure resulted in two different mean semi-major axis values (a difference of 0.0017737 m, as illustrated in Figure G.37). This bias in the initial semi-major axis is likely the culprit of the differences observed between the Cowell and SST cases. A more accurate representation of the initial mean conditions (possibly by fitting the Cowell ORB1 with SST) would likely produce results comparable to the Cowell case.

Based upon the differences observed for the J_2 case, other forces were individually added to the test protocol to determine the impact that the differences between FK4 and FK5 theories had on resulting orbits. However, because the second order zonal harmonic is the dominant effect, these additions had relatively negligible impact compared to the J_2 case.

It should be noted that at this point, testing of the implementation of solid earth tides and the instantaneous true of date coordinate system has not been

shown for the two orbit generators. Verification of proper incorporation is demonstrated in the testing associated with the differential correction and use of the POE vectors.

4.6 Testing of the Differential Correction

Validation of the Cowell and SST orbit generators using FK5 theory led to analysis of the differential correction process. Two tests (summarized in Table 4.9) were performed for differential correction validation.

Table 4.9 Differential Correction Test Cases

Test Case	Description	References in Appendix G
1	Cowell and SST differential corrections with truth ORB1 observations and perturbed initial conditions	Figures: G.48-G.62 Tables: G.18-G.19
2	Fit of Cowell truth ORB1 with SST techniques	Figures: G.63-G.74

Both Cowell and SST techniques were tested in a fashion similar to the process depicted in Figure 4.1. A truth ORB1 file based upon TOPEX orbital characteristics was produced using each of the two theories. The ORB1 files were used as observation sources for the respective differential corrections with slightly perturbed initial conditions. Force modeling included 50x50 geopotential, atmospheric drag, solar radiation pressure, solid earth tides, and third body effects, and integration was performed in the mean equator and equinox of J2000 reference frame.

Convergence to the initial conditions of the truth orbit indicated that the differential correction process, including the variational equations, was working properly. The truth and converged position vectors are shown below in Tables 4.10 and 4.11 along with the standard deviation of the coordinate residuals:

Table 4.10 Cowell Differences Between Truth and Converged States

	Truth (km)	Converged (km)	Δ (km)	1σ (km)
X	6107.1223364983	6107.1223364975	7.9945e-10	9.6775e-7
Y	-4337.566570945	-4337.566570946	9.3995e-10	6.7698e-7
Z	-1858.018949206	-1858.018949208	1.9998e-9	9.7018e-7
VX	3.0224246349983	3.0224246349997	1.4078e-12	8.9335e-8
VY	1.5404238300435	1.5404238300425	9.8321e-13	5.9140e-8
VZ	6.3370559318311	6.3370559318307	3.9879e-13	9.3149e-8

Table 4.11 SST Differences Between Truth and Converged States

	Truth (km)	Converged (km)	Δ (km)	1σ (km)
X	6105.1193296945	6105.1193446027	1.4908e-5	2.7894e-5
Y	-4335.062253693	-4335.062230911	2.2782e-5	2.6396e-5
Z	-1856.576096593	-1856.576111634	1.5041e-5	2.7805e-5
VX	3.0215542411922	3.0215542560749	1.4883e-8	2.7129e-6
VY	1.5426757579791	1.5426757799917	2.2013e-8	2.4183e-6
VZ	6.3372008864777	6.3372008684493	1.8028e-8	2.7122e-6

Although both cases converged to an estimate relatively close to the truth solution, the Cowell was a much tighter fit (as indicated by the standard deviation of the residuals and differences in Tables 4.10 and 4.11). This is a

result of the converged tolerance being more lenient for the SST case (see Figures G.48 and G.51).

Variation in the initial state for both generators translates into different orbits over the fit span. Comparison of the truth ORB1 file and the ORB1 generated from the converged solution shows that these errors are negligible, an indication that the differential correction works properly.

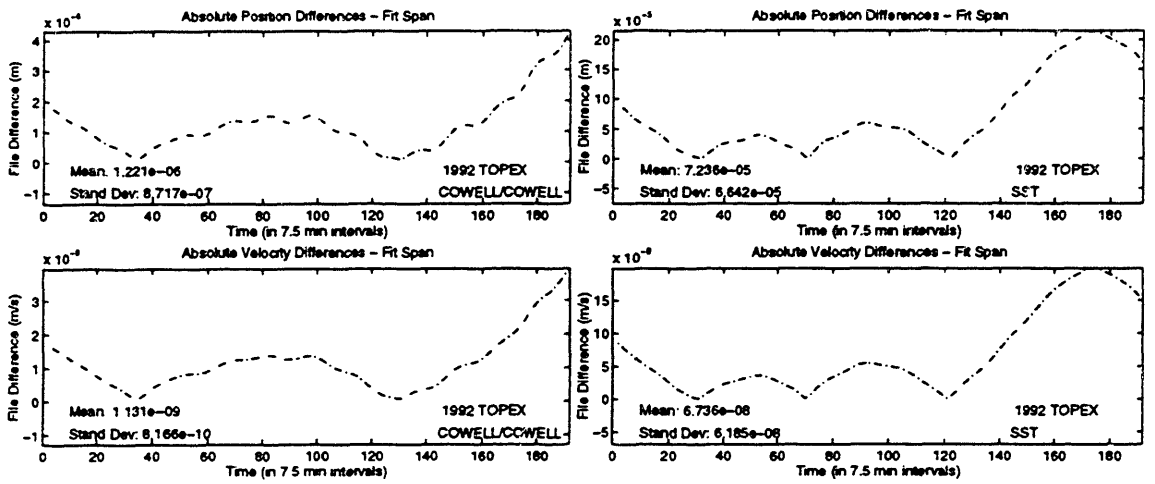

Figure 4.7 Accuracy of Converged Solutions in Differential Correction

Again, the Cowell fit is shown to be much tighter than the SST fit because of a stricter convergence tolerance. The position and velocity differences are an entire order of magnitude less for the Cowell case (see Figure 4.7).

An additional test case was performed to show the relative level of agreement between the differential correction process using the Cowell and SST orbit generators. This execution fit the semianalytic theory to the Cowell truth ORB1 file generated in the first differential correction test case (reference Figure 4.8). Because similar force models were used in the Cowell generation and the SST fit, comparison of the initial (Cowell) and resulting (SST)

ephemerides highlighted the fundamental differences between the two orbit generation techniques.

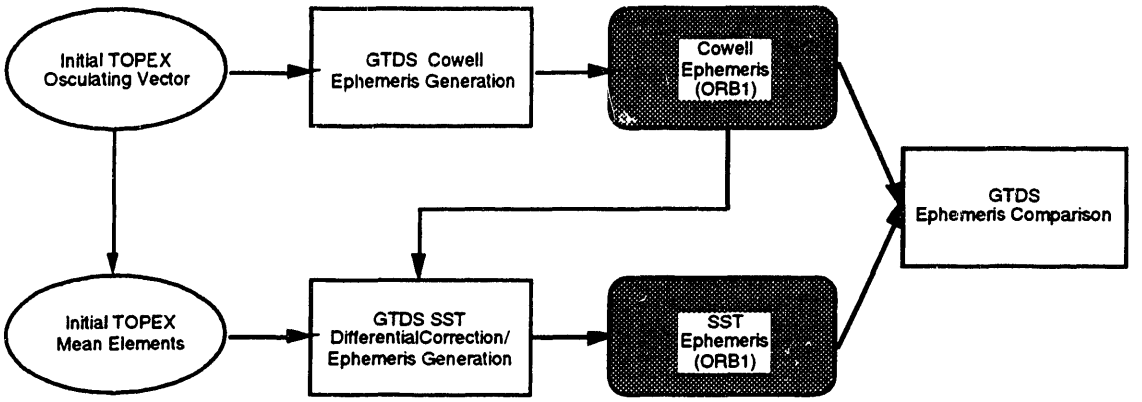

Figure 4.8 SST Fit to Cowell Truth Orbit

The results of this test are summarized by the statistics provided by the GTDS Ephemeris Comparison program and graphical representation of the ephemeris differences. The position and velocity RMS values are compared to results obtained by Fonte when he performed an analogous test in [20]. Table 4.12 shows the similarity between the results of the two tests.

Table 4.12 Comparison of SST/Cowell Orbits for LANDSAT 4 and TOPEX

	Position RMS (m)		Velocity RMS (cm/s)	
	LANDSAT	TOPEX	LANDSAT	TOPEX
Radial	0.50203	0.52057	2.0035	1.5541
Cross-Track	1.0954	0.39407	0.70972	0.46777
Along-Track	1.9867	1.7956	0.68605	0.79569
Total	2.3235	1.9106	2.2335	1.8076

Variation in the results of the two cases is a product of evaluating a different orbit (TOPEX vs. LANDSAT 4) with different force models (drag, solid earth

tides and a different geopotential were used for the TOPEX case). However, the similar magnitudes of SST variation exhibited provides additional confidence that the new capabilities are integrated properly into the differential correction process.

Variation in the Cowell and SST orbits was also plotted external to Draper R&D GTDS to facilitate transfer into this document. The absolute position and velocity differences are shown below in Figure 4.9.

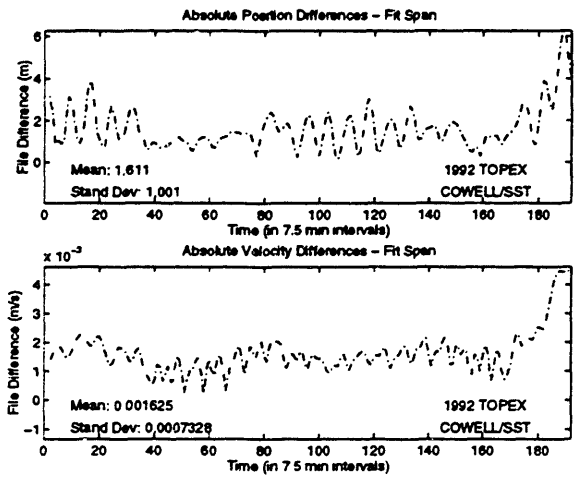

Figure 4.9 Relative Agreement of the Cowell and SST Orbit Propagators for a Synthesized TOPEX Orbit

4.7 Validation of Solid Earth Tide and ITOD Implementation Using the TOPEX POEs

The presence of a high quality external data source such as the TOPEX POEs provides a unique opportunity to test the accuracy of the orbit generators in Draper R&D GTDS. It also offers alternative methods for testing the incorporation of the solid earth tides and instantaneous true of date

coordinate system capabilities. Three categories of testing associated with the POEs were identified:

- Use POEs in differential correction to test accuracy of the force modeling in the Cowell and SST orbit generators
- Use POEs in differential correction to test implementation of the solid earth tide modeling
- Use POEs in differential correction to test implementation of the ITOD coordinate system

The TOPEX POE tests are summarized in Table 4.13.

Table 4.13 TOPEX POE Test Cases

Test Case	Description	References in Appendix G
1	Cowell fit of the TOPEX POEs with 21x21 geopotential; no solid earth tides	Figures: G.75-G.86
2	Cowell fit of the TOPEX POEs with 50x50 geopotential; no solid earth tides	Figures: G.87-G.98
3	Cowell fit of the TOPEX POEs with 21x21 geopotential; solid earth tides	Figures: G.99-G.110
4	Cowell fit of the TOPEX POEs with 50x50 geopotential; solid earth tides	Figures: G.111-G.122
5	SST fit of the TOPEX POEs with 50x50 geopotential; solid earth tides	Figures: G.123-G.134
6	Anticipated solid earth tide effects for Cowell propagator (based on TOPEX POE vector)	Figures: G.135-G.137 G.141-G.149
7	Anticipated solid earth tide effects for SST propagator (based on TOPEX POE vector)	Figures: G.138-G.140 G.141-G.149
8	Cowell fit to ECEF TOPEX POEs with 50x50 geopotential; solid earth tides	Figure: G.150

The most general application of the POEs in the testing phase involved using the high precision vectors as observations in a differential correction process to provide insight about the inherent accuracy of the force modeling in the Cowell and SST generators. The effects of the higher order (50x50) gravity model, solid earth tides, and FK4/FK5 theory differences were prime considerations for this application. A matrix of test cases was developed to highlight the impact that each of these considerations had on the accuracy of the fit process. Initially, the matrix included eight executions with the following combinations of the prime factors:

Table 4.14 Factors Considered in SST and Cowell POE Fits

	50x50	Solid Earth Tides	FK5
Procedure 1			
Procedure 2	•		
Procedure 3		•	
Procedure 4	•	•	
Procedure 5			•
Procedure 6	•		•
Procedure 7		•	•
Procedure 8	•	•	•

Procedures 5-8 in Table 4.14 correspond to test cases 1-4 in Table 4.13. Procedures 1-4 in Table 4.14 provided little additional information, and were not included as part of the TOPEX POE test cases presented here.

The initial fit of the TOPEX POEs (procedure 1 in Table 4.14) represented the capability present in the VAX version of Draper R&D GTDS prior to the work

of Fonte (i.e., 21x21 gravity field, no solid earth tides, FK4 theory). Each consideration was added to the modeling and fit process one at a time to isolate individual contributions until all existing capabilities were included.

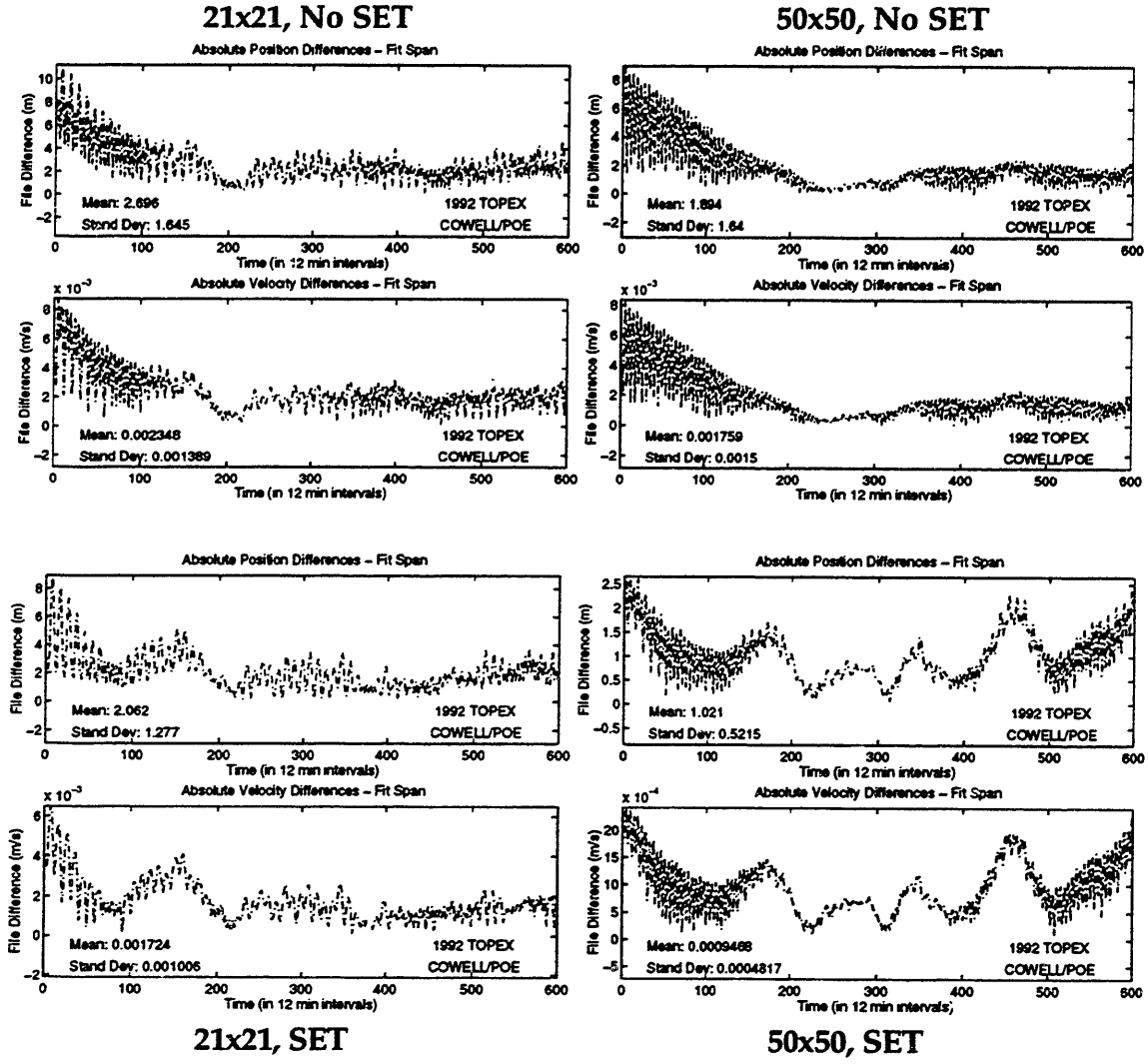

Figure 4.10 Cowell Fits to the POEs With Various Force Models

The primary effects were seen with the addition of the 50x50 and solid earth tides to the force modeling. Although it provides consistency between the

observation source and orbit determination process, the FK5 theory contributed little to the POE fit results. Therefore, comparison of the FK4 and FK5 results will not presented here. The fit results of the remaining combinations for the Cowell propagator in the FK5 systems are shown below in Figure 4.10.

Figure 4.10 shows that the addition of the higher order gravity field model and solid earth tides resulted in the anticipated improvement in fit accuracy. Increasing the order of the gravity field from 21 to 50 had a noticeable impact on the radial and along-track components, while introduction of solid earth tides resulted in significant reduction of the cross-track error. It is interesting to note that the *combination* of both 50x50 and solid earth tides provides a significant improvement in the overall fit accuracy (not consideration of one individual factor).

The semianalytic results revealed similar patterns in terms of improvement in the POE fit accuracy due to introduction of upgraded force modeling. Only the highest accuracy result (with 50x50 and solid earth tides) is shown here in Figure 4.11.

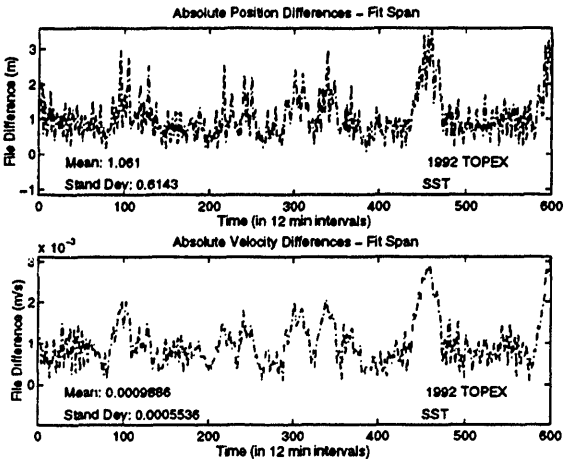

Figure 4.11 SST Fit to POEs With 50x50 and Solid Earth Tides

Although Figure 4.10 indicates that the solid earth tides were most likely implemented properly, there has been no verification thus far. One way to test the incorporation of the solid earth tides is to compare an orbit containing solid earth tide modeling with one that does not. By limiting the remaining force modeling to only third body effects over the time period for the orbit presented in Figure 4.11, comparison of these two orbits provided an estimate of the expected impact that solid earth tides had. Such a comparison was performed for both Cowell and SST perturbation techniques. The results are shown below in Figure 4.12.

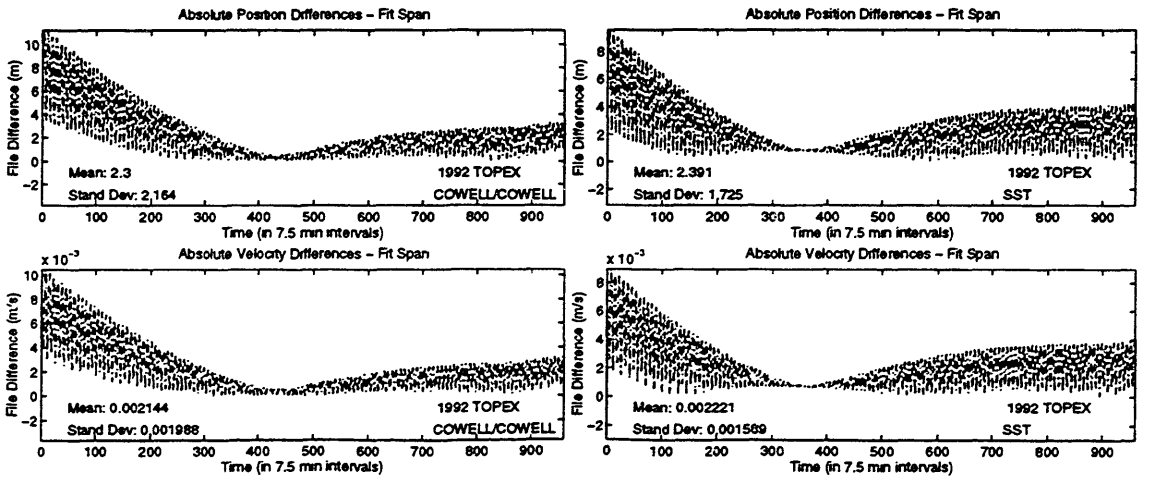

Figure 4.12 Expected Total Effects of Solid Earth Tides

The solid earth tides primarily affect the cross-track component for the TOPEX orbit. The signature associated with the expected cross-track errors (seen in Figure 4.13) matches that seen in the actual 50x50/No Solid Earth Tides fit to the POEs (see Figure G.94 in Appendix G), indicating that the implementation within the Cowell and SST perturbation methods is correct.

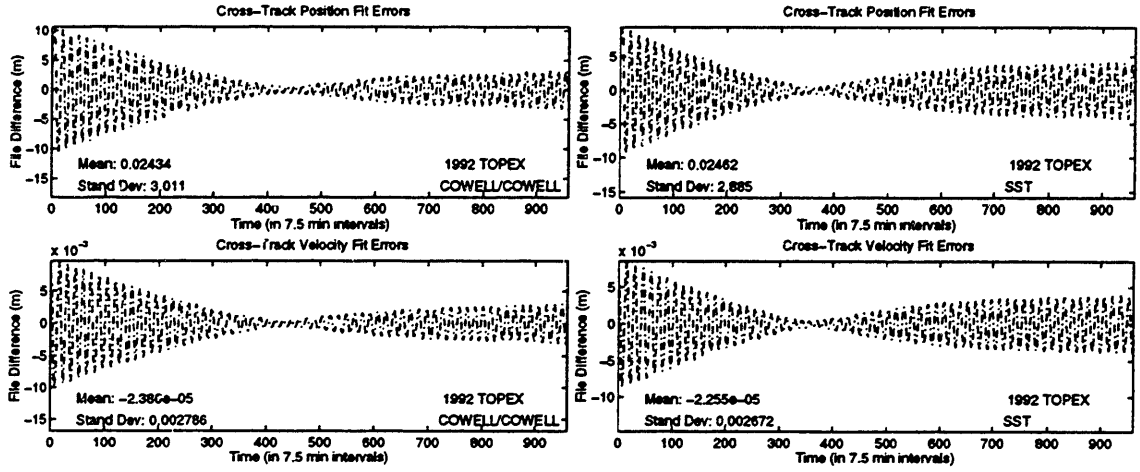

Figure 4.13 Expected Cross-Track Errors Due to Solid Earth Tides

Figure 4.10 also suggests that the ITOD coordinate system modeling and output options work properly, but falls short of absolute proof. Since the TOPEX POE vectors are provided in both the ITOD and ECEF coordinate systems, a fit using the ECEF POEs was compared to the results in Figure 4.10. The ECEF coordinate system is accepted as a viable input, modeling, and output option within R&D GTDS. The fit of the ECEF POEs was performed using 50x50, solid earth tides and FK5 theory for only the Cowell method. The absolute position and velocity residuals of the ECEF fit are shown below in Figure 4.14.

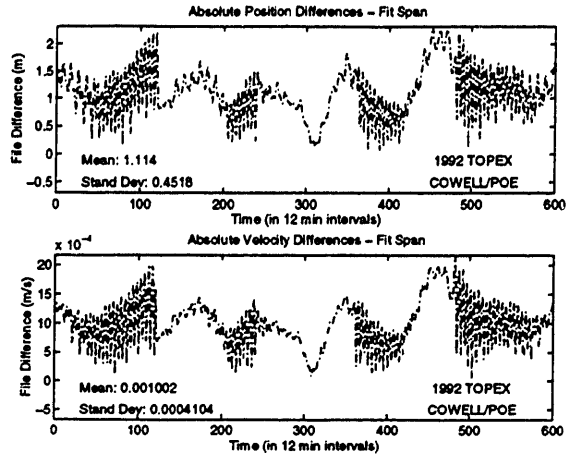

Figure 4.14 Cowell Fit to ECEF POEs

Although comparison of the ECEF orbital elements and radial/cross-track/along-track differences provides little insight (because of the rotation of the earth), the ECEF absolute position errors are analogous to the ITOD absolute position differences. Despite the slight variations existing between Figures 4.10 and 4.14, the magnitude of the fit errors is similar for both the ITOD and ECEF POEs, suggesting that the ITOD modeling and output options are properly implemented.

4.8 Chapter Summary

This chapter demonstrates that the J2000 and ITOD coordinate systems, and solid earth tide modeling were properly implemented in the VAX version of Draper R&D GTDS. The baseline source code was validated through a combination of test cases presented by Fonte [20] and Metzinger [47]. Proper incorporation of the FK5 theory was demonstrated by relating results to the existing FK4 theory (Figures G.14-47). Validation of the solid earth tide modeling and ITOD coordinate systems relied heavily upon fitting the high quality TOPEX POEs. Expected contributions of the solid earth tide

perturbation were synthesized and compared to observed effects (Figures G.90, G.94, G.141, and G.145), while a fit of the ITOD POEs was measured against an ECEF fit (Figure G.150). The POE fits indicate that Draper R&D GTDS has the ability to model the motion of a spacecraft with TOPEX orbital characteristics to about two meters, but error signatures suggest the possibility for futher improvement (Figures G.114-122 and G.126-134). The results presented in this chapter imply that the new capabilities are operating as intended and can be used in navigation solution experiments.

Chapter 5

Precision Orbits From GPSR Navigation Solutions

5.1 Introduction

The culmination of this research is the evaluation of the navigation solutions as an observation source in precision orbit determination. This chapter summarizes the results of a series of test cases for each of the three satellites introduced in section 1.7 (TOPEX, TAOS, and EUVE). The orbits derived by fitting the navigation solutions with the Draper R&D GTDS differential correction program using both Cowell and SST techniques are evaluated against the high accuracy POEs, and the content of the variations discussed. The TAOS and EUVE POEs are fit in a manner similar to the TOPEX POEs to indicate the ability of Draper R&D GTDS to model motion of spacecraft in low-earth orbit. The chapter concludes with a discussion of the feasibility of using navigation solutions in an orbit determination scheme.

5.2 Analysis Procedures

The primary analysis technique used to determine the accuracy of the orbits generated from navigation solutions was comparison to the POEs. The comparison process was performed by a combination of a set of FORTRAN

routines and MATLAB scripts. (Please reference Appendix C for a description of this software.) Where ITOD POEs were available (for TOPEX and TAOS), the differences were plotted in three manners:

- Cartesian coordinates
- Radial, cross-track and along-track components
- Orbital elements

Because the EUVE POEs were provided only in a non-inertial coordinate system (ECEF), only the Cartesian coordinates were compared.

5.3 TOPEX Experiments

TOPEX navigation solutions and POE vectors were obtained from JPL for the time period spanning December 23-29, 1992. A fit of the POE vectors, as described in the previous chapter, revealed that the ability of Draper R&D GTDS to model the spacecraft motion was around a couple of meters. With such tight agreement, it was thought that the navigation solutions from this spacecraft would provide a genuine assessment of the accuracy of the *process* of fitting the navigation solutions.

5.3.1 Accuracy Assessment of the Individual Navigation Solutions

Before any differential corrections were performed with the navigation solutions, it was deemed desirable to evaluate their individual accuracy. Comparison to the POEs indicated that use of individual navigation solutions to generate an ephemeris was impractical because of the uncertainty in the

solution. The typical (mean) errors highlighted in Figure 5.1 are unacceptable when propagated ahead over day-long time periods. In addition, there are several instances where large excursions (up to 4 km errors) from the normal error range occur and last over tens of minutes.

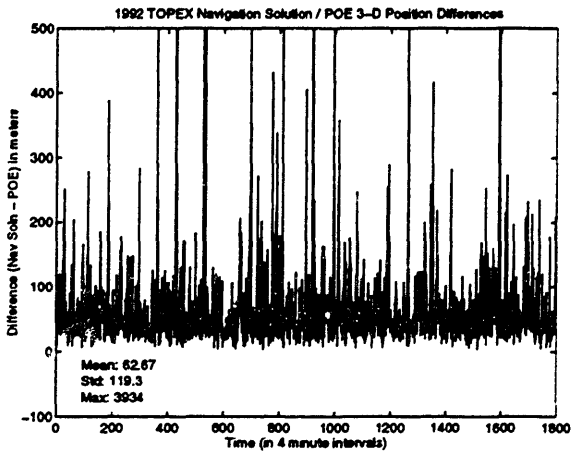

Figure 5.1 Differences Between TOPEX Navigation Solutions and POE Vectors

It should be noted that this comparison is based upon the actual navigation solutions provided (i.e., prior to accounting for the rotation bias discussed in section 2.6). However, the effects of rotating to a proper ECEF frame are lost in the noise of the individual solutions, such that comparison of the "rotated" solutions reveals similar statistics.

5.3.2 Orbit Determination from TOPEX GPSR Navigation Solutions

Although the inaccuracies of the navigation solutions prohibit their use individually, most of the noise in the representation of the orbit can be removed by fitting the information over time. Evaluation of orbit determination based upon a fit of the navigation solutions from the TOPEX Motorola GPS Demonstration Receiver (GPSDR) revolved around three

executions of the Draper R&D GTDS differential correction program. These cases are summarized below in Table 5.1.

Table 5.1 TOPEX Navigation Solution Experiments

Case	Description	References in Appendix H
1	Cowell five day fit of TOPEX navigation solutions with two day prediction	Figures: H.2-H.13
2	SST five day fit of TOPEX navigation solutions with two day prediction	Figures: H.14-H.24
3	Cowell four day fit of TOPEX navigation solutions with three day prediction	Figures: H.26-H.37

The first two experiments involved fitting a five day span of the "rotated" navigation solutions using Cowell and SST to generate ephemerides representative of a week-long period (extending two days past the end of the fit span) for comparison to the POEs. The third experiment, which used Cowell techniques, investigated the effects of reducing the observation span from a five day period to only four days. This test was designed to indicate how much data was necessary to obtain an estimate sufficiently representative of the satellite's orbit.

The dynamic models used in these studies included gravity, solar radiation pressure, lunar/solar point masses, atmospheric drag, and lunar/solar tidal effects. The Joint Gravity Model field 2 (JGM-2) of degree and order 50, implemented in the workstation version of Draper R&D GTDS in 1993 by Fonte [20], was used to model the geopotential effects. A 4x4 partial derivatives model was used for non-spherical potential in the variational

equations. The force due to solar radiation pressure, which is dependent upon the relative ratio of the surface area to the spacecraft mass (estimated to be 0.01167 for these studies), was determined from a cylindrical macro model that considers whether the satellite is in the sunlight or shadow of the earth. A standard Jacchia-Roberts atmospheric model that represents density as a function of altitude and exospheric temperature was used for drag effects. Solar and lunar point mass and tidal effects were included as well. Table 5.2 summarizes the dynamic models used for TOPEX studies. All executions utilized FK5 theory, and integration was performed in the mean equator and equinox of J2000 coordinate system.

Table 5.2 Orbit Dynamic Models Used in TOPEX Analysis

Perturbation	Description
Earth's gravity	JGM-2 50x50; 4x4 partials
Solar Radiation Pressure	Cylindrical macro model
Atmospheric Drag	Jacchia-Roberts
Lunar/Solar Third Body	Point Mass
Lunar/Solar Tides	Love number (0.29)

The estimated state included a representation of the satellite orbit and coefficients for atmospheric drag and solar radiation pressure. The different components of the state for Cowell and SST are identified in Table 5.3.

Table 5.3 Estimated State Parameters

Cowell	SST
Epoch position and velocity in integration coordinate system (mean of J2000)	Epoch mean equinoctial elements in integration coordinate system (mean of J2000)
Drag Parameter (ρ_1)	Drag Parameter (C_d)
SRP Parameter (C_r)	SRP Parameter (C_r)

Estimation of the solar radiation and drag parameters was designed to improve perturbation modeling.

The semianalytic method employed an averaged orbit generator (AOG) in conjunction with the short periodic generator (SPG) as discussed in section 2.3.3. The AOG included zonal harmonics, third body point mass, lunar/solar tidal effects, solar radiation pressure, drag and tesseral resonance in its force model. Resonance terms with periods greater than one day were considered, and a step size of a quarter of a day was used. Short periodic options included zonal, third body, M-daily, tesseral, J_2^2, and J_2/M-daily coupling. The runs were truncated based upon eccentricity to improve computational efficiency after a "full scale" run determined the significance of the short periodic coefficients. The specific terms truncated are seen in the overrides files found in Appendix H.

The first two executions used the ECEF navigation solutions over a five day period from December 23-28, 1992 to generate an estimate of the orbit over a

week-long span (extending two days past the end of the fit period). The difference between these two runs lies in the perturbation technique used; the first utilized the high precision Cowell method, while the second employed the computationally efficient semianalytic method. The results of these fits are summarized in Table 5.4.

Table 5.4 Statistics From the TOPEX Navigation Solution Fit

	Position 1σ (m)	Semi-major Axis 1σ (cm)	Drag Factor	SRP Factor
Cowell	3.2178	2.232	2.782	13.208
SST	2.9247	1.455	20.719	14.369

The standard deviation values of the position and semi-major axis provide an indication of how well the orbit has been fit. For these cases, the initial state was determined to within about three meters in absolute position terms, and two centimeters in the semi-major axis. These uncertainties are significant because they propagate throughout the entire orbit and result in error growth for periods following the fit interval. The drag and solar radiation pressure factors listed are indicators of how well the coefficients are defined. The value listed is the ratio of the solve-for parameter (ρ_1 or C_d, and C_r) to their associated standard deviation values. The larger the factor number, the better defined the parameter becomes. In general, a number of ten or greater suggests that the parameter is observable. Although the drag factor for the Cowell experiment raises some concern about the viability of the drag parameter (ρ_1), the orbit appears to be well defined for these cases.

The week-long orbit generated from the fit was broken into two intervals: the five day fit interval, and the two day predict interval. The differences between the fit-generated orbit and the POE ephemeris were plotted in Cartesian coordinates, radial/cross-track/along-track components, and orbital elements. The overall position errors are depicted below in Figures 5.2 and 5.3.

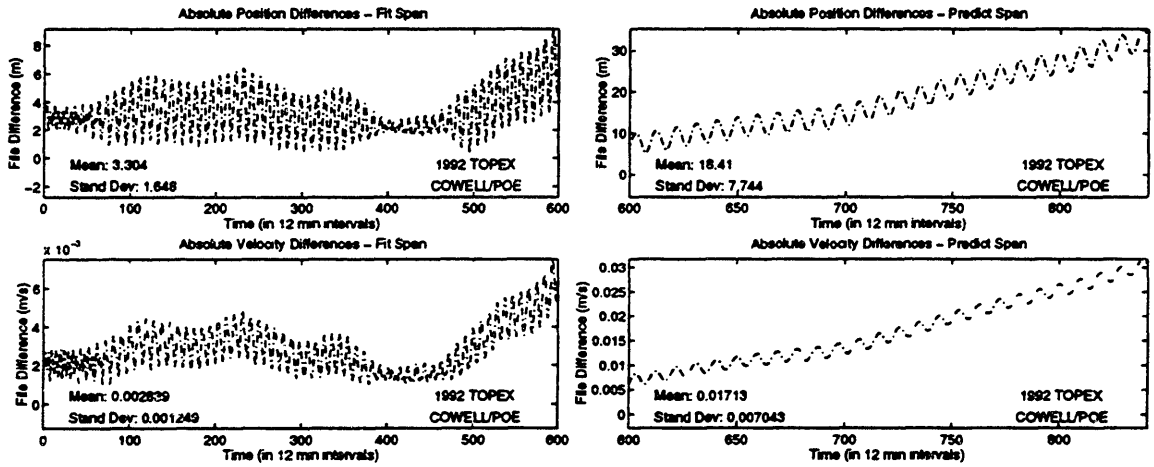

Figure 5.2 TOPEX Fit and Predict Position Errors for Cowell

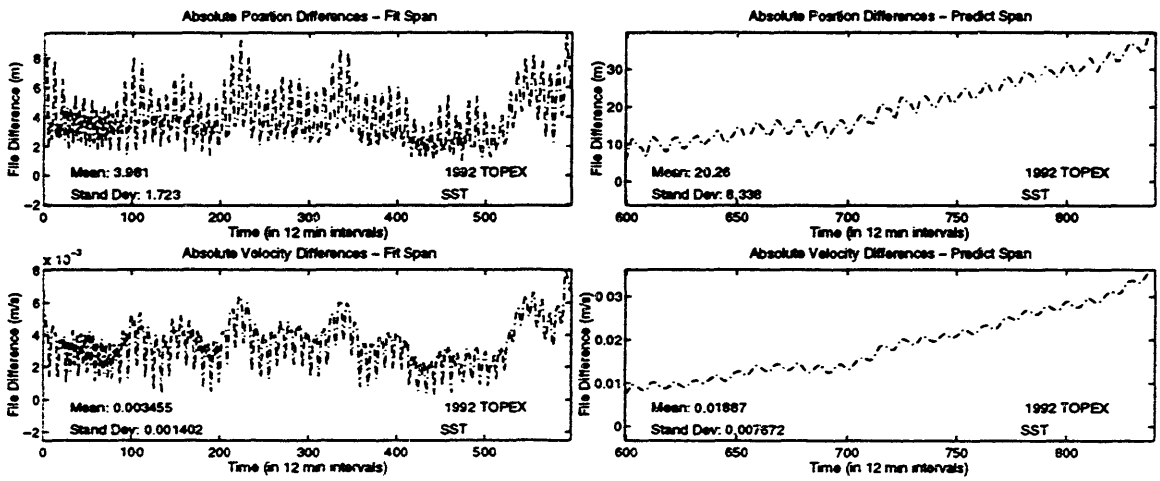

Figure 5.3 TOPEX Fit and Predict Position Errors for SST

The signatures seen in Figures 5.2 and 5.3 are typical, with the error bounded during the fit span, but experiencing growth in the predict interval. Two

items are of particular interest here. First, the orbits determined using SST methods are as accurate as the high precision Cowell techniques, but offer the opportunity to provide these results with reduced computational times. Also, the predict error growth is only about 10-15 meters per day, which is well within the navigation requirements for many applications.

The radial, cross-track, and along-track components of the errors offer an alternative expression that provides insight into how the differences manifest themselves with respect to the orbital plane. The maximum component variation and standard deviation of the errors for the fit and predict intervals are presented in Tables 5.5 and 5.6.

Table 5.5 TOPEX GTDS Solutions vs. NASA POEs (5 day fit)

	Radial		Cross-Track		Along-Track	
	Max Diff (m)	*1 σ (m)*	*Max Diff (m)*	*1 σ (m)*	*Max Diff (m)*	*1 σ (m)*
Cowell	1.4920	.9257	2.6768	1.3140	9.1519	3.2960
SST	2.2109	.9978	3.8940	2.0160	9.5222	3.6190

Table 5.6 TOPEX GTDS Solutions vs. NASA POEs (2 day predict)

	Radial		Cross-Track		Along-Track	
	Max Diff (m)	*1 σ (m)*	*Max Diff (m)*	*1 σ (m)*	*Max Diff (m)*	*1 σ (m)*
Cowell	1.5542	.9624	2.9418	1.7180	35.1854	7.7750
SST	1.4998	.6880	1.5530	.7900	39.7600	8.4590

These cases are derivatives of the TOPEX experiments presented in [8], with variations arising in the testing protocol due to introduction of the new capabilities discussed in Chapter 3. The differences are summarized by:

- FK5 theory was used in place of the existing FK4 theory.

- Ephemerides were generated in the ITOD coordinate frame and compared to the ITOD POEs. Previously output was generated in mean equator and equinox of 1950 and rotated to ITOD externally, while the POEs were rotated from ECEF to ITOD by the same process.

- Solid earth tides due to lunar and solar perturbations were modeled.

To highlight the impact that these improvements had on fitting the navigation solutions, the results from [8] and Tables 5.5/5.6 were compared and summarizes in Tables 5.7 and 5.8.

Table 5.7 Effect of Solid Earth Tides on TOPEX Results (Fit Span)

	Max Radial Error (m)		Max Cross-Track Error (m)		Max Along-Track Error (m)	
	No SET	*SET*	*No SET*	*SET*	*No SET*	*SET*
Cowell	1.464	1.492	11.100	2.677	7.784	9.152
SST	2.043	2.211	12.003	3.894	13.548	9.522

Table 5.8 Effect of Solid Earth Tides on TOPEX Results (Predict Span)

	Max Radial Error (m)		Max Cross-Track Error (m)		Max Along-Track Error (m)	
	No SET	*SET*	*No SET*	*SET*	*No SET*	*SET*
Cowell	1.523	1.554	11.764	2.942	22.244	35.185
SST	1.703	1.500	12.791	1.553	34.317	39.760

The impact of including solid earth tides was evident from the reduction in the cross-track errors in both the fit and predict spans. Review of the POE fits presented in the previous chapter and Appendix G (see Figures 4.10, 4.13, and G.130) shows that the same phenomenon occurred when solid earth tides were introduced and should be expected here as well.

The significant increase in the along-track error, however, for the Cowell case was unexpected. It can be attributed to the fact that the drag parameter was not as well defined for the solid earth tide case as it was previously (drag factor of 2.78 vs. 6.217). It is expected that either lengthening or shortening the fit span length may improve the observability of the drag parameter. Lengthening the fit span provides more information on the orbit to the fit process and could result in a more confident value for the drag parameter.

However, it could be the case that the fit span is too *long* for the drag coefficient the become well defined. Because Draper R&D GTDS only has the capability of solving for one drag parameter over the entire fit span, a highly dynamic atmosphere creates drifts in the error signatures during the fit span. A slight drift is observed in Figure 5.2 towards the end of the fit span, and could conceivably be the result of an improperly estimated drag parameter.

An additional test with a shorter fit span was introduced to test this hypothesis.

The final experiment for the TOPEX navigation solutions involved a four day fit span and three day predict interval. Because the drift was most notable using Cowell techniques, the final test was performed with this method. The remainder of the variables, including the presence of solid earth tides in the force modeling, were unaltered. The along-track errors, which dominate the total position differences, for the four and five day cases are shown below.

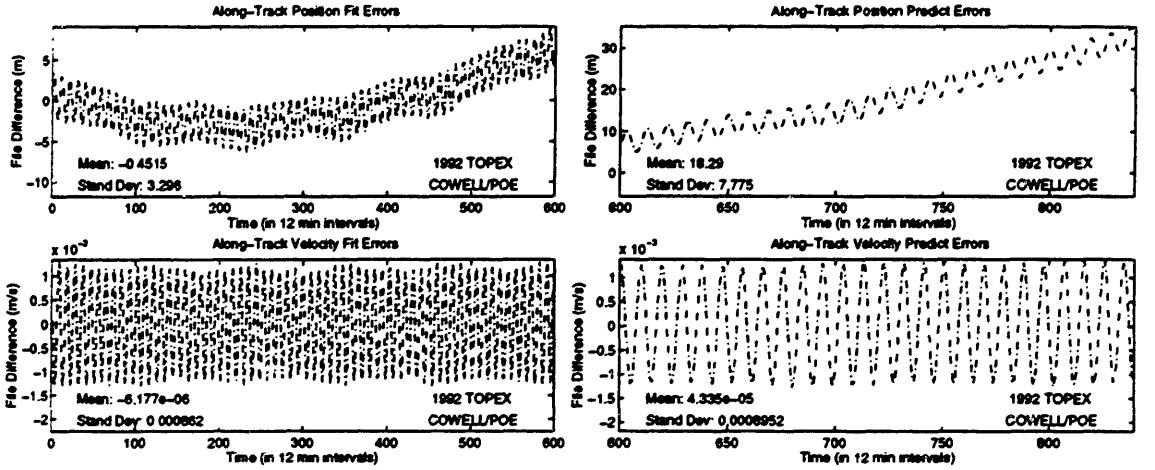

Figure 5.4 Along-Track Fit and Predict Errors for Five Day Fit Span

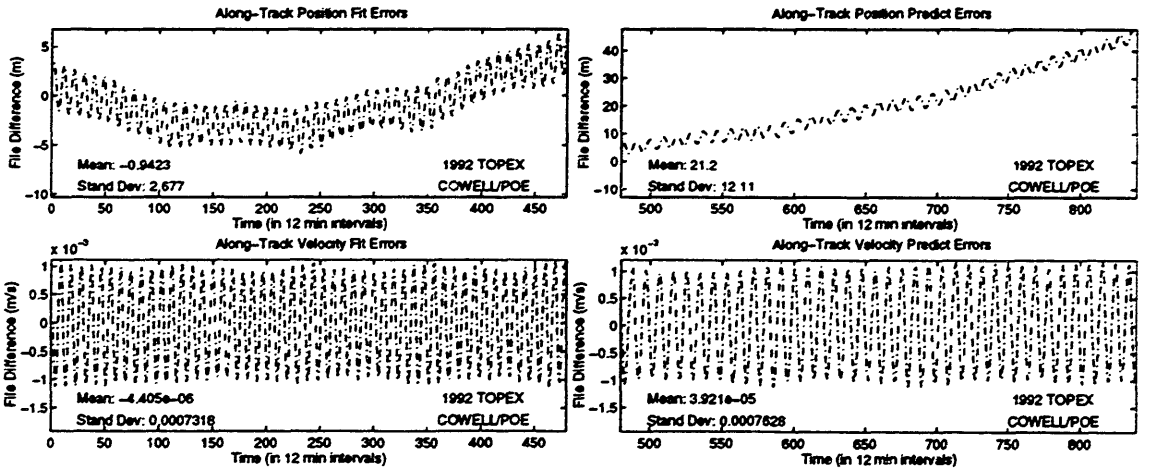

Figure 5.5 Along-Track Fit and Predict Errors for Four Day Fit Span

Figures 5.4 and 5.5 indicate that the reduction in the fit span had little impact on the overall fit or predict accuracy. The slight drift at the end of the fit span, although not as distinct, remained for the four day fit. The along-track drift, despite experiencing a maximum error of 47 meters due to the lengthened predict span, continued at an admirable rate of about 10-15 meters per day. The fit statistics, however, indicate that the orbit and drag parameter were not as defined for the four day case as it was for the five day experiment.

Table 5.9 Statistical Comparison of Cowell Four and Five Day Fits

	Position 1σ (m)	Semi-major Axis 1σ (cm)	Drag Factor	SRP Factor
Four Day	3.550	2.946	1.072	9.447
Five Day	3.218	2.232	2.782	13.208

One possibly significant source of error is the mismodeling of the geomagnetic activity level in the evaluation of the drag force acting on the satellite. The TOPEX experiments used the Jacchia-Roberts atmospheric density model file in representing the atmospheric activity during the time periods of interest. To evaluate the impact that geomagnetic mismodeling had on the five day experiment, the Jacchia-Roberts values were compared to a set of "truth" values distributed by the National Geophysical Data Center (NGDC). These geomagnetic activity levels (given here as a three hour K_p values) are determined from a network of thirteen ground-based observatories in a non-real time mode, and can be considered a "true" representation of the magnetic activity. The differences between the Jacchia-

Roberts and NGDC values are plotted below, along with the fit span along-track errors.

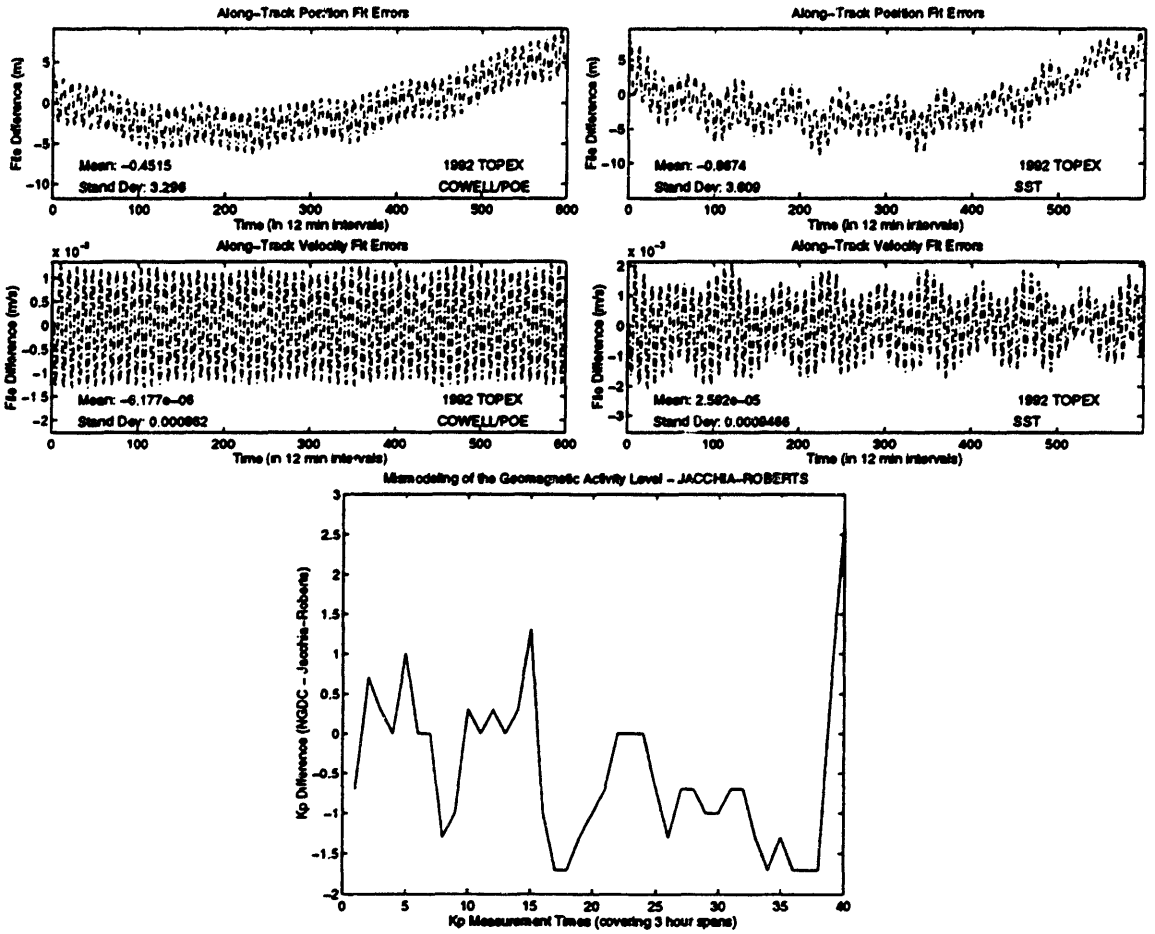

Figure 5.6 Correlation of Differences Between Jacchia-Roberts/NGDC Geomagnetic Activity Levels and Along-Track Errors

Although the along-track errors are small during the fit span, the signature experienced was somewhat similar to the pattern found in the errors in the geomagnetic activity level. No large excursions are seen in either plot that would help to validate the hypothesis that the remaining along-track errors are due to variation from the actual geomagnetic values.

The natural impulse is to attempt to fit the navigation solutions over a longer time span to better define the orbit and the drag parameter. However, at the altitude of TOPEX (~1330 km), the atmosphere has such a slight impact that it is very difficult to define its effects, and lengthening the fit span would not likely result in any significant improvements. Five days seems to be optimal for determining the orbit of a TOPEX-class satellite using navigation solutions.

Another feature evident in the TOPEX navigation solution analysis is the presence of a significant source of mismodeling in the fit process. This mismodeling is most evident in the element difference plots shown below.

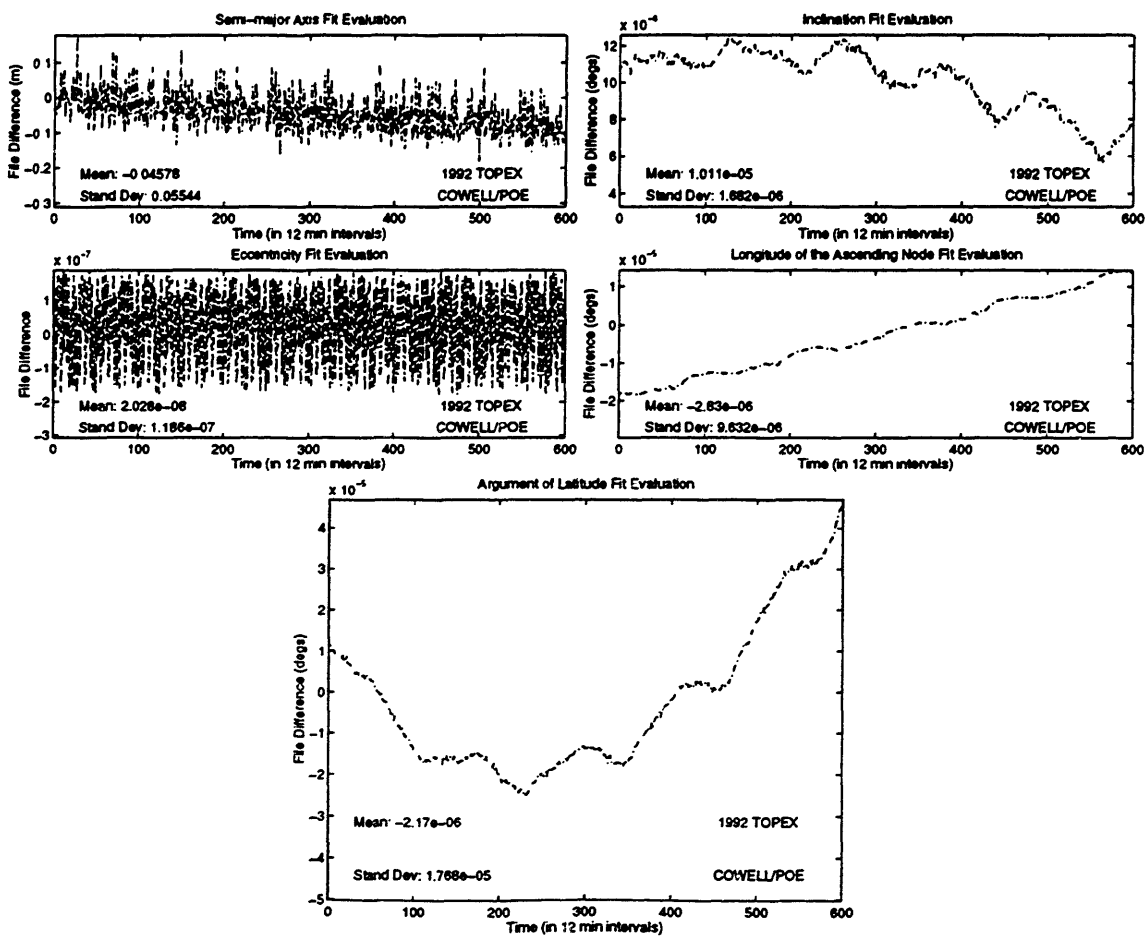

Figure 5.7 Cowell Orbital Element Differences for TOPEX Five Day Fit

The drift in the semi-major axis error and the quadratic signature of the argument of latitude differences are the two most striking features of Figure 5.7. In addition, there is a twenty-four hour signature (most noticeable in the inclination), all of which appear to be attributable to some sort of mismodeling. The SST plots revealed similar content, with the exception of an additional superimposed twelve hour signature in the inclination differences. This could be due to the truncation of the tesseral m-daily terms (reference Figure H.16).

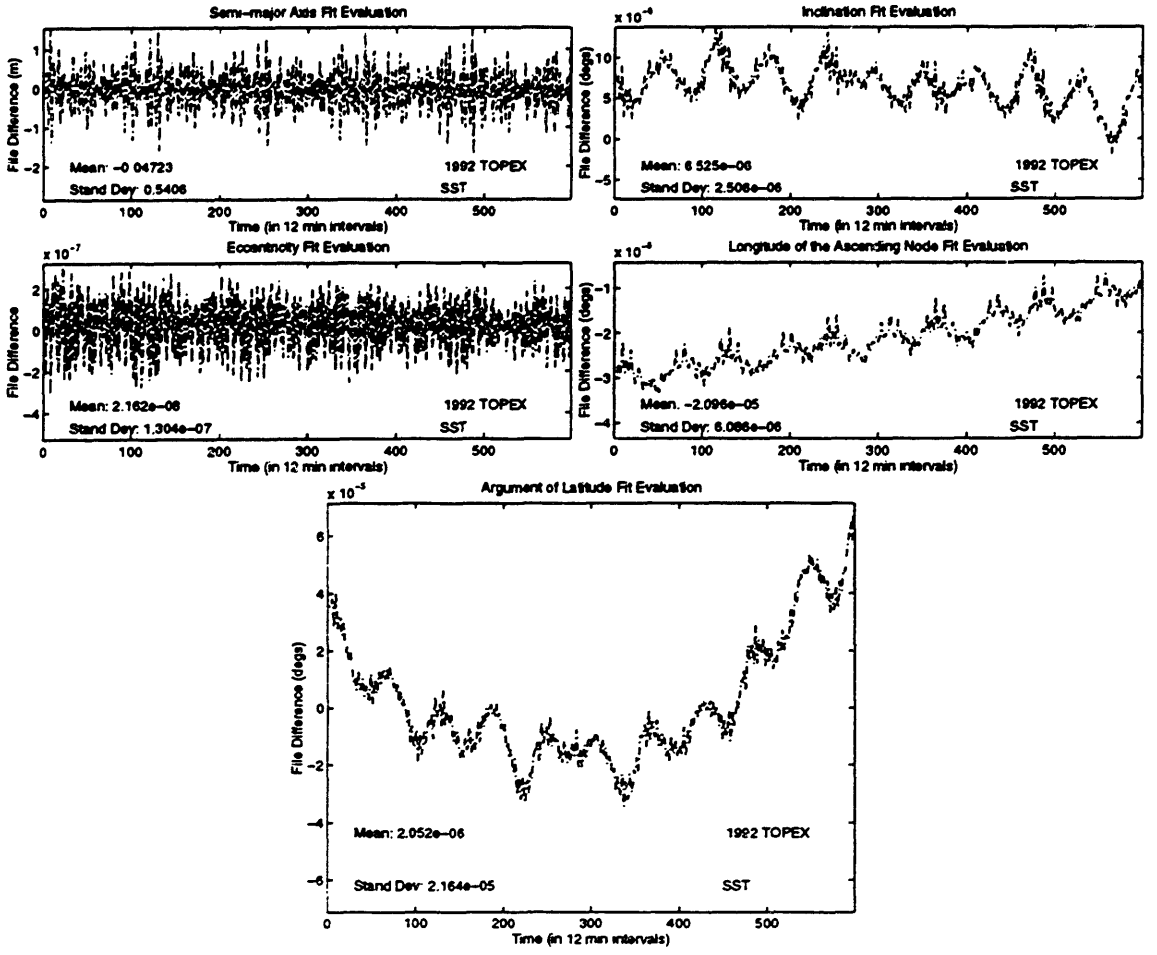

Figure 5.8 SST Orbital Element Differences for TOPEX Five Day Fit

Capturing the effects of this error source could significantly improve the fit (and predict) accuracies using navigation solutions. Possible sources of the mismodeling include earth albedo pressure and ocean tides.

5.4 TAOS Experiments

Prior to experimentation with the TAOS navigation solutions, the POEs were fit in a manner similar to the TOPEX POEs. These fits provided the unique opportunity to measure the ability of Draper R&D GTDS to model the forces acting on a satellite in low earth orbit. After the POE fits quantified the noise inherent to the orbit determination process, the navigation solutions were evaluated as an observation source for the heavily drag-perturbed spacecraft.

5.4.1 Orbit Determination from the TAOS POEs

Despite not possessing the level of accuracy of the TOPEX POEs (15 cm), the TAOS POEs (3 m) provided a valuable reference trajectory to compare against the orbits derived from the navigation solution fits. The noise introduced by the orbit determination process and the uncertainty in the POE solutions was investigated through three fits to the POEs of varying time intervals (five, two and one day periods), as indicated in Table 5.10.

Table 5.10 TAOS POE Experiments

Case	Description	References in Appendix H
1	Cowell one day fit of TAOS POEs	Figures: H.38-H.49
2	Cowell two day fit of TAOS POEs	Figures: H.50-H.61
3	Cowell three day fit of TAOS POEs	Figures: H.62-H.73

The dynamic models included for the TAOS orbit were similar to those considered for the TOPEX experiments (see Table 5.11). Because the altitude of TAOS is significantly lower than TOPEX, the solar radiation coefficient was not included as part of the solve-for state, but the force was still evaluated using a pre-stored default value for the coefficient. The drag parameter was expected to be an important factor in modeling the low earth orbit, and was solved-for in addition to the initial position and velocity. Integration was performed in the mean of J2000 coordinate system. The high level of agreement between the Cowell and SST techniques for the TOPEX fits to the POEs dictated that only one method was necessary to evaluate Draper R&D GTDS's ability to model the TAOS orbit. The Cowell techniques were chosen to perform this function.

Table 5.11 Orbit Dynamic Models Used in TAOS Analysis

Perturbation	Description
Earth's gravity	JGM-2 50x50; 4x4 partials
Solar Radiation Pressure	Cylindrical macro model
Atmospheric Drag	Schatten-Jacchia-Roberts
Lunar/Solar Third Body	Point Mass
Lunar/Solar Tides	Love number (0.29)

The first experiment with the TAOS POEs involved a five day fit over May 28-June 1, 1994, using the force models described in Table 5.11. This execution was designed to mirror the TOPEX process (with the exception of the modeling differences discussed above) so that the effects of drag at a lower altitude could be seen. The fit statistics are shown in Table 5.12.

Table 5.12 TAOS Five Day POE Fit Statistics

Position 1σ (cm)	Semi-major Axis 1σ (cm)	Drag Factor
21.2688	0.1375	5980.1050

The drag factor normally would indicate that the essence of the drag perturbation is effectively captured for this fit span. However, because drag is a much more dynamic factor at these lower altitudes, fitting an orbit over a five day period with only one drag parameter induces large residuals. In fact, the statistics in Table 5.12 are products of the orbit produced after twenty iterations in the differential correction process, indicating difficulty in fitting a full five days of information. Because drag acts in a direction opposite to the motion of the spacecraft, this phenomenon is best observed in plotting the along-track residuals (as seen below in Figure 5.9).

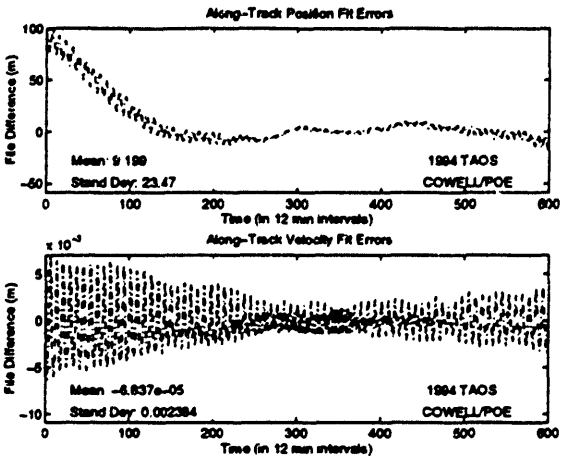

Figure 5.9 Along-Track Error Pattern for Five Day Fit Interval

The residuals at the beginning of the fit span indicate that the estimated drag parameter is more suited to the last three days or so of the fit interval than the beginning. Thus, despite the confidence in the drag parameter expressed in Table 5.12, residuals persisted during the fit span due to mismodeling of the drag over the entire period.

These large errors led to a second experiment, where the fit interval was reduced to two days, beginning on May 28. The intent of this case was to capture a time length where the drag parameter was more representative of the entire span. The fit statistics are summarized in Table 5.13.

Table 5.13 TAOS Two Day POE Fit Statistics

Position 1σ (cm)	Semi-major Axis 1σ (cm)	Drag Factor
6.9672	0.0836	1491.9744

The reduction in the position and semi-major axis standard deviations indicates that the two day interval is more conducive to providing a

confident representation of the orbit. The drag parameter remains well-defined for this time period, and, as indicated in Figure 5.10, the drag perturbations were modeled much more accurately for this fit interval.

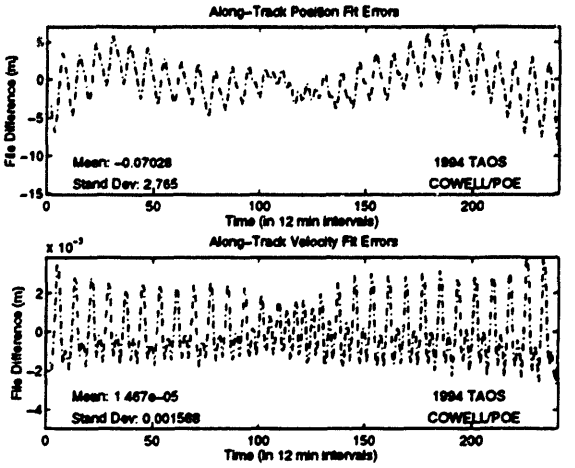

Figure 5.10 Along-Track Error Pattern for Two Day Fit Interval

The drift experienced in the beginning of the five day fit experiment is noticeably absent from Figure 5.10.

The final fit to the TAOS POEs involved a reduced fit span of one day duration, beginning on May 28. The purpose of the reduction was to test how much information was necessary to provide the same quality orbit as the two day fit.

Table 5.14 TAOS One Day POE Fit Statistics

Position 1σ (cm)	Semi-major Axis 1σ (cm)	Drag Factor
6.5365	0.1817	251.3853

The fit statistics for the one- and two-day intervals are not significantly different, even though the drag factor is an order of magnitude less for the one-day fit. The similarity in the estimated orbits is seen in Figure 5.11.

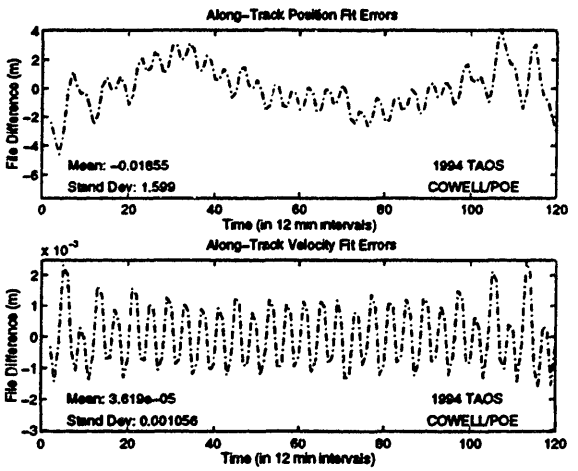

Figure 5.11 Along-Track Error Pattern for One Day Fit Interval

The beginning and end of the fit span for the two day case is slightly less accurate than the one day case, but the majority of the content is within the same range for both experiments.

One additional item of interest for the TAOS POE fits was a discrete jump observed at the day boundary. The jump was most noticeable in the inclination and nodal errors for the two day case (seen below in Figure 5.12).

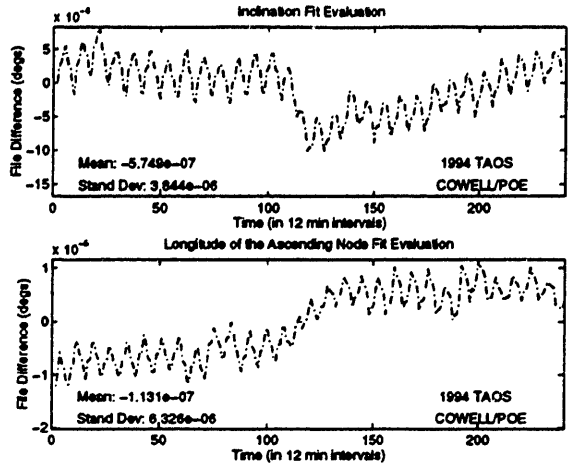

Figure 5.12 Inclination and Nodal Error Pattern for Two Day Fit Interval

This discrete jump is believed to be a product of the manner in which the POE files were created. Guinn indicates that the orbits were developed in thirty hour increments [28]. Since six hours of overlap exist between two adjacent time periods, a decision has to be made as to which solutions to use for that time period. It is unclear whether the orbits are continuous (smooth) over these overlapping time periods. Variations between the two overlapping orbits could create the artifacts in Figure 5.12.

The results from these three cases involving fitting the TAOS POEs indicated that the ability of Draper R&D GTDS to model the perturbations for the TAOS orbit was heavily dependent upon the length of the interval used for the fit process. In particular, for a TAOS-class, drag-perturbed orbit, an excessive fit span results in large residuals due to the dynamic nature of the drag parameter. One and two day intervals, which appear to be optimal, reveal that GTDS can model the spacecraft's motion to within about ten meters during the fit span.

5.4.2 Orbit Determination from TAOS GPSR Navigation Solutions

As was the case for TOPEX, the accuracy of the individual navigation solutions was assessed prior to orbit determination experimentation. The TAOS AST V receiver was evidently free from the rotation bias experienced with the GPSDRs on-board TOPEX and EUVE. The differences between the individual navigation solutions and POE vectors over a three day interval are shown below.

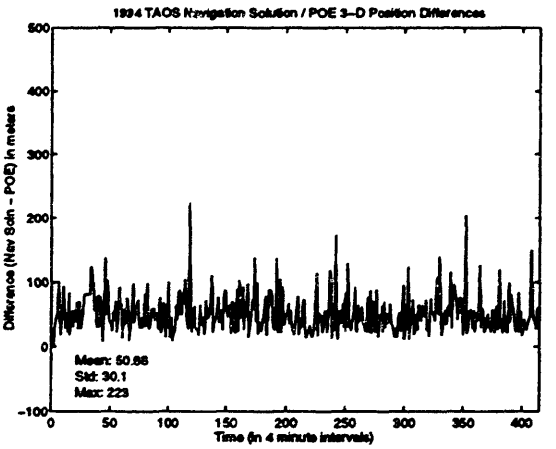

Figure 5.13 Differences Between TAOS Navigation Solutions and POE Vectors

The gross outliers noted for the TOPEX GPSDR (see Figure 5.1) are absent in the TAOS receiver. However, the typical 50 meter errors still prohibit use of individual navigation solutions for precision orbit prediction purposes.

The results of the TAOS POE fits presented in the previous section indicated that the selection of the fit length would be an important factor in the evaluation of the navigation solutions as an observation source.

Experiments with one-, two-, and three-day fit intervals with fit strategies identical to the POE cases were performed to investigate this effect.

Table 5.15 TAOS Navigation Solution Experiments

Case	Description	References in Appendix H
1	Cowell one day fit of TAOS navigation solutions with three day prediction; Schatten file used	Figures: H.74-H.85
2	Cowell two day fit of TAOS navigation solutions with two day prediction; Schatten file used	Figures: H.86-H.97
3	Cowell three day fit of TAOS navigation solutions with one day prediction; Schatten file used	Figures: H.98-H.109
4	SST three day fit of TAOS navigation solutions with one day prediction; Schatten file used	Figures: H.108-H.121
5	Cowell three day fit of TAOS navigation solutions with one day prediction; Near-real time density file used	Figures: H.122-H.133
6	SST three day fit of TAOS navigation solutions with one day prediction; Near-real time density file used	Figures: H.134-H.145

Although the fits to the TAOS POEs indicated that a one day interval provided sufficient information for orbit determination using the POE vectors, uncertainty remained about the validity of this short span for fits involving the noisier navigation solutions. The statistics from this Cowell fit are summarized below in Table 5.16.

Table 5.16 TAOS One Day Navigation Solution Fit Statistics

Position 1σ (m)	Semi-major Axis 1σ (cm)	Drag Factor
6.6693	19.8295	0.7368

The small drag factor (less than one) indicated that the drag parameter was not well-defined over this one day period. The confidence in the representation of the orbit was not high, as indicated by the position and semi-major axis standard deviations. The combination of these uncertainties are reflected not only in the one day fit span, but also on a much larger scale in the three day prediction.

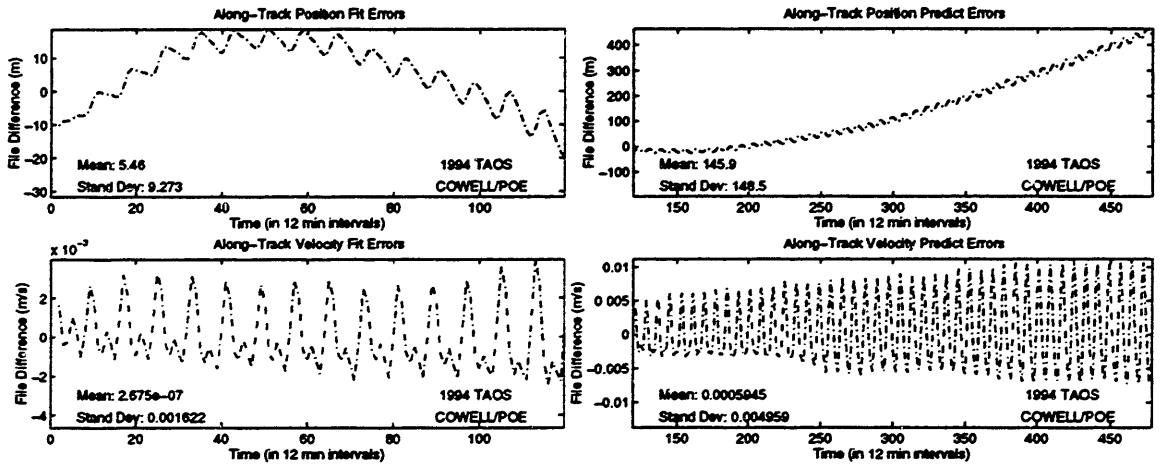

Figure 5.14 Along-Track Errors for One Day Fit and Three Day Predict Span

Table 5.17 TAOS GTDS Solutions vs. JPL POEs (1 day fit, 3 day predict)

	Radial		Cross-Track		Along-Track	
	Max Diff (m)	*1 σ (m)*	*Max Diff (m)*	*1 σ (m)*	*Max Diff (m)*	*1 σ (m)*
Fit	2.683	1.311	7.597	5.399	18.686	9.273
Predict	10.342	4.480	9.721	6.157	462.893	148.500

The parabolic shape of the along-track fit errors is representative of some sort of mismodeling (e.g., improper drag parameter), while the rapid drift (150 meters/day) seen in the prediction is a result of poorly defined initial conditions. In addition, the radial component experienced a slight growth (due to uncertainty in the semi-major axis), and the cross-track errors were at a level similar to the along-track differences, both indicators that the orbit was not well-defined (see Appendix H for the remainder of the error plots).

In an attempt to better capture the drag parameter and improve the estimate of the orbit, the fit span was then lengthened to two days. The remainder of the fit strategy was identical to the one day fit. The statistics of the two day fit indicate that increasing the amount of available information on the orbit boost the confidence in the estimate significantly.

Table 5.18 TAOS Two Day Navigation Solution Fit Statistics

Position 1σ (m)	Semi-major Axis 1σ (cm)	Drag Factor
4.9168	7.6999	12.3512

Although these numbers denote an improvement in the confidence of the orbit estimate, they do not translate into an improvement in the residual comparison to the POEs. The along-track plots (Figure 5.15) reveal a significant increase in the error, particularly at the beginning of the fit span.

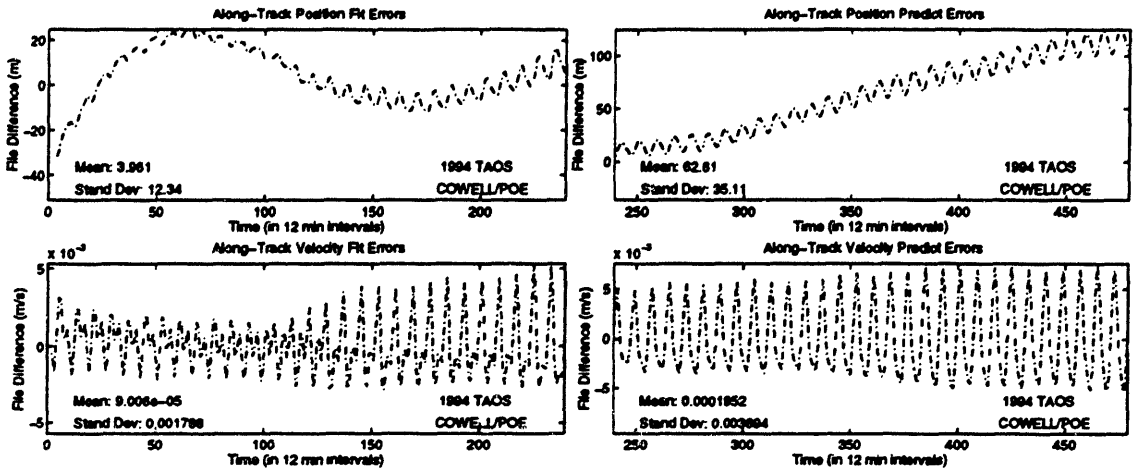

Figure 5.15 Along-Track Errors for Two Day Fit and Two Day Predict Spans

Table 5.19 TAOS GTDS Solutions vs. JPL POEs (2 day fit, 2 day predict)

	Radial		Cross-Track		Along-Track	
	Max Diff (m)	*1 σ (m)*	*Max Diff (m)*	*1 σ (m)*	*Max Diff (m)*	*1 σ (m)*
Fit	4.061	1.391	3.223	1.851	31.486	12.340
Predict	6.137	3.302	4.281	2.654	124.644	35.110

The imbalance in the error signature during the fit span indicates the possibility of a dynamic atmosphere during this time period, while the reduction in the predict growth rate (to about 50 meters/day) suggests the estimated initial conditions were much tighter than the one day case. The issue of the dynamic atmosphere is revisited in more depth following discussion of the third experiment.

Because the drag factor (~12) for the two day case raised some concern about the definition of the drag parameter, the fit interval was expanded to three days. In addition to the one- and two-day procedures, the SST perturbation techniques were employed for the three day experiment. The setup of the

AOG was the same as the TOPEX cases, while the SPG was not truncated to quite the degree as TOPEX. The overrides files exercising these options are found in Figure H.112.

Table 5.20 TAOS Three Day Navigation Solution Fit Statistics

	Position 1σ (m)	Semi-major Axis 1σ (cm)	Drag Factor
Cowell	4.1475	4.5432	42.3274
SST	4.1224	3.9358	201.4700

As expected, the extension to a three day fit interval resulted in improved observability of the drag parameter (see Table 5.20). However, once again, this increase did not represent a decrease in the overall fit errors, but rather a slight increase during the beginning of the span. The reduction of the uncertainty in the initial position and semi-major axis also resulted in improvement of the prediction errors (about 30 meters/day).

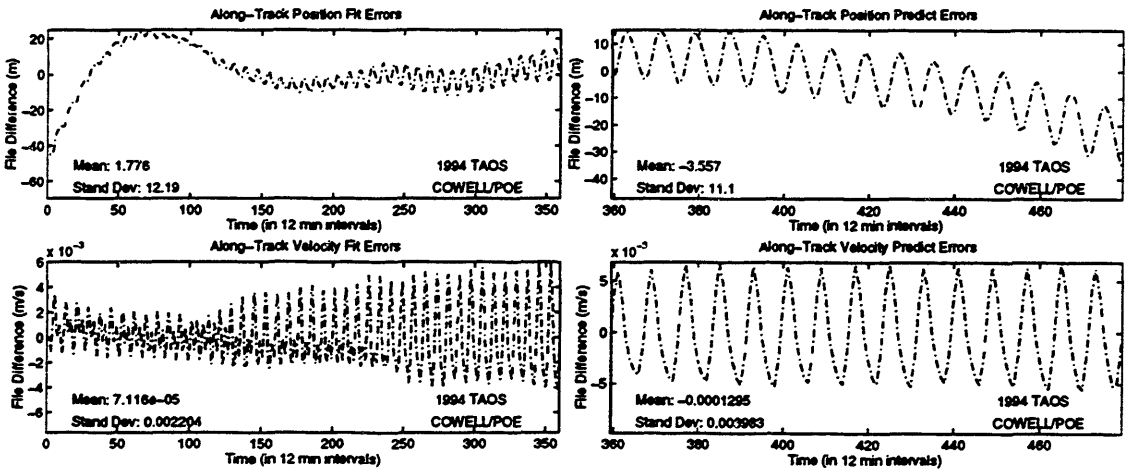

Figure 5.16 Cowell Along-Track Errors for Three Day Fit and One Day Predict Spans

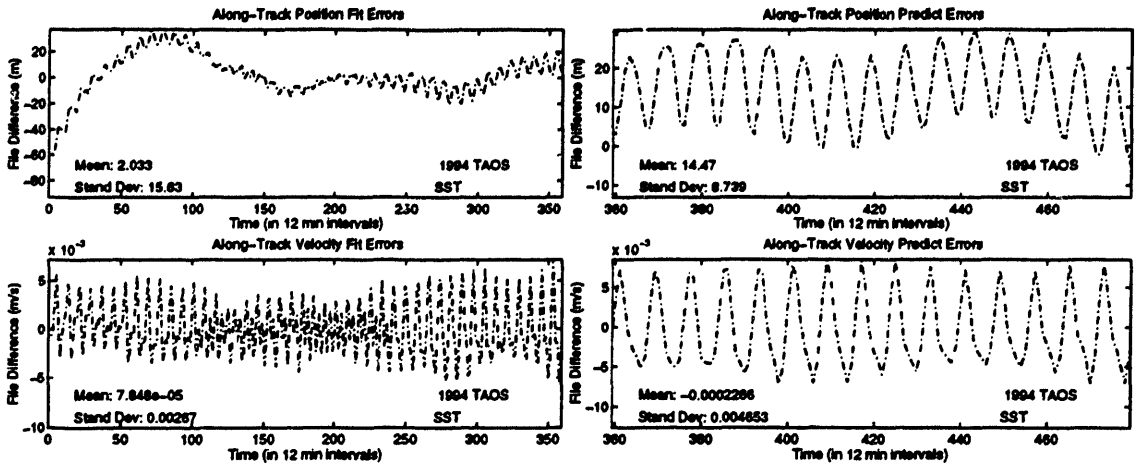

Figure 5.17 SST Along-Track Errors for Three Day Fit and One Day Predict Spans

The three day fit, one day predict cases were derivatives of cases presented in [8], with the new capabilities discussed in Chapter 3 included. The differences, again are the introduction of the FK5 theory, comparison to the ITOD POEs, and inclusion of solid earth tides in the force modeling. The effect of these factors is seen in Tables 5.21 and 5.22, which compare the results presented in [8] and those associated with Figures 5.16 and 5.17.

Table 5.21 Effect of New Capabilities on TOPEX Results (Fit Span)

	Max Radial Error (m)		Max Cross-Track Error (m)		Max Along-Track Error (m)	
	No SET	*SET*	*No SET*	*SET*	*No SET*	*SET*
Cowell	4.943	4.890	9.998	2.814	44.386	45.120
SST	4.646	5.421	10.609	3.627	46.976	59.365

Table 5.22 Effect of New Capabilities on TAOS Results (Predict Span)

	Max Radial Error (m)		Max Cross-Track Error (m)		Max Along-Track Error (m)	
	No SET	*SET*	*No SET*	*SET*	*No SET*	*SET*
Cowell	5.550	5.481	12.232	2.675	40.256	31.191
SST	6.189	6.738	13.760	3.195	30.636	29.626

As with the TOPEX orbit, the introduction of the new capabilities (solid earth tides most importantly) dramatically reduced the cross-track errors in both the fit and predict spans. Unlike the TOPEX results, however, the along-track prediction errors did not suffer from a transplant of the cross-track errors, but rather improved slightly.

The prevailing presence of the imbalance in the error signature at the beginning of the fit span reinforced the implication that a dynamic atmosphere is causing these variations. To test this hypothesis, the geomagnetic activity levels, which are used to derive atmospheric density profiles, were analyzed for this time period.

The TAOS fitting procedures thus far have used a derivative form of the Jacchia atmospheric density model of 1971, which determines exospheric temperature as a function of position, time, solar activity, and geomagnetic activity in the development of density profiles [6]. This model, referred to as a Schatten-Jacchia-Roberts, is stable and accurate over longer time periods (a week or greater), but susceptible to errors over shorter time spans [12].

To determine how accurate the Schatten atmospheric file was representing the geomagnetic activity levels, it was compared to an external data source provided by the National Geophysical Data Center (NGDC). The geomagnetic activity levels (given here as a three hour K_p values) are determined from a network of thirteen ground-based observatories in a non-real time mode, and can be considered a "true" representation of the magnetic activity. The differences between the Schatten and NGDC, along with the along-track errors experienced for these time periods, are shown below.

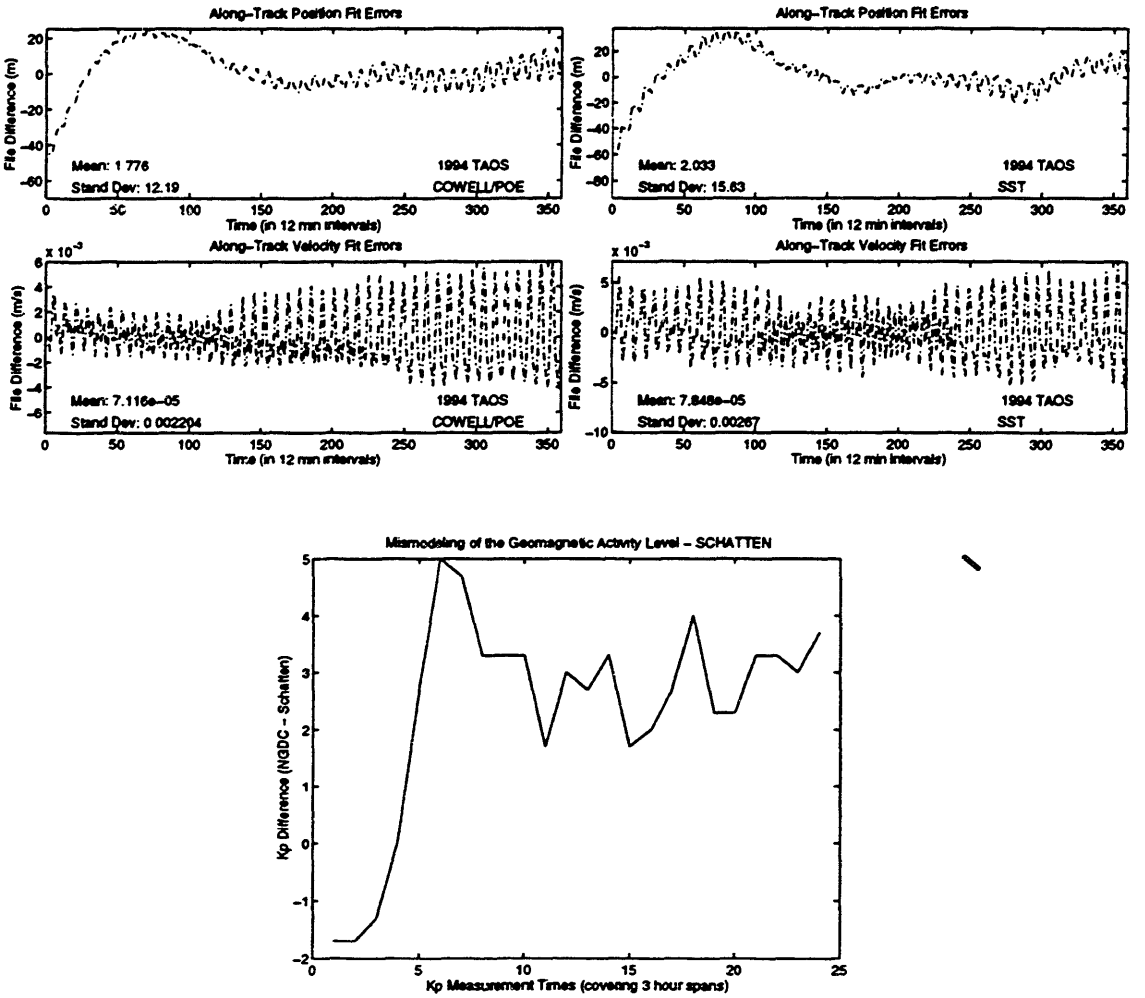

Figure 5.18 Correlation of the Differences Between Schatten/NGDC Geomagnetic Activity Levels and Along-Track Errors

The same general pattern can be seen in the differences between the Schatten and NGDC K_p values and the along-track errors for Cowell and SST techniques over the fit span. The fact that the K_p differences are not zero while the along-track errors are a minimum (during the final two days) is insignificant, as it is absorbed in the representation of the drag parameter. Correlation between the time periods of large variation and stability is the important characteristic to be taken from Figure 5.18. This indicates that the majority of the fit errors are a result of the current inability to predict atmospheric density.

In an attempt to improve the fit process, the three day Cowell and SST fits were reproduced using a separate atmospheric density file. The density file was created on a near-real time basis, such that the latest measurements of the geomagnetic levels were included in the prediction of the near-term future values [64]. The intent here was to determine if inclusion of the latest information available would improve the accuracy of the fit and/or predictions. The remainder of the test protocol was unchanged. The fit statistics for both Cowell and SST executions are summarized below in Table 5.23.

Table 5.23 TAOS Three Day Navigation Solution Fit Statistics with Near-Real Time Atmospheric Information

	Position 1σ (m)	Semi-major Axis 1σ (cm)	Drag Factor
Cowell	4.0352	3.6994	69.5389
SST	3.7509	2.8760	208.9558

Compared to the fit statistics based upon the Schatten files, it appears that the near-real time geomagnetic information provides a better representation of the orbit. However, further analysis reveals that while the majority of the along-track errors in the fit span are contained within ±5 meters, a drift begins at the end of the fit interval.

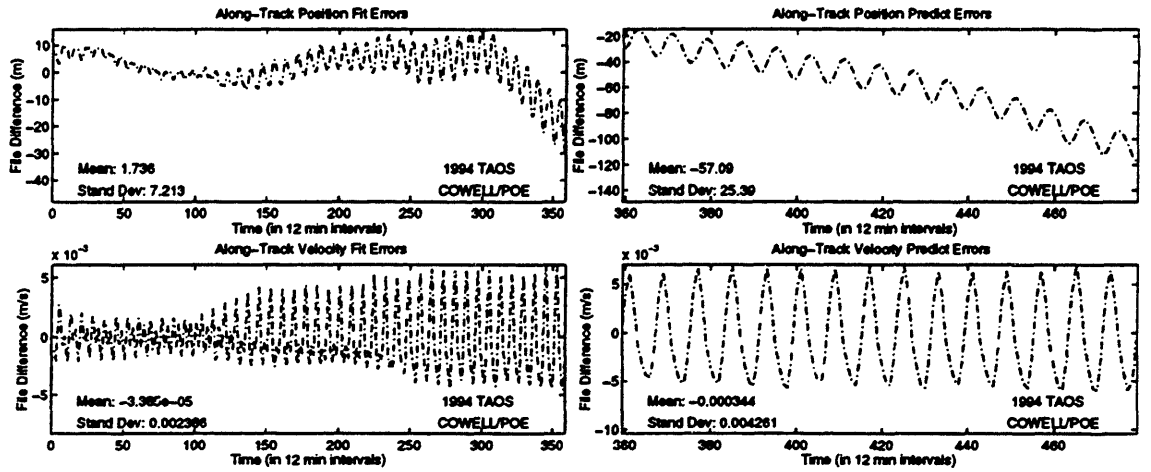

Figure 5.19 Cowell Along-Track Fit and Predict Errors with Near-Real Time Atmospheric Information

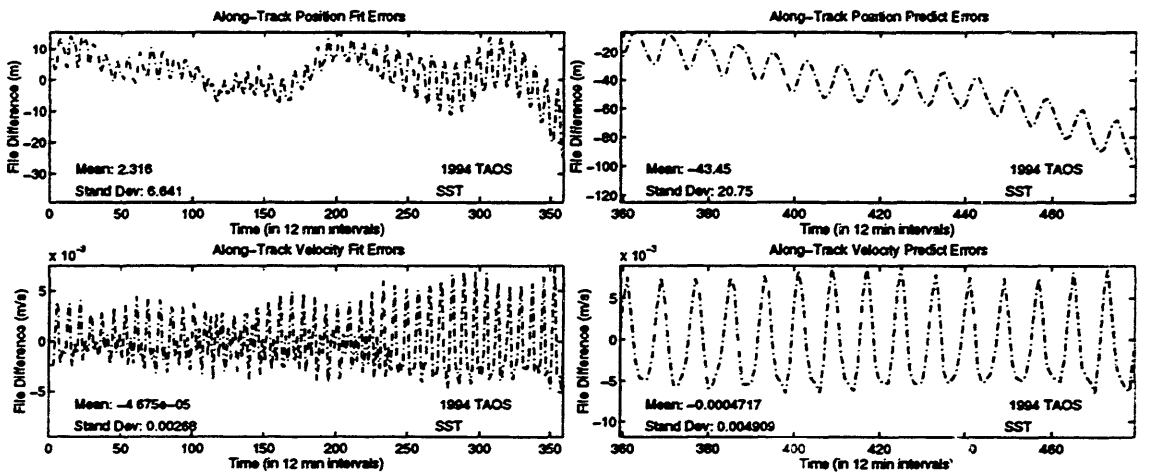

Figure 5.20 SST Along-Track Fit and Predict Errors with Near-Real Time Atmospheric Information

Figures 5.19 and 5.20 indicate the likelihood of a difference in the near-real time and NGDC geomagnetic representations toward the end of the three day

fit span. The estimated orbit is dominated by information from the first two and a half days of the fit span and cannot account for the relative change in the atmosphere toward the end of the interval. This error carries over into the predict interval, where the relative growth rate is significantly greater (about 100 meters/day) than the Schatten case (30 meters/day) and a result of the orbit being fit with the information from the relatively stable portion of the fit span.

As with the Schatten cases, the near-real time variations from the NGDC truth geomagnetic levels were compared to the along-track error signatures. Once again, the mismodeling of the atmospheric activity was highly correlated with the observed along-track errors.

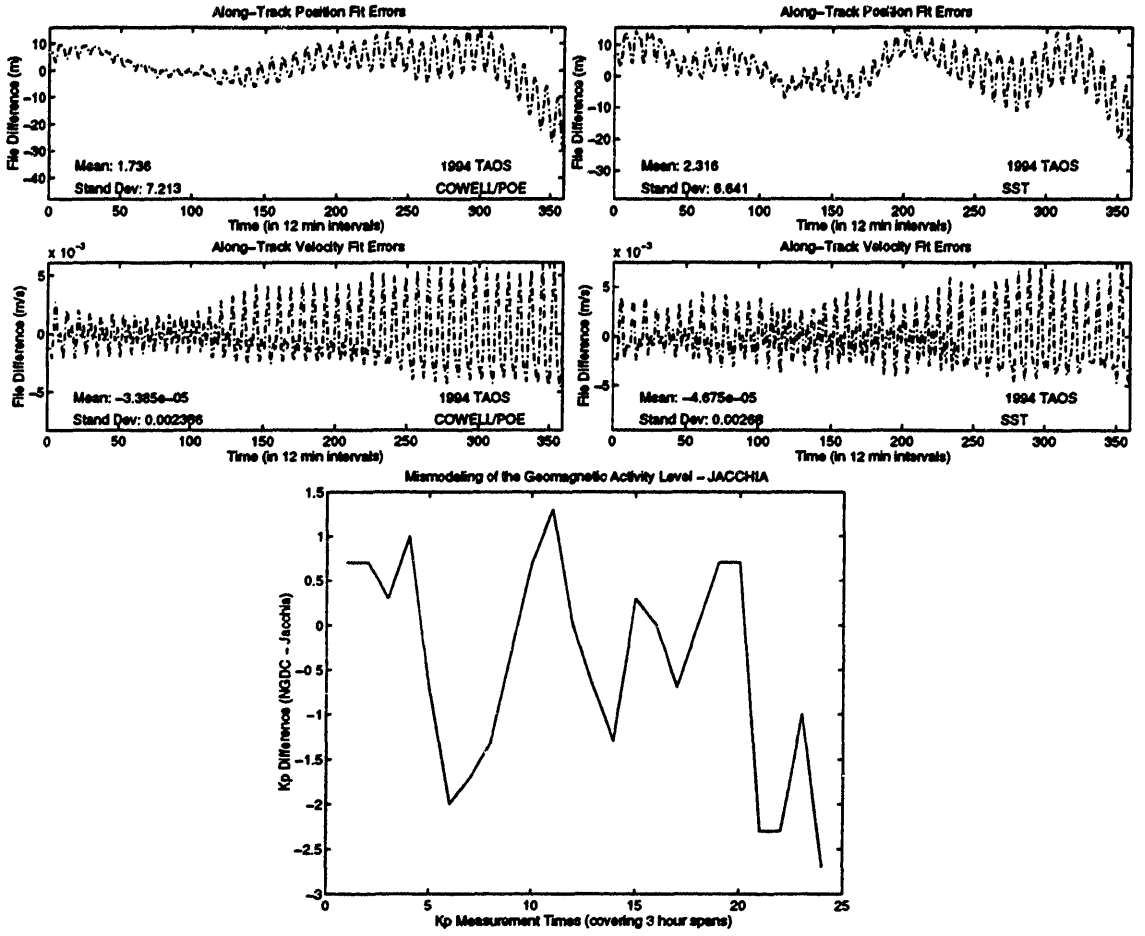

Figure 5.21 Correlation of the Differences Between Near-Real Time/NGDC Geomagnetic Activity Levels and Along-Track Errors

The TAOS results indicate that the accuracy of the orbits developed from navigation solution observations are heavily dependent upon both the length of the fit span and the ability to model atmospheric density accurately. The noise within the navigation solutions prohibits fit spans shorter than three days, but intervals of this length are susceptible to variations in atmospheric density models. The near-real time atmospheric model appears to be useful for applications where accuracy during a relatively short (on the order of a couple of days) fit interval is of importance. However, an atmospheric density model that is more stable over longer periods of time is

preferable in instances where prediction accuracies are the driving parameter. It would be interesting to fit the stable interval shown in Figure 5.16 to see how much improvement is observed in the orbit estimate and predictions.

5.5 EUVE Experiments

As was the case for the TAOS experiments, the EUVE POEs were fit using a similar strategy to TOPEX and TAOS before navigation solution experiments were performed. After the POE fits quantified the noise involved in the orbit determination fit process, the navigation solutions were evaluated as an observation source.

5.5.1 Orbit Determination from the EUVE POEs

The EUVE POEs were created by Gold at the University of Colorado at Boulder and have a reported accuracy of about one meter [26]. Because a limited amount of navigation solution and POE information was available, only one fit was performed for the EUVE POEs. The setup files and residual plots are found in Figures H.146-H.149.

The dynamic modeling for the EUVE POEs was similar to the TAOS experiments. The only variation existed in the atmospheric density model utilized for evaluation of the drag force. The Jacchia-Roberts atmospheric density model, which is an analytical representation of Jacchia's 1971 model, was used because the available Schatten file did not include the time periods of interest in its modeling capability. Only Cowell techniques were applied to the fit of the EUVE POEs.

Table 5.24 Orbit Dynamic Models Used in EUVE Analysis

Perturbation	Description
Earth's gravity	JGM-2 50x50; 4x4 partials
Solar Radiation Pressure	Cylindrical macro model
Atmospheric Drag	Jacchia-Roberts
Lunar/Solar Third Body	Point Mass
Lunar/Solar Tides	Love number (0.29)

Like the TAOS protocol, the EUVE experiments included the coefficient of drag as part of the solve-for state (along with the initial position and velocity vectors), but not the solar radiation pressure parameter.

The EUVE fit to the POEs involved a day and a half time interval (September 14-16, 1992) during which selective availability (SA) was turned off. This time period was one of only two time periods that were provided for the satellite (the other was similar in duration, but had SA activated). The Cowell fit statistics are summarized below:

Table 5.25 EUVE 1.5 Day POE Fit Statistics

Position 1σ (cm)	Semi-major Axis 1σ (cm)	Drag Factor
42.2756	.8773	1405.0726

While the drag factor indicates a well-defined parameter, the standard deviations on the absolute position and semi-major axis reveal that the orbit was not as tight as the fits to the TOPEX and TAOS POEs. Although the statistics are reminiscent of the TAOS five-day fits, the likelihood of an

extended fit span is small, a notion supported by the absolute position differences shown below. All comparisons for the EUVE experiments were performed in ECEF Cartesian coordinates due to the lack of an inertial representation of the POEs.

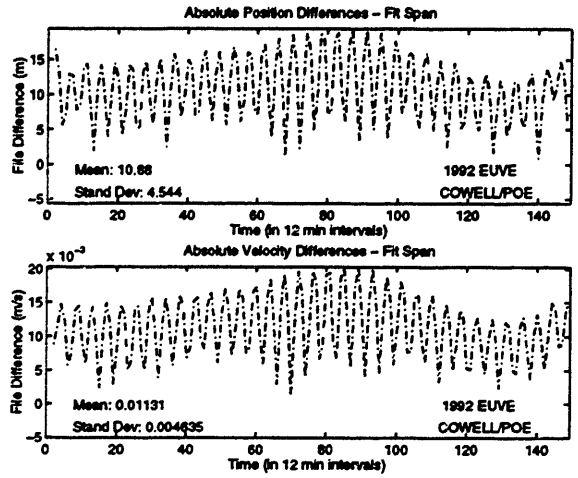

Figure 5.22 Absolute Position and Velocity Residuals for EUVE 1.5 Day POE Fit

The error signature in Figure 5.22 is very stable over the fit span, an indication that the satellite did not encounter a highly dynamic atmosphere during this time period. In fact, comparison of the NGDC geomagnetic levels and the values retrieved from the Jacchia-Roberts file revealed that the agreement between the two was exact for the entire span[1]. If the fit span was too long, a drift would be encountered either at the beginning or end of the interval. On the contrary, it is likely that the fit span should be lengthened in an effort to better define the nature of the orbit (i.e., absolute position and

---

1 The values were exact with the exception of those representing the third of an integer prior to an exact integer value (e.g., 2.6 for Jacchia-Roberts, or 2.7 for NGDC). The differences are simply a result of variation in the numbering convention adopted by each.

semi-major axis standard deviations) to improve the accuracy during the fit interval.

5.5.2 Orbit Determination from the EUVE Navigation Solutions

Similar to TOPEX and TAOS, the accuracy of the individual navigation solutions was determined prior to orbit determination experimentation. The EUVE Motorola GPSDR exhibited similar characteristics as the TOPEX Motorola GPSDR, including the rotation bias that is compatible with an offset of the FK4 equinox from the FK5 equinox at the time of the observation. The differences between the individual navigation solutions and the EUVE POE vectors over a four day span are shown below.

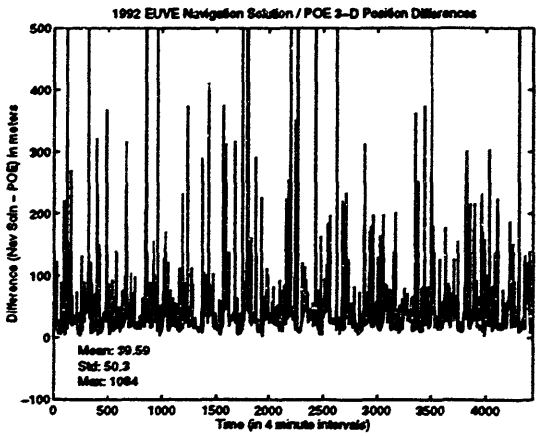

Figure 5.23 Differences Between EUVE Navigation Solutions and POE Vectors

The slightly lower mean value (as compared to the TOPEX GPSDR) is likely a result of SA being deactivated during this time period (September 14-17). The mean is quite a bit larger than the reported 5-20 meter accuracy associated with the navigation solutions when SA is not operating [40]; however, the representation in Figure 5.23 includes the large outliers, skewing the value significantly.

Because the longest contiguous time span with valid navigation data extended a mere two days, the expectations for determining a high precision orbit were slight. The inability to fit one and a half days of POE information to better than 15 meters substantiated this thought. Nonetheless, a two day interval of the GPSR navigation solutions was fit using similar models and strategy as the POE vectors. A second interval of POE vectors were identified as a reference for prediction errors. Figure 5.24 illustrates the fit and prediction intervals used for EUVE.

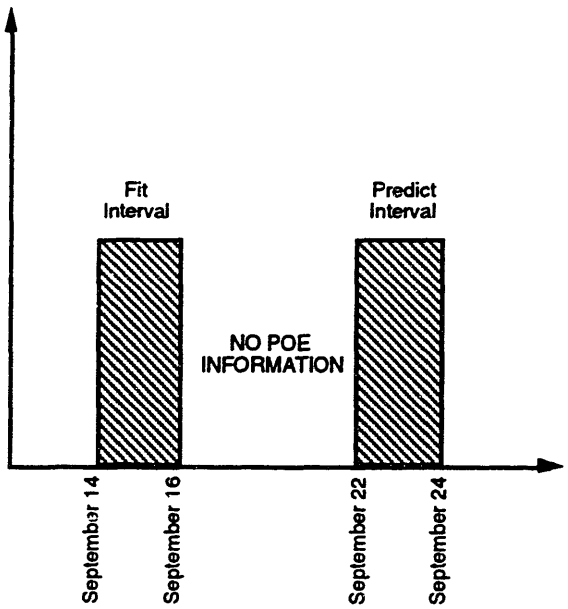

Figure 5.24 EUVE Fit and Predict Intervals

SST techniques were also employed in the fitting of the EUVE navigation solutions. The setup of the AOG and SPG were identical to the TAOS configuration, but step size and resonance periods were extended to a half day and five days, respectively. The fit statistics are summarized below in Table 5.26.

Table 5.26 EUVE Two Day Navigation Solution Fit Statistics

	Position 1σ (m)	Semi-major Axis 1σ (cm)	Drag Factor
Cowell	1.6077	2.2412	842.5050
SST	1.6124	2.2271	826.1789

These statistics are actually better than the three day TAOS fit process, but residuals are significantly larger, as shown by Figures 5.25 and 5.26.

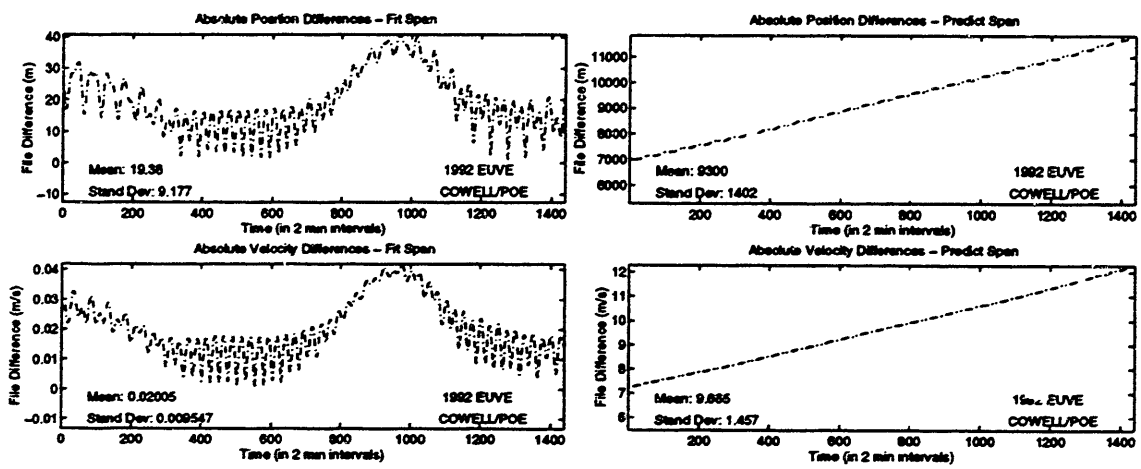

Figure 5.25 Cowell Absolute Position and Velocity Differences for Two Day Fit and Nine Day Predict

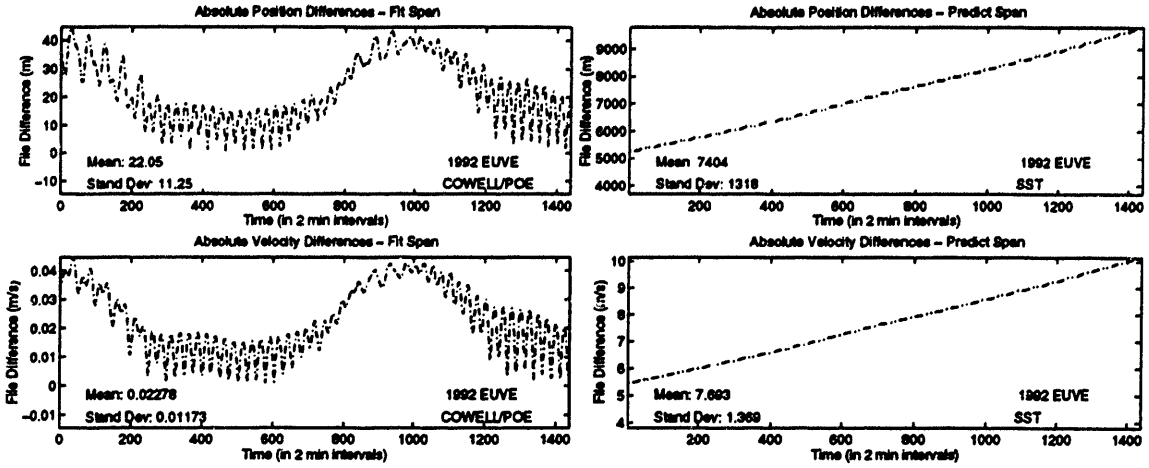

Figure 5.26 SST Absolute Position and Velocity Differences for Two Day Fit and Nine Day Predict

Despite the agreement between the Jacchia-Roberts and NGDC geomagnetic levels, the drag remains the likely culprit for the fit errors seen in Figures 5.25 and 5.26. Conversion of these differences into an inertial frame (not possible here because of the lack of Greenwich hour angle values) where radial, cross-track and along-track differences could be evaluated would assist in this analysis.

The predict errors, at first glance, appear irrational compared to the previous growth rates suggested by TOPEX and TAOS experiments. However, the beginning of the two-day predict interval was not encountered until five days after the completion of the fit interval because of the lack of POE vectors during this time period. Therefore, the end of the fit span is measured nine days after the beginning of the fit interval. If the primary error source is the suspected drag, these errors are not unreasonable. Because the along-track prediction errors for a drag-perturbed orbit grow at an exponential rate, errors on the order of ten kilometers over a nine day period might be expected. POE

vectors for the time period separating the fit and predict spans are necessary to substantiate this claim.

5.6 Evaluation of GPSR Navigation Solutions as an Observation Source

Use of navigation solutions as an observation source in a differential correction process appears to be a viable alternative for some applications. For orbits with altitudes in the TOPEX realm (~1330 km), Draper R&D GTDS fit the navigation solutions to an accuracy of within nine meters over a five day span. More impressive, however, was the predict growth rate associated with the navigation solution-derived orbit; a 10-15 meter/day error is suitable for many applications at this altitude.

As expected, the drag-perturbed spacecraft (altitude ~500 km) experienced a more difficult time in fitting the navigation solutions than the TOPEX case. The length of the fit interval appears to be significant in defining the orbit and drag parameter, and should be dependent upon the specific mission requirements. If fit accuracies are the driving factor, a shorter fit span (one to two days) is recommended. Reasonable predict accuracies rely upon the ability to capture the atmospheric activity levels that exist in the prediction intervals during the fit span, and could require three or more days of information. The shorter (one and two day) fit spans result in accuracies on the order of about 20 meters, the bulk of which is a product of mismodeling of the geomagnetic activity level. Experiments using a three day fit span that portrayed the same geomagnetic activity as the predict span result in growth rates of about 30 meters/day.

Finally, the TOPEX navigation solution fits, in particular, indicate that a significant source of mismodeling remains. Removal of the semi-major axis error growth and quadratic nature of the argument of latitude differences would likely improve the accuracy of using navigation solutions as an observation source.

[This page intentionally left blank.]

Chapter 6

Conclusions and Future Work

6.1 Summary

This work investigated the use of navigation solutions from a commercial-grade GPS receiver as a viable observation source in precision orbit determination. Initial experimentation led to identification of a secondary objective, evaluating the accuracy of force modeling within Draper R&D GTDS against a high quality independent data source (the precise orbit ephemerides, or POEs). Both subjects revealed a need to incorporate three new capabilities in the orbit determination software for analysis support and accuracy improvement. The existing orbit generation theory, which was based upon the Fourth Fundamental Catalogue (FK4), was augmented by the modern FK5 theory to ensure compatibility with the software products of the astrodynamics community external to Draper. The instantaneous true of date (ITOD) coordinate system was introduced as a modeling and output option in Draper R&D GTDS for processing of and comparison to the POE vectors. Modeling of perturbations due to lunar and solar solid earth tides was introduced for numerical integration techniques and revisited for the semianalytic propagator to improve fit accuracy. Introduction of these capabilities required development of several routines, substantial review of existing software, and extensive testing of the final product to ensure proper incorporation. A VAX station 4000/90 was chosen as the development

platform because of an existing VAX VMS GTDS with 50x50 gravity field models. The assistance provided by the VAX VMS system tools was a secondary feature available for the software development process.

The document begins with an introduction to the GPS constellation and fundamentals associated with application to the orbit determination arena. Previous high accuracy work is highlighted and related to the current focus of using navigation solutions as an observation source. The first chapter concludes with a background discussion of the three satellites (TOPEX, TAOS, and EUVE) chosen as subjects for analysis.

The second chapter helps the reader become oriented with the orbit determination software, Draper R&D GTDS, and the information contained in the navigation solutions. The perturbation techniques used in the analysis, with emphasis placed on Cowell and semianalytic methods, are presented along with a discussion of coordinate system options available in Draper R&D GTDS. A brief description of the navigation solution characteristics and efforts taken to ensure their compatibility with the orbit determination software completes the chapter.

The focus of the third chapter is on the new capabilities incorporated into Draper R&D GTDS. The need for the FK5 theory, ITOD coordinate system options, and ability to model solid earth tides is discussed along with the fundamental principles associated with each. Software design considerations are identified and provided to assist in future development projects. Code modifications are summarized, and include a total of 101 routines and 5527

lines of code (90 routines and 3887 lines of code modified, 11 routines and 1640 lines of code created).

The fourth chapter describes the testing philosophy for the final software product that includes the three capabilities outlined in previous chapter. Testing of the new capabilities encompasses the Draper R&D GTDS Ephemeris Generation, Differential Correction, Ephemeris Comparison, Data Management, and Permanent File Report functions. Merging of the baseline RADARSAT version of R&D GTDS with the 50x50 gravity field modifications is shown through replication of three test cases presented by Fonte [20]. A series of standard test cases that involves most of the major GTDS capabilities used at Draper was performed to show that none of the existing software was adversely affected by the modifications made. Results from incorporation of the FK5 theory were measured against the existing FK4 methods to verify proper implementation, while use of the ITOD coordinate system as a modeling and output option was shown through fitting the ITOD TOPEX POEs. Solid earth tide modeling was verified by creating a synthetic test case that highlighted the tidal effects over the time period of interest for the TOPEX POEs, and comparing these effects with what was witnessed when tides were added to the force modeling in the fit of the POEs. Individual contributions of the FK5 theory, 50x50 gravity field modeling, and solid earth tides were isolated, and suggest that no single factor was dominant in reducing the modeling errors to the two meter level, but rather all three elements were required to observe such improvement.

The fifth chapter covers the analysis of using GPSR navigation solutions as observations in an orbit determination process. Organized by satellite, the

results from TOPEX experiments are presented first, and indicate that fit accuracies for a five day period are within nine meters, and result in predictions that have errors growing on the order of 10-15 meters per day. The TAOS and EUVE POEs are fit in a manner similar to the TOPEX POEs in the previous chapter to indicate Draper R&D GTDS's ability to model low earth orbiting satellites. The apparent dependence of the fit accuracy upon the interval of information included is noted, and suggests that while three days of navigation solutions are necessary for adequate modeling of future spacecraft motion, one to two day periods are advised in the fit span to capture the essence of the perturbations (most notably drag). Results from the TAOS navigation solutions fits indicate errors in the fit interval of within 30 meters, and a prediction growth rate of about 30 meters per day. EUVE experiments were limited because of the lack of navigation solution and POE information, but the experiments performed showed the ability to fit with residuals around 30-40 meters, and an ambiguous growth rate that is estimated at best around 1 km per day.

6.2 Conclusions

The primary and secondary objectives of fitting the navigation solutions and POE vectors were successfully accomplished and offer extensive opportunities for future development. Two meter modeling accuracy for the TOPEX orbit is exceptional, but remaining error signatures indicate the possibility for further improvement. These results, combined with a rigorous and complete testing protocol, reflect proper implementation of the FK5 theory, ITOD coordinate system, and solid earth tide modeling capabilities. Coupled with the 50x50 class gravity fields and Draper's Semianalytic Orbit Propagator, integration of

these capabilities offer a unique tool for long-term, high accuracy orbit prediction.

Use of GPSR navigation solutions in a differential correction manner has been confirmed as a viable alternative to the more traditional tracking techniques for some applications. In particular, the prediction error growth rates of the TOPEX (10-15 meters per day) and TAOS (30 meters per day) orbits characterize orbit determination from GPSR navigation solutions as a low-cost, moderate accuracy technique.

6.3 Future Work

The progression of work in this document highlighted a number of areas that show potential for future projects. This section summarizes those opportunities, which can be divided into software and analysis related items.

6.3.1 Software-Related Work

The most prominent opportunity revealed in this work involved force model improvement to remove the remaining two meters existing in the fits to the TOPEX POEs. Expansion of the geopotential to a 70x70 class with normalized coefficients, and inclusion of albedo and ocean tidal effects are the most notable options for error reduction.

Another pressing item is the merger of the capabilities existing on the IBM, VAX, UNIX, and PC versions of Draper R&D GTDS. While the 50x50 gravity

field modeling[1], FK5 theory, ITOD coordinate system, and solid earth tide capabilities currently exist only on the VAX, the semianalytic short periodic input processor is found only in the UNIX and PC applications. The input processor offers a simple method of identifying options available to the user involving the averaged equations of motion and short periodic contributions. Incorporation into the VAX and IBM environments would eliminate the need for including the awkward overrides files. The advantages of the 50x50, FK5, ITOD and solid earth tide capabilities were discussed in Chapter 4. To obtain the maximum applicability for each of these tools, it is highly desirable to develop a common source code for the platforms identified above.

As explained in section 3.3.1.2, there are currently certain limitations on the interaction between FK4 and FK5 coordinate system options. Specifically, integration in one fundamental system and providing input, observations, or output in the true equator and equinox of date associated with the other fundamental system is not supported. Likewise, because the NORAD coordinate systems are inherently linked to the FK4 reference systems in Draper R&D GTDS, interaction with FK5 options is restricted. Because these limitations are a result of the existing SLP file structure, one remedy could involve replacing the SLP files with analytic formulae that serve the same functionalities.

The experiments in this work used observation files that contained only navigation solution or POE information because Draper R&D GTDS does not support the capability of accepting multiple observation types in the same

---

1 Initial efforts have been made toward incorporating the 50x50 gravity field models in the PC version; however, testing is not complete at this point.

execution. However, it might be desirable to use orbit information from multiple sources (e.g., ground-based tracking sources, satellite laser ranging (SLR) data, or high accuracy optical data) in many instances to supplement the navigation solutions. This is particularly applicable for missions where power or bandwidth restrictions prohibit use of navigation solutions all the time. Development of the capability to use information from multiple information sources in Draper R&D GTDS could prove to be well worth the effort.

In analyzing the error signatures in the TOPEX POE fits, it was noted that the timing convention used by Draper R&D GTDS could introduce errors into the fit process. Currently, the software only calculates the UT-UT1 offset once per day despite the fact that this is a continuously varying value. The absolute position errors induced by these slight timing differences can be up to about one meter over the day period for a TOPEX-class orbit, which is a significant portion of the remaining error. Although the process of accounting for these variations could become quite cumbersome, it might be required in order to eliminate the remaining errors seen in the TOPEX fits.

The TAOS experiments revealed the tremendous importance of being able to properly evaluate a drag coefficient representative of the entire fit span. Although solving for this drag parameter is a viable option in Draper R&D GTDS, only one value can be obtained for the entire span. To account for a highly dynamic atmosphere, it is desirable to have the option of solving for several drag parameters over this same interval. Along the same lines, the introduction of a navigation solution observation bias solve-for capability is

also appealing. This is a particularly enticing notion for GPS-related observations because of the current presence of Selective Availability.

A Graphical User Interface (GUI) simplifies the interaction between the user and software by providing a "point and click" capability. Draper R&D GTDS could be enhanced to offer a simplified process for identifying options (input card data files, command procedures, etc.) and highlighting results (summarizing key findings, enhanced plotting, etc.). Automation of these processes would reduce both the likelihood of typographical errors and the required operational manpower.

6.3.2 Analysis-Related Work

The high accuracy results obtained by fitting the TOPEX POEs spawned the idea of utilizing other precision observation information in a similar manner. These data types include satellite laser ranging data and the GPS observables (pseudorange and carrier phase). Expansion of the available observation options would not only help to support the findings presented here, but also increase the types of orbits available for analysis and model improvement.

Specifically, the next logical step is to incorporate a capability to model raw pseudorange observations. Definitive GPS satellite ephemerides (SA removed) are available on the internet (NOAA post-fit data is found on an anonymous FTP site at *gracie.grdl.noaa.gov*) and can be used in conjunction with the pseudorange measurements to improve the estimate of the orbit. The resulting orbits could serve as a reference for navigation solution-based

orbits, thus providing an alternative to the high precision DGPS or SLR sources, which are not available for every satellite.

The presence of a high accuracy reference orbit from an independent source also offers the opportunity to evaluate a variety of existing orbit theories. By fitting the TOPEX POEs with the NAVSPASUR PPT2 theory, it has been demonstrated that a major error source associated with the theory is the lack of tesseral m-daily terms [9]. Other existing orbit theories (the NORAD analytic perturbation theories, for example) could be evaluated in a similar fashion.

The high accuracy reference orbit could also be used to analyze the effects of orbital maneuvers on the differential correction process. The current lack of an ability to detect the times and duration of maneuvers limits the utility of fitting the data in time periods adjacent to these burns. This is a significant factor for propulsion systems using low thrust with longer burn times. The high accuracy reference orbits could help to detect these maneuvers and the effects that they have on orbit determination. Ultimately, an ability to model these maneuvers during the fit process would greatly improve orbit determination during these time periods of interest.

The TAOS experiments, in particular, revealed a high correlation between mismodeling of the geomagnetic activity levels and the along-track errors in the fit span. Improvements in the density and geomagnetic activity models could result in orbit determination accuracies using GPSR navigation solutions for low earth orbiting satellites to levels approaching those seen for TOPEX.

An alternative approach to the atmospheric model improvements is to apply the concepts presented here to a real-time filtering strategy. Filters generally handle highly dynamic systems better than the batch orbit determination method presented here. Such a strategy may allow for autonomous navigation of a satellite based upon GPSR solutions.

The bulk of the navigation solution information obtained for analysis in this work was created during time periods where SA was active for the GPS constellation. The EUVE navigation solutions were developed in a period of deactivation, but the lack of information over significant intervals of time limited the utility of these solutions. Vice-president Gore's initiative to eliminate all dithering of the GPS signals by the year 2006 improves the prospects of using navigation solutions as an observation source [32]. Further analysis using non-SA solutions would provide a better indication of the accuracy of these techniques in the environment anticipated ten years from now.

Appendix A

Summary of Available GPS Space-Based Receivers

The advent of GPS-based spacecraft navigation has prompted several GPSR suppliers to expand receiver development from the terrestrial realm into the space industry. Because the market for ground-based GPS applications is immense compared to the space-based demand, most of the existing spaceborne receivers are upgrades of existing ground models. An abbreviated list of some of the more common options available to spaceborne users is provided on the following page [49].

Table A.1 summarizes some of the space-qualified GPSRs that have or will be launched on-board spacecraft for navigation or attitude determination purposes. Receiver designation is composed of the supplier and model identification, and is accompanied by a description of the fundamental receiver characteristics, including the number of available channels, dual frequency capability, and weight and size parameters. Although not comprehensive, this list does provide the reader with a feel for the options that have been or are available.

Table A.1 Available GPS Space-Based Receivers

SUPPLIER	MODEL	MISSION	CHANNEL/ FREQ/CODE	WT(LB)	SIZE(IN)
Motorola	GPSDR	Explorer	12 L1 C/A or P	10	5.5x6.9x7.5
Motorola	GPSDR	TOPEX	6 L1, L2 C/A, P	14	5.5x6.9x10.4
Motorola	Seastar	NASA Seastar	12 L1 C/A	3.4	5.2x6x1.7
Motorola	Monarch upgrade	none	6 L1, L2 C/A, P	3.7	6x5.2x2.7
Rockwell	AST V	TAOS	6 L1, L2 C/A or P	8	7.8x7.1x5.1
Rockwell	3M upgrade	NASA-JSC Shuttle	5 L1 or L2 C/A or P	11	3.1x6.8x12
Rockwell	Spaceborne 5-channel	P91-1 ARGOS (USAF)	5 L1 or L2 C/A or P	5	7x7x2.5
Rockwell	SPINSAT	SPINSAT (cancelled)	2 L1 or L2 C/A or P	2.6	7.95x5.75x1.25
Trimble	TANS II upgrade	APEX, Pegasus, LEAP	6 L1 C/A	2.9	5x9.5x2.04
Trimble	TANS Quadrex	RADCAL	6 L1 C/A	3.2	5x9.5x2.04
Texas Instruments	SNR	DOD	1 L1, L2 C/A, Y	50	3000 cubic
Texas Instruments	ASNR	none	6 L1, L2 C/A, Y	20	570 cubic
Ashtec and E-systems	3DF upgrade P-12 upgrade OEM upgrade	none none none	24,L1,C/A 12,L1/2,C/A, P 12,L1,C/A	14 7 1	7x7x5 7x5x3.5 4x3x1
Magnavox	GPSPAC	Landsat 4,5 DOD	2 L1, L2 C/A, P	43	16.4x12x8.1

Appendix B

Software Modifications Made to Support the Earth-Centered, Earth-Fixed (ECEF) Input Option in VAX Draper R&D GTDS

Prior to inception of work on this project, Cefola introduced the capability to provide Draper R&D GTDS (PC/DOS version) with an input vector for the ephemeris generation or differential correction programs in an earth-centered, earth-fixed (ECEF) coordinate system. These modifications, previously not integrated into the VAX VMS version, were intended to allow GPSR navigation solutions (provided in ECEF) to be processed without having to transform the initial state to another coordinate system that Draper R&D GTDS could already interpret. Because ECEF modeling and output options were available, only the software involving the input coordinate system needed to be addressed.

Four routines were identified for modification to support this new input option. Table B.1 lists these modules and summarizes the changes made.

Table B.1 Modifications Made to Support ECEF Input Capability

Routine	Modification
CRDLBL	Expand labeling options to include Earth-Centered, Earth-Fixed input
INTOGN	Rotate ECEF input to the true of reference frame and reset input coordinate system to reflect this
ESTFLGBD	Alter default values for modeling coordinate system and source to be ECEF input from an observation card
SETRUN	Expand range of valid input options on ELEMENT1 card to include ECEF (option 10)

Appendix C

Summary of Software Tools Developed to Support This Project

Several software tools were developed to support the objectives of this document. The software listings, due to their length, are not included here; however, a summary of the tools is provided, and accompanied by directions for proper execution. The developed software can be grouped into three categories, including

- GTDS preprocessing
- MATLAB preparation
- MATLAB comparison scripts

Preprocessing routines were written in VAX FORTRAN and serve to transform navigation solution and/or POE information from their existing format (reference section 2.5 for a discussion of the various types) to an observation file that GTDS can interpret. Because the formats of the navigation solution files for the cases studied were satellite-dependent, the preparation routines were case-specific as well. Preprocessing of the POE vectors was somewhat simpler, as the TOPEX and TAOS POEs were provided in the same format. The EUVE POEs were packaged in an SP1 format similar in nature to the TAOS navigation solutions. An additional routine was developed to transform the high precision vectors into the format dictated by

the TOPEX and TAOS POEs. In this manner, one routine could be used to convert the POE information into the GTDS observation file format. The preprocessing routines are summarized in Table C.1.

Table C.1 Preprocessing Software

Routine Name	Description
TOPEX_PREP.FOR	Converts TOPEX navigation solutions from SP3 format into a GTDS observation file
TAOS_NAV_PREP.FOR	Converts TAOS navigation solutions from SP1 format into a GTDS observation file
EUVE_PREP.FOR	Converts EUVE navigation solutions from modified RINEX format into a GTDS observation file
SP1_TO_POE.FOR	Converts file in SP1 format into POE file standards
POE_PREP.FOR	Converts POE file into a GTDS observation file

These tools are maintained in the author's personal Code Management System (CMS) library, specified by:

FDS$DISKA:[SSC2414.CHANGES.CHANGES_REF]

Each tool has an associated file that links the appropriate objects and a command procedure that executes the desired function. The naming convention for these link files and command procedures is as follows:

LINK_XXXX.COM
RUN_XXXX.COM

where *XXXX* is the name of the tool being executed.

The essence of the command procedure structure is to provide a method of defining the input navigation solution/POE file and the output GTDS observation card file. The file names are assigned to logical variables (*INPUT_FILE* and *OUTPUT_FILE*) used by the FORTRAN routines. Thus, to execute the preprocessing package for TAOS navigation solutions, the user would:

1) Ensure the command procedure is pointing to appropriate navigation solutions file. This file might look something like the following:

```
$ !  RUN_TAOS_NAV_PREP.COM
$ !
$ assign/table=lnm$job taos_nav_solns.dat input_file
$ assign/table=lnm$job taos_obs_card.dat output_file
$ run/nodebug fds$diska:[ssc2414.changes.changes_ref]taos_nav_prep
```

2) Execute the command procedure by entering:

```
$ @run_taos_nav_prep
```

The other preprocessing routines operate in a similar fashion.

The MATLAB preparation software (see Table C.2) links orbital information (in the form of GTDS ORB1 files, POE files or navigation solution files) to a plotting package. This set of FORTRAN routines retrieves information from the appropriate sources and places it into a binary array format compatible with MATLAB. The products of this software, referred to as MATfiles, are then interpreted by a set of MATLAB scripts that compare and plot the results.

Table C.2 MATLAB Preparation Software

Routine Name	Description
ORB1_TOOL.FOR	Produces MATfiles for comparison of ORB1/POE or ORB1/ORB1 information; optionally produces GTDS observation files from ORB1/POE files
NAV_CARD_POE_COMPARE.FOR	Produces MATfiles for comparison of GTDS observation card (nominally containing navigation solutions) and POE file
NAV_POE_COMPARE.FOR	Produces MATfiles for comparison of navigation solutions (SP3 format only) and POE files
EUVE_NAV_POE_COMPARE.FOR	Produces MATfiles for comparison of navigation solutions (modified RINEX format only) and POE files

ORB1_TOOL provides the capability to either compare two GTDS ORB1 files, or an ORB1 file and a POE file. Information from a GTDS observation card or navigation solution file is compared to the POE solutions by one of the three remaining tools listed in Table C.2 (*NAV_CARD_POE_COMPARE*, *NAV_POE_COMPARE*, or *EUVE_NAV_POE_COMPARE*).

The protocol for executing these routines is the same as for the preprocessing software. The command procedures entitled *RUN_XXXX.COM* access these tools from the author's CMS library. However, because the products are different from those generated by the preprocessing software, the associated

command procedures take on a different form. An example of a command procedure that might be used to execute *ORB1_TOOL* is shown below.

```
$!     RUN_ORB1_TOOL.COM
$
$      assign/table=lnm$job sys$command for090
$      assign/table=lnm$job sys$command for091
$      assign/table=lnm$job topex_poe_itod_dc_1.orb1 orb1
$      assign/table=lnm$job jplpoe010.dat poe_file
$      assign/table=lnm$job jplpoe010.hdr poe_header_file
$      assign/table=lnm$job 92dec22-92dec30.uta poe_a1_file
$      assign/table=lnm$job topex.print print_file
$      assign/table=lnm$job char_file.dat char_file
$      run/nodebug [ssc2414.changes.changes_ref]orb1_tool
```

This command procedure configures the *ORB1_TOOL* to compare the GTDS ORB1 file *topex_poe_itod_dc_1.orb1* to a POE file denoted by *jplpoe010.dat*. The .hdr and .uta files provide information about the POE solutions (such as start and stop times and A1-UTC offsets) required for proper interpolation of the POE vectors. *Char_file.dat* is an ASCII file required for proper character labeling in the MATLAB scripts. The information in this file is obtained during execution of *ORB1_TOOL* by prompting the user for information on the type of comparison being performed (ORB1 vs. POE, or ORB1 vs. ORB1), orbit generation theory used (Cowell, SST, etc.), and length of fit and predict spans (where applicable). In addition, the user has the option of producing GTDS observation card(s) from the retrieved ORB1/POE information. The *sys$command* assignments define the keyboard and screen as the appropriate locations for prompting the user and interpreting options.

Products of the *ORB1_TOOL* software package include three MATfiles and one ASCII file used in the MATLAB comparison process. These files are stored in the local directory and denoted by:

MF_A_DAT.MAT
MF_B_DAT.MAT
INT_INFO.MAT
CHAR_FILE.DAT

The first two MATfiles (.MAT) contain the ephemeris information from the appropriate sources (in this case, ORB1 and POE files). *INT_INFO.MAT* is a binary array of integer values (such as the year of the comparison, and switches describing whether the comparison is over the fit and/or predict span) used in the execution of the MATLAB scripts. *CHAR_FILE.DAT* , defined in the command procedure, contains the alphanumeric representations of the character strings used in the plotting functions. It is required because the version of MATLAB employed in this work (version 4.2 on the VAX node SHIRE) does not have the capability of accessing information from a file that contains anything other than numeric values (integer or real).

The lower three routines listed in Table C.2 support the MATLAB scripts that compare individual navigation solutions to the appropriate POE vectors. An example of a command procedure that might be used to execute these routines is shown below.

```
$    assign/table=lnm$job 92dec22-92dec30.hdr header_file
$    assign/table=lnm$job jplpoe010.uta uta_file
$    assign/table=lnm$job topex.print print_file
$    assign/table=lnm$job jplpoe010.dat in_poe_file
$    assign/table=lnm$job 92dec23-27.poscard in_nav_file
$    run/nodebug [ssc2414.changes.changes_ref]nav_card_poe_compare
```

This command procedure executes a FORTRAN routine (*NAV_CARD_POE_COMPARE*) to produce MATfiles in support of the comparison of individual navigation solutions from a GTDS observation card (*92DEC23-27.POSCARD*) and the POE vectors (*JPLPOE010.DAT*). The .hdr, .uta, and .print files serve the same purpose as in the *ORB1_TOOL* example presented above.

The MATfiles produced in this example (and for the *NAV_POE_COMPARE* and *EUVE_NAV_POE_COMPARE* programs) are limited to ephemeris information, and include:

NAV_FILE.MAT
POE_NPM_FILE.MAT
POE_PM_FILE.MAT

The two MATfiles containing POE solutions differ in that one represents vectors with the effects of polar motion removed (*POE_NPM_FILE*) while the other retains these effects (*POE_PM_FILE*).

After production in the FORTRAN processes, the MATfiles are used by a set of MATLAB scripts for ephemeris comparison. For files that contain information derived from an inertial coordinate system, the differences can be represented in Cartesian coordinates, radial/cross-track/along-track components, and orbital elements. Non-inertial ephemerides (ECEF) are compared only in Cartesian coordinates.

The scripts that perform these functions are summarized in Table C.3 on the following page. Each requires the four files (three MATfiles and one ASCII

data file) discussed in the MATLAB preparation phase for proper execution. By default, the scripts assume the names of these files to be exactly as they are represented previously (*MF_A_DAT, MF_B_DAT, INT_INFO, CHAR_INFO.DAT*). If existing MATfiles with different names are to be used, the LOAD commands found in each of the three differencing scripts (XYZ_PLOTS, RCA_PLOTS, and ORBELS_PLOTS) should be commented out, and the character information array renamed to CHAR_FILE. Thus, if a previous execution of the ORB1_TOOL produced MATLAB files with the names,

EXAMPLE_ORB1_DAT.MAT
EXAMPLE_POE_DAT.MAT
EXAMPLE_INT_INFO.MAT
EXAMPLE_CHAR_INFO.DAT

the MATLAB commands required prior to using any of the comparison scripts would be:

```
> load EXAMPLE_ORB1_DAT.MAT
> load EXAMPLE_POE_DAT.MAT
> load EXAMPLE_INT_INFO.MAT
> load EXAMPLE_CHAR_INFO.DAT
> char_info = example_char_info;
```

Table C.3 MATLAB Comparison Software

Routine Name	Description
XYZ_PLOTS.M	Cartesian coordinate differences plotted from MATfile position and velocity information
RCA_PLOTS.M	Radial/cross-track/along-track differences plotted from MATfile position and velocity information
ORBELS_PLOTS.M	Orbital element differences plotted from MATfile position and velocity information
ALL_FIT_PLOTS.M	Cartesian coordinate, radial/cross-track/along-track difference postscript plots produced, named in predefined manner (assumes fit plots only)
ALL_FIT_PRED_PLOTS.M	Cartesian coordinate, radial/cross-track/along-track difference postscript plots produced, named in predefined manner (assumes fit and predict plots)
ALL_FIT_PLOTS_DEPS.M	Cartesian coordinate, radial/cross-track/along-track difference encapsulated postscript plots produced, named in predefined manner (assumes fit plots only)
ALL_PLOTS_DEPS.M	Cartesian coordinate, radial/cross-track/along-track difference encapsulated postscript plots produced, named in predefined manner (assumes fit and predict plots)

NAV_POE_COMPARE.M	Compares individual navigation solutions and POE vectors from MATfiles to produce 3-D difference plots

Once the proper files have been loaded into MATLAB, the comparison scripts can be utilized. The first three scripts listed in Table C.3 read the information in the MATfiles and produce difference plots as described. Thus, if the following commands were entered into MATLAB,

```
> xyz_plots
> rca_plots
> orbels_plots
```

a total of nine (fit *or* predict span only MATfiles) or eighteen (fit *and* predict span MATfiles) plots would be generated and remain on the screen. Each script produces either three (fit *or* predict span only) or six (fit *and* predict span) plots.

A series of print files associated with these plots can be generated by using one of the four routines listed after the three comparison scripts in Table C.3. These scripts generate plots for each of the comparison routines, convert them to either postscript (for direct printing to an on-line printer) or encapsulated postscript (for printing to a file, usually inserted in a document) files, and close the figures. Although the user does not have the opportunity to view these figures on the screen, the process becomes much more automated and simpler than typing in each of the MATLAB commands for execution of the scripts and printing of the files. Because these scripts utilize the three comparison routines, the same MATfile naming protocol is used.

The files produced by the print scripts are dependent upon which one is being executed. Execution of the script *ALL_FIT_PLOTS.M* results in creation of the following postscript files in the local directory:

XYZ_POSVEL.PS
XYZ_XP.PS
XYZ_XV.PS
RCA_RAD.PS
RCA_CT.PS
RCA_AT.PS
OE_SMA.PS
OE_INC.PS
OE_AOL.PS

Encapsulated postscript files differ only in the file extension (.DEPS vs. .PS). Fit and predict plots are distinguishable by 'FIT' and 'PRED' identifiers in between the two character strings seen above. Thus, fit and predict cross-track differences would be denoted by:

RCA_FIT_CT.PS
RCA_PRED_CT.PS

At this point, a simple VAX VMS command procedure could be designed to rename these print files to a more descriptive naming convention.

The final script presented in Table C.3 performs a comparison between individual navigation solutions and the POE vectors. The *NAV_FILE* and *POE_NPM_FILE* arrays are required for proper execution of this script, which plots only the three-dimensional position differences, and must be loaded

prior to execution. The MATfiles can be titled anything with an .MAT extension, as long as they were created by one of the FORTRAN routines listed in Table C.2.

Appendix D

Card Modifications

This appendix describes the modifications to R&D GTDS cards due to introduction of the FK5 and instantaneous true of date coordinate systems, and solid earth tidal modelling. Additional options have been defined for: ELEMENT1, IMPULSE, OBSINPUT, ORBTYPE, OUTCOORD, OUTOPT, OUTPUT, and SLPCOORD. In addition, one new GTDS keyword card has been introduced (SETIDE). The following keyword card descriptions should be used in conjunction with the R&D GTDS User's Guide when utilizing J2000, instantaneous true of date, or solid earth tide options.

ELEMENT1

- Card format: (A8, 3I3, 3G21.14)
- Applicable programs: EPHEM, DC
- Detailed format:

Columns	Format	Description
1-8	A8	ELEMENT1- keyword to set the first three components of the initial state vector and to identify the coordinate system and reference central body of the initial state.
9-11	I3	Input coordinate system orientation: = 1, mean Earth equator and equinox of 1950.0 = 2, true of reference, earth equator and equinox (FK4 based) = 3, true of reference, earth equator and equinox (FK4 based) = 4, mean ecliptic and equinox of 1950.0 = 5, true of reference ecliptic and equinox (FK4 based) = 6, NORAD true equator, mean equinox of date = 8, NORAD true equator, mean equinox of epoch = 10, earth-centered, earth-fixed **= 11, mean Earth equator and equinox of 2000.0** **= 12, true of reference, earth equator and equinox (FK5 based)** **= 14, mean ecliptic and equinox of 2000.0** **= 15, true of reference ecliptic and equinox (FK5 based)**
12-14	I3	Input coordinate system type: = 1, Cartesian = 2, Keplerian = 3, Spherical = 4, Mean Keplerian (used with the Brouwer, Brouwer-Lyddane, Brouwer-Gordon and Vinti analytic theories)

ELEMENT1 Cont'd

= 5, DODS Flight parameters
= 6, Averaged Keplerian (used with the Averaged VOP integrator)
= 7, Keplerian selenographic (body-fixed, moon-centered)
= 8, Averaged equinoctial (used with the Averaged VOP integrator)
= 9, Equinoctial
= 10, NORAD SGP elements (GTDS Keplerian format)
= 11, NORAD GP4/DP4 elements (GTDS Keplerian format)
= 12, NORAD HANDE elements (GTDS Keplerian format)
= 13, NORAD SALT elements (GTDS Keplerian format)
= 14, NORAD SGP elements (SPADOC format)
= 15, NORAD GP4/DP4 elements (SPADOC format)
= 16, NORAD HANDE elements (SPADOC format)
= 17, NORAD SALT elements (SPADOC format)
= 18, NORAD SGP elements (from the NORAD Historical Data System) (SPADOC format)
= 19, NAVSPASUR PPT2 elements -- GTDS Keplerian format (not currently found in VAX VMS version)
= 20, NAVSPASUR PPT2 elements -- NAVSPASUR format (not currently found in VAX VMS version)

15-17	I3	Input reference central body of the initial state[1,2]

---

1 Body Indices

1 = Earth	4 = Mars	7 = Uranus	10 = Mercury
2 = Moon	5 = Jupiter	8 = Neptune	11 = Venus
3 = Sun	6 = Saturn	9 = Pluto	

2 When Keplerian selenographic coordinates are used, the reference central body must be the moon.

ELEMENT1 Cont'd

The next three fields contain the elements[3] corresponding to the coordinate system type specified in field 3 (card columns 12-14) of this card:

Column	18-38	39-54	60-80
Format	G21.14	G21.14	G21.14
Cartesian	X position	Y position	Z position
Keplerian	Semimajor axis (a)	Eccentricity (e)	Inclination (i)
Spherical	Right ascension (α)	Declination (δ)	Vertical flight path angle
DODS	East longitude	Geodetic latitude	Horizontal flight path angle
Equinoctial	Semimajor axis (a)	Equinoctial variable h	Equinoctial variable k
SPADOC	mean motion (revs/day)	Eccentricity (e)	Inclination (i)

This keyword has no default variables.

3 Units are km, seconds, and degrees unless otherwise noted.

IMPULSE

- Card format: (A8, 3I3, 3G21.14)
- Applicable programs: EPHEM, DC
- Detailed format:

Columns	Format	Description
1-8	A8	IMPULSE - keyword to set the impulsive maneuver velocity increments.
9-11	I3	Maneuver number (1,2,...,5)
12-14	I3	Coordinate system reference for the maneuver: = 1, mean Earth equator and equinox of 1950.0 = 2, true of reference, earth equator and equinox (FK4 based) **= 11, mean Earth equator and equinox of 2000.0** **= 12, true of reference, earth equator and equinox (FK5 based)**
15-17	I3	Type of maneuver: =1, normal impulsive maneuver: X, Y, Z =2, maneuver uses Δv in R1 field, to be used with pitch and yaw from ATTANG1 and ATTANG2 cards. =3, ERTS type maneuver. =4,5 two IMPULSE cards must be real in order to change final default values (constants) in the ERTS gating maneuver model. =4, constants C1, C2, and C3 are contained in the three real fields. =5, constants C4 and C5 are contained in the first two real fields. =6, RADARSAT maneuvers, in radial, cross-track, and along-track components.
18-38	G21.14	X velocity increment (km/sec)
39-59	G21.14	Y velocity increment (km/sec)
60-80	G21.14	Z velocity increment (km/sec)

OBSINPUT

- Card format: (A8, 3I3, 3G21.14)
- Applicable programs: DC, FILTER, EARLYORB
- Detailed format:

Columns	Format	Description
1-8	A8	OBSINPUT - keyword to specify observations input sources.
9-11	I3	Source of input observations[1]
12-14	I3	Source of input observations
15-17	I3	Source of input observations
18-38	G21.14	Start time of observations span (yymmddhhmmss.ssss) (default = run epoch)
39-59	G21.14	End time of observations span (yymmddhhmmss.ssss) (default = run epoch plus three months)
60-80	G21.14	Satellite ID for second satellite (Applicable only when processing satellite to satellite data).

---

1 There are no default observation sources. Any desired source must be specified. If more than three sources are required, multiple OBSINPUT cards must be used. There are two options for inputing observation sources. Option 1 is used when there is no satellite to satellite tracking involved. Option 2 is used when the case involves satellite to satellite tracking. The two options can be intermixed but only one indicator from option 2 may be used on any set of OBSINPUT cards. No source number may be used in both options. The source numbers for options 1 and 2 are given below.

OBSINPUT Cont'd

Option 1

Source Number	Source
1	GTDS observations tape (29)[2]
2	GTDS observations disk (31)
3	DODS observations tape (30)
4	DODS permanent data base (32)
5	GTDS tracking data card file (15)
6	OABIAS data tape (94)
7	G-WWW tape, 9-track (40)
8	60 byte data base (96)
9	PCE ORB1 file in GTDS True of Reference Date coordinates -- FK4-based (24) - this ORB1 file usually would have been generated by a GTDS numerical integration process
10	Landmark data cards
11	Observations working file previously created (17)
12	General data handler tape (91)
13	LANDTRAK picture earth-edge data on cards (15)
14	GPS data tape
15	**PCE ORB1 file in Mean of 1950.0 (M50) coordinates (24)**

---

2 FORTRAN reference numbers associated with the various sources are within parentheses.

OBSINPUT Cont'd

- this ORB1 file usually would have been generated by a GTDS orbit generation process.

16 PCE ORB1 file in Earth-Centered Earth-Fixed (ECEF) coordinates (24)
- this ORB1 file usually would have been generated by a GTDS orbit generation process.

17 PCE ORB1 file in GTDS NORAD True of Reference coordinates (24)
- this ORB1 file usually would have been generated by a GTDS NORAD GP or SALT orbit generator.

18 PCE position and velocity in GTDS True of Reference Date coordinates (FK4-based) in observation card file format (15)
- this data would usually be generated externally to GTDS

19 PCE position and velocity in Mean of 1950.0 (M50) coordinates in observation card file format (15)
- this data would usually be generated externally to GTDS

20 PCE position and velocity in Earth-Centered Earth-Fixed (ECEF) coordinates in observation card file format (15)
- this data would usually be generated externally to GTDS

21 PCE position and velocity in NORAD True of Date coordinates in observation card file format (15)
- this data would usually be generated externally to GTDS

22 PCE ORB1 file in GTDS True of Reference Date coordinates -- FK5-based (24)
- this ORB1 file usually would have been generated by a GTDS numerical integration process

23 PCE ORB1 file in Mean of 2000.0 coordinates (24)

- this ORB1 file usually would have been generated by a GTDS orbit generation process.

24 PCE position and velocity in GTDS True of Reference Date coordinates (FK5-based) in observation card file format (15)
- this data would usually be generated externally to GTDS

25 PCE position and velocity in Mean of 2000.0 coordinates in observation card file format (15)
- this data would usually be generated externally to GTDS

26 PCE ORB1 in Instantaneous True of Date (ITOD) coordinates -- FK4-based (24)
- this ORB1 file usually would have been generated by a GTDS orbit generation process.

27 PCE ORB1 in Instantaneous True of Date (ITOD) coordinates -- FK5-based (24)
- this ORB1 file usually would have been generated by a GTDS orbit generation process.

28 PCE position and velocity in Instantaneous True of Date (ITOD) coordinates in observation card file format -- FK4-based (15)
- this data would usually be generated externally to GTDS

29 PCE position and velocity in Instantaneous True of Date (ITOD) coordinates in observation card file format -- FK5-based (15)
- this data would usually be generated externally to GTDS

Option 2

The source indicator IJK is a packed integer where

I indicates source of the satellite-to-satellite relay data

OBSINPUT Cont'd

J indicates source of ATS tracking data

K indicates source of target satellite tracking data

The following source numbers apply to I,J, and K.

Source Number	Source
1	No data of this type
2	General data handler tape (91)
3	DODS observations tape (30)
4	DODS permanent data base (32)

ORBTYPE

- Card format: (A8, 3I3, 3G21.14)
- Applicable programs: DC, FILTER, EARLYORB
- Detailed format:

Columns	Format	Description
1-8	A8	ORBTYPE - keyword to select orbit generator type.
9-11	I3	Orbit generator type (see Table tbs on the next page for types and additional options).
12-14	I3	See Table on next page.
15-17	I3	See Table on next page.
18-38	G21.14	See Table on next page.
39-59	G21.14	See Table on next page.
60-80	G21.14	See Table on next page.

ORBTYPE Cont'd

COLUMN	9-11	12-14	15-17	18-38	39-59	60-80
FORMAT	I3	I3	I3	G21.14	G21.14	G21.14
1	TIME-REGULAR-IZED COWELL = 1	INTEGRA-TION STEP MODE	COORD. SYSTEM ORIENT-ATION	NUMBER OF STEPS PER REVOLUTION (DEFAULT = 200)	--	TIME REGULATIZA-TION CONSTANT (DEFAULT = 1.5)
2	COWELL (DEFAULT) = 2	INTEGRA-TION STEP MODE	COORD. SYSTEM ORIENT-ATION	INTEGRA-TION STEPSIZE IN SECONDS (DEFAULT = 24)	--	--
3	BROUWER = 3	SECULAR THEORY OPTIONS 1 - YES 0 - NO (DEFAULT)	OSCULATING TO MEAN OPTIONS	RATE FOR SEMI-MAJOR AXIS	--	--
4	BROUWER-LYDDANE = 4	SECULAR THEORY OPTIONS	OSCULATING TO MEAN OPTIONS	RATE FOR SEMI-MAJOR AXIS	--	--
5	AVERAGED VARIATION OF PARAMETER (VOP) = 5	INTEGRA-TION STEP MODE	COORD. SYSTEM ORIENT-ATION	INTEGRA-TION STEPSIZE IN SECONDS (DEFAULT = 86400)	INTEGRA-TION METHOD OPTIONS BLANK = USE MULTISTEP (SEE NOTES) 1 = USE RUNGE-KUTTA	TYPE OF VOP PARAMETER (DEFAULT = 12, AVERAGED EQUI-NOCTIAL)
6	PRE-GENERATED ORBIT FILE = 6	LEVEL OF ORBIT FILE = 0 (ZERO) FOR SEQUENTIAL	FRN OF THE ORBIT FILE	--	--	--
7	OSCULATING VARIATION OF PARAMETER (VOP) = 7	INTEGRA-TION STEP MODE	COORD. SYSTEM ORIENT-ATION	INTEGRA-TION STEPSIZE IN SECONDS (DEFAULT = 7200)	--	TYPE OF VOP PARAMETER (DEFAULT = 2)
8	NOT USED IN DRAPER R&D GTDS					
9	CHEBYSHEV SERIES INTEGRATOR = 9	INTEGRA-TION STEP MODE	COORD. SYSTEM ORIENT-ATION	ARC LENGTH IN SECONDS (DEFAULT = 5400)	ORDER OF CHEBYSHEV POLY-NOMIAL (DEFAULT = 36)	TOLERANCE (DEFAULT = 1.D-6)
10	RUNGE-KUTTA-FEHLBERG = 10	INTEGRA-TION STEP MODE	COORD. SYSTEM ORIENT-ATION	INTEGRA-TION STEPSIZE IN SECONDS (DEFAULT = 24)	--	--

ORBTYPE Cont'd

COLUMN	9-11	12-14	15-17	18-38	39-59	60-80
FORMAT	I3	I3	I3	G21.14	G21.14	G21.14
11	BROUWER-GORDON = 11	SECULAR THEORY OPTIONS	OSCULATING TO MEAN OPTIONS	RATE FOR SEMI-MAJOR AXIS	--	--
12	VINTI = 12	RESIDUAL 4TH HARMONIC OPTION 1 - YES 0 - NO (DEFAULT)	MEAN RATE OPTION 1 - AVERAGED 2 - SECULAR (DEFAULT)	RATE FOR SEMI-MAJOR AXIS	--	--
13	NORAD SGP = 13	OSCULATING OR MEAN OUTPUT 1 - OSCULATING 2 - MEAN (NOT OPERA-TIONAL)	COORD. SYSTEM ORIENT-ATION = 8	COMPUTE METHOD FOR REFERENCE TIME = 1, CONSIDER A.1-UTC OFFSET = 2, ZERO TIME CONSTANTS	--	--
14	NORAD GP4/DP4 (AUTOMATIC SELECTION) = 14	OSCULATING OR MEAN OUTPUT 1 - OSCULATING 2 - MEAN (NOT OPERA-TIONAL)	COORD. SYSTEM ORIENT-ATION = 8	COMPUTE METHOD FOR REFERENCE TIME = 1, CONSIDER A.1-UTC OFFSET = 2, ZERO TIME CONSTANTS	--	--
15	NORAD DP4 = 15	OSCULATING OR MEAN OUTPUT 1 - OSCULATING 2 - MEAN (NOT OPERA-TIONAL)	COORD. SYSTEM ORIENT-ATION = 8	COMPUTE METHOD FOR REFERENCE TIME = 1, CONSIDER A.1-UTC OFFSET = 2, ZERO TIME CONSTANTS	--	--

ORBTYPE Cont'd

COLUMN	9-11	12-14	15-17	18-38	39-59	60-80
FORMAT	I3	I3	I3	G21.14	G21.14	G21.14
16	NORAD HANDE (7 parameter input) = 16	OSCULATING OR MEAN OUTPUT 1 - OSCULATING 2 - MEAN (NOT OPERA-TIONAL)	COORD. SYSTEM ORIENT-ATION = 8	COMPUTE METHOD FOR REFERENCE TIME = 1, CONSIDER A.1-UTC OFFSET = 2, ZERO TIME CONSTANTS	--	--
17	NORAD HANDE (16 parameter input) = 17	OSCULATING OR MEAN OUTPUT 1 - OSCULATING 2 - MEAN (NOT OPERA-TIONAL)	COORD. SYSTEM ORIENT-ATION = 8	COMPUTE METHOD FOR REFERENCE TIME = 1, CONSIDER A.1-UTC OFFSET = 2, ZERO TIME CONSTANTS	--	--
18	NORAD SALT	OSCULATING OR MEAN OUTPUT 1 - OSCULATING 2 - MEAN (NOT OPERA-TIONAL)	COORD. SYSTEM ORIENT-ATION = 8	COMPUTE METHOD FOR REFERENCE TIME = 1, CONSIDER A.1-UTC OFFSET = 2, ZERO TIME CONSTANTS	SALT NUM. INT. SCHEME 1, RK 4-4 2, RK FAST MODE (NOT OPERA-TIONAL IN GTDS)	SALT NUM. INT. STEPSIZE IN REVS.
19	NAVSPASUR PPT2	OSCULATING OR MEAN OUTPUT 1 - OSCULATING 2 - MEAN (NOT OPERA-TIONAL)	COORD. SYSTEM ORIENT-ATION = 8	COMPUTE METHOD FOR REFERENCE TIME = 1, CONSIDER A.1-UTC OFFSET = 2, ZERO TIME CONSTANTS	--	TESSERAL SHORT PERIODIC OPTION = 1, NAVSPASUR ROUTINE LUNAR =2, DRAPER M-DAILY MODEL =3, NONE (DEFAULT)

ORBTYPE Cont'd

Notes to ORBTYPE options:

- Integration step modes

  1 - Fixed step (default)

  2 - Regular vary step

  3 - Shell mode vary step (not available for VOP orbit generators)

  4 - Halving-doubling

  Tolerances for the automatic variable step options (2 - regular vary step, and 4 - halving-doubling) are specified by the TOLER, LOWBOUND, UPPBOUND, and NOMBOUND keywords.

  The radial distances and corresponding stepsizes for the semi-automatic variable step option (3 - shell mode vary step) are specified on the SHELLRAD card.

- Coordinate system orientation

  1 - Mean equator and equinox of 1950.0 (default)[1]

  2 - True of reference -- FK4 based (Precession and nutation are ignored in coordinate system transformations during integration. Therefore, this coordinate system orientation is only desireable when the integration span is short and in proximity to the reference date).

  8 - NORAD True of reference (only used with NORAD and NAVSPASUR theories)

  11 - Mean equator and equinox of 2000.0 (default)[1]

  12 - True of reference -- FK5 based (Precession and nutation are ignored in coordinate system transformations during

---

1 The default value depends upon the fundamental reference system used (either FK4 or FK5). If FK4, the default is mean of 1950.0; for FK5, it is mean of 2000.0

integration. Therefore, this coordinate system orientation is only desireable when the integration span is short and in proximity to the reference date).

- Integration stepsize

  The initial stepsize and mode are used for all flight sections unless overridden by the keyword cards STEPSIZE and INTMODE, respectively.

  When using the time-regularized option, the stepsize is determined by the period divided by the number of steps per revolution.

- Time regularization constant (n)

  The type of independent variables in time regularization are defined by:

$$\frac{dt}{ds} = \frac{r^n}{\sqrt{\mu}} \qquad 1 \leq n \leq 2$$

- Type of VOP parameter

1 = Dallas	6 = Kustaanheimo-Stiefel (KS)
2 = Equinoctial (mean longitude)	7 = Delaunay-Stiefel (DS)
3 = Equinoctial (ecc. longitude)	8 = Keplerian
4 = Ideal (true longitude)	12 = Averaged Equinoctial
5 = Ideal (ecc. longitude)	18 = Averaged Keplerian

- Osculating-to-mean options:

  0 = Osculating to mean conversion in Cartesian mean space (default)

ORBTYPE Cont'd

1 = Osculating to mean conversion in Keplerian space

2 = 1st order osculating to mean conversion

- Integration Method for the Averaged Variation of Parameter Formulation

  The Runge-Kutta method with fixed stepsize must be employed if short periodics are on. The multistep method with fixed stepsize may be employed if short periodics are off. The multistep method is recommended for long arc (several months or years) integration.

OUTCOORD

- Card format: (A8, 3I3, 3G21.14)
- Applicable programs: EPHEM
- Detailed format:

Columns	Format	Description
1-8	A8	OUTCOORD - keyword to set the output coordinate system orientation by flight sections.
9-11	I3	Flight section I.
12-14	I3	Flight section J.
15-17	I3	Flight section K.
18-38	G21.14	Indicator for output coordinate system orientation for section I.[1]
39-59	G21.14	Indicator for output coordinate system orientation for section I.
60-80	G21.14	Indicator for output coordinate system orientation for section I.

The maximum number of flight sections is ten (10).

---

1 The following values are used to specify the coordinate system orientation:

1 - Mean of 1950.0 body-centered

2 - Body-centered true of date (or reference)[2] -- FK4-based.

3 - Body-fixed true of date (or reference)[2]

11 - Mean of 2000.0 body-centered

12 - Body-centered true of date (or reference)[2] -- FK5-based.

2 This output will be true of date if integrating in the 1950.0 system, otherwise, it will be in the true of reference system.

OUTOPT

- Card format: (A8, 3I3, 3G21.14)
- Applicable programs: EPHEM, DC, FILTER
- Detailed format:

Columns	Format	Description
1-8	A8	OUTOPT - keyword to select ephemeris output.
9-11	I3	Type of ephemeris file to be generated:[1] = 0, ORBIT file on primary unit = 1, ORB1 file (9-track) on primary unit = 2, ORB1 file (9-track) and ORBIT file on primary units = 3, EPHEM file on primary unit[2] = 4, ORBIT file and EPHEM file on primary units = 5, EDFP file[3] = 20, ORBIT file on secondary unit = 21, ORB1 file (9-track) on secondary unit = 22, ORB1 file (9-track) and ORBIT file on secondary units = 23, EPHEM file on secondary unit = 24, ORBIT file and EPHEM file on secondary units
12-14	I3	For ORBIT file (i.e., when value in columns 9-11 is 0,2,4,20,22, or 24), partial derivatives switch[4] = 1, partial derivatives are included = 2, partial derivatives are not included (default). For EPHEM files (i.e., when the value in columns 9-11 is 3 or 23), central body indicator.
15-17	I3	For ORBIT files (i.e., when the value in columns 9-

1 see Note 1.

2 see Note 2.

3 see Note 3.

4 In these cases, the EPHEM file will default to Earth-centered true of date.

11 is 0,2,4,20,22, or 24):[1]
= 0, means sequential
> 0, indicates the level of direct access file to be generated

For EPHEM files (i.e., when the value in columns 9-11 is 3 or 23), the coordinate frame indicator:[5]
= 1, Mean of 1950.0
= 2, True of Reference -- FK4-based (default)
= 9, Instantaneous True of Date -- FK4-based
= 11, Mean of 2000.0
= 12, True of Reference -- FK5-based (default)
= 19, Instantaneous True of Date -- FK5-based

18-38	G21.14	Start time of arc (yymmddhhmmss.ssss)
39-59	G21.14	End time of arc (yymmddhhmmss.ssss)
60-80	G21.14	Output interval for ORB1 or EPHEM file (default = 60 seconds)

NOTES: 1. The ORBIT file will be referenced to the same central body and coordinate system as teh integrator. The primary unit is the standard unit assignment when any output ephemeris file is needed. The secondary unit is used when a file is being generated for immediate use in the COMPARE program. The FRNs for the files are:

Primary Unit	Secondary Unit	File
19	86	ORBIT disk file with partial derivatives
20	88	ORBIT disk file without partial derivatives

---

5 In these cases, the default reference system will be dependent upon the fundamental integration coordinate system. For integration in FK4 (M50)-based systems, the default will be 2; for FK5(J2000)-based systems, the default will be 12.

21	82	ORBIT tape file with partial derivatives

OUTOPT Cont'd

22	84	ORBIT tape file without partial derivatives
24	81,83,85,87	ORB1 or EPHEM file
54	None	EDPF file

2. In stacked cases when multiple EPHEM files are generated, the FRN is cicularly updated with each case starting with unit 24, then 81 followed by 83, 85, and 87. The user may specify the first unit to be written as unit 81 by setting the secondary EPHEM indicator.

3. The EDPF file is an ephemeris data file for the PDP-11 computer.

OUTPUT

- Card format: (A8, 3I3, 3G21.14)
- Applicable programs: EPHEM
- Detailed format:

Columns	Format	Description
1-8	A8	OUTPUT - keyword to select orbit generator printer output.
9-11	I3	Output coordinate system orientation: = 1, mean Earth equator and equinox of 1950.0 = 2, true of reference, earth equator and equinox - inertial (FK4 based) (default) = 3, true of reference, earth equator and equinox - body-fixed = 4, mean ecliptic and equinox of 1950.0 = 5, true of reference ecliptic and equinox (FK4 based) = 6, NORAD true equator, mean equinox of date = 8, NORAD true equator, mean equinox of epoch **= 9, instantaneous true of date, earth equator and equinox - inertial (FK4 based)** **= 11, mean Earth equator and equinox of 2000.0** **= 12, true of reference, earth equator and equinox - inertial (FK5 based)** **= 14, mean ecliptic and equinox of 2000.0** **= 15, true of reference ecliptic and equinox (FK5 based)** **=19, instantaneous true of date, earth equator and equinox - inertial (FK5 based)**
12-14	I3	Output Reference System: = 1, Cartesian (position, velocity, latitude, height) = 2, Cartesian, Keplerian, and spherical (default) = 3, Cartesian, Keplerian, spherical and mean[1]

[1] Osculating instead of mean when using the VOP integrator averaging types. Mean elements are those associated with the Brouwer-Lyddane orbit theory.

OUTPUT Cont'd

		= 91, same as 1 plus coordinates in Earth/Moon-Sun L-1 rotating systems = 92, same as 2 plus rotating coordinates = 93, same as 3 plus rotating coordinates This field may take the form NM where M is defined above (column 14) and N indicates special nodal crossing printout (column 13): N = 1, print at ascending nodes N = 2, print at descending nodes N = 3, print at ascending and descending nodes
15-17	I3	Output reference body (other than central body): = 1, Earth = 2, Sun = 4, Moon = 8, target body (defined as central body of the final section)
18-38	G21.14	Year, month, day of end print arc (yymmdd)
39-59	G21.14	Hours, minutes, seconds of end of print arc (hhmmss.ssss)
60-80	G21.14	Output print interval in seconds OR Nodal print frequency if I2>9 (i.e., print every Nth crossing)

The start time of the print arc is epoch by default or can be set using the keyword card TIMES in the OGOPT subdeck.

The initial output coordinate system orientation, output coordinate system type, and output reference body will be used for all flight sections unless overridden by the keyword cards OUTCOORD, OUTTYPE, and OUTBODY, respectively.

SLPCOORD

- Card format: (A8, 3I3, 3G21.14)
- Applicable programs: EPHEM, DC, FILTER, DATAMGT, ANALYSIS, DATASIM
- Detailed format:

Columns	Format	Description
1-8	A8	SLPCOORD - keyword to specify SLP ephemeris coordinate system reference
9-11	I3	Coordinate system reference: = 1, mean equator and equinox of 1950.0 (default) = 2, true equator and equinox of date (FK4-based) **= 3, mean equator and equinox of 2000.0 (default)** **= 4, true equator and equinox of date (FK5-based)**
12-17	2I3	Blank
18-80	G21.14	Blank

SETIDE

- Card format: (A8, 3I3, 3G21.14)
- Applicable programs: EPHEM, DC, FILTER[1]
- Detailed format:

Columns	Format	Description
1-8	A8	SETIDE - keyword set the solid earth tide force model option
9-11	I3	Model options: = 1, include both solar and lunar tidal effects = 2, include only solar tidal effects = 3, include only lunar tidal effects =4, include neither solar or lunar tidal effects (default)
12-17	2I3	Blank
18-38	G21.14	Love's constant (default = 0.30 for FK4 systems, 0.29 for FK5 systems)
39-80	2G21.14	Blank

1 Only one section.

[This page intentionally left blank.]

Appendix E

Typical VAX VMS Draper R&D GTDS Setup

This appendix provides a more in-depth discussion of the operation of the VAX VMS version of Draper R&D GTDS. Section 2.2.1 indicates that a typical setup involves three files: the input card data file, a command file, and an overrides file. Although not currently implemented, these files could be tied to a system that would simplify program execution, such as a Graphical User Interface (GUI)*.

The purpose of the input card data file is to specify the program to be executed and the desired options associated with that program. The content of the input card data file is dependent upon the program being executed, but certain information must be included in every Draper R&D GTDS program. A CONTROL card defines the specific program being executed, while a FIN card indicates the termination of this particular application. Mandatory cards follow the CONTROL card in the data file; the number of these cards is program specific. Subdecks contain various options available to the user for that specific application.

When input card data files are concatenated into one data file, Draper R&D GTDS has the capability to interpret multiple input card data files in the same

---

* Initial efforts have been made toward a GUI for the PC-based version of R&D GTDS at the U.S. Air Force's Phillips Laboratory. Also, RADARSAT Flight Dynamics software is in a GUI environment.

execution. In this manner, one application can create working files to be used in later programs. Also, final results from one program can be passed through a COMMON block as initial conditions for the next application. The following figure illustrates a typical concatenated input card data file.

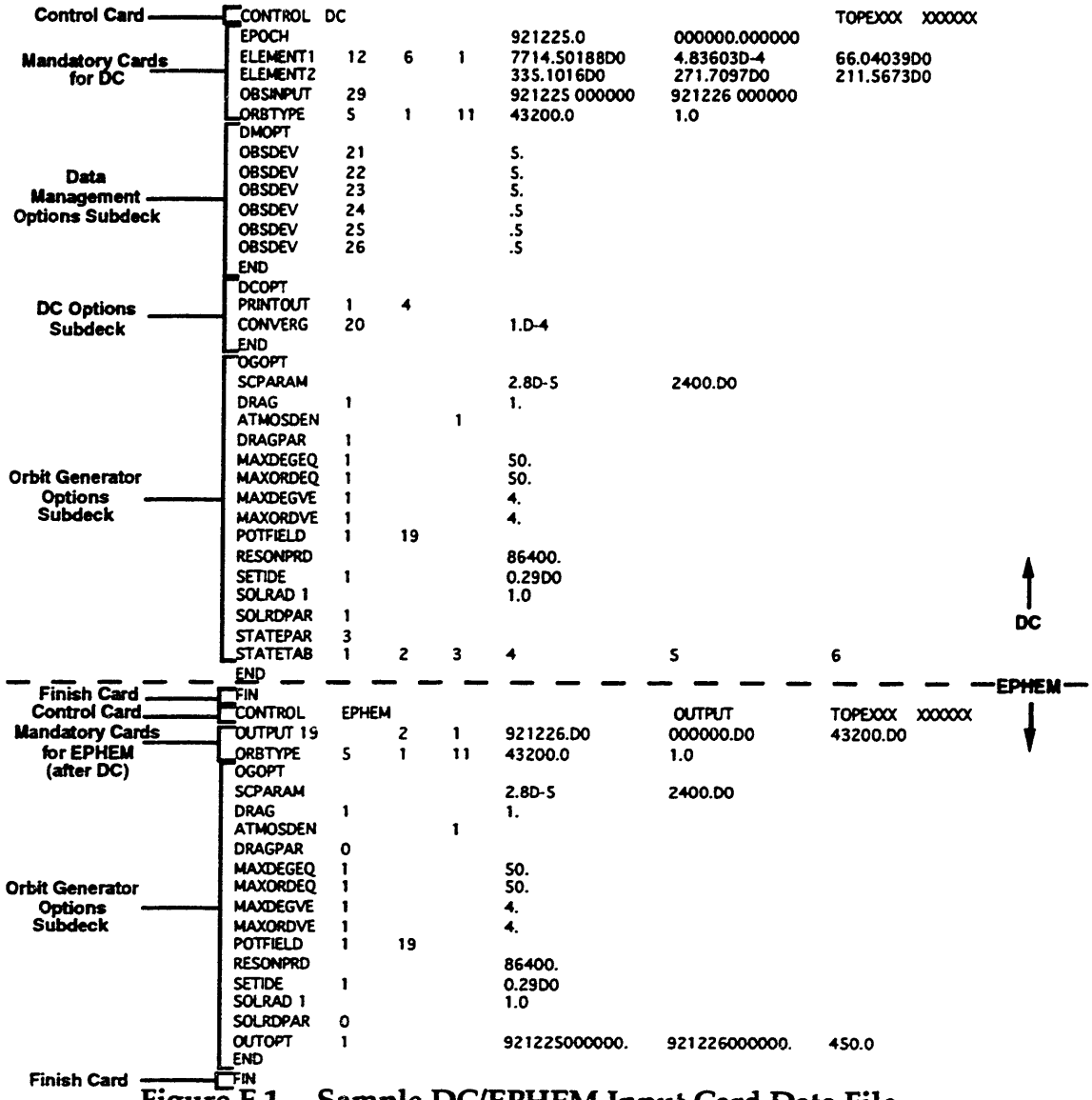

Figure E.1 Sample DC/EPHEM Input Card Data File

In this example, observations from an external source (in the form of a GTDS observation card) are used in a differential correction orbit determination

scheme over a one day period. The resulting initial conditions are then used to generate an ephemeris over the one day fit span, which is written to a GTDS ORB1 file.

The differential correction step in Figure E.1 has five mandatory cards that describe the initial state (ELEMENT1, ELEMENT2, and EPOCH cards), the observation source and associated times (OBSINPUT), and the orbit generator to be used (ORBTYPE). This particular card data file uses instantaneous true equator and equinox of date Cartesian positions and velocities from an observation card as input to the differential correction. A semianalytic integrator referenced to the mean equator and equinox of J2000 coordinate system is used to generate an ephemeris during the fit process.

Options from the data management (DMOPT), differential correction (DCOPT), and orbit generator (OGOPT) subdecks are used. Observation noise standard deviations for the Cartesian positions and velocities are specified in the DMOPT subdeck (OBSDEV). The DCOPT subdeck requests printouts of the residual reports for the first and last iteration (PRINTOUT), and sets the convergence criteria to an RMS value of 0.0001, limiting the number of iterations to 20 (CONVERG). The OGOPT subdeck sets perturbation parameters for drag (DRAG and ATMOSDEN), the gravitational potential (MAXDEGEQ, MAXORDEQ, MAXDEGVE, MAXORDVE, and POTFIELD), solid earth tides (SETIDE), and solar radiation pressure (SOLRAD). The minimum resonant perturbation period is set to one day (RESONPRD). The drag and solar radiation parameters are solved-for via the DRAGPAR and SOLRDPAR cards, respectively, and the spacecraft area and mass parameters

are set with the SCPARAM card. The averaged equinoctial elements are defined as state solve-for parameters (STATEPAR and STATETAB).

After the best estimate of the initial conditions is developed by the DC, these conditions are passed to the EPHEM for orbit generation (as a result of the OUTPUT found in the CONTROL EPHEM card). Since elements are passed from the DC to the EPHEM, no ELEMENT1, ELEMENT2, or EPOCH cards are required (the epoch of the EPHEM is assumed to be the same as the epoch of the DC). Perturbation modeling in the DC and EPHEM are the same. Note that the drag and solar radiation pressure parameters are no longer part of the solve-for vector. An ORB1 file over the one day fit span at 7.5 minute intervals is produced (OUTOPT).

A separate command file is used to spawn Draper R&D GTDS and accept the input card data file for execution. This command file typically contains file assignments for data bases required in the specific application. The executable file for the version of GTDS being used is also identified.

```
$!-------------------------------------------------------------------
$! topex_nav_sst_fit_1.com
$!
$!
$!-------------------------------------------------------------------
$!
$! Set default for batch run
$!
$  SET DEFAULT fds$diska:[ssc2414.work.new_gtds.nav_solns]
$!
$!              Assign debug overrides
$!
$  ASSIGN/TABLE=LNM$JOB   [ssc2414.work.new_gtds.nav_solns]topex_nav_sst_fit_1.OVERRIDES          DBG$INIT
$!
$!              Assign various perturbation-related files
$!
$  ASSIGN/TABLE=lnm$job fds$diska:[djf1230.bianca]dan_potential.dat gtds$047
$  ASSIGN/TABLE=lnm$job fds$diska:[djf1230.bianca]moon.dat     gtds$048
$  ASSIGN/TABLE=LNM$JOB fds_dbf:jacchia_roberts.dat  gtds$075
$  ASSIGN/TABLE=LNM$JOB fds$diska:[ssc2414.work.new_gtds.test]newcomb.dat  gtds$023
$!
$!              Assign SLP files
$!
$  ASSIGN/TABLE=lnm$job elrond$dka0:[ssc2414]june95_msgen_slp_mn2000.dat gtds$014
$  ASSIGN/TABLE=lnm$job elrond$dka0:[ssc2414]june95_msgen_slp_tod2000.dat gtds$078
$!
$!              Assign Timing Coefficients file
$!
$  ASSIGN/TABLE=lnm$job elrond$dka0:[ssc2414]june95_msgen_slp_timecoef.dat gtds$038
$!
$!              Assign Observations file
$!
$  ASSIGN/TABLE=lnm$job fds$diska:[ssc2414.topex.obscard]92dec23-27_pbias.poscard gtds$015
$!
$!              Assign ORB1 file
$!
$  ASSIGN/TABLE=LNM$JOB fds$diska:[ssc2414.work.new_gtds.nav_solns]topex_nav_sst_fit_1.ORB1 gtds$024
$!
$!              Assign Fundamental Constants file
$!
$  ASSIGN/TABLE=LNM$JOB fds$diska:[ssc2414.work.new_gtds.mods]j2000_csconst.dat gtds$099
$!
$!
$!            Execute the J2000 version of GTDS using TOPEX_NAV_COWELL_FIT_1.GTDS as the input card data file
$!
$  @[ssc2414.work.new_gtds.test]j2000_SWAT_GTDS [ssc2414.work.new_gtds.nav_solns]topex_nav_sst_fit_1
$!
$  EXIT
```

Figure E.2 Sample DC/EPHEM GTDS Command File

To simplify matters, the names of the input card data, command and overrides files are usually the same (file extensions are usually .GTDS, .COM, and .OVERRIDES, respectively). This example shows the name of the files being executed to be *'TOPEX_NAV_SST_FIT_1'*. The command file assigns logical names that GTDS understands prior to execution. After the overrides file is assigned to DBG$INIT, a series of GTDS logicals (GTDS$xxx) are assigned to appropriate files. The files allocated for this execution included perturbation-related data bases, SLP files, timing coefficient files, the observations file, the output ORB1 file, and the fundamental constants file.

Once these GTDS logicals were pointed to the proper files, execution of GTDS could take place. A second command procedure (J2000_SWAT_GTDS.COM) is used to assign the names of the input card data file and tabulated output report to the appropriate GTDS logicals. It then executes the appropriate version (in this case, the executable resulting from this project) of Draper R&D GTDS.

Because the short periodics input processor is not included in the VAX VMS versions of Draper R&D GTDS, an overrides file is necessary to change certain semianalytic capabilities from their default values. This file breaks the execution of the application in three subroutines (where applicable) - HWIRE, ESTSET, and SKFSET. It then 'deposits' the desired value into memory location associated with that specific parameter.

```
SET OUTPUT LOG
SET LOG
SET BREAK/return ESTSET DO -
      (DEPOSIT  IDIFF  = 3; -
       DEPOSIT  IDRVAR = 1; -
       DEPOSIT  ISRVAR = 1; -
       DEPOSIT  KPAR   = 1; -
       DEPOSIT  KATMOS = 1; -
       EXAMINE  KATMOS   ; -
       EXAMINE  IDIFF    ; -
       EXAMINE  IDRVAR   ; -
       EXAMINE  ISRVAR   ; -
       EXAMINE  KPAR     ; -
       GO -
    ); -
GO
SET BREAK/return HWIRE  DO -
      (DEPOSIT  LZN   = 4; -
       DEPOSIT  JZN   = 25; -
       DEPOSIT  LMD   = 4; -
       DEPOSIT  MMD   = 28;-
       DEPOSIT  MTS   = 41;-
       DEPOSIT  NJ2MD  = 12; -
       DEPOSIT  MJ2MD  = 12; -
       DEPOSIT  LJ2MD  = 4; -
       DEPOSIT  IDRMD  = 2; -
       DEPOSIT  NTH(1)  = 4; -
       DEPOSIT  NTH(2)  = 4; -
       DEPOSIT  JMAXTH(1)= 5; -
       DEPOSIT  LTH(1)  = 4; -
       DEPOSIT  LTH(2)  = 4; -
       DEPOSIT  JMAXTS  = 25;-
       DEPOSIT  JMINTS  =-25;-
       EXAMINE  LZN    ; -
       EXAMINE  JZN    ; -
       EXAMINE  LMD    ; -
       EXAMINE  NJ2MD  ; -
       EXAMINE  MJ2MD  ; -
       EXAMINE  LJ2MD  ; -
       EXAMINE  IDRMD  ; -
       EXAMINE  NTH(1)  ; -
       EXAMINE  NTH(2)  ; -
       EXAMINE  JMAXTH(1); -
       EXAMINE  LTH(1)  ; -
       EXAMINE  LTH(2)  ; -
       GO -
    ); -
GO
```

Figure E.3 Sample GTDS Overrides File

This overrides file breaks execution in two locations, routines ESTSET and HWIRE. Various parameter switches associated with the Average Partial Generator (APG) and Short Periodic Partial Generator (SPPG) are deposited in ESTSET. Other parameters involved in the averaged equations of motion and short periodics recovery are deposited in HWIRE. After the values are deposited, they are 'examined' to ensure that the values were properly deposited.

[This page intentionally left blank.]

Appendix F

Fundamental Constants File Description

The numerical values for several astrodynamic constants are different between the fundamental systems used by the FK4 and FK5 catalogues. These differences are primarily a result of improvements in measurement techniques or natural phenomena (e.g., earth's rotation rate). Table 3.1 summarizes the various constants that have different representations.

Because these values are dependent upon the theory being executed, some distinction had to exist between the two sets of constants. It was decided to access the values from an external ASCII file that contained either the FK4 or FK5 representation, depending upon the theory being implemented (the active SLP files were the distinguishing factor). This places the burden of responsibility on the user to ensure that the constants being read from this external file and the information on the SLP files are compatible.

This appendix summarizes the content and format of the ASCII file. The file has been assigned to the GTDS logical file number 99 in routine FILESBD. The standard FK4 and FK5 files are presented, along with a description of the contents. Also, the FK5 fundamental constants file used in the TAOS experiments is presented separately. Analysis of the TAOS POE file indicated that the fundamental value associated with the earth's rotation rate was different than that of TOPEX. The remainder of the values are the same. The

FK4 constants are based upon the values existing in Draper R&D GTDS prior to this work.

Table F.1 Format of Fundamental Constants File

	Columns 1-24	Columns 27-50	Columns 53-76	Columns 79-102	Columns 105-128
Row 1	REF_DA2	A1_EPOCH	MJD_CORR		
Row 2	GHA(1)	GHA(2)	GHA(3)	GHA(4)	GHA(5)
Row 3	MN_OBL(1)	MN_OBL(2)	MN_OBL(3)	MN_OBL(4)	
Row 4	LAN_M(1)	LAN_M(2)	LAN_M(3)	LAN_M(4)	LAN_M(5)
Row 5	LONG_M(1)	LONG_M(2)	LONG_M(3)	LONG_M(4)	LONG_M(5)
Row 6	LOP_M(1)	LOP_M(2)	LOP_M(3)	LOP_M(4)	LOP_M(5)
Row 7	LONG_S(1)	LONG_S(2)	LONG_S(3)	LONG_S(4)	LONG_S(5)
Row 8	LOP_S(1)	LOP_S(2)	LOP_S(3)	LOP_S(4)	LOP_S(5)
Row 9	NUT_OB(1)	NUT_OB(2)	NUT_OB(3)	NUT_OB(4)	NUT_OB(5)
Row 10	NUT_OB(6)	NUT_OB(7)	NUT_OB(8)	NUT_OB(9)	NUT_OB(10)
Row 11	NUT_OB(11)	NUT_OB(12)	NUT_OB(13)	NUT_OB(14)	NUT_OB(15)
Row 12	NUT_OB(16)	NUT_OB(17)	NUT_OB(18)		
Row 13	GCON	GM	AB	OMEGA	FLAT
Row 14	EYE	BESJUL	RE	AU	
Row 15	LIBR_I(1)	LIBR_I(2)	LIBR_I(3)	MA_M(1)	MA_M(2)
Row 16	LIBR_M(1)	LIBR_M(2)	LIBR_M(3)	AOP_M(1)	AOP_M(2)
Row 17	LIBR_N(1)	LIBR_N(2)	LIBR_N(3)	MA_S(1)	MA_S(2)
Row 18	PREC_S(1)	PREC_S(2)	PREC_S(3)		
Row 19	PREC_U(1)	PREC_U(2)	PREC_U(3)		
Row 20	PREC_Z(1)	PREC_Z(2)	PREC_Z(3)		
Row 21	DELLAC(1)	DELLAC(2)	DELLAC(3)		
Row 22	GM_S	GM_M	CLOVE		

Variable	Common Block	Meaning
REFDA2	FRC	Modified Julian Date of Fundamental Epoch (B1950 or J2000)
A1_EPOCH	CSCONST	A1-UTC at Fundamental Epoch
MJD_CORR	CSCONST	Number of days from JD 2430000 and 1900 (for B1950 cases) or 2000 (for J2000 cases)
GHA(1-5)	CSCONST	Coefficients for Greenwich hour angle
MN_OBL(1-4)	CSCONST	Coefficients for mean obliquity of date
LAN_M(1-5)	CSCONST	Coefficients for longitude of ascending node of the moon
LONG_M(1-5)	CSCONST	Coefficients for longitude of the moon
LOP_M(1-5)	CSCONST	Coefficients for longitude of perigee of the moon
LONG_S(1-5)	CSCONST	Coefficients for longitude of the sun
LOP_S(1-5)	CSCONST	Coefficients for longitude of perigee of the sun
NUT_OB(1-18)	CSCONST	Coefficients for nutation in obliquity
GCON	FRC	Universal gravitational constant
GM	FRC	Gravitational constant for the earth
AB	FRC	Radius of the earth
OMEGA	FRC	Rotation rate of the earth
FLAT	FRC	Flattening coefficient of the earth
EYE	CSCONST	Inclination of mean lunar equator to ecliptic
BESJUL	CSCONST	Conversion from Besselian to Julian time
RE	CETBL1	Radius of the earth
AU	CETBL1	One astronomical unit
LIBR_I(1-3)	CSCONST	Coefficients for lunar libration in inclination
LIBR_M(1-3)	CSCONST	Coefficients for lunar libration in mean longitude
LIBR_N(1-3)	CSCONST	Coefficients for lunar libration in longitude of the ascending node
MA_M(1-2)	CSCONST	Coefficients for lunar mean anomaly
AOP_M(1-2)	CSCONST	Coefficients for lunar argument of perigee
MA_S(1-2)	CSCONST	Coefficients for solar mean anomaly
PREC_S(1-3)	CSCONST	Coefficients for precession
PREC_U(1-3)	CSCONST	Coefficients for precession

PREC_Z(1-3)	CSCONST	Coefficients for precession
DELLAC(1-3)	CSCONST	Coefficients for difference between geodetic and geocentric latitude
GM_S	FRC	Gravitational constant for sun
GM_M	FRC	Gravitational constant for moon
CLOVE	FRC	Love number for solid earth tides

```
3282.423000000000D0   3.070000000000D0   14980.000000000000D0
   1.739935893717D0 628.331950990899D0      6.75587864626D-6   0.000000000000D0   6.300388098446D0
  23.445758700000D0   -.013094040000D0   -.000000880000D0    .000000500000D0
  12.112790000000D0   -.052953922000D0    .002079500000D0    .002081000000D0    .000002000000D0
  64.375452000000D0  13.176397000000D0   -.001131575000D0   -.001130150000D0    .000001900000D0
 208.843990000000D0    .111404080000D0   -.010334000000D0   -.010343000000D0   -.000012000000D0
 280.081210000000D0    .985647340000D0    .000303000000D0    .000303000000D0    .000000000000D0
 282.080530000000D0    .000047068400D0    .000455250000D0    .000457500000D0    .000003000000D0
  25.584400000000D0   -.251100000000D0   1.533600000000D0    .066600000000D0   -.025800000000D0
   -.018300000000D0   -.006700000000D0    .245600000000D0    .050800000000D0    .036900000000D0
   -.013900000000D0   -.008600000000D0    .008300000000D0    .006100000000D0    .006400000000D0
   0.000000000000D0   0.000000000000D0   0.000000000000D0
   6.6730000000D-23   3.986008000000D5 6378.140000000000D0   7.29211585494D-5  298.250000000000D0
   0.026790804000D0   0.075643000000D0 6378.149200000000D0   1.495979000000D8
  -0.51875025100D-3   0.17937970500D-3  -0.53329407900D-4   3.761884939000D0   0.228027127200D0
  -0.58171824000D-4   0.28603852000D-3   0.87266462600D-4   3.433859067800D0   0.28685987000D-2
  -0.52844550000D-3   0.17937970500D-3  -0.53329407900D-4   6.248436972000D0   0.17201973800D-1
   0.011174940810D0   0.14641373000D-5   0.86781649000D-7
   0.97171109000D-2  -0.20653063000D-6  -0.20168249000D-6
   0.011174940810D0   0.52299013600D-5   0.93084227000D-7
 695.663500000000D0   1.173100000000D0  -0.002600000000D0
   1.32715445000D11   4.902778000000D3   0.300000000000D0
```

Figure F.1 FK4 Fundamental Constants

```
21545.000000000000D0   3.070000000000D0  -21545.000000000000D0
   1.753368559233D0 628.331970688841D0      6.77071394490D-6  -4.50876723430-10   6.300387741877D0
  23.439291110000D0   -.013004166000D0    -.000000163889D0    .000000503611D0
 135.044522222222D0   -.052953764841D0    0.000000000000D0    .002070833333D0    .000002222222D0
 228.316432500000D0    .131763964758D0    0.000000000000D0   -.000016116667D0    .000000052778D0
  93.353451111111D0    .111403528520D0    0.000000000000D0   -.010308888889D0   -.000012500000D0
 290.466069444000D0    .985647359267D0    0.000000000000D0    .000302500000D0    0.000000000000D0
 292.938346111111D0    .000047076173D0    0.000000000000D0    .000462777778D0    .000003333333D0
  25.562500000000D0   -.248611111111D0    1.593333333330D0    .062222222222D0    0.000000000000D0
  -.019444444444D0    0.000000000000D0    .271388888889D0     .055555555556D0    .035833333333D0
  -.014722222220D0    -.009166666667D0    .008888888889D0     .007222222222D0    .007500000000D0
  -.006666666667D0    0.015000000000D0    -.026388888890D0
   6.6720000000D-23   3.986004480000D5 6378.140000000000D0   7.29211544199D-5  298.257000000000D0
   0.026920249000D0   0.000000000000D0 6378.140000000000D0   1.495978700000D8
  -0.51875025100D-3   0.17937970500D-3  -0.53329407900D-4   0.000000000000D0   0.000000000000D0
  -0.58171824000D-4   0.28603852000D-3   0.87266462600D-4   0.000000000000D0   0.000000000000D0
  -0.52844550000D-3   0.17937970500D-3  -0.53329407900D-4   0.000000000000D0   0.000000000000D0
   0.011180861350D0   0.14635555405D-5   0.87256766321D-7
   0.97171734552D-2  -0.20684575705D-6  -0.20305484059D-6
   0.011180860865D0   0.53071584044D-5   0.88250634372D-7
 692.740000000000D0  -1.160000000000D0   0.000000000000D0
   1.32712440000D11   4.902799062815D3   0.290000000000D0
```

Figure F.2 FK5 Fundamental Constants

```
21545.000000000000D0   3.070000000000D0  -21545.000000000000D0
   1.753368559233D0 628.331970688841D0      6.77071394490D-6  -4.50876723430-10   6.300388381608D0
  23.439291110000D0   -.013004166000D0    -.000000163889D0    .000000503611D0
 135.044522222222D0   -.052953764841D0    0.000000000000D0    .002070833333D0    .000002222222D0
 228.316432500000D0    .131763964758D0    0.000000000000D0   -.000016116667D0    .000000052778D0
  93.353451111111D0    .111403528520D0    0.000000000000D0   -.010308888889D0   -.000012500000D0
 290.466069444000D0    .985647359267D0    0.000000000000D0    .000302500000D0    0.000000000000D0
 292.938346111111D0    .000047076173D0    0.000000000000D0    .000462777778D0    .000003333333D0
  25.562500000000D0   -.248611111111D0    1.593333333330D0    .062222222222D0    0.000000000000D0
  -.019444444444D0    0.000000000000D0    .271388888889D0     .055555555556D0    .035833333333D0
  -.014722222220D0    -.009166666667D0    .008888888889D0     .007222222222D0    .007500000000D0
  -.006666666667D0    0.015000000000D0    -.026388888890D0
   6.6720000000D-23   3.986004480000D5 6378.140000000000D0   7.29211618242D-5  298.257000000000D0
   0.026920249000D0   0.000000000000D0 6378.140000000000D0   1.495978700000D8
  -0.51875025100D-3   0.17937970500D-3  -0.53329407900D-4   0.000000000000D0   0.000000000000D0
  -0.58171824000D-4   0.28603852000D-3   0.87266462600D-4   0.000000000000D0   0.000000000000D0
  -0.52844550000D-3   0.17937970500D-3  -0.53329407900D-4   0.000000000000D0   0.000000000000D0
   0.011180861350D0   0.14635555405D-5   0.87256766321D-7
   0.97171734552D-2  -0.20684575705D-6  -0.20305484059D-6
   0.011180860865D0   0.53071584044D-5   0.88250634372D-7
 692.740000000000D0  -1.160000000000D0   0.000000000000D0
   1.32712440000D11   4.902799062815D3   0.290000000000D0
```

Figure F.3 TAOS FK5 Fundamental Constants

[This page intentionally left blank.]

Appendix G

Summary of Test Cases

This appendix is designed as a reference to the test cases performed for validation of the software modifications made to support this work. It contains the input card data files, command procedures, and overrides files used to generate the results, as well as a summary of the key findings. It is organized according to test function, and contains the following:

- Testing of the Merged RADARSAT/50x50 Code
- Testing of the Permanent File Report
- Testing of the Cowell and SST Orbit Generators
- Testing of the Differential Correction
- Testing against the TOPEX POEs

The VAX file names for each test case are indicated in parentheses in the test header. The files presented here are stored on the VAX node ELROND under the author's home directory [SSC2414.WORK.NEW_GTDS.THESIS]. They are separated according to function. The [.gtds], [.com], and [.overrides] subdirectories contain the input card data files, command procedures, and overrides files, respectively, for the executions being discussed here. The [.output] subdirectory houses the tabulated file output of each of the runs, while the [.orb1] structure is comprised of the GTDS ORB1 files that are produced.

G.1 Testing of the Merged RADARSAT/50x50 Code

The merger of the RADARSAT and 50x50 capabilities was tested through three cases to ensure that both groups of functionalities were preserved. The three test cases are summarized below in Table G.1.

Table G.1 Summary of RADARSAT/50x50 Merger Testing

Test Case	Description	References in Appendix G
1	Cowell orbit generator	Figures: G.1-G.2 Table: G.2
2	Cowell differential correction with perturbed initial conditions	Figures: G.3-G.4 Table: G.3
3	21x21 SST fit of orbit created with 50x50 modeling using SST	Figures: G.5-G.8

The first test case tested the Cowell orbit generator using the ephemeris generation program. It involved a simple propagation with only 50x50 gravity field and third body effects included in the force modeling. The input card data file and command procedure associated with this execution (Figures G.1 and G.2) precede the results (Table G.2).

Test Case 1: 50x50 Cowell Orbit Generation
(TEST_50X50_COWELL_EPHEM)

```
CONTROL   EPHEM                                          LNDSAT-4  8207201
EPOCH                        820224.0        0.0
ELEMENT1  1     2     1      7077.8          0.0011      98.2
ELEMENT2                     158.1           89.4        176.0
OUTPUT    1     2     1      820227.0        0.0         43200.
ORBTYPE   2     1     1      10.0
OGOPT
MAXDEGEQ  1                  50.
MAXORDEQ  1                  50.
POTFIELD  1     10
END
FIN
```

Figure G.1 Cowell 50x50 Ephemeris Generation Input Card Data File

```
$!-------------------------------------------------------
$! TEST_50x50_COWELL_EPHEM.COM -- Test setup for generating a COWELL run
$!
$!-------------------------------------------------------
$!
$       set default [ssc2414.work.new_gtds.test]
$!
$! Set up the logical links to the standard gtds databases.
$!
$       @[ssc2414.work.new_gtds.test]50x50_validation_setup
$!
$! Assign field related files
$!
$       assign/table=lnm$job fds$diska:[RJP9045.bianca.fonte]newcomb.dat       gtds$023
$       assign/table=lnm$job fds$diska:[dj1230.bianca.changes.changes_com]radarsat.dat  gtds$047
$       ASSIGN/table=lnm$job fds$diska:[dj1230.bianca.changes.changes_com]moon.dat  gtds$048
$!
$! Assign fundamental constants file
$!
$       assign/table=lnm$job fds$diska:[ssc2414.work.new_gtds.mods]b1950_csconst.dat   gtds$099
$!
$!
$! Assign ORB1 files
$!
$       assign/table=lnm$job fds$diska:[ssc2414.work.new_gtds.test]test_50x50_cowell_ephem.orb1    gtds$024
$!
$! Make the run using input cards in
$!
$       @[ssc2414.work.new_gtds.test]2000_swat_gtds fds$diska:[ssc2414.work.new_gtds.test]test_50x50_cowell_ephem
$!
$       EXIT
$!
$!-------------------------------------------------------
```

Figure G.2 Cowell 50x50 Ephemeris Generation Command Procedure

Sub-millimeter differences in the end conditions of Fonte's initial 50x50 execution and the execution performed here were encountered. These differences appear to be the result of switching operating environments from the VAX 8820 model (BIGSIM) that Fonte used to the VAX 4000/90 used in this work. The end conditions of the Cowell orbit generation are shown below in Table G.2.

Table G.2 Validation of the Cowell 50x50 Orbit Generator

End conditions	Fonte's Results	New GTDS Results	Δ
X Position (km)	3873.119562949189	3873.119562*82987*	3.3798e-8
Y Position (km)	-430.5243130203381	-430.5243130*354492*	1.5111e-8
Z Position (km)	5925.145802534543	5925.145802*511251*	2.3292e-8
X Velocity (km/s)	5.793182527061727	5.793182527*036600*	2.5127e-11
Y Velocity (km/s)	-2.597763108551348	-2.597763108*548536*	2.8120e-12
Z Velocity (km/s)	-3.978183663971041	-3.97818366*4009602*	3.8561e-11

The second test case validated the operation of the Cowell orbit generator in the differential correction process. A Cowell truth ORB1 file was created using 50x50 gravity modeling by the ephemeris generation program. The ORB1 file was then used as an observation source for a Cowell differential correction. While the force modeling was identical for the truth ORB1 and differential correction process, the initial conditions were perturbed for the differential correction. The input card data file and command procedure associated with this test case are shown in Figures G.3 and G.4.

Test Case 2: 50x50 Cowell Differential Correction (50X50_COWELL_FIT_VALIDATION)

```
CONTROL  EPHEM                                                    RADARSAT  8202230
ELEMENT1 1     2     1     7173.495209009536  .8209321703559D-03   98.70377436252944
ELEMENT2                   120.5944568455971  87.98279452954401    250.1704964150892
EPOCH                      820102.0           000240.6
OUTPUT   1     2     1     820107.0           003241.0             86400.0
ORBTYPE  2     1     1     10.0
OGOPT
DRAG     1                1
ATMOSDEN             1
DRAGPAR  3     0           3.0
SOLRAD   1                1
SCPARAM                    14.680D-6          2830.000
MAXDEGEQ1                  50.0
MAXORDEQ1                  50.0
POTFIELD 1     10
OUTOPT   1                 820102000241.0     820107003241.0       1800.
END
FIN
CONTROL  DC                                                       RADARSAT  8202230
ELEMENT1 1     2     1     7173.48434         0.8209043439900D-03  98.70378044247322
ELEMENT2                   120.5944241036     87.9862755708162     250.16721
EPOCH                      820102.0           000240.6
ORBTYPE  2     1     1     10.
OBSINPUT 15                820102 000340.6    820105 000340.6
DMOPT
OBSDEV   21 22       23    10.                10.                  10.
OBSDEV   24 25       26    1.                 1.                   1.
END
OGOPT
DRAG     1                1
ATMOSDEN             1
DRAGPAR  3     0           3.0
SOLRAD   1                1.0
SCPARAM                    14.680D-6          2830.000
MAXDEGEQ1                  50
MAXORDEQ1                  50
POTFIELD 1     10
END
DCOPT
PRINTOUT 1           4
CONVERG  25    6           1.D-3
END
FIN
CONTROL  EPHEM                                 OUTPUT               RADARSAT  8202230
OUTPUT   1     2     1     820107.0           003241.0                   86400.0
ORBTYPE  2     1     1     10.0
OGOPT
DRAG     1                1
ATMOSDEN             1
DRAGPAR  3      0          3.0
SOLRAD   1                1
SCPARAM                    14.680D-6          2830.000
MAXDEGEQ1                  50.0
MAXORDEQ1                  50.0
POTFIELD 1     10
OUTOPT   21                820102000241.0     820107003241.0       1800.
END
FIN
CONTROL  COMPARE                                                  RADARSAT  8202230
COMPOPT
CMPEPHEM 1     102   102   820102000241.0     820105003241.0       30.
CMPPLOT  3                                                        2.
HISTPLOT 1     102   102   820102000241.0     820105003241.0       1800.
END
FIN
CONTROL  COMPARE                                                  RADARSAT  8202230
COMPOPT
CMPEPHEM 1     102   102   820105000241.0     820107003241.0       30.
CMPPLOT  3                                                        2.
HISTPLOT 1     102   102   820105000241.0     820107003241.0       1800.
END
FIN
```

Figure G.3 RADARSAT/50x50 Test Case 2 Input Card Data File

```
$!-------------------------------------------------------------
$! GRAV_DC -- This differential correction (DC) run processes range and
$!             range rate data for St. Hubert over a three day period.
$!             The DC physical model differs from the Datasim physical
$!             model as follows:
$!                  Datasim Gravity model  -- GEMT3
$!                  DC     Gravity model  -- GEMT3 Clone
$!
$!             Three day fit span and two day predict span plots are
$!             generated.
$!
$!-------------------------------------------------------------- $!
$! CLR
$!
$       set def [ssc2414.work.new_gtds.test]
$!
$! Set up the logical links to the standard gtds databases.
$       @[ssc2414.work.new_gtds.test]50x50_validation_setup.com
$!
$!
$! Assign Earth geopotential file
$       ASSIGN/table=lnm$job [dj11230.bianca.changes.changes_com]earth.dat gtds$047
$       ASSIGN/table=lnm$job [dj11230.bianca.changes.changes_com]moon.dat gtds$048
$       ASSIGN/table=lnm$job ids$diska:[ssc2414.work.new_gtds.mods]b1950_csconst.dat   GTDS$099
$!
$! Assign ORB1 truth file
$       ASSIGN/table=lnm$job [ssc2414.work.new_gtds.test]50x50_cowell_truth_validation.ORB1                    GTDS$024
$!
$! Assign ORB1 truth file
$       ASSIGN/table=lnm$job [ssc2414.work.new_gtds.test]50x50_cowell_fit_validation.ORB1  GTDS$081
$!
$!
$! Make the run using input cards in GRAV_DC.GTDS
$       @[ssc2414.work.new_gtds.test]j2000_swat_gtds 50x50_ccwell_fit_validation
$!
$       EXIT
$!
$!-------------------------------------------------------------
```

Figure G.4 RADARSAT/50x50 Test Case 2 Command Procedure

The differential correction converged back to the initial truth conditions, indicating that the 50x50 modeling is compatible with the differential correction process. The actual truth and converged solutions are shown with the fit statistics in Table G.3.

Table G.3 Comparison of Truth Initial Conditions and Converged Solutions

	Actual Initial Condition (km and km/s)	Converged Solution (km and km/s)	Δ (km and km/s)	1 σ (km and km/s)
X	-3736.803593965437	-3736.803593***80256***	1.4819e-8	1.8207e-5
Y	5523.017887591180	5523.01788***7676010***	8.4829e-8	2.7646e-5
Z	-2649.590848037073	-2649.590***847838223***	1.9885e-7	3.1081e-5
VX	-.5134002749726257	-.513400274***8553410***	1.1728e-10	1.8916e-6
VY	2.924254086071665	2.92425408***5898364***	1.7330e-10	2.8533e-6
VZ	6.835193797081531	6.83519379***7165048***	8.3517e-11	3.0873e-6

The final test case involved a fit of a GEMT3 50x50 ephemeris with a GEMT3 21x21 model. The two resulting orbits were compared using the GTDS ephemeris comparison program. The input card data file, command procedure, and overrides files are shown in the following pages.

Test Case 3: 21x21 Fit to 50x50 Orbit

(50X50_SST_VALIDATION)

```
CONTROL  EPHEM                                          DMSPBL-6  1234567
EPOCH                        820223.0          0.0
ELEMENT1 1     6     1       7272.0            0.001125          99.0
ELEMENT2                     65.931            90.0              0.0
OUTPUT   1     2     1       820911.0          0.0               864000.
ORBTYPE  5     1     1       43200.            1.0
OGOPT
NCBODY   1
RESONPRD                     432000.0
MAXDEGEQ 1                   50.
MAXORDEQ 1                   50.
POTFIELD 1     10
OUTOPT   1                   820223000000.0    820911000000.0    14400.
END
FIN
CONTROL  DC                                             DMSPBL-6  1234567
EPOCH                        820223.0          0.0
ELEMENT1 1     6     1       7271.99999        0.0011235         98.9999
ELEMENT2                     65.93136          89.66716          0.322
OBSINPUT 15                  820223000000.0    820911000000.0
ORBTYPE  5     1     1       43200.            1.0
DMOPT
OBSDEV   21    22    23      100.              100.              100.
OBSDEV   24    25    26      10.               10.               10.
END
OGOPT
NCBODY   1
MAXDEGEQ 1                   21.
MAXORDEQ 1                   21.
POTFIELD 1     10
STATEPAR 3
STATETAB 1     2     3       4.0               5.0               6.0
END
DCOPT
PRINTOUT 1           4
CONVERG  30          1       1.D-4
END
FIN
CONTROL  EPHEM                                  OUTPUT          DMSPBL-6  1234567
OUTPUT   1     2     1       820911.0          0.0               864000.0
ORBTYPE  5     1     1       43200.            1.0
OGOPT
NCBODY   1
MAXDEGEQ 1                   21.
MAXORDEQ 1                   21.
POTFIELD 1     10
OUTOPT   21                  820223000000.0    820911000000.0    14400.
END
FIN
CONTROL  COMPARE                                DMSPBL-6  1234567
COMPOPT
CMPEPHEM 1     102   102     820223000000.0    820911000000.0    3600.0
CMPPLOT  1                                                       2.0
HISTPLOT 1     102   102     820223000000.0    820911000000.0    216000.0
END
FIN
CONTROL  COMPARE                                DMSPBL-6  1234567
COMPOPT
CMPEPHEM 1     102   102     820223000000.0    820911000000.0    1200.0
CMPPLOT  1                                                       2.0
HISTPLOT 1     102   102     820223000000.0    820911000000.0    72000.0
END
FIN
```

Figure G.5 RADARSAT/50x50 Test Case 3 Input Card Data File

```
$!-------------------------------------------------------
$! THESIS_DEEP_RESONANCE--Test setup for Precise Conversion of Elements (PCE)
$!              generation of precision mean elements from a Cowell
$!              Truth File
$!-------------------------------------------------------
$!
$! Set default for batch run
$       SET DEFAULT [ssc2414.work.new_gtds.test]
$!
$! Set up the logical links to the standard gtds databases.
$       @[ssc2414.work.new_gtds.test]50x50_validation_setup.com
$!
$       ASSIGN/table=lnm$job fds$diska:[ssc2414.work.new_gtds.test]50x50_sst_validation.overrides      dbg$init
$       ASSIGN/table=lnm$job fds$diska:[RJP9045.bianca.fonte]NEWCOMB.DAT          GTDS$023
$       ASSIGN/table=lnm$job fds$diska:[djf1230.bianca.changes.changes_com]radarsat.DAT  GTDS$047
$       ASSIGN/table=lnm$job fds$diska:[djf1230.bianca.changes.changes_com]MOON.DAT    GTDS$048
$       ASSIGN/table=lnm$job fds$diska:[ssc2414.work.new_gtds.mods]b1950_csconst.dat   GTDS$099
$!
$! Assign ORB1 files
$!
$       ASSIGN/table=lnm$job    fds$diska:[ssc2414.work.new_gtds.test]50x50_sst_validation_50x50_orb1.DAT    GTDS$024
$       ASSIGN/table=lnm$job    fds$diska:[ssc2414.work.new_gtds.test]50x50_sst_validation_21x21_orb1.DAT    GTDS$081
$!
$!
$! Make the run using input cards in
$!
$       @[ssc2414.work.new_gtds.test]j2000_swat_gtds fds$diska:[ssc2414.work.new_gtds.test]50x50_sst_validation
$!
$       EXIT
$!
$!-------------------------------------------------------
```

Figure G.6 RADARSAT/50x50 Test Case 3 Command Procedure

```
SET OUTPUT LOG

SET BREAK/return HWIRE DO -

        (DEPOSIT IZONAL = 3;
         DEPOSIT IMDALY = 3;
         DEPOSIT ITHIRD = 3;
         DEPOSIT ITESS  = 3;
         DEPOSIT IJ2MD  = 3;
         DEPOSIT IJ2J2  = 3; -

         GO -
        ); -
GO
```

Figure G.7 RADARSAT/50x50 Test Case 3 Overrides File

The purpose of this test was to replicate the results that Fonte obtained in his master's thesis [20]. He summarized the results of the ephemeris comparison by:

	POSITION RMS (km)	VELOCITY RMS (km/sec)
RADIAL	3.3576D-02	1.6680D-03
CROSS-TRACK	1.7800D-02	1.6002D-05
ALONG-TRACK	1.6392D+00	3.4504D-05
TOTAL	1.6396D+00	1.6684D-03

Figure G.8 Test Case 3 Results: 200 Day GEMT3 Fit of 21x21 AOG to 50x50 AOG

The results using the newly-developed code were identical to Fonte's to the level presented in Figure G.8.

G.2 Standard Test Cases

A series of twenty-one standard test cases that utilize a large subset of commonly used Draper R&D GTDS functionalities is presented in [47]. These test cases were executed on the VAX 8820 (BIGSIM) by Mr. Rick Metzinger in 1993 to validate the porting of GTDS to the SGI platform. Fourteen of these test cases were reproduced on the VAX 4000/90 for this work to demostrate that existing functionalities were not disturbed. Cases 15, 16, 17, 18, and 21 listed in Table G.4 were not performed due to ambiguity in their setup (missing command procedures and overrides files). Two cases (19 and 20) were not performed due to the lack of existing VAX values in [47].

Table G.4 Summary of Standard Test Cases

Test Case	Designation	Description
1	L6_PCE_SETUP	SST and Cowell orbit generations
2	L6_PCE_SST	SST DC from ORB1; ephemeris comparison
3	DC_M50_COWELL	Cowell DC from NORAD RAER data

4	EARLY_ORB	Orbit estimate from five sets of observations
5	FILERPT_ATM	File report of Harris-Priester atmospheric density file
6	FILERPT_EPOT	File report of Earth potential file
7	FILERPT_JACC	File report of Jacchia-Roberts atmospheric density file
8	L6_PCE_BL	Brouwer-Lyddane DC from ORB1; ephemeris comparison
9	L6_PCE_BL_DRAG	Brouwer-Lyddane DC from ORB1 considering drag as solve-for; ephemeris comparison
10	EPHEM_BROUWER	Three day ephemeris generation using Brouwer-Lyddane
11	EPHEM_M50_COWELL	Three day ephemeris generation using Cowell
12	EPHEM_M50_COWELL _JACCHIA	Three day ephemeris generation using Cowell with Jacchia-Roberts file
13	EPHEM_TWOBODY	Two day ephemeris generation using Cowell with no perturbations
14	COMPARE	Ephemeris comparison of cases 11 and 12
15	DATASIM	Generates simulated set of observations from given ephemeris
16	DC_SALT	NORAD SALT DC from NORAD RAER data
17	DC_HANDE	HANDE DC from NORAD RAER data
18	DC_GP4	GP4 DC from NORAD RAER data
19	EPHEM_NORAD	One day ephemeris generation using SGP, GP4/DP4, and DP4
20	EPHEM_NORAD_GP4	One day ephemeris generation using GP4
21	L6_PCE_GP4	GP4 DC from ORB1 file

The results of the fourteen test cases are summarized below along with a description of each case. Differences are likely a result of the executions being performed in different environments (VAX 8820 vs. VAX 4000/90).

- **L6_PCE_SETUP:** This run utilizes the SST and Cowell orbit generators to create a Cowell ORB1 file used in later experiments. The end state for the Cowell ephemeris is shown below:

Table G.5 L6_PCE_SETUP Results

	1993 Testing	J2000/ITOD/SET Testing	Δ
X (km)	-6324.740968949820	-6324.740968*39076*	1.0748e-8
Y (km)	2072.818657993558	2072.818657*994833*	1.2747e-9
Z (km)	2268.217443661746	2268.217443*689772*	2.8026e-8
VX (km/s)	2.709923724270893	2.709923724*299650*	2.8757e-11
VY (km/s)	0.3235086740483813	0.323508674*0389620*	9.4919e-12
VZ (km/s)	7.047377494509693	7.047377494*499316*	1.0376e-11

- **L6_PCE_SST:** This run performs a differential correction based upon one of the ORB1 files generated in L6_PCE_SETUP using Draper's semianalytic theory. The solved-for state is shown below:

Table G.6 L6_PCE_SST Results

	1993 Testing	J2000/ITOD/SET Testing	Δ
X (km)	2436.099038388797	2436.09903838*8076*	7.2123e-10
Y (km)	-1955.65370799763	-1955.65370799*7032*	5.9799e-10
Z (km)	-6435.497322441975	-6435.49732244*2321*	3.4470e-10
VX (km/s)	-6.442632610100174	-6.44263261010*0478*	3.0465e-13
VY (km/s)	2.019981434787018	2.019981434787*258*	2.3981e-13
VZ (km/s)	-3.087797126902613	-3.08779712690*1821*	7.9137e-13

- **DC_M50_COWELL_ADC10299:** This run performs a differential correction based upon a Cowell numerical integration technique using NORAD range, azimuth, elevation, and range-rate (RAER) observations. The solved-for state (including the drag coefficient) is shown below:

Table G.7 DC_M50_COWELL_ADC10299 Results

	1993 Testing	J2000/ITOD/SET Testing	Δ
X (km)	3544.240550741282	3544.240550*743849*	2.5670e-9
Y (km)	-5517.406430407821	-5517.406430*372417*	3.5404e-8
Z (km)	1140.664960853038	1140.664960*787514*	6.5524e-8
VX (km/s)	2.655752612308443	2.655752612*263857*	4.4587e-11
VY (km/s)	0.1150406527182320	0.1150406527*875791*	6.9347e-11
VZ (km/s)	-7.260206531868176	-7.260206531*932220*	6.4044e-11
ρ1	-0.0789931033621219	-0.07899310*263206641*	7.3006e-10

- **EARLY_ORB:** This run exercises the early orbit function in Draper R&D GTDS to generate an estimate of the satellite state based upon five sets of range, azimuth and elevation (RAE) observations. The derived states are shown below:

Table G.8 EARLY_ORB Results

	1993 Testing	J2000/ITOD/SET Testing	Δ
X (km)	6853.142060304291	6853.142060304*690*	3.9927e-10
Y (km)	1396.079727347051	1396.079727346*225*	8.2628e-10
Z (km)	-1091.926305710841	-1091.926305710*225*	6.1596e-10
VX (km/s)	1.332880203268265	1.33288020326*7043*	1.2217e-12
VY (km/s)	-0.8374482809904740	-0.837448280990*8338*	3.5982e-13
VZ (km/s)	7.336093037596076	7.33609303759*6123*	4.5297e-14

- **FILERPT_ATM:** This run produces a file report on the GTDS Harris-Priester atmospheric density file. A file difference between the original and latest testing files indicated no differences. A sample of the output is provided below:

```
1                              GTDS  FILERPT  PROGRAM                              PAGE   3
                    DATA MANAGEMENT REPORT OF THE PERMANENT FILES -- ATMOSPHERIC DENSITY
MODEL NUMBER:  1
NUMBER OF ENTRIES IN DENSITY ARRAY: 56
MODEL NAME:
     1964 HARRIS/PRIESTER ATMOSPHERE %MIN-MAX< 0-1000 KM  F#65

ATMOSPHERIC DENSITY MODEL

          ALTITUDE          MINIMUM DENSITY          MAXIMUM DENSITY
          (IN KM)           (IN KG/KM**3)            (IN KG/KM**3)

       0.0000000D+00     1.2250000D+09     1.2250000D+09
       2.0000000D+01     8.8910000D+07     8.8910000D+07
       4.0000000D+01     3.9957000D+06     3.9957000D+06
       6.0000000D+01     3.0592000D+05     3.0592000D+05
       8.0000000D+01     1.9990000D+04     1.9990000D+04
       1.0000000D+02     4.9740000D+02     4.9740000D+02
       1.1000000D+02     7.8000000D+01     7.8000000D+01
       1.2000000D+02     2.4900000D+01     2.4900000D+01
       1.3000000D+02     8.9780000D+00     9.3310000D+00
       1.4000000D+02     4.0690000D+00     4.2120000D+00
       1.5000000D+02     2.0860000D+00     2.1680000D+00
       1.6000000D+02     1.1460000D+00     1.2360000D+00
       1.7000000D+02     6.6160000D-01     7.5580000D-01
       1.8000000D+02     4.0160000D-01     4.8850000D-01
       1.9000000D+02     2.5300000D-01     3.2740000D-01
       2.0000000D+02     1.6280000D-01     2.2840000D-01
       2.1000000D+02     1.0760000D-01     1.6340000D-01
       2.2000000D+02     7.2870000D-02     1.1920000D-01
       2.3000000D+02     5.0380000D-02     8.8510000D-02
       2.4000000D+02     3.5490000D-02     6.6660000D-02
       2.5000000D+02     2.5410000D-02     5.0830000D-02
       2.6000000D+02     1.8460000D-02     3.9190000D-02
```

Figure G.9 FILERPT_ATM Results

- **FILERPT_EPOT:** This run produces a file report on the GEM10B Earth potential coefficients file. A sample of the output is provided below:

```
0                              MODEL NUMBER      MODEL DESCRIPTION
                                    6            GEM 10B Earth potential coefficients.

0GRAV CON*M(KM**3/SEC**2)                0.39860044D+06
 MEAN RADIUS(KM)                         0.63781360D+04

1                                                    GTDS FILERPT PROGRAM                                    PAGE 12
                                                PERMANENT FILE REPORT - PHYSICAL CONSTANTS PERMANENT FILE
 .                          HARMONIC COEFFICIENTS  EARTH                                  MAXIMUM DEGREE = 21
                                                                                                MAXIMUM ORDER = 21
0     ZONALS
      INDEX  VALUE        INDEX  VALUE        INDEX  VALUE        INDEX  VALUE        INDEX  VALUE        INDEX  VALUE
      N M                 N M                 N M                 N M                 N M                 N M
      2 0   -0.108263D-02 3 0    0.253641D-05 4 0    0.162335D-05 5 0   -0.226086D-06 6 0   -0.542488D-06 7 0    0.383193D-06
      8 0    0.207726D-06 9 0    0.117150D-06 10 0   0.241565D-06 11 0  -0.228942D-06 12 0   0.195700D-06 13 0   0.223162D-06
     14 0   -0.125018D-06 15 0   0.141511D-07 16 0  -0.357389D-07 17 0   0.928094D-07 18 0   0.632760D-07 19 0   0.108517D-07
     20 0    0.156833D-06 21 0  -0.583605D-08

0     SECTORALS AND TESSERALS
            INDEX          VALUE                INDEX          VALUE                INDEX          VALUE
            N M        C           S            N M        C           S            N M        C           S
            2 1   0.1253023D-08 -.1987932D-10     2 2   0.1570270D-05 -.9018561D-06     3 1   0.2193737D-05 0.2737775D-06
            3 2   0.3053705D-06 -.2122137D-06     3 3   0.9945011D-07 0.1978112D-06     4 1  -.5057939D-06 -.4488828D-06
            4 2   0.7872106D-07 0.1497794D-06     4 3   0.5920478D-07 -.1224908D-07     4 4  -.4086442D-08 0.6486244D-08
            5 1  -.4660619D-07 -.8220881D-07     5 2   0.1055672D-06 -.5261555D-07     5 3  -.1524811D-07 -.7140907D-08
            5 4  -.2347814D-08 0.3604744D-09     5 5   0.3870879D-09 -.1636973D-08     6 1  -.6055275D-07 0.2096056D-07
            6 2   0.5767671D-08 -.4472656D-07     6 3   0.1263087D-08 0.9294532D-10     6 4  -.3681644D-09 -.1755995D-08
            6 5  -.2131442D-09 -.4350628D-09     6 6   0.1200458D-11 -.5497075D-10     7 1   0.2005654D-06 0.7173705D-07
            7 2   0.3241958D-07 0.1044491D-07     7 3   0.3475753D-08 -.3005489D-08     7 4  -.5925421D-09 -.2662401D-09
            7 5   0.2142472D-11 0.9454587D-11     7 6  -.2517948D-10 0.9480444D-11     7 7  -.8809011D-13 0.4151520D-12
            8 1   0.1903821D-07 0.3490608D-07     8 2   0.5914020D-08 0.5872106D-08     8 3  -.1777463D-09 -.9446808D-09
            8 4  -.3226866D-09 0.9675626D-10     8 5  -.3553729D-11 0.1540599D-10     8 6  -.1880534D-11 0.8723576D-11
            8 7   0.3391291D-12 0.3677650D-12     8 8  -.1598049D-12 0.1547572D-12     9 1   0.9896576D-07 0.1033361D-07
            9 2   0.1647813D-08 -.1932820D-08     9 3  -.1273033D-08 -.6626066D-09     9 4  -.1682983D-10 0.9309273D-11
            9 5  -.1890843D-11 -.5396508D-11     9 6   0.7283723D-12 0.2870706D-11     9 7  -.2087645D-12 -.1713608D-12
            9 8   0.6288644D-13 -.2624323D-14     9 9  -.3772475D-14 0.7457226D-14    10 1   0.4905926D-07 -.8003425D-07
           10 2  -.5267134D-08 -.1802995D-08    10 3  -.5753886D-10 -.9177374D-09    10 4  -.5444888D-10 -.4177777D-10
           10 5  -.3456931D-11 -.2636747D-11    10 6  -.2764476D-12 -.5411966D-12    10 7   0.7055851D-14 0.5003418D-14
           10 8   0.4679786D-14 -.9401778D-14    10 9   0.2348547D-14 -.8608738D-15   10 10  0.4226862D-15 -.1243606D-15
```

Figure G.10 FILERPT_EPOT Results

- **FILERPT_JACC:** This run produces a file report on the GTDS Jacchia-Roberts atmospheric density file. A file difference between the original and latest testing files indicated no differences. A sample of the output is provided below:

DATE	MJD	8 KP VALUES				TC
28 FEB 65	8820					
		2720	713	1320	2013	
		1013	313	2333	1713	622.1046143
		13	1313	2033	3320	622.4346924
		3337	4030	3347	4740	620.8735352
		4060	4033	2013	1007	620.3510132
		7	2033	2017	2017	620.3561401
		1010	307	310	2023	621.6163940
		3017	1717	2320	1003	622.4537964
		303	710	703	300	622.7766113
		1007	1707	1707	313	619.4966431
		1300	3	1000	300	617.3215942
		1713	1007	307	1003	617.4553223
		3	300	2313	2320	615.6673584
		1720	2333	3327	1303	617.6614380
		320	1010	2317	2027	620.0644531
		3320	3327	1327	3310	618.7006836
		1320	310	303	323	616.0836182
		710	1310	1723	2003	613.9752808
		303	700	703	0	614.1195068
		3	1717	1303	717	618.4918213
		2000	320	2307	1713	620.8992920
20 MAR 65	8840					
		2000	320	2307	1713	
		2710	1017	2717	1333	617.3973389
		703	703	713	3040	616.6856079
		2037	4330	3043	5043	614.8270264
		1317	3040	3720	2023	615.1741333
		2033	5043	2317	4023	614.3955688
		4330	3723	1717	2023	616.0908203
		2723	2717	1320	3013	615.4318848
		720	2713	713	303	613.7769775
		2017	1307	2017	2010	613.1734619
		0	307	1010	1003	613.4844971
		1320	1317	303	310	612.7573853
		2317	1303	1007	703	612.9622192
		310	1007	3	7	612.4902954
		10	703	1307	707	612.9674683
		320	2720	2320	1003	612.7227783
		327	703	303	710	612.4945068
		1320	1307	2327	1723	612.2316895
		3033	1313	2717	710	612.7243652
		1003	307	1010	717	612.8178101
		3040	3007	720	1727	613.0369263

Figure G.11 FILERPT_JACC Results

- **L6_PCE_BL:** This run implements the differential correction program with the Cowell ORB1 file created in L6_PCE_SETUP using Brouwer-Lydane theory. The resulting orbit (from the converged solution) is then

compared to the initial observations on the ORB1 file. The end conditions are shown below:

Table G.9 L6_PCE_BL Results

	1993 Testing	J2000/ITOD/SET Testing	Δ
X (km)	-6335.067992844939	-6335.067992841848	3.0905e-9
Y (km)	2071.574264439482	2071.574264439849	3.6653e-10
Z (km)	2241.258740256925	2241.258740265022	8.0968e-9
VX (km/s)	2.682144313934302	2.682144313942642	8.3404e-12
VY (km/s)	0.3325457059431656	0.3325457059404381	2.7275e-12
VZ (km/s)	7.057307838314064	7.057307838311121	2.9416e-12

- **L6_PCE_BL_DRAG:** This run is an extension of the previous test case, with the drag parameter added as a solve-for parameter. The end conditions are shown below:

Table G.10 L6_PCE_BL_DRAG Results

	1993 Testing	J2000/ITOD/SET Testing	Δ
X (km)	-6314.638707371847	-6314.638707373753	1.9050e-9
Y (km)	2074.024479177335	2074.024479177109	2.2555e-10
Z (km)	2294.396123801316	2294.396123796392	4.9240e-9
VX (km/s)	2.736859239915806	2.736859239910734	5.0724e-12
VY (km/s)	0.3146076041345148	0.3146076041351802	6.6541e-13
VZ (km/s)	7.037640237917411	7.037640237919270	1.8581e-12

- **EPHEM_BROUWER:** This run generates a three day ephemeris from an initial Brouwer mean Keplerian state vector using the Brouwer-Lydane orbit generator. The end conditions are shown below:

Table G.11 EPHEM_BROUWER Results

	1993 Testing	J2000/ITOD/SET Testing	Δ
X (km)	6108.649784212740	6108.649784212*582*	1.5825e-10
Y (km)	-1610.744279405818	-1610.744279405*709*	1.0891e-10
Z (km)	3189.939349801162	3189.939349801*520*	3.5743e-10
VX (km/s)	2.940060415415718	2.940060415*416088*	3.6948e-13
VY (km/s)	-2.015408676637255	-2.015408676*637354*	9.9032e-14
VZ (km/s)	-6.607887347277723	-0.6607887347*277527*	1.9540e-14

- **EPHEM_M50_COWELL:** This run generates a three day ephemeris from an initial osculating Keplerian state vector using the Cowell orbit generator. The end conditions are shown below:

Table G.12 EPHEM_M50_COWELL Results

	1993 Testing	J2000/ITOD/SET Testing	Δ
X (km)	3878.022960507109	3878.022960*492259*	1.4850e-8
Y (km)	-432.7688049065612	-432.7688*048998769*	6.6844e-9
Z (km)	5921.894232556308	5921.894232*566628*	1.0320e-8
VX (km/s)	5.789509857424832	5.789509857*435914*	1.1082e-11
VY (km/s)	-2.597331172114242	-2.597331172*115489*	1.2474e-12
VZ (km/s)	-3.983585468383628	-3.983585468*366592*	1.7036e-11

- **EPHEM_M50_COWELL_JACCHIA:** This run is similar to the previous execution, with the exception that the Jacchia-Roberts atmospheric density model is used in place of the Harris-Priester. The end conditions are shown below:

Table G.13 EPHEM_M50_COWELL_JACCHIA Results

	1993 Testing	J2000/ITOD/SET Testing	Δ
X (km)	3882.676588702401	3882.676588*693646*	8.7548e-9
Y (km)	-434.8618543843906	-434.8618543*804595*	3.9012e-9
Z (km)	5918.655169829135	5918.655169*835250*	6.1164e-9
VX (km/s)	5.786037189568382	5.786037189*574945*	6.5628e-12
VY (km/s)	-2.596944882530031	-2.596944882530*755*	7.2387e-13
VZ (km/s)	-3.988921240445654	-3.988921240*435552*	1.0102e-11

- **EPHEM_TWOBODY:** This execution disables the contributions of the perturbation sources, restricting motion to two-body mechanics. The end conditions are shown below:

Table G.14 EPHEM_TWOBODY Results

	1993 Testing	J2000/ITOD/SET Testing	Δ
X (km)	1267.817114245432	1267.817114*232916*	1.2516e-8
Y (km)	574.4416036480912	574.4416036*534028*	5.3116e-9
Z (km)	6931.786079953686	6931.786079955*604*	1.9180e-9
VX (km/s)	6.852965234435398	6.852965234437*976*	2.5793e-12
VY (km/s)	-2.906948956067391	-2.906948956066*185*	1.2057e-12
VZ (km/s)	-1.016218195985223	-1.016218195*970914*	1.4309e-11

- **COMPARE:** This run compares the two ephemerides generated in test cases 11 and 12. The RMS values for the position and velocity differences in radial, cross-track, and along-track components are shown below:

Table G.15 COMPARE Results

RMS	1993 Testing	J2000/ITOD/SET Testing
Radial position (km)	1.6783D-2	1.6783D-2
Cross-track position (km)	4.7932D-4	4.7932D-4
Along-track position (km)	2.6399D0	2.6399D0
Total position (km)	2.6400D0	2.6400D0
Radial velocity (km/s)	2.7902D-3	2.7902D-3
Cross-track velocity (km/s)	1.2083D-6	1.2083D-6
Along-track velocity (km/s)	1.0627D-5	1.0627D-5
Total velocity (km/s)	2.7902D-3	2.7902D-3

G.3 Permanent File Report Testing

A file report was performed on the FK5-based SLP files to ensure their compatibility with the existing SLP file structure within Draper R&D GTDS. The report provided information about the positions of the sun, moon, and planets, as well as transformation matrices from mean equator and equinox of date to selenographic and true of date frames. The input card data file and command procedure (*2000_FLRPT*) used for this test are shown below in Figures G.12 and G.13.

```
CONTROL  FILERPT
PFROPT
SLPRPT   8
END
FIN
```

Figure G.12 SLP File Report Input Card Data File

```
$!-------------------------------------------------
$! 2000_FLRPT
$!
$!    Test to ensure proper access of FK5-based SLP files.
$!
$!-------------------------------------------------
$!
$! Set default for batch run
$!
$     SET DEFAULT fds$diska:[ssc2414.work.new_gtds.test]
$!
$! Assign the body potential files
$!
$     assign/table=lnm$job fds$diska:[djf1230.bianca]dan_potential.dat gtds$047
$     assign/table=lnm$job fds$diska:[djf1230.bianca]moon.dat      gtds$048
$!
$! Assign the SLP files
$!
$     assign/table=lnm$job elrond$dka0:[ssc2414]june95_msgen_slp_mn2000.dat gtds$014
$     assign/table=lnm$job elrond$dka0:[ssc2414]june95_msgen_slp_timecoef.dat gtds$038
$     assign/table=lnm$job elrond$dka0:[ssc2414]june95_msgen_slp_tod2000.dat gtds$078
$!
$! Assign the fundamental constants file
$!
$     assign/table=lnm$job fds$diska:[ssc2414.work.new_gtds.mods]jj2000_csconst.dat gtds$099
$!
$     @[ssc2414.work.new_gtds.test]jj2000_SWAT_GTDS [ssc2414.work.new_gtds.test]2000_FLRPT
$!
$     EXIT
```

Figure G.13 SLP File Report Command Procedure

G.4 Orbit Generator Testing

Two sets of tests were performed for validating the incorporation of the FK5 theory into the orbit generation process. These tests relied upon relating orbits generated by FK5 theory to those generated by FK4 theory, and are summarized in Table G.16.

Table G.16 FK5 Orbit Generator Test Cases

Test Case	Description	References in Appendix G
1	Two orbits (one based on FK4 theory; the other on FK5) generated using two body mechanics only; ephemerides compared	Figures: G.14-G.30
2	Two orbits (one based on FK4 theory; the other on FK5) generated considering J_2 effects; ephemerides compared	Figures: G.31-G.47

Using a mean of 1950 vector as an initial satellite state, orbits represented in the mean of 2000 coordinate system were produced using both FK4 and FK5 theory. The ephemerides were then compared to reveal any theory-dependent effects. The differences for each case are presented along with the setup files in Figures G.14-G.47.

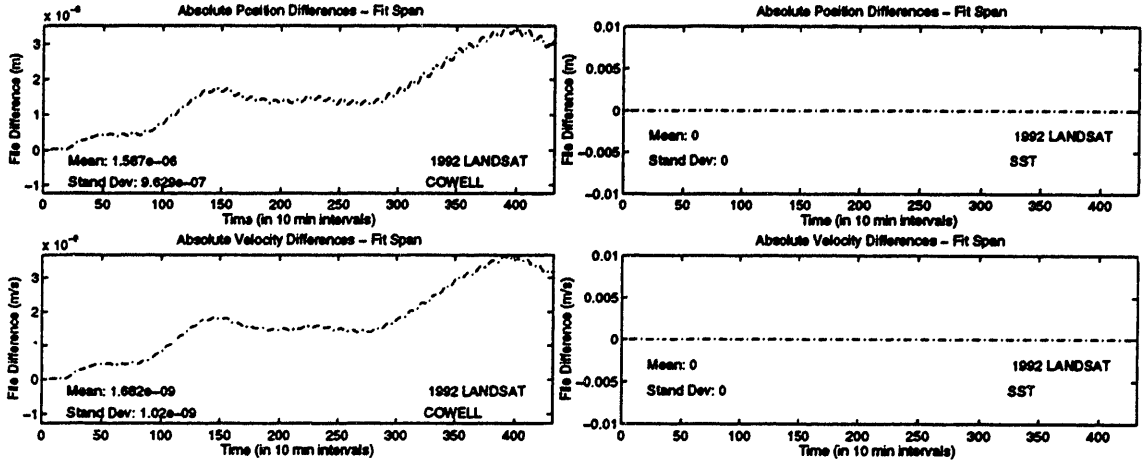

Figure G.14 Absolute FK4/FK5 Differences for Two-Body Case

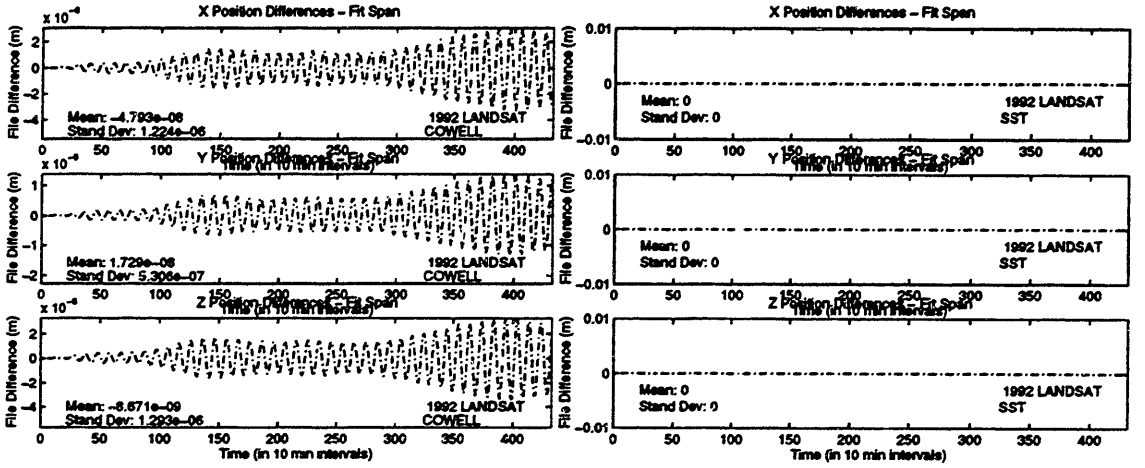

Figure G.15 FK4/FK5 Position Differences for Two-Body Case

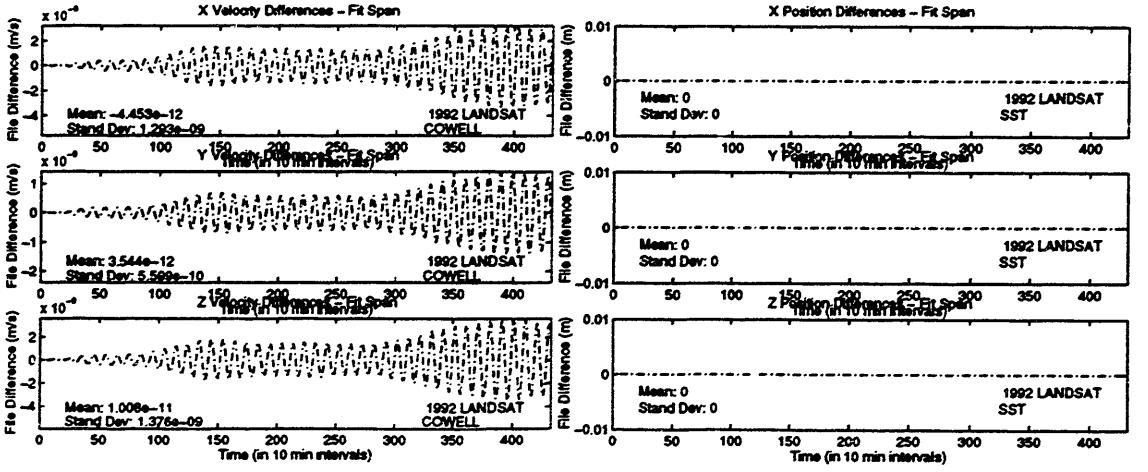

Figure G.16 FK4/FK5 Velocity Differences for Two-Body Case

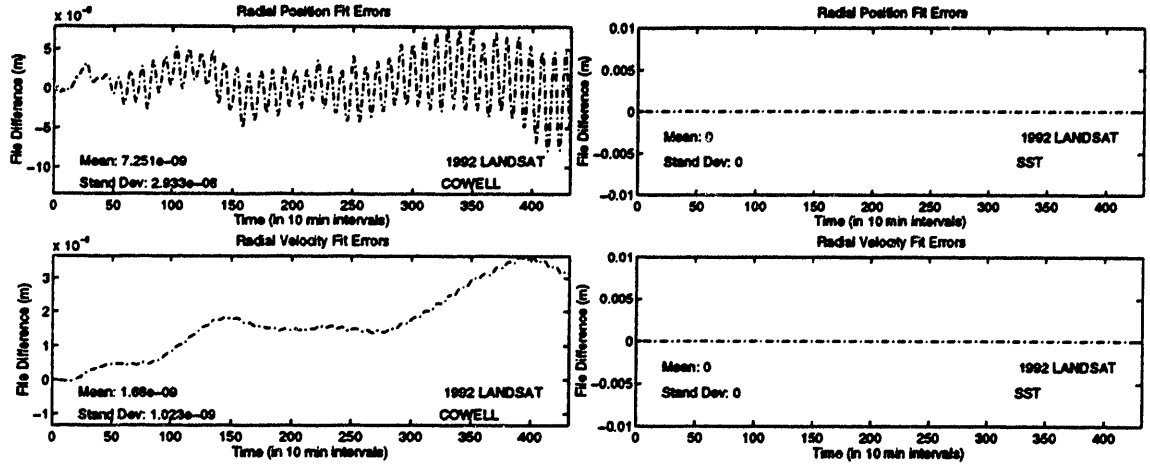

Figure G.17 FK4/FK5 Radial Differences for Two-Body Case

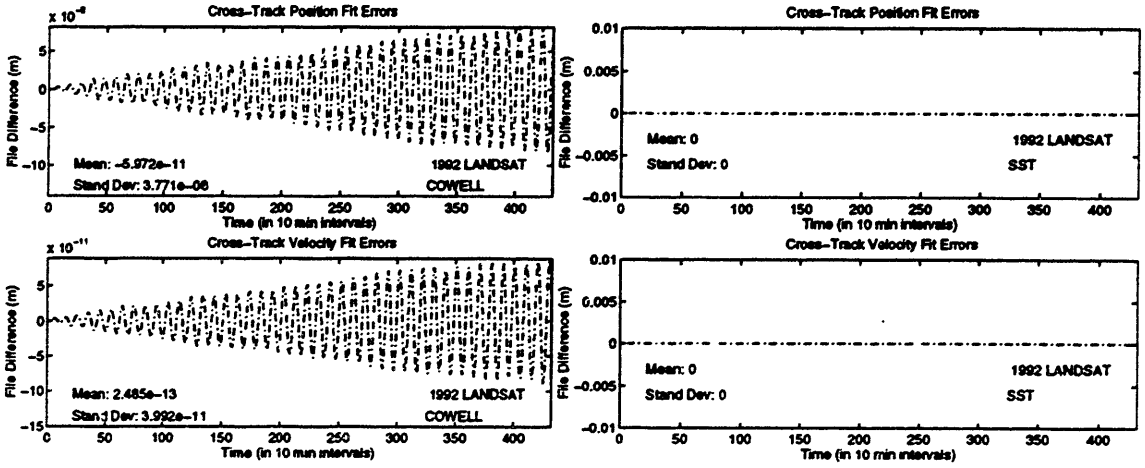

Figure G.18 FK4/FK5 Cross-Track Differences for Two-Body Case

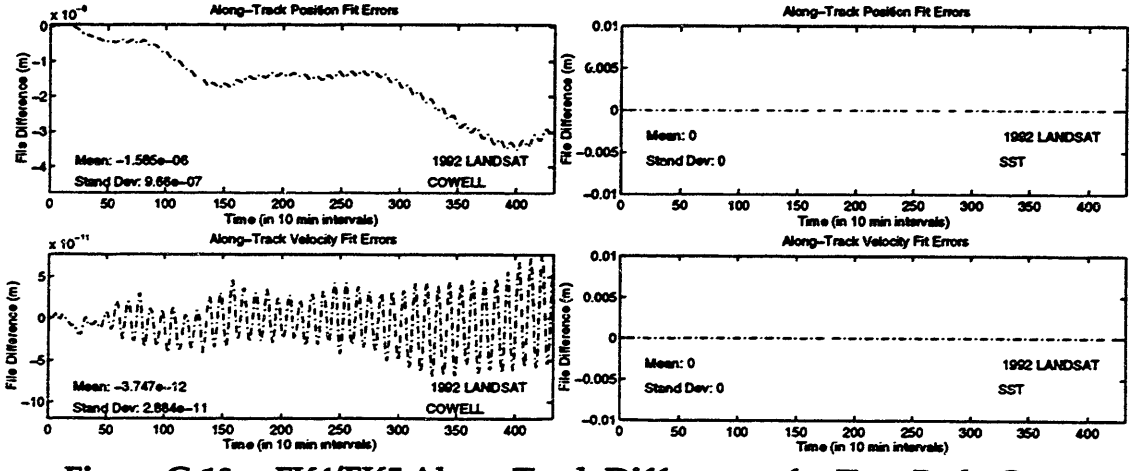

Figure G.19 FK4/FK5 Along-Track Differences for Two-Body Case

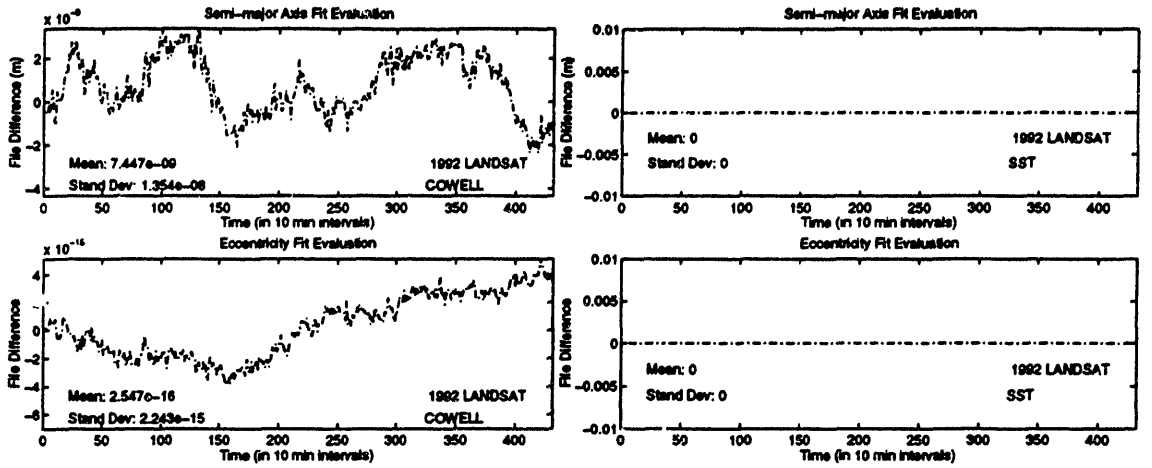

Figure G.20 FK4/FK5 *a/e* Differences for Two-Body Case

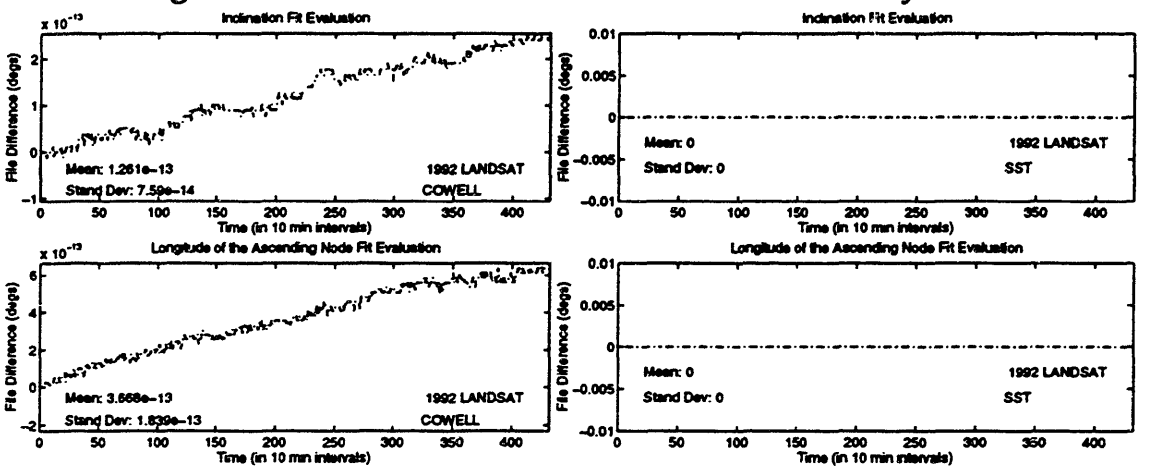

Figure G.21 FK4/FK5 *i/Ω* Differences for Two-Body Case

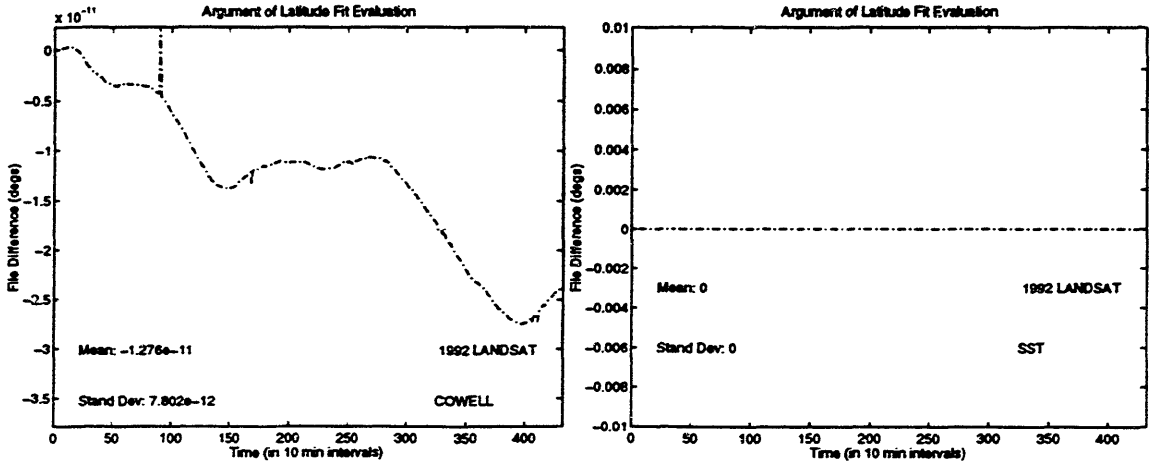

Figure G.22 FK4/FK5 Argument of Latitude Differences for Two-Body Case

Cowell FK4 Two-Body Orbit (T10_F1)

```
CONTROL  EPHEM                                                    TOPEXXX  XXXXXX
EPOCH                        920224.0          000000.000000
ELEMENT1 1     2     1       7077.6D0          0.0011D0          98.2D0
ELEMENT2                     158.1D0           89.4D0            176.D0
OUTPUT   11    2     1       920227.D0         0.D0              43200.D0
ORBTYPE  2     1     1       60.0
OGOPT
NCBODY   1
CNM      3     2     0       1.D-10                              1.0
MAXDEGEQ1                    2.0
MAXORDEQ1                    0.0
POTFIELD 1     6
OUTOPT   1                   920224000000.0    920227000000.0    60.0
END
FIN
```

Figure G.23 Cowell FK4 Two-Body Input Card Data File

```
$!-------------------------------------------------------------
$! tod_to_ecef  test setup to generate a valid test case
$!
$!
$!-------------------------------------------------------------
$!
$      SET DEFAULT fds$diska:[ssc2414.work.new_gtds.thesis]
$!
$! Assign the body potential files
$!
$      assign/table=lnm$job fds$diska:[djf1230.bianca]dan_potential.dat gtds$047
$      assign/table=lnm$job fds$diska:[djf1230.bianca]moon.dat     gtds$048
$!
$! Assign the density file
$!
$      assign/table=lnm$job fds_dbf:jacchia_roberts.dat   gtds$075
$!
$! Assign the SLP and timing files
$!
$      assign/table=lnm$job fds_dbf:june94_msgen_slp_mn1950.dat gtds$014
$      assign/table=lnm$job fds_dbf:june94_msgen_slp_timcof.dat gtds$038
$      assign/table=lnm$job fds_dbf:june94_msgen_slp_tod1950.dat gtds$078
$!
$! Assign ORB1 files
$!
$      assign/table=lnm$job fds$diska:[ssc2414.work.new_gtds.thesis]t10_f1.ORB1 gtds$024
$!
$! Assign fundamental constants file
$!
$      assign/table=lnm$job fds$diska:[ssc2414.work.new_gtds.mods]b1950_csconst.dat gtds$099
$!
$! Execute the local version of debug executable
$!
$      @[ssc2414.work.new_gtds.test]2000_SWAT_GTDS [ssc2414.work.new_gtds.thesis]T10_F1
$!
$      EXIT
```

Figure G.24 Cowell FK4 Two-Body Command Procedure

Cowell FK5 Two-Body Orbit
(T10_F2)

```
CONTROL  EPHEM                                          TOPEXXX  XXXXXX
EPOCH                    920224.0        000000.000000
ELEMENT1 1    2    1     7077.8D0        0.0011D0        98.2D0
ELEMENT2                 158.1D0         89.4D0          176.D0
OUTPUT   11   2    1     920227.D0       0.D0            43200.D0
ORBTYPE  2    1    11    60.0
OGOPT
NCBODY   1
CNM      3    2    0     1.D-10                          1.0
MAXDEGEQ 1                2.0
MAXORDEQ 1                0.0
POTFIELD 1    6
OUTOPT   1                920224000000.0  920227000000.0  60.0
END
FIN
CONTROL  COMPARE                                        TOPEXXX  XXXXXX
COMPOPT
CMPEPHEM 1    102  102    920224000000.   920227000000    30.
CMPPLOT  3                                              2.
END
FIN
```

Figure G.25 Cowell FK5/COMPARE Two-Body Input Card Data File

```
$!-------------------------------------------------------------
$! tod_to_ecef  test setup to generate a valid test case
$!
$!
$!-------------------------------------------------------------
$!
$       SET DEFAULT fds$diska:[ssc2414.work.new_gtds.thesis]
$!
$! Assign the body potential files
$!
$       assign/table=lnm$job fds$diska:[dj1230.bianca]dan_potential.dat gtds$047
$       assign/table=lnm$job fds$diska:[dj1230.bianca]moon.dat     gtds$048
$!
$! Assign the density file
$!
$       assign/table=lnm$job fds_dbf:jacchia_roberts.dat   gtds$075
$!
$! Assign the SLP and timing files
$!
$      assign/table=lnm$job elrond$dka0:[ssc2414]june95_megen_slp_mn2000.dat gtds$014
$       assign/table=lnm$job elrond$dka0:[ssc2414]:june95_megen_slp_timcof.dat gtds$038
$       assign/table=lnm$job elrond$dka0:[ssc2414]:june95_megen_slp_tod2000.dat gtds$078
$!
$! Assign ORB1 files
$!
$       assign/table=lnm$job fds$diska:[ssc2414.work.new_gtds.thesis]t10_f2.ORB1 gtds$024
$       assign/table=lnm$job fds$diska:[ssc2414.work.new_gtds.thesis]t10_f1.ORB1 gtds$081
$!
$! Assign fundamental constants file
$!
$       assign/table=lnm$job fds$diska:[ssc2414.work.new_gtds.mods]j2000_csconst.dat gtds$099
$!
$! Execute the local version of debug executable
$!
$       @[ssc2414.work.new_gtds.test]j2000_SWAT_GTDS [ssc2414.work.new_gtds.thesis]T10_F2
$!
$       EXIT
```

Figure G.26 Cowell FK5/COMPARE Two-Body Command Procedure

SST FK4 Two-Body Orbit:
(T10_F1_SST)

```
CONTROL  EPHEM                                          TOPEXXX  XXXXXX
EPOCH                    920224.0        000000.000000
ELEMENT1 1    2    1     7077.8D0        0.0011D0        98.2D0
ELEMENT2                 158.1D0         89.4D0          176.D0
OUTPUT   11   2    1     920227.D0       0.D0            43200.D0
ORBTYPE  5    1    1     43200.0         1.0
OGOPT
NCBODY   1
CNM      3    2    0     1.D-10                          1.0
MAXDEGEQ 1                2.0
MAXORDEQ 1                0.0
POTFIELD 1    6
OUTOPT   1                920224000000.0  920227000000.0  60.0
END
FIN
```

Figure G.27 SST FK4 Two-Body Input Card Data File

```
$!-------------------------------------------------
$! tod_to_ecef  test setup to generate a valid test case
$!
$!
$!-------------------------------------------------
$!
$       SET DEFAULT fds$diska:[ssc2414.work.new_gtds.thesis]
$!
$! Assign debug overrides
$!
$       assign/table=lnm$job  [ssc2414.work.new_gtds.thesis]t10_f1_sst.overrides dbg$init
$!
$! Assign the body potential files
$!
$       assign/table=lnm$job fds$diska:[dj1230.bianca]dan_potential.dat gtds$047
$       assign/table=lnm$job fds$diska:[dj1230.bianca]moon.dat     gtds$048
$!
$! Assign the density file
$!
$       assign/table=lnm$job fds_dbf:jacchia_roberts.dat   gtds$075
$!
$! Assign the SLP and timing files
$!
$       assign/table=lnm$job fds_dbf:june94_msgen_slp_mn1950.dat gtds$014
$       assign/table=lnm$job fds_dbf:june94_msgen_slp_timcof.dat gtds$038
$       assign/table=lnm$job fds_dbf:june94_msgen_slp_tod1950.dat gtds$078
$!
$! Assign ORB1 files
$!
$       assign/table=lnm$job fds$diska:[ssc2414.work.new_gtds.thesis]t10_f1_sst.orb1 gtds$024
$!
$! Assign fundamental constants file
$!
$       assign/table=lnm$job fds$diska:[ssc2414.work.new_gtds.mods]b1950_csconst.dat gtds$099
$!
$! Execute the local version of debug executable
$!
$       @[ssc2414.work.new_gtds.test]j2000_swat_gtds [ssc2414.work.new_gtds.thesis]T10_F1_SST
$!
$       EXIT
```

Figure G.28 SST FK4 Two-Body Command Procedure

SST FK5 Two-Body Orbit:
(T10_F2_SST)

```
CONTROL  EPHEM                                              TOPEXXX  XXXXXX
EPOCH                    920224.0        000000.000000
ELEMENT1 1    2    1     7077.8D0        0.0011D0         98.2D0
ELEMENT2                 158.1D0         89.4D0           176.D0
OUTPUT   11   2    1     920227.D0       0.D0             43200.D0
ORBTYPE  5    1    11    43200.0         1.0
OGOPT
NCBODY   1
CNM      3    2    0     1.D-10                           1.0
MAXDEGEQ 1                2.0
MAXORDEQ 1                0.0
POTFIELD 1    6
OUTOPT   1                920224000000.0  920227000000.0   60.0
END
FIN
CONTROL  COMPARE                                            TOPEXXX  XXXXXX
COMPOPT
CMPEPHEM 1    102  102    920224000000.   920227000000     30.
CMPPLOT  3                                                  2.
END
FIN
```

Figure G.29 SST FK5/COMPARE Two-Body Input Card Data File

```
$!-------------------------------------------------------
$! tod_to_ecef  test setup to generate a valid test case
$!
$!
$!-------------------------------------------------------
$!
$     SET DEFAULT fds$diska:[ssc2414.work.new_gtds.thesis]
$!
$! Assign debug overrides
$!
$     assign/table=lnm$job  [ssc2414.work.new_gtds.thesis]t10_f2_sst.overrides dbg$init
$!
$! Assign the body potential files
$!
$     assign/table=lnm$job fds$diska:[dj1230.bianca]dan_potential.dat gtds$047
$     assign/table=lnm$job fds$diska:[dj1230.bianca]moon.dat     gtds$048
$!
$! Assign the density file
$!
$     assign/table=lnm$job fds_dbf:jacchia_roberts.dat  gtds$075
$!
$! Assign the SLP and timing files
$!
$    assign/table=lnm$job elrond$dka0:[ssc2414]june95_megen_slp_mn2000.dat gtds$014
$     assign/table=lnm$job elrond$dka0:[ssc2414]june95_megen_slp_timcof.dat gtds$038
$     assign/table=lnm$job elrond$dka0:[ssc2414]june95_megen_slp_tod2000.dat gtds$078
$!
$! Assign ORB1 files
$!
$     assign/table=lnm$job fds$diska:[ssc2414.work.new_gtds.thesis]t10_f2_sst.orb1 gtds$024
$     assign/table=lnm$job fds$diska:[ssc2414.work.new_gtds.thesis]t10_f1_sst.orb1 gtds$081
$!
$! Assign fundamental constants file
$!
$     assign/table=lnm$job fds$diska:[ssc2414.work.new_gtds.mods]2000_csconst.dat gtds$099
$!
$! Execute the local version of debug executable
$!
$     @[ssc2414.work.new_gtds.test]2000_swat_gtds [ssc2414.work.new_gtds.thesis]t10_f2_sst
$!
$     EXIT
```

Figure G.30 SST FK5/COMPARE Two-Body Command Procedure

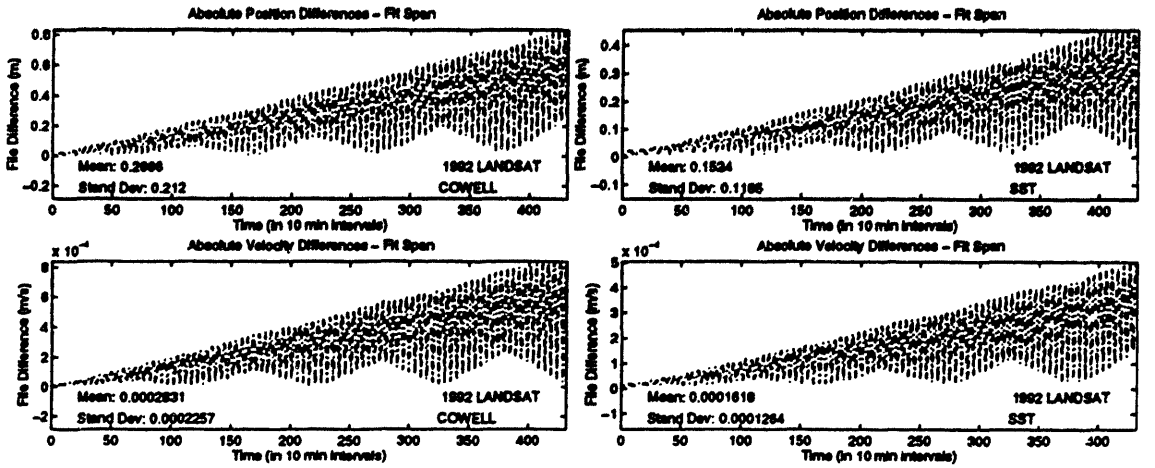

Figure G.31 Absolute FK4/FK5 Differences for J_2 Case

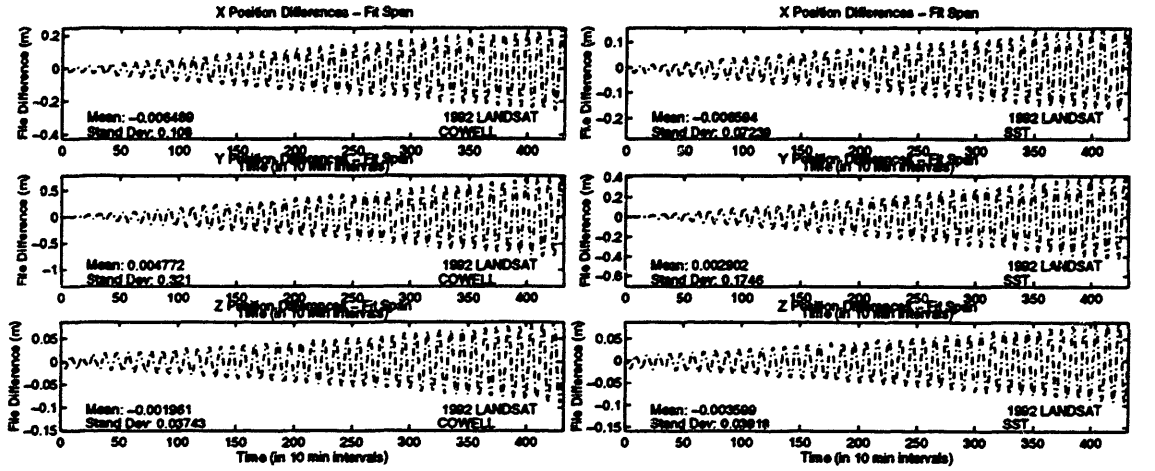

Figure G.32 FK4/FK5 Position Differences for J_2 Case

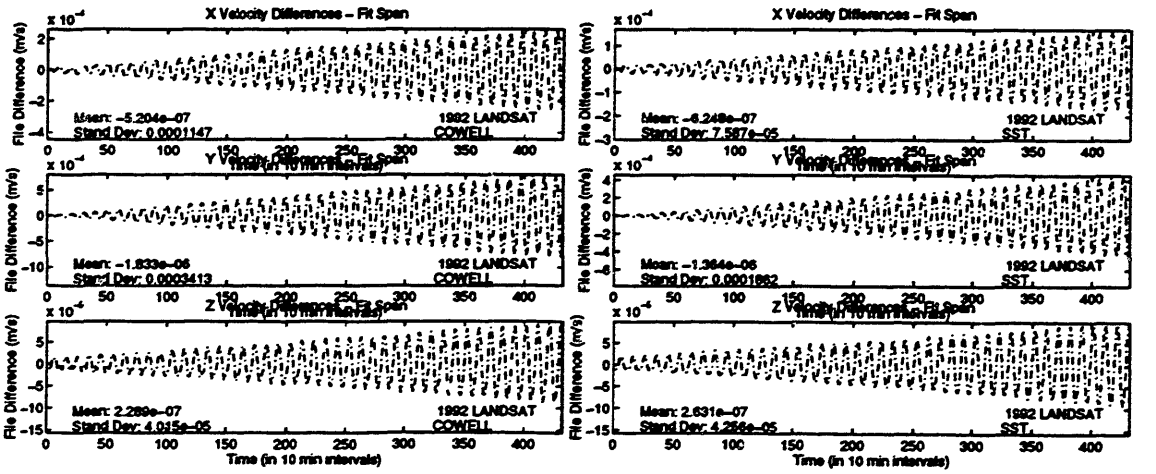

Figure G.33 FK4/FK5 Velocity Differences for J_2 Case

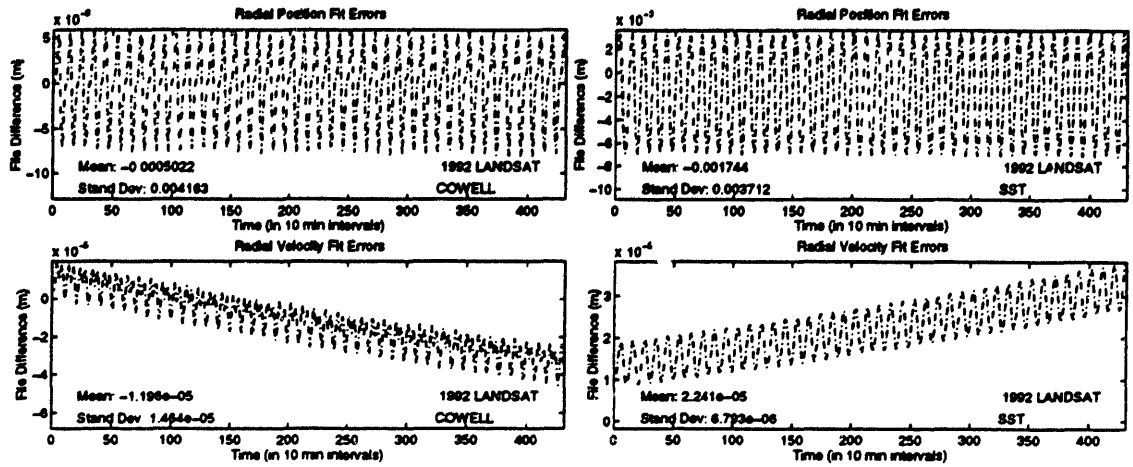

Figure G.34 FK4/FK5 Radial Differences for J_2 Case

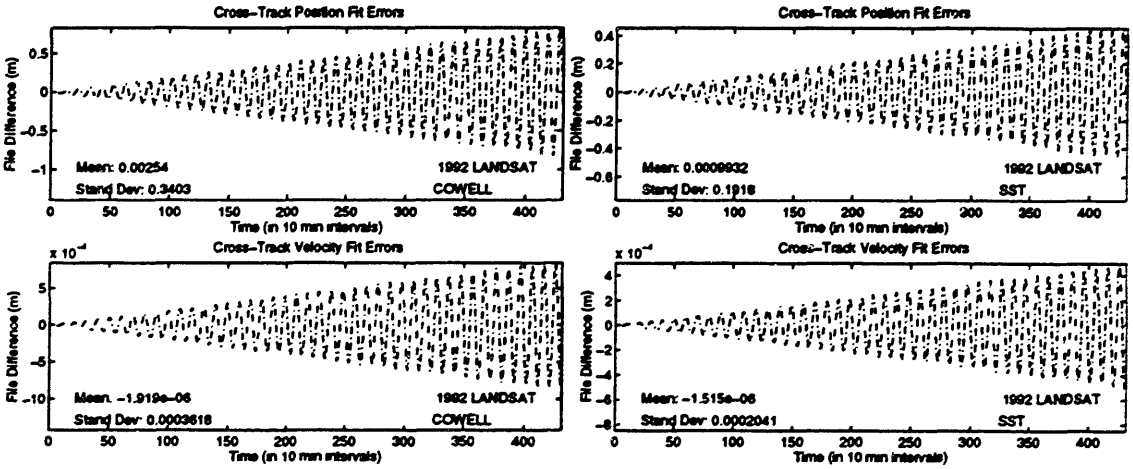

Figure G.35 FK4/FK5 Cross-Track Differences for J_2 Case

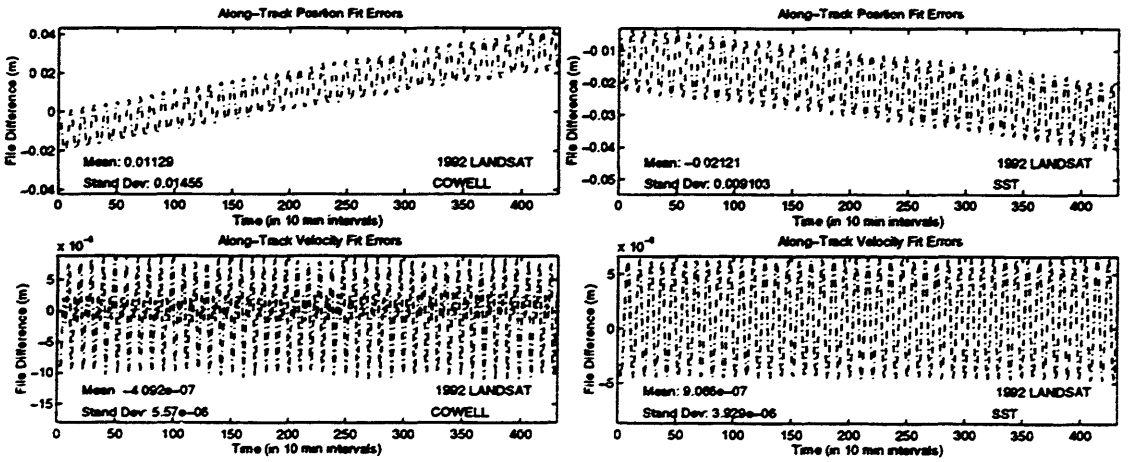

Figure G.36 FK4/FK5 Along-Track Differences for J_2 Case

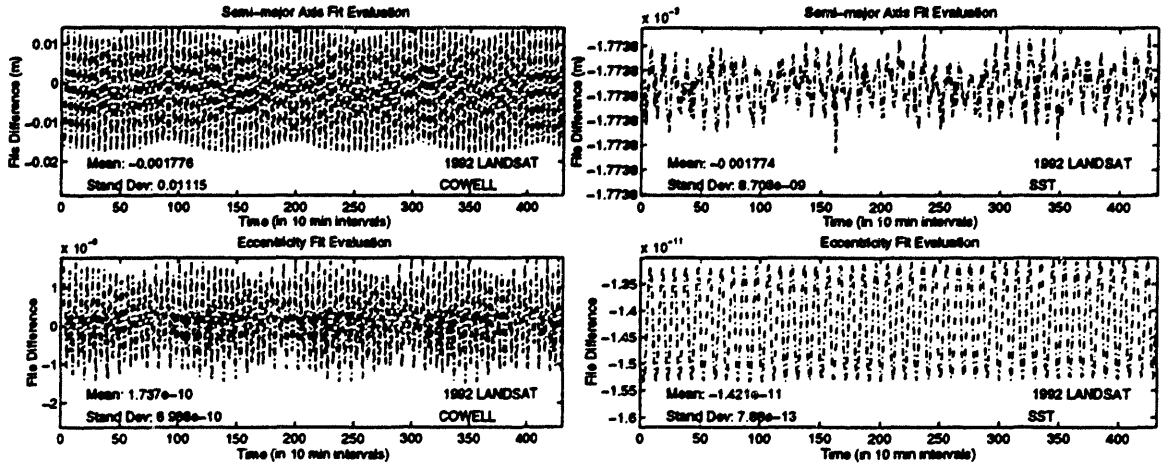

Figure G.37 FK4/FK5 *a/e* Differences for J_2 Case

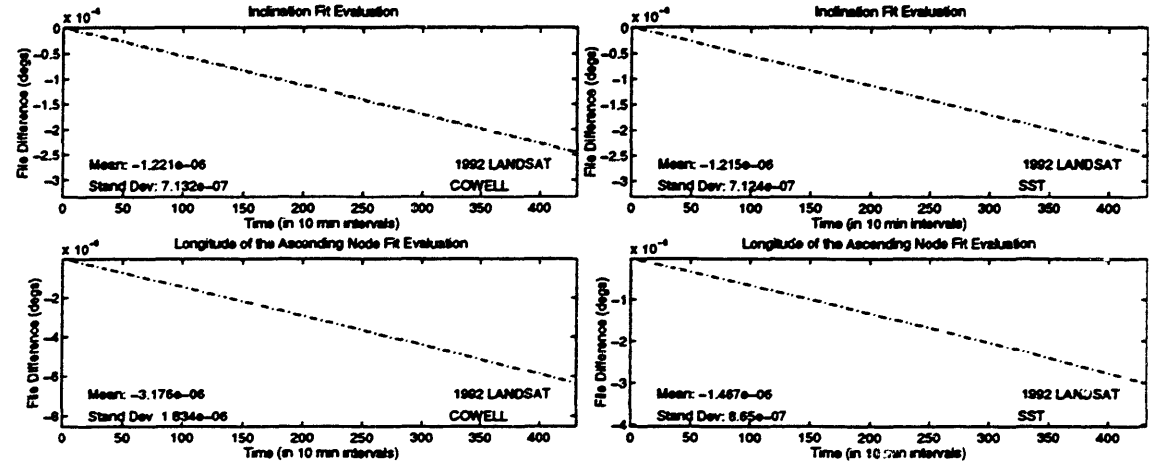

Figure G.38 FK4/FK5 i/Ω Differences for J_2 Case

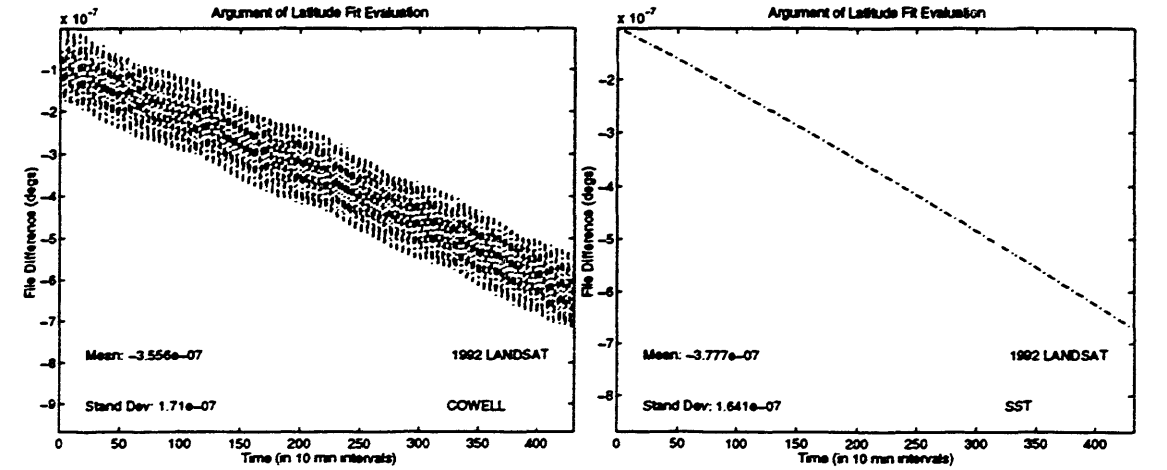

Figure G.39 FK4/FK5 Argument of Latitude Differences for J_2 Case

Cowell FK4 J_2 Orbit
(T4_F1)

```
CONTROL  EPHEM                                          TOPEXXX  XXXXXX
EPOCH                    920224.0        000000.000000
ELEMENT1 1    2    1     7077.8D0        0.0011D0        98.2D0
ELEMENT2                 158.1D0         89.4D0          176.D0
OUTPUT   11   2    1     920227.D0       0.D0            43200.D0
ORBTYPE  2    1    1     60.0
OGOPT
NCBODY   1
MAXDEGEQ 1               2.0
MAXORDEQ 1               0.0
POTFIELD 1    6
OUTOPT   1               920224000000.0  920227000000.0  60.0
END
FIN
```

Figure G.40 Cowell FK4 J_2 Input Card Data File

```
$!-------------------------------------------------------------
$! tod_to_ecef  test setup to generate a valid test case
$!
$!
$!-------------------------------------------------------------
$!
$     SET DEFAULT fds$diska:[ssc2414.work.new_gtds.thesis]
$!
$! Assign the body potential files
$!
$     assign/table=lnm$job fds$diska:[djf1230.bianca]dan_potential.dat gtds$047
$     assign/table=lnm$job fds$diska:[djf1230.bianca]moon.dat     gtds$048
$!
$! Assign the density file
$!
$     assign/table=lnm$job fds_dbf:jacchia_roberts.dat  gtds$075
$!
$! Assign the SLP and timing files
$!
$     assign/table=lnm$job fds_dbf:june94_megen_slp_mn1950.dat gtds$014
$     assign/table=lnm$job fds_dbf:june94_megen_slp_timcof.dat gtds$038
$     assign/table=lnm$job fds_dbf:june94_megen_slp_tod1950.dat gtds$078
$!
$! Assign ORB1 files
$!
$     assign/table=lnm$job fds$diska:[ssc2414.work.new_gtds.thesis]t4_f1.ORB1 gtds$024
$!
$! Assign fundamental constants file
$!
$     assign/table=lnm$job fds$diska:[ssc2414.work.new_gtds.mods]b1950_csconst.dat gtds$099
$!
$! Execute the local version of debug executable
$!
$     @[ssc2414.work.new_gtds.test]2000_SWAT_GTDS [ssc2414.work.new_gtds.thesis]T4_F1
$!
$     EXIT
```

Figure G.41 Cowell FK4 J_2 Command Procedure

Cowell FK5 J_2 Orbit

(T4_F2)

```
CONTROL  EPHEM                                                  TOPEXXX  XXXXXX
EPOCH                        920224.0          000000.000000
ELEMENT1 1     2     1       7077.8D0          0.0011D0        98.2D0
ELEMENT2                     156.1D0           89.4D0          178.D0
OUTPUT   11    2     1       920227.D0         0.D0            43200.D0
ORBTYPE  2     1     11      60.0
OGOPT
NCBODY   1
MAXDEGEQ 1                   2.0
MAXORDEQ 1                   0.0
POTFIELD 1     6
OUTOPT   1                   920224000000.0    920227000000.0  60.0
END
FIN
CONTROL  COMPARE                                                TOPEXXX  XXXXXX
COMPOPT
CMPEPHEM 1     102   102     920224000000.     920227000000    30.
CMPPLOT  3                                                      2.
END
FIN
```

Figure G.42 Cowell FK5/COMPARE J_2 Input Card Data File

```
$!-------------------------------------------------
$! tod_to_ecef  test setup to generate a valid test case
$!
$!
$!-------------------------------------------------
$!
$     SET DEFAULT fds$disku:[sec2414.work.new_gtds.thesis]
$!
$! Assign the body potential files
$!
$     assign/table=lnm$job fds$disku:[dj1230.bianca]dan_potential.dat gtds$047
$     assign/table=lnm$job fds$disku:[dj1230.bianca]moon.dat     gtds$048
$!
$! Assign the density file
$!
$     assign/table=lnm$job fds_dbf:jacchia_roberts.dat  gtds$075
$!
$! Assign the SLP and timing files
$!
$     assign/table=lnm$job elrond$dka0:[sec2414]june95_magen_slp_mn2000.dat gtds$014
$     assign/table=lnm$job elrond$dka0:[sec2414]june95_magen_slp_timcof.dat gtds$038
$     assign/table=lnm$job elrond$dka0:[sec2414]june95_magen_slp_tod2000.dat gtds$078
$!
$! Assign ORB1 files
$!
$     assign/table=lnm$job fds$disku:[sec2414.work.new_gtds.thesis]t4_f2.ORB1 gtds$024
$     assign/table=lnm$job fds$disku:[sec2414.work.new_gtds.thesis]t4_f1.ORB1 gtds$061
$!
$! Assign fundamental constants file
$!
$     assign/table=lnm$job fds$disku:[sec2414.work.new_gtds.mods]2000_cconst.dat gtds$099
$!
$! Execute the local version of debug executable
$!
$     @[sec2414.work.new_gtds.test]2000_SWAT_GTDS [sec2414.work.new_gtds.thesis]T4_F2
$!
$     EXIT
```

Figure G.43 Cowell FK5/COMPARE J_2 Command Procedure

SST FK4 J_2 Orbit
(T4_F1_SST)

```
CONTROL  EPHEM                                                  TOPEXXX  XXXXXX
EPOCH                    920224.0          000000.000000
ELEMENT1 1    2    1     7077.8D0          0.0011D0          98.2D0
ELEMENT2                 158.1D0           89.4D0            176.D0
OUTPUT   11   2    1     920227.D0         0.D0              43200.D0
ORBTYPE  5    1    1     43200.0           1.0
OGOPT
NCBODY   1
MAXDEGEQ 1               2.0
MAXORDEQ 1               0.0
POTFIELD 1    6
OUTOPT   1               920224000000.0    920227000000.0    60.0
END
FIN
```

Figure G.44 SST FK4 J_2 Input Card Data File

```
$!-------------------------------------------------------------
$! tod_to_ecef  test setup to generate a valid test case
$!
$!
$!-------------------------------------------------------------
$!
$     SET DEFAULT fds$diska:[ssc2414.work.new_gtds.thesis]
$!
$! Assign debug overrides
$!
$     assign/table=lnm$job  [ssc2414.work.new_gtds.thesis]t4_f1_sst.overrides dbg$init
$!
$! Assign the body potential files
$!
$     assign/table=lnm$job fds$diska:[djf1230.bianca]dan_potential.dat gtds$047
$     assign/table=lnm$job fds$diska:[djf1230.bianca]moon.dat      gtds$048
$!
$! Assign the density file
$!
$     assign/table=lnm$job fds_dbf:jacchia_roberts.dat   gtds$075
$!
$! Assign the SLP and timing files
$!
$     assign/table=lnm$job fds_dbf:june94_msgen_slp_mn1950.dat gtds$014
$     assign/table=lnm$job fds_dbf:june94_msgen_slp_timcof.dat gtds$038
$     assign/table=lnm$job fds_dbf:june94_msgen_slp_tod1950.dat gtds$078
$!
$! Assign ORB1 files
$!
$     assign/table=lnm$job fds$diska:[ssc2414.work.new_gtds.thesis]t4_f1_sst.orb1 gtds$024
$!
$! Assign fundamental constants file
$!
$     assign/table=lnm$job fds$diska:[ssc2414.work.new_gtds.mods]b1950_csconst.dat gtds$099
$!
$! Execute the local version of debug executable
$!
$     @[ssc2414.work.new_gtds.test]j2000_swat_gtds [ssc2414.work.new_gtds.thesis]T4_F1_SST
$!
$     EXIT
```

Figure G.45 SST FK4 J_2 Command Procedure

SST FK4 J_2 Orbit
(T4_F2_SST)

```
CONTROL  EPHEM                                          TOPEXXX  XXXXXX
EPOCH                    920224.0        000000.000000
ELEMENT1 1    2    1     7077.8D0        0.0011D0        98.2D0
ELEMENT2                 158.1D0         89.4D0          176.D0
OUTPUT   11   2    1     920227.D0       0.D0            43200.D0
ORBTYPE  5    1    11    43200.0         1.0
OGOPT
NCBODY   1
MAXDEGEQ 1               2.0
MAXORDEQ 1               0.0
POTFIELD 1    6
OUTOPT   1               920224000000.0  920227000000.0  60.0
END
FIN
CONTROL  COMPARE                                        TOPEXXX  XXXXXX
COMPOPT
CMPEPHEM 1    102  102   920224000000.   920227000000    30.
CMPPLOT  3                                              2.
END
FIN
```

Figure G.46 SST FK5/COMPARE J_2 Input Card Data File

```
$!-------------------------------------------------------
$! tod_to_ecef  test setup to generate a valid test case
$!
$!
$!-------------------------------------------------------
$!
$       SET DEFAULT fds$diska:[ssc2414.work.new_gtds.thesis]
$!
$! Assign debug overrides
$!
$       assign/table=lnm$job  [ssc2414.work.new_gtds.thesis]j4_f2_sst.overrides dbg$init
$!
$! Assign the body potential files
$!
$       assign/table=lnm$job fds$diska:[dj1230.bianca]dan_potential.dat gtds$047
$       assign/table=lnm$job fds$diska:[dj1230.bianca]moon.dat     gtds$048
$!
$! Assign the density file
$!
$       assign/table=lnm$job fds_dbf:jacchia_roberts.dat   gtds$075
$!
$! Assign the SLP and timing files
$!
$      assign/table=lnm$job elrond$dka0:[ssc2414]june95_msgen_slp_mn2000.dat gtds$014
$       assign/table=lnm$job elrond$dka0:[ssc2414]june95_msgen_slp_timcof.dat gtds$038
$       assign/table=lnm$job elrond$dka0:[ssc2414]june95_msgen_slp_tod2000.dat gtds$078
$!
$! Assign ORB1 files
$!
$       assign/table=lnm$job fds$diska:[ssc2414.work.new_gtds.thesis]j4_f2_sst.orb1 gtds$024
$       assign/table=lnm$job fds$diska:[ssc2414.work.new_gtds.thesis]j4_f1_sst.orb1 gtds$081
$!
$! Assign fundamental constants file
$!
$       assign/table=lnm$job fds$diska:[ssc2414.work.new_gtds.mods]j2000_csconst.dat gtds$099
$!
$! Execute the local version of debug executable
$!
$       @[ssc2414.work.new_gtds.test]j2000_swat_gtds [ssc2414.work.new_gtds.thesis]j4_f2_sst
$!
$       EXIT
```

Figure G.47 SST FK5/COMPARE J_2 Command Procedure

G.5 Differential Correction Testing

A total of three tests were performed to show that the differential correction process was undisturbed by the introduction of the new capabilities. These cases are summarized in Table G.17.

Table G.17 Differential Correction Test Cases

Test Case	Description	References in Appendix G
1	Cowell and SST differential corrections with truth ORB1 observations and perturbed initial conditions	Figures: G.48-G.62 Tables: G.18-G.19
2	Fit of Cowell truth ORB1 with SST techniques	Figures: G.63-G.74

The first two involved fitting Cowell and SST truth ORB1 files with similar force models, but with perturbed initial conditions. The converged solution was shown to be a virtual representation of the truth initial conditions, indicating that the differential correction process (including the variational equations) was working properly. The final test of the differential correction involved fitting the truth Cowell ORB1 file with semianalytic theory to show variations in the perturbation techniques. The results were similar to ones presented by Fonte in [20]. The file setups and plots associated with these tests are provided in the following pages.

Differential Correction Test Case 1: Cowell Differential Correction (TOPEX_TEST_COWELL_ITOD)

```
CONTROL  EPHEM                                                    TOPEXXX  XXXXXX
EPOCH                          921225.0              000000.000000
ELEMENT1 12   1    1           6107.12233649834D0    -4337.56757094521D0   -1858.01894920629D0
ELEMENT2                       3.02242463499831D0    1.54042383004345D0    6.337055931831127D0
OUTPUT   19   2    1           921226.D0             000000.D0             43200.D0
ORBTYPE  2    1    11          10.0
OGOPT
SCPARAM                        2.8D-5                2400.D0
DRAG     1                     1.0
ATMOSDEN           1
DRAGPAR  0
MAXDEGEQ 1                     50.
MAXORDEQ 1                     50.
MAXDEGVE 1                     4.
MAXORDVE 1                     4.
POTFIELD 1    19
SETIDE   1                     0.29D0
SOLRAD   1                     1.0
SOLRDPAR 0
OUTOPT   1                     921225000000.         921226000000.         450.0
END
FIN
CONTROL  DC                                                       TOPEXXX  XXXXXX
EPOCH                          921225.0              000000.000000
ELEMENT1 12   1    1           6107.D0               -4337.5D0             -1858.D0
ELEMENT2                       3.02D0                1.54D0                6.34D0
OBSINPUT 27                    921225 000000         921226 000000
ORBTYPE  2    1    11          10.0
DMOPT
OBSDEV   21                    100.
OBSDEV   22                    100.
OBSDEV   23                    100.
OBSDEV   24                    10.
OBSDEV   25                    10.
OBSDEV   26                    10.
END
DCOPT
PRINTOUT 1    4
CONVERG  20                    1.D-5                                       1.0
END
OGOPT
SCPARAM                        2.8D-5                2400.D0
DRAG     1                     1.0
ATMOSDEN           1
DRAGPAR  0
MAXDEGEQ 1                     50.
MAXORDEQ 1                     50.
MAXDEGVE 1                     4.
MAXORDVE 1                     4.
POTFIELD 1    19
SETIDE   1                     0.29D0
SOLRAD   1                     1.0
SOLRDPAR 0
STATEPAR 1
STATETAB 1    2    3           4                     5                     6
END
FIN
CONTROL  EPHEM                                OUTPUT              TOPEXXX  XXXXXX
OUTPUT   19   2    1           921226.D0             000000.D0             43200.D0
ORBTYPE  2    1    11          10.0
OGOPT
SCPARAM                        2.8D-5                2400.D0
DRAG     1                     1.0
ATMOSDEN           1
DRAGPAR  0
MAXDEGEQ 1                     50.
MAXORDEQ 1                     50.
MAXDEGVE 1                     4.
MAXORDVE 1                     4.
POTFIELD 1    19
SETIDE   1                     0.29D0
SOLRAD   1                     1.0
SOLRDPAR 0
OUTOPT   21                    921225000000.0        921226000000.0        450.0
END
FIN
CONTROL  COMPARE                                                  TOPEXXX  XXXXXX
COMPOPT
CMPEPHEM 1    102  102         921225000000.0        921226000000.0        7.5
CMPPLOT  3
HISTPLOT 1    102  102         921225000000.0        921226000000.0        450.0
END
FIN
```

Figure G.48 Cowell Differential Correction Test Input Card Data File

```
$!-------------------------------------------------------------
$! TOPEX_TEST_COWELL_ITOD.COM
$!
$!
$!-------------------------------------------------------------
$!
$! Set default for batch run from CSDL0:[GTDS.GTDS_TEST]
$!
$       set default fds$diska:[ssc2414.work.new_gtds.test]
$!
$! Assign debug overrides
$       assign/table=lnm$job [ssc2414.work.new_gtds.test]topex_test_cowell_itod.overrides   dbg$init
$!
$! Assign the body potential files
$!
$       assign/table=lnm$job fds$diska:[rjp9045.bianca.fonte]newcomb.dat gtds$023
$       assign/table=lnm$job fds$diska:[djf1230.bianca]dan_potential.dat gtds$047
$       assign/table=lnm$job fds$diska:[djf1230.bianca]moon.dat     gtds$048
$!
$! Assign the density
$!
$       assign/table=lnm$job fds_dbf:jacchia_roberts.dat   gtds$075
$!
$! Assign the SLP and timing files
$!
$       assign/table=lnm$job elrond$dka0:[ssc2414]june95_msgen_slp_mn2000.dat gtds$014
$       assign/table=lnm$job elrond$dka0:[ssc2414]june95_msgen_slp_timecoef.dat gtds$038
$       assign/table=lnm$job elrond$dka0:[ssc2414]june95_msgen_slp_tod2000.dat gtds$078
$!
$! Assign ORB1 files
$       assign/table=lnm$job fds$diska:[ssc2414.work.new_gtds.test]topex_poe_cowell_seed_8_new.orb1 gtds$024
$       assign/table=LNM$JOB fds$diska:[ssc2414.work.new_gtds.test]topex_test_cowell_itod.orb1 gtds$081
$       ASSIGN/TABLE=LNM$JOB fds$diska:[ssc2414.work.new_gtds.mods]j2000_csconst.dat gtds$099
$!
$! Execute the local version of debug executable
$!
$       @[ssc2414.work.new_gtds.test]j2000_SWAT_GTDS [ssc2414.work.new_gtds.test]topex_test_cowell_itod
$!
$       EXIT
```

Figure G.49 Cowell Differential Correction Test Command Procedure

```
SET OUTPUT LOG
SET LOG
SET BREAK/return ESTSET DO -
                        (DEPOSIT   IDIFF      = 0; -
                        DEPOSIT    IDRVAR     = 0; -
                        DEPOSIT    ISRVAR     = 0; -
                        DEPOSIT    KPAR       = 0; -
                        DEPOSIT    KATMOS     = 1; -
                        EXAMINE    KATMOS     ; -
                        EXAMINE    IDIFF      ; -
                        EXAMINE    IDRVAR     ; -
                        EXAMINE    ISRVAR     ; -
                        EXAMINE    KPAR       ; -
                        GO -
                );-
GO
```

Figure G.50 Cowell Differential Correction Test Overrides File

Differential Correction Test Case 2: SST Differential Correction (TOPEX_TEST_SST_ITOD)

```
CONTROL  EPHEM                                                    TOPEXXX  XXXXXX
EPOCH                          921225.0              000000.000000
ELEMENT1 12    6     1         7714.433648444437D0   1.108026791140940-4   66.04264029108742D0
ELEMENT2                       330.94791911507570    73.151643720448550    271.59201524024160
OUTPUT   19    2     1         921226.D0             000000.D0             43200.D0
ORBTYPE  5     1     11        43200.0               1.0
OGOPT
SCPARAM                        2.8D-5                2400.D0
DRAG     1                     1.0
ATMOSDEN               1
DRAGPAR  0
MAXDEGEQ 1                     50.
MAXORDEQ 1                     50.
MAXDEGVE 1                     4.
MAXORDVE 1                     4.
POTFIELD 1     19
RESONPRD                       259200.D0
SETIDE   1                     0.29D0
SOLRAD   1                     1.0
SOLRDPAR 0
OUTOPT   1                     921225000000.         921226000000.         450.0
END
FIN
CONTROL  DC                                                       TOPEXXX  XXXXXX
EPOCH                          921225.0              000000.000000
ELEMENT1 12    6     1         7714.4D0              1.108D-4              66.D0
ELEMENT2                       330.9D0               73.2D0                271.D0
OBSINPUT 27                    921225 000000         921226 000000
ORBTYPE  5     1     11        43200.0                                     1.0
DMOPT
OBSDEV   21                    100.
OBSDEV   22                    100.
OBSDEV   23                    100.
OBSDEV   24                    10.
OBSDEV   25                    10.
OBSDEV   26                    10.
END
DCOPT
PRINTOUT 1     4
CONVERG  20                    1.D-4                                       1.0
END
OGOPT
SCPARAM                        2.8D-5                2400.D0
DRAG     1                     1.0
ATMOSDEN               1
DRAGPAR  0
MAXDEGEQ 1                     50.
MAXORDEQ 1                     50.
MAXDEGVE 1                     4.
MAXORDVE 1                     4.
POTFIELD 1     19
RESONPRD                       259200.D0
SETIDE   1                     0.29D0
SOLRAD   1                     1.0
SOLRDPAR 0
STATEPAR 3
STATETAB 1     2     3         4                     5                     6
END
FIN
CONTROL  EPHEM                          OUTPUT                          TOPEXXX  XXXXXX
OUTPUT   19    2     1         921226.D0             000000.D0             43200.D0
ORBTYPE  5     1     11        43200.0               1.0
OGOPT
SCPARAM                        2.8D-5                2400.D0
DRAG     1                     1.0
ATMOSDEN               1
DRAGPAR  0
MAXDEGEQ 1                     50.
MAXORDEQ 1                     50.
MAXDEGVE 1                     4.
MAXORDVE 1                     4.
POTFIELD 1     19
RESONPRD                       259200.D0
SETIDE   1                     0.29D0
SOLRAD   1                     1.0
SOLRDPAR 0
OUTOPT   21                    921225000000.0        921226000000.0        450.0
END
FIN
CONTROL  COMPARE                                                  TOPEXXX  XXXXXX
COMPOPT
CMPEPHEM 1     102   102       921225000000.0        921226000000.0        7.5
CMPPLOT  3
HISTPLOT 1     102   102       921225000000.0        921226000000.0        450.0
END
FIN
```

Figure G.51 SST Differential Correction Test Input Card Data File

```
$!-----------------------------------------------------
$! TOPEX_TEST_COWELL_ITOD.COM
$!
$!
$!-----------------------------------------------------
$!
$! Set default for batch run from CSDL0:[GTDS.GTDS_.TEST]
$!
$       set default fds$diska:[ssc2414.work.new_gtds.test]
$!
$! Assign debug overrides
$       assign/table=lnm$job [ssc2414.work.new_gtds.test]topex_test_sst_itod.overrides   dbg$init
$!
$! Assign the body potential files
$!
$       assign/table=lnm$job fds$diska:[rjp9045.bianca.fonte]newcomb.dat gtds$023
$       assign/table=lnm$job fds$diska:[djf1230.bianca]dan_potential.dat gtds$047
$       assign/table=lnm$job fds$diska:[djf1230.bianca]moon.dat     gtds$048
$!
$! Assign the density
$!
$       assign/table=lnm$job fds_dbf:jacchia_roberts.dat  gtds$075
$!
$! Assign the SLP and timing files
$!
$       assign/table=lnm$job elrond$dka0:[ssc2414]june95_magen_slp_mn2000.dat gtds$014
$       assign/table=lnm$job elrond$dka0:[ssc2414]june95_magen_slp_timecoef.dat gtds$038
$       assign/table=lnm$job elrond$dka0:[ssc2414]june95_magen_slp_tod2000.dat gtds$078
$!
$! Assign ORB1 files
$       assign/table=lnm$job fds$diska:[ssc2414.work.new_gtds.test]topex_poe_sst_seed_1_new.orb1 gtds$024
$       assign/table=lnm$job fds$diska:[ssc2414.work.new_gtds.test]topex_test_sst_itod.orb1 gtds$081
$       assign/table=lnm$job fds$diska:[ssc2414.work.new_gtds.mods]j2000_csconst.dat gtds$099
$!
$! Execute the local version of debug executable
$!
$       @[ssc2414.work.new_gtds.test]j2000_SWAT_GTDS [ssc2414.work.new_gtds.test]topex_test_sst_itod
$!
$       EXIT
```

Figure G.52 SST Differential Correction Test Command Procedure

```
SET OUTPUT LOG
SET LOG
SET BREAK/return ESTSET DO -
                 (DEPOSIT   IDIFF     = 0; -
                 DEPOSIT    IDRVAR    = 0; -
                 DEPOSIT    ISRVAR    = 0; -
                 DEPOSIT    KPAR      = 0; -
                 DEPOSIT    KATMOS    = 1; -
                 EXAMINE    KATMOS    ; -
                 EXAMINE    IDIFF     ; -
                 EXAMINE    IDRVAR    ; -
                 EXAMINE    ISRVAR    ; -
                 EXAMINE    KPAR      ; -
                 GO -
        ); -
GO
```

Figure G.53 SST Differential Correction Test Overrides File

The accuracy of the differential correction process is measured in two manners here. First, the converged solution is compared in absolute terms to the initial truth conditions (Tables G.18 and G.19). Because they are slightly

different, the ephemeris generated from the converged solution varies somewhat from the truth ephemeris. These differences are plotted in Cartesian coordinates, radial/cross-track/along track components, and orbit elements in Figures G.48-G.74.

Table G.18 Cowell Differences Between Truth and Converged States

	Truth (km)	Converged (km)	Δ (km)	1σ (km)
X	6107.1223364983	6107.1223364975	7.9945e-10	9.6775e-7
Y	-4337.566570945	-4337.566570946	9.3995e-10	6.7698e-7
Z	-1858.018949206	-1858.018949208	1.9998e-9	9.7018e-7
VX	3.0224246349983	3.0224246349997	1.4078e-12	8.9335e-8
VY	1.5404238300435	1.5404238300425	9.8321e-13	5.9140e-8
VZ	6.3370559318311	6.3370559318307	3.9879e-13	9.3149e-8

Table G.19 SST Differences Between Truth and Converged States

	Truth (km)	Converged (km)	Δ (km)	1σ (km)
X	6105.1193296945	6105.1193446027	1.4908e-5	2.7894e-5
Y	-4335.062253693	-4335.062230911	2.2782e-5	2.6396e-5
Z	-1856.576096593	-1856.576111634	1.5041e-5	2.7805e-5
VX	3.0215542411922	3.0215542560749	1.4883e-8	2.7129e-6
VY	1.5426757579791	1.5426757799917	2.2013e-8	2.4183e-6
VZ	6.3372008864777	6.3372008684493	1.8028e-8	2.7122e-6

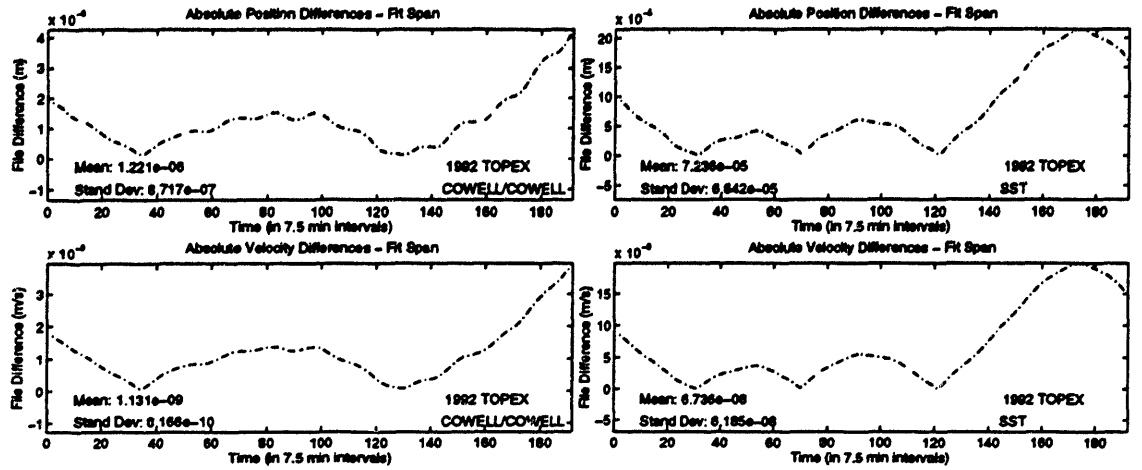

Figure G.54 Absolute Differences Between Truth and Converged Orbits

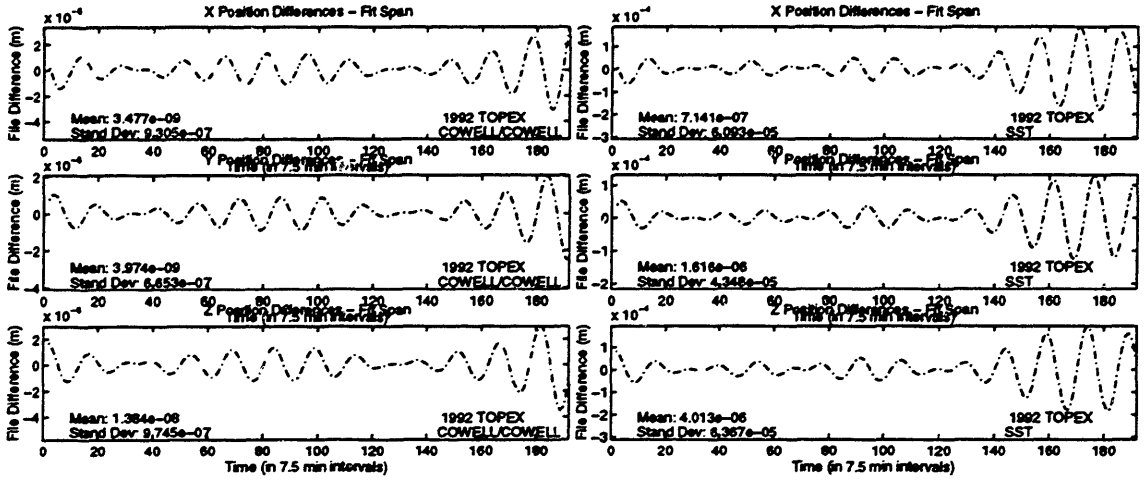

Figure G.55 Position Differences Between Truth and Converged Orbits

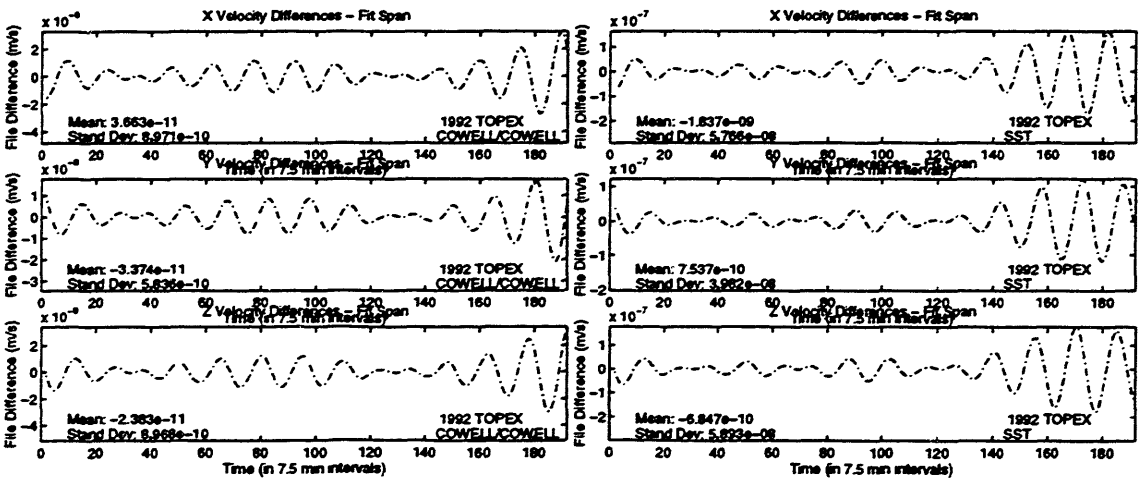

Figure G.56 Velocity Differences Between Truth and Converged Orbits

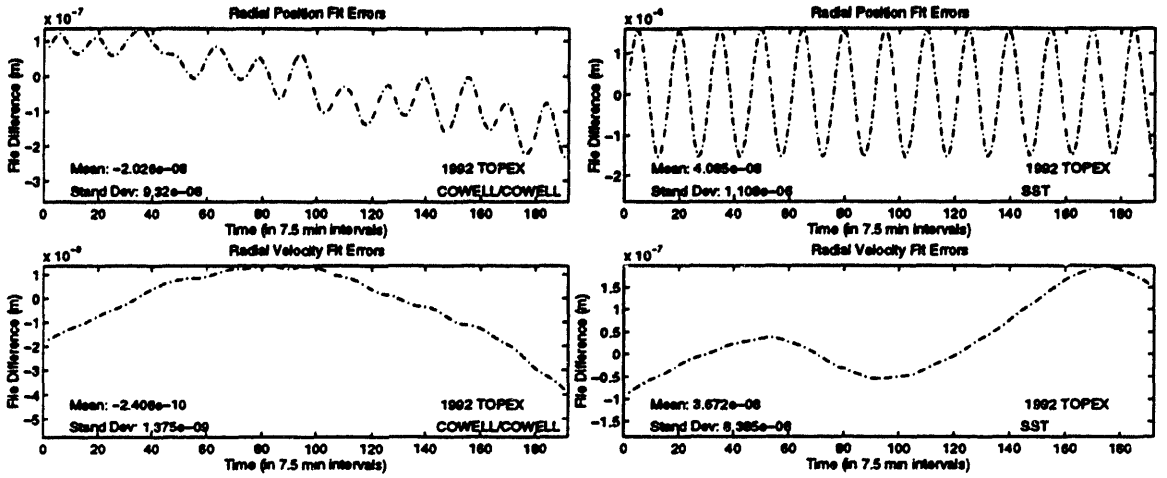

Figure G.57 Radial Differences Between Truth and Converged Orbits

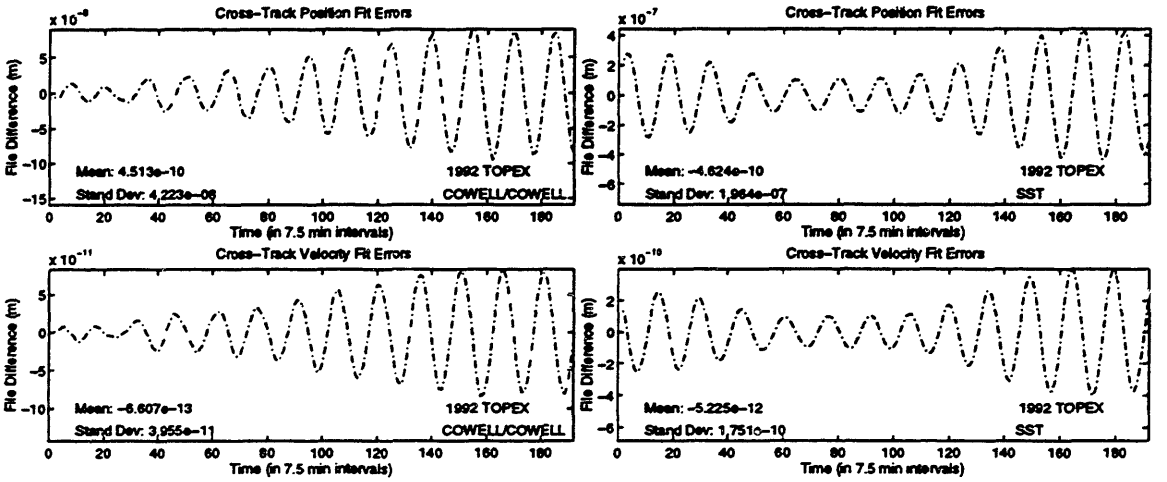

Figure G.58 Cross-Track Differences Between Truth and Converged Orbits

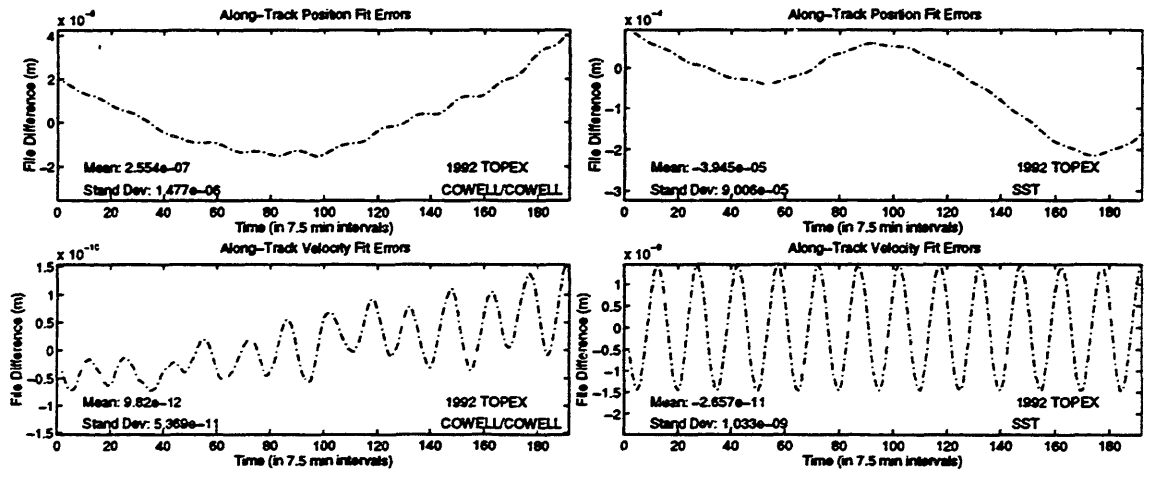

Figure G.59 Along-Track Differences Between Truth and Converged Orbits

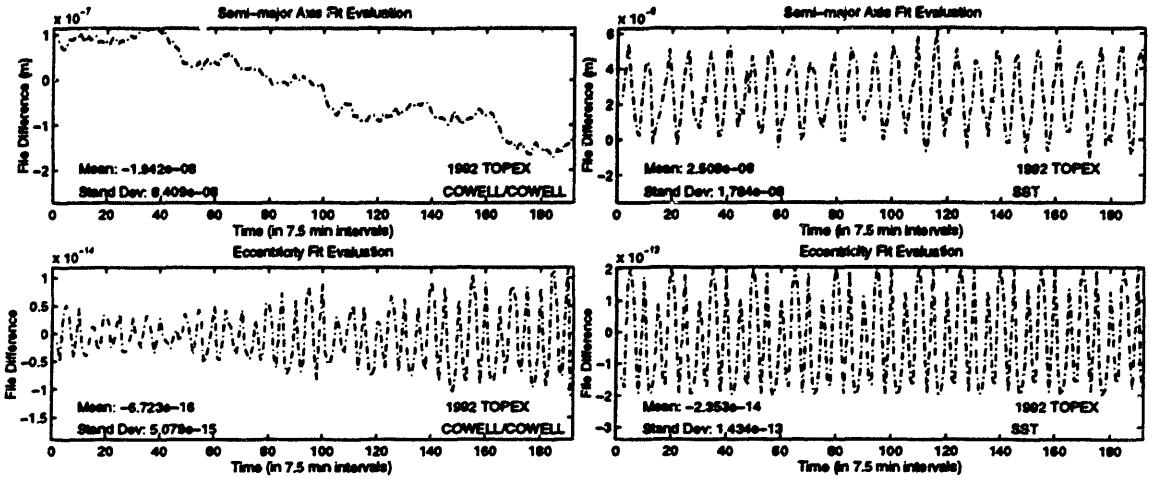

Figure G.60 *a/e* Differences Between Truth and Converged Orbits

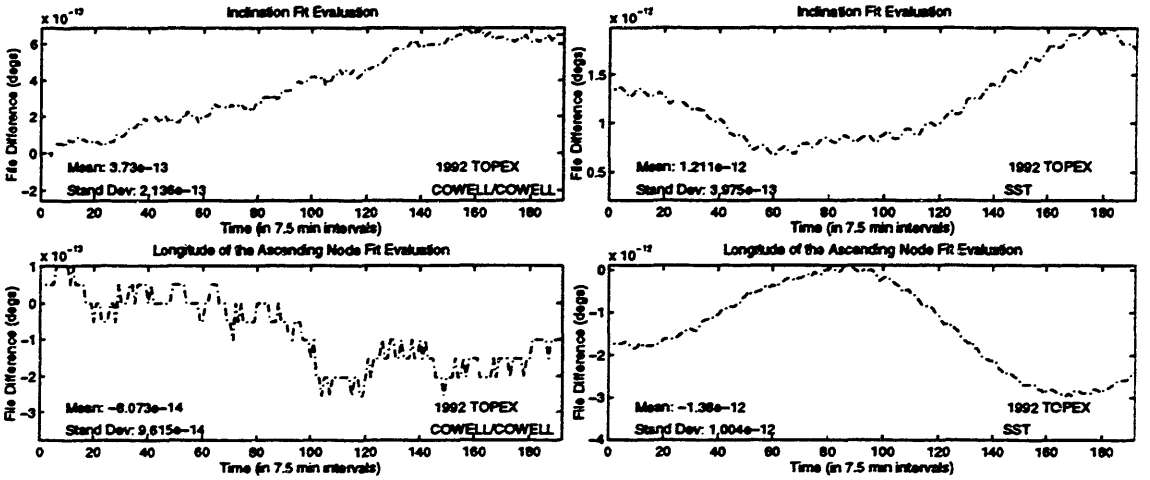

Figure G.61 *i/Ω* Differences Between Truth and Converged Orbits

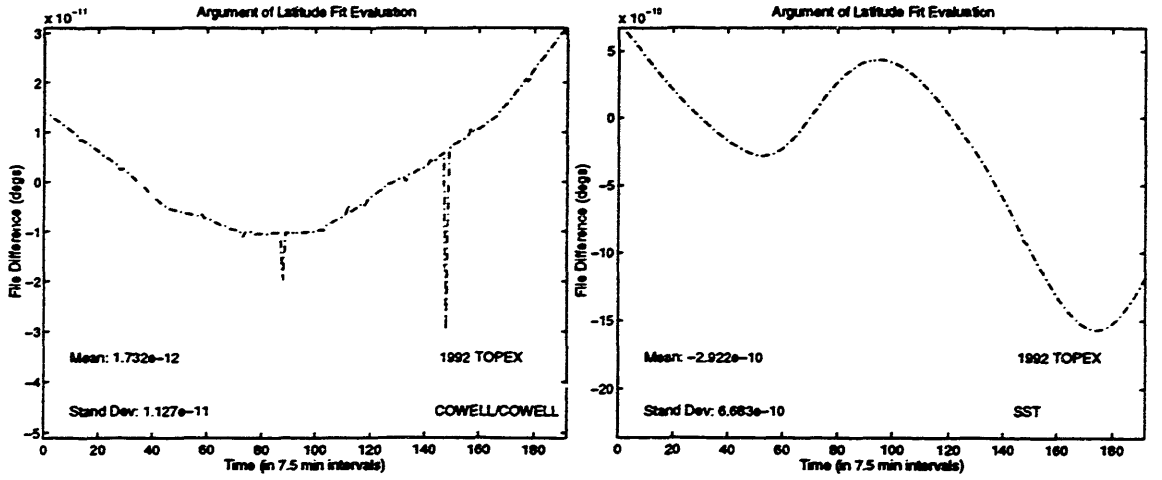

Figure G.62 Argument of Latitude Differences Between Truth and Converged Orbits

Differential Correction Test Case 3: SST Fit to Cowell Truth Orbit (TOPEX_POE_M20_SST_DC_7_NEW)

```
CONTROL  DC                                                          TOPEXXX  XXXXXX
EPOCH                    921225.0          000000.000000
ELEMENT1 12  6      1    7714.4D0          1.108D-4          66.D0
ELEMENT2                 330.9D0           73.2D0            271.D0
OBSINPUT 27              921225 000000     921226 000000
ORBTYPE  5   1      11   43200.0           1.0
DMOPT
OBSDEV   21              100.
OBSDEV   22              100.
OBSDEV   23              100.
OBSDEV   24              10.
OBSDEV   25              10.
OBSDEV   26              10.
END
DCOPT
PRINTOUT 1   4
CONVERG  20              1.D-4                               1.0
END
OGOPT
SCPARAM                  2.8D-5            2400.D0
DRAG     1               1.0
ATMOSDEN          1
DRAGPAR  0
MAXDEGEQ 1               50.
MAXORDEQ 1               50.
MAXDEGVE 1               4.
MAXORDVE 1               4.
POTFIELD 1   19
RESONPRD                 259200.
SETIDE   1               0.29D0
SOLRAD   1               1.0
SOLRDPAR 0
STATEPAR 3
STATETAB 1   2      3    4                 5                 6
END
FIN
CONTROL  EPHEM                OUTPUT                         TOPEXXX  XXXXXX
OUTPUT   19  2        1    921226.D0         000000.D0         43200.D0
ORBTYPE  5   1      11   43200.0           1.0
OGOPT
SCPARAM                  2.8D-5            2400.D0
DRAG     1               1.0
ATMOSDEN          1
DRAGPAR  0
MAXDEGEQ 1               50.
MAXORDEQ 1               50.
MAXDEGVE 1               4.
MAXORDVE 1               4.
RESONPRD                 259200.
POTFIELD 1   19
SETIDE   1               0.29D0
SOLRAD   1               1.0
SOLRDPAR 0
OUTOPT   21              921225000000.0    921226000000.0    450.0
END
FIN
CONTROL  COMPARE                                                     TOPEXXX  XXXXXX
COMPOPT
CMPEPHEM 1       102 102 921225000000.0    921226000000.0    7.5
CMPPLOT  3
HISTPLOT 1       102 102 921225000000.0    921226000000.0    450.0
END
FIN
```

Figure G.63 SST Fit to Cowell Truth Orbit Input Card Data File

```
$!-------------------------------------------------------
$! TOPEX_POE_M20_SST_DC_7_NEW.COM
$!
$!
$!-------------------------------------------------------
$!
$! Set default for batch run from CSDL0:[GTDS.GTDS_TEST]
$!
$  set default fds$diska:[ssc2414.work.new_gtds.test]
$!
$! Assign debug overrides
$  assign/table=lnm$job [ssc2414.work.new_gtds.test]topex_poe_m20_sst_dc_7_new.overrides dbg$init
$!
$! Assign the body potential files
$!
$  assign/table=lnm$job fds$diska:[ssc2414.work.new_gtds.test]newcomb.dat gtds$023
$  assign/table=lnm$job fds$diska:[dj1230.bianca]dan_potential.dat gtds$047
$  assign/table=lnm$job fds$diska:[dj1230.bianca]moon.dat      gtds$048
$!
$! Assign the density file
$!
$  assign/table=lnm$job fds_dbf:jacchia_roberts.dat   gtds$075
$!
$! Assign the SLP and timing files
$!
$  assign/table=lnm$job elrond$dka0:[ssc2414]june95_magen_slp_mn2000.dat gtds$014
$  assign/table=lnm$job elrond$dka0:[ssc2414]june95_magen_slp_timecoef.dat gtds$038
$  assign/table=lnm$job elrond$dka0:[ssc2414]june95_magen_slp_tod2000.dat gtds$078
$!
$! Assign ORB1 files
$!
$  assign/table=lnm$job fds$diska:[ssc2414.work.new_gtds.test]topex_poe_cowell_seed_8_new.ORB1 gtds$024
$  assign/table=lnm$job fds$diska:[ssc2414.work.new_gtds.test]topex_poe_m20_sst_dc_7_new.ORB1 gtds$081
$!
$! Assign the fundamental constants file
$!
$  assign/table=lnm$job fds$diska:[ssc2414.work.new_gtds.mods]j2000_csconst.dat gtds$099
$!
$! Execute the local version of debug executable
$!
$  @[ssc2414.work.new_gtds.test]j2000_SWAT_GTDS [ssc2414.work.new_gtds.test]topex_poe_m20_sst_dc_7_new
$!
$  EXIT
```

Figure G.64 SST Fit to Cowell Truth Orbit Command Procedure

```
SET OUTPUT LOG
SET LOG
SET BREAK/return ESTSET DO -
                 (DEPOSIT   IDIFF     = 0; -
                 DEPOSIT    IDRVAR    = 0; -
                 DEPOSIT    ISRVAR    = 0; -
                 DEPOSIT    KPAR      = 0; -
                 DEPOSIT    KATMOS    = 1; -
                 EXAMINE    KATMOS    ; -
                 EXAMINE    IDIFF     ; -
                 EXAMINE    IDRVAR    ; -
                 EXAMINE    ISRVAR    ; -
                 EXAMINE    KPAR      ; -
                 GO -
        ); -
GO
```

Figure G.65 SST Fit to Cowell Truth Orbit Overrides File

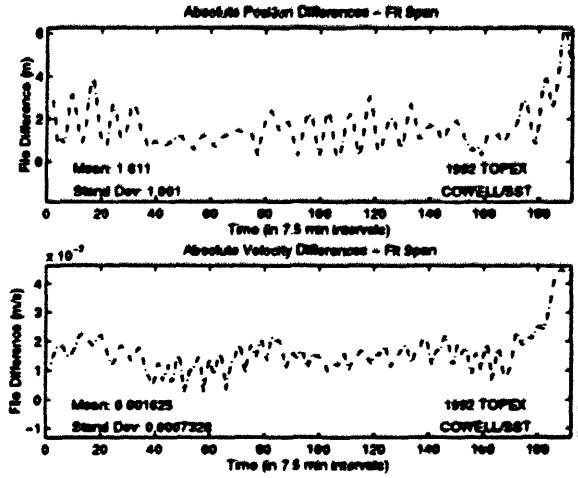

Figure G.66 Absolute SST/Cowell Differences

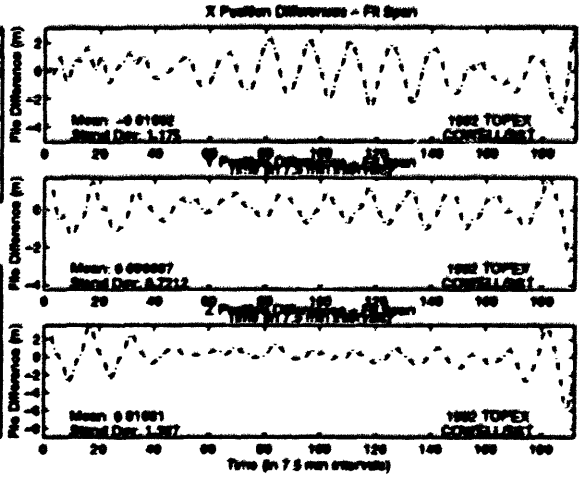

Figure G.67 SST/Cowell Position Differences

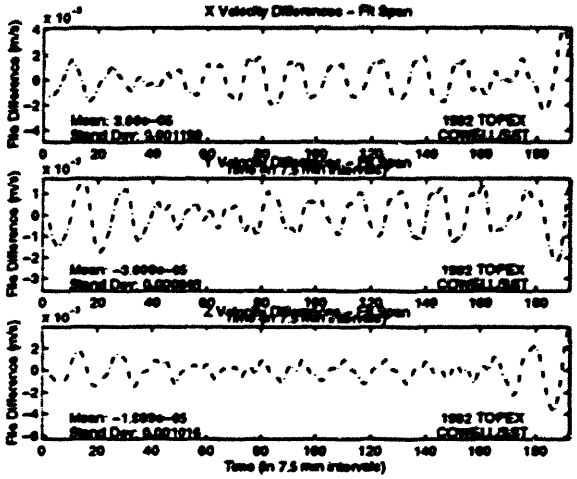

Figure G.68 SST/Cowell Velocity Differences

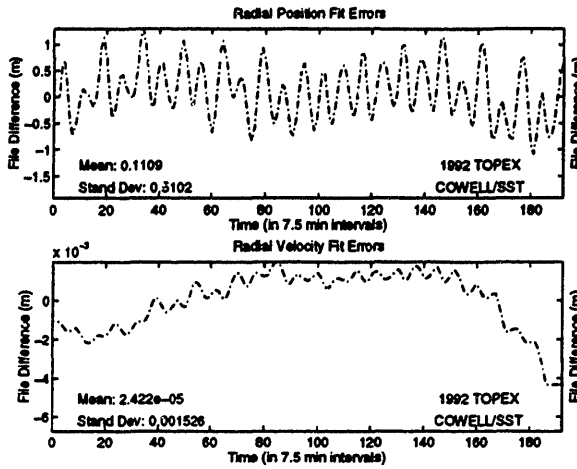

Figure G.69 SST/Cowell Radial Differences

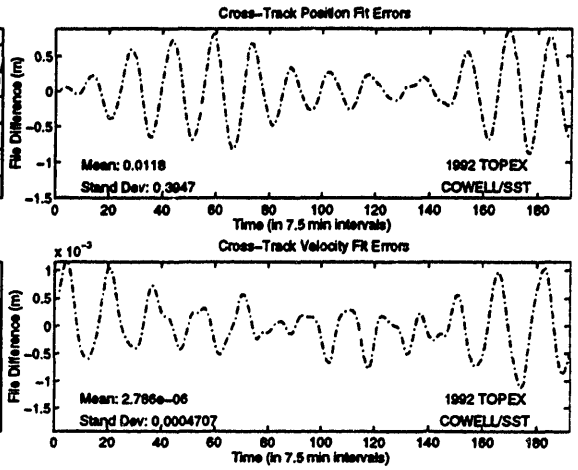

Figure G.70 SST/Cowell Cross-Track Differences

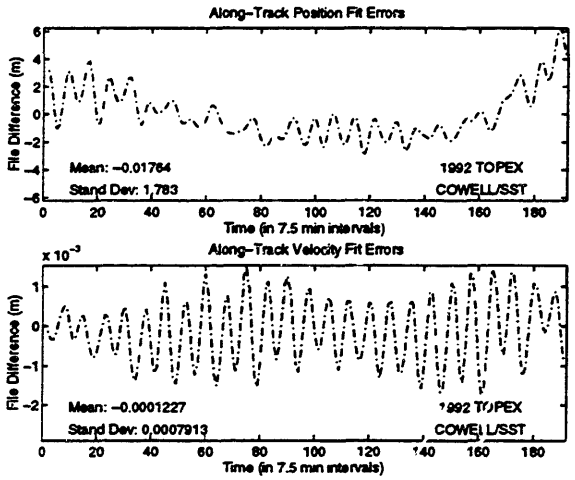

Figure G.71 SST/Cowell Along-Track Differences

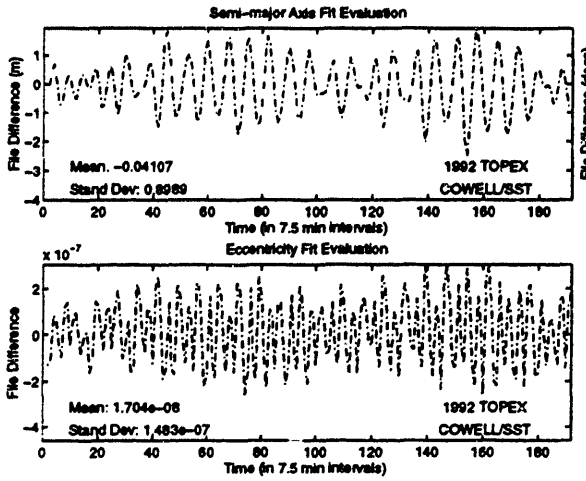

Figure G.72 SST/Cowell *a/e* Differences

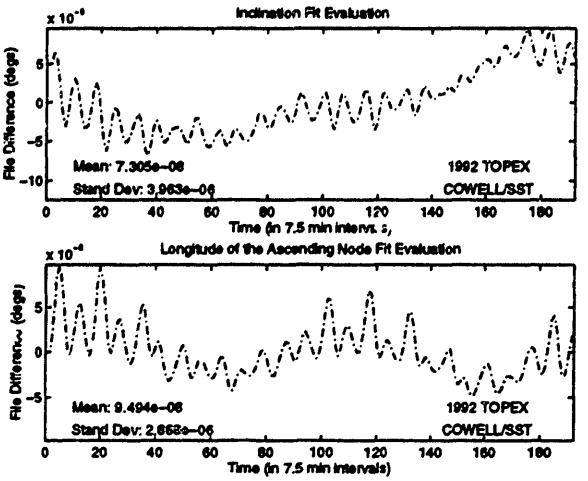

Figure G.73 SST/Cowell *i/Ω* Differences

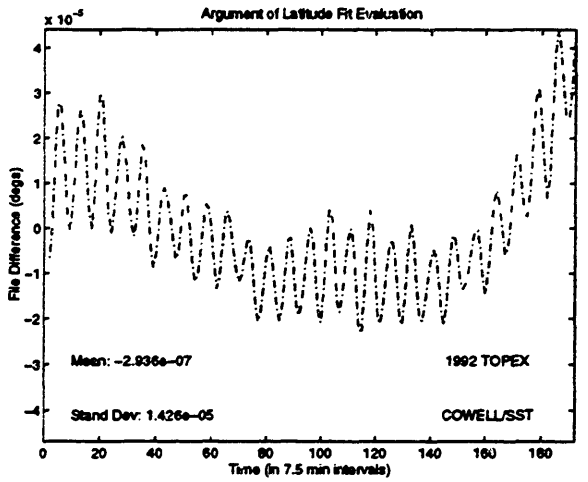

Figure G.74 SST/Cowell Argument of Latitude Differences

G.6 Testing with the TOPEX POEs

The POEs provided a unique opportunity to test the accuracy of the Draper R&D GTDS Cowell and SST propagators, as well as evaluation of the solid earth tide and instantaneous true of date incorporations. Three categories of applications involving the POEs during the testing phase were identified.

- Use POEs in differential correction to test accuracy of the force modeling in the Cowell and SST orbit generators

- Use POEs in differential correction to test implementation of the solid earth tide modeling

- Use POEs in differential correction to test implementation of the ITOD coordinate system

The TOPEX POE tests are summarized in Table G.20.

Table G.20 TOPEX POE Test Cases

Test Case	Description	References in Appendix G
1	Cowell fit of the TOPEX POEs with 21x21 geopotential; no solid earth tides	Figures: G.75-G.86
2	Cowell fit of the TOPEX POEs with 50x50 geopotential; no solid earth tides	Figures: G.87-G.98
3	Cowell fit of the TOPEX POEs with 21x21 geopotential; solid earth tides	Figures: G.99-G.110
4	Cowell fit of the TOPEX POEs with 50x50 geopotential; solid earth tides	Figures: G.111-G.122
5	SST fit of the TOPEX POEs with 50x50 geopotential; solid earth tides	Figures: G.123-G.134
6	Anticipated solid earth tide effects for Cowell propagator (based on TOPEX POE vector)	Figures: G.135-G.137 G.141-G.149
7	Anticipated solid earth tide effects for SST propagator (based on TOPEX POE vector)	Figures: G.138-G.140 G.141-G.149
8	Cowell fit to ECEF TOPEX POEs with 50x50 geopotential; solid earth tides	Figure: G.150

The first category tests the absolute accuracy of the Cowell and SST propagators by using the high accuracy POE vectors as observations. The effects of both solid earth tides and 50x50 gravity field modeling were isolated and shown to be significant for fit accuracy improvement. The file setups and plots are presented for each of the FK5-based test cases (switching from FK4 to FK5 revealed little improvement in the fit of the POEs).

TOPEX POE Test Case 1: Cowell Fit of POEs with 21x21 JGM-2, No Solid Earth Tides

(TOPEX_POE_ITOD_DC_2)

```
CONTROL  DC                                                    TOPEXXX  XXXXXX
EPOCH                    921225.0          000000.000000
ELEMENT1 12   1    1     6107.1205886653D0 -4337.5682058825D0 -1858.0201149621D0
ELEMENT2                 3.0224258514177D0 1.5404220636548D0  6.3370559518274D0
OBSINPUT 29              921225 000000     921230 000100
ORBTYPE  2    1    11    10.0
DMOPT
OBSDEV   21              5.
OBSDEV   22              5.
OBSDEV   23              5.
OBSDEV   24              .5
OBSDEV   25              .5
OBSDEV   26              .5
END
DCOPT
PRINTOUT 1    4
CONVERG  20              1.D-4                                 1.0
END
OGOPT
DRAG     1               1.
ATMOSDEN          1
DRAGPAR  2    1          0.15D0
SCPARAM                  2.8D-5            2400.0D0
MAXDEGEQ 1               21.
MAXORDEQ 1               21.
MAXDEGVE 1               4.
MAXORDVE 1               4.
POTFIELD 1    19
SOLRAD   1               1
SOLRDPAR 1
STATEPAR 1
STATETAB 1    2    3     4                 5                     6
END
FIN
CONTROL  EPHEM             OUTPUT                               TOPEXXX  XXXXXX
OUTPUT   19   2    1     921230.D0         000000.D0             43200.D0
ORBTYPE  2    1    11    10.0
OGOPT
DRAG     1               1
ATMOSDEN          1
DRAGPAR  0
SCPARAM                  2.8D-5            2400.0D0
MAXDEGEQ 1               21.
MAXORDEQ 1               21.
MAXDEGVE 1               4.
MAXORDVE 1               4.
POTFIELD 1    19
SOLRAD   1               1
SOLRDPAR 0
OUTOPT   1               921225000000.0    921230000000.0        120.0
END
FIN
```

Figure G.75 Cowell 21x21, No SET Fit to POEs Input Card Data File

```
$!-------------------------------------------------------
$! TOPEX_POE_ITOD_DC_2.COM
$!
$!
$!-------------------------------------------------------
$!
$! Set default for batch run from CSDL0:[GTDS.GTDS_TEST]
$!
$  set default fds$diska:[ssc2414.work.new_gtds.test]
$!
$! Assign debug overrides
$!
$  assign/table=lnm$job  [ssc2414.work.new_gtds.test]topex_poe_itod_dc_2.overrides          dbg$init
$!
$! Assign the body potential files
$!
$  assign/table=lnm$job fds$diska:[dj1230.bianca]dan_potential.dat gtds$047
$  assign/table=lnm$job fds$diska:[dj1230.bianca]moon.dat      gtds$048
$!
$! Assign the density file
$!
$  assign/table=lnm$job fds_dbf:jacchia_roberts.dat   gtds$075
$!
$! Assign the SLP and timing files
$!
$  assign/table=lnm$job elrond$dka0:[ssc2414]june95_msgen_slp_mn2000.dat gtds$014
$  assign/table=lnm$job elrond$dka0:[ssc2414]june95_msgen_slp_timecoef.dat gtds$038
$  assign/table=lnm$job elrond$dka0:[ssc2414]june95_msgen_slp_tod2000.dat gtds$078
$!
$! Assign the observation card and ORB1 files
$!
$  assign/table=lnm$job fds$diska:[ssc2414.topex.obscard]topex_poe_itod_2.poscard gtds$015
$  assign/table=lnm$job fds$diska:[ssc2414.work.new_gtds.test]topex_poe_itod_dc_2.orb1 gtds$024
$!
$! Assign the fundamental constants file
$!
$  assign/table=lnm$job fds$diska:[ssc2414.work.new_gtds.mods]j2000_csconst.dat gtds$099
$!
$! Execute the local version of debug executable
$!
$  @[ssc2414.work.new_gtds.test]j2000_SWAT_GTDS [ssc2414.work.new_gtds.test]topex_poe_itod_dc_2
$!
$  EXIT
```

Figure G.76 Cowell 21x21, No SET Fit to POEs Command Procedure

```
SET OUTPUT LOG
SET LOG
SET BREAK/return: ESTSET DO -
      (DEPOSIT  IDIFF      = 3; -
       DEPOSIT  IDRVAR     = 1; -
       DEPOSIT  ISRVAR     = 1; -
       DEPOSIT  KPAR       = 0; -
       DEPOSIT  KATMOS     = 1; -
       EXAMINE  KATMOS     ; -
       EXAMINE  IDIFF      ; -
       EXAMINE  IDRVAR     ; -
       EXAMINE  ISRVAR     ; -
       EXAMINE  KPAR       ; -
       GO -
    ); -
GO
```

Figure G.77 Cowell 21x21, No SET Fit to POEs Overrides File

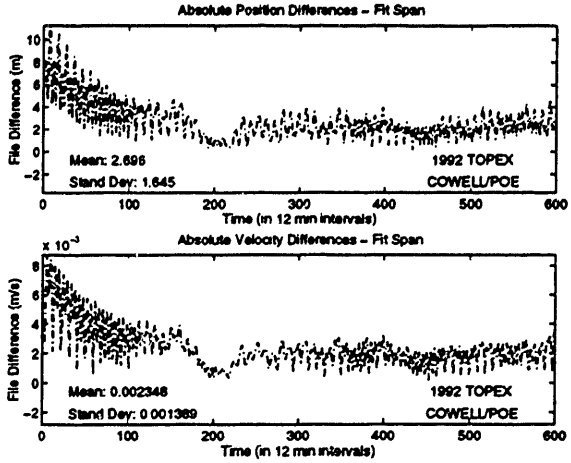

Figure G.78 Cowell 21x21/No SET Absolute Differences

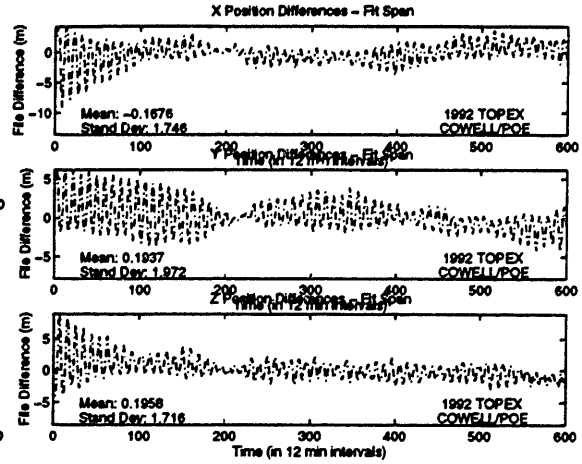

Figure G.79 Cowell 21x21/No SET Position Differences

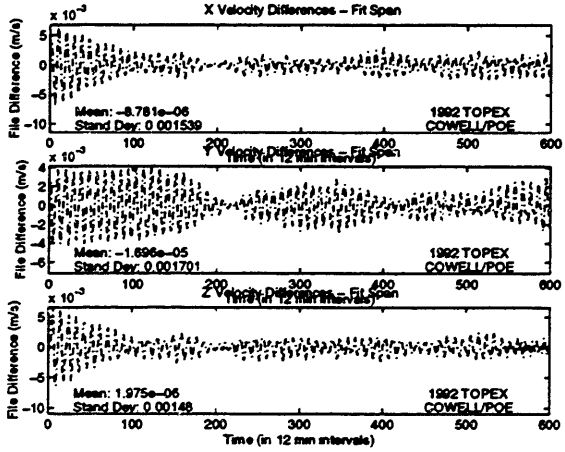

Figure G.80 Cowell 21x21/No SET Velocity Differences

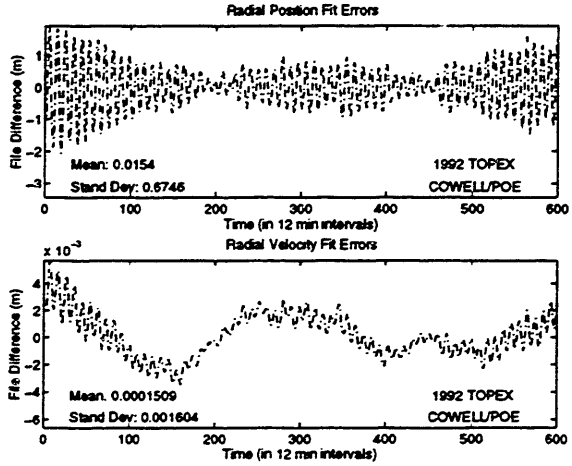

Figure G.81 Cowell 21x21/No SET Radial Differences

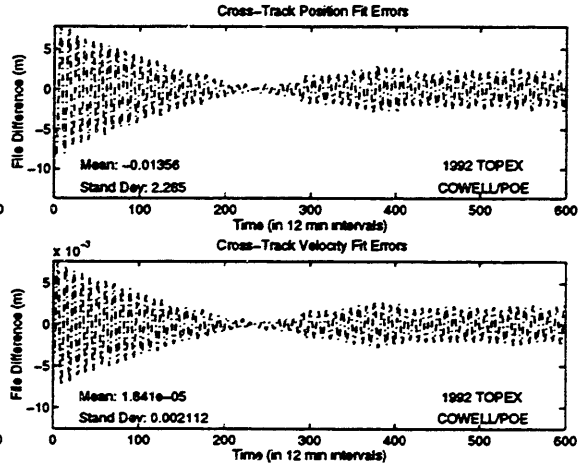

Figure G.82 Cowell 21x21/No SET Cross-Track Differences

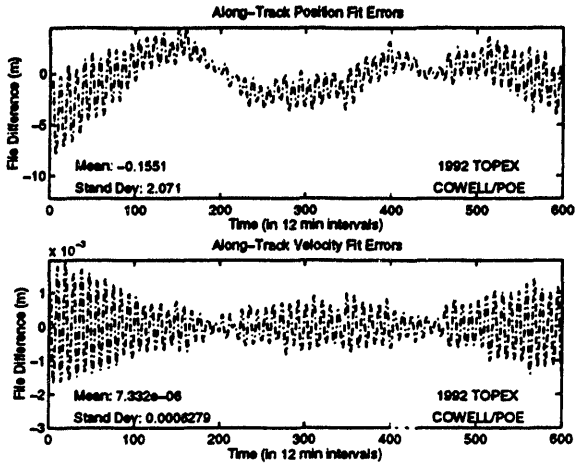

Figure G.83 Cowell 21x21/No SET Along-Track Differences

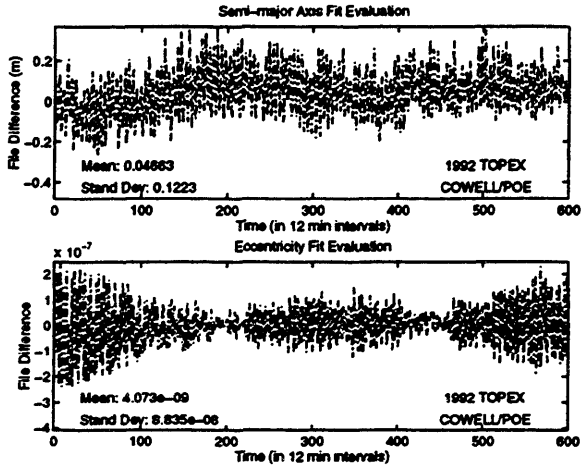

Figure G.84 Cowell 21x21/No SET *a/e* Differences

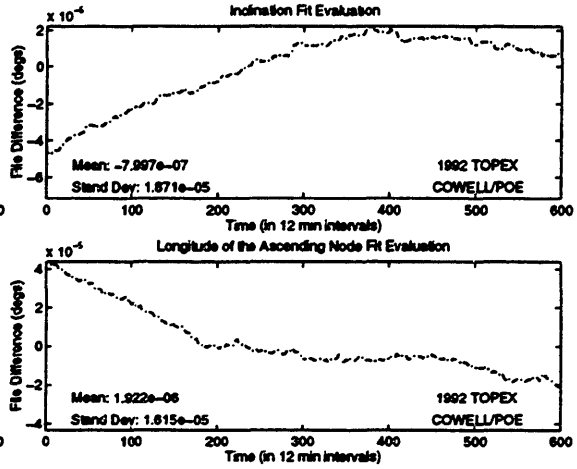

Figure G.85 Cowell 21x21/No SET *i/Ω* Differences

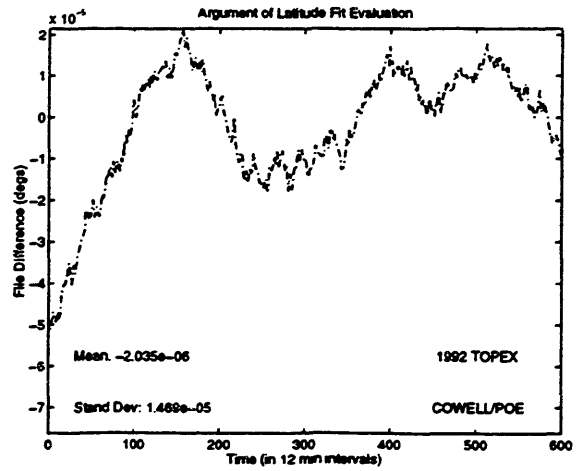

Figure G.86 Cowell 21x21/No SET Argument of Latitude Differences

TOPEX POE Test Case 2: Cowell Fit of POEs with 50x50 JGM-2, No Solid Earth Tides

(TOPEX_POE_ITOD_DC_3)

```
CONTROL  DC                                                    TOPEXXX  XXXXXX
EPOCH                    921225.0              000000.000000
ELEMENT1  12   1    1    6107.1205886653D0     -4337.5682058825D0    -1858.0201149621D0
ELEMENT2                 3.0224258514177D0     1.5404220636548D0     6.3370559518274D0
OBSINPUT  29             921225 000000         921230 000100
ORBTYPE   2    1    11   10.0
DMOPT
OBSDEV    21             5.
OBSDEV    22             5.
OBSDEV    23             5.
OBSDEV    24             .5
OBSDEV    25             .5
OBSDEV    26             .5
END
DCOPT
PRINTOUT  1    4
CONVERG   20             1.D-4                                 1.0
END
OGOPT
DRAG      1              1.
ATMOSDEN             1
DRAGPAR   2    1         0.15D0
SCPARAM                  2.8D-5                2400.0D0
MAXDEGEQ  1              50.
MAXORDEQ  1              50.
MAXDEGVE  1              4.
MAXORDVE  1              4.
POTFIELD  1    19
SOLRAD    1              1
SOLRDPAR  1
STATEPAR  1
STATETAB  1    2    3    4                     5                     6
END
FIN
CONTROL  EPHEM                OUTPUT                                 TOPEXXX  XXXXXX
OUTPUT    19   2    1    921230.D0             000000.D0             43200.D0
ORBTYPE   2    1    11   10.0
OGOPT
DRAG      1              1
ATMOSDEN             1
DRAGPAR   0
SCPARAM                  2.8D-5                2400.0D0
MAXDEGEQ  1              50.
MAXORDEQ  1              50.
MAXDEGVE  1              4.
MAXORDVE  1              4.
POTFIELD  1    19
SOLRAD    1              1
SOLRDPAR  0
OUTOPT    1              921225000000.0        921230000000.0        120.0
END
FIN
```

Figure G.87 Cowell 50x50, No SET Fit to POEs Input Card Data File

```
$!-------------------------------------------------------------
$! TOPEX_POE_ITOD_DC_3.COM
$!
$!
$!-------------------------------------------------------------
$!
$! Set default for batch run from CSDL0:[GTDS.GTDS_TEST]
$!
$  set default fds$diska:[ssc2414.work.new_gtds.test]
$!
$! Assign debug overrides
$!
$  assign/table=lnm$job  [ssc2414.work.new_gtds.test]topex_poe_itod_dc_3.overrides          dbg$init
$!
$! Assign the body potential files
$!
$  assign/table=lnm$job fds$diska:[djf1230.bianca]dan_potential.dat gtds$047
$  assign/table=lnm$job fds$diska:[djf1230.bianca]moon.dat     gtds$048
$!
$! Assign the density file
$!
$  assign/table=lnm$job fds_dbf:jacchia_roberts.dat   gtds$075
$!
$! Assign the SLP and timing files
$!
$  assign/table=lnm$job elrond$dka0:[ssc2414]june95_msgen_slp_mn2000.dat gtds$014
$  assign/table=lnm$job elrond$dka0:[ssc2414]june95_msgen_slp_timecoef.dat gtds$038
$  assign/table=lnm$job elrond$dka0:[ssc2414]june95_msgen_slp_tod2000.dat gtds$078
$!
$! Assign the observation card and ORB1 files
$!
$  assign/table=lnm$job fds$diska:[ssc2414.topex.obscard]topex_poe_itod_2.poscard gtds$015
$  assign/table=lnm$job fds$diska:[ssc2414.work.new_gtds.test]topex_poe_itod_dc_3.orb1 gtds$024
$!
$! Assign the fundamental constants file
$!
$  assign/table=lnm$job fds$diska:[ssc2414.work.new_gtds.mods]j2000_csconst.dat gtds$099
$!
$! Execute the local version of debug executable
$!
$  @[ssc2414.work.new_gtds.test]j2000_SWAT_GTDS [ssc2414.work.new_gtds.test]topex_poe_itod_dc_3
$!
$  EXIT
```

Figure G.88 Cowell 50x50, No SET Fit to POEs Command Procedure

```
SET OUTPUT LOG
SET LOG
SET BREAK/return ESTSET DO -
      (DEPOSIT  IDIFF      = 3; -
       DEPOSIT  IDRVAR     = 1; -
       DEPOSIT  ISRVAR     = 1; -
       DEPOSIT  KPAR       = 0; -
       DEPOSIT  KATMOS     = 1; -
       EXAMINE  KATMOS     ; -
       EXAMINE  IDIFF      ; -
       EXAMINE  IDRVAR     ; -
       EXAMINE  ISRVAR     ; -
       EXAMINE  KPAR       ; -
       GO -
    ); -
GO
```

Figure G.89 Cowell 50x50, No SET Fit to POEs Overrides File

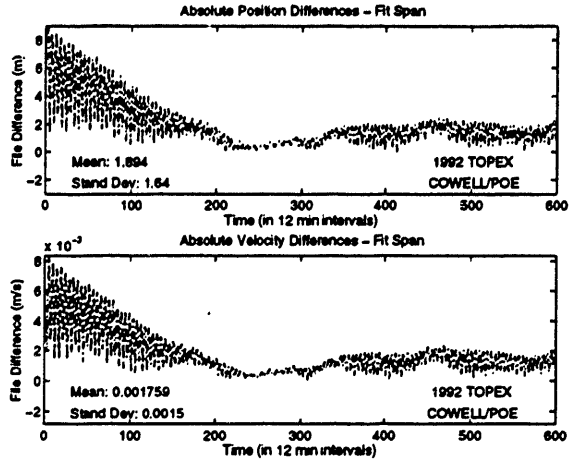

Figure G.90 Cowell 50x50/No SET Absolute Differences

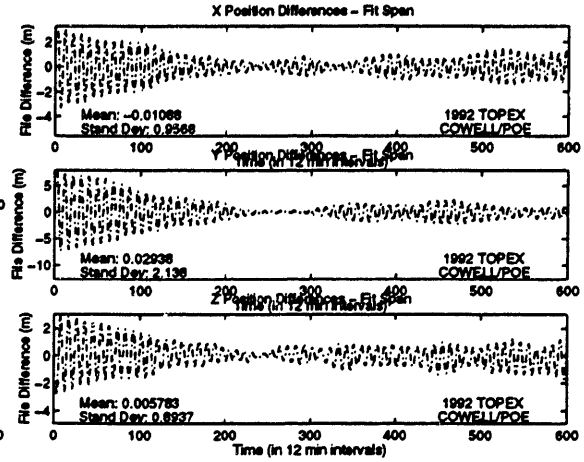

Figure G.91 Cowell 50x50/No SET Position Differences

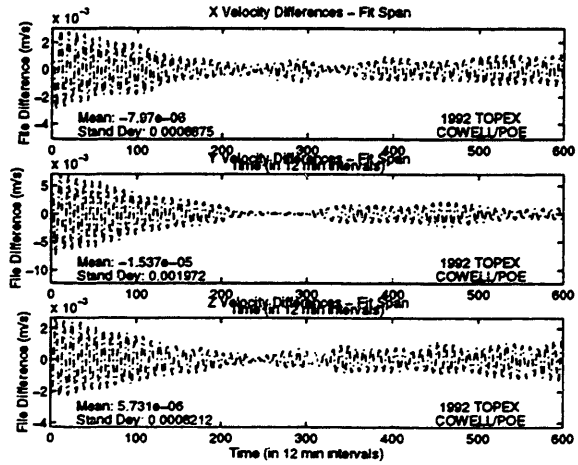

Figure G.92 Cowell 50x50/No SET Velocity Differences

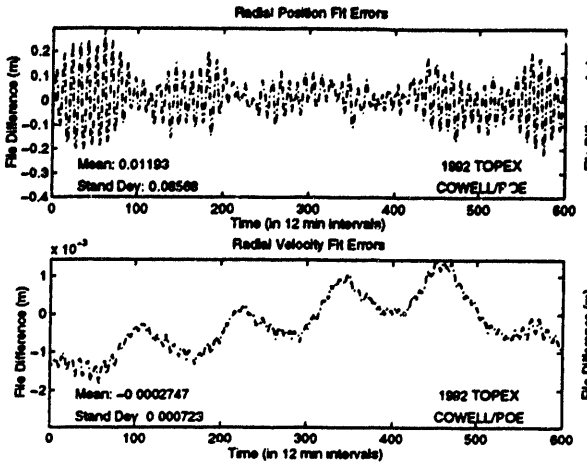

Figure G.93 Cowell 50x50/No SET Radial Differences

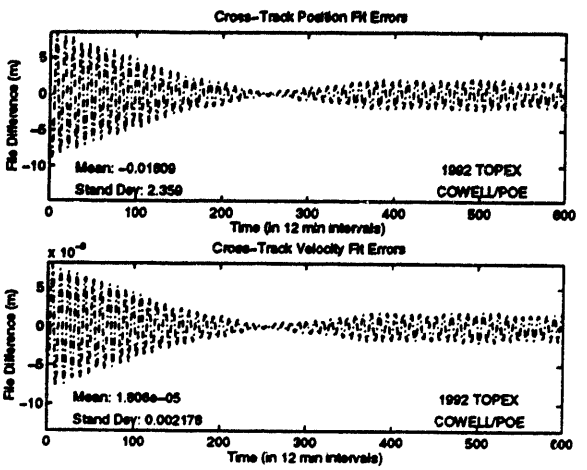

Figure G.94 Cowell 50x50/No SET Cross-Track Differences

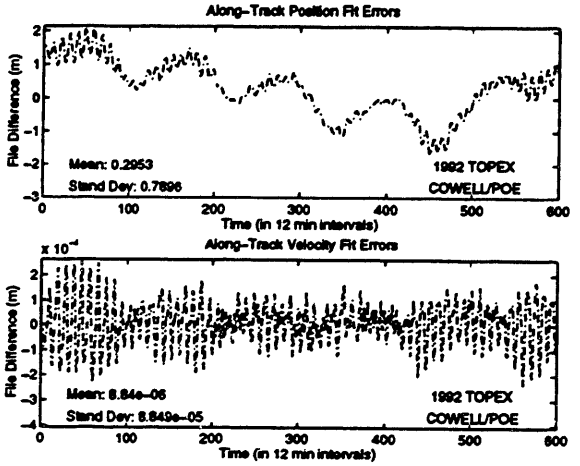

Figure G.95 Cowell 50x50/No SET Along-Track Differences

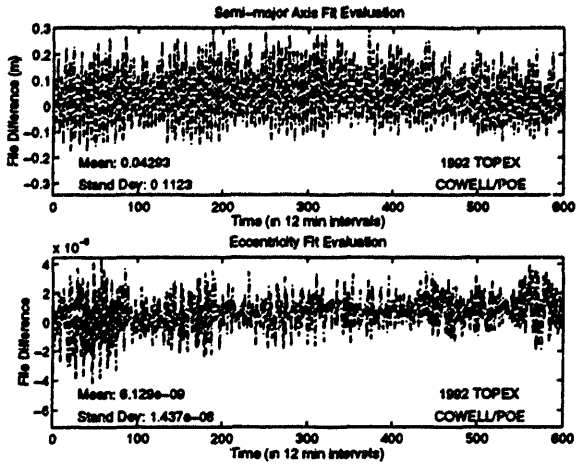

Figure G.96 Cowell 50x50/No SET *a/e* Differences

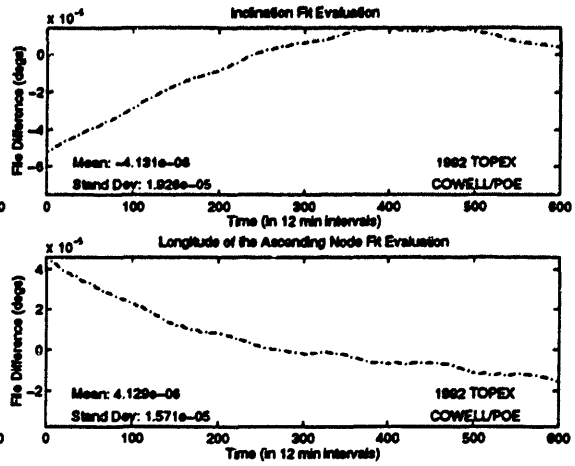

Figure G.97 Cowell 50x50/No SET *i/Ω* Differences

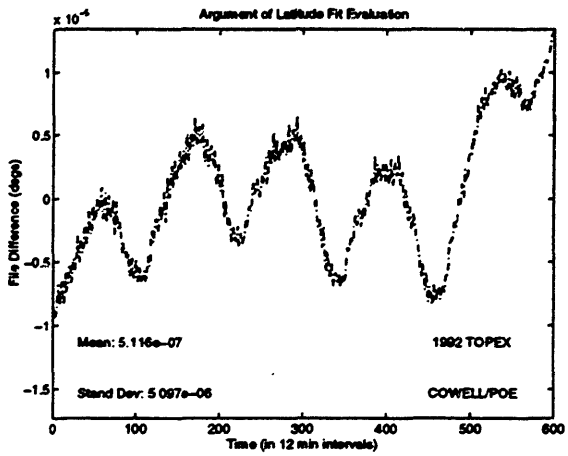

Figure G.98 Cowell 50x50/No SET Argument of Latitude Differences

TOPEX POE Test Case 3: Cowell Fit of POEs with 21x21 JGM-2, Solid Earth Tides

(TOPEX_POE_ITOD_DC_4)

```
CONTROL  DC                                                    TOPEXXX  XXXXXX
EPOCH                    921225.0              000000.000000
ELEMENT1  12    1    1   6107.1205886653D0     -4337.568205682626D0   -1858.020114962 1D0
ELEMENT2                 3.0224258514177D0     1.5404220636548D0      6.2370566618274D0
OBSINPUT  29             921225 000000         921230 000100
ORBTYPE   2     1    11  10.0
DMOPT
OBSDEV    21             5.
OBSDEV    22             5.
OBSDEV    23             5.
OBSDEV    24             .5
OBSDEV    25             .5
OBSDEV    26             .5
END
DCOPT
PRINTOUT  1     4
CONVERG   20             1.D-4                                 1.0
END
OGOPT
DRAG      1              1.
ATMOSDEN                 1
DRAGPAR   2     1        0.15D0
SCPARAM                  2.8D-5                2400.0D0
MAXDEGEQ  1              21.
MAXORDEQ  1              21.
MAXDEGVE  1              4.
MAXORDVE  1              4.
POTFIELD  1     19
SETIDE    1              0.29D0
SOLRAD    1              1
SOLRDPAR  1
STATEPAR  1
STATETAB  1     2    3   4                     5                     6
END
FIN
CONTROL  EPHEM                 OUTPUT                                TOPEXXX  XXXXXX
OUTPUT    19    2    1   921230.D0             000000.D0             43200.D0
ORBTYPE   2     1    11  10.0
OGOPT
DRAG      1              1
ATMOSDEN                 1
DRAGPAR   0
SCPARAM                  2.8D-5                2400.0D0
MAXDEGEQ  1              21.
MAXORDEQ  1              21.
MAXDEGVE  1              4.
MAXORDVE  1              4.
POTFIELD  1     19
SETIDE    1              0.29D0
SOLRAD    1              1
SOLRDPAR  0
OUTOPT    1              921225000000.0        921230000000.0        120.0
END
FIN
```

Figure G.99 Cowell 21x21, SET Fit to POEs Input Card Data File

```
$!-----------------------------------------------------------------
$! TOPEX_POE_ITOD_DC_4.COM
$!
$!
$!-----------------------------------------------------------------
$!
$! Set default for batch run from CSDL0:[GTDS.GTDS_TEST]
$!
$  set default fds$diska:[ssc2414.work.new_gtds.test]
$!
$! Assign debug overrides
$!
$  assign/table=lnm$job  [ssc2414.work.new_gtds.test]topex_poe_itod_dc_4.overrides          dbg$init
$!
$! Assign the body potential files
$!
$  assign/table=lnm$job fds$diska:[djf1230.bianca]dan_potential.dat gtds$047
$  assign/table=lnm$job fds$diska:[djf1230.bianca]moon.dat      gtds$048
$!
$! Assign the density file
$!
$  assign/table=lnm$job fds_dbf:jacchia_roberts.dat   gtds$075
$!
$! Assign the SLP and timing files
$!
$  assign/table=lnm$job elrond$dka0:[ssc2414]june95_msgen_slp_mn2000.dat gtds$014
$  assign/table=lnm$job elrond$dka0:[ssc2414]june95_msgen_slp_timecoef.dat gtds$038
$  assign/table=lnm$job elrond$dka0:[ssc2414]june95_msgen_slp_tod2000.dat gtds$078
$!
$! Assign the observation card and ORB1 files
$!
$  assign/table=lnm$job fds$diska:[ssc2414.topex.obscard]topex_poe_itod_2.poscard gtds$015
$  assign/table=lnm$job fds$diska:[ssc2414.work.new_gtds.test]topex_poe_itod_dc_4.orb1 gtds$024
$!
$! Assign the fundamental constants file
$!
$  assign/table=lnm$job fds$diska:[ssc2414.work.new_gtds.mods]j2000_csconst.dat gtds$099
$!
$! Execute the local version of debug executable
$!
$  @[ssc2414.work.new_gtds.test]j2000_SWAT_GTDS [ssc2414.work.new_gtds.test]topex_poe_itod_dc_4
$!
$  EXIT
```

Figure G.100 Cowell 21x21, SET Fit to POEs Command Procedure

```
SET OUTPUT LOG
SET LOG
SET BREAK/return ESTSET DO -
      (DEPOSIT  IDIFF      = 3; -
       DEPOSIT  IDRVAR     = 1; -
       DEPOSIT  ISRVAR     = 1; -
       DEPOSIT  KPAR       = 0; -
       DEPOSIT  KATMOS     = 1; -
       EXAMINE  KATMOS     ; -
       EXAMINE  IDIFF      ; -
       EXAMINE  IDRVAR     ; -
       EXAMINE  ISRVAR     ; -
       EXAMINE  KPAR       ; -
       GO -
    ); -
GO
```

Figure G.101 Cowell 21x21, SET Fit to POEs Overrides File

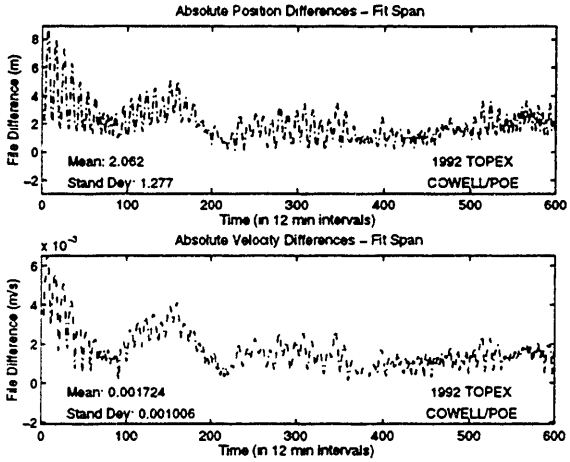

Figure G.102 Cowell 21x21/SET Absolute Differences

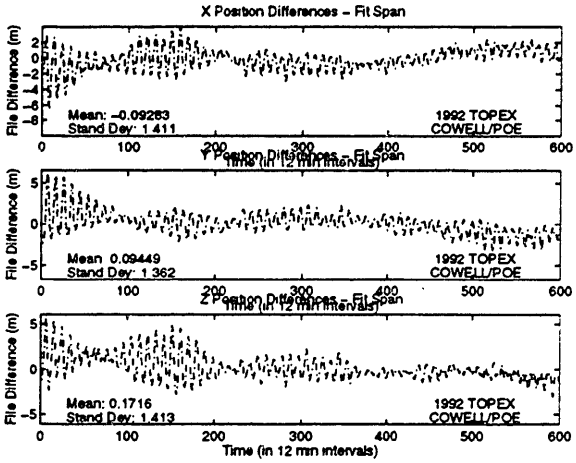

Figure G.103 Cowell 21x21/SET Position Differences

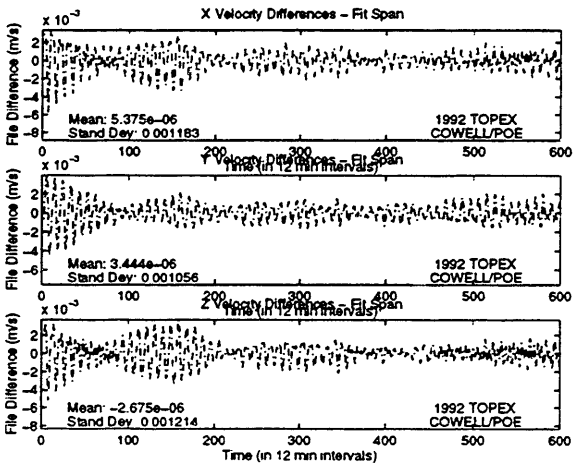

Figure G.104 Cowell 21x21/SET Velocity Differences

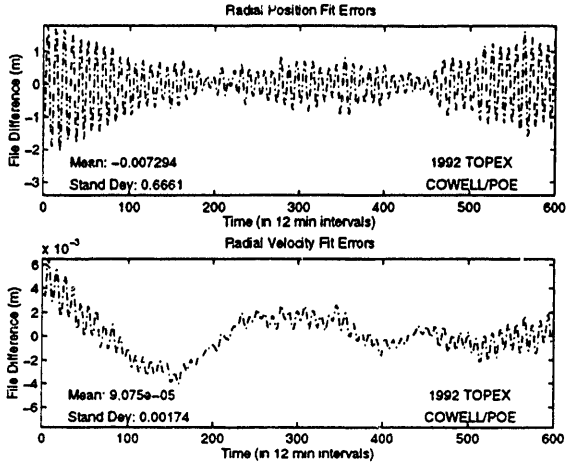

Figure G.105 Cowell 21x21/SET Radial Differences

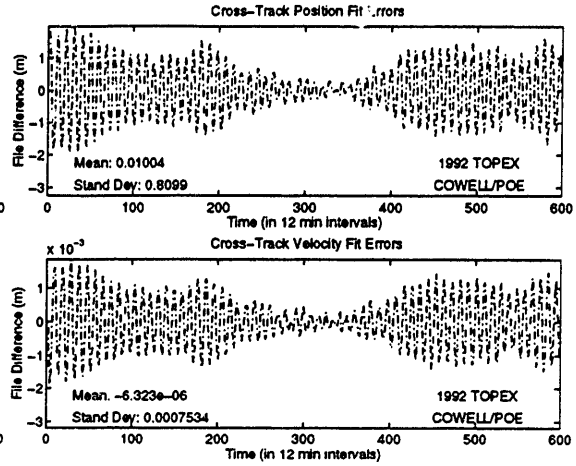

Figure G.106 Cowell 21x21/SET Cross-Track Differences

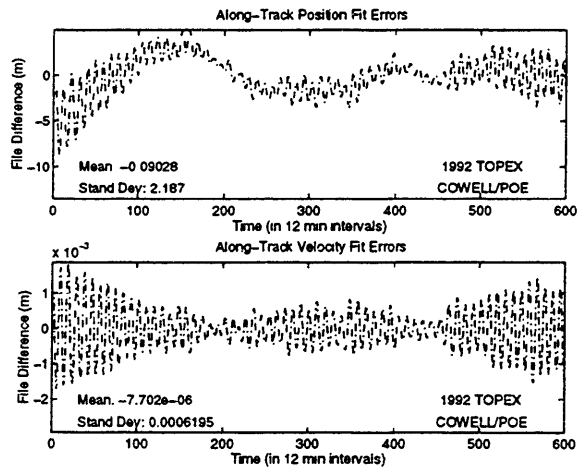

Figure G.107 Cowell 21x21/SET Along-Track Differences

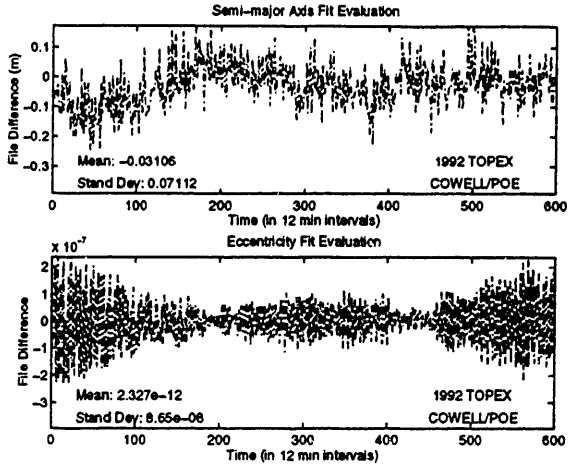

Figure G.108 Cowell 21x21/SET *a/e* Differences

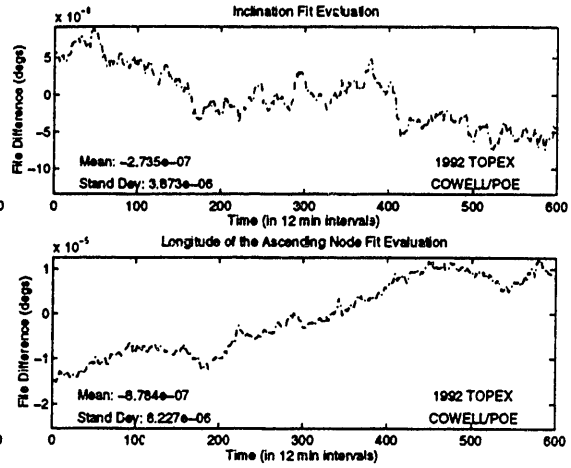

Figure G.109 Cowell 21x21/SET *i/Ω* Differences

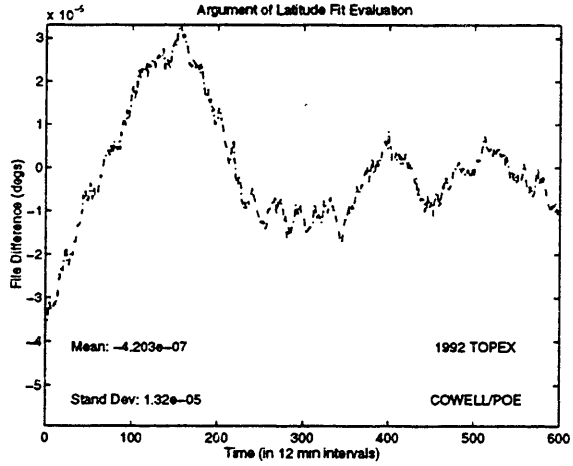

Figure G.110 Cowell 21x21/SET Argument of Latitude Differences

TOPEX POE Test Case 4: Cowell Fit of POEs with 50x50 JGM-2, Solid Earth Tides

(TOPEX_POE_ITOD_DC_5)

```
CONTROL  DC                                                    TOPEXXX  XXXXXX
EPOCH                    921225.0          000000.000000
ELEMENT1 12    1    1    6107.1205886653D0 -4337.5682058825D0 -1858.0201149621D0
ELEMENT2                 3.0224258514177D0 1.5404220636548D0  6.3370559518274D0
OBSINPUT 29              921225 000000     921230 000100
ORBTYPE  2     1    11   10.0
DMOPT
OBSDEV   21              5.
OBSDEV   22              5.
OBSDEV    23             5.
OBSDEV   24              .5
OBSDEV   25              .5
OBSDEV   26              .5
END
DCOPT
PRINTOUT 1     4
CONVERG  20              1.D-4                                 1.0
END
OGOPT
DRAG     1               1.
ATMOSDEN          1
DRAGPAR  2     1         0.15D0
SCPARAM                  2.8D-5            2400.0D0
MAXDEGEQ1                50.
MAXORDEQ1                50.
MAXDEGVE 1               4.
MAXORDVE 1               4.
POTFIELD 1     19
SETIDE   1               0.29D0
SOLRAD   1               1
SOLRDPAR 1
STATEPAR 1
STATETAB 1     2    3    4                 5                 6
END
FIN
CONTROL  EPHEM             OUTPUT                              TOPEXXX  XXXXXX
OUTPUT   19    2    1     921230.D0         000000.D0         43200.D0
ORBTYPE  2     1    11    10.0
OGOPT
DRAG     1               1
ATMOSDEN          1
DRAGPAR  0
SCPARAM                  2.8D-5            2400.0D0
MAXDEGEQ1                50.
MAXORDEQ1                50.
MAXDEGVE 1               4.
MAXORDVE 1               4.
POTFIELD 1     19
SETIDE   1               0.29D0
SOLRAD   1               1
SOLRDPAR 0
OUTOPT   1               921225000000.0    921230000000.0    120.0
END
FIN
```

Figure G.111 Cowell 50x50, SET Fit to POEs Input Card Data File

```
$!-------------------------------------------------------------------
$! TOPEX_POE_ITOD_DC_5.COM
$!
$!
$!-------------------------------------------------------------------
$!
$! Set default for batch run from CSDL0:[GTDS.GTDS_TEST]
$!
$  set default fds$diska:[ssc2414.work.new_gtds.test]
$!
$! Assign debug overrides
$!
$  assign/table=lnm$job  [ssc2414.work.new_gtds.test]topex_poe_itod_dc_5.overrides          dbg$init
$!
$! Assign the body potential files
$!
$  assign/table=lnm$job fds$diska:[djf1230.bianca]dan_potential.dat gtds$047
$  assign/table=lnm$job fds$diska:[djf1230.bianca]moon.dat      gtds$048
$!
$! Assign the density file
$!
$  assign/table=lnm$job fds_dbf:jacchia_roberts.dat   gtds$075
$!
$! Assign the SLP and timing files
$!
$  assign/table=lnm$job elrond$dka0:[ssc2414]june95_msgen_slp_mn2000.dat gtds$014
$  assign/table=lnm$job elrond$dka0:[ssc2414]june95_msgen_slp_timecoef.dat gtds$038
$  assign/table=lnm$job elrond$dka0:[ssc2414]june95_msgen_slp_tod2000.dat gtds$078
$!
$! Assign the observation card and ORB1 files
$!
$  assign/table=lnm$job fds$diska:[ssc2414.topex.obscard]topex_poe_itod_2.poscard gtds$015
$  assign/table=lnm$job fds$diska:[ssc2414.work.new_gtds.test]topex_poe_itod_dc_5.orb1 gtds$024
$!
$! Assign the fundamental constants file
$!
$  assign/table=lnm$job fds$diska:[ssc2414.work.new_gtds.mods]jj2000_csconst.dat gtds$099
$!
$! Execute the local version of debug executable
$!
$  @[ssc2414.work.new_gtds.test]jj2000_SWAT_GTDS [ssc2414.work.new_gtds.test]topex_poe_itod_dc_5
$!
$  EXIT
```

Figure G.112 Cowell 50x50, SET Fit to POEs Command Procedure

```
SET OUTPUT LOG
SET LOG
SET BREAK/return ESTSET DO -
      (DEPOSIT  IDIFF      = 3; -
       DEPOSIT  IDRVAR     = 1; -
       DEPOSIT  ISRVAR     = 1; -
       DEPOSIT  KPAR       = 0; -
       DEPOSIT  KATMOS     = 1; -
       EXAMINE  KATMOS     ; -
       EXAMINE  IDIFF      ; -
       EXAMINE  IDRVAR     ; -
       EXAMINE  ISRVAR     ; -
       EXAMINE  KPAR       ; -
       GO -
    ); -
GO
```

Figure G.113 Cowell 50x50, SET Fit to POEs Overrides File

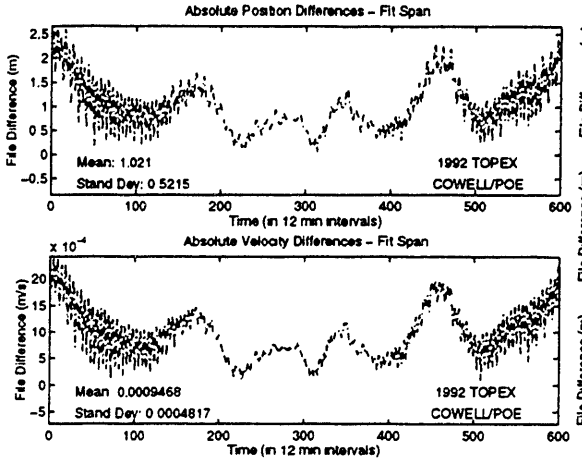

Figure G.114 Cowell 50x50/SET Absolute Differences

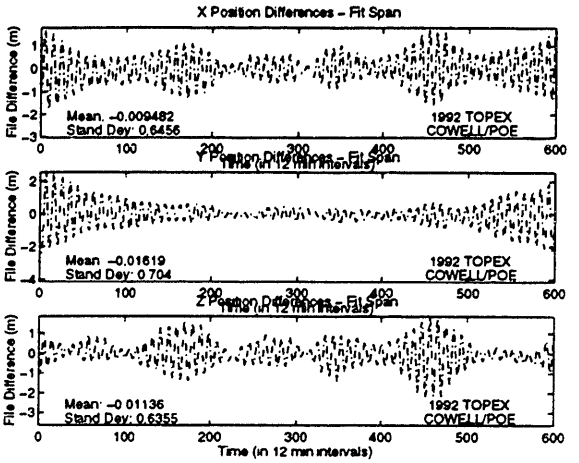

Figure G.115 Cowell 50x50/SET Position Differences

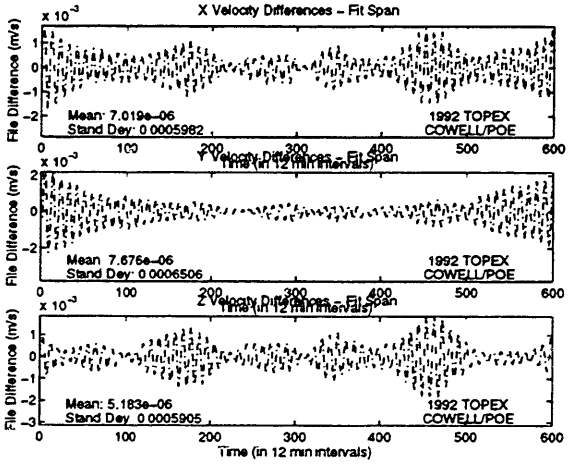

Figure G.116 Cowell 50x50/SET Velocity Differences

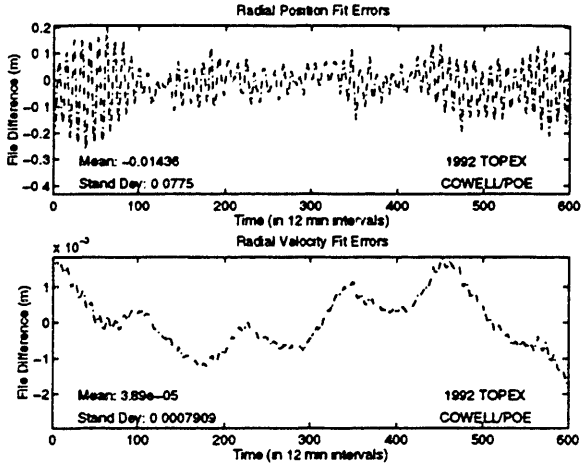

Figure G.117 Cowell 50x50/SET Radial Differences

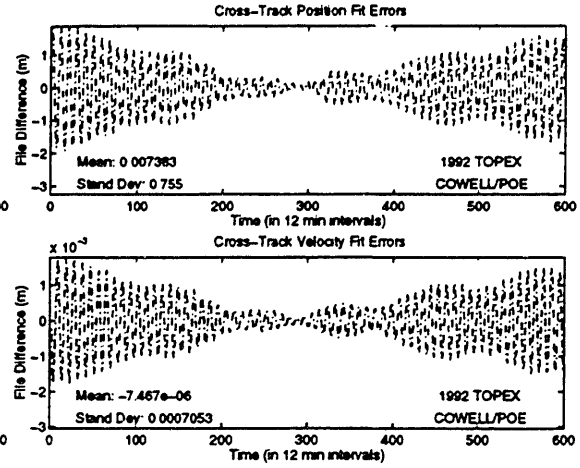

Figure G.118 Cowell 50x50/SET Cross-Track Differences

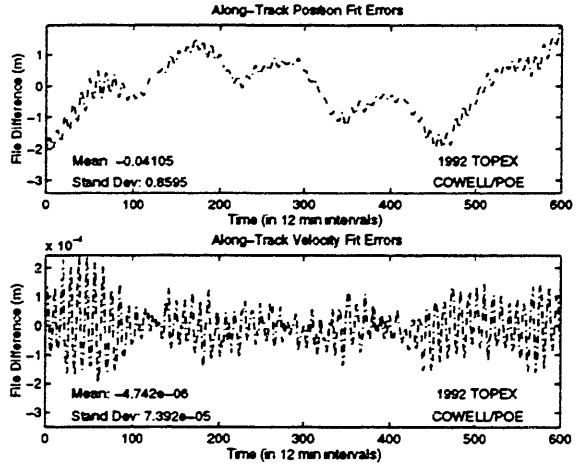

Figure G.119 Cowell 50x50/SET Along-Track Differences

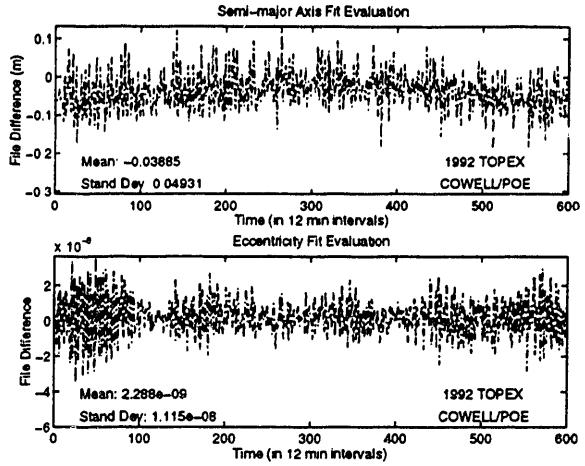

Figure G.120 Cowell 50x50/SET *a/e* Differences

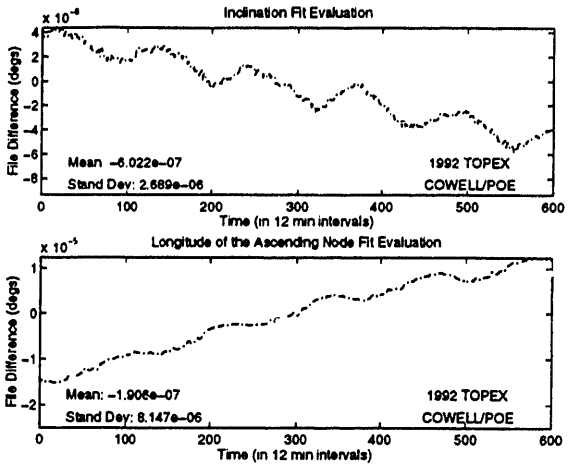

Figure G.121 Cowell 50x50/SET i/Ω Differences

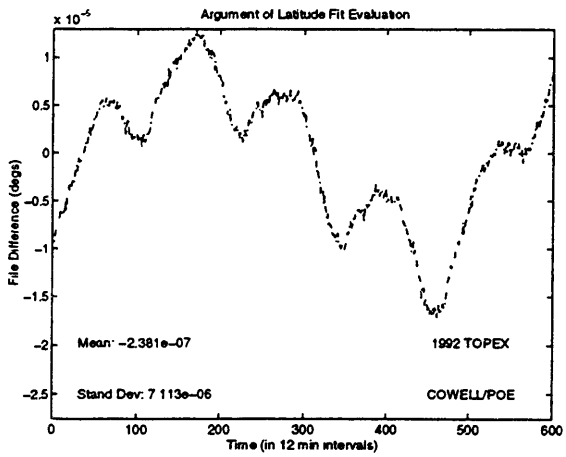

Figure G.122 Cowell 50x50/SET Argument of Latitude Differences

TOPEX POE Test Case 5: SST Fit of POEs with 50x50 JGM-2, Solid Earth Tides

(TOPEX_POE_ITOD_SST_DC_6)

```
CONTROL  DC                                                          TOPEXXX  XXXXXX
EPOCH                      921225.0          000000.000000
ELEMENT1  12    6     1    7714.4D0          1.108D-4          66.D0
ELEMENT2                   330.9D0           73.2D0            271.D0
OBSINPUT  29               921225 000000     921230 000100
ORBTYPE   5     1    11   21600.0           1.0
DMOPT
OBSDEV    21               5.
OBSDEV    22               5.
OBSDEV    23               5.
OBSDEV    24               .5
OBSDEV    25               .5
OBSDEV    26               .5
END
DCOPT
PRINTOUT  1     4
CONVERG   20               1.D-4                                     1.0
END
OGOPT
DRAG      1                1.
ATMOSDEN                   1
DRAGPAR   1
SCPARAM                    2.8D-5            2400.0D0
MAXDEGEQ  1                50.
MAXORDEQ  1                50.
MAXDEGVE  1                4.
MAXORDVE  1                4.
POTFIELD  1     19
RESONPRD                   86400.D0
SETIDE    1                0.29D0
SOLRAD    1                1
SOLRDPAR  1
STATEPAR  3
STATETAB  1     2     3    4                 5                 6
END
FIN
CONTROL  EPHEM                OUTPUT                             TOPEXXX  XXXXXX
OUTPUT    19    2     1      921230.D0         000000.D0         43200.D0
ORBTYPE   5     1    11   21600.0           1.0
OGOPT
DRAG      1                1
ATMOSDEN                   1
DRAGPAR   0
SCPARAM                    2.8D-5            2400.0D0
MAXDEGEQ  1                50.
MAXORDEQ  1                50.
MAXDEGVE  1                4.
MAXORDVE  1                4.
POTFIELD  1     19
RESONPRD                   86400.D0
SETIDE    1                0.29D0
SOLRAD    1                1
SOLRDPAR  0
OUTOPT    1                921225000000.0    921230000000.0    120.0
END
FIN
```

Figure G.123 SST 50x50, SET Fit to POEs Input Card Data File

```
$!----- ------------------------------------------------------------------
$! TOPEX_POE_ITOD_SST_DC_6.COM
$!
$!
$!------------------------------------------------------------------------
$!
$! Set default for batch run from CSDL0:[GTDS.GTDS_TEST]
$!
$  set default fds$diska:[ssc2414.work.new_gtds.test]
$!
$! Assign debug overrides
$!
$  assign/table=lnm$job  [ssc2414.work.new_gtds.test]topex_poe_itod_sst_dc_6.overrides          dbg$init
$!
$! Assign the body potential files
$!
$  assign/table=lnm$job fds$diska:[djf1230.bianca]dan_potential.dat gtds$047
$  assign/table=lnm$job fds$diska:[djf1230.bianca]moon.dat     gtds$048
$!
$! Assign the density file
$!
$  assign/table=lnm$job fds_dbf:jacchia_roberts.dat   gtds$075
$!
$! Assign the SLP and timing files
$!
$  assign/table=lnm$job elrond$dka0:[ssc2414]june95_msgen_slp_mn2000.dat gtds$014
$  assign/table=lnm$job elrond$dka0:[ssc2414]june95_msgen_slp_timecoef.dat gtds$038
$  assign/table=lnm$job elrond$dka0:[ssc2414]june95_msgen_slp_tod2000.dat gtds$078
$!
$! Assign the observation card and ORB1 files
$!
$  assign/table=lnm$job fds$diska:[ssc2414.topex.obscard]topex_poe_itod_2.poscard gtds$015
$  assign/table=lnm$job fds$diska:[ssc2414.work.new_gtds.test]topex_poe_itod_sst_dc_6.orb1 gtds$024
$!
$! Assign the fundamental constants file
$!
$  assign/table=lnm$job fds$diska:[ssc2414.work.new_gtds.mods]j2000_csconst.dat gtds$099
$!
$! Execute the local version of debug executable
$!
$  @[ssc2414.work.new_gtds.test]j2000_swat_gtds[ssc2414.work.new_gtds.test]topex_poe_itod_sst_dc_6
$!
$  EXIT
```

Figure G.124 SST 50x50, SET Fit to POEs Command Procedure

```
SET OUTPUT LOG
SET LOG
SET BREAK/return ESTSET DO -
      (DEPOSIT  IDIFF       = 3; -
       DEPOSIT  IDRVAR      = 1; -
       DEPOSIT  ISRVAR      = 1; -
       DEPOSIT  KPAR        = 1; -
       DEPOSIT  KATMOS      = 1; -
       EXAMINE  KATMOS      ; -
       EXAMINE  IDIFF       ; -
       EXAMINE  IDRVAR      ; -
       EXAMINE  ISRVAR      ; -
       EXAMINE  KPAR        ; -
       GO -
   ); -
GO
SET BREAK/return HWIRE  DO -
      (DEPOSIT  LZN         = 4; -
       DEPOSIT  JZN         = 25; -
       DEPOSIT  LMD         = 4; -
       DEPOSIT  MMD         = 28;-
       DEPOSIT  MTS         = 41;-
       DEPOSIT  NJ2MD       = 12; -
       DEPOSIT  MJ2MD       = 12; -
       DEPOSIT  LJ2MD       = 4; -
       DEPOSIT  IDRMD       = 2; -
       DEPOSIT  NTH(1)      = 4; -
       DEPOSIT  NTH(2)      = 4; -
       DEPOSIT  JMAXTH(1)   = 5; -
       DEPOSIT  LTH(1)      = 4; -
       DEPOSIT  LTH(2)      = 4; -
       DEPOSIT  JMAXTS      = 25;-
       DEPOSIT  JMINTS      =-25;-
       EXAMINE  LZN         ; -
       EXAMINE  JZN         ; -
       EXAMINE  LMD         ; -
       EXAMINE  NJ2MD       ; -
       EXAMINE  MJ2MD       ; -
       EXAMINE  LJ2MD       ; -
       EXAMINE  IDRMD       ; -
       EXAMINE  NTH(1)      ; -
       EXAMINE  NTH(2)      ; -
       EXAMINE  JMAXTH(1)   ; -
       EXAMINE  LTH(1)      ; -
       EXAMINE  LTH(2)      ; -
       GO -
   ); -
GO
```

Figure G.125 SST 50x50, SET Fit to POEs Overrides File

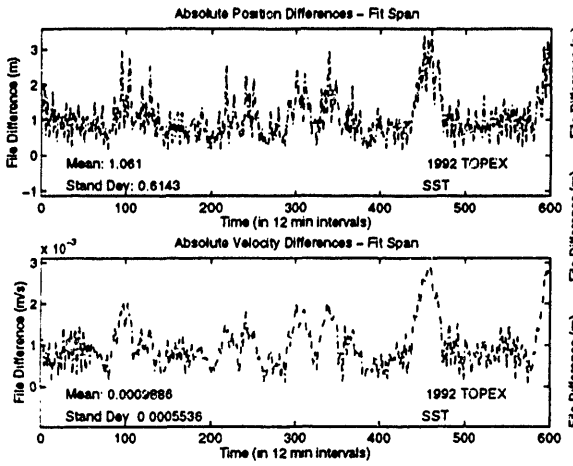

Figure G.126 SST 50x50/SET Absolute Differences

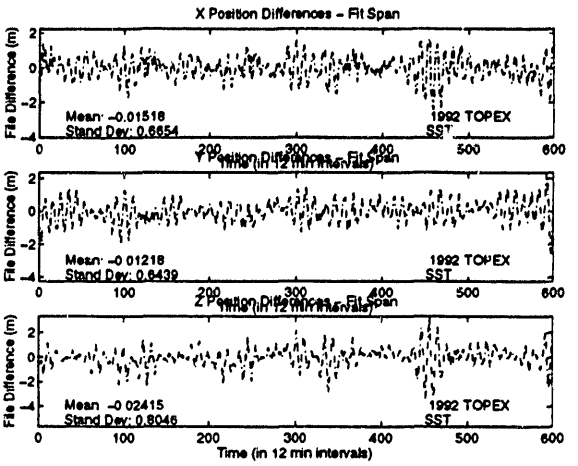

Figure G.127 SST 50x50/SET Position Differences

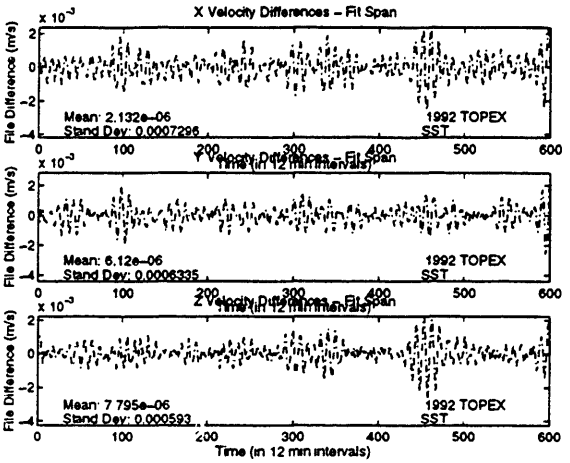

Figure G.128 SST 50x50/SET Velocity Differences

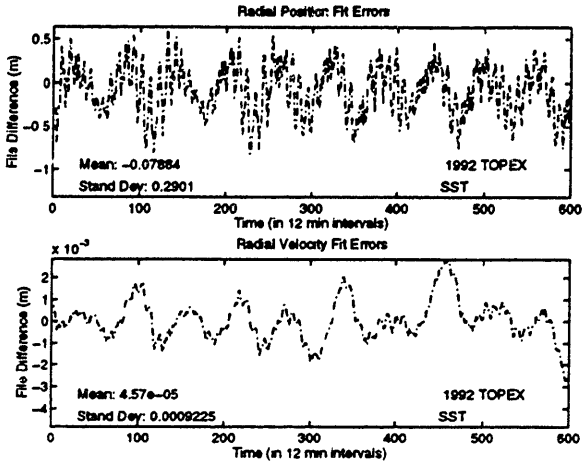

Figure G.129 SST 50x50/SET Radial Differences

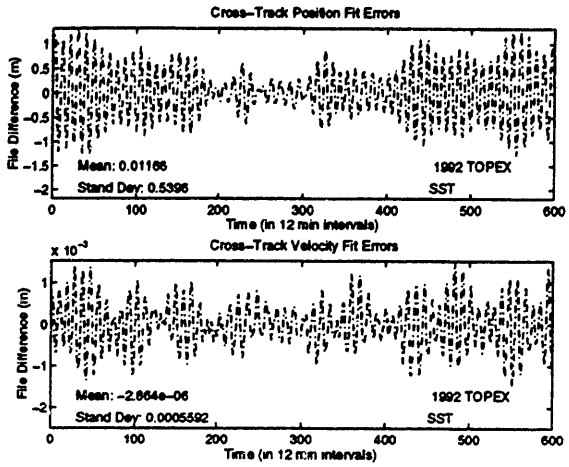

Figure G.130 SST 50x50/SET Cross-Track Differences

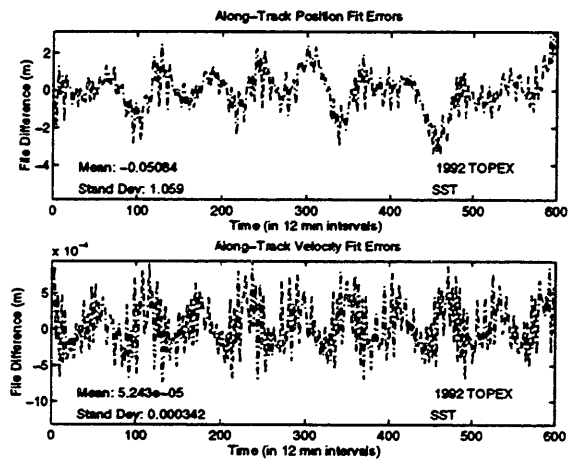

Figure G.131 SST 50x50/SET Along-Track Differences

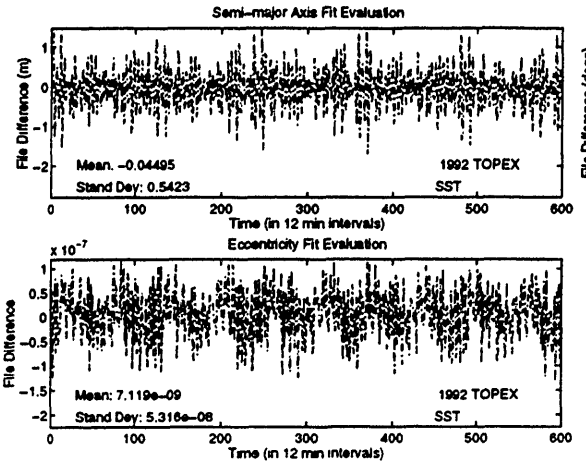

Figure G.132 SST 50x50/SET *a/e* Differences

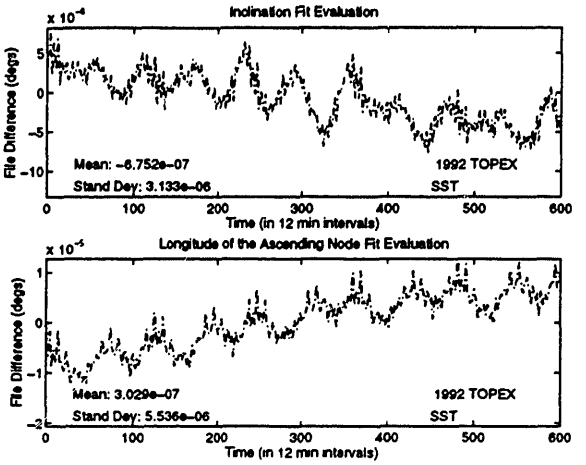

Figure G.133 SST 50x50/SET *i/Ω* Differences

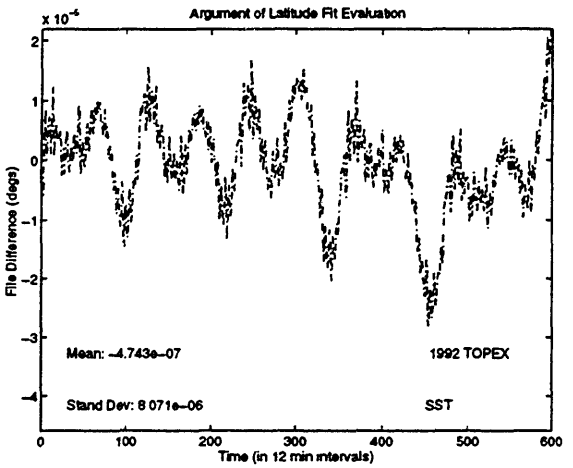

Figure G.134 SST 50x50/SET Argument of Latitude Differences

The second category of testing involving the POEs dealt with validation of the implementation of the solid earth tide models for both the Cowell and SST perturbation methods. One orbit was generated using TOPEX orbital characteristics representative of the period involved in the above set of figures, including only third-body effects in the force model. A second orbit with solid earth tides added to the force modeling was generated and compared to the first to show the expected tidal effects. The impact was then related to the cross-track errors actually observed in Figure G.94. The file

setups and plots for both Cowell and SST perturbation techniques are given here.

TOPEX POE Test Case 6: Anticipated Effects of Solid Earth Tides (SHOW_SET_EFFECTS)

```
CONTROL  EPHEM                                                    TOPEXXX  XXXXXX
EPOCH                      921225.0              000000.000000
ELEMENT1 12    1    1      6107.12233649834D0    -4337.56657094521D0   -1858.01894920629D0
ELEMENT2                   3.02242463499831D0    1.5404238300434 5D0   6.337055931831127D0
OUTPUT   11    2    1      921226.D0             000000.D0             43200.D0
ORBTYPE  2     1    11     10.0
OGOPT
POTFIELD 1     19
SETIDE   1                 0.29D0
OUTOPT   1                 921225000000.0        921230000000.0        450.0
END
FIN
CONTROL  DC                                                       TOPEXXX  XXXXXX
EPOCH                      921225.0              000000.000000
ELEMENT1 12    1    1      6107.12233649834D0    -4337.56657094521D0   -1858.01894920629D0
ELEMENT2                   3.02242463499831D0    1.5404238300434 5D0   6.337055931831127D0
ORBTYPE  2     1    11     10.0
OBSINPUT 23                921225000000.0        921230000000.0
DMOPT
OBSDEV   21    22   23     100.                  100.                  100.
OBSDEV   24    25   26     10.                   10.                   10.
END
OGOPT
POTFIELD 1     19
END
DCOPT
PRINTOUT 1     4
CONVERG  25    6           1.D-4
END
FIN
CONTROL  EPHEM                 OUTPUT                                 TOPEXXX  XXXXXX
OUTPUT   11    2    1      921226.D0             000000.D0             43200.D0
ORBTYPE  2     1    11     10.0
OGOPT
POTFIELD 1     19
OUTOPT   21                921225000000.0        921230000000.0        450.0
END
FIN
CONTROL  COMPARE                                                  TOPEXXX  XXXXXX
COMPOPT
CMPEPHEM 1     102  102    921225000000.0        921230000000.0        30.
CMPPLOT  3                                                        2.
HISTPLOT 1     102  102    921225000000.0        921230000000.0        1800.
END
FIN
```

Figure G.135 Cowell Solid Earth Tide Test Input Data Card File

```
$!-------------------------------------------------------------------
$! SHOW_SET_EFFECTS.COM
$!
$!
$!-------------------------------------------------------------------
$!
$! Set default for batch run from CSDL0:[GTDS.GTDS_TEST]
$!
$  set default fds$diska:[ssc2414.work.new_gtds.test]
$!
$! Assign debug overrides
$!
$  assign/table=lnm$job    [ssc2414.work.new_gtds.test]show_set_effects.overrides          dbg$init
$!
$! Assign the body potential files
$!
$  assign/table=lnm$job fds$diska:[rjp9045.bianca.fonte]newcomb.dat gtds$023
$  assign/table=lnm$job fds$diska:[djf1230.bianca]dan_potential.dat gtds$047
$  assign/table=lnm$job fds$diska:[djf1230.bianca]moon.dat      gtds$048
$!
$! Assign the density file
$!
$  assign/table=lnm$job fds_db1:jacchia_roberts.dat   gtds$075
$!
$! Assign the SLP and timing files
$!
$  assign/table=lnm$job elrond$dka0:[ssc2414]june95_msgen_slp_mn2000.dat gtds$014
$  assign/table=lnm$job elrond$dka0:[ssc2414]june95_msgen_slp_timecoef.dat gtds$038
$  assign/table=lnm$job elrond$dka0:[ssc2414]june95_msgen_slp_tod2000.dat gtds$078
$!
$! Assign ORB1 files
$!
$  assign/table=lnm$job fds$diska:[ssc2414.work.new_gtds.test]show_set_effects_set.orb1 gtds$024
$  assign/table=lnm$job fds$diska:[ssc2414.work.new_gtds.test]show_set_effects_noset.orb1 gtds$081
$!
$! Assign ORB1 files
$!
$  assign/table=lnm$job fds$diska:[ssc2414.work.new_gtds.mods]j2000_csconst.dat gtds$099
$!
$! Execute the local version of debug executable
$!
$  @[ssc2414.work.new_gtds.test]j2000_SWAT_GTDS [ssc2414.work.new_gtds.test]show_set_effects
$!
$  EXIT
```

Figure G.136 Cowell Solid Earth Tide Test Command Procedure

```
SET OUTPUT LOG
SET LOG
SET BREAK/return ESTSET DO -
                    (DEPOSIT   IDIFF      = 0; -
                    DEPOSIT    IDRVAR     = 0; -
                    DEPOSIT    ISRVAR     = 0; -
                    DEPOSIT    KPAR       = 0; -
                    DEPOSIT    KATMOS     = 1; -
                    EXAMINE    KATMOS     ; -
                    EXAMINE    IDIFF      ; -
                    EXAMINE    IDRVAR     ; -
                    EXAMINE    ISRVAR     ; -
                    EXAMINE    KPAR       ; -
                    GO -
            ); -
GO
```

Figure G.137 Cowell Solid Earth Tide Test Overrides File

```
CONTROL  EPHEM                                                    TOPEXXX  XXXXXX
EPOCH                    921225.0              000000.000000
ELEMENT1 12  1       1   6107.12233649834D0    -4337.56657094521D0   -1858.01894920629D0
ELEMENT2                 3.02242463499831D0    1.54042383004345D0    6.337055931831127D0
OUTPUT   11  2       1   921226.D0             000000.D0             43200.D0
ORBTYPE  5     1     11  43200.0               1.0
OGOPT
POTFIELD 1     19
SETIDE   1               0.29D0
OUTOPT   1               921225000000.0        921230000000.0        450.0
END
FIN
CONTROL  DC                                                       TOPEXXX  XXXXXX
EPOCH                    921225.0              000000.000000
ELEMENT1 12  1       1   6107.12233649834D0    -4337.56657094521D0   -1858.01894920629D0
ELEMENT2                 3.02242463499831D0    1.54042383004345D0    6.337055931831127D0
ORBTYPE  5     1     11  43200.0                                     1.0
OBSINPUT 23              921225000000.0        921230000000.0
DMOPT
OBSDEV   21    22    23  100.                  100.                  100.
OBSDEV   24    25    26  10.                   10.                   10.
END
OGOPT
POTFIELD 1     19
END
DCOPT
PRINTOUT 1     4
CONVERG  25  6           1.D-4
STATEPAR 3
STATETAV 1     2     3   4                     5                     6
END
FIN
CONTROL  EPHEM             OUTPUT                                   TOPEXXX  XXXXXX
OUTPUT   11  2       1   921226.D0             000000.D0             43200.D0
ORBTYPE  5     1     11  43200.0               1.0
OGOPT
POTFIELD 1     19
OUTOPT   21              921225000000.0        921230000000.0        450.0
END
FIN
CONTROL  COMPARE                                                  TOPEXXX  XXXXXX
COMPOPT
CMPEPHEM 1     102 102   921225000000.0        921230000000.0        30.
CMPPLOT  3                                                        2.
HISTPLOT 1     102 102   921225000000.0        921230000000.0        1800.
END
FIN
```

Figure G.138 SST Solid Earth Tide Test Input Data Card File

```
$!-------------------------------------------------------------------
$! SHOW_SET_EFFECTS_SST.COM
$!
$!
$!-------------------------------------------------------------------
$!
$! Set default for batch run from CSDL0:[GTDS.GTDS_TEST]
$!
$  set default fds$diska:[ssc2414.work.new_gtds.test]
$!
$! Assign debug overrides
$!
$  assign/table=lnm$job   [ssc2414.work.new_gtds.test]show_set_effects_sst.overrides          dbg$init
$!
$! Assign the body potential files
$!
$  assign/table=lnm$job fds$diska:[rjp9045.bianca.fonte]newcomb.dat gtds$023
$  assign/table=lnm$job fds$diska:[djf1230.bianca]dan_potential.dat gtds$047
$  assign/table=lnm$job fds$diska:[djf1230.bianca]moon.dat     gtds$048
$!
$! Assign the density file
$!
$  assign/table=lnm$job fds_dbf:jacchia_roberts.dat   gtds$075
$!
$! Assign the SLP and timing files
$!
$  assign/table=lnm$job elrond$dka0:[ssc2414]june95_msgen_slp_mn2000.dat gtds$014
$  assign/table=lnm$job elrond$dka0:[ssc2414]june95_msgen_slp_timecoef.dat gtds$038
$  assign/table=lnm$job elrond$dka0:[ssc2414]june95_msgen_slp_tod2000.dat gtds$078
$!
$! Assign ORB1 files
$!
$  assign/table=lnm$job fds$diska:[ssc2414.work.new_gtds.test]show_set_effects_sst_set.orb1 gtds$024
$  assign/table=lnm$job fds$diska:[ssc2414.work.new_gtds.test]show_set_effects_sst_noset.orb1 gtds$081
$!
$! Assign ORB1 files
$!
$  assign/table=lnm$job fds$diska:[ssc2414.work.new_gtds.mods]j2000_csconst.dat gtds$099
$!
$! Execute the local version of debug executable
$!
$  @[ssc2414.work.new_gtds.test]j2000_SWAT_GTDS [ssc2414.work.new_gtds.test]show_set_effects_sst
$!
$  EXIT
```

Figure G.139 SST Solid Earth Tide Test Command Procedure

```
SET OUTPUT LOG
SET BREAK/return HWIRE DO -
      (DEPOSIT IZONAL      = 3; -
       DEPOSIT IMDALY      = 3; -
       DEPOSIT ITHIRD      = 3; -
       DEPOSIT ITESS       = 3; -
       DEPOSIT IJ2MD       = 3; -
       DEPOSIT IJ2J2       = 3; -
       GO -
   ); -
GO
```

Figure G.140 SST Solid Earth Tide Test Overrides File

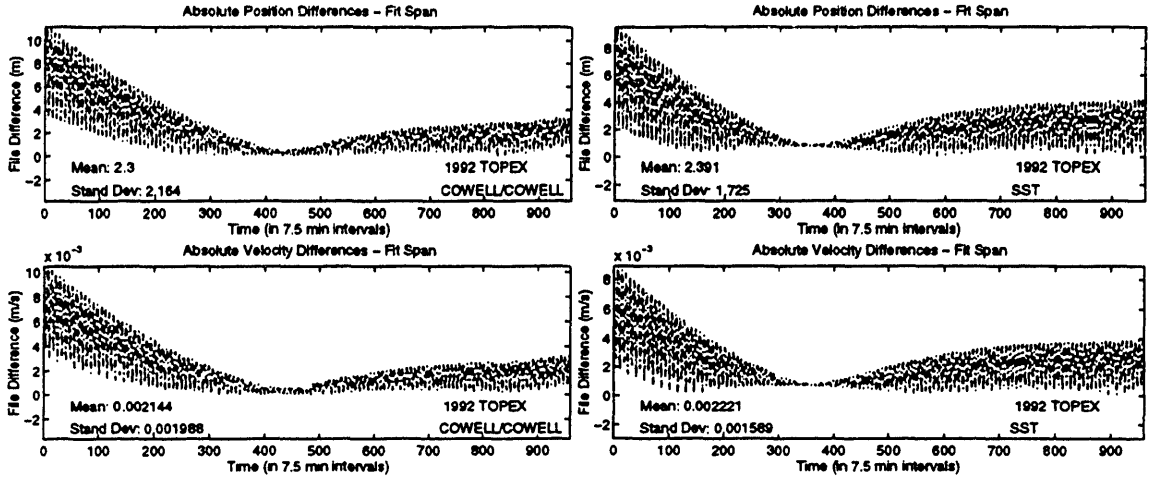

Figure G.141 Cowell and SST SET Test Absolute Differences

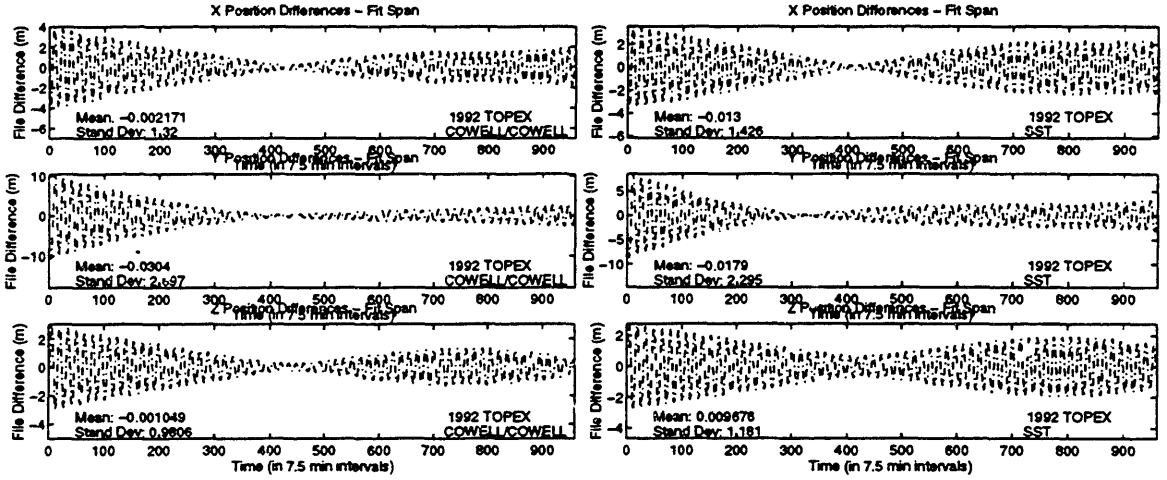

Figure G.142 Cowell and SST SET Test Position Differences

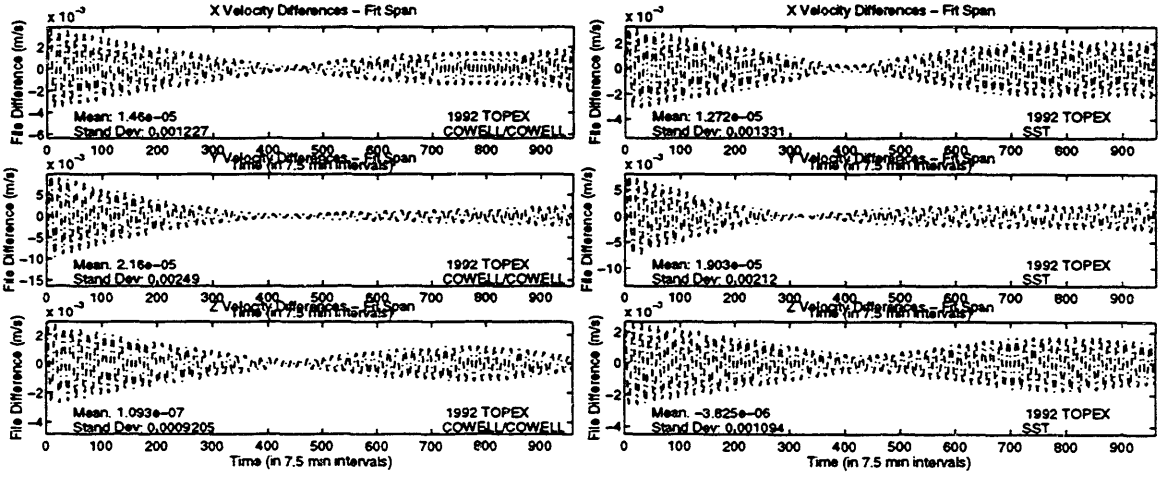

Figure G.143 Cowell and SST SET Test Velocity Differences

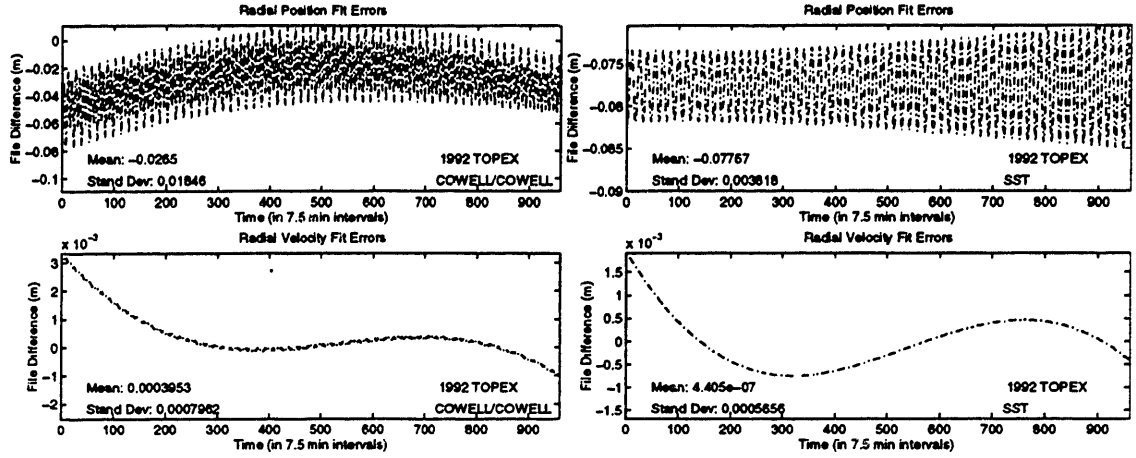

Figure G.144 Cowell and SST SET Test Radial Differences

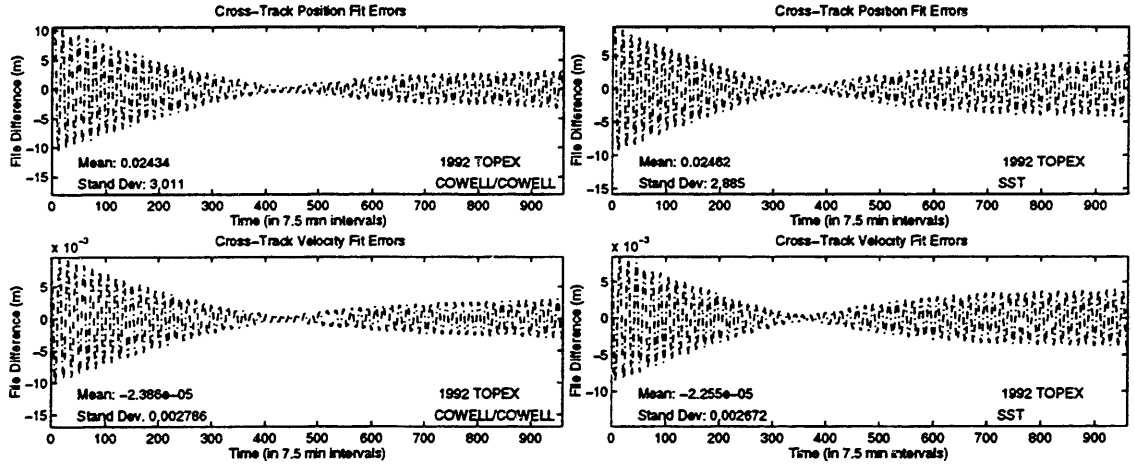

Figure G.145 Cowell and SST SET Test Cross-Track Differences

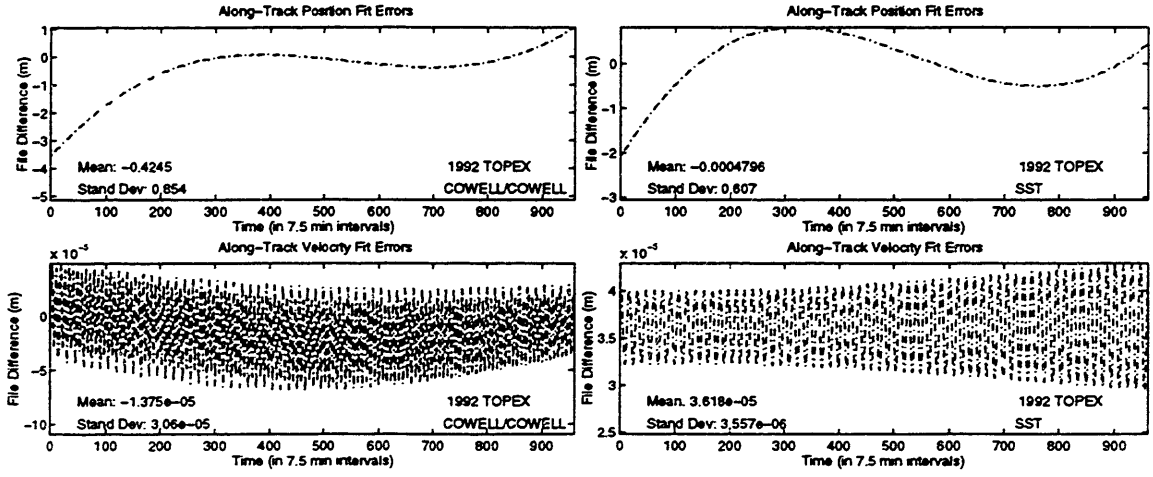

Figure G.146 Cowell and SST SET Test Along-Track Differences

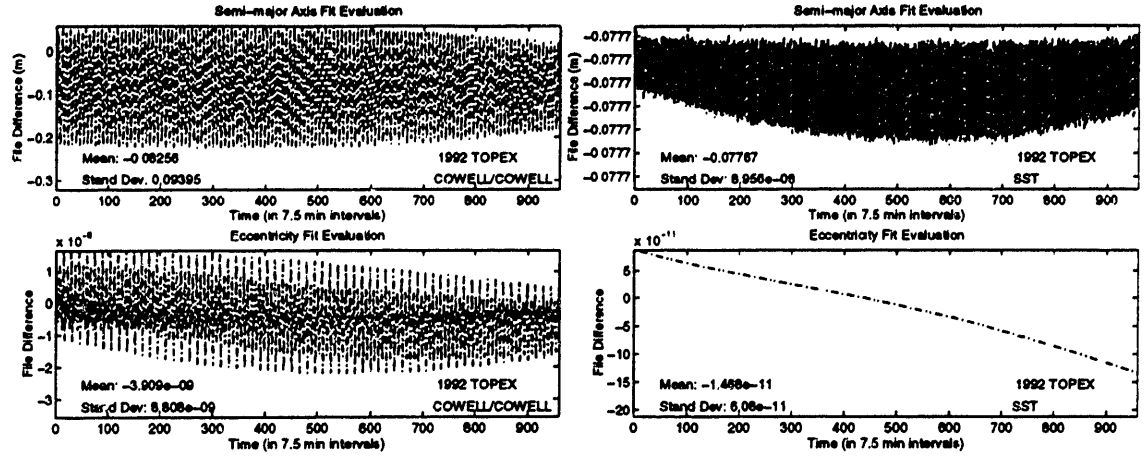

Figure G.147 Cowell and SST SET Test *a/e* Differences

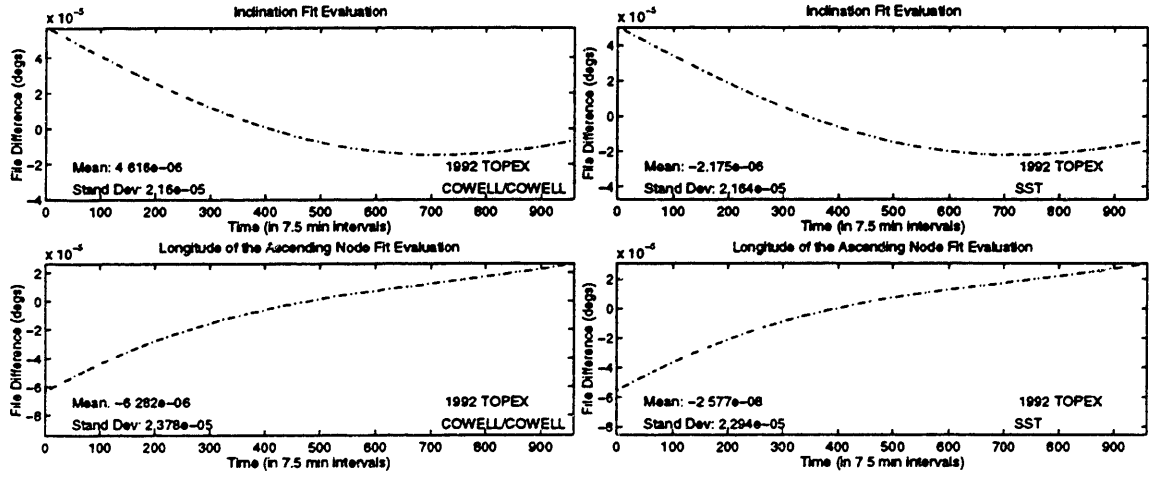

Figure G.148 Cowell and SST SET Test i/Ω Differences

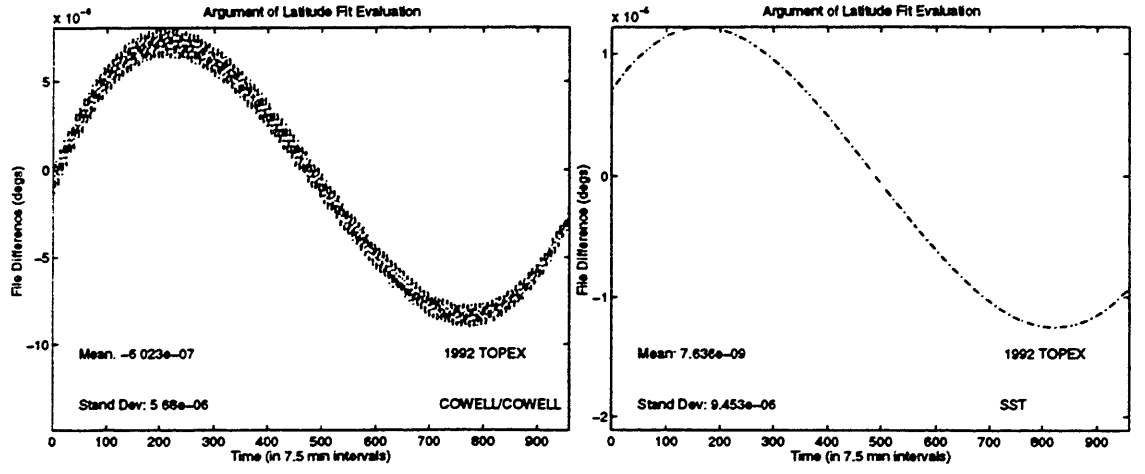

Figure G.149 Cowell and SST SET Test Argument of Latitude Differences

The final category of testing associated with the TOPEX POEs involved verification of the ITOD coordinate system as a modeling and output option. Because the POE vectors were provided in both ITOD and ECEF frames, and the ECEF options were accepted as viable options within Draper R&D GTDS, the ECEF POEs could be used to validate the incorporation of the ITOD capabilities. The similarity of the ITOD and ECEF fit errors indicated that the ITOD coordinate system was implemented properly.

ITOD **ECEF**

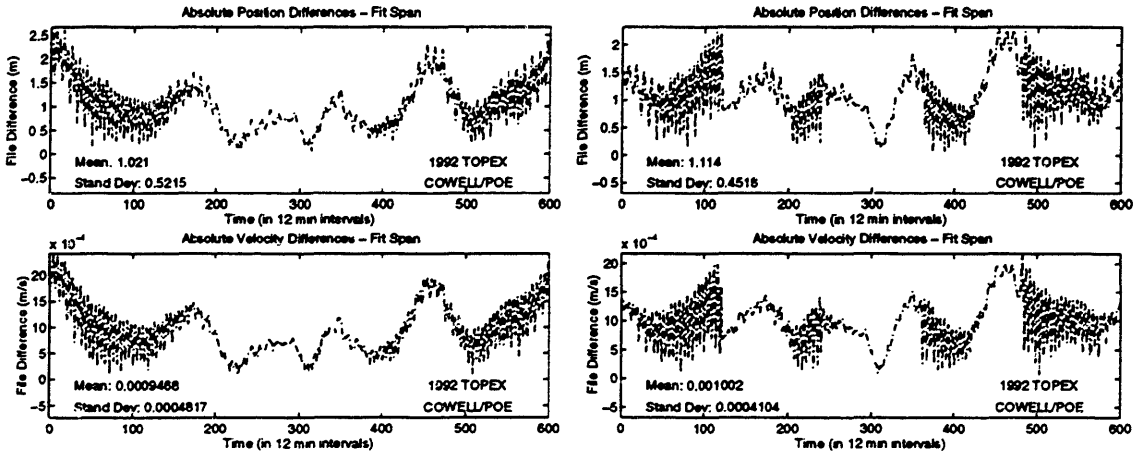

Figure G.150 Magnitude of Fit Error Using ITOD and ECEF POEs

[This page intentionally left blank.]

Appendix H

Summary of GPSR Navigation Solution Results

This appendix is designed as a reference to the experiments performed in the evaluation of navigation solutions as an observation source in an orbit determination process. It contains the input card data files, command procedures, and overrides files used to generate the results, as well as a summary of the key findings, and is organized according to satellite:

- TOPEX Results
- TAOS Results
- EUVE Results

The files presented here are stored on the VAX node ELROND under the author's home directory. They are separated according to function.

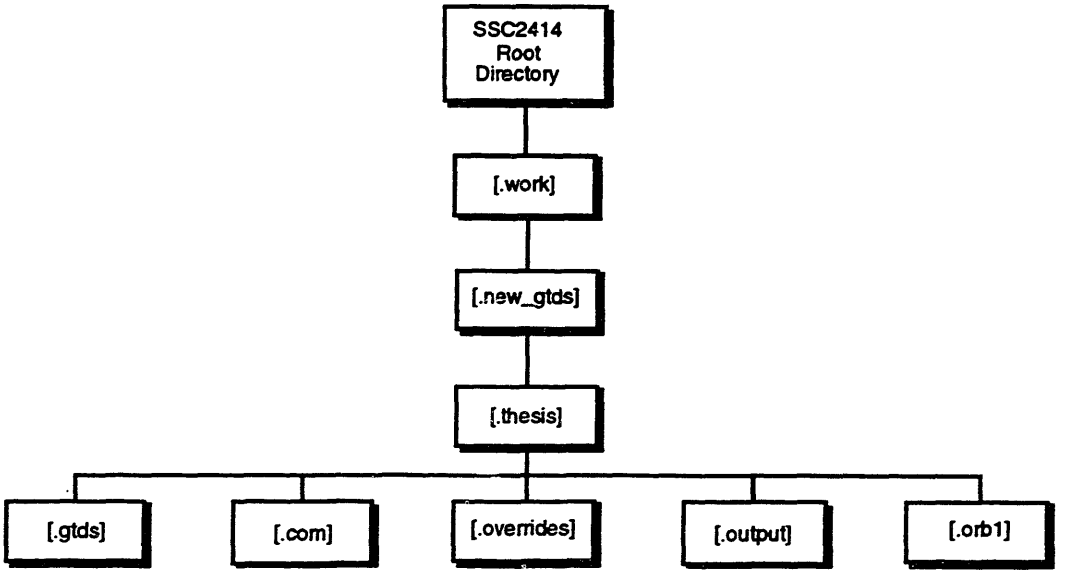

Figure H.1 Directory System for Results

The [.gtds], [.com], and [.overrides] subdirectories contain the input card data files, command procedures, and overrides files, respectively, for the executions being discussed here. The [.output] subdirectory houses the tabulated file output of each of the runs, while the [.orb1] structure is comprised of the GTDS ORB1 files produced. The file names are indicated here in parentheses by the experiment header.

H.1 TOPEX Experiments

Three experiments were performed in which the TOPEX navigation solutions were fit in order to acquire an estimate of the orbit. The three cases are summarized in Table H.1 below.

Table H.1 TOPEX Navigation Solution Experiments

Case	Description	References in Appendix H
1	Cowell five day fit of TOPEX navigation solutions with two day prediction	Figures: H.2-H.13
2	SST five day fit of TOPEX navigation solutions with two day prediction	Figures: H.14-H.24
3	Cowell four day fit of TOPEX navigation solutions with three day prediction	Figures: H.26-H.37

The force modeling was similar for all three cases and included:

Table H.2 Orbit Dynamic Models Used in TOPEX Analysis

Perturbation	Description
Earth's gravity	JGM-2 50x50; 4x4 partials
Solar Radiation Pressure	Cylindrical macro model
Atmospheric Drag	Jacchia-Roberts
Lunar/Solar Third Body	Point Mass
Lunar/Solar Tides	Love number (0.29)

Integration was performed in the mean equator and equinox of J2000 coordinate system.

The first two test cases involved a five day fit of the navigation solutions with a two day prediction interval, and were differentiated by the perturbation techniques used in the force modeling procedures (Cowell for the first experiment, and SST for the second). The final TOPEX experiment consisted of a Cowell four day fit and three day predict interval to determine how much data was necessary to obtain a sufficiently accurate estimate of the satellite's orbit. The input card data files, command procedures, and overrides files used in these three experiments precede a summary of the accuracy obtained in terms of Cartesian coordinates, radial/cross-track/along-track components, and orbital elements.

Experiment 1: Cowell Five Day Fit, Two Day Predict Using TOPEX Navigation Solutions (TOPEX_NAV_COWELL_FIT_1)

```
CONTROL  DC                                                          TOPEXXX  XXXXXX
EPOCH                          921223.0          000006.062256
ELEMENT1 10     1     1        4244.0405454594D0 2604.2124253247D0 5893.7520000000D0
ELEMENT2                       1.4617104691037D0 5.7771779442207D0 -3.601910156000D0
OBSINPUT 20                    921223 000010     921227 234810
ORBTYPE  2      1     11       10.0
DMOPT
OBSDEV   21                    100.
OBSDEV   22                    100.
OBSDEV   23                    125.
OBSDEV   24                    75.
OBSDEV   25                    75.
OBSDEV   26                    100.
END
DCOPT
PRINTOUT 1      4
CONVERG  20                    1.D-4                                 1.0
END
OGOPT
DRAG     1                     1.
ATMOSDEN                 1
DRAGPAR  2      1             0.15D0
SCPARAM                        2.8D-5            2400.0D0
MAXDEGEQ 1                     50.
MAXORDEQ 1                     50.
MAXDEGVE 1                     4.
MAXORDVE 1                     4.
POTFIELD 1      19
SETIDE   1                     0.29D0
SOLRAD   1      1
SOLRDPAR 1
STATEPAR 1
STATETAB 1      2     3        4                 5                   6
END
FIN
CONTROL  EPHEM                       OUTPUT                          TOPEXXX  XXXXXX
OUTPUT   19     2     1        921230.D0         000000.D0           43200.D0
ORBTYPE  2      1     11       10.0
OGOPT
DRAG     1                     1
ATMOSDEN                 1
DRAGPAR  0
SCPARAM                        2.8D-5            2400.0D0
MAXDEGEQ 1                     50.
MAXORDEQ 1                     50.
MAXDEGVE 1                     4.
MAXORDVE 1                     4.
POTFIELD 1      19
SETIDE   1                     0.29D0
SOLRAD   1      1
SOLRDPAR 0
OUTOPT   1                     921223000000.0    921230000000.0      120.0
END
FIN
```

Figure H.2 TOPEX Cowell Five Day Fit Input Card Data File

```
$!-------------------------------------------------------------------
$! TOPEX_NAV_COWELL_FIT_1
$!
$!
$!-------------------------------------------------------------------
$!
$! Set default for batch run from CSDL0:[GTDS.GTDS_TEST]
$  set default fds$diska:[ssc2414.work.new_gtds.thesis.com]
$!
$! Assign debug overrides
$!
$  assign/table=lnm$job [ssc2414.work.new_gtds.thesis.overrides]topex_nav_cowell_fit_1.overrides dbg$init
$!
$! Assign the observation card file
$!
$  assign/table=lnm$job fds$diska:[ssc2414.topex.obscard]92dec23-27_pbias.poscard gtds$015
$!
$! Assign the body potential files
$!
$  assign/table=lnm$job fds$diska:[rjp9045.bianca.fonte]newcomb.dat gtds$023
$  assign/table=lnm$job fds$diska:[djf1230.bianca]dan_potential.dat gtds$047
$  assign/table=lnm$job fds$diska:[djf1230.bianca]moon.dat      gtds$048
$!
$! Assign the SLP and timing files
$!
$  assign/table=lnm$job elrond$dka0:[ssc2414]june95_msgen_slp_mn2000.dat gtds$014
$  assign/table=lnm$job elrond$dka0:[ssc2414]june95_msgen_slp_timecoef.dat gtds$038
$  assign/table=lnm$job elrond$dka0:[ssc2414]june95_msgen_slp_tod2000.dat gtds$078
$!
$! Assign ORB1 files
$!
$  assign/table=lnm$job fds$diska:[ssc2414.work.new_gtds.thesis.orb1]topex_nav_cowell_fit_1.orb1 gtds$024
$!
$! Assign atmospheric density files
$!
$  assign/table=lnm$job fds_dbf:jacchia_roberts.dat   gtds$075
$!
$! Assign fundamental constants file
$!
$  assign/table=lnm$job fds$diska:[ssc2414.work.new_gtds.mods]j2000_csconst.dat gtds$099
$!
$! Execute the local version of debug executable
$!
$  @[ssc2414.work.new_gtds.test]j2000_SWAT_GTDS [ssc2414.work.new_gtds.thesis.gtds]topex_nav_cowell_fit_1
$  rename [-.thesis.gtds]topex_nav_cowell_fit_1.output [-.thesis.output]topex_nav_cowell_fit_1.output
$!
$  assign/table=lnm$job fds_dbf:schatten_jacchia_roberts.dat gtds$075
$  EXIT
```

Figure H.3 TOPEX Cowell Five Day Fit Command Procedure

```
SET OUTPUT LOG
SET LOG
SET BREAK/return ESTSET DO -
      (DEPOSIT  IDIFF      = 3; -
       DEPOSIT  IDRVAR     = 1; -
       DEPOSIT  ISRVAR     = 1; -
       DEPOSIT  KPAR       = 0; -
       DEPOSIT  KATMOS     = 1; -
       EXAMINE  KATMOS     ; -
       EXAMINE  IDIFF      ; -
       EXAMINE  IDRVAR     ; -
       EXAMINE  ISRVAR     ; -
       EXAMINE  KPAR       ; -
       GO -
    ); -
GO
```

Figure H.4 TOPEX Cowell Five Day Fit Overrides File

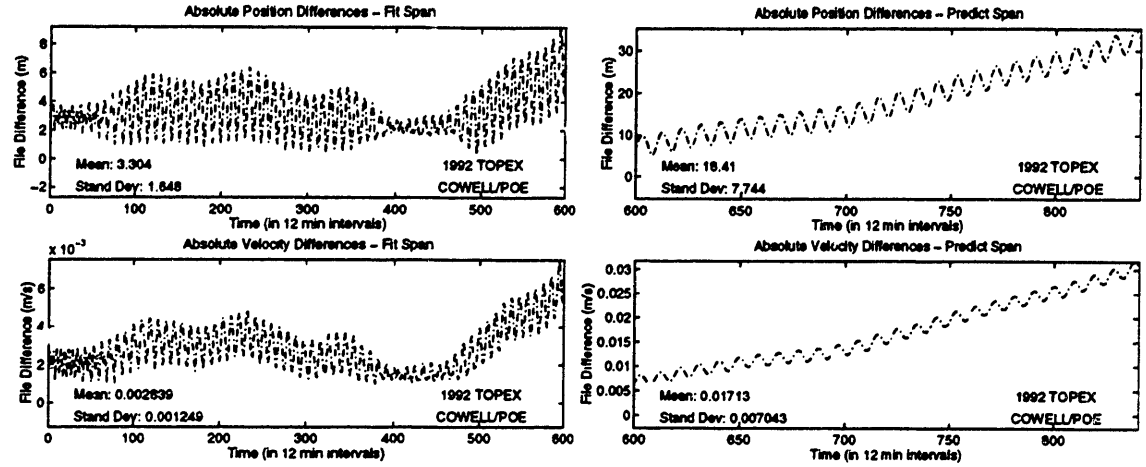

Figure H.5 TOPEX Position and Velocity Errors for Cowell Five Day Fit and Two Day Predict

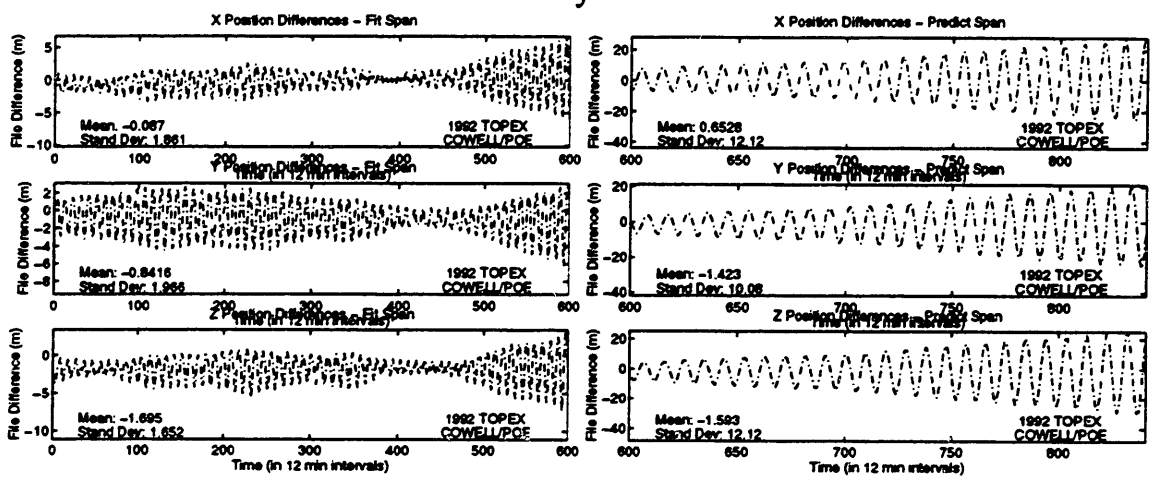

Figure H.6 TOPEX Position Errors for Cowell Five Day Fit and Two Day Predict

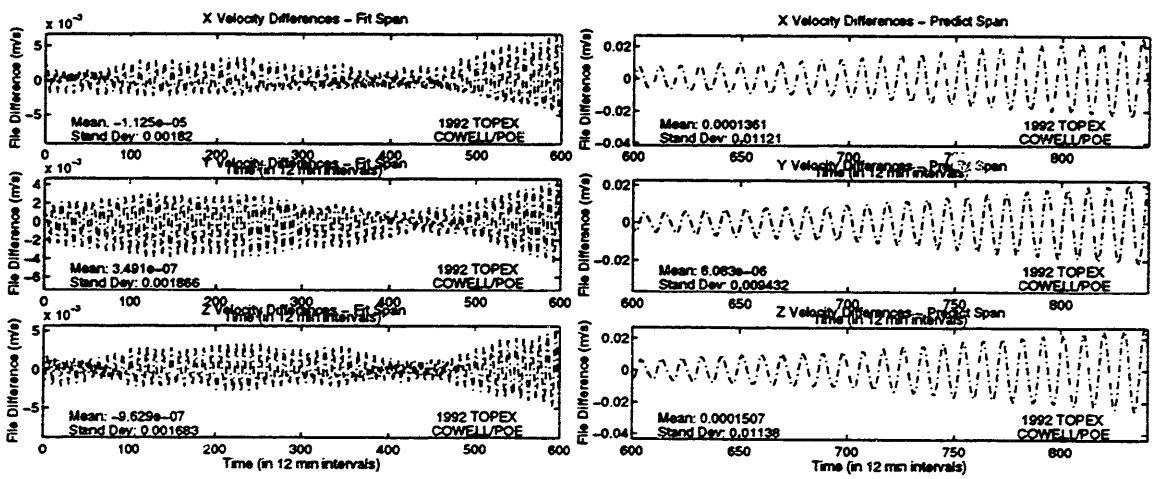

Figure H.7 TOPEX Velocity Errors for Cowell Five Day Fit and Two Day Predict

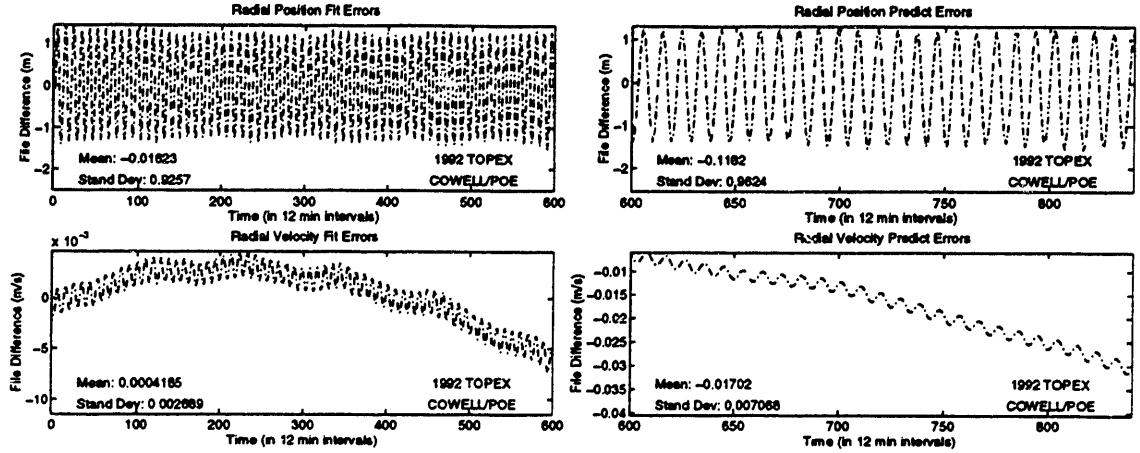

Figure H.8 TOPEX Radial Errors for Cowell Five Day Fit and Two Day Predict

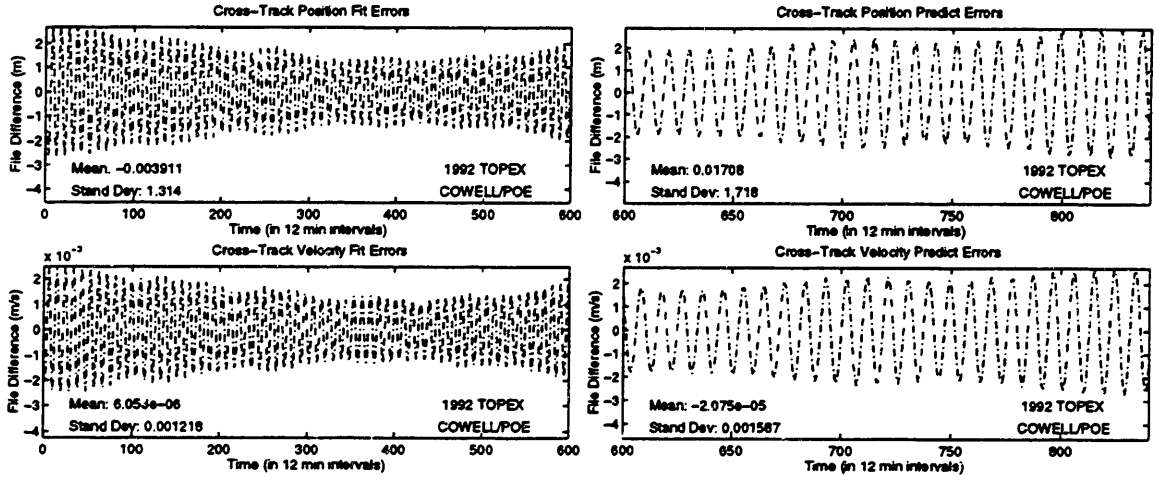

Figure H.9 TOPEX Cross-Track Errors for Cowell Five Day Fit and Two Day Predict

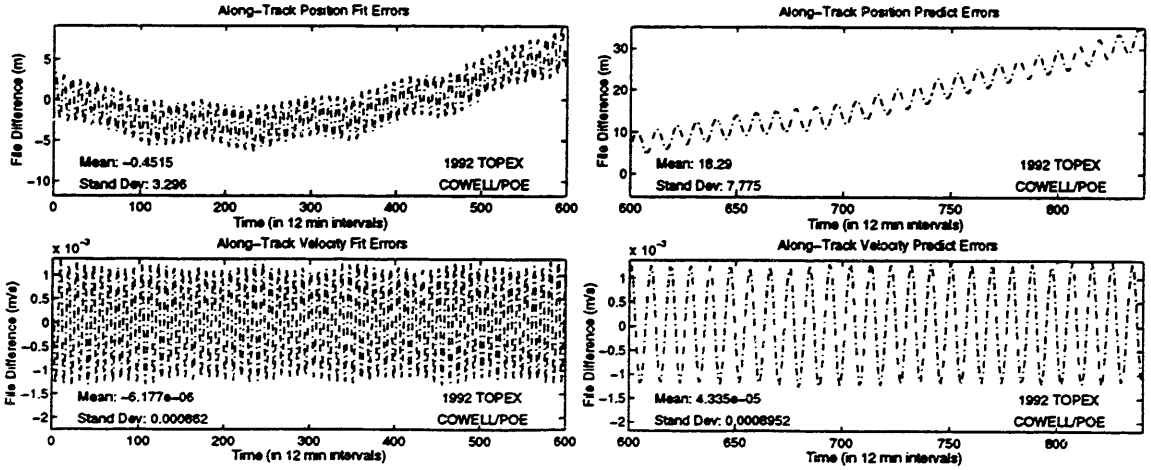

Figure H.10 TOPEX Along-Track Errors for Cowell Five Day Fit and Two Day Predict

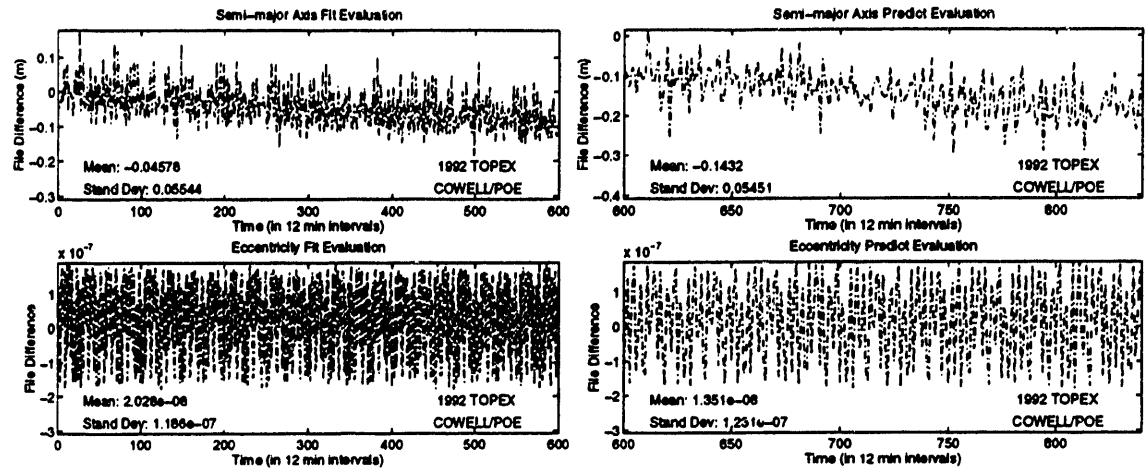

Figure H.11 TOPEX *a/e* Errors for Cowell Five Day Fit and Two Day Predict

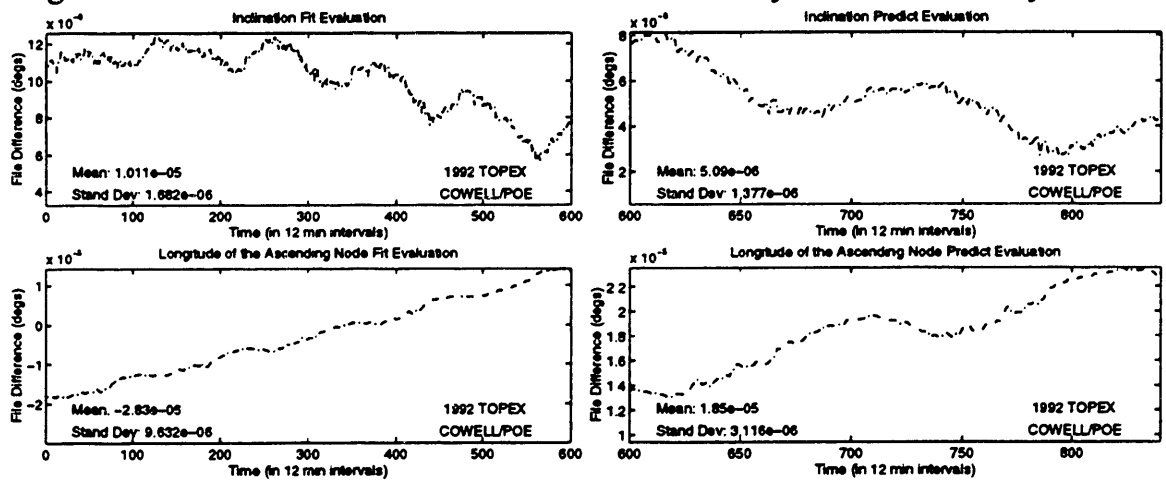

Figure H.12 TOPEX i/Ω Errors for Cowell Five Day Fit and Two Day Predict

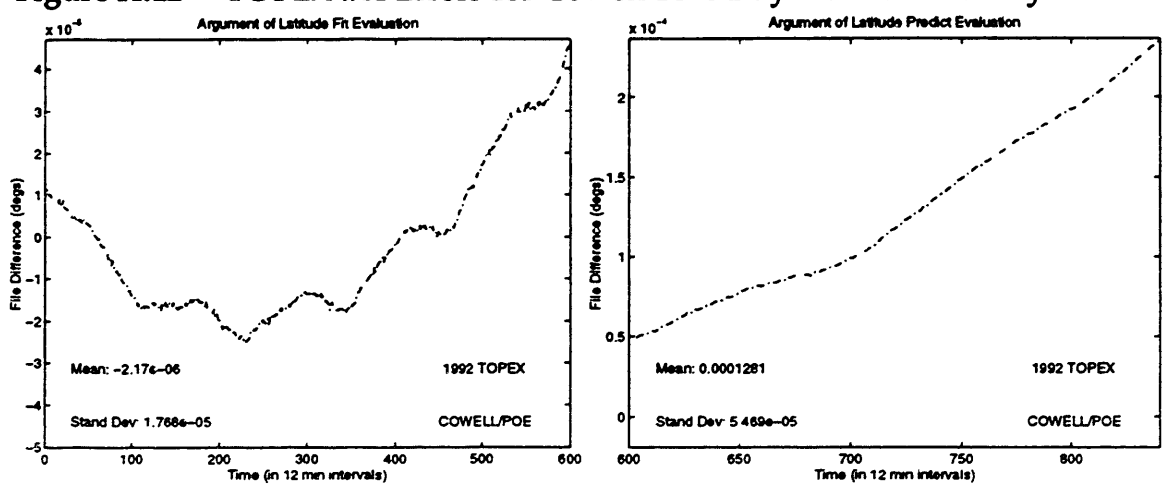

Figure H.13 TOPEX Argument of Latitude Errors for Cowell Five Day Fit and Two Day Predict

Experiment 2 SST Five Day Fit, Two Day Predict Using TOPEX Navigation Solutions (TOPEX_NAV_SST_FIT_1)

```
CONTROL  DC                                                          TOPEXXX  XXXXXX
EPOCH                          921223.0                 000006.062256
ELEMENT1  12    6     1        7714.501880367606D0      4.8360361713957D-4       66.04039556435517D0
ELEMENT2                       335.1015957617251D0      271.709682192564D0       211.5673105250555D0
OBSINPUT  20                   921223 000010            921227 234810
ORBTYPE   5     1     11       21600.0                  1.0
DMOPT
OBSDEV    21                   100.
OBSDEV    22                   100.
OBSDEV    23                   125.
OBSDEV    24                   75.
OBSDEV    25                   75.
OBSDEV    26                   100.
END
DCOPT
PRINTOUT  1     4
CONVERG   20                   1.D-4                                  1.0
END
OGOPT
DRAG      1                    1.
ATMOSDEN            1
DRAGPAR   1
SCPARAM                        2.8D-5                   2400.0D0
MAXDEGEQ  1                    50.
MAXORDEQ  1                    50.
MAXDEGVE  1                    4.
MAXORDVE  1                    4.
POTFIELD  1     19
RESONPRD                       86400.
SETIDE    1                    0.29D0
SOLRAD    1     1
SOLRDPAR  1
STATEPAR  3
STATETAB  1     2     3        4                        5                        6
END
FIN
CONTROL  EPHEM                      OUTPUT                                    TOPEXXX  XXXXXX
OUTPUT    19    2     1        921230.D0                000000.D0                43200.D0
ORBTYPE   5     1     11       21600.0                  1.0
OGOPT
DRAG      1                    1
ATMOSDEN            1
DRAGPAR   0
SCPARAM                        2.8D-5                   2400.0D0
MAXDEGEQ  1                    50.
MAXORDEQ  1                    50.
MAXDEGVE  1                    4.
MAXORDVE  1                    4.
POTFIELD  1     19
RESONPRD                       86400.
SETIDE    1                    0.29D0
SOLRAD    1     1
SOLRDPAR  0
OUTOPT    1                    921223000000.0           921230000000.0           120.0
END
FIN
```

Figure H.14 TOPEX SST Five Day Fit Input Card Data File

```
$!-------------------------------------------------------------
$! TOPEX_NAV_SST_FIT_1
$!
$!
$!-------------------------------------------------------------
$!
$! Set default for batch run from CSDL0:[GTDS.GTDS_TEST]
$  set default fds$diska:[ssc2414.work.new_gtds.thesis.com]
$!
$! Assign debug overrides
$!
$  assign/table=lnm$job [ssc2414.work.new_gtds.thesis.overrides]topex_nav_sst_fit_1.overrides dbg$init
$!
$! Assign the observation card file
$!
$  assign/table=lnm$job fds$diska:[ssc2414.topex.obscard]92dec23-27_pbias.poscard gtds$015
$!
$! Assign the body potential files
$!
$  assign/table=lnm$job fds$diska:[rjp9045.bianca.fonte]newcomb.dat gtds$023
$  assign/table=lnm$job fds$diska:[dj1230.bianca]dan_potential.dat gtds$047
$  assign/table=lnm$job fds$diska:[dj1230.bianca]moon.dat      gtds$048
$!
$! Assign the SLP and timing files
$!
$  assign/table=lnm$job elrond$dka0:[ssc2414]june95_msgen_slp_mn2000.dat gtds$014
$  assign/table=lnm$job elrond$dka0:[ssc2414]june95_msgen_slp_timecoef.dat gtds$038
$  assign/table=lnm$job elrond$dka0:[ssc2414]june95_msgen_slp_tod2000.dat gtds$078
$!
$! Assign ORB1 files
$!
$  assign/table=lnm$job fds$diska:[ssc2414.work.new_gtds.thesis.orb1]topex_nav_sst_fit_1.orb1 gtds$024
$!
$! Assign atmospheric density files
$!
$  assign/table=lnm$job fds_dbf:jacchia_roberts.dat   gtds$075
$!
$! Assign fundamental constants file
$!
$  assign/table=lnm$job fds$diska:[ssc2414.work.new_gtds.models]j2000_csconst.dat gtds$099
$!
$! Execute the local version of debug executable
$!
$  @[ssc2414.work.new_gtds.test]j2000_SWAT_GTDS [ssc2414.work.new_gtds.thesis.gtds]topex_nav_sst_fit_1
$  rename [-.thesis.gtds]topex_nav_sst_fit_1.output [-.thesis.output]topex_nav_sst_fit_1.output
$!
$  assign/table=lnm$job fds_dbf:schatten_jacchia_roberts.dat gtds$075
$  EXIT
```

Figure H.15 TOPEX SST Five Day Fit Command Procedure

```
SET OUTPUT LOG
 SET LOG
 SET BREAK/return ESTSET DO -
       (DEPOSIT  IDIFF        = 3; -
        DEPOSIT  IDRVAR       = 1; -
        DEPOSIT  ISRVAR       = 1; -
        DEPOSIT  KPAR         = 1; -
        DEPOSIT  KATMOS       = 1; -
        EXAMINE  KATMOS       ; -
        EXAMINE  IDIFF        ; -
        EXAMINE  IDRVAR       ; -
        EXAMINE  ISRVAR       ; -
        EXAMINE  KPAR         ; -
        GO -
    ); -
GO
 SET BREAK/return HWIHE  DO -
       (DEPOSIT  LZN          = 4; -
        DEPOSIT  JZN          = 25; -
        DEPOSIT  LMD          = 4; -
        DEPOSIT  MMD          = 28;-
        DEPOSIT  MTS          = 41;-
        DEPOSIT  NJ2MD        = 12; -
        DEPOSIT  MJ2MD        = 12; -
        DEPOSIT  LJ2MD        = 4; -
        DEPOSIT  IDRMD        = 2; -
        DEPOSIT  NTH(1)       = 4; -
        DEPOSIT  NTH(2)       = 4; -
        DEPOSIT  JMAXTH(1)    = 5; -
        DEPOSIT  LTH(1)       = 4; -
        DEPOSIT  LTH(2)       = 4; -
        DEPOSIT  JMAXTS       = 25;-
        DEPOSIT  JMINTS       =-25;-
        EXAMINE  LZN          ; -
        EXAMINE  JZN          ; -
        EXAMINE  LMD          ; -
        EXAMINE  NJ2MD        ; -
        EXAMINE  MJ2MD        ; -
        EXAMINE  LJ2MD        ; -
        EXAMINE  IDRMD        ; -
        EXAMINE  NTH(1)       ; -
        EXAMINE  NTH(2)       ; -
        EXAMINE  JMAXTH(1)    ; -
        EXAMINE  LTH(1)       ; -
        EXAMINE  LTH(2)       ; -
        GO -
    ); -
GO
```

Figure H.16 TOPEX SST Five Day Fit Overrides File

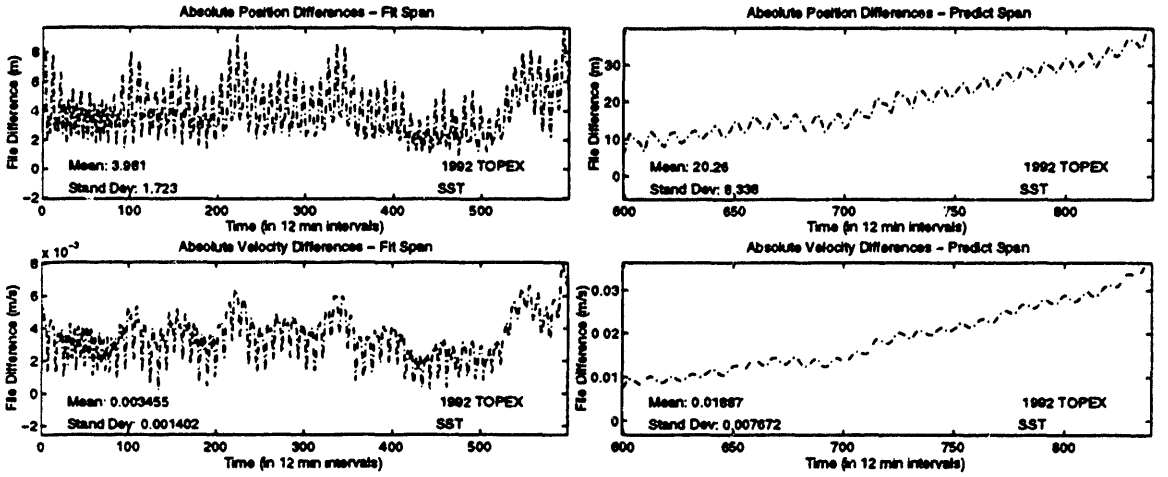

Figure H.17 TOPEX Position and Velocity Errors for SST Five Day Fit and Two Day Predict

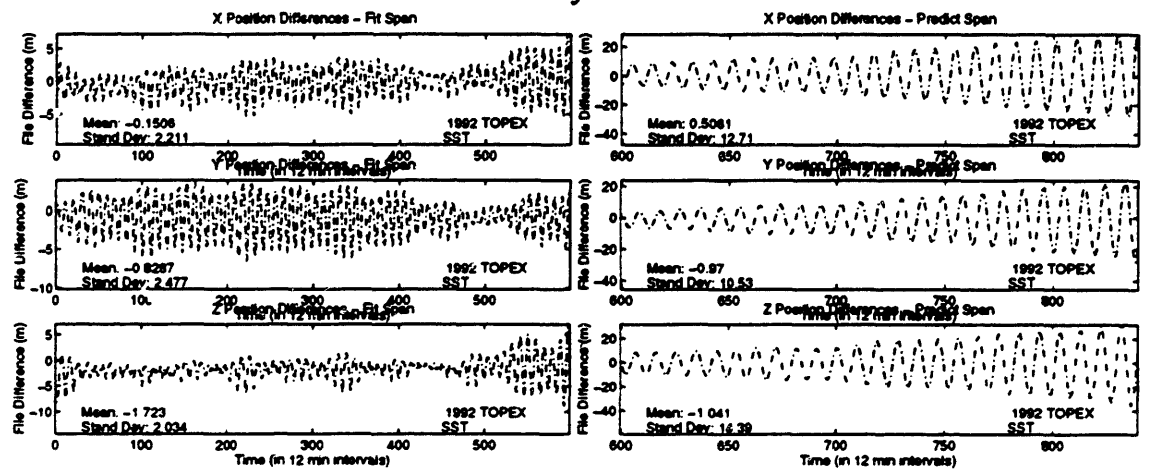

Figure H.18 TOPEX Position Errors for SST Five Day Fit and Two Day Predict

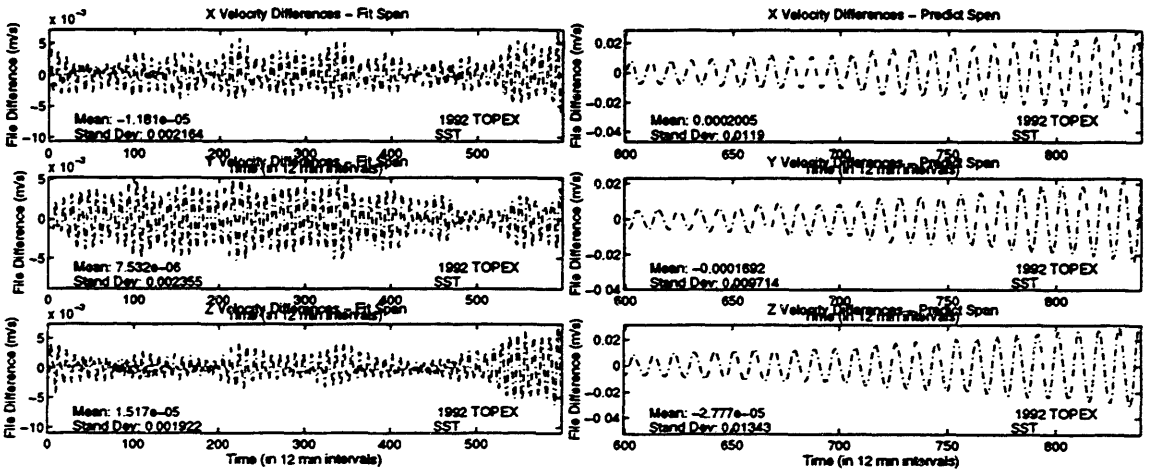

Figure H.19 TOPEX Velocity Errors for SST Five Day Fit and Two Day Predict

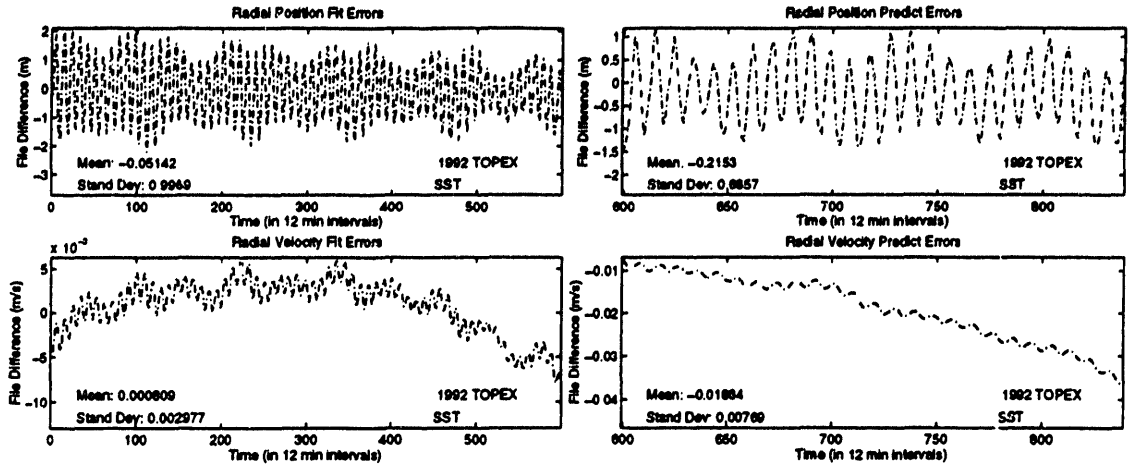

Figure H.20 TOPEX Radial Errors for SST Five Day Fit and Two Day Predict

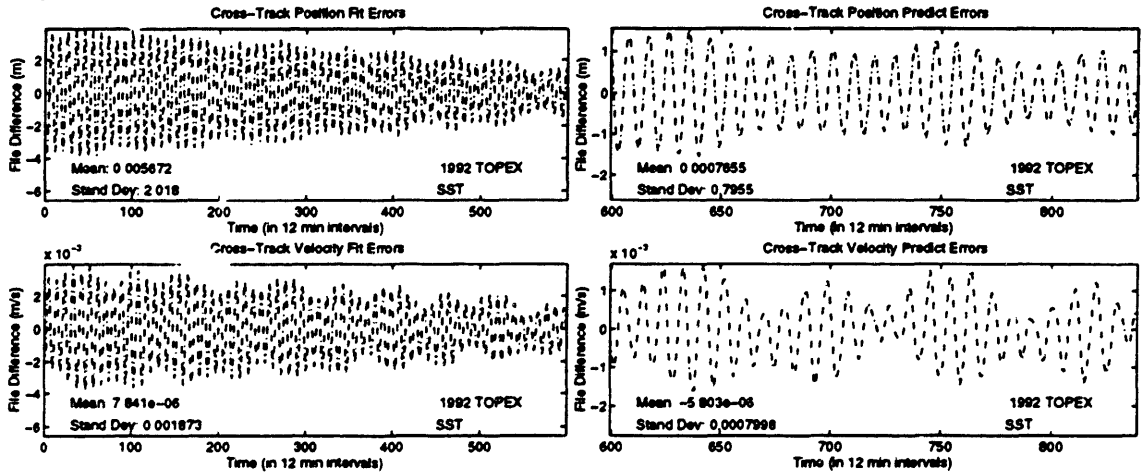

Figure H.21 TOPEX Cross-Track Errors for SST Five Day Fit and Two Day Predict

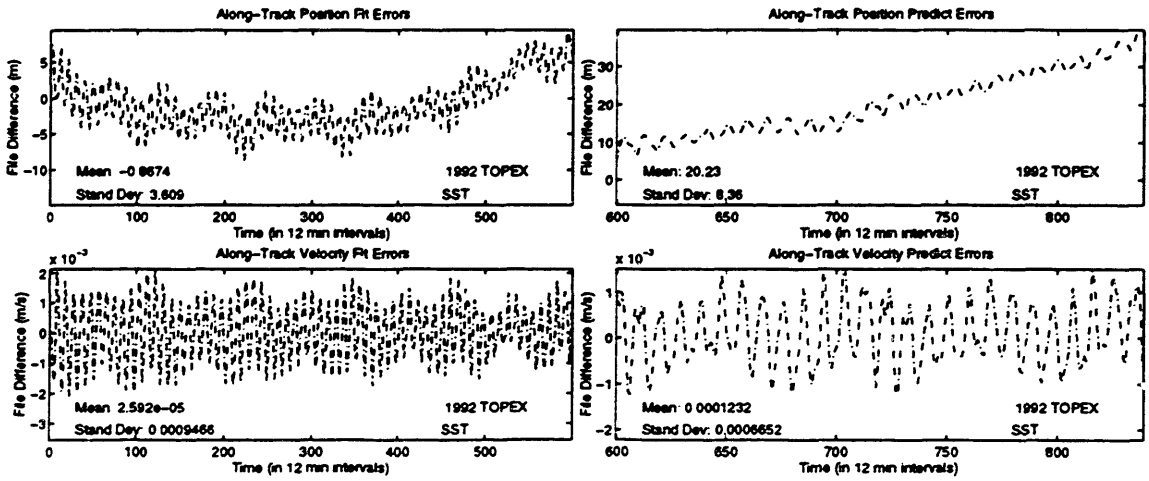

Figure H.22 TOPEX Along-Track Errors for SST Five Day Fit and Two Day Predict

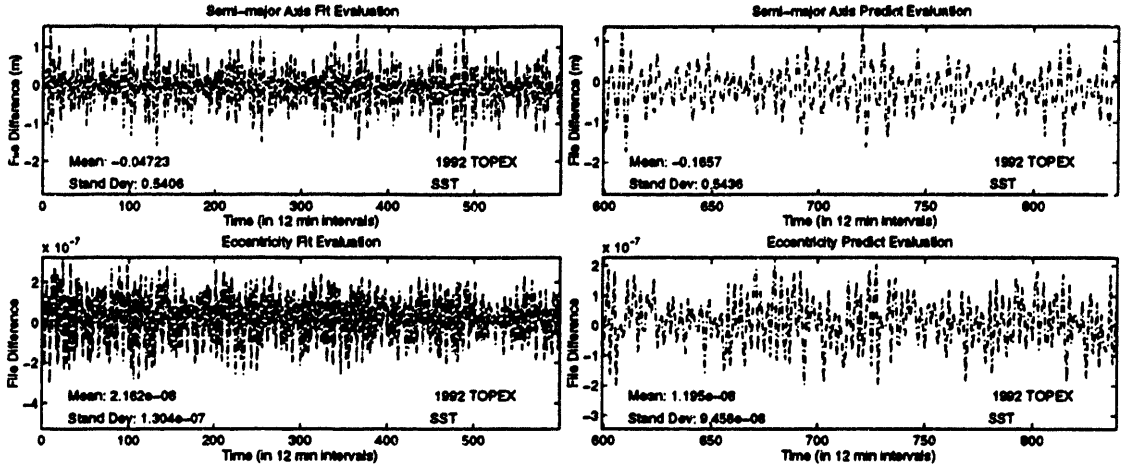

Figure H.23 TOPEX *a/e* Errors for SST Five Day Fit and Two Day Predict

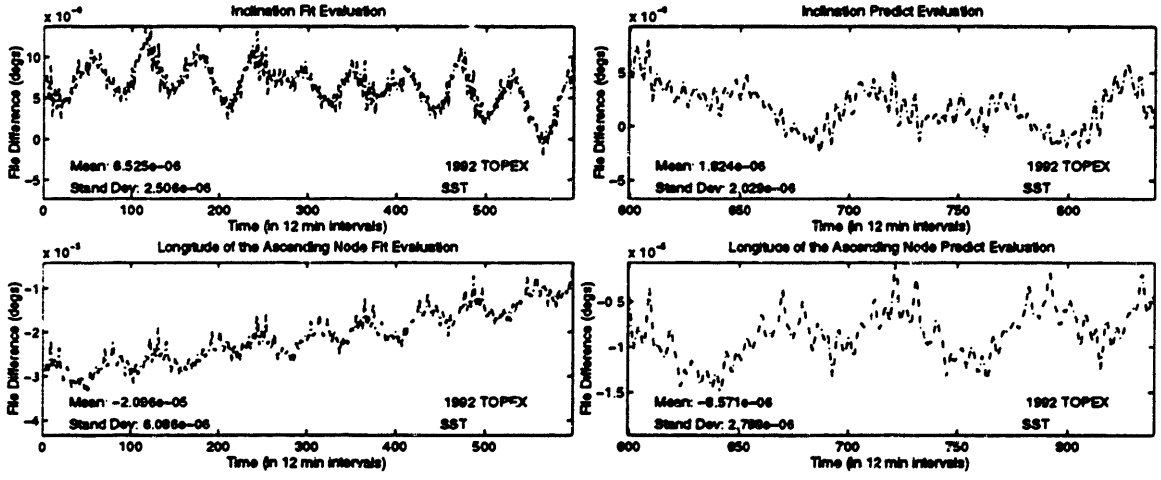

Figure H.24 TOPEX i/Ω Errors for SST Five Day Fit and Two Day Predict

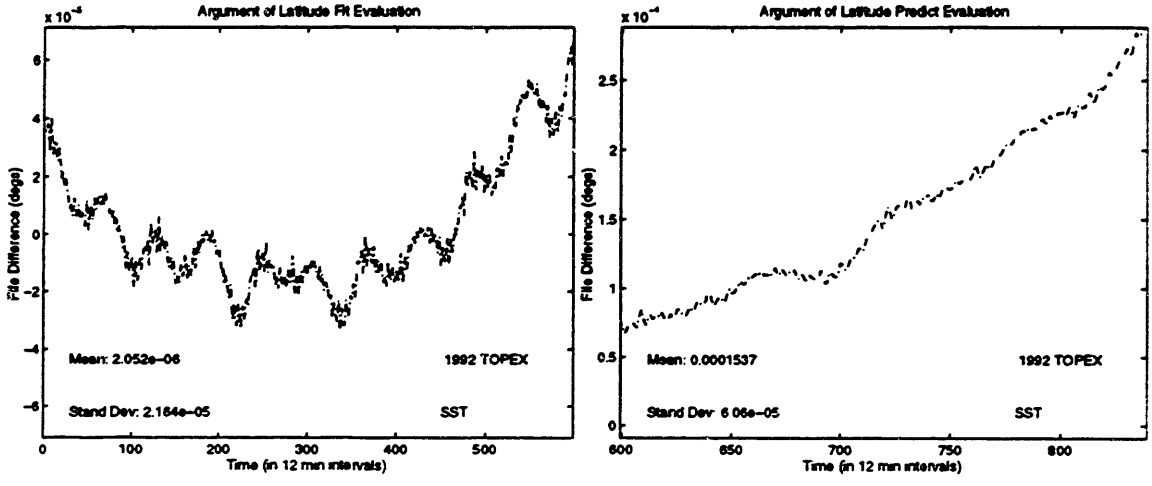

Figure H.25 TOPEX Argument of Latitude Errors for SST Five Day Fit and Two Day Predict

Experiment 3: Cowell Four Day Fit, Three Day Predict Using TOPEX Navigation Solutions (TOPEX_NAV_COWELL_FIT_2)

```
CONTROL  DC                                                          TOPEXXX  XXXXXX
EPOCH                        921223.0            000006.062256
ELEMENT1 10    1    1        4244.0405454594D0   2604.2124253247D0   5893.752000000000
ELEMENT2                     1.4617104691037D0   5.7771779442207D0   -3.601910156000D0
OBSINPUT 20                  921223 000010       921227 000010
ORBTYPE  2     1    11       10.0
DMOPT
OBSDEV   21                  100.
OBSDEV   22                  100.
OBSDEV   23                  125.
OBSDEV   24                  75.
OBSDEV   25                  75.
OBSDEV   26                  100.
END
DCOPT
PRINTOUT 1     4
CONVERG  20                  1.D-4                                   1.0
END
OGOPT
DRAG     1                   1.
ATMOSDEN          1
DRAGPAR  2     1             0.15D0
SCPARAM                      2.8D-5              2400.0D0
MAXDEGEQ 1                   50.
MAXORDEQ 1                   50.
MAXDEGVE 1                   4.
MAXORDVE 1                   4.
POTFIELD 1     19
SETIDE   1                   0.29D0
SOLRAD   1     1
SOLRDPAR 1
STATEPAR 1
STATETAB 1     2    3        4                   5                   6
END
FIN
CONTROL  EPHEM                    OUTPUT                            TOPEXXX  XXXXXX
OUTPUT   19    2    1           921230.D0           000000.D0           43200.D0
ORBTYPE  2     1    11          10.0
OGOPT
DRAG     1                     1
ATMOSDEN          1
DRAGPAR  0
SCPARAM                      2.8D-5              2400.0D0
MAXDEGEQ 1                   50.
MAXORDEQ 1                   50.
MAXDEGVE 1                   4.
MAXORDVE 1                   4.
POTFIELD 1     19
SETIDE   1                   0.29D0
SOLRAD   1     1
SOLRDPAR 0
OUTOPT   1                   921223000000.0      921230000000.0      120.0
END
FIN
```

Figure H.26 TOPEX Cowell Four Day Fit Input Card Data File

```
$!-------------------------------------------------------------
$! TOPEX_NAV_COWELL_FIT_2
$!
$!
$!-------------------------------------------------------------
$!
$! Set default for batch run from CSDL0:[GTDS.GTDS_TEST]
$  set default fds$diska:[ssc2414.work.new_gtds.thesis.com]
$!
$! Assign debug overrides
$!
$  assign/table=lnm$job [ssc2414.work.new_gtds.thesis.overrides]topex_nav_cowell_fit_2.overrides dbg$init
$!
$! Assign the observation card file
$!
$  assign/table=lnm$job fds$diska:[ssc2414.topex.obscard]92dec23-26_pbias.poscard gtds$015
$!
$! Assign the body potential files
$!
$  assign/table=lnm$job fds$diska:[rjp9045.bianca.fonte]newcomb.dat gtds$023
$  assign/table=lnm$job fds$diska:[djf1230.bianca]dan_potential.dat gtds$047
$  assign/table=lnm$job fds$diska:[djf1230.bianca]moon.dat      gtds$048
$!
$! Assign the SLP and timing files
$!
$  assign/table=lnm$job elrond$dka0:[ssc2414]june95_msgen_slp_mn2000.dat gtds$014
$  assign/table=lnm$job elrond$dka0:[ssc2414]june95_msgen_slp_timecoef.dat gtds$038
$  assign/table=lnm$job elrond$dka0:[ssc2414]june95_msgen_slp_tod2000.dat gtds$078
$!
$! Assign ORB1 files
$!
$  assign/table=lnm$job fds$diska:[ssc2414.work.new_gtds.thesis.orb1]topex_nav_cowell_fit_2.orb1 gtds$024
$!
$! Assign atmospheric density files
$!
$  assign/table=lnm$job fds_dbf:jacchia_roberts.dat   gtds$075
$!
$! Assign fundamental constants file
$!
$  assign/table=lnm$job fds$diska:[ssc2414.work.new_gtds.mods]j2000_csconst.dat gtds$099
$!
$! Execute the local version of debug executable
$!
$  @[ssc2414.work.new_gtds.test]j2000_SWAT_GTDS [ssc2414.work.new_gtds.thesis.gtds]topex_nav_cowell_fit_2
$  rename [-.thesis.gtds]topex_nav_cowell_fit_2.output [-.thesis.output]topex_nav_cowell_fit_2.output
$!
$  assign/table=lnm$job fds_dbf:schatten_jacchia_roberts.dat gtds$075
$  EXIT
```

Figure H.27 TOPEX Cowell Four Day Fit Command Procedure

```
SET OUTPUT LOG
SET LOG
SET BREAK/return ESTSET DO -
      (DEPOSIT  IDIFF      = 3; -
       DEPOSIT  IDRVAR     = 1; -
       DEPOSIT  ISRVAR     = 1; -
       DEPOSIT  KPAR       = 0; -
       DEPOSIT  KATMOS     = 1; -
       EXAMINE  KATMOS     ; -
       EXAMINE  IDIFF      ; -
       EXAMINE  IDRVAR     ; -
       EXAMINE  ISRVAR     ; -
       EXAMINE  KPAR       ; -
       GO -
    ); -
GO
```

Figure H.28 TOPEX Cowell Four Day Fit Overrides File

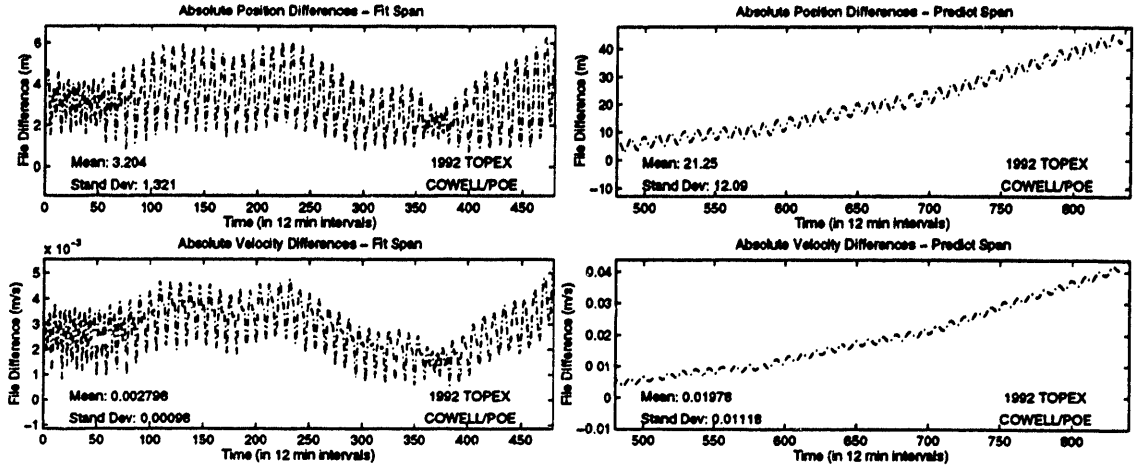

Figure H.29 TOPEX Position and Velocity Errors for Cowell Four Day Fit and Three Day Predict

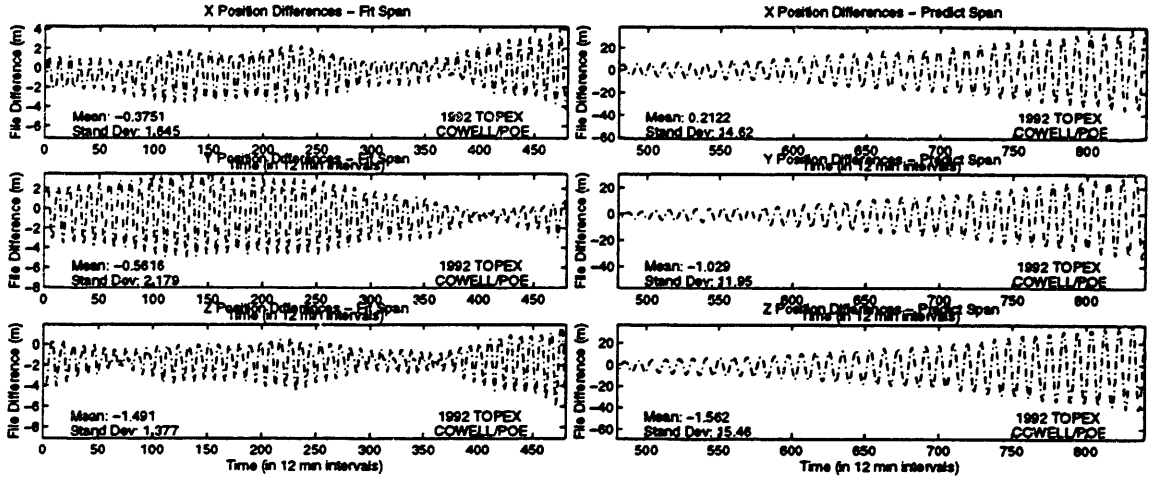

Figure H.30 TOPEX Position Errors for Cowell Four Day Fit and Three Day Predict

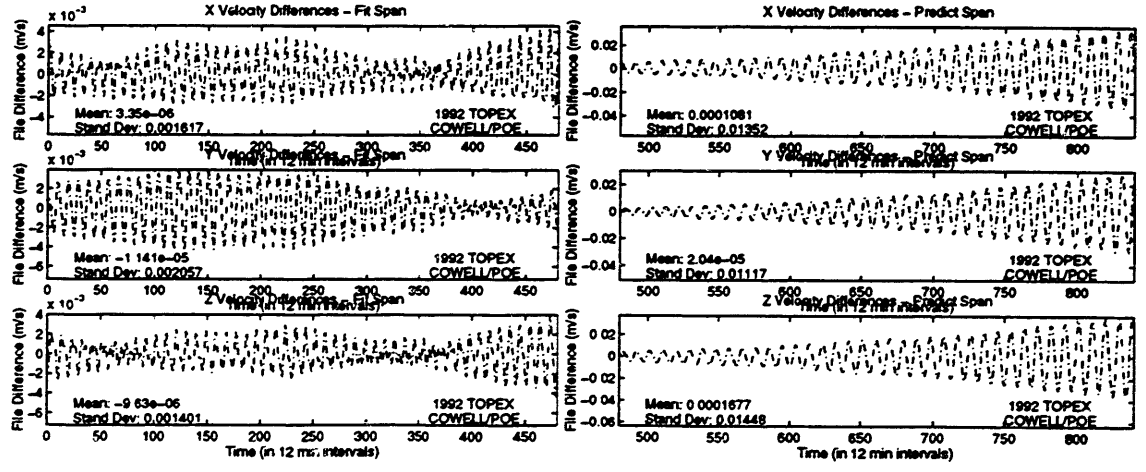

Figure H.31 TOPEX Velocity Errors for Cowell Four Day Fit and Three Day Predict

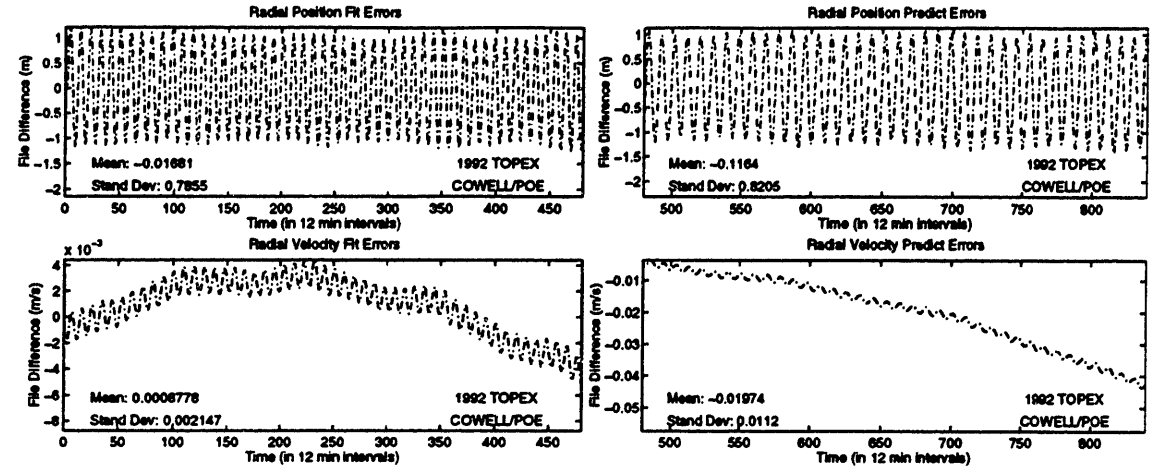

Figure H.32 TOPEX Radial Errors for Cowell Four Day Fit and Three Day Predict

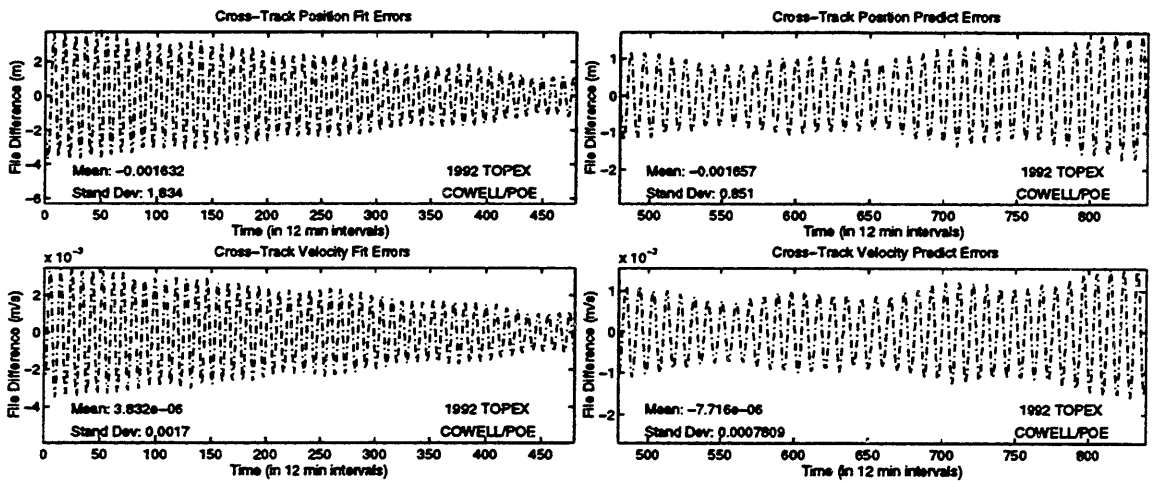

Figure H.33 TOPEX Cross-Track Errors for Cowell Four Day Fit and Three Day Predict

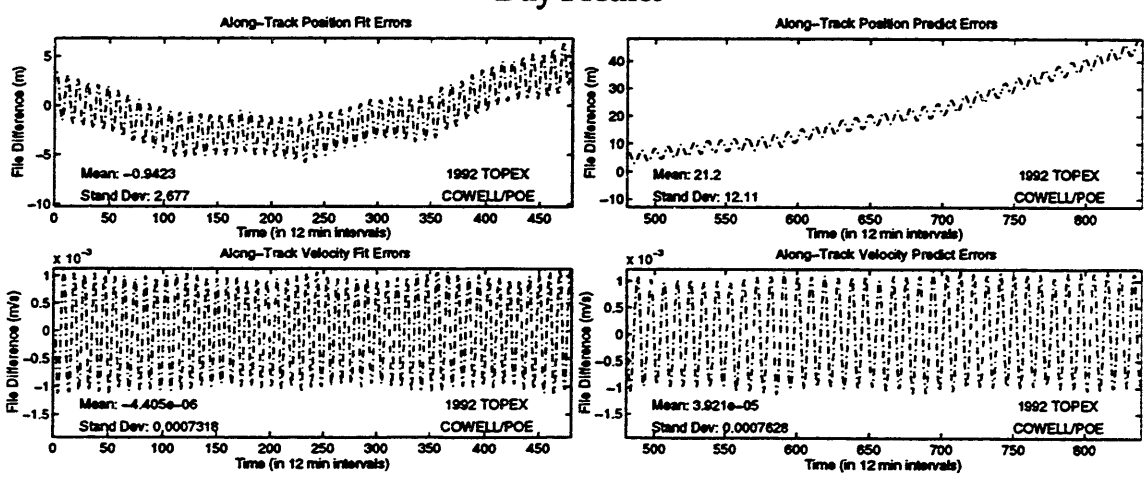

Figure H.34 TOPEX Along-Track Errors for Cowell Four Day Fit and Three Day Predict

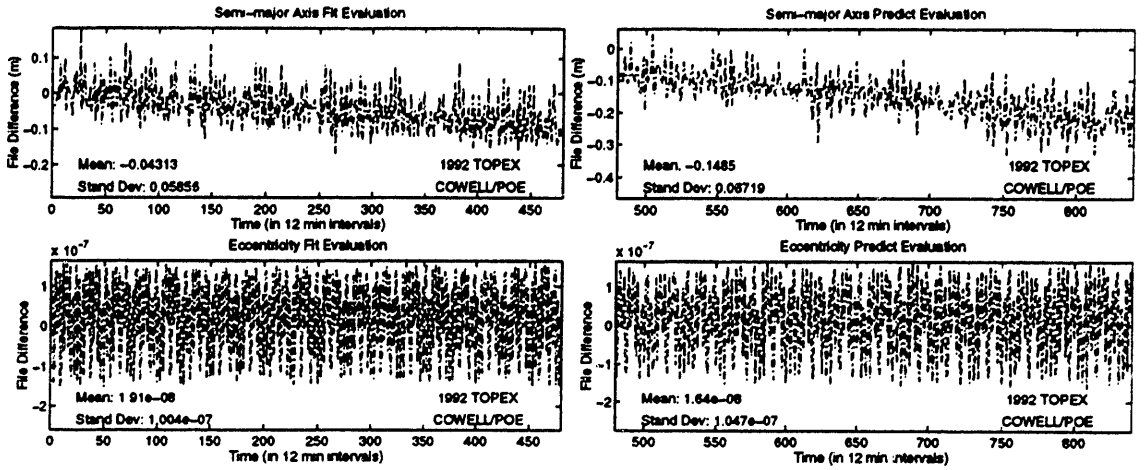

Figure H.35 TOPEX *a/e* Errors for Cowell Four Day Fit and Three Day Predict

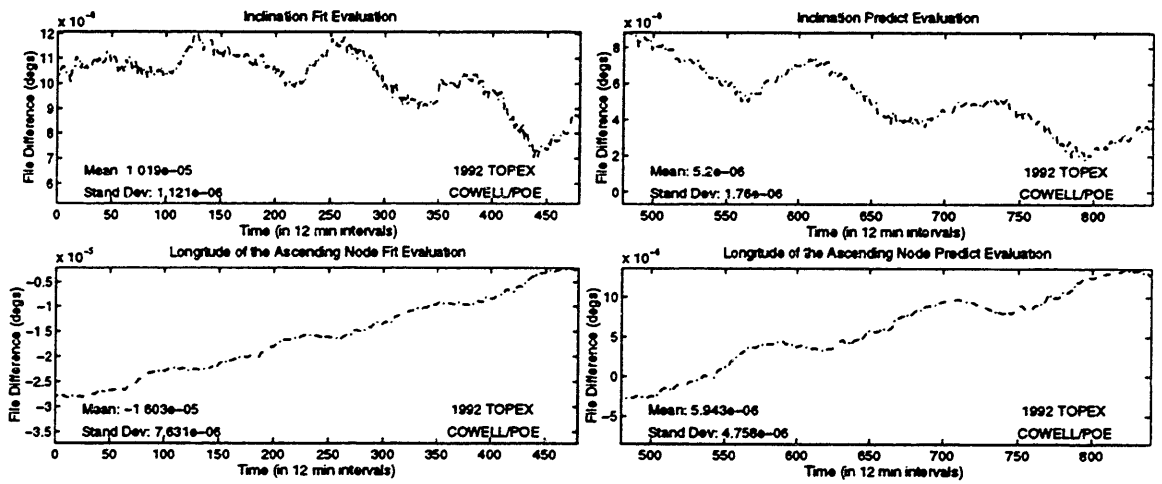

Figure H.36 TOPEX *i/Ω* Errors for Cowell Four Day Fit and Three Day Predict

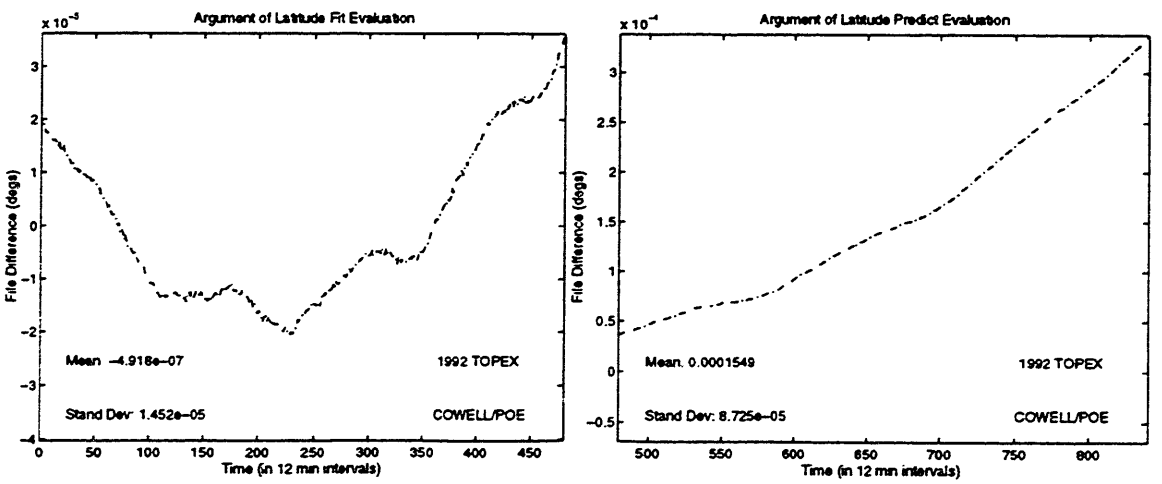

Figure H.37 TOPEX Argument of Latitude Errors for Cowell Four Day Fit and Three Day Predict

H.2 TAOS Experiments

H.2.1 Orbit Determination from the TAOS POEs

Initial experiments involving the TAOS data revolved around the fitting of the POE vectors, a high quality representations of the orbit (~3 meter 1σ) provided by Dr. Joseph Guinn of JPL. It was desirable to determine the accuracy to which Draper R&D GTDS could model the "truth" prior to experimentation with the navigation solutions because the errors represent a type of process noise that is going to exist in the navigation solutions fits as well. Quantification with the POE vectors would provide an estimate of what to expect with the navigation solutions.

Three experiments of varying fit interval lengths were performed with the TAOS POEs. The three cases are summarized in Table H.3.

Table H.3 TAOS POE Experiments

Case	Description	References in Appendix H
1	Cowell one day fit of TAOS POEs	Figures: H.38-H.49
2	Cowell two day fit of TAOS POEs	Figures: H.50-H.61
3	Cowell three day fit of TAOS POEs	Figures: H.62-H.73

After a five day fit indicated GTDS's inability to accurately portray the drag parameter for the entire fit span, the information content was reduced to one-

and two-day periods. The force modeling associated with the TAOS runs was similar to the TOPEX configuration.

Table H.4 Orbit Dynamic Models Used in TAOS Analysis

Perturbation	Description
Earth's gravity	JGM-2 50x50; 4x4 partials
Solar Radiation Pressure	Cylindrical macro model
Atmospheric Drag	Schatten-Jacchia-Roberts
Lunar/Solar Third Body	Point Mass
Lunar/Solar Tides	Love number (0.29)

Because TAOS's altitude is significantly lower than that of TOPEX, the solar radiation pressure coefficient was dropped from the solve-for vector, which now included the initial position and velocity at epoch and the drag parameter. The input card data files, command procedures, and overrides files are contained along with the results of these three Cowell POE fits in this section.

Experiment 1: TAOS Five Day Fit of the POE Vectors

(TAOS_POE_ITOD_DC_1)

```
CONTROL  DC                                                          TAOSXXXX  XXXXXX
EPOCH                        940528.0              000000.0
ELEMENT1  12  1       1      6135.0929862214D0     -1114.1967011652D0    -3058.3210851343D0
ELEMENT2                     2.7550108887691D0     -2.7235147364250D0    6.5097125101216D0
OBSINPUT  29                 940528 000000         940602 000000
ORBTYPE  2     1      11  10.0
DMOPT
OBSDEV   21                  10.
OBSDEV   22                  10.
OBSDEV   23                  10.
OBSDEV   24                  1.
OBSDEV   25                  1.
OBSDEV   26                  1.
END
DCOPT
PRINTOUT  1    4
CONVERG  20                  1.D-4                                 1.0
END
OGOPT
DRAG     1                   1.
ATMOSDEN                 1
DRAGPAR  2     1             0.15D0
SCPARAM                      2.8D-5                2400.0D0
MAXDEGEQ 1                   50.
MAXORDEQ 1                   50.
MAXDEGVE 1                   4.
MAXORDVE 1                   4.
POTFIELD  1    19
SETIDE   1                   0.29D0
SOLRAD   1     1
STATEPAR 1
STATETAB 1     2      3      4                     5                     6
END
FIN
CONTROL  EPHEM                    OUTPUT                                TOPEXXX  XXXXXX
OUTPUT   19    2      1      940602.0              000000.0              43200.0
ORBTYPE  2     1      11  10.0
OGOPT
DRAG     1                   1.
ATMOSDEN                 1
DRAGPAR  0
SCPARAM                      2.8D-5                2400.0D0
MAXDEGEQ 1                   50.
MAXORDEQ 1                   50.
MAXDEGVE 1                   4.
MAXORDVE 1                   4.
POTFIELD  1    19
SETIDE   1                   0.29D0
SOLRAD   1     1
OUTOPT   1                   940528000000.0        940602000000.0        120.0
END
FIN
```

Figure H.38 TAOS Cowell Five Day POE Fit Input Card Data File

```
$!-----------------------------------------------------------------
$! TAOS_POE_ITOD_DC_1
$!
$!
$!-----------------------------------------------------------------
$!
$! Set default for batch run from CSDL0:[GTDS.GTDS_TEST]
$  set default fds$diska:[ssc2414.work.new_gtds.thesis.com]
$!
$! Assign debug overrides
$!
$  assign/table=lnm$job [ssc2414.work.new_gtds.thesis.overrides]taos_poe_itod_dc_1.overrides dbg$init
$!
$! Assign the observation card file
$!
$  assign/table=lnm$job fds$diska:[ssc2414.taos.obscard]taos_poe_itod.poscard gtds$015
$!
$! Assign the body potential files
$!
$  assign/table=lnm$job fds$diska:[djf1230.bianca]dan_potential.dat gtds$047
$  assign/table=lnm$job fds$diska:[djf1230.bianca]moon.dat      gtds$048
$!
$! Assign the SLP and timing files
$!
$  assign/table=lnm$job elrond$dka0:[ssc2414]june95_msgen_slp_mn2000.dat gtds$014
$  assign/table=lnm$job elrond$dka0:[ssc2414]june95_msgen_slp_timecoef.dat gtds$038
$  assign/table=lnm$job elrond$dka0:[ssc2414]june95_msgen_slp_tod2000.dat gtds$078
$!
$! Assign ORB1 files
$!
$  assign/table=lnm$job fds$diska:[ssc2414.work.new_gtds.thesis.orb1]taos_poe_itod_dc_1.orb1 gtds$024
$!
$! Assign atmospheric density file
$!
$  assign/table=lnm$job fds$diskb:[rjp9045.jacchia]jac_real_jun95.dat   gtds$075
$!
$! Assign fundamental constants file
$!
$  assign/table=lnm$job fds$diska:[ssc2414.work.new_gtds.mods]taos_j2000_csconst.dat gtds$099
$!
$! Execute the local version of debug executable
$!
$  @[ssc2414.work.new_gtds.test]j2000_SWAT_GTDS [ssc2414.work.new_gtds.thesis.gtds]taos_poe_itod_dc_1
$  rename [-.gtds]taos_poe_itod_dc_1.output [-.output]taos_poe_itod_dc_1.output
$  assign/table=lnm$job fds_dbf:schatten_jacchia_roberts.dat gtds$075
$!
$  EXIT
```

Figure H.39 TAOS Cowell Five Day POE Fit Command Procedure

```
SET OUTPUT LOG
SET LOG
SET BREAK/return ESTSET DO -
      (DEPOSIT  IDIFF      = 3; -
       DEPOSIT  IDRVAR     = 1; -
       DEPOSIT  ISRVAR     = 0; -
       DEPOSIT  KPAR       = 0; -
       DEPOSIT  KATMOS     = 1; -
       EXAMINE  KATMOS     ; -
       EXAMINE  IDIFF      ; -
       EXAMINE  IDRVAR     ; -
       EXAMINE  ISRVAR     ; -
       EXAMINE  KPAR       ; -
       GO -
    ); -
GO
```

Figure H.40 TAOS Cowell Five Day POE Fit Overrides File

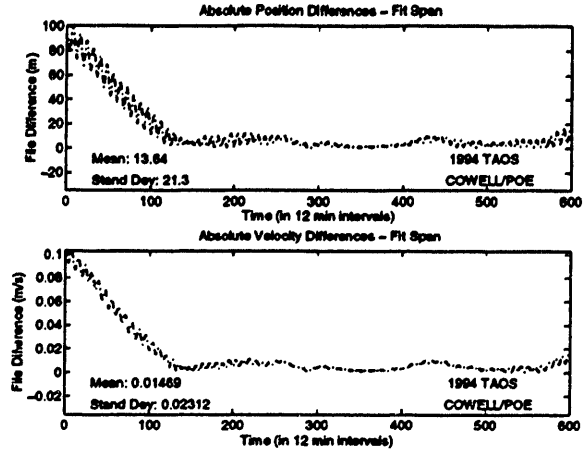

Figure H.41 TAOS Position and Velocity Errors for Cowell Five Day POE Fit

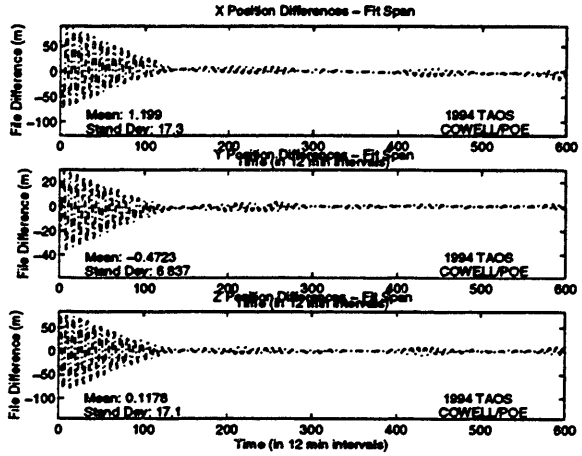

Figure H.42 TAOS Position Errors for Cowell Five Day POE Fit

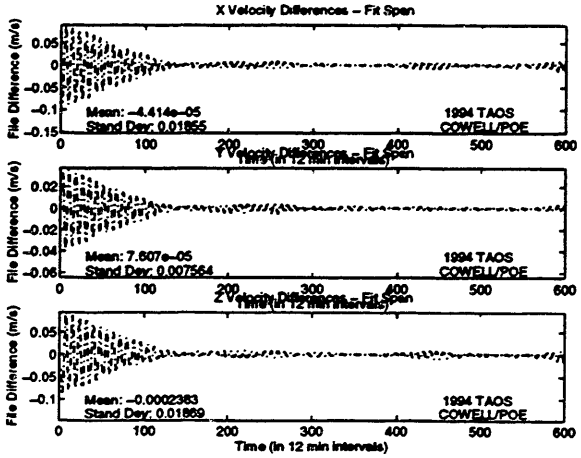

Figure H.43 TAOS Velocity Errors for Cowell Five Day POE Fit

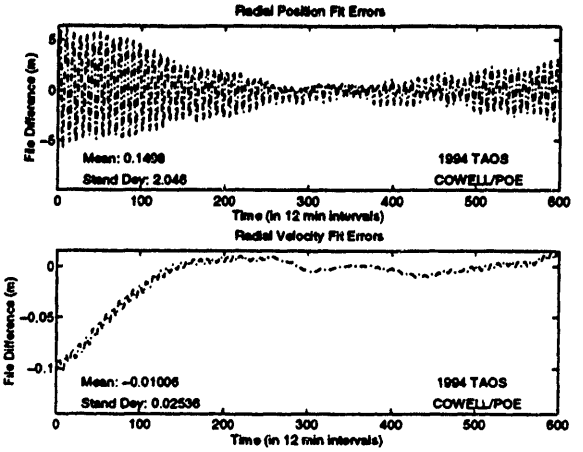

Figure H.44 TAOS Radial Errors for Cowell Five Day POE Fit

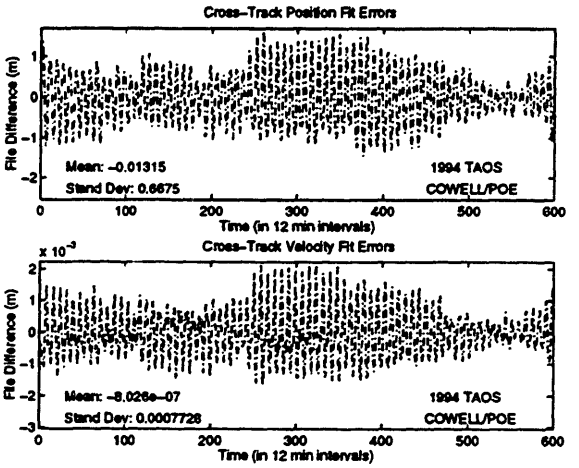

Figure H.45 TAOS Cross-Track Errors for Cowell Five Day POE Fit

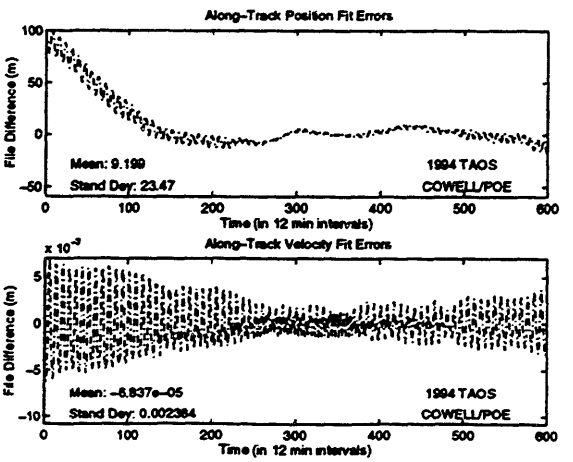

Figure H.46 TAOS Along-Track Errors for Cowell Five Day POE Fit

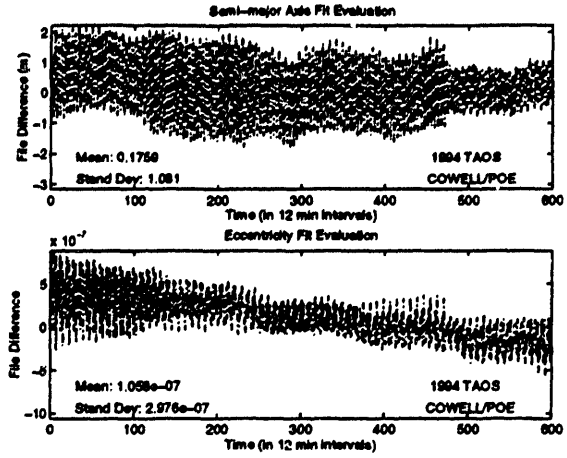

Figure H.47 TAOS *a/e* Errors for Cowell Five Day POE Fit

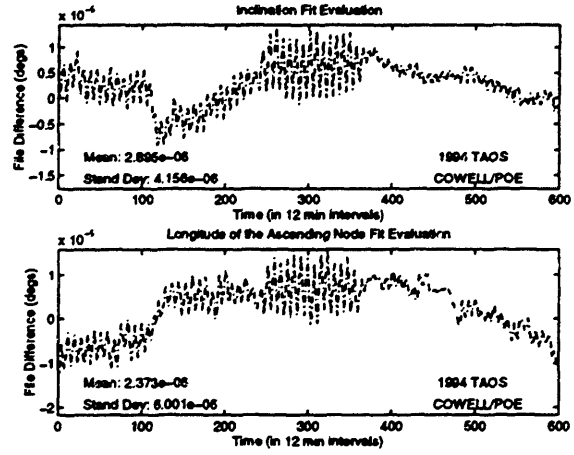

Figure H.48 TAOS *i/Ω* Errors for Cowell Five Day POE Fit

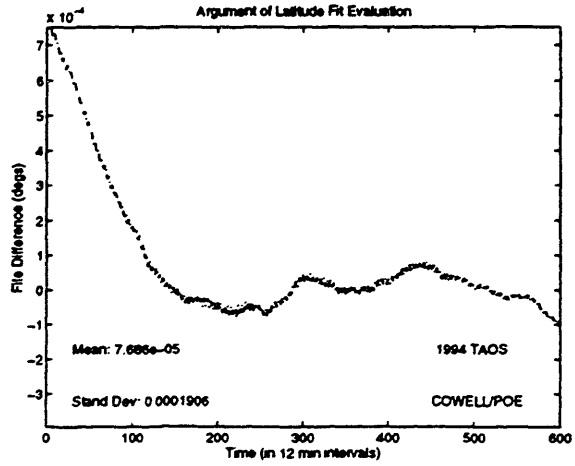

Figure H.49 TAOS Argument of Latitude Errors for Cowell Five Day POE Fit

Experiment 2: TAOS Two Day Fit of the POE Vectors

(TAOS_POE_ITOD_DC_4)

```
CONTROL  DC                                                          TAOSXXXX  XXXXXX
EPOCH                    940528.0            000000.0
ELEMENT1  12  1      1   6135.0929862214D0   -1114.1967011652D0   -3058.3210851343D0
ELEMENT2                 2.7550106887691D0   -2.7235147364250D0   6.5097125101216D0
OBSINPUT  29             940528 000000       940530 000000
ORBTYPE   2    1    11  10.0
DMOPT
OBSDEV    21             10.
OBSDEV    22             10.
OBSDEV    23             10.
OBSDEV    24             1.
OBSDEV    25             1.
OBSDEV    26             1.
END
DCOPT
PRINTOUT  1    4
CONVERG   20             1.D-4                                       1.0
END
OGOPT
DRAG      1              1.
ATMOSDEN             1
DRAGPAR   2    1         0.15D0
SCPARAM                  2.8D-5              2400.0D0
MAXDEGEQ  1              50.
MAXORDEQ  1              50.
MAXDEGVE  1              4.
MAXORDVE  1              4.
POTFIELD  1    19
SETIDE    1              0.29D0
SOLRAD    1    1
STATEPAR  1
STATETAB  1    2    3    4                   5                   6
END
FIN
CONTROL  EPHEM                OUTPUT                                 TOPEXXX  XXXXXX
OUTPUT    19   2    1    940530.0            000000.0            43200.0
ORBTYPE   2    1    11  10.0
OGOPT
DRAG      1              1.
ATMOSDEN             1
DRAGPAR   0
SCPARAM                  2.8D-5              2400.0D0
MAXDEGEQ  1              50.
MAXORDEQ  1              50.
MAXDEGVE  1              4.
MAXORDVE  1              4.
POTFIELD  1    19
SETIDE    1              0.29D0
SOLRAD    1    1
OUTOPT    1              940528000000.0      940530000000.0      120.0
END
FIN
```

Figure H.50 TAOS Cowell Two Day POE Fit Input Card Data File

```
$!-------------------------------------------------------------
$! TAOS_POE_ITOD_DC_4
$!
$!
$!-------------------------------------------------------------
$!
$! Set default for batch run from CSDL0:[GTDS.GTDS_TEST]
$  set default fds$diska:[ssc2414.work.new_gtds.thesis.com]
$!
$! Assign debug overrides
$!
$  assign/table=lnm$job [ssc2414.work.new_gtds.thesis.overrides]taos_poe_itod_dc_4.overrides dbg$init
$!
$! Assign the observation card file
$!
$  assign/table=lnm$job fds$diska:[ssc2414.taos.obscard]taos_poe_itod_2day.poscard gtds$015
$!
$! Assign the body potential files
$!
$  assign/table=lnm$job fds$diska:[djf1230.bianca]dan_potential.dat gtds$047
$  assign/table=lnm$job fds$diska:[djf1230.bianca]moon.dat      gtds$048
$!
$! Assign the SLP and timing files
$!
$  assign/table=lnm$job elrond$dka0:[ssc2414]june95_msgen_slp_mn2000.dat gtds$014
$  assign/table=lnm$job elrond$dka0:[ssc2414]june95_msgen_slp_timecoef.dat gtds$038
$  assign/table=lnm$job elrond$dka0:[ssc2414]june95_msgen_slp_tod2000.dat gtds$078
$!
$! Assign ORB1 files
$!
$  assign/table=lnm$job fds$diska:[ssc2414.work.new_gtds.thesis.orb1]taos_poe_itod_dc_4.orb1 gtds$024
$!
$! Assign atmospheric density file
$!
$  assign/table=lnm$job fds$diskb:[rjp9045.jacchia]jac_real_jun95.dat   gtds$075
$!
$! Assign fundamental constants file
$!
$  assign/table=lnm$job fds$diska:[ssc2414.work.new_gtds.mods]taos_j2000_csconst.dat gtds$099
$!
$! Execute the local version of debug executable
$!
$  @[ssc2414.work.new_gtds.test]j2000_SWAT_GTDS [ssc2414.work.new_gtds.thesis.gtds]taos_poe_itod_dc_4
$  rename [-.gtds]taos_poe_itod_dc_4.output [-.output]taos_poe_itod_dc_4.output
$  assign/table=lnm$job fds_dbf:schatten_jacchia_roberts.dat gtds$075
$!
$  EXIT
```

Figure H.51 TAOS Cowell Two Day POE Fit Command Procedure

```
SET OUTPUT LOG
SET LOG
SET BREAK/return ESTSET DO -
      (DEPOSIT  IDIFF      = 3; -
       DEPOSIT  IDRVAR     = 1; -
       DEPOSIT  ISRVAR     = 0; -
       DEPOSIT  KPAR       = 0; -
       DEPOSIT  KATMOS     = 1; -
       EXAMINE  KATMOS     ; -
       EXAMINE  IDIFF      ; -
       EXAMINE  IDRVAR     ; -
       EXAMINE  ISRVAR     ; -
       EXAMINE  KPAR       ; -
       GO -
    ); -
GO
```

Figure H.52 TAOS Cowell Two Day POE Fit Overrides File

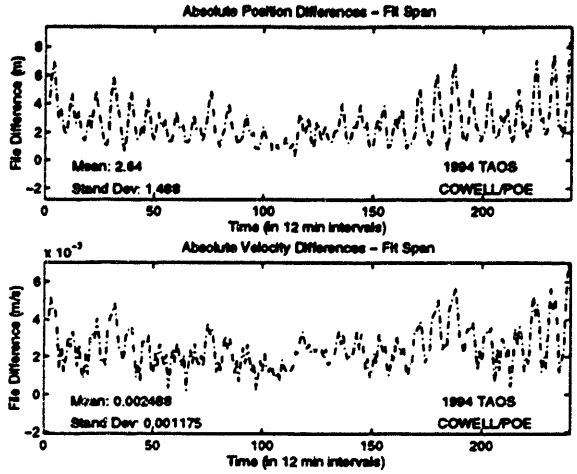

Figure H.53 TAOS Position and Velocity Errors for Cowell Two Day POE Fit

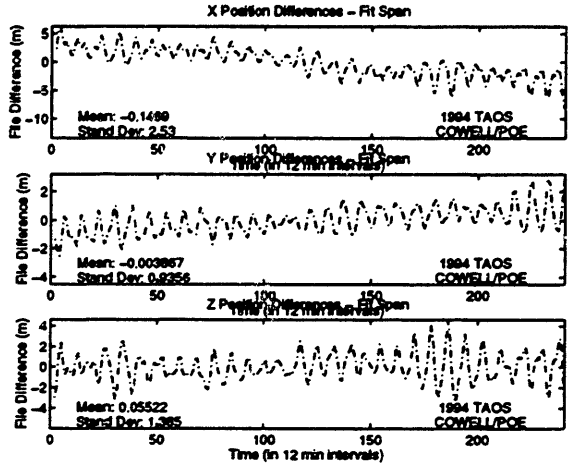

Figure H.54 TAOS Position Errors for Cowell Two Day POE Fit

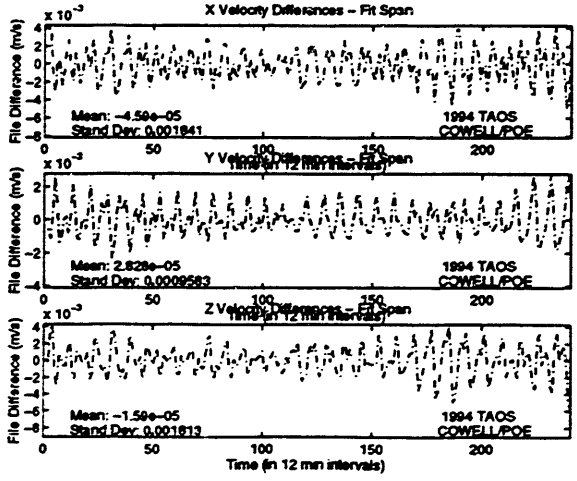

Figure H.55 TAOS Velocity Errors for Cowell Two Day POE Fit

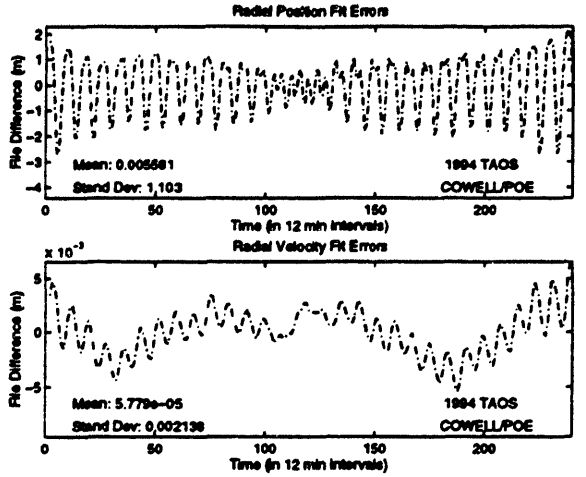

Figure H.56 TAOS Radial Errors for Cowell Two Day POE Fit

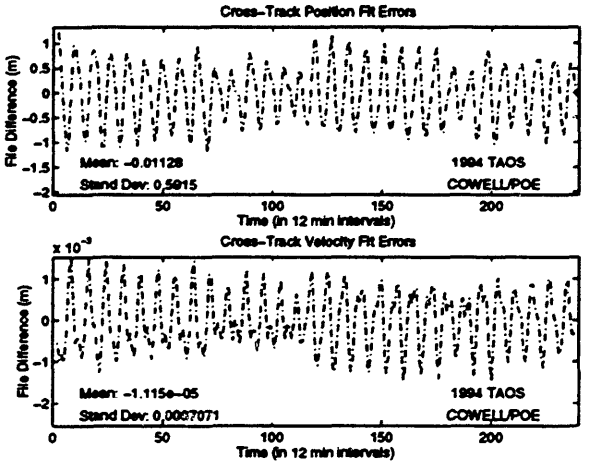

Figure H.57 TAOS Cross-Track Errors for Cowell Two Day POE Fit

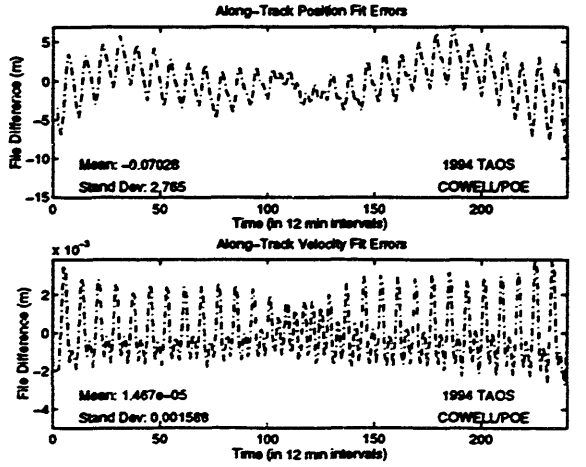

Figure H.58 TAOS Along-Track Errors for Cowell Two Day POE Fit

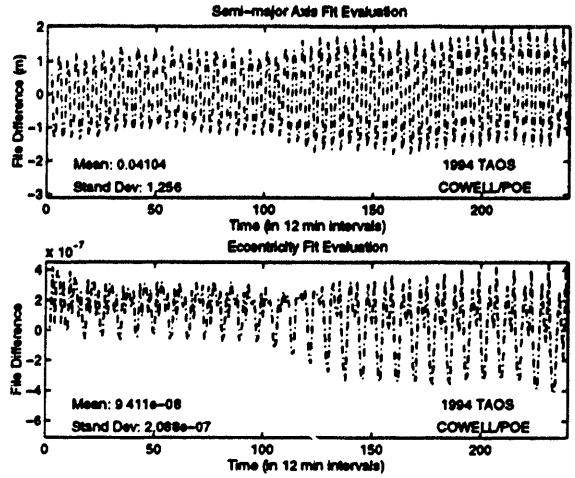

Figure H.59 TAOS *a/e* Errors for Cowell Two Day POE Fit

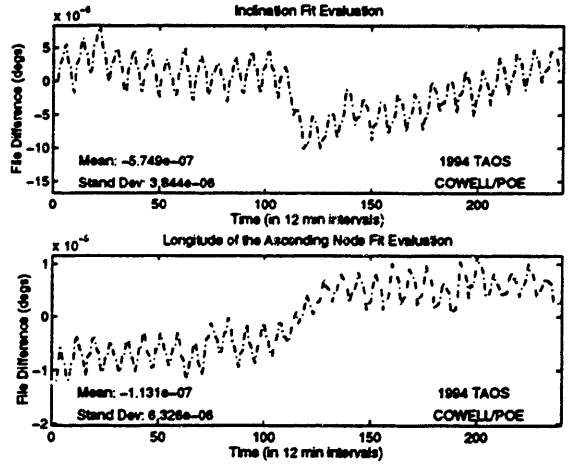

Figure H.60 TAOS *i/Ω* Errors for Cowell Two Day POE Fit

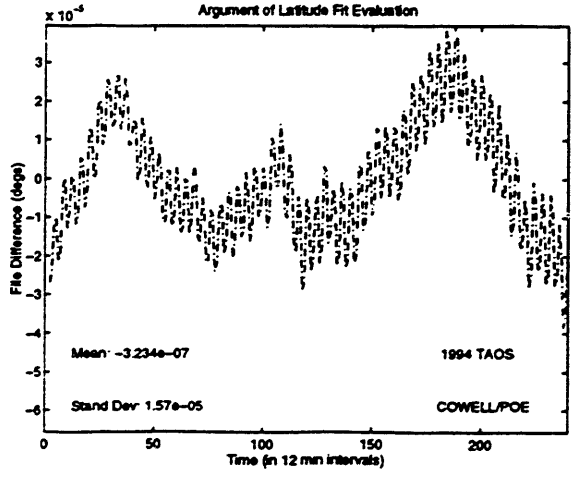

Figure H.61 TAOS Argument of Latitude Errors for Cowell Two Day POE Fit

Experiment 3: TAOS One Day Fit of the POE Vectors (TAOS_POE_ITOD_DC_5)

```
CONTROL  DC                                                          TAOSXXXX  XXXXXX
EPOCH                    940528.0              000000.0
ELEMENT1  12  1      1   6135.0929862214D0     -1114.1967011652D0    -3058.3210851343D0
ELEMENT2                 2.7550106887691D0     -2.7235147364250D0    6.5097125101216D0
OBSINPUT  29             940528 000000         940529 000000
ORBTYPE   2    1    11  10.0
DMOPT
OBSDEV    21             10.
OBSDEV    22             10.
OBSDEV    23             10.
OBSDEV    24             1.
OBSDEV    25             1.
OBSDEV    26             1.
END
DCOPT
PRINTOUT  1    4
CONVERG   20             1.D-4                                       1.0
END
OGOPT
DRAG      1              1.
ATMOSDEN             1
DRAGPAR   2    1         0.15D0
SCPARAM                  2.8D-5                2400.0D0
MAXDEGEQ  1              50.
MAXORDEQ  1              50.
MAXDEGVE  1              4.
MAXORDVE  1              4.
POTFIELD  1    19
SETIDE    1              0.29D0
SOLRAD    1    1
STATEPAR  1
STATETAB  1    2    3    4                     5                     6
END
FIN
CONTROL  EPHEM                OUTPUT                                 TOPEXXX  XXXXXX
OUTPUT    19   2    1    940529.0              000000.0              43200.0
ORBTYPE   2    1    11  10.0
OGOPT
DRAG      1              1.
ATMOSDEN             1
DRAGPAR   0
SCPARAM                  2.8D-5                2400.0D0
MAXDEGEQ  1              50.
MAXORDEQ  1              50.
MAXDEGVE  1              4.
MAXORDVE  1              4.
POTFIELD  1    19
SETIDE    1              0.29D0
SOLRAD    1    1
OUTOPT    1              940528000000.0        940529000000.0        120.0
END
FIN
```

Figure H.62 TAOS Cowell One Day POE Fit Input Card Data File

```
$!-------------------------------------------------------------
$! TAOS_POE_ITOD_DC_5
$!
$!
$!-------------------------------------------------------------
$!
$! Set default for batch run from CSDL0:[GTDS.GTDS_TEST]
$  set default fds$diska:[ssc2414.work.new_gtds.thesis.com]
$!
$! Assign debug overrides
$!
$  assign/table=lnm$job [ssc2414.work.new_gtds.thesis.overrides]taos_poe_itod_dc_5.overrides dbg$init
$!
$! Assign the observation card file
$!
$  assign/table=lnm$job fds$diska:[ssc2414.taos.obscard]taos_poe_itod_1day.poscard gtds$015
$!
$! Assign the body potential files
$!
$  assign/table=lnm$job fds$diska:[djf1230.bianca]dan_potential.dat gtds$047
$  assign/table=lnm$job fds$diska:[djf1230.bianca]moon.dat      gtds$048
$!
$! Assign the SLP and timing files
$!
$  assign/table=lnm$job elrond$dka0:[ssc2414]june95_msgen_slp_mn2000.dat gtds$014
$  assign/table=lnm$job elrond$dka0:[ssc2414]june95_msgen_slp_timecoef.dat gtds$038
$  assign/table=lnm$job elrond$dka0:[ssc2414]june95_msgen_slp_tod2000.dat gtds$078
$!
$! Assign ORB1 files
$!
$  assign/table=lnm$job fds$diska:[ssc2414.work.new_gtds.thesis.orb1]taos_poe_itod_dc_5.orb1 gtds$024
$!
$! Assign atmospheric density file
$!
$  assign/table=lnm$job fds$diskb:[rjp9045.jacchia]jac_real_jun95.dat   gtds$075
$!
$! Assign fundamental constants file
$!
$  assign/table=lnm$job fds$diska:[ssc2414.work.new_gtds.mods]taos_j2000_csconst.dat gtds$099
$!
$! Execute the local version of debug executable
$!
$  @[ssc2414.work.new_gtds.test]j2000_SWAT_GTDS [ssc2414.work.new_gtds.thesis.gtds]taos_poe_itod_dc_5
$  rename [-.gtds]taos_poe_itod_dc_5.output [-.output]taos_poe_itod_dc_5.output
$  assign/table=lnm$job fds_dbf:schatten_jacchia_roberts.dat gtds$075
$!
$  EXIT
```

Figure H.63 TAOS Cowell One Day POE Fit Command Procedure

```
SET OUTPUT LOG
SET LOG
SET BREAK/return ESTSET DO -
      (DEPOSIT  IDIFF      = 3; -
       DEPOSIT  IDRVAR     = 1; -
       DEPOSIT  ISRVAR     = 0; -
       DEPOSIT  KPAR       = 0; -
       DEPOSIT  KATMOS     = 1; -
       EXAMINE  KATMOS     ; -
       EXAMINE  IDIFF      ; -
       EXAMINE  IDRVAR     ; -
       EXAMINE  ISRVAR     ; -
       EXAMINE  KPAR       ; -
       GO -
    ); -
GO
```

Figure H.64 TAOS Cowell One Day POE Fit Overrides File

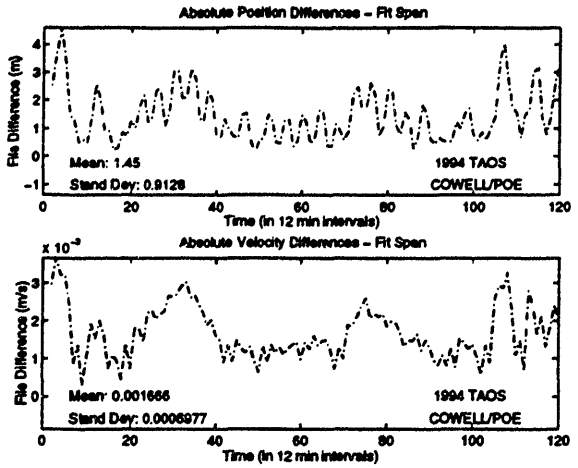

Figure H.65 TAOS Position and Velocity Errors for Cowell One Day POE Fit

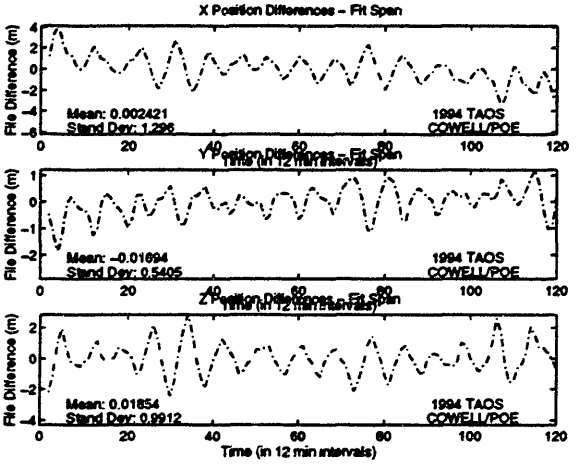

Figure H.66 TAOS Position Errors for Cowell One Day POE Fit

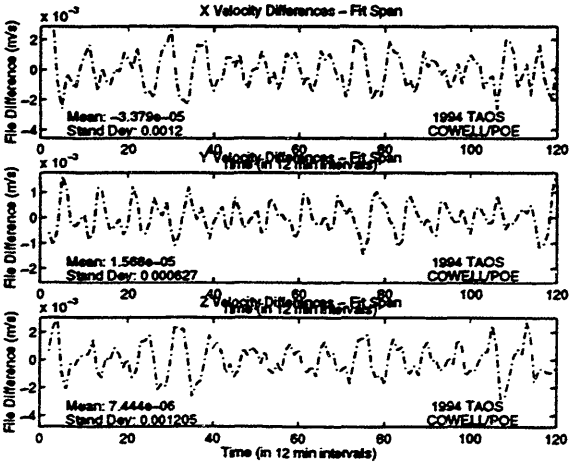

Figure H.67 TAOS Velocity Errors for Cowell One Day POE Fit

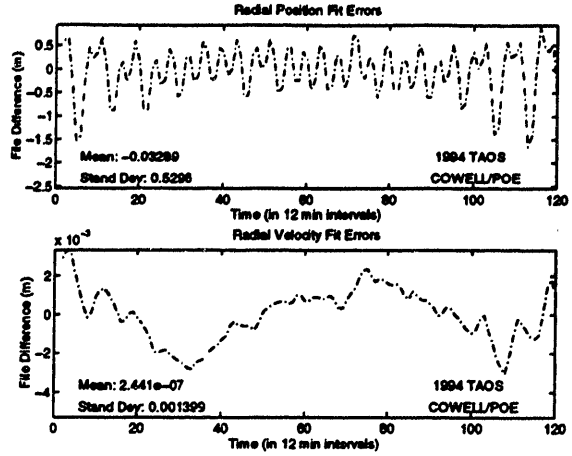

Figure H.68 TAOS Radial Errors for Cowell One Day POE Fit

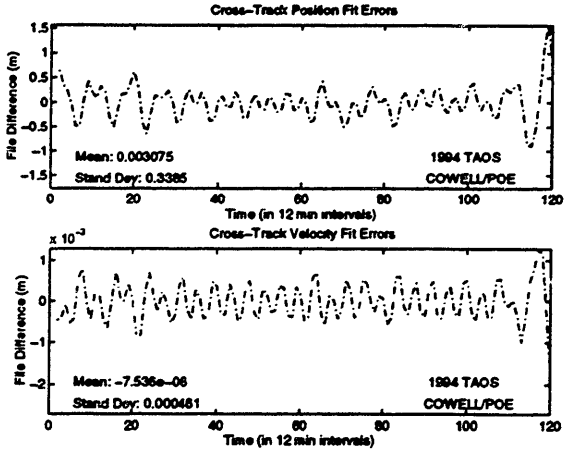

Figure H.69 TAOS Cross-Track Errors for Cowell One Day POE Fit

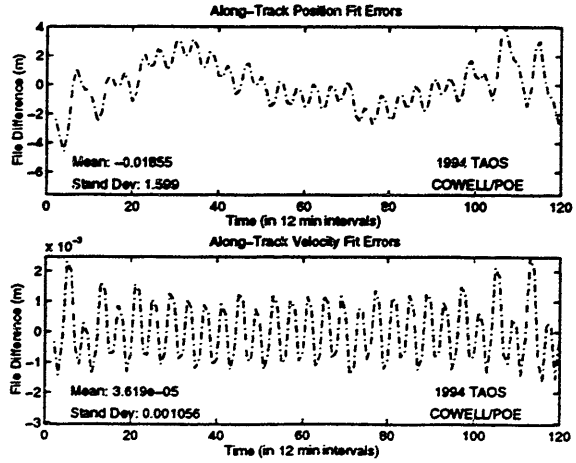

Figure H.70 TAOS Along-Track Errors for Cowell One Day POE Fit

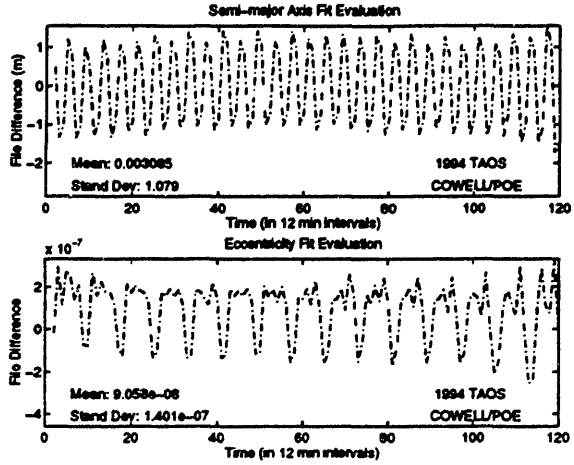

Figure H.71 TAOS *a/e* Errors for Cowell One Day POE Fit

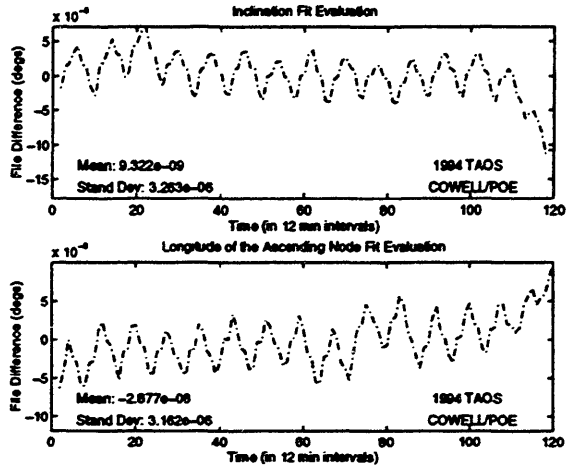

Figure H.72 TAOS *i/Ω* Errors for Cowell One Day POE Fit

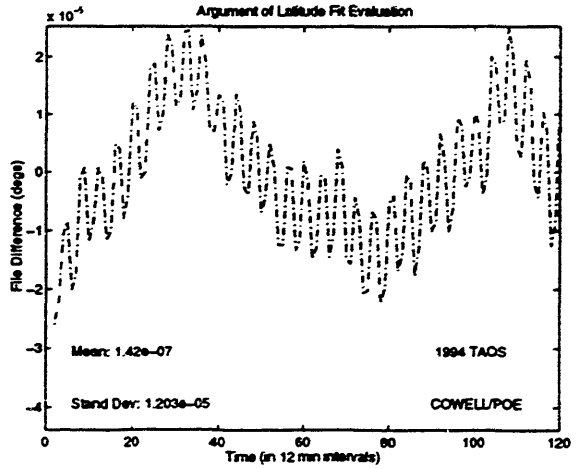

Figure H.73 TAOS Argument of Latitude Errors for Cowell One Day POE Fit

H.2.2 Orbit Determination from the TAOS Navigation Solutions

After the TAOS POEs were fit to provide an indication of the process noise associated with the differential correction fit, the use of navigation solutions for a drag-perturbed satellite was evaluated for TAOS. The POE fits indicated the susceptibility of the drag parameter to become mismodeled over long periods of time (five days), while shorter periods (one to two days) may not capture the essence of the geomagnetic level during the predictions. Because of the fit and prediction accuracies' heavy dependence upon the fit span length, three intervals were initially tested over four experiments with the Schatten-Jacchia-Roberts atmospheric model. The first three experiments were one, two and three days in fit span duration using Cowell techniques, and possessed the same modeling as the POE fits. The fourth experiment was a replica of the three day fit using semianalytic theory with a setup described in Chapter 5. These experiments are summarized below in Table H.5.

Table H.5 TAOS Navigation Solution Experiments

Case	Description	References in Appendix H
1	Cowell one day fit of TAOS navigation solutions with three day prediction; Schatten file used	Figures: H.74-H.85
2	Cowell two day fit of TAOS navigation solutions with two day prediction; Schatten file used	Figures: H.86-H.97
3	Cowell three day fit of TAOS navigation solutions with one day prediction; Schatten file used	Figures: H.98-H.109
4	SST three day fit of TAOS navigation solutions with one day prediction; Schatten file used	Figures: H.108-H.121
5	Cowell three day fit of TAOS navigation solutions with one day prediction; Near-real time density file used	Figures: H.122-H.133
6	SST three day fit of TAOS navigation solutions with one day prediction; Near-real time density file used	Figures: H.134-H.145

Experiment 1: TAOS One Day Fit of the Navigation Solutions (TAOS_NAV_COWELL_FIT_4)

```
CONTROL  DC                                                          TAOSXXXX  XXXXXX
EPOCH                    940528.0                 000000.0
ELEMENT1 10   1    1     -1550.6273944874D0       6039.5657891884D0  -3058.3210851343D0
ELEMENT2                 1.76398296192709D0       3.7539218851281D0  6.5097125101215SD0
OBSINPUT 20              940528 000950            940529 000950
ORBTYPE  2    1    11    10.0
DMOPT
OBSDEV   21              50.
OBSDEV   22              50.
OBSDEV   23              50.
OBSDEV   24              100.
OBSDEV   25              75.
OBSDEV   26              125.
END
DCOPT
PRINTOUT 1    4
CONVERG  20              1.D-4                                       1.0
END
OGOPT
DRAG     1               1.
ATMOSDEN          1
DRAGPAR  2    1          0.15D0
SCPARAM                  2.8D-5                   2400.0D0
MAXDEGEQ 1               50.
MAXORDEQ 1               50.
MAXDEGVE 1               4.
MAXORDVE 1               4.
POTFIELD 1    19
SETIDE   1               0.29D0
SOLRAD   1               1
STATEPAR 1
STATETAB 1    2    3     4                        5                  6
END
FIN
CONTROL  EPHEM                    OUTPUT                             TOPEXXX  XXXXXX
OUTPUT   19   2    1     940601.0                 000000.0           43200.0
ORBTYPE  2    1    11    10.0
OGOPT
DRAG     1               1.
ATMOSDEN          1
DRAGPAR  0
SCPARAM                  2.8D-5                   2400.0D0
MAXDEGEQ 1               50.
MAXORDEQ 1               50.
MAXDEGVE 1               4.
MAXORDVE 1               4.
POTFIELD 1    19
SETIDE   1               0.29D0
SOLRAD   1               1
OUTOPT   1               940528000200.0           940601000000.0     120.0
END
FIN
```

Figure H.74 TAOS Cowell One Day Navigation Solution Fit Input Card Data File

```
$!-------------------------------------------------------------
$! TAOS_NAV_COWELL_FIT_4
$!
$!
$!-------------------------------------------------------------
$!
$! Set default for batch run from CSDL0:[GTDS.GTDS_TEST]
$  set default fds$diska:[ssc2414.work.new_gtds.thesis.com]
$!
$! Assign debug overrides
$!
$  assign/table=lnm$job [ssc2414.work.new_gtds.thesis.overrides]taos_nav_cowell_fit_4.overrides dbg$init
$!
$! Assign the observation card file
$!
$  assign/table=lnm$job fds$diska:[ssc2414.taos.obscard]148.poscard gtds$015
$!
$! Assign the body potential files
$!
$  assign/table=lnm$job fds$diska:[djf1230.bianca]dan_potential.dat gtds$047
$  assign/table=lnm$job fds$diska:[djf1230.bianca]moon.dat     gtds$048
$!
$! Assign the SLP and timing files
$!
$  assign/table=lnm$job elrond$dka0:[ssc2414]june95_msgen_slp_mn2000.dat gtds$014
$  assign/table=lnm$job elrond$dka0:[ssc2414]june95_msgen_slp_timecoef.dat gtds$038
$  assign/table=lnm$job elrond$dka0:[ssc2414]june95_msgen_slp_tod2000.dat gtds$078
$!
$! Assign ORB1 files
$!
$  assign/table=lnm$job fds$diska:[ssc2414.work.new_gtds.thesis.orb1]taos_nav_cowell_fit_4.orb1 gtds$024
$!
$! Assign atmospheric density files
$!
$  assign/table=lnm$job fds_dbf:schatten_jacchia_roberts.dat  gtds$075
$!
$! Assign fundamental constants file
$!
$  assign/table=lnm$job fds$diska:[ssc2414.work.new_gtds.mods]taos_j2000_csconst.dat gtds$099
$!
$! Execute the local version of debug executable
$!
$  @[ssc2414.work.new_gtds.test]j2000_SWAT_GTDS [ssc2414.work.new_gtds.thesis.gtds]taos_nav_cowell_fit_4
$  rename [-.gtds]taos_nav_cowell_fit_4.output [-.output]taos_nav_cowell_fit_4.output
$!
$  assign/table=lnm$job fds_dbf:schatten_jacchia_roberts.dat gtds$075
$  EXIT
```

Figure H.75 TAOS Cowell One Day Navigation Solution Fit Command Procedure

```
SET OUTPUT LOG
SET LOG
SET BREAK/return ESTSET DO -
      (DEPOSIT  IDIFF      = 3; -
       DEPOSIT  IDRVAR     = 1; -
       DEPOSIT  ISRVAR     = 0; -
       DEPOSIT  KPAR       = 0; -
       DEPOSIT  KATMOS     = 1; -
       EXAMINE  KATMOS     ; -
       EXAMINE  IDIFF      ; -
       EXAMINE  IDRVAR     ; -
       EXAMINE  ISRVAR     ; -
       EXAMINE  KPAR       ; -
       GO -
    ); -
GO
```

Figure H.76 TAOS Cowell One Day Navigation Solution Fit Overrides File

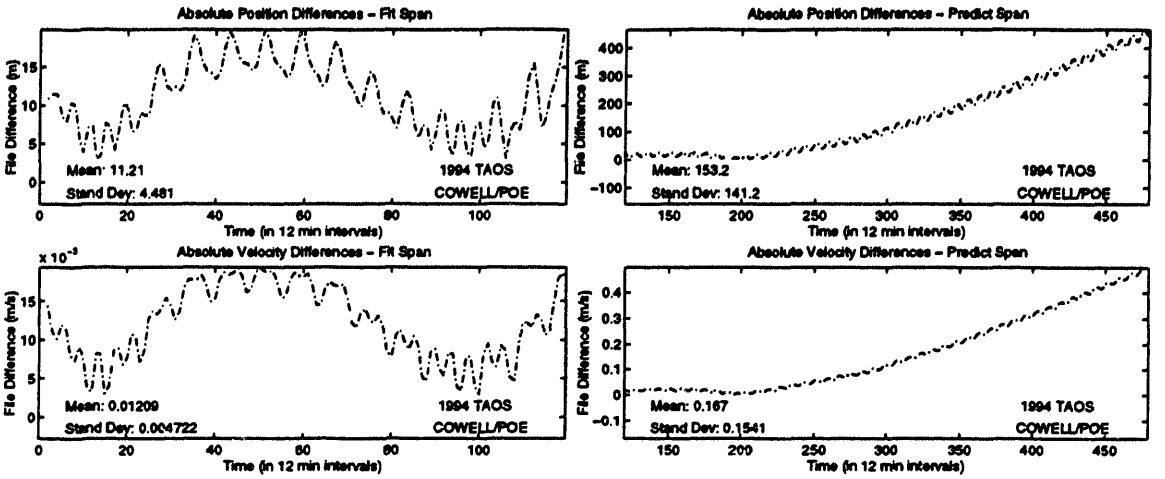

Figure H.77 TAOS Position and Velocity Errors for Cowell One Day Fit and Three Day Predict Using Navigation Solutions

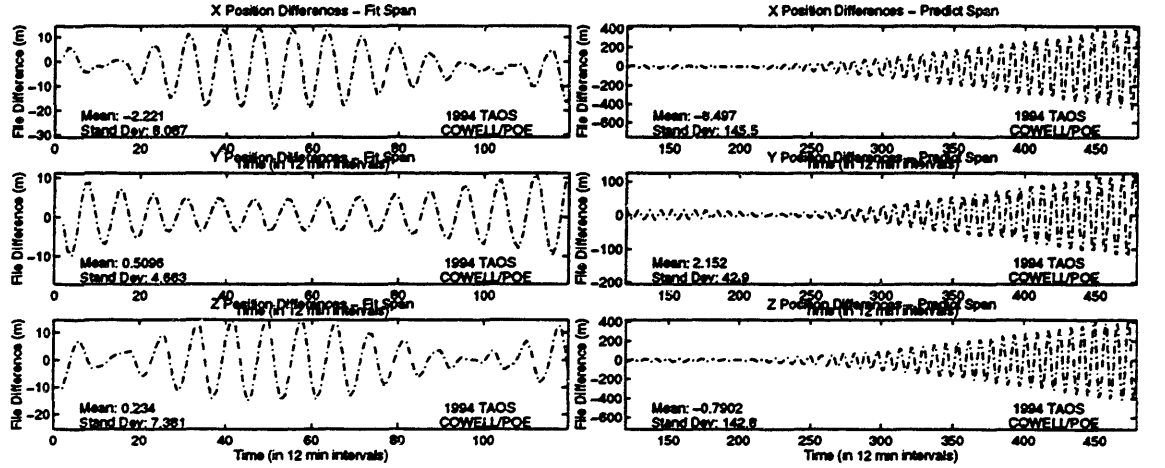

Figure H.78 TAOS Position Errors for Cowell One Day Fit and Three Day Predict Using Navigation Solutions

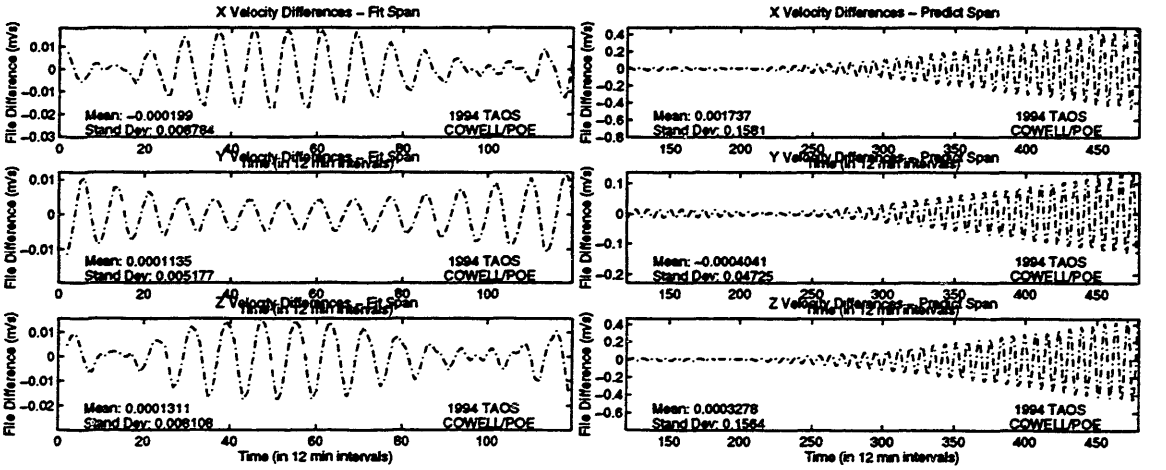

Figure H.79 TAOS Velocity Errors for Cowell One Day Fit and Three Day Predict Using Navigation Solutions

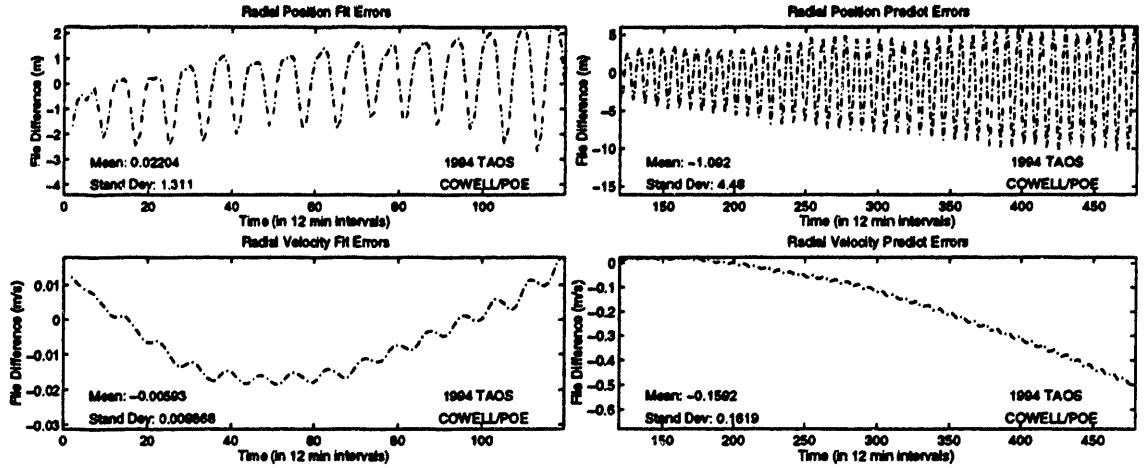

Figure H.80 TAOS Radial Errors for Cowell One Day Fit and Three Day Predict Using Navigation Solutions

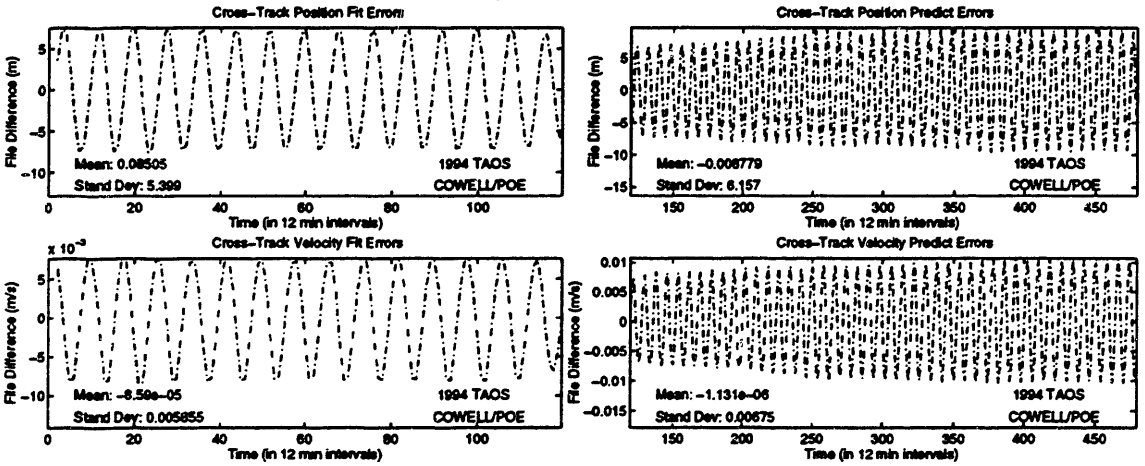

Figure H.81 TAOS Cross-Track Errors for Cowell One Day Fit and Three Day Predict Using Navigation Solutions

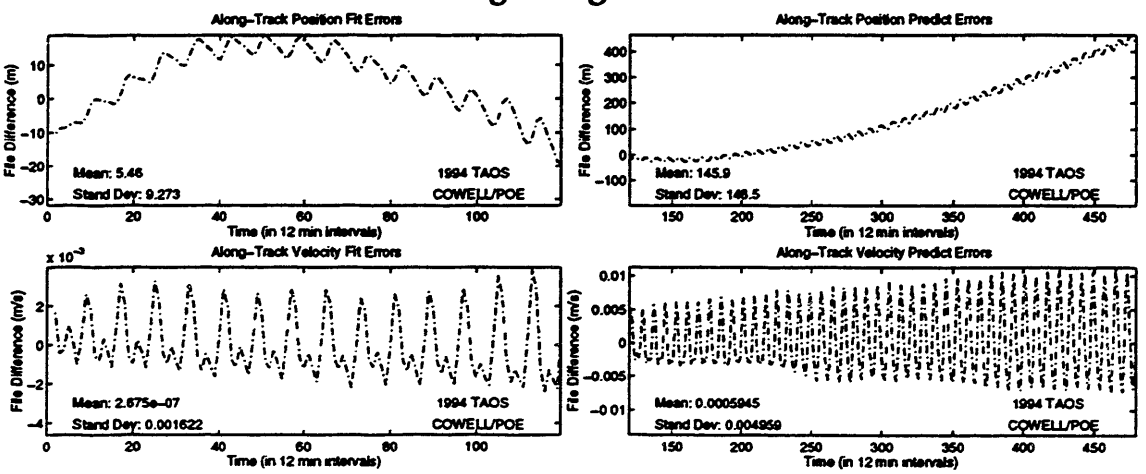

Figure H.82 TAOS Along-Track Errors for Cowell One Day Fit and Three Day Predict Using Navigation Solutions

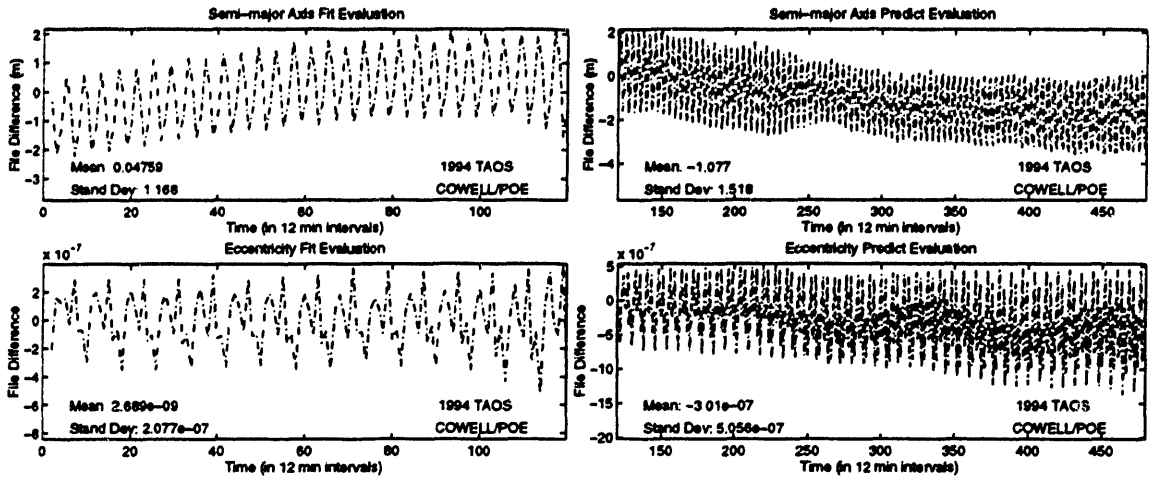

Figure H.83 TAOS *a/e* Errors for Cowell One Day Fit and Three Day Predict Using Navigation Solutions

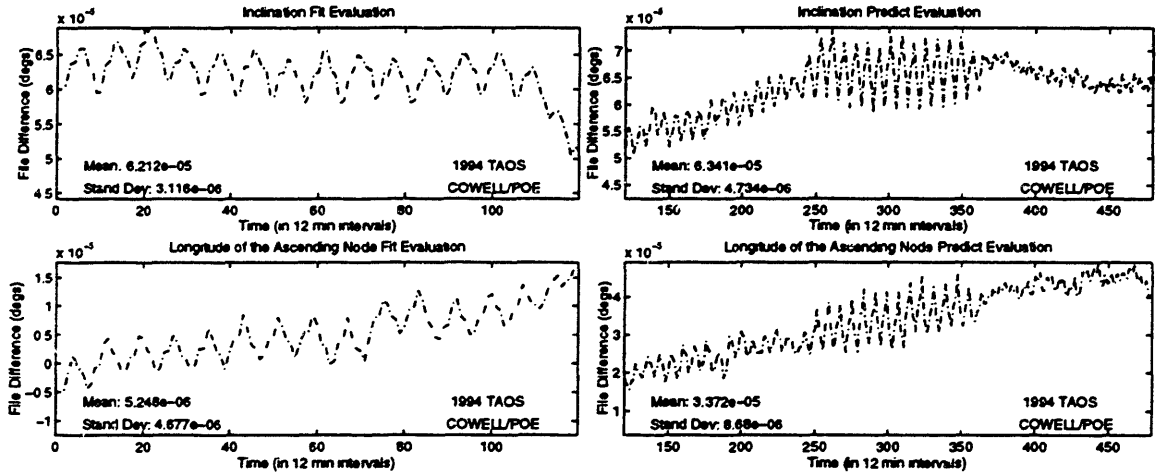

Figure H.84 TAOS i/Ω Errors for Cowell One Day Fit and Three Day Predict Using Navigation Solutions

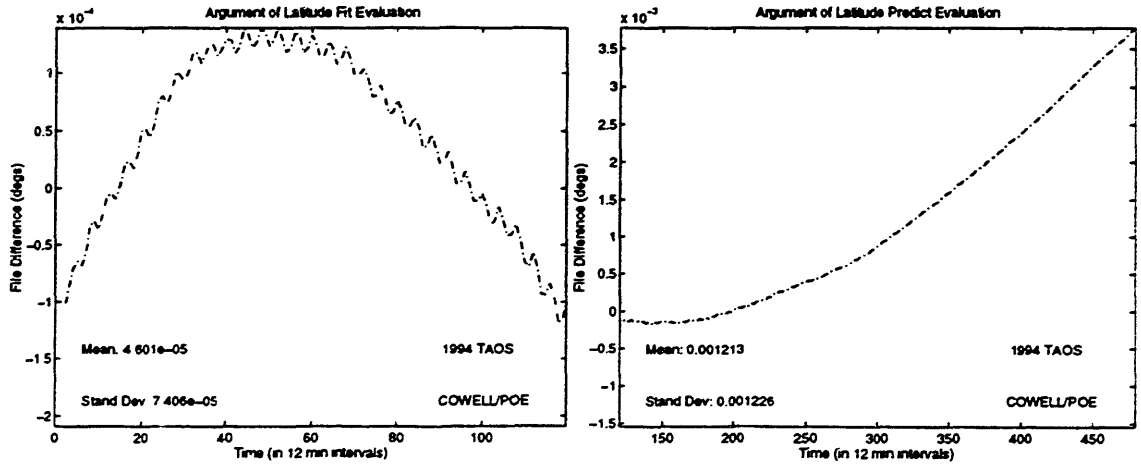

Figure H.85 TAOS Argument of Latitude Errors for Cowell One Day Fit and Three Day Predict Using Navigation Solutions

Experiment 2: TAOS Two Day Fit of the Navigation Solutions (TAOS_NAV_COWELL_FIT_6)

```
CONTROL  DC                                                          TAOSXXXX  XXXXXX
EPOCH                        940528.0                 000000.0
ELEMENT1  10    1     1      -1550.6273944874D0       6039.5657891884D0       -3058.3210851343D0
ELEMENT2                     1.76398296192709D0       3.7539218851281D0       6.50971251012155D0
OBSINPUT  20                 940528 000950            940530 000950
ORBTYPE   2     1     11     10.0
DMOPT
OBSDEV    21                 50.
OBSDEV    22                 50.
OBSDEV    23                 50.
OBSDEV    24                 100.
OBSDEV    25                 75.
OBSDEV    26                 125.
END
DCOPT
PRINTOUT  1     4
CONVERG   20                 1.D-4                                   1.0
END
OGOPT
DRAG      1                  1.
ATMOSDEN                1
DRAGPAR   2     1            0.15D0
SCPARAM                      2.8D-5                  2400.0D0
MAXDEGEQ  1                  50.
MAXORDEQ  1                  50.
MAXDEGVE  1                  4.
MAXORDVE  1                  4.
POTFIELD  1     19
SETIDE    1                  0.29D0
SOLRAD    1                  1
STATEPAR  1
STATETAB  1     2     3      4                       5                       6
END
FIN
CONTROL  EPHEM                      OUTPUT                                   TOPEXXX  XXXXXX
OUTPUT    19    2     1      940601.0                 000000.0                43200.0
ORBTYPE   2     1     11     10.0
OGOPT
DRAG      1                  1.
ATMOSDEN                1
DRAGPAR   0
SCPARAM                      2.8D-5                  2400.0D0
MAXDEGEQ  1                  50.
MAXORDEQ  1                  50.
MAXDEGVE  1                  4.
MAXORDVE  1                  4.
POTFIELD  1     19
SETIDE    1                  0.29D0
SOLRAD    1                  1
OUTOPT    1                  940528000200.0           940601000000.0          120.0
END
FIN
```

Figure H.86 TAOS Cowell Two Day Navigation Solution Fit Input Card Data File

```
$!-------------------------------------------------------------
$! TAOS_NAV_COWELL_FIT_4
$!
$!
$!-------------------------------------------------------------
$!
$! Set default for batch run from CSDL0:[GTDS.GTDS_TEST]
$  set default fds$diska:[ssc2414.work.new_gtds.thesis.com]
$!
$! Assign debug overrides
$!
$  assign/table=lnm$job [ssc2414.work.new_gtds.thesis.overrides]taos_nav_cowell_fit_6.overrides dbg$init
$!
$! Assign the observation card file
$!
$  assign/table=lnm$job fds$diska:[ssc2414.taos.obscard]148-149.poscard gtds$015
$!
$! Assign the body potential files
$!
$  assign/table=lnm$job fds$diska:[djf1230.bianca]dan_potential.dat gtds$047
$  assign/table=lnm$job fds$diska:[djf1230.bianca]moon.dat     gtds$048
$!
$! Assign the SLP and timing files
$!
$  assign/table=lnm$job elrond$dka0:[ssc2414]june95_magen_slp_mn2000.dat gtds$014
$  assign/table=lnm$job elrond$dka0:[ssc2414]june95_magen_slp_timecoef.dat gtds$038
$  assign/table=lnm$job elrond$dka0:[ssc2414]june95_magen_slp_tod2000.dat gtds$078
$!
$! Assign ORB1 files
$!
$  assign/table=lnm$job fds$diska:[ssc2414.work.new_gtds.thesis.orb1]taos_nav_cowell_fit_6.orb1 gtds$024
$!
$! Assign atmospheric density files
$!
$  assign/table=lnm$job fds_dbf:schatten_jacchia_roberts.dat  gtds$075
$!
$! Assign fundamental constants file
$!
$  assign/table=lnm$job fds$diska:[ssc2414.work.new_gtds.mods]taos_j2000_cscnst.dat gtds$099
$!
$! Execute the local version of debug executable
$!
$  @[ssc2414.work.new_gtds.test]j2000_SWAT_GTDS [ssc2414.work.new_gtds.thesis.gtds]taos_nav_cowell_fit_6
$  rename [-.gtds]taos_nav_cowell_fit_6.output [-.output]taos_nav_cowell_fit_6.output
$!
$  assign/table=lnm$job fds_dbf:schatten_jacchia_roberts.dat gtds$075
$  EXIT
```

Figure H.87 TAOS Cowell Two Day Navigation Solution Fit Command Procedure

```
SET OUTPUT LOG
SET LOG
SET BREAK/return ESTSET DO -
      (DEPOSIT  IDIFF      = 3; -
       DEPOSIT  IDRVAR     = 1; -
       DEPOSIT  ISRVAR     = 0; -
       DEPOSIT  KPAR       = 0; -
       DEPOSIT  KATMOS     = 1; -
       EXAMINE  KATMOS     ; -
       EXAMINE  IDIFF      ; -
       EXAMINE  IDRVAR     ; -
       EXAMINE  ISRVAR     ; -
       EXAMINE  KPAR       ; -
       GO -
    ): -
GO
```

Figure H.88 TAOS Cowell Two Day Navigation Solution Fit Overrides File

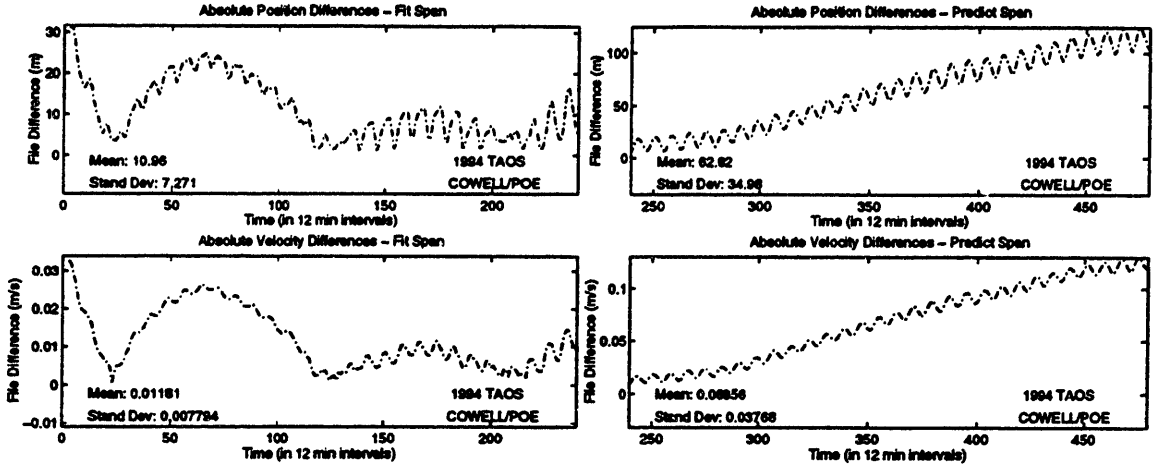

Figure H.89 TAOS Position and Velocity Errors for Cowell Two Day Fit and Two Day Predict Using Navigation Solutions

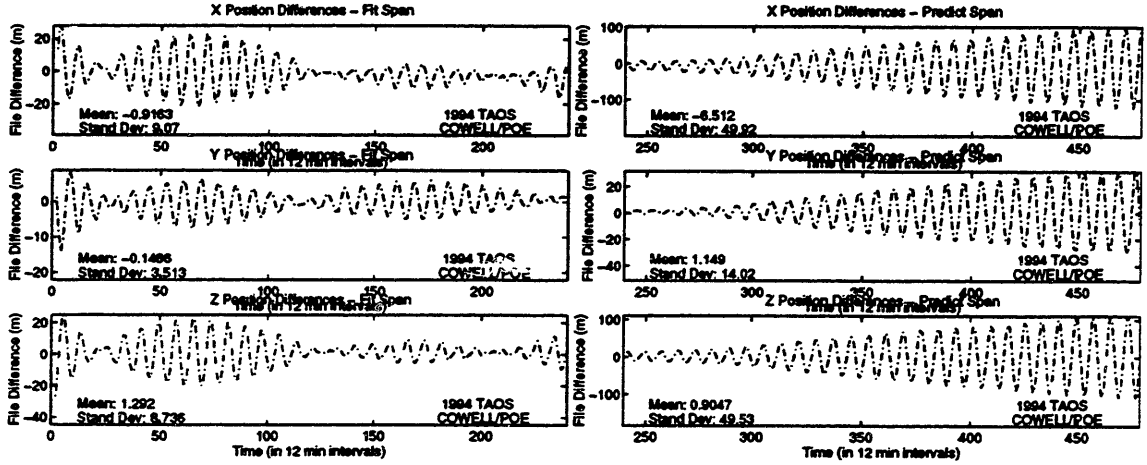

Figure H.90 TAOS Position Errors for Cowell Two Day Fit and Two Day Predict Using Navigation Solutions

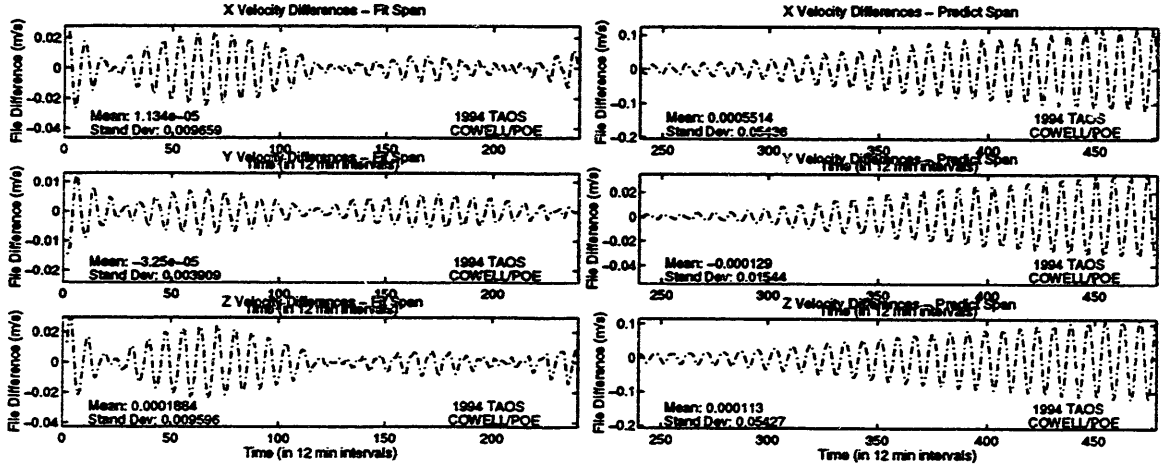

Figure H.91 TAOS Velocity Errors for Cowell Two Day Fit and Two Day Predict Using Navigation Solutions

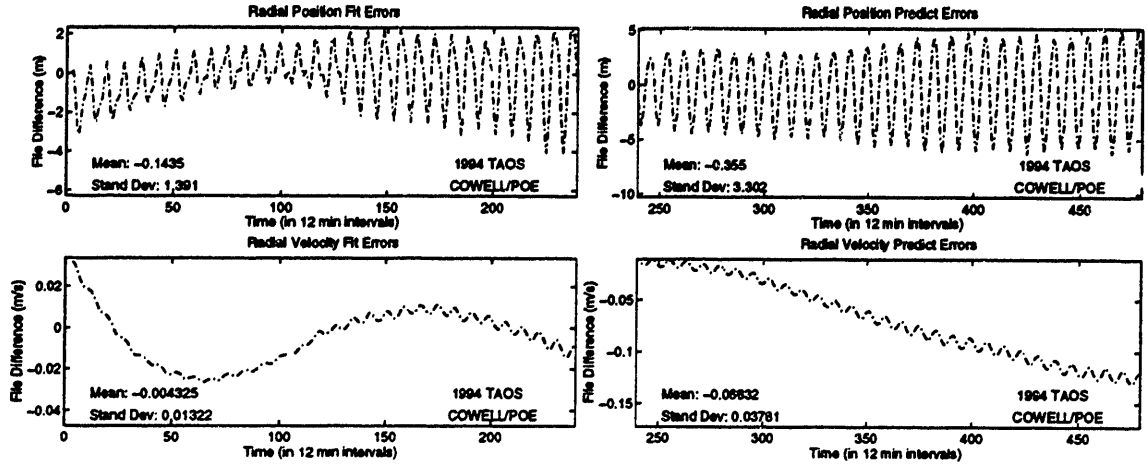

Figure H.92 TAOS Radial Errors for Cowell Two Day Fit and Two Day Predict Using Navigation Solutions

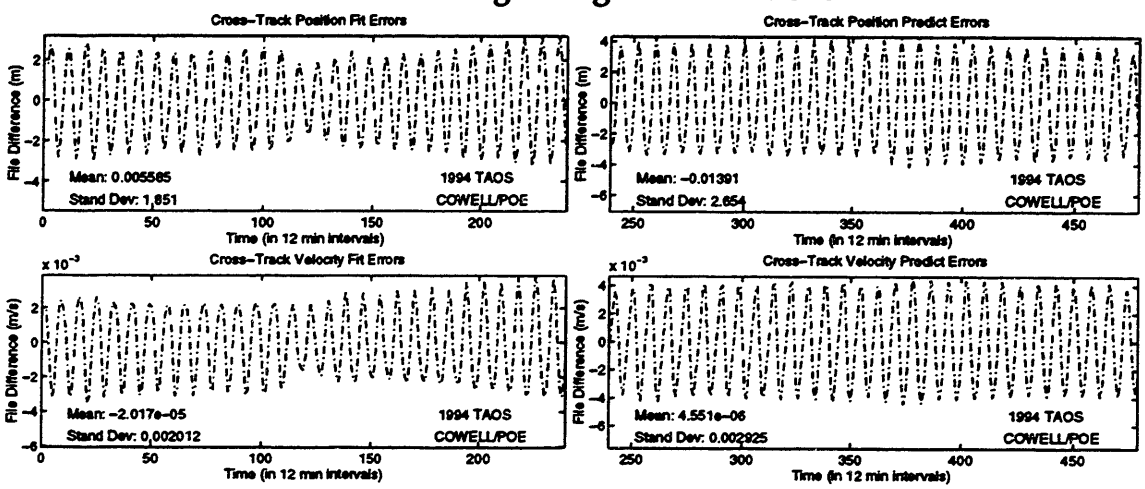

Figure H.93 TAOS Cross-Track Errors for Cowell Two Day Fit and Two Day Predict Using Navigation Solutions

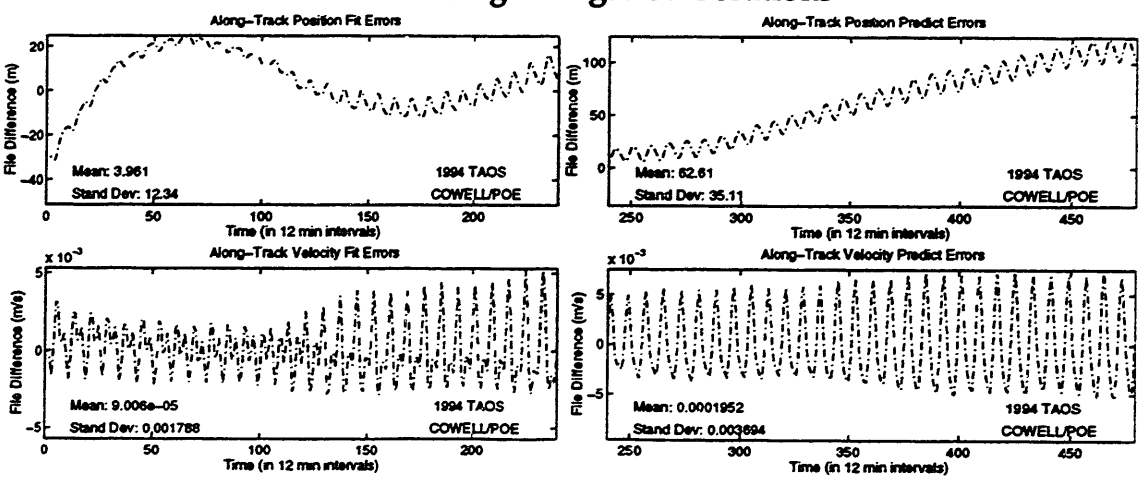

Figure H.94 TAOS Along-Track Errors for Cowell Two Day Fit and Two Day Predict Using Navigation Solutions

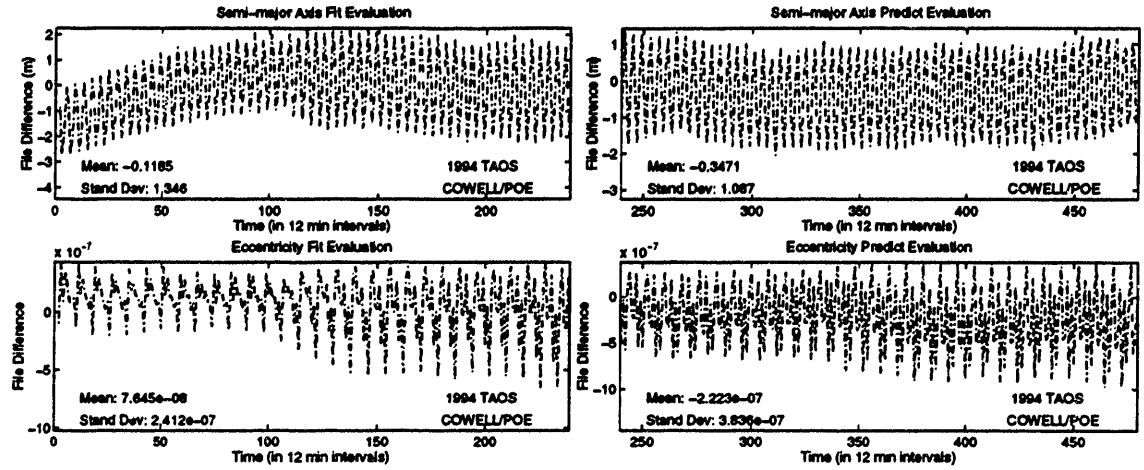

Figure H.95 TAOS *a/e* Errors for Cowell Two Day Fit and Two Day Predict Using Navigation Solutions

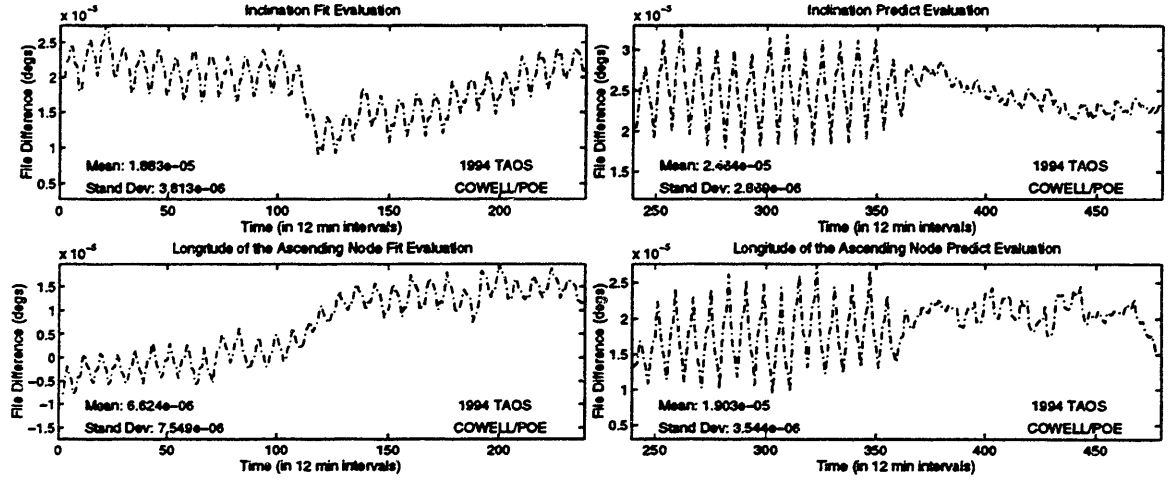

Figure H.96 TAOS *i/Ω* Errors for Cowell Two Day Fit and Two Day Predict Using Navigation Solutions

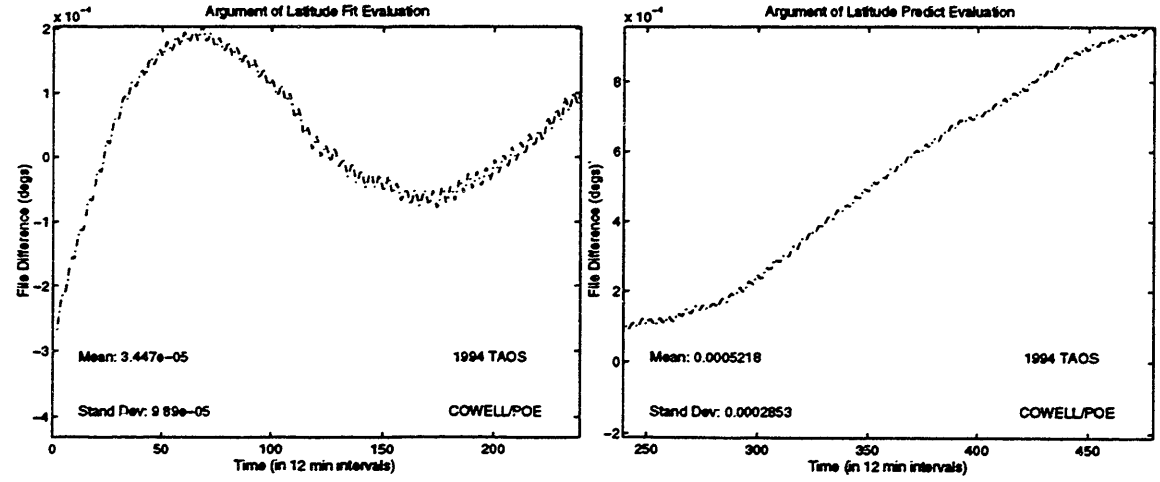

Figure H.97 TAOS Argument of Latitude Errors for Cowell Two Day Fit and Two Day Predict Using Navigation Solutions

Experiment 3: TAOS Three Day Fit of the Navigation Solutions (TAOS_NAV_COWELL_FIT_1)

```
CONTROL  DC                                                          TAOSXXXX  XXXXXX
EPOCH                        940528.0                 000000.0
ELEMENT1 10    1    1        -1550.6273844874D0       6039.5657891884D0       -3058.3210851343D0
ELEMENT2                     1.76398296192709D0       3.7539218851281D0       6.5097125101215 5D0
OBSINPUT 20                  940528 000950            940530 230000
ORBTYPE  2     1    11       10.0
DMOPT
OBSDEV   21                  50.
OBSDEV   22                  50.
OBSDEV   23                  50.
OBSDEV   24                  100.
OBSDEV   25                  75.
OBSDEV   26                  125.
END
DCOPT
PRINTOUT 1     4
CONVERG  20                  1.D-4                                   1.0
END
OGOPT
DRAG     1                   1.
ATMOSDEN          1
DRAGPAR  2     1             0.15D0
SCPARAM                      2.8D-5                  2400.0D0
MAXDEGEQ 1                   50.
MAXORDEQ 1                   50.
MAXDEGVE 1                   4.
MAXORDVE 1                   4.
POTFIELD 1     19
SETIDE   1                   0.29D0
SOLRAD   1                   1
STATEPAR 1
STATETAB 1     2    3        4                       5                       6
END
FIN
CONTROL  EPHEM                        OUTPUT                                 TOPEXXX  XXXXXX
OUTPUT   19    2    1        940601.0                 000000.0                43200.0
ORBTYPE  2     1    11       10.0
OGOPT
DRAG     1                   1.
ATMOSDEN          1
DRAGPAR  0
SCPARAM                      2.8D-5                  2400.0D0
MAXDEGEQ 1                   50.
MAXORDEQ 1                   50.
MAXDEGVE 1                   4.
MAXORDVE 1                   4.
POTFIELD 1     19
SETIDE   1                   0.29D0
SOLRAD   1                   1
OUTOPT   1                   940528000200.0          940601000000.0          120.0
END
FIN
```

Figure H.98 TAOS Cowell Three Day Navigation Solution Fit Input Card Data File

```
$!-------------------------------------------------------------
$! TAOS_NAV_COWELL_FIT_2
$!
$!
$!-------------------------------------------------------------
$!
$! Set default for batch run from CSDL0:[GTDS.GTDS_TEST]
$  set default fds$diska:[ssc2414.work.new_gtds.thesis.com]
$!
$! Assign debug overrides
$!
$  assign/table=lnm$job [ssc2414.work.new_gtds.thesis.overrides]taos_nav_cowell_fit_2.overrides dbg$init
$!
$! Assign the observation card file
$!
$  assign/table=lnm$job fds$diska:[ssc2414.taos.obscard]148-151.poscard gtds$015
$!
$! Assign the body potential files
$!
$  assign/table=lnm$job fds$diska:[djf1230.bianca]dan_potential.dat gtds$047
$  assign/table=lnm$job fds$diska:[djf1230.bianca]moon.dat      gtds$048
$!
$! Assign the SLP and timing files
$!
$  assign/table=lnm$job elrond$dka0:[ssc2414]june95_msgen_slp_mn2000.dat gtds$014
$  assign/table=lnm$job elrond$dka0:[ssc2414]june95_msgen_slp_timecoef.dat gtds$038
$  assign/table=lnm$job elrond$dka0:[ssc2414]june95_msgen_slp_tod2000.dat gtds$078
$!
$! Assign ORB1 files
$!
$  assign/table=lnm$job fds$diska:[ssc2414.work.new_gtds.thesis.orb1]taos_nav_cowell_fit_2.orb1 gtds$024
$!
$! Assign atmospheric density files
$!
$  assign/table=lnm$job fds_dbf:schatten_jacchia_roberts.dat   gtds$075
$!
$! Assign fundamental constants file
$!
$  assign/table=lnm$job fds$diska:[ssc2414.work.new_gtds.mods]taos_j2000_csconst.dat gtds$099
$!
$! Execute the local version of debug executable
$!
$  @[ssc2414.work.new_gtds.test]j2000_SWAT_GTDS [ssc2414.work.new_gtds.thesis.gtds]taos_nav_cowell_fit_2
$  rename [-.gtds]taos_nav_cowell_fit_2.output [-.output]taos_nav_cowell_fit_2.output
$!
$  assign/table=lnm$job fds_dbf:schatten_jacchia_roberts.dat gtds$075
$  EXIT
```

Figure H.99 TAOS Cowell Three Day Navigation Solution Fit Command Procedure

```
SET OUTPUT LOG
SET LOG
SET BREAK/return ESTSET DO -
      (DEPOSIT  IDIFF      = 3; -
       DEPOSIT  IDRVAR     = 1; -
       DEPOSIT  ISRVAR     = 0; -
       DEPOSIT  KPAR       = 0; -
       DEPOSIT  KATMOS     = 1; -
       EXAMINE  KATMOS     ; -
       EXAMINE  IDIFF      ; -
       EXAMINE  IDRVAR     ; -
       EXAMINE  ISRVAR     ; -
       EXAMINE  KPAR       ; -
       GO -
    ): -
GO
```

Figure H.100 TAOS Cowell Three Day Navigation Solution Fit Overrides File

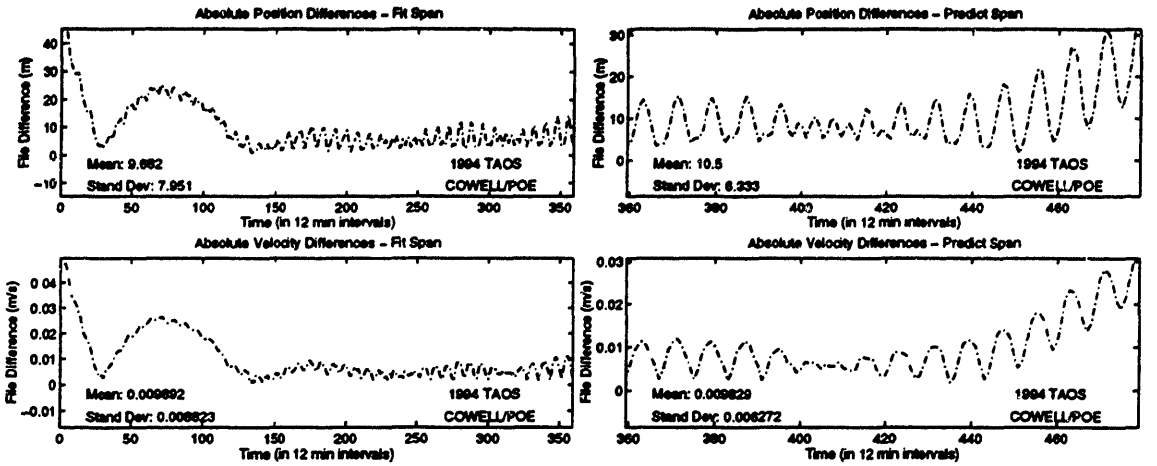

Figure H.101 TAOS Position and Velocity Errors for Cowell Three Day Fit and One Day Predict Using Navigation Solutions

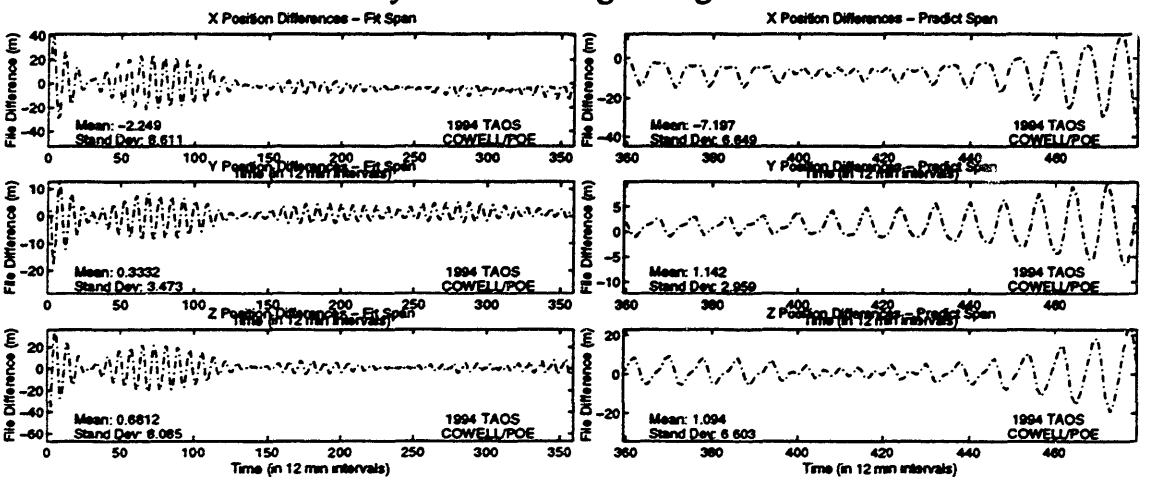

Figure H.102 TAOS Position Errors for Cowell Three Day Fit and One Day Predict Using Navigation Solutions

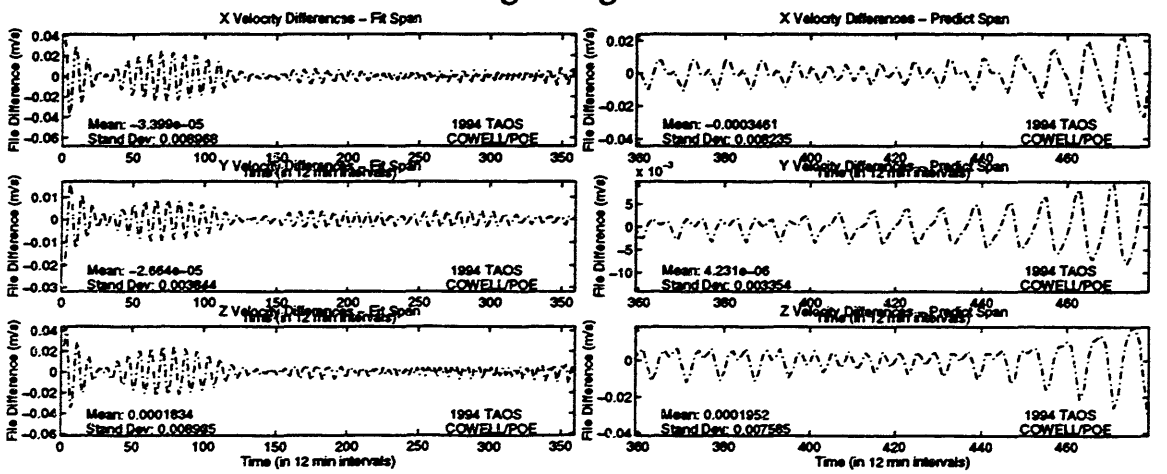

Figure H.103 TAOS Velocity Errors for Cowell Three Day Fit and One Day Predict Using Navigation Solutions

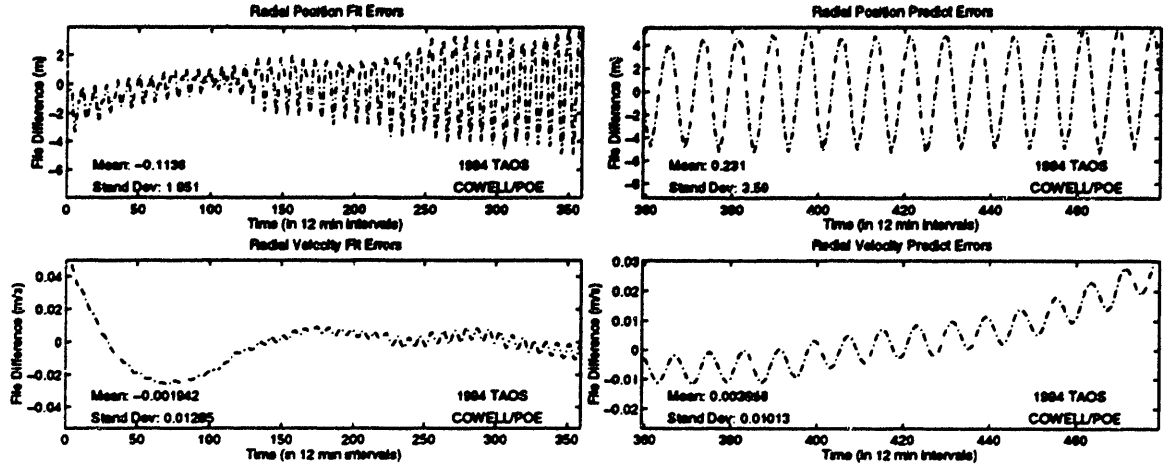

Figure H.104 TAOS Radial Errors for Cowell Three Day Fit and One Day Predict Using Navigation Solutions

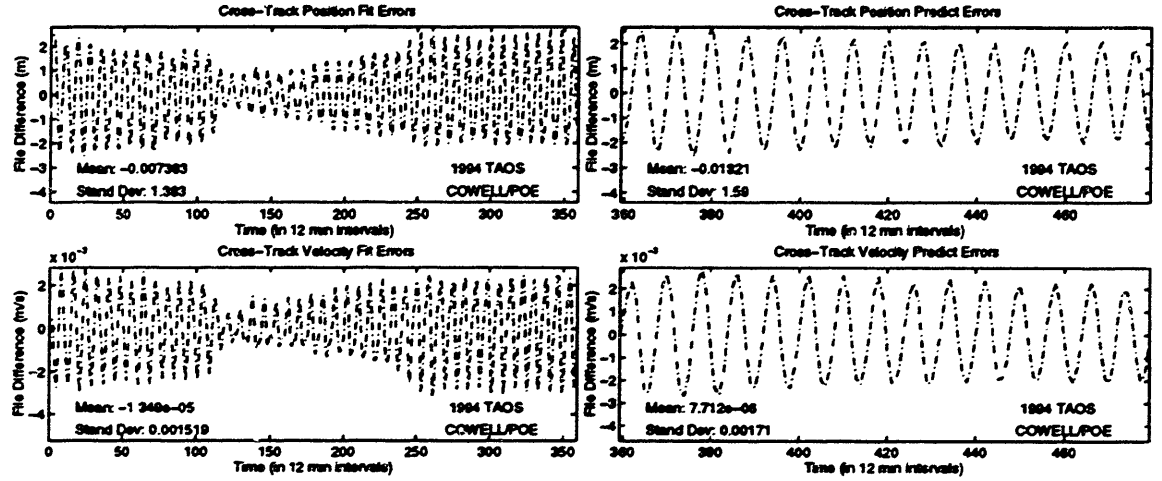

Figure H.105 TAOS Cross-Track Errors for Cowell Three Day Fit and One Day Predict Using Navigation Solutions

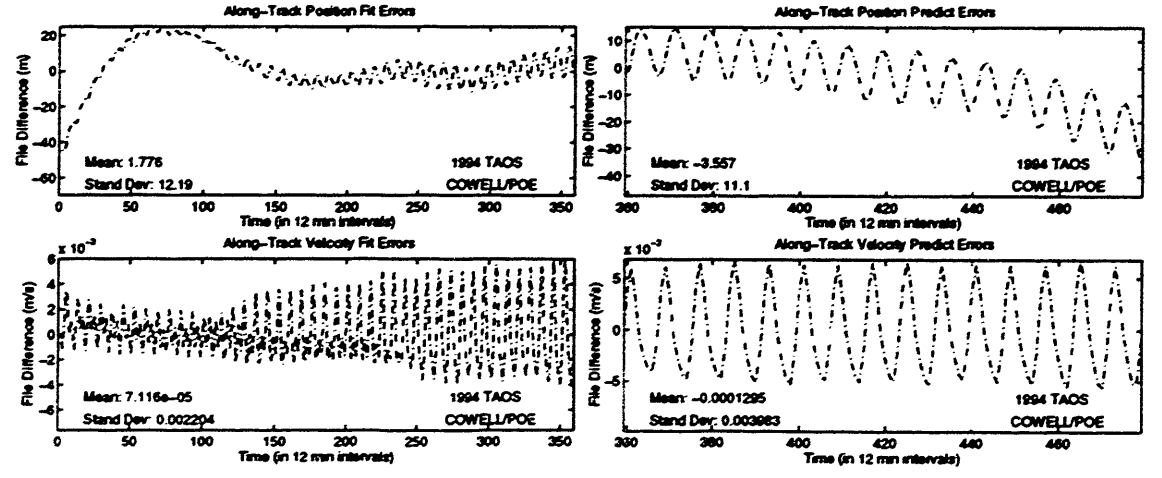

Figure H.106 TAOS Along-Track Errors for Cowell Three Day Fit and One Day Predict Using Navigation Solutions

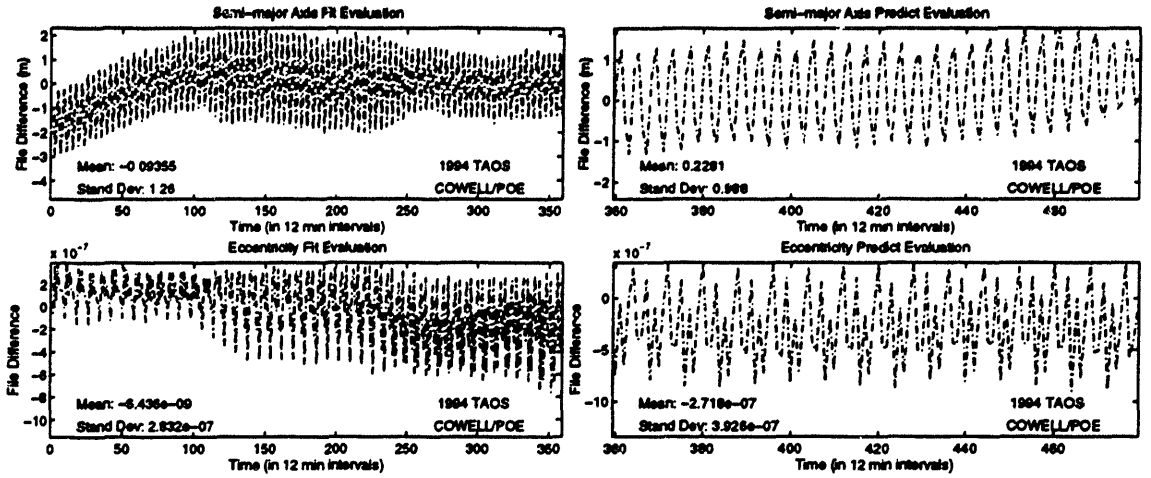

Figure H.107 TAOS *a/e* Errors for Cowell Three Day Fit and One Day Predict Using Navigation Solutions

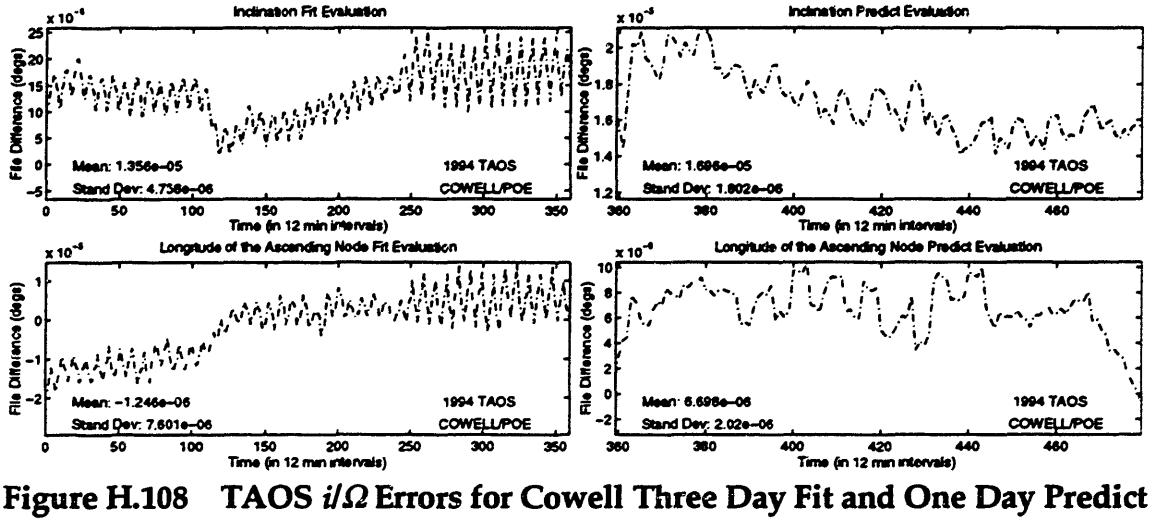

Figure H.108 TAOS i/Ω Errors for Cowell Three Day Fit and One Day Predict Using Navigation Solutions

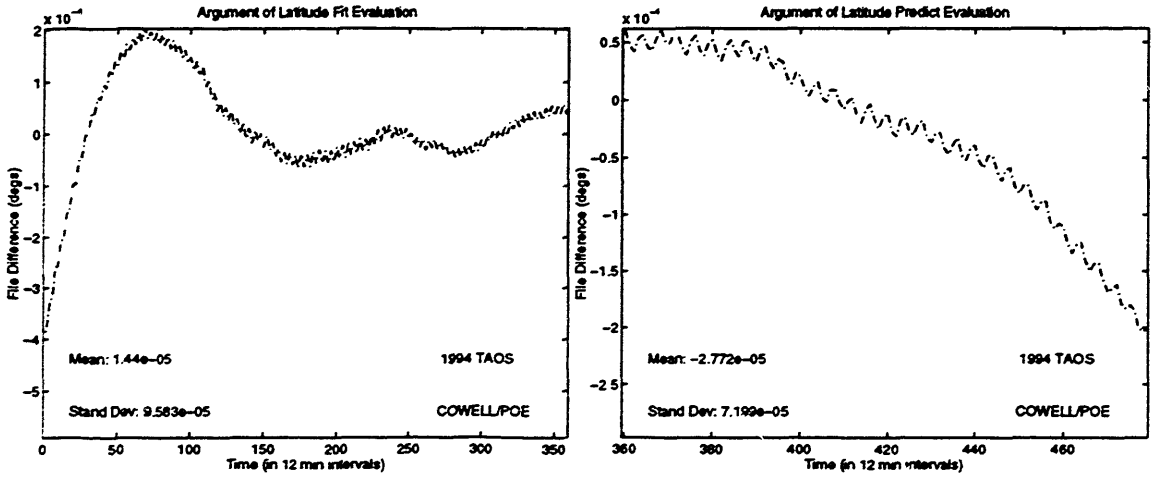

Figure H.109 TAOS Argument of Latitude Errors for Cowell Three Day Fit and One Day Predict Using Navigation Solutions

Experiment 4: TAOS Three Day Fit of the Navigation Solutions Using SST (TAOS_NAV_SST_FIT_1)

```
CONTROL  DC                                                          TAOSXXXX  XXXXXX
EPOCH                          940528.0                 000000.0
ELEMENT1 10     1     1        -1550.6273944874D0       6039.5657891884D0       -3058.3210851343D0
ELEMENT2                       1.76398296192709D0       3.7539218851281D0       6.50971251012155D0
OBSINPUT 20                    940528 000950            940530 230000
ORBTYPE  5      1     11       21600.0                  1.0
DMOPT
OBSDEV   21                    50.
OBSDEV   22                    50.
OBSDEV   23                    50.
OBSDEV   24                    100.
OBSDEV   25                    75.
OBSDEV   26                    125.
END
DCOPT
PRINTOUT 1      4
CONVERG  20                    1.D-4                                 1.0
END
OGOPT
DRAG     1                     1.
ATMOSDEN                 1
DRAGPAR  1
SCPARAM                        2.8D-5                   2400.0D0
MAXDEGEQ 1                     50.
MAXORDEQ 1                     50.
MAXDEGVE 1                     4.
MAXORDVE 1                     4.
POTFIELD 1      19
RESONPRD                       432000.D0
SETIDE   1                     0.29D0
SOLRAD   1                     1
STATEPAR 3
STATETAB 1      2     3        4                        5                       6
END
FIN
CONTROL  EPHEM                       OUTPUT                                  TOPEXXX  XXXXXX
OUTPUT   19     2     1        940601.0                 000000.0                43200.0
ORBTYPE  5      1     11       21600.0                  1.0
OGOPT
DRAG     1                     1.
ATMOSDEN                 1
DRAGPAR  0
SCPARAM                        2.8D-5                   2400.0D0
MAXDEGEQ 1                     50.
MAXORDEQ 1                     50.
MAXDEGVE 1                     4.
MAXORDVE 1                     4.
POTFIELD 1      19
RESONPRD                       432000.D0
SETIDE   1                     0.29D0
SOLRAD   1                     1
OUTOPT   1                     940528000200.0           940601000000.0          120.0
END
FIN
```

Figure H.110 TAOS SST Three Day Navigation Solution Fit Input Card Data File

```
$!-------------------------------------------------------------
$! TAOS_NAV_SST_FIT_5
$!
$!
$!-------------------------------------------------------------
$!
$! Set default for batch run from CSDL0:[GTDS.GTDS_TEST]
$  set default fds$diska:[ssc2414.work.new_gtds.thesis.com]
$!
$! Assign debug overrides
$!
$  assign/table=lnm$job [ssc2414.work.new_gtds.thesis.overrides]taos_nav_sst_fit_5.overrides dbg$init
$!
$! Assign the observation card file
$!
$  assign/table=lnm$job fds$diska:[ssc2414.taos.obscard]148-151.poscard gtds$015
$!
$! Assign the body potential files
$!
$  assign/table=lnm$job fds$diska:[djf1230.bianca]dan_potential.dat gtds$047
$  assign/table=lnm$job fds$diska:[djf1230.bianca]moon.dat      gtds$048
$!
$! Assign the SLP and timing files
$!
$  assign/table=lnm$job elrond$dka0:[ssc2414]june95_msgen_slp_mn2000.dat gtds$014
$  assign/table=lnm$job elrond$dka0:[ssc2414]june95_msgen_slp_timecoef.dat gtds$038
$  assign/table=lnm$job elrond$dka0:[ssc2414]june95_msgen_slp_tod2000.dat gtds$078
$!
$! Assign ORB1 files
$!
$  assign/table=lnm$job fds$diska:[ssc2414.work.new_gtds.thesis.orb1]taos_nav_sst_fit_5.orb1 gtds$024
$!
$! Assign atmospheric density files
$!
$  assign/table=lnm$job fds_dbf:schatten_jacchia_roberts.dat   gtds$075
$!
$! Assign fundamental constants file
$!
$  assign/table=lnm$job fds$diska:[ssc2414.work.new_gtds.mods]taos_j2000_csconst.dat gtds$099
$!
$! Execute the local version of debug executable
$!
$  @[ssc2414.work.new_gtds.test]j2000_SWAT_GTDS [ssc2414.work.new_gtds.thesis.gtds]taos_nav_cowell_fit_5
$  rename [-.gtds]taos_nav_sst_fit_5.output [-.output]taos_nav_sst_fit_5.output
$!
$  assign/table=lnm$job fds_dbf:schatten_jacchia_roberts.dat gtds$075
$  EXIT
```

Figure H.111 TAOS SST Three Day Navigation Solution Fit Command Procedure

```
SET OUTPUT LOG
SET LOG
SET BREAK/return ESTSET DO -
      (DEPOSIT  IDIFF        = 3; -
       DEPOSIT  IDRVAR       = 1; -
       DEPOSIT  ISRVAR       = 0; -
       DEPOSIT  KPAR         = 1; -
       DEPOSIT  KATMOS       = 1; -
       EXAMINE  KATMOS       ; -
       EXAMINE  IDIFF        ; -
       EXAMINE  IDRVAR       ; -
       EXAMINE  KPAR         ; -
       GO -
   ); -
GO
SET BREAK/return HWIRE  DO -
      (DEPOSIT  LZN          = 4; -
       DEPOSIT  JZN          = 25; -
       DEPOSIT  MTS          = 41;-
       DEPOSIT  JMAXTH(1)    = 5; -
       DEPOSIT  JMAXTS       = 25;-
       DEPOSIT  JMINTS       =-25;-
       EXAMINE  LZN          ; -
       EXAMINE  JZN          ; -
       EXAMINE  JMAXTH(1)    ; -
       GO -
   ); -
GO
```

Figure H.112 TAOS SST Three Day Navigation Solution Fit Overrides File

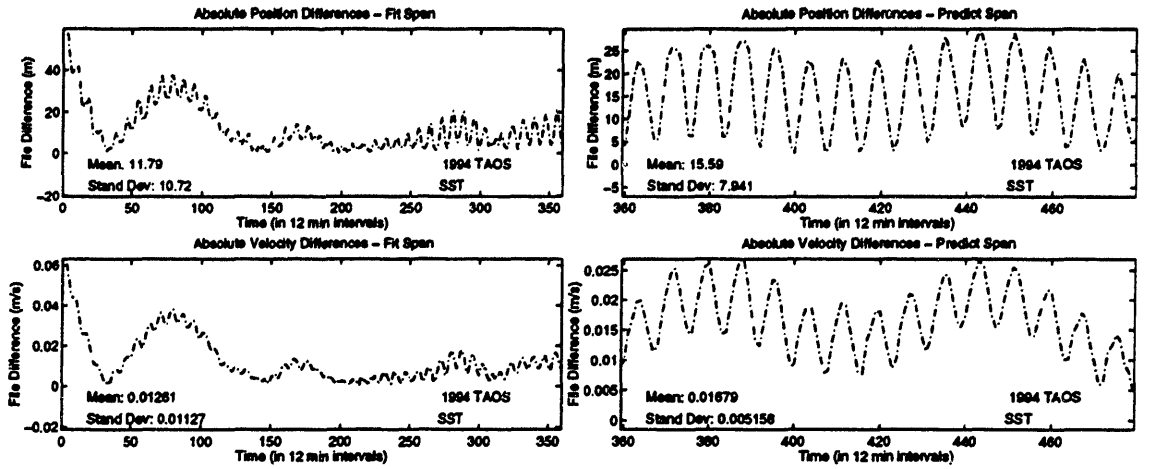

Figure H.113 TAOS Position and Velocity Errors for SST Three Day Fit and One Day Predict Using Navigation Solutions

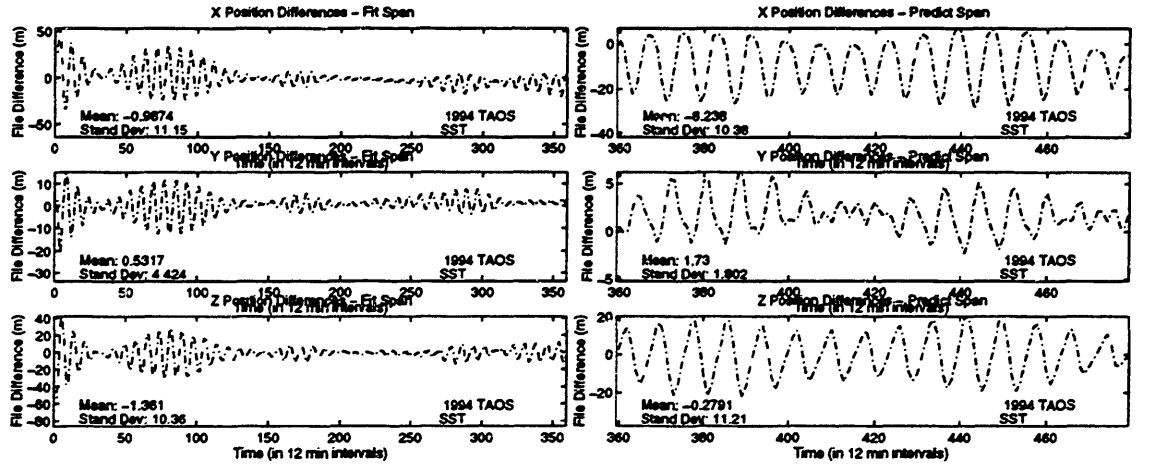

Figure H.114 TAOS Position Errors for SST Three Day Fit and One Day Predict Using Navigation Solutions

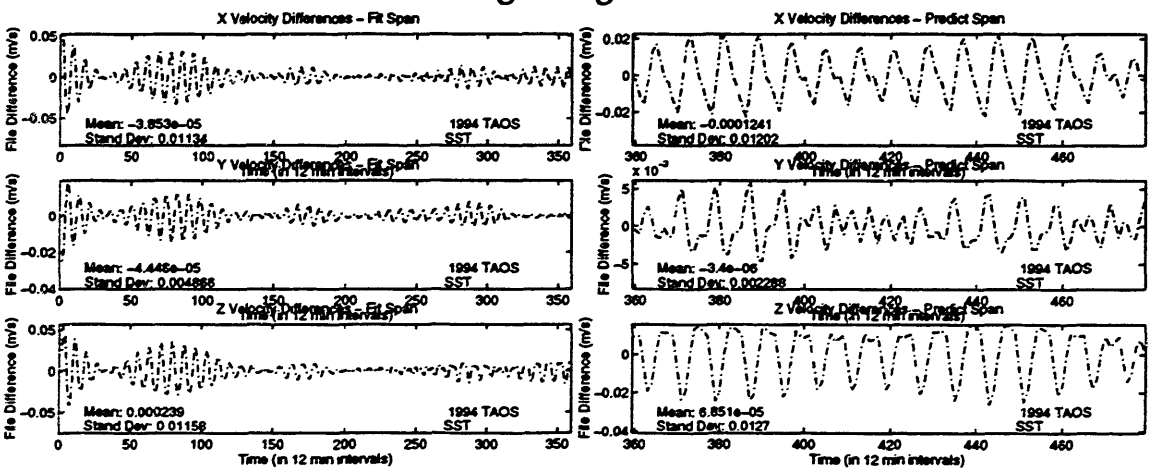

Figure H.115 TAOS Velocity Errors for SST Three Day Fit and One Day Predict Using Navigation Solutions

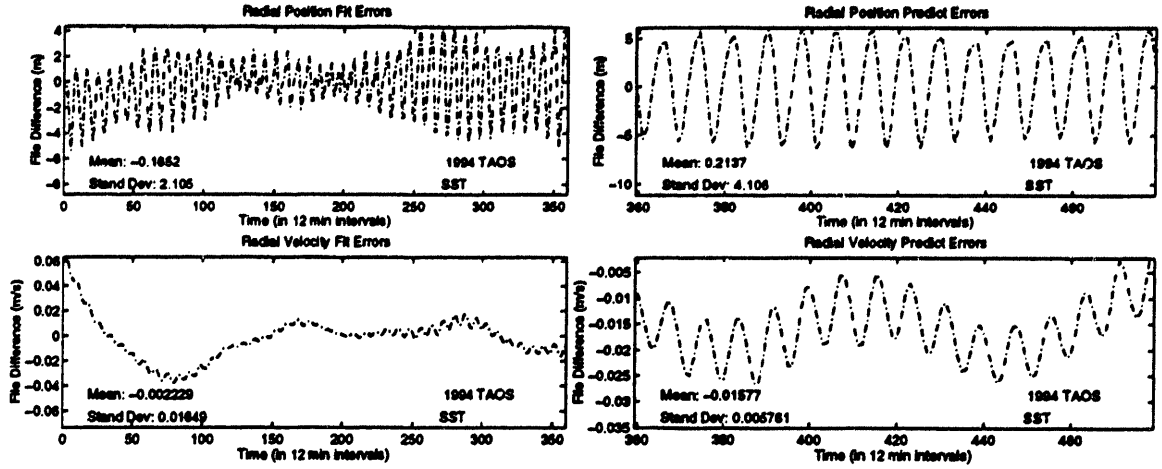

Figure H.116 TAOS Radial Errors for SST Three Day Fit and One Day Predict Using Navigation Solutions

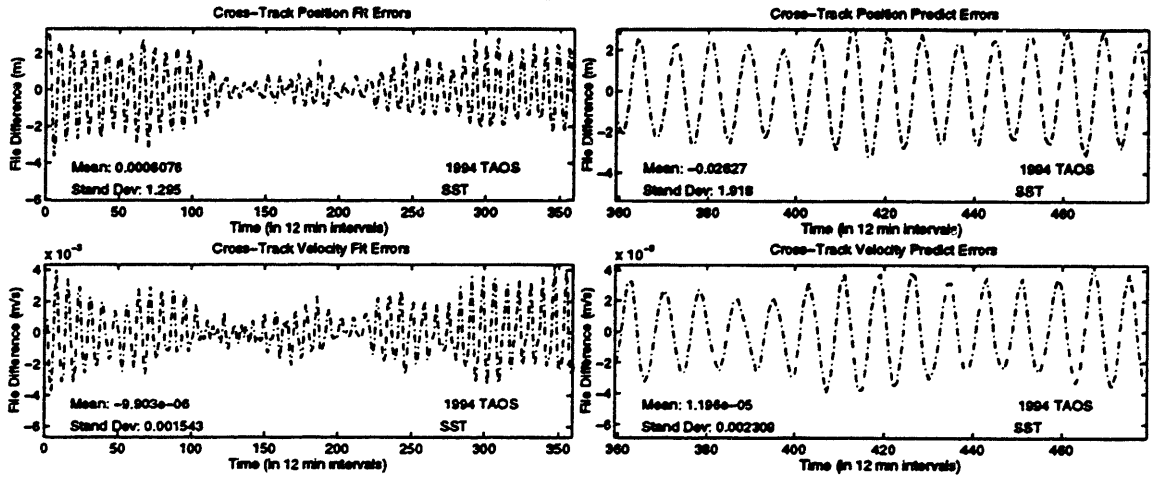

Figure H.117 TAOS Cross-Track Errors for SST Three Day Fit and One Day Predict Using Navigation Solutions

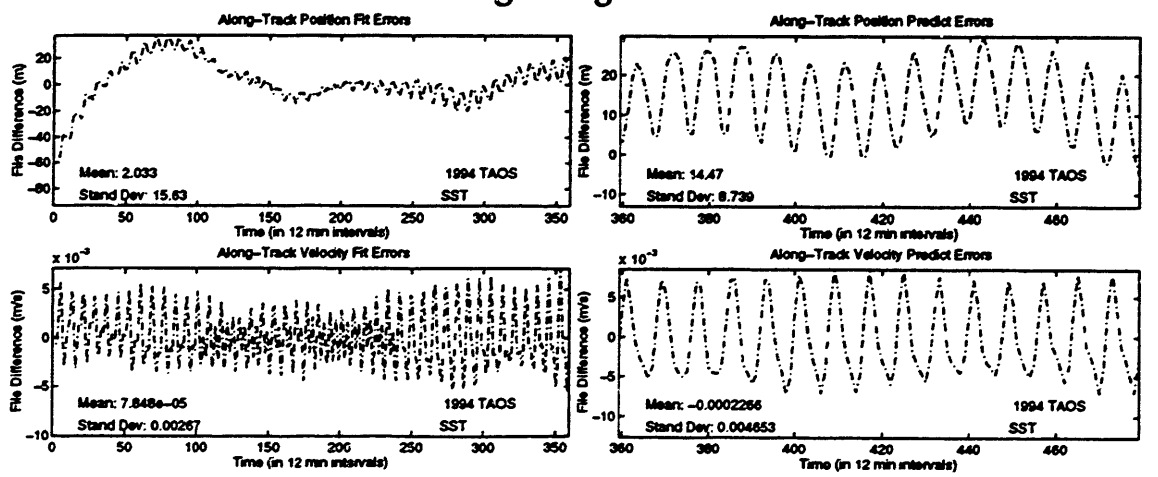

Figure H.118 TAOS Along-Track Errors for SST Three Day Fit and One Day Predict Using Navigation Solutions

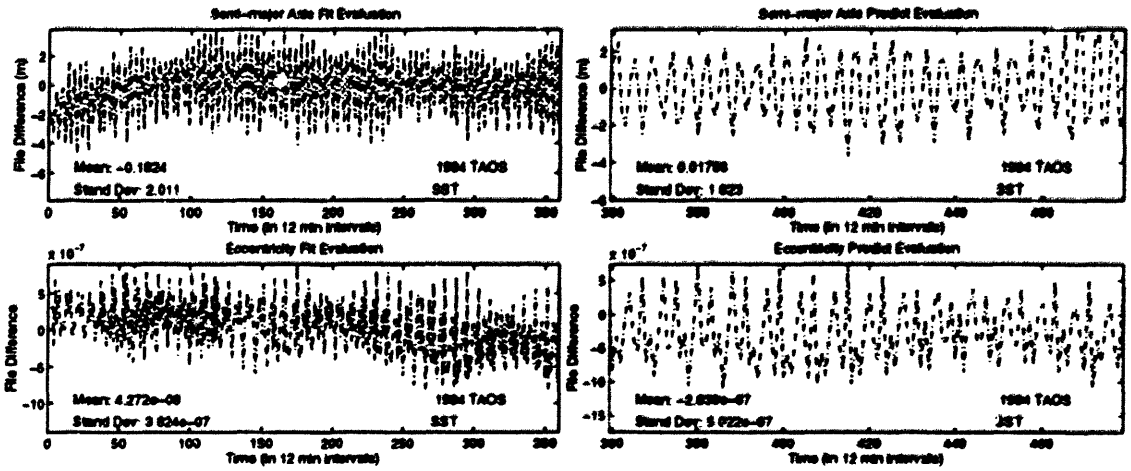

Figure H.119 TAOS *a/e* Errors for SST Three Day Fit and One Day Predict Using Navigation Solutions

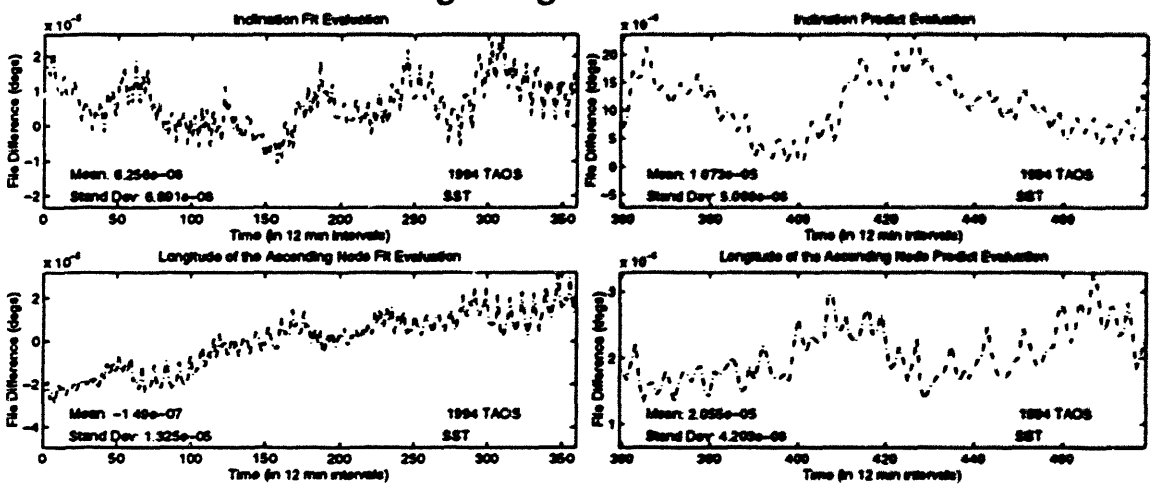

Figure H.120 TAOS *i/Ω* Errors for SST Three Day Fit and One Day Predict Using Navigation Solutions

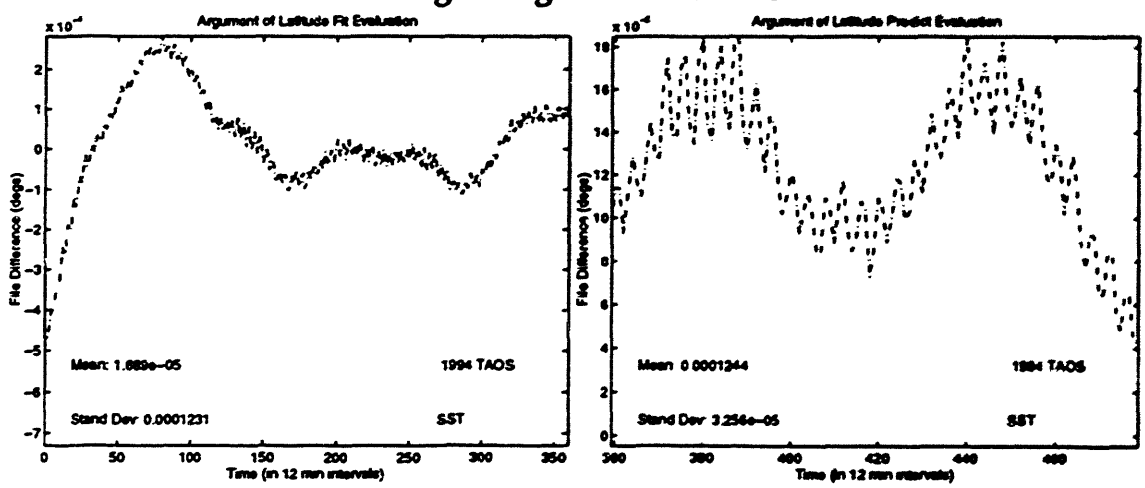

Figure H.121 TAOS Argument of Latitude Errors for SST Three Day Fit and One Day Predict Using Navigation Solutions

In an attempt to improve the fit process, the three day Cowell and SST fits were reproduced using a separate atmospheric density file. The density file was created on a near-real time basis, such that the latest measurements of the geomagnetic levels were included in the prediction of the near-term future values [64]. The intent here was to determine if inclusion of the latest information available would improve the accuracy of the fit and/or predictions. The remainder of the test protocol was unchanged. The associated files and results of fitting the navigation solutions with this near-real time atmospheric data file are provided in the following pages.

Experiment 5: TAOS Three Day Fit of the Navigation Solutions Using Cowell with Near-Real Time Atmospheric Information

(TAOS_NAV_COWELL_FIT_1)

```
CONTROL  DC                                                          TAOSXXXX  XXXXXX
EPOCH                          940528.0          000000.0
ELEMENT1 10    1     1         -1550.62739[illegible]74D0  6039.5657891884D0  -3058.3210851343D0
ELEMENT2                       1.76398296192709D0  3.7539218851281D0  6.50971251012155D0
OBSINPUT 20                    940528 000950     940530 230000
ORBTYPE  2     1     11        10.0
DMOPT
OBSDEV   21                    50.
OBSDEV   22                    50.
OBSDEV   23                    50.
OBSDEV   24                    100.
OBSDEV   25                    75.
OBSDEV   26                    125.
END
DCOPT
PRINTOUT 1     4
CONVERG  20                    1.D-4                                 1.0
END
OGOPT
DRAG     1                     1.
ATMOSDEN       1
DRAGPAR  2     1               0.15D0
SCPARAM                        2.8D-5            2400.0D0
MAXDEGEQ 1                     50.
MAXORDEQ 1                     50.
MAXDEGVE 1                     4.
MAXORDVE 1                     4.
POTFIELD 1     19
SETIDE   1                     0.29D0
SOLRAD   1                     1
STATEPAR 1
STATETAB 1     2     3         4                 5                   6
END
FIN
CONTROL  EPHEM                       OUTPUT                          TOPEXXX  XXXXXX
OUTPUT   19    2     1         940601.0          000000.0            43200.0
ORBTYPE  2     1     11        10.0
OGOPT
DRAG     1                     1.
ATMOSDEN       1
DRAGPAR  0
SCPARAM                        2.8D-5            2400.0D0
MAXDEGEQ 1                     50.
MAXORDEQ 1                     50.
MAXDEGVE 1                     4.
MAXORDVE 1                     4.
POTFIELD 1     19
SETIDE   1                     0.29D0
SOLRAD   1                     1
OUTOPT   1                     940528000200.0    940601000000.0      120.0
END
FIN
```

Figure H.122 TAOS Cowell Three Day Navigation Solution Fit with Near-Real Time Atmospheric Information Input Card Data File

```
$!-------------------------------------------------------------
$! TAOS_NAV_COWELL_FIT_1
$!
$!
$!-------------------------------------------------------------
$!
$! Set default for batch run from CSDL0:[GTDS.GTDS_TEST]
$  set default fds$diska:[ssc2414.work.new_gtds.thesis.com]
$!
$! Assign debug overrides
$!
$  assign/table=lnm$job [ssc2414.work.new_gtds.thesis.overrides]taos_nav_cowell_fit_1.overrides dbg$init
$!
$! Assign the observation card file
$!
$  assign/table=lnm$job fds$diska:[ssc2414.taos.obscard]148-151.poscard gtds$015
$!
$! Assign the body potential files
$!
$  assign/table=lnm$job fds$diska:[djf1230.bianca]dan_potential.dat gtds$047
$  assign/table=lnm$job fds$diska:[djf1230.bianca]moon.dat      gtds$048
$!
$! Assign the SLP and timing files
$!
$  assign/table=lnm$job elrond$dka0:[ssc2414]june95_msgen_slp_mn2000.dat gtds$014
$  assign/table=lnm$job elrond$dka0:[ssc2414]june95_msgen_slp_timecoef.dat gtds$038
$  assign/table=lnm$job elrond$dka0:[ssc2414]june95_msgen_slp_tod2000.dat gtds$078
$!
$! Assign ORB1 files
$!
$  assign/table=lnm$job fds$diska:[ssc2414.work.new_gtds.thesis.orb1]taos_nav_cowell_fit_1.orb1 gtds$024
$!
$! Assign atmospheric density files
$!
$  assign/table=lnm$job fds$diskb:[rjp9045.jacchia]jac_real_jun95.dat   gtds$075
$!
$! Assign fundamental constants file
$!
$  assign/table=lnm$job fds$diska:[ssc2414.work.new_gtds.mods]taos_j2000_csconst.dat gtds$099
$!
$! Execute the local version of debug executable
$!
$  @[ssc2414.work.new_gtds.test]j2000_SWAT_GTDS [ssc2414.work.new_gtds.thesis.gtds]taos_nav_cowell_fit_1
$  rename [-.gtds]taos_nav_cowell_fit_1.output [-.output]taos_nav_cowell_fit_1.output
$!
$  assign/table=lnm$job fds_dbf:schatten_jacchia_roberts.dat gtds$075
$  EXIT
```

Figure H.123 TAOS Cowell Three Day Navigation Solution Fit with Near-Real Time Atmospheric Information Command Procedure

```
SET OUTPUT LOG
SET LOG
SET BREAK/return ESTSET DO -
      (DEPOSIT  IDIFF      = 3; -
       DEPOSIT  IDRVAR     = 1; -
       DEPOSIT  ISRVAR     = 0; -
       DEPOSIT  KPAR       = 0; -
       DEPOSIT  KATMOS     = 1; -
       EXAMINE  KATMOS     ; -
       EXAMINE  IDIFF      ; -
       EXAMINE  IDRVAR     ; -
       EXAMINE  ISRVAR     ; -
       EXAMINE  KPAR       ; -
       GO -
    ); -
GO
```

Figure H.124 TAOS Cowell Three Day Navigation Solution Fit with Near-Real Time Atmospheric Information Overrides File

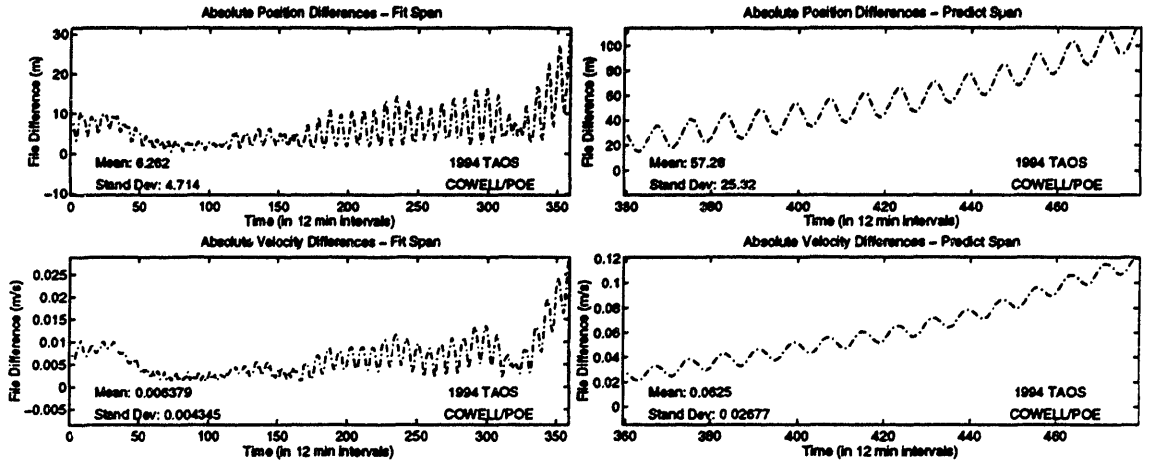

Figure H.125 TAOS Position and Velocity Errors for Cowell Experiment with Near-Real Time Atmospheric Information

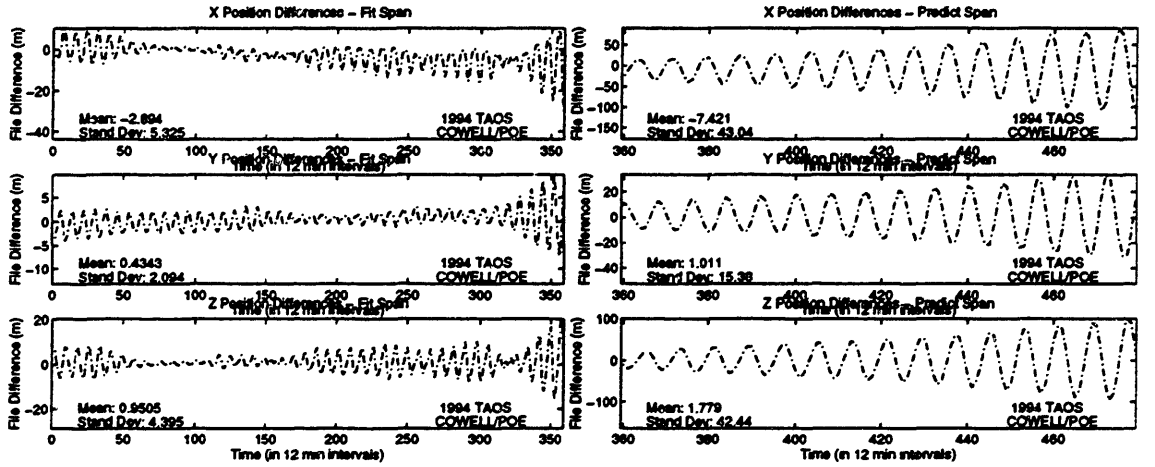

Figure H.126 TAOS Position Errors for Cowell Experiment with Near-Real Time Atmospheric Information

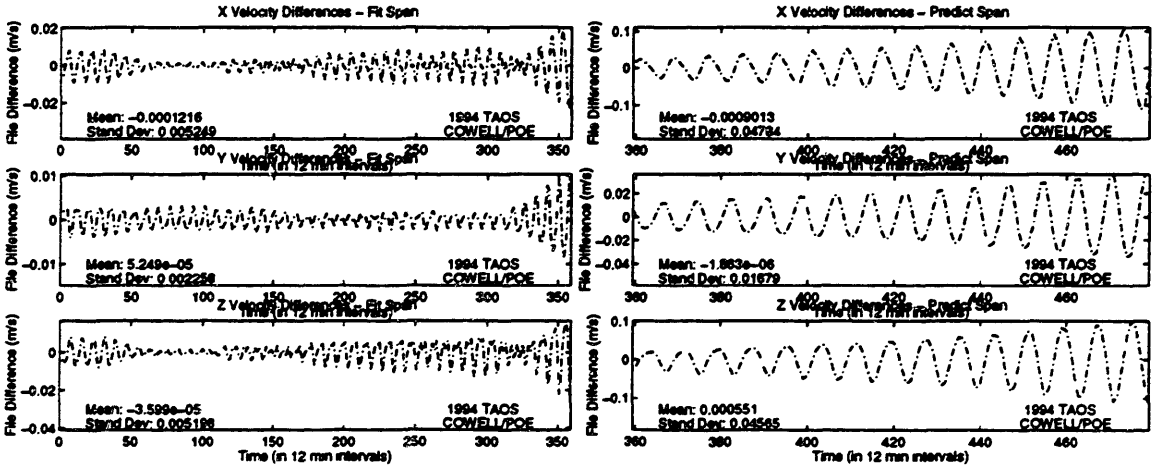

Figure H.127 TAOS Velocity Errors for Cowell Experiment with Near-Real Time Atmospheric Information

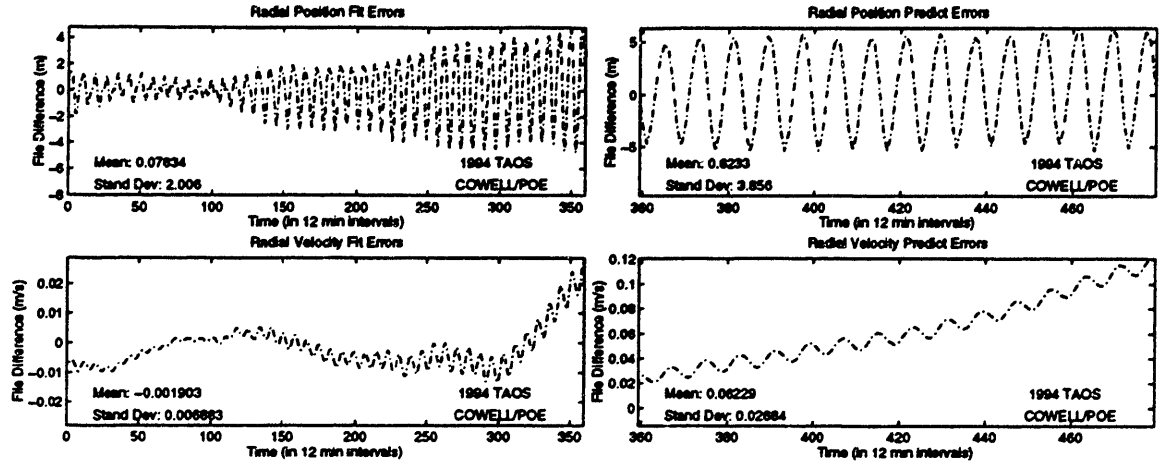

Figure H.128 TAOS Radial Errors for Cowell Experiment with Near-Real Time Atmospheric Information

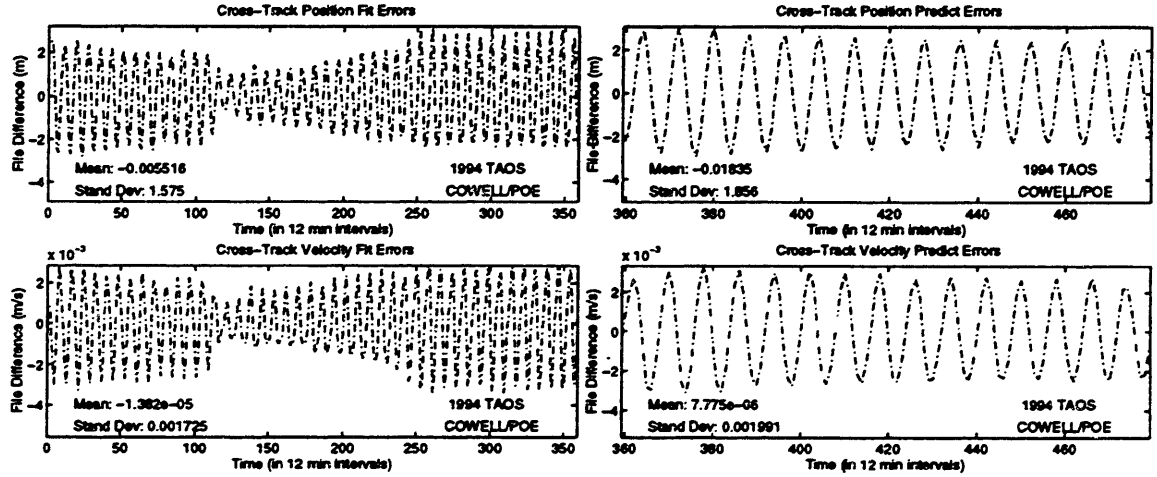

Figure H.129 TAOS Cross-Track Errors for Cowell Experiment with Near-Real Time Atmospheric Information

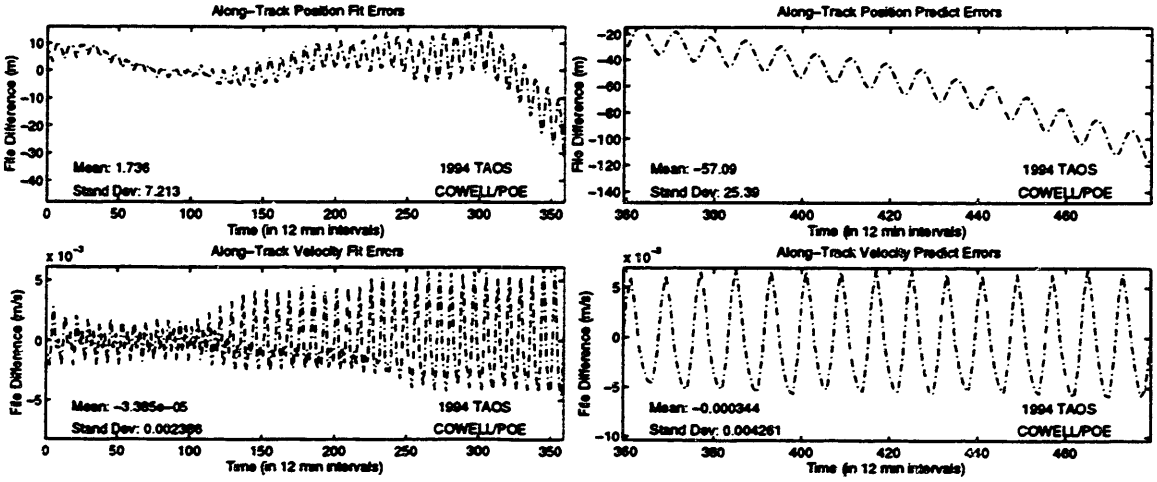

Figure H.130 TAOS Along-Track Errors for Cowell Experiment with Near-Real Time Atmospheric Information

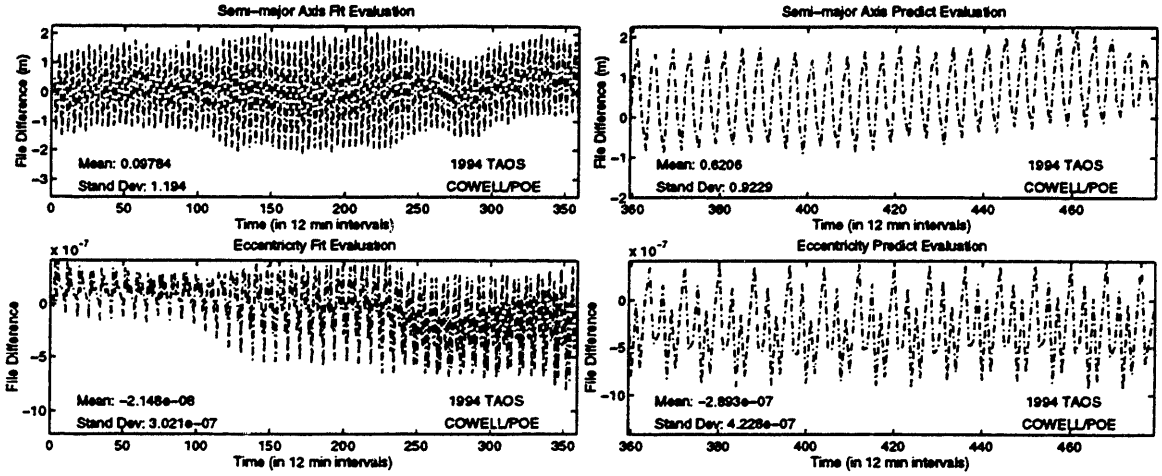

Figure H.131 TAOS *a/e* Errors for Cowell Experiment with Near-Real Time Atmospheric Information

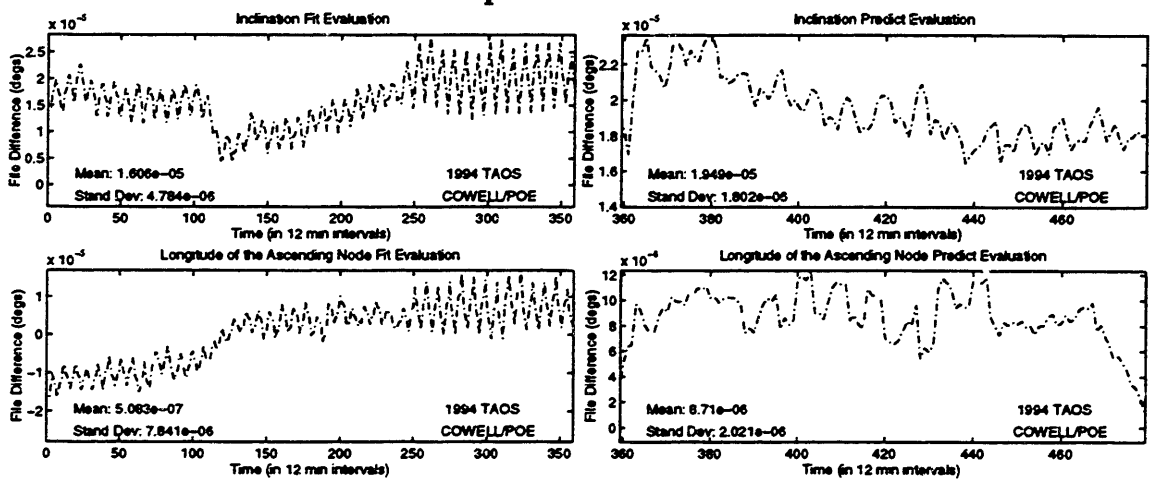

Figure H.132 TAOS *i/Ω* Errors for Cowell Experiment with Near-Real Time Atmospheric Information

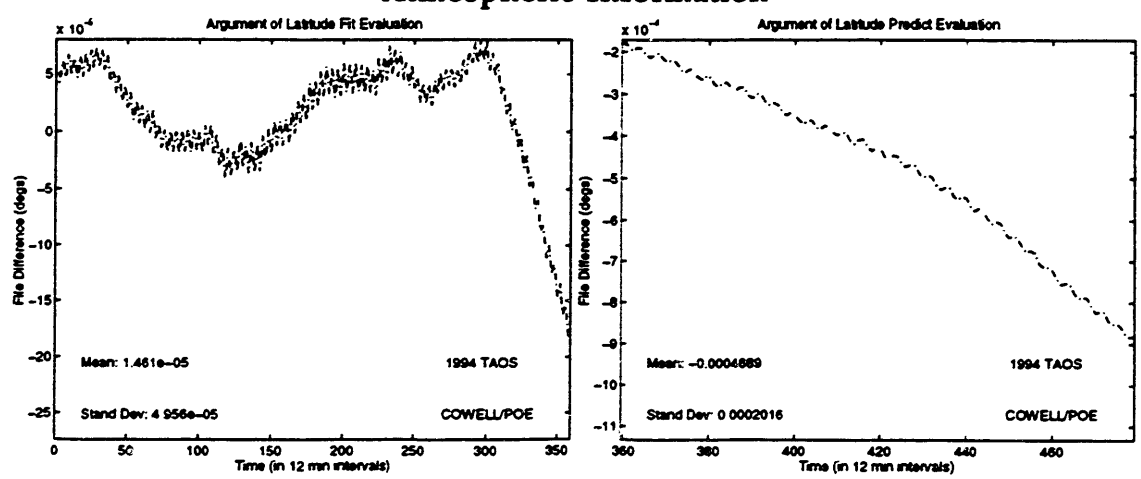

Figure H.133 TAOS Argument of Latitude Errors for Cowell Experiment with Near-Real Time Atmospheric Information

Experiment 6: TAOS Three Day Fit of the Navigation Solutions Using SST with Near-Real Time Atmospheric Information

(TAOS_NAV_SST_FIT_4)

```
CONTROL  DC                                                          TAOSXXXX  XXXXXX
EPOCH                          940528.0              000000.0
ELEMENT1 10    1     1         -1550.6273944874D0    6039.5657891884D0     -3058.3210851343D0
ELEMENT2                       1.76398296192709D0    3.7539218851281D0     6.50971251012155D0
OBSINPUT 20                    940528 000950         940530 230000
ORBTYPE  5     1     11        21600.0               1.0
DMOPT
OBSDEV   21                    50.
OBSDEV   22                    50.
OBSDEV   23                    50.
OBSDEV   24                    100.
OBSDEV   25                    75.
OBSDEV   26                    125.
END
DCOPT
PRINTOUT 1     4
CONVERG  20                    1.D-4                                 1.0
END
OGOPT
DRAG     1                     1.
ATMOSDEN               1
DRAGPAR  1
SCPARAM                        2.8D-5                2400.0D0
MAXDEGEQ 1                     50.
MAXORDEQ 1                     50.
MAXDEGVE 1                     4.
MAXORDVE 1                     4.
POTFIELD 1     19
RESONPRD                       432000.D0
SETIDE   1                     0.29D0
SOLRAD   1                     1
STATEPAR 3
STATETAB 1     2     3         4                     5                     6
END
FIN
CONTROL  EPHEM                       OUTPUT                          TOPEXXX  XXXXXX
OUTPUT   19    2     1         940601.0              000000.0              43200.0
ORBTYPE  5     1     11        21600.0               1.0
OGOPT
DRAG     1                     1.
ATMOSDEN               1
DRAGPAR  0
SCPARAM                        2.8D-5                2400.0D0
MAXDEGEQ 1                     50.
MAXORDEQ 1                     50.
MAXDEGVE 1                     4.
MAXORDVE 1                     4.
POTFIELD 1     19
RESONPRD                       432000.D0
SETIDE   1                     0.29D0
SOLRAD   1                     1
OUTOPT   1                     940528000200.0        940601000000.0        120.0
END
FIN
```

Figure H.134 TAOS SST Three Day Navigation Solution Fit with Near-Real Time Atmospheric Information Input Card Data File

```
$!-------------------------------------------------------
$! TAOS_NAV_SST_FIT_4
$!
$!
$!-------------------------------------------------------
$!
$! Set default for batch run from CSDL0:[GTDS.GTDS_TEST]
$  set default fds$diska:[ssc2414.work.new_gtds.thesis.com]
$!
$! Assign debug overrides
$!
$  assign/table=lnm$job [ssc2414.work.new_gtds.thesis.overrides]taos_nav_sst_fit_4.overrides dbg$init
$!
$! Assign the observation card file
$!
$  assign/table=lnm$job fds$diska:[ssc2414.taos.obscard]148-151.poscard gtds$015
$!
$! Assign the body potential files
$!
$  assign/table=lnm$job fds$diska:[djf1230.bianca]dan_potential.dat gtds$047
$  assign/table=lnm$job fds$diska:[djf1230.bianca]moon.dat      gtds$048
$!
$! Assign the SLP and timing files
$!
$  assign/table=lnm$job elrond$dka0:[ssc2414]june95_msgen_slp_mn2000.dat gtds$014
$  assign/table=lnm$job elrond$dka0:[ssc2414]june95_msgen_slp_timecoef.dat gtds$038
$  assign/table=lnm$job elrond$dka0:[ssc2414]june95_msgen_slp_tod2000.dat gtds$078
$!
$! Assign ORB1 files
$!
$  assign/table=lnm$job fds$diska:[ssc2414.work.new_gtds.thesis.orb1]taos_nav_sst_fit_4.orb1 gtds$024
$!
$! Assign atmospheric density files
$!
$  assign/table=lnm$job fds$diskb:[rjp9045.jacchia]jac_real_jun95.dat   gtds$075
$!
$! Assign fundamental constants file
$!
$  assign/table=lnm$job fds$diska:[ssc2414.work.new_gtds.mods]taos_j2000_csconst.dat gtds$099
$!
$! Execute the local version of debug executable
$!
$  @[ssc2414.work.new_gtds.test]j2000_SWAT_GTDS [ssc2414.work.new_gtds.thesis.gtds]taos_nav_cowell_fit_4
$  rename [-.gtds]taos_nav_sst_fit_4.output [-.output]taos_nav_sst_fit_4.output
$!
$  assign/table=lnm$job fds_dbf:schatten_jacchia_roberts.dat gtds$075
$  EXIT
```

Figure H.135 TAOS SST Three Day Navigation Solution Fit with Near-Real Time Atmospheric Information Command Procedure

```
SET OUTPUT LOG
SET LOG
SET BREAK/return ESTSET DO -
      (DEPOSIT  IDIFF      = 3; -
       DEPOSIT  IDRVAR     = 1; -
       DEPOSIT  ISRVAR     = 0; -
       DEPOSIT  KPAR       = 1; -
       DEPOSIT  KATMOS     = 1; -
       EXAMINE  KATMOS     ; -
       EXAMINE  IDIFF      ; -
       EXAMINE  IDRVAR     ; -
       EXAMINE  KPAR       ; -
       GO -
   ); -
GO
SET BREAK/return HWIRE  DO -
      (DEPOSIT  LZN        = 4; -
       DEPOSIT  JZN        = 25; -
       DEPOSIT  MTS        = 41;-
       DEPOSIT  JMAXTH(1)  = 5; -
       DEPOSIT  JMAXTS     = 25;-
       DEPOSIT  JMINTS     =-25;-
       EXAMINE  LZN        ; -
       EXAMINE  JZN        ; -
       EXAMINE  JMAXTH(1)  ; -
       GO -
   ); -
GO
```

Figure H.136 TAOS SST Three Day Navigation Solution Fit with Near-Real Time Atmospheric Information Overrides File

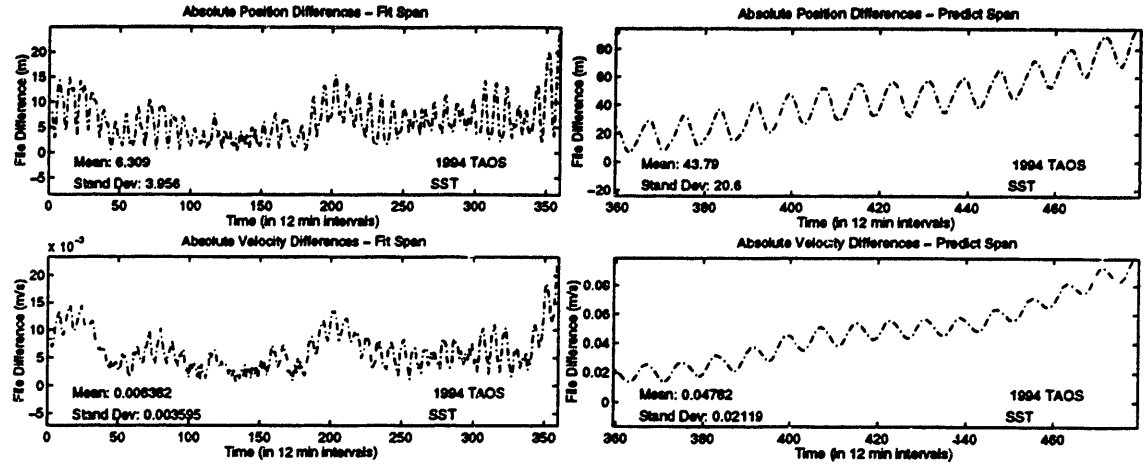

Figure H.137 TAOS Position and Velocity Errors for SST Experiment with Near-Real Time Atmospheric Information

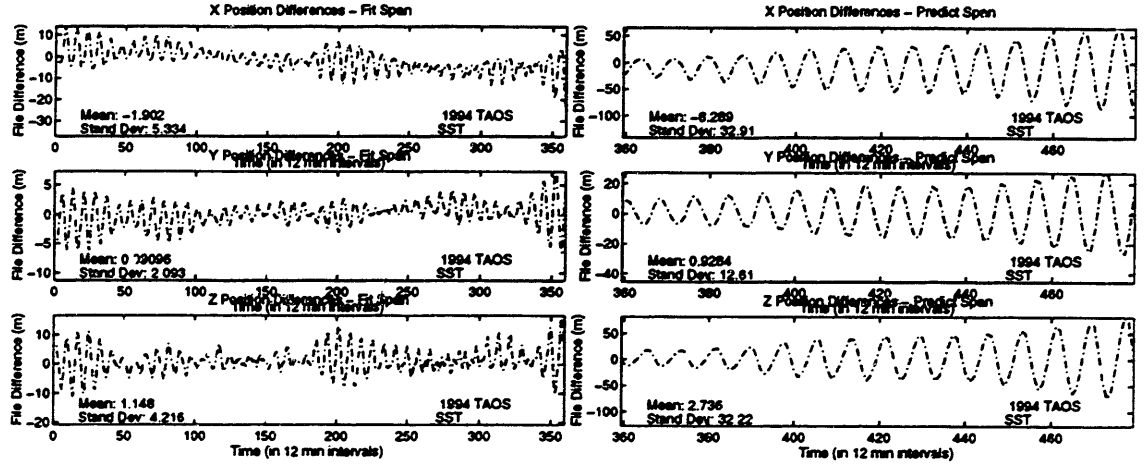

Figure H.138 TAOS Position Errors for SST Experiment with Near-Real Time Atmospheric Information

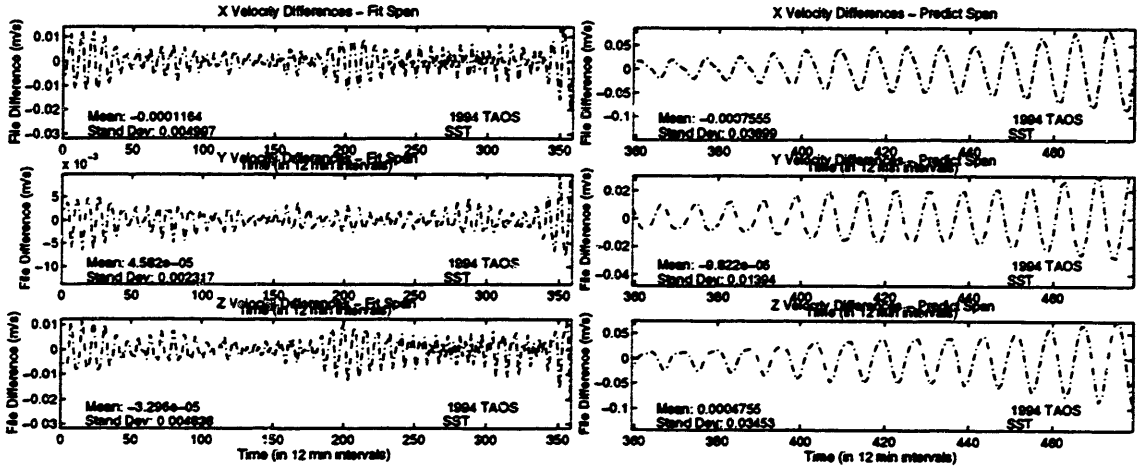

Figure H.139 TAOS Velocity Errors for SST Experiment with Near-Real Time Atmospheric Information

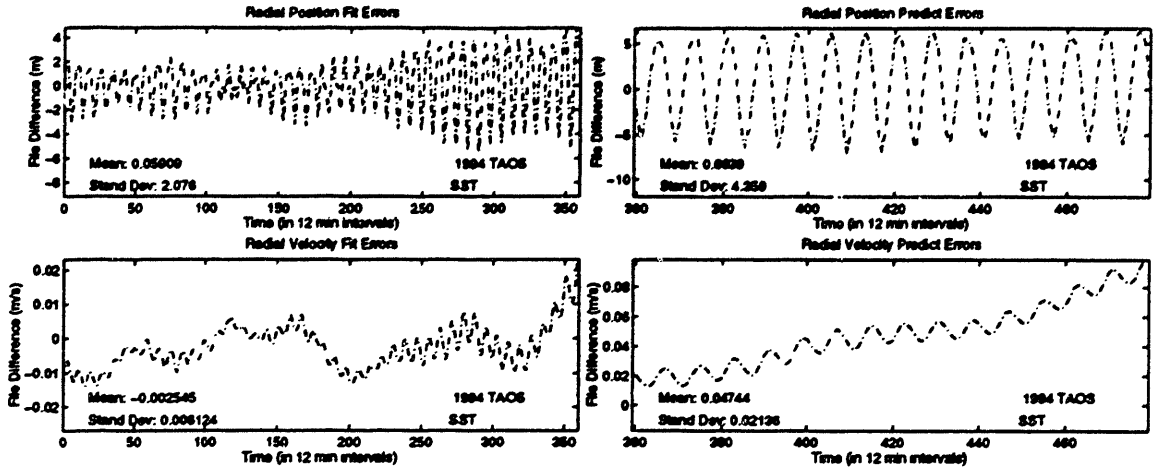

Figure H.140 TAOS Radial Errors for SST Experiment with Near-Real Time Atmospheric Information

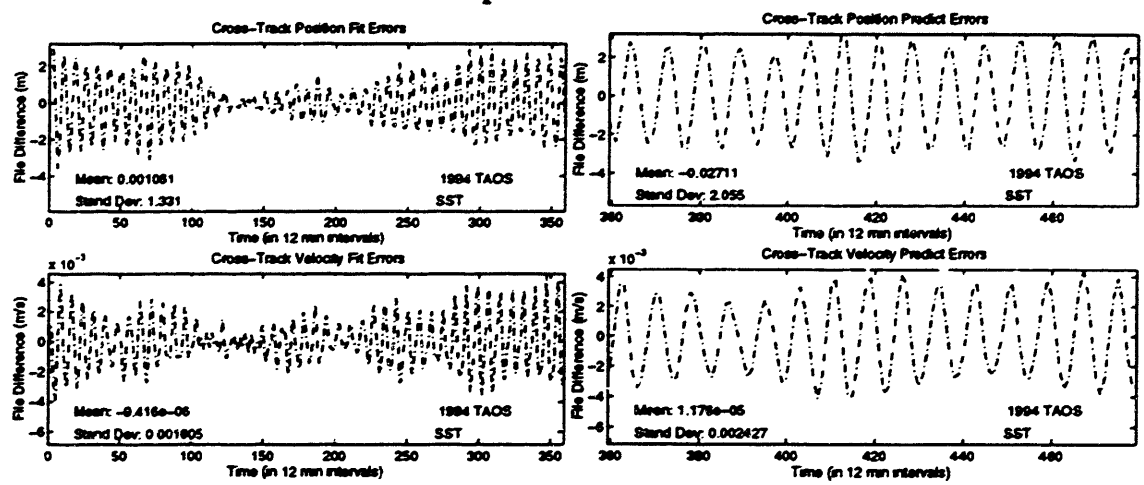

Figure H.141 TAOS Cross-Track Errors for SST Experiment with Near-Real Time Atmospheric Information

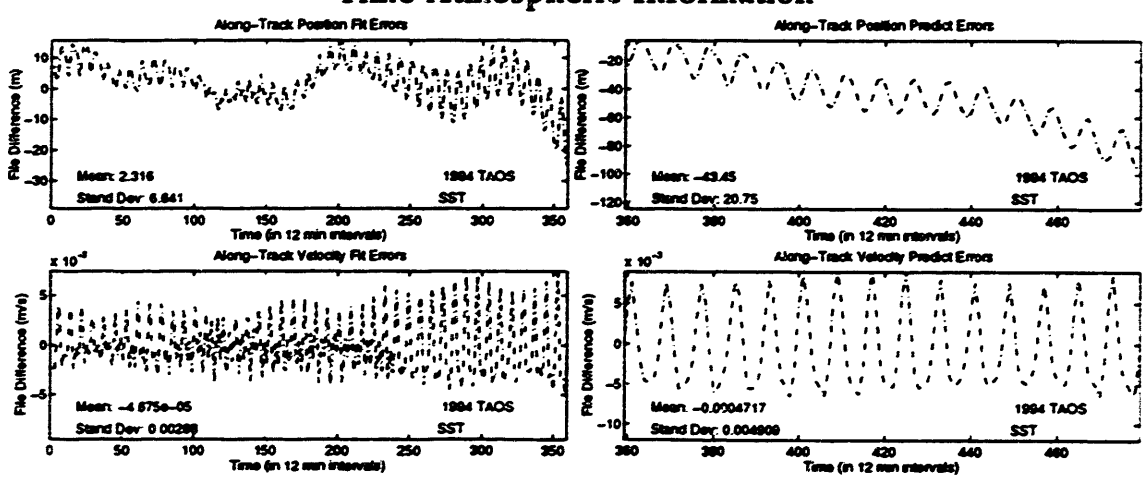

Figure H.142 TAOS Along-Track Errors for SST Experiment with Near-Real Time Atmospheric Information

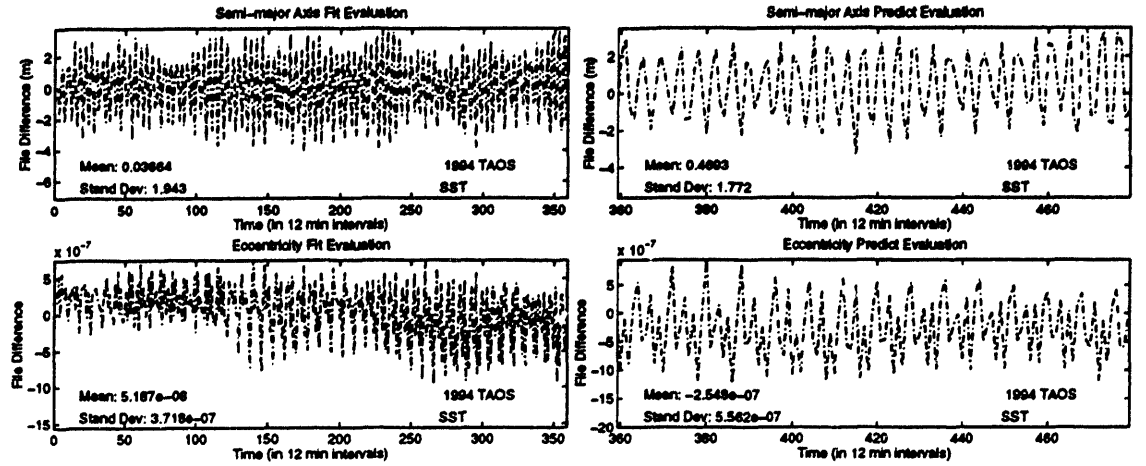

Figure H.143 TAOS *a/e* Errors for SST Experiment with Near-Real Time Atmospheric Information

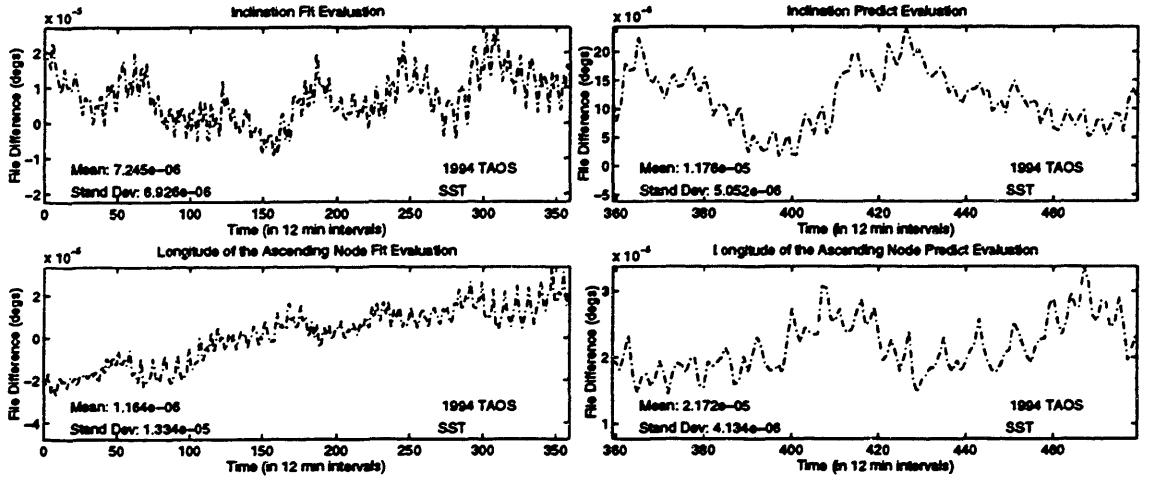

Figure H.144 TAOS i/Ω Errors for SST Experiment with Near-Real Time Atmospheric Information

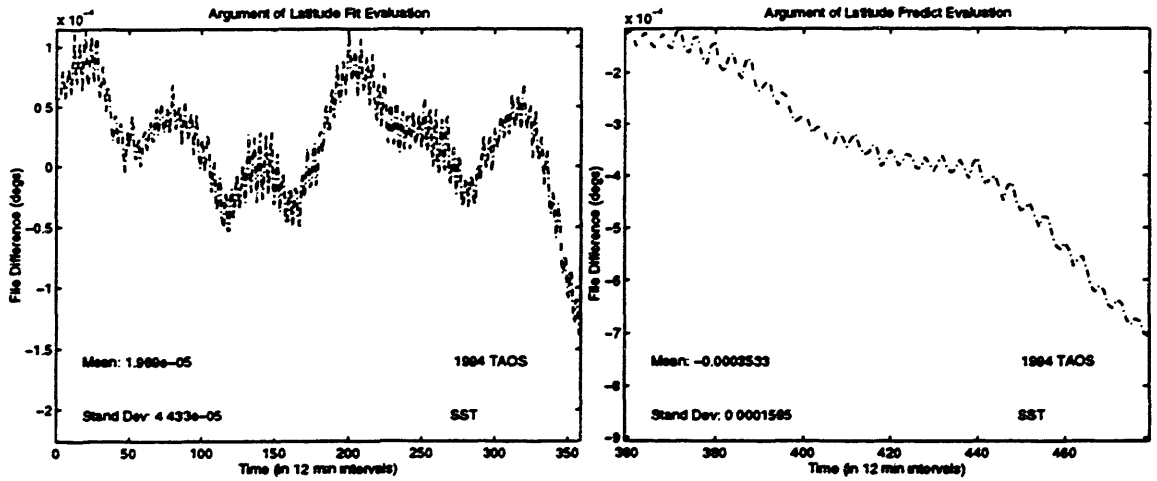

Figure H.145 TAOS Argument of Latitude Errors for SST Experiment with Near-Real Time Atmospheric Information

H.3 EUVE Experiments

Testing of the EUVE data was limited to two experiments due to the unavailability of the navigation solutions and POEs. The POEs were initially fit in the same manner as the TOPEX and TAOS POEs to provide an estimate of how well Draper R&D GTDS was modeling the EUVE perturbations. The navigation solutions were then fit with Cowell and SST over a two day period, the longest interval where contiguous data was available.

H.3.1 Orbit Determination from the EUVE POEs

Gold reports that the EUVE POEs produced at the University of Colorado at Boulder have an accuracy of about one meter [26]. Because EUVE's orbit can be characterized in many ways similar to TAOS's orbit, the configuration for fitting the POEs was comparable. The Cowell fit to the POEs contained the following dynamic models.

Table H.6 Orbit Dynamic Models Used in EUVE Analysis

Perturbation	Description
Earth's gravity	JGM-2 50x50; 4x4 partials
Solar Radiation Pressure	Cylindrical macro model
Atmospheric Drag	Jacchia-Roberts
Lunar/Solar Third Body	Point Mass
Lunar/Solar Tides	Love number (0.29)

The only significant difference noted in comparison of Tables H.2 and H.3 is the atmospheric density files used. One and a half days of POE vectors were included in the fit span to estimate the EUVE orbit and drag parameter.

Experiment 1: EUVE 1.5 Day Fit of the POE Vectors (EUVE_POE_ECF_DC_1)

```
CONTROL  DC                                                          TOPEXXX  XXXXXX
EPOCH        920914.0        210052.000000
ELEMENT1 10    1     1       4817.1444600000D0   4623.183680000000D0  -1755.744600000000D0
ELEMENT2                    -3.864213500000D0   5.191890700000000D0  3.058730300000000D0
OBSINPUT 20                 920914 210152       920916 025852
ORBTYPE  2     1     11      10.0
DMOPT
OBSDEV   21                 5.
OBSDEV   22                 5.
OBSDEV   23                 5.
OBSDEV    24                .5
OBSDEV   25                 .5
OBSDEV   26                 .5
END
DCOPT
PRINTOUT 1     4
CONVERG  20                 1.D-4                                    1.0
END
OGOPT
DRAG     1                  1.
ATMOSDEN               1
DRAGPAR  2     1            0.15D0
SCPARAM                     2.8D-5              2400.0D0
MAXDEGEQ 1                  50.
MAXORDEQ 1                  50.
MAXDEGVE 1                  4.
MAXORDVE 1                  4.
POTFIELD 1     19
SETIDE   1                  0.29D0
SOLRAD   1                  1
STATEPAR 1
STATETAB 1     2     3      4                   5                    6
END
FIN
CONTROL  EPHEM                    OUTPUT                             TOPEXXX  XXXXXX
OUTPUT   3     2     1      920916.D0           025852.D0            43200.D0
ORBTYPE  2     1     11     10.0
OGOPT
DRAG     1                  1
ATMOSDEN               1
DRAGPAR  0
SCPARAM                     2.8D-5              2400.0D0
MAXDEGEQ 1                  50.
MAXORDEQ 1                  50.
MAXDEGVE 1                  4.
MAXORDVE 1                  4.
POTFIELD 1     19
SETIDE   1                  0.29D0
SOLRAD   1                  1
OUTOPT   1                  920914210152.0      920916024952.0       120.0
END
FIN
```

Figure H.146 EUVE Cowell 1.5 Day POE Fit Input Card Data File

```
$!-------------------------------------------------------------------------
$! EUVE_POE_ECF_DC_1
$!
$!
$!-------------------------------------------------------------------------
$!
$! Set default for batch run from CSDL0:[GTDS.GTDS_TEST]
$  set default fds$diska:[ssc2414.work.new_gtds.thesis.com]
$!
$! Assign debug overrides
$!
$  assign/table=lnm$job [ssc2414.work.new_gtds.thesis.overrides]euve_poe_ecf_dc_1.overrides dbg$init
$!
$! Assign the observation card file
$!
$  assign/table=lnm$job fds$diska:[ssc2414.explorer.obscard]sep15_poe.poscard gtds$015
$!
$! Assign the body potential files
$!
$  assign/table=lnm$job fds$diska:[djf1230.bianca]dan_potential.dat gtds$047
$  assign/table=lnm$job fds$diska:[djf1230.bianca]moon.dat      gtds$048
$!
$! Assign the body potential files
$!
$  assign/table=lnm$job elrond$dka0:[ssc2414]june95_msgen_slp_mn2000.dat gtds$014
$  assign/table=lnm$job elrond$dka0:[ssc2414]june95_msgen_slp_timecoef.dat gtds$038
$  assign/table=lnm$job elrond$dka0:[ssc2414]june95_msgen_slp_tod2000.dat gtds$078
$!
$! Assign ORB1 files
$!
$  assign/table=lnm$job fds$diska:[ssc2414.work.new_gtds.thesis.orb1]euve_poe_ecf_dc_1.orb1 gtds$024
$!
$! Assign atmospheric density file
$!
$  assign/table=lnm$job fds_dbf:jacchia_roberts.dat  gtds$075
$!
$! Assign fundamental constants file
$!
$  assign/table=lnm$job fds$diska:[ssc2414.work.new_gtds.mods]j2000_csconst.dat gtds$099
$!
$! Execute the local version of debug executable
$!
$  @[ssc2414.work.new_gtds.test]j2000_SWAT_GTDS [ssc2414.work.new_gtds.thesis.gtds]euve_poe_ecf_dc_1
$  rename [-.gtds]euve_poe_ecf_dc_1.output [-.output]euve_poe_ecf_dc_1.output
$!
$  assign/table=lnm$job fds_dbf:schatten_jacchia_roberts.dat  gtds$075
$  EXIT
```

Figure H.147 EUVE Cowell 1.5 Day POE Fit Command Procedure

```
SET OUTPUT LOG
SET LOG
SET BREAK/return ESTSET DO -
      (DEPOSIT  IDIFF      = 3; -
       DEPOSIT  IDRVAR     = 1; -
       DEPOSIT  ISRVAR     = 0; -
       DEPOSIT  KPAR       = 0; -
       DEPOSIT  KATMOS     = 1; -
       EXAMINE  KATMOS     ; -
       EXAMINE  IDIFF      ; -
       EXAMINE  IDRVAR     ; -
       EXAMINE  ISRVAR     ; -
       EXAMINE  KPAR       ; -
       GO -
    ); -
GO
```

Figure H.148 EUVE Cowell 1.5 Day POE Fit Overrides File

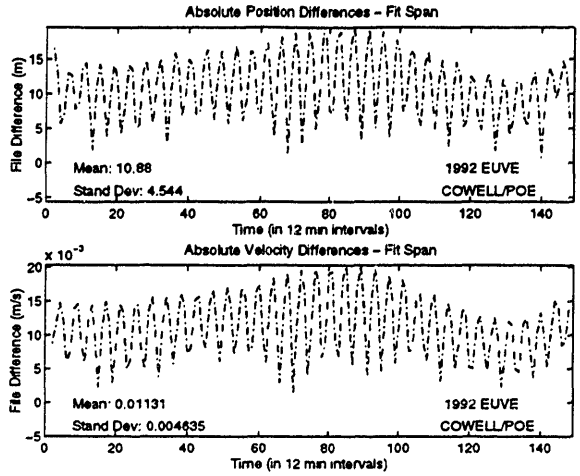

Figure H.149 EUVE Position and Velocity Errors for Cowell 1.5 Day POE Fit

H.3.2 Orbit Determination from the EUVE Navigation Solutions

After the EUVE POEs were fit to provide an indication of the process noise associated with the differential correction fit, the use of navigation solutions for a drag-perturbed satellite was evaluated for EUVE. Because of the lack of valid navigation solutions over periods longer than two days, the experimentation for EUVE was limited to one Cowell and one SST fit and predict. The predict interval was somewhat unorthodox, as it begins five days after the conclusion of the fit span, and lasts for two days, resulting in a difference in the beginning of the fit span and end of the predict span of nine days. This delay in measuring variation in the predict span was a result of a lack of POE information in the interim period. Error analysis was limited to the absolute position and velocity differences because the EUVE POEs were provided in a non-inertial frame (ECEF).

Experiment 1: EUVE Two Day Fit of the Navigation Solutions with Cowell

(EUVE_NAV_COWELL_FIT_1)

```
CONTROL  DC                                                        EUVEXXX  XXXXXX
EPOCH                        920915.D0          000010.064087D0
ELEMENT1 10    1     1       4559.8545571997D0  -4135.8961409612D0  -4135.8961409612D0
ELEMENT2                     5.1654390121014D0  4.8243172194616D0   1.1366040000000D0
OBSINPUT 20                  920915 000040      920917 000000
ORBTYPE  2     1     11      10.0
DMOPT
OBSDEV   21                  50.
OBSDEV   22                  50.
OBSDEV   23                  50.
OBSDEV    24                 100.
OBSDEV   25                  75.
OBSDEV   26                  125.
END
DCOPT
PRINTOUT 1   4
CONVERG  20                  1.D-4                                 1.0
END
OGOPT
DRAG     1                   1.
ATMOSDEN           1
DRAGPAR  2     1             0.15D0
SCPARAM                      2.8D-5             2400.0D0
MAXDEGEQ 1                   50.
MAXORDEQ 1                   50.
MAXDEGVE 1                   4.
MAXORDVE 1                   4.
POTFIELD 1     19
SETIDE   1                   0.29D0
SOLRAD   1                   1
STATEPAR 1
STATETAB 1     2     3       4                  5                   6
END
FIN
CONTROL  EPHEM                     OUTPUT                          TOPEXXX  XXXXXX
OUTPUT   3     2     1       920917.0           0.0                 43200.D0
ORBTYPE  2     1     11      10.0
OGOPT
DRAG     1                   1
ATMOSDEN           1
DRAGPAR  0
SCPARAM                      2.8D-5             2400.0D0
MAXDEGEQ 1                   50.
MAXORDEQ 1                   50.
MAXDEGVE 1                   4.
MAXORDVE 1                   4.
POTFIELD 1     19
SETIDE   1                   0.29D0
SOLRAD   1                   1
OUTOPT   1                   920915000100.0     920917000100.0      120.0
END
FIN
```

Figure H.150 EUVE Cowell Two Day Navigation Solution Fit Input Card Data File

```
$!-------------------------------------------------------------
$! EUVE_NAV_COWELL_FIT_1
$!
$!
$!-------------------------------------------------------------
$!
$! Set default for batch run from CSDL0:[GTDS.GTDS_TEST]
$  set default fds$diska:[ssc2414.work.new_gtds.thesis.com]
$!
$! Assign debug overrides
$!
$  assign/table=lnm$job [ssc2414.work.new_gtds.thesis.overrides]euve_nav_cowell_fit_1.overrides dbg$init
$!
$! Assign the observations card file
$!
$  assign/table=lnm$job fds$diska:[ssc2414.explorer.obscard]259_260_pbias.poscard gtds$015
$!
$! Assign the body potential files
$!
$  assign/table=lnm$job fds$diska:[djf1230.bianca]dan_potential.dat gtds$047
$  assign/table=lnm$job fds$diska:[djf1230.bianca]moon.dat      gtds$048
$!
$! Assign the atmospheric density file
$!
$  assign/table=lnm$job fds_dbf:jacchia_roberts.dat   gtds$075
$!
$! Assign the SLP and timing files
$!
$  assign/table=lnm$job elrond$dka0:[ssc2414]june95_msgen_slp_mn2000.dat gtds$014
$  assign/table=lnm$job elrond$dka0:[ssc2414]june95_msgen_slp_timecoef.dat gtds$038
$  assign/table=lnm$job elrond$dka0:[ssc2414]june95_msgen_slp_tod2000.dat gtds$078
$!
$! Assign ORB1 files
$!
$  assign/table=lnm$job fds$diska:[ssc2414.work.new_gtds.thesis.orb1]euve_nav_cowell_fit_1.orb1 gtds$024
$!
$! Assign fundamental constants file
$!
$  assign/table=lnm$job fds$diska:[ssc2414.work.new_gtds.mods]j2000_csconst.dat gtds$099
$!
$! Execute the local version of debug executable
$!
$  @[ssc2414.work.new_gtds.test]j2000_SWAT_GTDS [ssc2414.work.new_gtds.thesis.gtds]euve_nav_cowell_fit_1
$  rename [-.gtds]euve_nav_cowell_fit_1.output [-.output]euve_nav_cowell_fit_1.output
$!
$  assign/table=lnm$job fds_dbf:schatten_jacchia_roberts.dat gtds$075
$
$  EXIT
```

Figure H.151 EUVE Cowell Two Day Navigation Solution Fit Command Procedure

```
SET OUTPUT LOG
SET LOG
SET BREAK/return ESTSET DO -
      (DEPOSIT  IDIFF      = 3; -
       DEPOSIT  IDRVAR     = 1; -
       DEPOSIT  ISRVAR     = 0; -
       DEPOSIT  KPAR       = 0; -
       DEPOSIT  KATMOS     = 1; -
       EXAMINE  KATMOS     ; -
       EXAMINE  IDIFF      ; -
       EXAMINE  IDRVAR     ; -
       EXAMINE  ISRVAR     ; -
       EXAMINE  KPAR       ; -
       GO -
    ); -
GO
```

Figure H.152 EUVE Cowell Two Day Navigation Solution Fit Overrides File

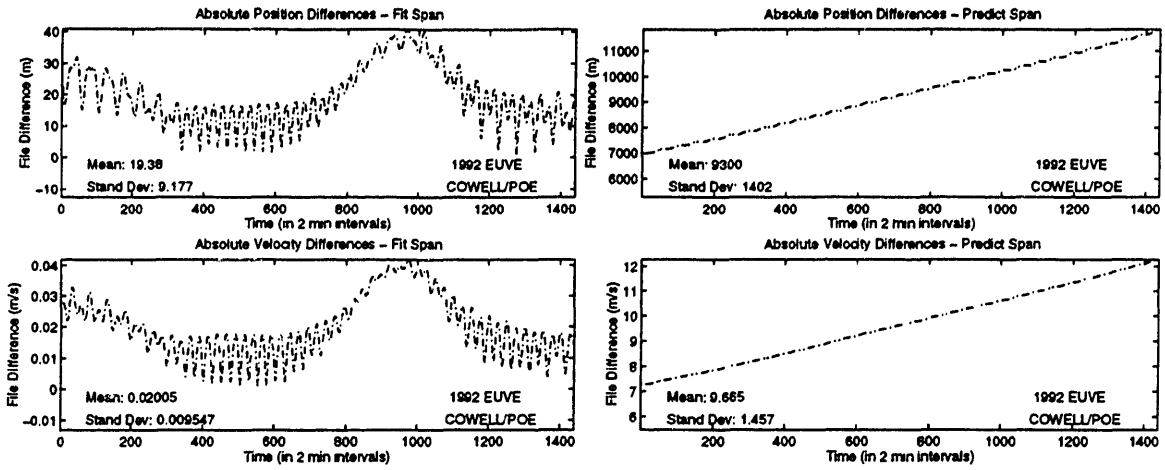

Figure H.153 EUVE Position and Velocity Errors for Cowell Two Day Navigation Solution Fit and Two Day Predict

Experiment 2: EUVE Two Day Fit of the Navigation Solutions with SST (EUVE_NAV_SST_FIT_1)

```
CONTROL  DC                                                          EUVEXXX  XXXXXX
EPOCH                        920915.D0          000010.064087D0
ELEMENT1 10    1     1       4559.8545571997D0  -4135.8961409612D0  -4135.8961409612D0
ELEMENT2                     5.1654390121014D0  4.8243172194616D0   1.1366040000000D0
OBSINPUT 20                  920915 000040      920917 000000
ORBTYPE  5     1     11      43200.0            1.0
DMOPT
OBSDEV   21                  50.
OBSDEV   22                  50.
OBSDEV   23                  50.
OBSDEV   24                  100.
OBSDEV   25                  75.
OBSDEV   26                  125.
END
DCOPT
PRINTOUT 1     4
CONVERG  20                  1.D-4                                   1.0
END
OGOPT
DRAG     1                   1.
ATMOSDEN           1
DRAGPAR  1
SCPARAM                      2.8D-5             2400.0D0
MAXDEGEQ 1                   50.
MAXORDEQ 1                   50.
MAXDEGVE 1                   4.
MAXORDVE 1                   4.
POTFIELD 1     19
RESONPRD                     432000.D0
SETIDE   1                   0.29D0
SOLRAD   1                   1
STATEPAR 3
STATETAB 1     2     3       4                  5                   6
END
FIN
CONTROL  EPHEM                     OUTPUT                            TOPEXXX  XXXXXX
OUTPUT   3     2     1       920917.0           0.0                 43200.D0
ORBTYPE  5     1     11      43200.0            1.0
OGOPT
DRAG     1                   1
ATMOSDEN           1
DRAGPAR  0
SCPARAM                      2.8D-5             2400.0D0
MAXDEGEQ 1                   50.
MAXORDEQ 1                   50.
MAXDEGVE 1                   4.
MAXORDVE 1                   4.
POTFIELD 1     19
RESONPRD                     432000.D0
SETIDE   1                   0.29D0
SOLRAD   1                   1
OUTOPT   1                   920915000100.0     920917000100.0      120.0
END
FIN
```

Figure H.154 EUVE SST Two Day Navigation Solution Fit Input Card Data File

```
$!-------------------------------------------------------------
$! EUVE_NAV_SST_FIT_1
$!
$!
$!-------------------------------------------------------------
$!
$! Set default for batch run from CSDL0:[GTDS.GTDS_TEST]
$  set default fds$diska:[ssc2414.work.new_gtds.thesis.com]
$!
$! Assign debug overrides
$!
$  assign/table=lnm$job [ssc2414.work.new_gtds.thesis.overrides]euve_nav_sst_fit_1.overrides dbg$init
$!
$! Assign the observations card file
$!
$  assign/table=lnm$job fds$diska:[ssc2414.explorer.obscard]259_260_pbias.poscard gtds$015
$!
$! Assig. the body potential files
$!
$  assign/table=lnm$job fds$diska:[djf1230.bianca]dan_potential.dat gtds$047
$  assign/table=lnm$job fds$diska:[djf1230.bianca]moon.dat      gtds$048
$!
$! Assign the atmospheric density file
$!
$  assign/table=lnm$job fds_dbf:jacchia_roberts.dat   gtds$075
$!
$! Assign the SLP and timing files
$!
$  assign/table=lnm$job elrond$dka0:[ssc2414]june95_msgen_slp_mn2000.dat gtds$014
$  assign/table=lnm$job elrond$dka0:[ssc2414]june95_msgen_slp_timecoef.dat gtds$038
$  assign/table=lnm$job elrond$dka0:[ssc2414]june95_msgen_slp_tod2000.dat gtds$078
$!
$! Assign ORB1 files
$!
$  assign/table=lnm$job fds$diska:[ssc2414.work.new_gtds.thesis.orb1]euve_nav_sst_fit_1.orb1 gtds$024
$!
$! Assign fundamental constants file
$!
$  assign/table=lnm$job fds$diska:[ssc2414.work.new_gtds.mods]jj2000_csconst.dat gtds$099
$!
$! Execute the local version of debug executable
$!
$  @[ssc2414.work.new_gtds.test]jj2000_SWAT_GTDS [ssc2414.work.new_gtds.thesis.gtds]euve_nav_sst_fit_1
$  rename [-.gtds]euve_nav_sst_fit_1.output [-.output]euve_nav_cowell_sst_1.output
$!
$  assign/table=lnm$job fds_dbf:schatten_jacchia_roberts.dat gtds$075
$
$  EXIT
```

Figure H.155 EUVE SST Two Day Navigation Solution Fit Command Procedure

```
SET OUTPUT LOG
 SET LOG
 SET BREAK/return ESTSET DO -
       (DEPOSIT  IDIFF       = 3; -
        DEPOSIT  IDRVAR      = 1; -
        DEPOSIT  ISRVAR      = 0; -
        DEPOSIT  KPAR        = 1; -
        DEPOSIT  KATMOS      = 1; -
        EXAMINE  KATMOS      ; -
        EXAMINE  IDIFF       ; -
        EXAMINE  IDRVAR      ; -
        EXAMINE  KPAR        ; -
        GO -
    ); -
GO
 SET BREAK/return HWIRE  DO -
       (DEPOSIT  LZN         = 4; -
        DEPOSIT  JZN         = 25; -
        DEPOSIT  LMD         = 4; -
        DEPOSIT  MMD         = 28;-
        DEPOSIT  MTS         = 41;-
        DEPOSIT  NJ2MD       = 12; -
        DEPOSIT  MJ2MD       = 12; -
        DEPOSIT  LJ2MD       = 4; -
        DEPOSIT  IDRMD       = 2; -
        DEPOSIT  JMAXTH(1)   = 5; -
        DEPOSIT  JMAXTS      = 25;-
        DEPOSIT  JMINTS      =-25;-
        EXAMINE  LZN         ; -
        EXAMINE  JZN         ; -
        EXAMINE  LMD         ; -
        EXAMINE  NJ2MD       ; -
        EXAMINE  MJ2MD       ; -
        EXAMINE  LJ2MD       ; -
        EXAMINE  IDRMD       ; -
        EXAMINE  JMAXTH(1)   ; -
        GO -
    ); -
GO
```

Figure H.156 EUVE SST Two Day Navigation Solution Fit Overrides File

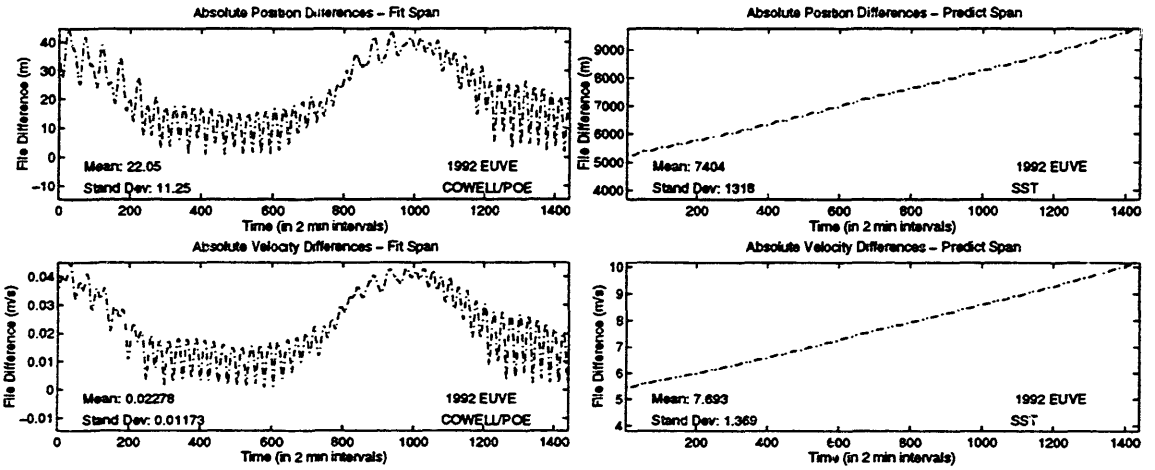

Figure H.157 EUVE Position and Velocity Errors for SST Two Day Navigation Solution Fit and Two Day Predict

[This page intentionally left blank.]

Appendix I

SLP Files Used in This Project

This appendix provides a brief description of the SLP files used for this project. The information contained in the files used by Draper R&D GTDS programs is initially stored on a tape provided by the Jet Propulsion Laboratory. Personnel at the Goddard Space Flight Center translate the information from the JPL tape into SLP files via the Testing, Report, and Maintenance Program (TRAMP). The files are then distributed to interested parties, including Draper Laboratory.

The FK-5 based files were requested from GSFC in July 1995, and provided in August 1995. The files were removed from the tape sent by GSFC personnel and placed on Draper's IBM mainframe by Mr. James Ogletree. Dr. Paul Cefola then named the files in the following manner:

Table I.1 IBM Naming Convention for August 1995 SLP Files

File Description	IBM Mainframe File Name
Time Observation File (TRAMP)	*PJC1787.TEMP.1995.FILE1.DATA*
UTC Leap Second File (TRAMP)	*PJC1787.TEMP.1995.FILE2.DATA*
GTDS Timing Coefficient File	*PJC1787.TEMP.1995.FILE3.DATA*
SLP Ephemeris File (mean equator and equinox of B1950.0)	*PJC1787.TEMP.1995.FILE4.DATA*
SLP Ephemeris File (true equator and equinox -- FK4-based)	*PJC1787.TEMP.1995.FILE5.DATA*
SLP Ephemeris File (mean equator and equinox of J2000.0)	*PJC1787.TEMP.1995.FILE6.DATA*
SLP Ephemeris File (true equator and equinox -- FK5-based)	*PJC1787.TEMP.1995.FILE7.DATA*

The timing coefficient and FK5-based SLP files were then converted from their IBM binary format into text for transfer to the VAX environment. Once the transfer had taken place, the files were then reconverted to a VAX binary format for use by VAX R&D GTDS. Currently, these files are located in the author's directory (ELROND$DKA0:[SSC2414]) and named as follows:

Table I.2 VAX Naming Convention for August 1995 SLP Files

File Description	VAX File Name
GTDS Timing Coefficient File	*JUNE95_MSGEN_TIMECOEF.DAT*
SLP Ephemeris File (mean equator and equinox of J2000.0)	*JUNE95_MSGEN_SLP_MN2000.DAT*
SLP Ephemeris File (true equator and equinox -- FK5-based)	*JUNE95_MSGEN_SLP_TOD2000.DAT*

The JUNE95 designation was chosen because that was the time period when the timing coefficient files were last updated.

[This page intentionally left blank.]

References

[1] Aoki, S. *et al. Conversion Matrix of Epoch B1950.0 FK4-based Positions of Stars to Epoch J2000.0 Positions in Accordance with the New IAU Resolutions.* Astronomy and Astrophysics. Vol. 128. 1983.

[2] *The Astronomical Almanac* (1992). U.S. Government Printing Office, Washington, and HM Stationery Office, London.

[3] Bate, Roger R. *et al. Fundamentals of Astrodynamics.* New York: Dover Publications, Inc. 1971.

[4] Battin, Richard H. *An Introduction to the Mathematics and Methods of Astrodynamics.* New York: AIAA Education Series. 1987.

[5] Bertiger, Willy I. Jet Propulsion Laboratory. Personal Discussion. (818) 354-4990.

[6] Blitzer, Leon. *Handbook of Orbital Perturbations.* Professor of Physics, University of Arizona. Partially re-printed and used as course text for Astronautics 422 at the United States Air Force Academy (Spring 1993). Colorado Springs, CO. Copy available from Department of Astronautics at the United States Air Force Academy.

[7] Broucke, Roger. *On the Matrizant of the Two-Body Problem.*

Astronomy and Astrophysics. Vol. 6, 173-182, 1980.

[8] Carter, Scott S., Paul J. Cefola, and Ronald J. Proulx. *The Determination of Precision Mean Element Sets From GPS Receiver On-Board Navigation Solutions.* Paper presented at the *AIAA/AAS Astrodynamics Conference.* August 14-17, 1995. Halifax, Nova Scotia, Canada.

[9] Cefola, Paul J, Daniel J. Fonte, and Naresh Shah. *The Inclusion of the Naval Space Command Satellite Theory PPT2 in the R&D GTDS Orbit Determination System.* Paper presented at the *AAS/AIAA Space Flight Mechanics Meeting.* February 12-15, 1996. Austin, TX.

[10] Cefola, Paul J. *Equinoctial Orbit Elements - Application to Artificial Satellite Orbits.* AIAA Paper #72-937. *AIAA/AAS Astrodynamics Conference.* Palo Alto, CA. September 1972.

[11] Cefola, Paul J. *On the Formulation of the Gravitational Potential in Terms of Equinoctial Variables.* Paper presented at the *13th AIAA Aerospace Sciences Meeting,* January 20-22, 1975. Pasadena, CA.

[12] Cefola, Paul J. Personal Discussions. August 1994 through May 1996. (617) 258-1787.

[13] Cefola, Paul J. *R&D GTDS Semianalytical Satellite Theory Input Processor.* Draper Laboratory IOC, ESD-92-582/SGI GTDS-92-001, December 17, 1992. Copy available through Dr. Paul Cefola. (617) 258-

1787.

[14] Cefola, Paul J. *Semianalytic Orbit Generation (N00014-81-C-0206) Long Arc Observation Data Processiong Progress Review.* Prepared for the Naval Surface Weapons Center (NSWC). June 1983.

[15] *Explanatory Supplement to the Astronomical Ephemeris and the American Ephemeris and Nautical Almanac.* London: Her Majesty's Stationery Office, 1961.

[16] *Explorer Interface Control Document,* 408-EP-240-002. Goddard Space Flight Center.

[17] Fennessey, Richard *et al. GPS as an Orbit Determination Subsystem.* Space Test Engineering Contract #F04690-92-C-0529, U.S. Air Force Materiel Command, presented at the *NASA GSFC Flight Mechanics Meeting,* May 1995. (NASA CP-3299).

[18] Ferguson, Jack. *Statistical Orbit Determination.* Reprinted for Astronautics 422 course at the United States Air Force Academy (Spring 1993). Colorado Springs, CO. Copy available from Department of Astronautics at the United States Air Force Academy.

[19] Fonte, Daniel J. *An Introduction to Perturbation Theory.* Summary of notes made during 16.601, an advanced special topic course at the Massachusetts Institute of Technology. Department of Aeronautics and Astronautics. Spring Term, 1992. Copy available from Dr. Paul Cefola

(617) 258-1787.

[20] Fonte, Daniel J. *Implementing a 50x50 Gravity Field Model in an Orbit Determination System.* Master of Science Thesis. Department of Aeronautics and Astronautics, Massachusetts Institute of Technology. CSDL-T-1169. June 1993.

[21] Fonte, Daniel J. *PC Based Orbit Determination.* Paper presented at the *AIAA/AAS Astrodynamics Conference.* August 1-3, 1994. Scottsdale, AZ.

[22] Fricke, W. *Determination of the Equinox and Equator of the FK5.* Astronomy and Astrophysics. Vol. 107, L13-16, 1982.

[23] Gaposchkin, E.M. *Satellite Dynamics.* 1973 Smithsonian Standard Earth (III). Cambridge, MA: Smithsonian Institution Astrophysical Observatory, 1974.

[24] *Goddard Trajectory Determination System (GTDS) Mathematical Theory.* NASA's Operational GTDS Mathematical Specification. Revision 1. Edited by Computer Sciences Corporation and NASA Goddard Space Flight Center. Contract NAS 5-31500. Task 213. July 1989.

[25] *Goddard Trajectory Determination System (GTDS) User's Guide.* NASA's Operational GTDS User's Guide. Revision 2, Update 8. Edited by Computer Sciences Corporation and NASA Goddard Space Flight

Center. Contract NAS 5-31500. Task 52 617. September 1994.

[26] Gold, Kenn L. *GPS Orbit Determination for the Extreme Ultraviolet Explorer.* Ph.D. Thesis, Department of Aerospace Engineering Sciences, University of Colorado. November 1994.

[27] Guinn, Joseph, and Peter Wolff. *TOPEX/POSEIDON Operational Orbit Determination Results Using Global Positioning Satellites.* Advances in the Astronautical Sciences. Vol. 85, Part II, 143-158, 1993.

[28] Guinn, Joseph *et al. TAOS Orbit Determination Results Using Global Positioning Satellites.* AAS Pre-print 95-146, presented at the *AAS/AIAA Spaceflight Mechanics Meeting,* Albuquerque, NM, February, 1995.

[29] Guinn, Joseph. Jet Propulsion Laboratory. Personal Discussion. July 1995. (818) 354-0425.

[30] Guinn, Joseph R., Timothy N. Munson, and Mark A. Vincent. *Autonomous Spacecraft Navigation for Earth Ground Track Repeat Orbits Using GPS.* Presented at the *AAS/AIAA Space Flight Mechanics Meeting,* Austin, TX, February 1996.

[31] Gurtner, W., G. Mader, and D. MacArthur. *A Common Exchange Format for GPS Data.* CSTG GPS Bulletin, Vol. 2, No. 3, May/June 1989, National Geodetic Survey, Rockville, MD.

[32] Heronema, Jennifer. *Pentagon Must Give Equal Time to Commercial Users of GPS.* Defense News. April 1-7, 1996. p.58.

[33] Irish, Kelly *et al. Precision Orbit Determination for GFO and GFO-2.* Presented at the *AAS/AIAA Space Flight Mechanics Meeting,* Austin, TX, February 1996.

[34] Jablonski (Boelitz), Carole A. *Application of Semianalytic Satellite Theory to Maneuver Planning.* Master of Science Thesis, Department of Aeronautics and Astronautics, Massachusetts Institute of Technology. CSDL-T-1086. May 1991.

[35] Kaplan, G. H. *et al. Mean and Apparent Place Computations in the New IAU System. III. Apparent, Topocentric, and Astrometric Places of Planets and Stars.* The Astronomical Journal. Vol.97, No.4. April 1989.

[36] Kaplan, G. H. *The IAU Resolutions on Astronomical Constants, Time Scales, and the Fundamental Reference Frame.* USNO Circular No. 163 (United States Naval Observatory). Washington, D.C., 1981.

[37] Kawano, Isao *et al. The Application of GPS to the H-II Orbiting Plane.* Navigation. Vol. 38, No. 4, 317-322, Winter 1991-1992.

[38] Langer, John V. *et al. RADCAL: Precision Orbit Determination with a Commercial Grade GPS Receiver.* 1992 National Technical Meeting of The Institute of Navigation, January 1994.

[39] Laubscher, Roy. Personal Discussion. 22 March 1996. (805) 968-7473.

[40] Leick, A. *GPS Satellite Surveying.* New York:Wiley-Interscience. 1995.

[41] Lieske, J. H. *et al. Expressions for the Precession Quantities Based upon the IAU (1976) System of Astronomical Constants.* Astronomy and Astrophysics. Vol. 58, 1-16, 1977.

[42] Lieske, Jay H. *Precession Matrix Based on IAU(1976) System of Astronomical Constants.* Astronomy and Astrophysics. Vol. 73. 1979.

[43] Lowery, Stephanie. Johnson Space Center. Personal Discussion. October 1994. (713) 483-0187.

[44] McClain, Wayne. *A Recursively Formulated First-Order Semianalytic Artificial Satellite Theory Based on the Generalized Method of Averaging.* Volume 1. Contract NAS 5-24300, Task Assignment 880. June 1978.

[45] McClain, Wayne D., Intralab Memorandum, "GTDS Implementation of the NORAD C and B Matrices," Charles Stark Draper Laboratory, Cambridge, MA, 14 September 1987.

[46] Melbourne, William G., E.S. Davis, and Thomas P. Yunck. *The GPS Flight Experiment on TOPEX/POSEIDON.* Geophysical Research Letters. Vol. 21, No. 19, 2171-2174, September 15, 1994.

[47] Metzinger, Richard. *Validation of the Workstation Version of R&D GTDS.* February 1993. Copy available through Dr. Paul Cefola. (617) 258-1787.

[48] Milani, Andrea, Anna Maria Nobili, and Paolo Farinella. *Non-Gravitational Perturbations and Satellite Geodesy.* Bristol, England: Adam Hilger, 1987.

[49] Munjal, Prem, William Feess, and Mohan Ananda. *A Review of Spaceborne Applications of GPS.* ION GPS-92 Meeting Proceedings. September 1992.

[50] Murata, Masaaki, Masatoshi Harigae, and Toshiaki Tsuji. *Orbit Determination of the Orbital Re-Entry Experiment (OREX) Spacecraft by GPS.* Presented at the *AAS/AIAA Space Flight Mechanics Meeting,* Austin, TX, February 1996.

[51] Murray, C. A. *The Transformation of Coordinates Between the Systems of B1950.0 and J2000.0, and the Principal Galactic Axes Referred to J2000.0.* Astronomy and Astrophysics. Vol. 218, 325-329, 1989.

[52] O'Toole, James W. *CELEST Computer Program for Computing Satellite Orbits,* Naval Surface Weapons Center, TR-3565. October 1976.

[53] *Recommended Practice: Astrodynamics - Concepts,Terms, and Symbols - Part 1.* ANSI/AIAA R-064-1995. October 1995.

[54] *Research and Development Goddard Trajectory Determination System (R&D GTDS) User's Guide.* Edited jointly by Computer Sciences Corporation and Systems Development and Analysis Branch, Goddard Space Flight Center. July 1978.

[55] Rim, Hyung J., George W. Davis, and Bob E. Schutz. *Dynamic Orbit Determination for the EOS Laser Altimeter Satellite (EOS ALT/GLAS) Using GPS Measurements.* Presented at the *AAS/AIAA Space Flight Mechanics Meeting,* Austin, TX, February 1996.

[56] Roy, A. E. *Orbital Motion.* New York: Adam Hilger. 1991.

[57] Schroeder, C. , B. Schutz, and P. Abusali. *STS-69 Relative Positioning GPS Experiment.* Presented at the *AAS/AIAA Space Flight Mechanics Meeting,* Austin, TX, February 1996.

[58] Seidelmann, Kenneth. *Explanatory Supplement to the Astronomical Almanac.* Mill Valley, CA: University Science Books, 1992.

[59] Sfeir, R. and R. Weninger. *Six Channel Spaceborne GPS Receiver.* Presented at the *5th Annual AIAA/USU Conference on Small Satellites,* Logan, UT, August, 1991.

[60] Swift, Everett R., Michael J. Merrigan, and M. Wendel Gouldman. *Orbit Estimation for TOPEX/POSEIDON Based on GPS Tracking Data.* Presented at the *AAS/AIAA Space Flight Mechanics Meeting,* Austin,

TX, February 1996.

[61] Tapley, Byron D. *et al. Precision Orbit Determination for TOPEX/POSEIDON.* Journal of Geophysical Research. Vol. 99, No. C12, 24383-24404, December 15, 1994.

[62] *Testing, Reporting, and Maintenance Program (TRAMP) User's Guide.* Revision 1. Prepared for NASA/Goddard Space Flight Center by Computer Sciences Corporation. Contract NAS 5-27600. Task Assignment 210-751. April 1988.

[63] Vannicola, Francine. U.S. Naval Observatory. Personal Discussion. October 1994. (202) 653-1525.

[64] Wallace, Scott T. U. S. Air Force, Phillips Laboratory, Kirtland AFB, New Mexico. Provided near-real time atmospheric density data file based upon information from the NOAA Bulletin Board.

[65] Wilson, Andrew. *Jane's Space Directory, 10th edition.* Alexandria, VA: Jane's Information Group, Inc. 1994.

[66] Wright, James. *Variation of Parameters for Definitive Geocentric Orbits.* AIAA-92-4361-CP. *AIAA/AAS Astrodynamics Conference,* Hilton Head, SC. August 1992.

[67] Zelensky, Nikita. Goddard Space Flight Center. Personal Discussion. June 1995. (301) 441-4107.

[68] Zelensky, Nikita. *Topex GSFC Precision Orbit Determination Production System (PDOPS) Development.* Document from FTP site *bodhi.jpl.nasa.gov.*